Electronic Structure and Photochemical Reactivity of Binuclear Metal Complexes

Thesis by

David Charles Smith

In Partial Fulfillment of the Requirements

for the Degree of

Doctor of Philosophy

California Institute of Technology

Pasadena, California

1989

(Submitted February 20, 1989)

To Mom, Dad, and Gunilla

Acknowledgments

Well, it is finally over. All that remains for me to do is to acknowledge the many people who have enriched my experience at Cal Tech.

I first must thank Harry and Bill for giving me the opportunity (and the money) to explore my own interests. The freedom you gave me has taught me how to develop and pursue an idea, and my interaction with you has been invaluable. You have shown me what it takes to be a great scientist. Harry has also shown me that one should not take life too seriously.

While I have valued my independence, I could not have achieved the end result without numerous interactions. Vinny Miskowski and Tad Fox have been through thick and thin with me for the past years: Vinny showing me the ins and outs of electronic spectroscopy; Tad being a friend with whom I have shared many experiences. Bill Schaefer and Dick Marsh have been invaluable for all of the crystallographic work that was necessary for the research. I have come away from this interaction with a deep appreciation and respect for those who still approach x-ray crystallography as an art form and not simply as another analytical tool. Special thanks go to Roy Mason and Tom Loehr, those voices on the other end of the telephone line, who provided some of the crucial data for this work. I owe special thanks to Adria McMillan. Thanks for caring, taking time out to sit and listen, and to ask how things were going. Other comrades in arms whom I would like to mention and thank are Tony Vlcek (he taught me a lot about inorganic photochemistry), John Brewer, Miriam Zeitlow, Adel Naylor, Mary Selman, Janet Marshall (thanks for the Schlenk line), Cindy St. Clair, Mike Hopkins, Walther Ellis (ligand field theory forever), Al Stiegman, Catherine May, Ged Parkin, Rita Upmacis, Mark Brusich, John Low, and Tom Zeitlow. These are but a few of the people who were part of the Cal Tech experience.

Special thanks go to Mark Neifeld. He has been a true friend and a good roommate.

All that I have accomplished here at Cal Tech could not have been realized without the help of three very special people. My parents have stood by me for the many long years with words of encouragement and support. Gunilla Persson has made these past four years at Cal Tech my happiest. I do not know how I could have survived the ordeal of graduate school without the love and encouragement she has offered so unselfishly.

I would also like to acknowledge the financial support of the Sun Oil Company and the National Science Foundation.

Abstract

A valence bond (VB) "weak coupling" model of the electronic structure for $[Ir_2(TMB)_4](B(C_6H_5)_4)_2$ is developed and generalized to the class of dimeric systems in which the metals are nonbonded, in a formal sense, and can be viewed as weakly coupled. With the VB model, the energies and widths of the previously observed optical absorption bands can be rationalized; in addition, plausible assignments are made for bands that were not interpreted satisfactorily or not observed in earlier work. The VB model does not change any of the molecular orbital-based interpretations of the thermal chemistry, photochemistry, or photophysics of these systems.

Photophysical characterization of the $^{1,3}(d\sigma^* p\sigma)$ excited state of $Ir_2(TMB)_4{}^{2+}$ finds a system quite comparable to other binuclear d^8 complexes. Both fluorescence (λ_{max} 735 nm, τ ~ 70 ± 30 ps) and phosphorescence (λ_{max} 1080 nm, τ = 210 ± 20 ns) are observed.

The relatively long lifetime of the $^3(d\sigma^* p\sigma)$ excited state of $Ir_2(TMB)_4{}^{2+}$ suggests that it should be able to participate in bimolecular photochemical reactions. The diradical-like structure of the excited state, an electron (or oxidizing hole) localized on the exterior of the M_2 unit (the $d\sigma^*$ orbital) and an electron localized in the interior of the dimer cage (the $p\sigma$ orbital), implies that one-electron chemistry will be observed. Reactions of the ground state follow two-electron pathways, similar to those observed for mononuclear d^8 complexes.

The $^3(d\sigma^* p\sigma)$ excited state of $Ir_2(TMB)_4{}^{2+}$ is found to be a powerful reductant, $E^0(Ir_2(TMB)_4{}^{3+}/{}^3(Ir_2(TMB)_4{}^{2+})^*)$ ~ -1.0 V (SSCE). Excited-state electron-transfer quenching by pyridinium acceptors is observed to follow classical Marcus theory for outer-sphere electron transfer. No "inverted" behavior is found. The bimolecular electron-transfer reaction is highly nonadiabatic, κ ~ 0.0001, because of the large donor-acceptor separation, ~ 8 Å. The results for $Ir_2(TMB)_4{}^{2+}$ are discussed in comparison to those for $[Ir(\mu\text{-pz})COD]_2$.

$Ir_2(TMB)_4^{2+}$ is found to react photochemically with alkyl halides. Although the $^3(d\sigma^*p\sigma)$ excited state is a good reductant, outer-sphere electron transfer seems unlikely ($E^0(RX/RX^{\bullet-}) < -1.5$ V (SSCE)). An $S_{RN}1$ pathway has been suggested to explain the alkyl halide photoreduction reaction observed for metal complexes with $E^0(M_2^+/^3M_2^*) < -1.5$ V (SSCE); however, atom transfer to the $^3(d\sigma^*p\sigma)$ excited state is the favored reaction mechanism for the alkyl halide photoreduction reaction of $Ir_2(TMB)_4^{2+}$. The generality of this reaction is discussed.

While there is some ambiguity as to the primary photoprocess for alkyl halide photoreactivity, $^3(d\sigma^*p\sigma)$ excited-state hydrogen-atom transfer has been established as the mechanism of the reaction of $Ir_2(TMB)_4^{2+}$ and a number of organic substrates. The atom-transfer reactivity of the $^3(d\sigma^*p\sigma)$ excited state is attributed to the presence of a hole in the $d\sigma^*$ orbital, analogous to the $^3n\pi^*$ state of organic ketones. Interaction of the oxidizing hole with the electron pair of the C-H bond is the presumed pathway.

Electrochemical oxidation of $Rh_2(TMB)_4^{2+}$ generates the d^8-d^7 species $Rh_2(TMB)_4^{3+}$. This complex reacts with 1,4-cyclohexadiene to abstract a hydrogen atom mimicking the initial step of the $^3(d\sigma^*p\sigma)$ photoreaction. The importance of this result is discussed in terms of energy storage systems and extension of the range of hydrocarbon oxidations with binuclear d^8 complexes.

The d^7-d^7 dihydride product obtained from the photoreaction of $Ir_2(TMB)_4^{2+}$ and 1,4-cyclohexadiene is isolated and characterized. In addition to NMR, UV-Vis, IR, and Raman spectra, the complex is characterized crystallographically. The reactivity of this complex is also discussed.

Table of Contents

List of Figures

Chapter 1

Chapter 2

Chapter 3

Chapter 4

Chapter 5

Chapter 6

List of Tables

Chapter 2

Chapter 3

Chapter 4

Chapter 5

Appendix 1

Appendix 3

Chapter 1

Introduction

Binuclear metal complexes are attractive systems for the activation of organic and inorganic substrates because they offer the possibility of cooperative involvement of their active sites: multiple binding sites for substrates; multielectron redox capabilities; and for heteronuclear complexes, distinct metal centers that can interact differently with a given substrate.[1-5] Numerous studies have focused on the thermal reactivity of binuclear complexes with a variety of substrates, with less attention having been given to the activation of substrates by the electronic excited states of these complexes.[6-8] Since a photoexcited molecule is best envisioned as a new species possessing physical and chemical properties distinct from its corresponding ground state molecule, photoexcited binuclear complexes may possess reactivity very different from the ground state.[9,10] It is therefore of interest to investigate the possibility of the conversion of light to net chemical energy through a photochemical process.[11-13] Binuclear d^8 complexes with the general structure shown in Figure 1.1 have been

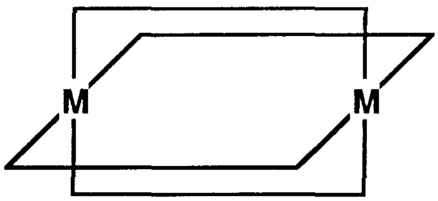

M = Rh(I), Ir(I), Pt(II)

Figure 1.1. General Structure for a face-to-face binuclear d^8 complex. Bidentate ligands are diisocyanoalkanes or $P_2O_5H_2^{4-}$ (e.g., $Rh_2b_4^{2+}$ (b = 1,3-diisocyanopropane), $Rh_2(TMB)_4^{2+}$ (TMB = 2,5-diisocyano-2,5-dimethylhexane), $Pt_2(P_2O_5H_2)_4^{4-}$). For A-frame d^8 complexes two bridging ligands (e.g., [Ir(μ-pz)COD]$_2$, pz = pyrazole, COD = 1,5-cyclooctadiene).

studied for several years because of their unique spectral properties, thermal reactivity, and photochemical reactivity. The work in this area grew out of studies of the spectroscopic properties of Rh(I) isocyanide complexes.

For years Rh(I) and Ir(I) isocyanide complexes have been suspected of existing as oligomers owing to the intense color, uncharacteristic of d^8 complexes possessing π-acceptor ligands.[14,15] It was not until Mann demonstrated that the bands in the visible and near-infrared region of the spectrum for $Rh(CNC_6H_5)_4^+$ were not linearly related to the concentration of monomer but to some root (e.g., square, cubic, etc.) of monomer concentration that the extent of oligomerization was realized.[16] The existence of discrete species was later confirmed by x-ray diffraction analysis.[17,18]

Stacking of square planar d^8 complexes has been observed in the solid state.[19] Electrostatic binding (attraction of oppositely charged, square planar units) was thought to be the important interaction. Oligomerization of similarly charged, square planar units could be understood to occur only from some favorable metal-metal interaction. Metal-metal interactions for the stacked linear chain complexes have been discussed in reference to the d/p band structure and the observed electrical conductivities. The dark colors of the linear chain salts and the solid-state emission are discussed in terms of d $\rightarrow$ p transitions.[20]

Binuclear Rh species were later synthesized using a series of diisocyanoalkanes, ligands chosen to favor formation of dimeric complexes.[21,22] Characterization of these complexes found them to be analogous to the oligomeric Rh species studied earlier.

The electronic structure of binuclear d^8 complexes has been understood in terms of a simple molecular orbital (MO) model (Figure 1.2).[16] Starting from a monomer orbital scheme, two square planar units are brought together in a face-to-face orientation. The orbitals perpendicular to the molecular plane, d_{z^2} and p_z, interact strongly, yielding $d\sigma/\sigma^*$ and $p\sigma/\sigma^*$ orbitals. To a first approximation the ground state is expected to be nonbonding since both the $d\sigma$ and $d\sigma^*$ orbitals are filled. However,

Figure 1.2. Molecular orbital diagram for the interaction of two square planar d^8 metal ions.

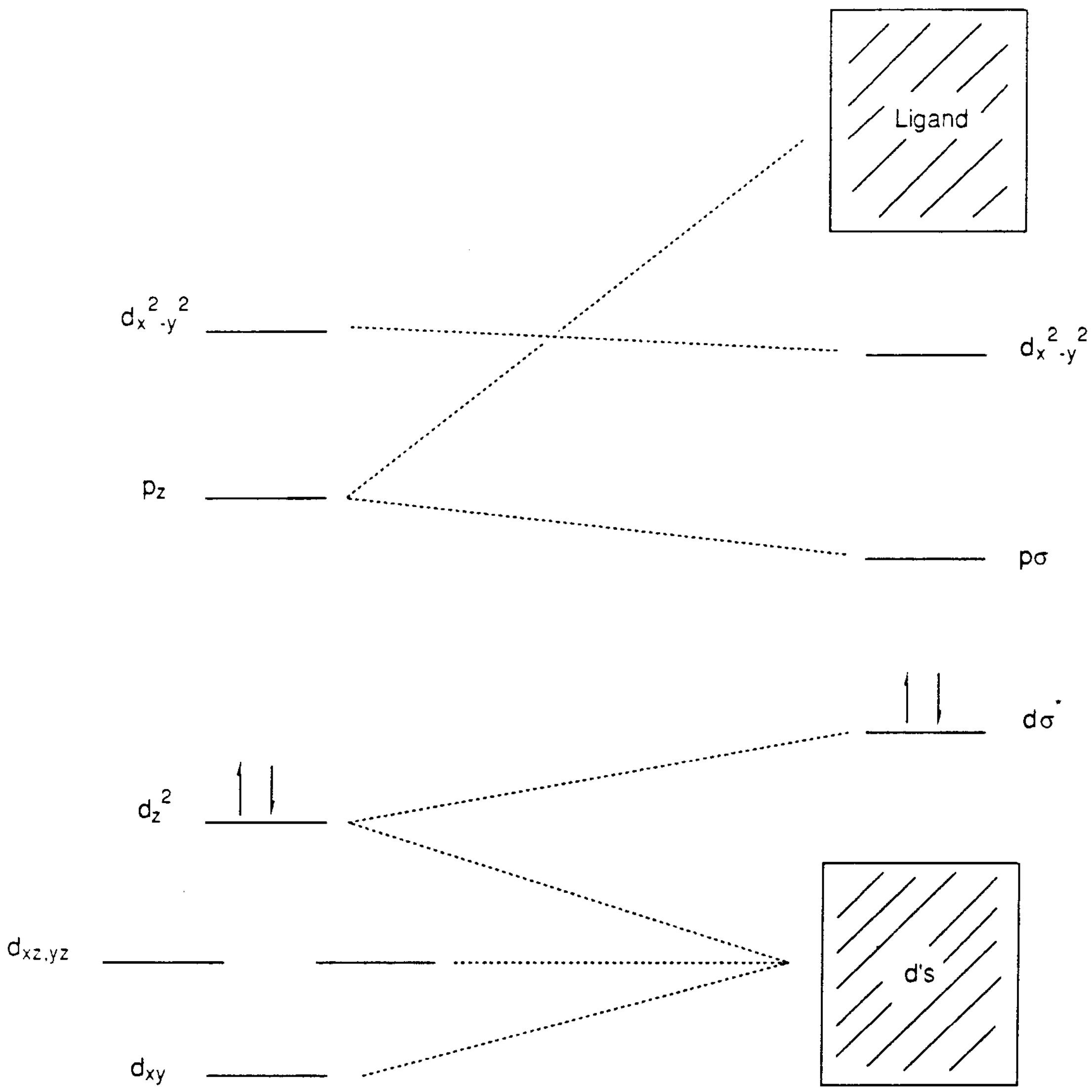
Ligand
$d_{x^2-y^2}$
$d_{x^2-y^2}$
p_z
$p\sigma$
$d\sigma^*$
d_{z^2}
$d_{xz,yz}$
d's
d_{xy}

extensive spectroscopic studies of binuclear complexes have established that the metal-metal interaction in the $^{1}A_{1g}(d\sigma^{*})^{2}$ ground state is weakly bonding.[23,24] Perturbational mixing of orbitals of the same symmetry will stabilize the lower set and destabilize the uppers ones; stabilization of the filled lower set is viewed as a source of metal-metal bonding.

As suggested by the MO model and well established for numerous other studies, the lowest energy transition is $d\sigma^{*} \rightarrow p\sigma$.[22,25] This excitation results in formation of a metal-metal single bond in the excited state. The spectral and photophysical properties of all binuclear d^8 complexes are found to be dominated by the large contraction along the metal-metal coordinate that occurs upon excitation.[25-27] The $d\sigma^{*} \rightarrow p\sigma$ transition is metal-localized and can be viewed as movement of an electron from an orbital localized on the exterior of the M_2 unit (the $d\sigma^{*}$ orbital) to an orbital localized in the interior of the dimer cage (the $p\sigma$ orbital). The excitation results in hole formation on a metal center at an open coordination site (Figure 1.3). The diradical picture of the excited state is important in discussing the photochemistry and the electrochemistry of these systems.

Additional studies of the binuclear Rh(I) complexes revealed that the lowest energy singlet and triplet excited states derived form the $(d\sigma)^2(d\sigma^{*})^1(p\sigma)^1$ electronic configuration are luminescent at ambient temperatures in fluid solution.[22-24,28] (For stacked linear chain complexes luminescence has been observed in the solid state and discussed in terms of a dp excited state.)[20] The $^{1}(d\sigma^{*}p\sigma)$ excited-state lifetime, in most cases, is less than 1 ns. The $^{3}(d\sigma^{*}p\sigma)$ excited-state lifetime is found to range from 30 ns to 10 μs. Ground-state and excited-state Raman studies found that the metal-metal vibrational frequency increases upon excitation, an increase in the metal-metal bond strength.[26] The increased metal-metal interaction is also manifest in the low-temperature absorption spectra.[25,27] The band at 670 nm in the spectrum of $Rh_2b_4^{2+}$

Figure 1.3. Pictorial representation of the M_2-localized hole in a $^3(d\sigma^* p\sigma)$ state.

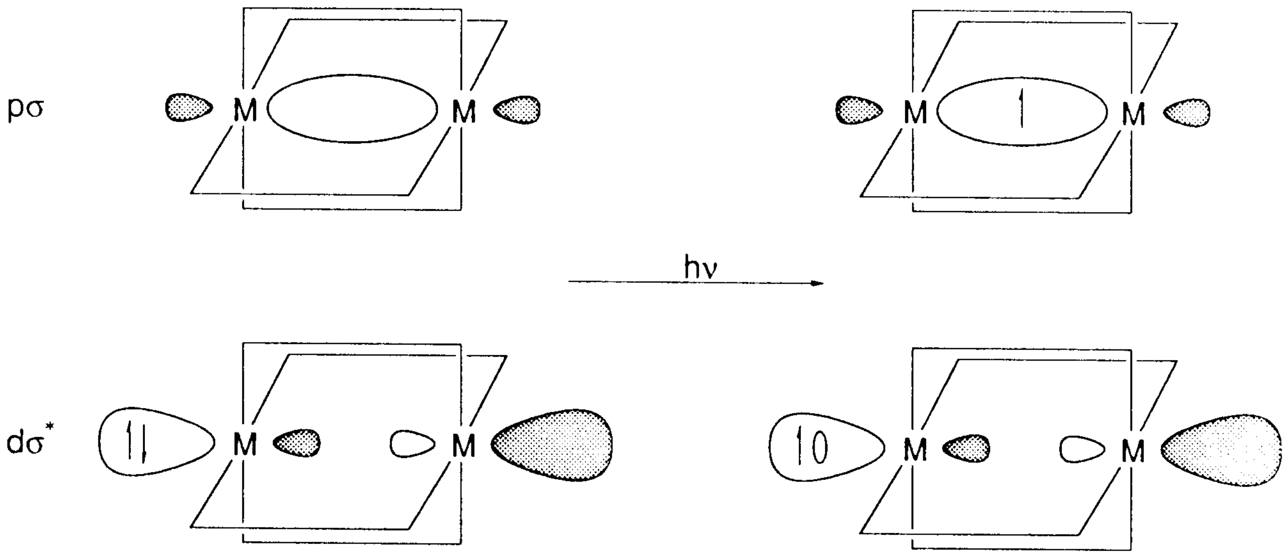
pσ
dσ*
M
hν

assigned to the $^1A_{1g} \rightarrow {}^3E_u$ transition shows a vibrational progression in a frequency of ~150 cm^{-1}, consistent with the Rh-Rh stretching frequency of 144 cm^{-1} obtained from the Raman studies. (The ground-state Rh-Rh vibrational frequency is 79 cm^{-1}.) Analysis of the band shape suggests that the Rh-Rh distance decreases 0.3 Å in the $^3(d\sigma^*p\sigma)$ excited state, consistent with the increased metal-metal bonding interaction in the excited state.

The MO picture also yields insight into the chemistry of these systems. For monomeric d^8 complexes, the predominant mode of reaction is oxidative addition.[29] The chemistry is controlled by the $(d_{z^2})^2$ electron configuration, and while most reactions are classified as oxidative addition, the pathways followed are electron transfer, nucleophilic attack by the metal center, or acid/base. For binuclear d^8 complexes, the chemistry of the ground state is expected to be controlled by the $(d\sigma^*)^2$ electron configuration. Similar to the monomeric species, the binuclear complexes, undergo oxidative addition reactions. Many complexes have been found to undergo two-electron oxidative addition reactions with dihalides and alkyl halides.[21,30,31] The pathway for these reactions are not well understood. In analogy to the monomeric complexes, the dimers are expected to undergo electron transfer, nucleophilic attack by the metal, and acid/base reactions. The transfer of two $d\sigma^*$ electrons results in the formation of a metal-metal single bond. The presence of this bond has been verified by x-ray diffraction.[32,33] Other manifestations of the metal-metal bond have been observed spectroscopically.[34]

The lifetime of the $^3(d\sigma^*p\sigma)$ excited state, normally in between 100 ns and 10 μs, makes binuclear d^8 complexes attractive for bimolecular photoprocesses. An electronic excited state of a metal complex is both a stronger reductant and a stronger oxidant than the ground state.[10] Excitation of an electron from a low-energy to a high-energy orbital reduces the ionization potential and increases the electron affinity of a molecule. Therefore, binuclear d^8 complexes with relatively long-lived excited states can participate in intermolecular electron-transfer reactions that are uphill for the corresponding ground-state species. Such excited-state electron-transfer reactions often play key roles in multistep schemes for the conversion of light to chemical energy.[9]

While electron-transfer processes are common in inorganic photochemistry, excited-state atom transfer is limited to a small class of inorganic complexes. For UO_2^{2+}, the diradical excited state (•U-O•) is active in alcohol oxidation.[35] The primary photoprocess is hydrogen atom abstraction by the oxygen-centered radical. Photoaddition to a metal center via atom transfer has been observed for binuclear metal complexes such as $Re_2(CO)_{10}$.[36-39] The primary photoprocess is metal-metal bond homolysis. The photogenerated metal radical undergoes thermal atom-abstraction reactions. Until recently, atom transfer to a metal-localized excited state had not been observed.

Atom transfer to a metal complex is facilitated if localized electron or hole generation occurs at one or more open coordination sites. Binuclear d^8 complexes have been found to undergo photochemical atom transfer to one of the metal centers.[40-43] These complexes possess open coordination sites in addition to an electronic structure that localizes the electron (hole) necessary for atom transfer to the metal center.

The initial interest in the binuclear d^8 complexes was stimulated by observations of their photochemical electron-transfer reactivity.[41] From spectroscopic and electrochemical studies, the $^3(d\sigma^*p\sigma)$ excited state is predicted to be a powerful reductant, with $E^0(M_2^+/^3M_2^*)$ estimated to range from -0.8 to -2.0 V vs SSCE in CH_3CN. That this state is a powerful reductant has been confirmed by investigation of the electron-transfer quenching of $^3M_2^*$ by a series of pyridinium acceptors with varying reduction potentials. For several binuclear complexes, the excited-state reduction potential cannot be calculated accurately because of the irreversibility of the ground-state electrochemistry, but it can be estimated from bimolecular electron-transfer quenching experiments.

For systems that are powerful excited-state reductants, photoreduction of alkyl halides is observed.[41,44] This reaction was initially interpreted to be an outer-sphere electron transfer to form an alkyl-halide radical anion, which rapidly decomposes to yield R· and X⁻. Subsequent thermal reactions give the observed products, an $S_{RN}1$ mechanism (Figure 1.4). While such a mechanism, $S_{RN}1$, appears plausible for a metal complex with $E^0(M_2^+/^3M_2^*) < -1.5$ V (SSCE), it seems unlikely for complexes with $E^0(M_2^+/^3M_2^*) > -1.0$ V (SSCE). Reduction potentials for alkyl halides of interest are generally more negative than -1.5 V (SSCE).[45] An alternative pathway to outer-sphere electron transfer, which yields similar photoredox products with alkyl halides, is excited-state atom transfer (Figure 1.5).

Although the primary photoprocess for alkyl-halide photoreduction may not be atom transfer in all cases, $^3(d\sigma^*p\sigma)$ excited-state hydrogen atom transfer has been established as the mechanism of the reaction between $Pt_2(P_2O_5H_2)_4^{4-}$ and a number of organic and organometallic substrates.[40-43] Initial work in this area focused on the catalytic conversion of isopropanol to acetone (Equation 1.1).[46]

$$Pt_2(P_2O_5H_2)_4^{4-} + (CH_3)_2CHOH \xrightarrow{h\nu} Pt_2(P_2O_5H_2)_4^{4-} + H_2 + (CH_3)_2CO \quad 1.1$$

From detailed studies of this system, it was concluded that the primary photoprocess is abstraction of the α-hydrogen by the $^3Pt_2^*$ to form a monohydride species (directly observed by transient absorption spectroscopy for a number of substrates) and the organic radical (Equation 1.2), with the final photoproduct being Pt_2H_2 and acetone (Equation 1.3). The Pt_2H_2 complex has been characterized by NMR, UV-Vis, and IR (but has not been successfully isolated).[47]

Figure 1.4. $S_{RN}1$ mechanistic scheme for halocarbon photooxidative addition to binuclear d^8 complexes.

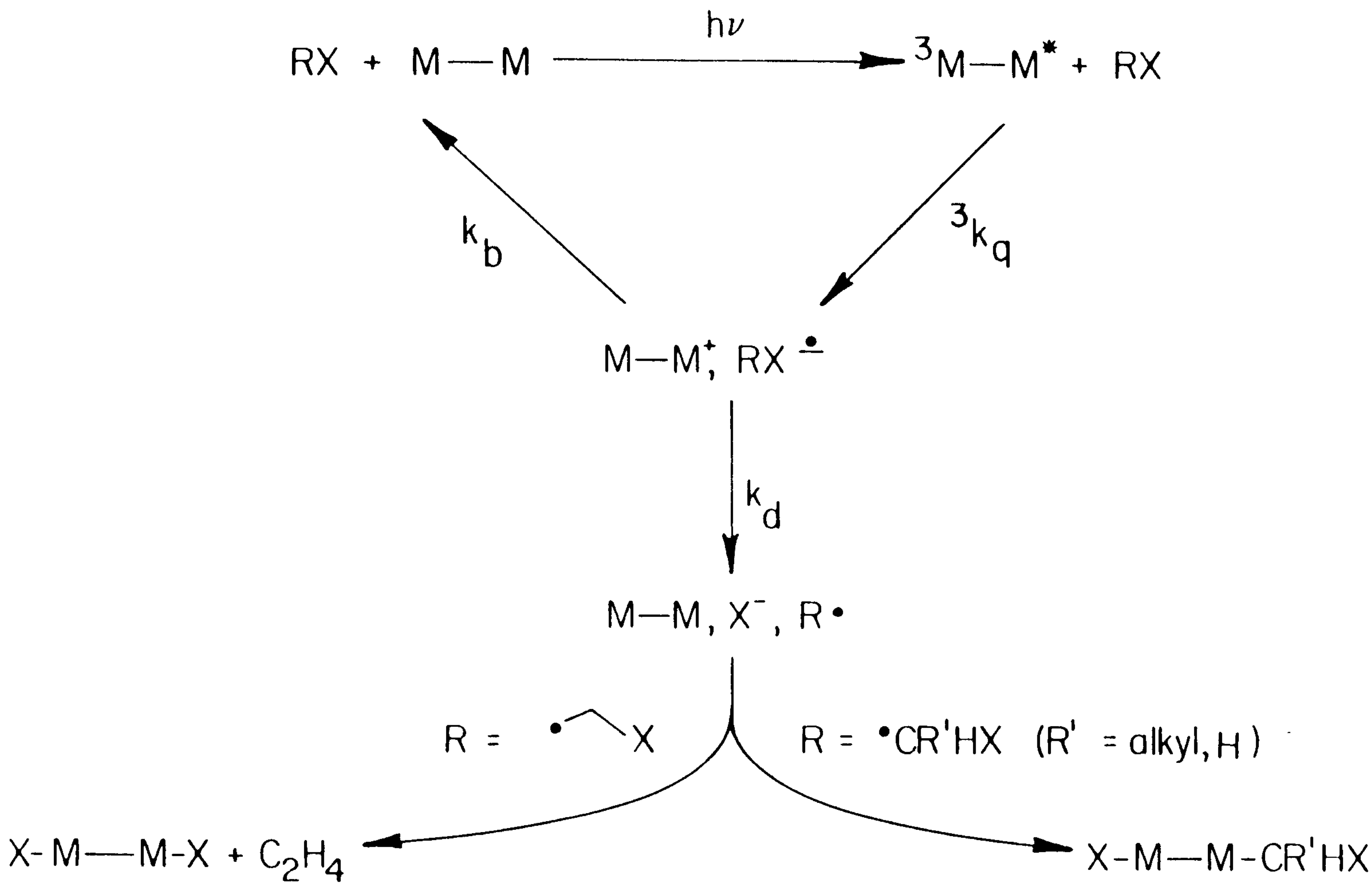
RX + M—M
hν
³M—M* + RX
k_b
³k_q
M—M⁺, RX⁻
k_d
M—M, X⁻, R•
R = •CH2CH2X
R = •CR'HX (R' = alkyl, H)
X-M—M-X + C2H4
X-M—M-CR'HX

Figure 1.5. Atom-transfer mechanism for halocarbon photooxidative addition.

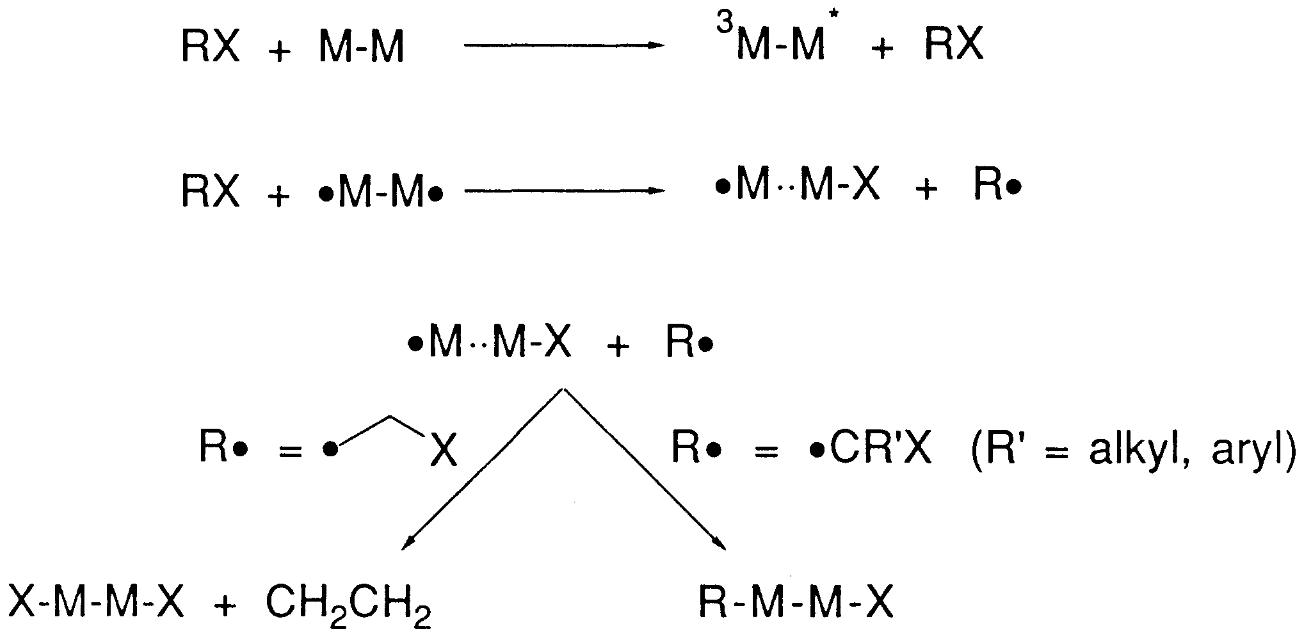
RX + M-M
³M-M* + RX
RX + •M-M•
•M··M-X + R•
•M··M-X + R•
R• =
X
R• = •CR'X (R' = alkyl, aryl)
X-M-M-X + CH2CH2
R-M-M-X

$$^{3}Pt_2^{*} + (CH_3)_2CHOH \rightarrow Pt_2H + (CH_3)_2COH \quad 1.2$$

$$Pt_2H + (CH_3)_2COH \rightarrow Pt_2H_2 + (CH_3)_2CO \quad 1.3$$

To further extend the understanding of the chemistry and spectroscopy of binuclear d^8 complexes, an Ir(I) analog of the Rh(I) species was prepared, $Ir_2(TMB)_4^{2+}$.[30] This complex was found to compare well to the Rh(I) dimers with the expected red shift of the $d\sigma^* \rightarrow p\sigma$ transition. The $^3(d\sigma^*p\sigma)$ excited state was found to have a temperature-independent lifetime of approximately 200 ns.

The crystal structure of the $B(C_6H_5)_4^-$ salt of $Ir_2(TMB)_4^{2+}$ is described in Chapter 2. The optical absorption spectrum is presented and discussed in reference to a large number of binuclear d^8 complexes. Photophysical characterization of the emissive $^{1,3}(d\sigma^*p\sigma)$ excited states is reported along with Raman vibrational data for the ground state and the $^3(d\sigma^*p\sigma)$ excited state.

A detailed study of the electronic spectrum of $Ir_2(TMB)_4^{2+}$ is presented in Chapter 3. A change in the metal from rhodium to iridium should perturb the electronic structure, thereby altering the characteristic d^8-d^8 electronic spectrum and allowing key aspects of the MO model to be tested. Electronic absorption and magnetic circular dichroism spectra of $Rh_2(TMB)_4^{2+}$ and $Ir_2(TMB)_4^{2+}$ are reported along with polarized single-crystal absorption spectra of $[Ir_2(TMB)_4](B(C_6H_5)_4)_2 \cdot CH_3C_6H_5$.

Earlier work found that $Rh_2b_4^{2+}$, $Rh_2(TMB)_4^{2+}$, $Pt_2(P_2O_5H_2)_4^{4-}$, and $[Ir(\mu\text{-}pz)COD]_2$ react with dihalides to yield the corresponding d^7-d^7 dimer, X-M-M-X.[21,40,31] $Pt_2(P_2O_5H_2)_4^{4-}$ and $[Ir(\mu\text{-}pz)COD]_2$ were also found to oxidatively add CH_3I to yield CH_3-M-M-I. It was found that $Ir_2(TMB)_4^{2+}$ oxidatively adds dihalides (Cl_2, Br_2, I_2), CH_3I, HCl, and $CH_2(CN)_2$ to yield the corresponding d^7-d^7 complex, X-M-M-Y (X = Y, Cl_2, Br_2, I_2; X = I, Y = CH_3; X = Cl, Y = H; X = $CH(CN)_2$, Y = H).[30] Because of the greater reactivity expected for Ir and the interest in the photochemical reactivity of the excited states of $Ir_2(TMB)_4^{2+}$, extension of the thermal chemistry was pursued. Thermal reactions with nonpolar and low-polarity reagents (H_2, R_3CH, R_3SiH, R_3SnH), and electrophilic reagents (X_2, RX, HX, CH_3COCl) are discussed in Chapter 4.

The relatively long lifetime of the $^3(d\sigma^*p\sigma)$ excited state of $Ir_2(TMB)_4^{2+}$ in fluid solution suggests that it should be able to participate in bimolecular photochemical reactions. In light of the favorable absorption and emission properties of this complex, it is of interest to examine the possibility of the conversion of visible light to net chemical energy through a photochemical process, either electron transfer or atom transfer. The excited-state electron-transfer reactivity of $Ir_2(TMB)_4^{2+}$ with pyridinium acceptors is reported and analyzed in the context of classical Marcus theory for outer-sphere electron transfer in Chapter 4. The photochemical reactions of $Ir_2(TMB)_4^{2+}$ with alkyl halides and hydrogen-atom donors are reported.

Hydrogen-atom transfer has been established as an important reaction pathway for the triplet $d\sigma^*p\sigma$ excited state of binuclear d^8 complexes. Substrates that serve as hydrogen-atom donors include hydrocarbons (e.g., cyclohexene and 1,4-cyclohexadiene), alcohols with α(C-H) bonds, and triorganosilanes, -germanes, and -stannanes. Irradiation of the metal complex in the presence of these substrates produces complexes of the type M_2H_2. Earlier work has characterized the product formed with $Pt_2(P_2O_5H_2)_4^{4-}$ as the binuclear platinium(III) dihydride, $Pt_2(P_2O_5H_2)_4H_2^{4-}$ (Pt_2H_2). In Chapter 5, the characterization of the dihydride of $Ir_2(TMB)_4^{2+}$ (Ir_2H_2) is reported. In addition to NMR, UV-Vis, IR, and Raman spectra, the complex has been characterized crystallographically. The reactivity of Ir_2H_2 is also reported.

Theoretical studies have also contributed to the study of the electronic structure and the spectral properties of metal dimers.[48,49] Results of *ab initio* calculations of $Re_2Cl_8^{2-}$ designed to provide accurate bond energies and torsion barriers as well as accurate shapes for the potential curves are reported in Chapter 6. These studies use the generalized valence bond (GVB) approach in which electron correlations are included for all eight electrons available for the quadruple bond, while solving self-consistently for all orbitals.

References

1. Poilblanc, R. *Inorg. Chim. Acta.* **1982**, *62*, 75-78, and references therein.

2. Halpern, J. *Inorg. Chim. Acta.* **1982**, *62*, 31-37, and references therein.

3. Poilblanc, R. *Nouv. J. Chim.* **1978**, *2*, 145-150.

4. McCleverty, J.A. *Inorg. Chim. Acta.* **1982**, *62*, 67-73.

5. Chisholm, M.H. *ACS Symp. Ser.* **1980**, *155*, 17-39.

6. Wrighton, M.S.; Graff, J.L.; Luong, J.C.; Reichel, C.L.; Robbins, J.L. *ACS Symp. Ser.* **1980**, *155*, 85-110.

7. Nocera, D.G.; Maverick, A.W.; Winkler, J.R.; Che, C.-M.; Gray, H.B. *ACS Symp. Ser.* **1983**, *211*, 21-33.

8. Gray, H.B.; Maverick, A.W. *Science* **1981**, *214*, 1201-1205.

9. Balzani, V.; Scandola, F. In *Energy Resources through Photochemistry and Catalysis*; Gratzel M., Ed.; Academic Press: New York, 1983; Chapter 1.

10. Balzani, V.; Bolletta, F.; Gandolfi, M.T.; Maestri M. *Top. Curr. Chem.* **1978**, *75*, 1-64.

11. Rabani, J., Ed. *Photochemical Conversion and Storage of Solar Energy*; Weizmann Science Press: Jerusalem, 1982.

12. Gratzel, M., Ed. *Energy Resources through Photochemistry and Catalysis*; Academic Press: New York, 1983.

13. Connolly, J.S., Ed. *Photochemical Conversion and Storage of Solar Energy*; Academic Press: New York, 1981.

14. Kawakami, K.; Haga, M.-A.; Tanaka, T. *J. Organomet. Chem.* **1973**, *60*, 363-373.

15. Malatesta, L.; Bonati, F. *Isocyanide Complexes of Metals*; Wiley: New York, 1969.

16. Mann, K.R.; Gordon, J.G. II; Gray, H.B. *J. Am. Chem. Soc.* **1975**, *97*, 3553-3555.

17. Mann, K.R.; Lewis, N.S.; Williams, R.M.; Gray, H.B.; Gordon, J.G., II *Inorg. Chem.* **1978**, *17*, 828-834.

18. Endres, H.; Gottstein, N.; Keller, H.J.; Martin, R.; Rodemer, W.; Steiger, W. *Z. Naturforsch.* **1979**, *34B*, 827-833.

19. Miller, J.S., Ed. *Extended Linear Chain Compounds*; Plenum Press: New York, 1982, and references therein.

20. Moreau-Colin, M.L. *Struct. Bonding* **1972**, *10*, 167-190.

21. Lewis, N.S.; Mann, K.R.; Gordon, J.G. II; Gray, H.B. *J. Am. Chem. Soc.* **1976**, *98*, 7461-7463.

22. Mann, K.R.; Thich, J.A.; Bell, R.A.; Coyle, C.L.; Gray, H.B. *Inorg. Chem.* **1980**, *19*, 2462-2468.

23. Mann, K.R.; Gray, H.B. *Adv. Chem. Ser.* **1979**, *173*, 225-235.

24. Rice, S.F.; Milder, S.J.; Goldbeck, R.A.; Kliger, D.S.; Gray, H.B. *Coord. Chem. Rev.* **1982**, *43*, 349-354.

25. Rice, S.F.; Miskowski, V.M.; Gray, H.B. *Inorg. Chem.* **1988**, *27*, 4704-4708.

26. Dallinger, R.F.; Miskowski, V.M.; Gray, H.B.; Woodruff, W.H. *J. Am. Chem. Soc.* **1981**, *103*, 1595-1596.

27. Rice, S.F.; Gray, H.B. *J. Am. Chem. Soc.* **1981**, *103*, 1593-1595

28. Miskowski, V.M.; Nobinger, G.L.; Kliger, D.S.; Hammond, G.S.; Lewis, N.S.; Mann, K.R.; Gray, H.B. *J. Am. Chem. Soc.* **1978**, *100*, 485-488.

29. Collman, J.P.; Hegedus, L.S.; Norton, J.R.; Finke, R.G. *Principles and Applications of Organotransition Metal Chemistry*; University Science Books: Mill Valley, California, 1987.

30. Smith, T.P., Ph.D. Dissertation, California Institute of Technology, 1982.

31. Marshall, J.L., Ph.D. Dissertation, California Institute of Technology, 1987.

32. Mann, K.R.; Bell, R.A.; Gray, H.B. *Inorg. Chem.* **1979**, *18*, 2671-2673.

33. Maverick, A.W.; Smith, T.P.; Maverick, E.F.; Gray, H.B. *Inorg. Chem.* **1987**, *26*, 4336-4341.

34. Miskowski, V.M.; Smith, T.P.; Loehr, T.M.; Gray, H.B. *J. Am. Chem. Soc.* **1985**, *107*, 7925-7934.

35. Bergamini, P.; Sostero, S.; Traverso, O. In *Fundamental and Technological Aspects of Organo-f-Element Chemistry*; Marks, T.J.; Fragala, I.L., Eds.; D. Reidel: Boston, 1985; pp. 361-385.

36. Stiegman, A.E.; Tyler, D.R. *Comm. Inorg. Chem.* **1986**, *5*, 215-245.

37. Hanckel, J.M.; Lee, K.-W.; Rushman, P.; Brown, T.L. *Inorg. Chem.* **1986**, *25*, 1852-1856.

38. Wayland, B.B.; Del Rossi, K.J. *J. Organomet. Chem.* **1984**, *276*, C27-C30.

39. Tyler, D.R. *Prog. Inorg. Chem.* **1988**, *36*, 125-194.

40. Roundhill, D.M.; Gray, H.B.; Che, C.-M. *Accts. Chem. Res.*, in press.

41. Marshall, J.L.; Stiegman, A.E.; Gray, H.B. In *Excited States and Reactive Intermediates*; Lever, A.B.P., Ed.; ACS Symp. Ser. 307; American Chemical Society: Washington, D.C., 1986; pp 166-176.

42. Vlcek, A., Jr.; Gray, H.B. *J. Am. Chem. Soc.* **1987**, *109*, 286-287.

43. Vlcek, A., Jr.; Gray, H.B. *Inorg. Chem.* **1987**, *26*, 1997-2001.

44. Caspar, J.V.; Gray, H.B. *J. Am. Chem. Soc.* **1984**, *106*, 3029-3030.

45. Hawley, M.D. In *Encyclopedia of Electrochemistry of the Elements. Vol. XIV*; Bard, A.J., Ed.; Marcel Dekker: New York, 1980; pp. 1-135.

46. Roundhill, D.M. *J. Am. Chem. Soc.* **1985**, *107*, 4354-4356.

47. Harvey, E.L.; Stiegman, A.E.; Vlcek, A., Jr.; Gray, H.B. *J. Am. Chem. Soc.* **1987**, *109*, 5233-5235.

48. Cotton, F.A.; Walton, R.A. *Multiple Bonds Between Metal Atoms*; Wiley: New York, 1982.

49. Hoffman, D.M.; Hoffmann, R. *Inorg. Chem.* **1981**, *20*, 3543-3555.

Chapter 2

Structure, Optical Absorption Spectrum, and Photophysics of $Ir_2(TMB)_4^{2+}$

Introduction

Extensive studies of binuclear d^8 complexes have revealed a class of compounds that are spectroscopically unique and chemically very interesting. The ground state of these complexes, while formally nonbonding, does possess a weak metal-metal bond. The electronic excited states have a formal metal-metal single bond. This arises from excitation of an electron from the $d\sigma^*$ orbital to the $p\sigma$ orbital. Such a nonbonding-to-bonding transition is unique among inorganic complexes. In studying binuclear d^8 complexes, one wishes to understand how the metal-metal interaction in the ground state and excited states influence the spectroscopy and chemistry.

Many of the binuclear d^8 complexes are found to be emissive. Excited states formed by absorption of a photon rather than merely by undergoing thermal deactivation to the ground state decay by emission of a photon. The emissive states have been shown to be the $^{1,3}(d\sigma^*p\sigma)$ excited states. The $^1(d\sigma^*p\sigma)$ excited state lifetime, in most cases, is less than 1 ns. The $^3(d\sigma^*p\sigma)$ lifetime is found to range from 30 ns to 10 μs. The structure and properties of these excited states have been the focus of much work. One would like to characterize these states much as one would characterize the ground state.

To further extend the understanding of the chemistry and spectroscopy of binuclear d^8 complexes, a study of an Ir(I) complex, $Ir_2(TMB)_4^{2+}$, was undertaken. The synthesis and preliminary characterization of $Ir_2(TMB)_4^{2+}$ has been reported.[1] The crystal structure of the $B(C_6H_5)_4^-$ salt of $Ir_2(TMB)_4^{2+}$ is presented. The optical absorption spectrum of $Ir_2(TMB)_4^{2+}$ is discussed in reference to a large number of binuclear d^8 complexes. It is shown that the energy of the $^1(d\sigma^* \rightarrow p\sigma)$ transition is dictated by excited-state properties, not by ground-state interactions as prescribed by the MO model. Photophysical characterization of the emissive $^{1,3}(d\sigma^*p\sigma)$ excited states is reported along with Raman vibrational data for the ground state and the $^3(d\sigma^*p\sigma)$ excited state.

Experimental

Synthesis

All synthetic procedures were carried out with standard Schlenk techniques. All solvents were from freshly opened bottles with no further purification. All solvents were Schlenk-degassed prior to use. Standard procedures were used to prepare 2,5-diisocyano-2,5-dimethylhexane (TMB)[2] and $[Ir(COD)Cl]_2$ (COD = 1,4-cyclooctadiene)[3]. All other chemicals were of reagent grade or comparable quality and were used as received. The ^1H NMR spectra were obtained on a 400-MHz JNM-GX400 FT NMR spectrometer. The IR spectra were measured on a Beckman IR 4240.

$[Ir_2(TMB)_4](B(C_6H_5)_4)_2$

To a filtered acetonitrile solution of $[Ir(COD)Cl]_2$ (0.1 g in 10 ml CH_3CN), a filtered solution of TMB (0.1g in a minimum of CH_3CN) was added with stirring. The solution immediately turned dark blue. The mixture was allowed to stir for approximately 15 minutes, at which time the solvent and COD were removed under vacuum. The resulting metallic-brown solid was dissolved in methanol. A filtered methanol solution of $NaB(C_6H_5)_4$ (0.11g, 10 ml) was added to the stirred methanol solution of $[Ir_2(TMB)_4]Cl_2$. Immediate precipitation of a blue solid occurred. The solution was filtered and the blue powder washed with cold methanol. The solid could be recrystallized from acetone or acetonitrile. Yields were quite variable. Calculated for $[Ir_2(TMB)_4](B(C_6H_5)_4)_2$: C, 62.91; H, 6.24; N, 6.67. Found: C, 62.61; H, 6.43; N, 6.40. NMR: δ (CD_3CN, 20 °C); 1.49 (broad singlet, CH_3, 48H), 1.86 (broad singlet, CH_2, 16H), 6.83(triplet-of-triplets, 8H), 6.98 (triplet, 16H), 7.25 (multiplet, 16H). IR: ν, cm^{-1} (Nujol mull, NaCl plates); 2140 (vs, N≡C). Free ligand IR: ν, cm^{-1} (Nujol mull, NaCl plates); 2120 (vs, N≡C).

X-ray Data Collection and Reduction for $[Ir_2(TMB)_4](B(C_6H_5)_4)_2 \cdot 2CH_3CN$

Crystal data are given in Table 2.1. Oscillation and Weissenberg photographs showed monoclinic symmetry. Bright-blue crystals, freshly grown from acetonitrile, were cut to size with a razor blade. An irregular chunk was glued to a glass fiber and then quickly covered with epoxy glue to retard decomposition. It was centered on a Nonius CAD-4 diffractometer equipped with graphite-monochromated MoKα radiation, and the cell dimensions plus an orientation matrix were obtained from the setting angles of 25 reflections with $22° < 2\vartheta < 25°$. Two crystals were used to measure 6332 reflections with an ω scan. A scale factor relating the two data sets was calculated from the three check reflections, which were measured every 10,000 seconds of x-ray exposure. These showed a linear decay of about 9% in I for each crystal, and the data were corrected for this decay. Backgrounds were measured for each reflection at each end of the scan; an average background as a function of 2ϑ was calculated and used to correct the measured scan counts. Absences in the data of 0k0, k=2n+1 and h0l, h+l=2n+1 identify the space group as $P2_1/n$, #14. After deleting space-group absences and merging equivalent reflections, 5562 reflections used in the structure solution and refinement remained, of which 5116 had $F_o^2 > 0$ and 4333 had $F_o^2 > 3\sigma(F_o^2)$. The data were corrected for Lorentz and polarization factors but not for absorption; the epoxy glue on the crystals prevented their measurement and identifying the crystal faces. Variances of the individual reflections were assigned, based on counting statistics plus an additional term, $0.014I^2$. Variances for the merged reflections were obtained by standard propagation of error plus another additional term, $0.014I^2$. Scattering factors were taken from Reference 4.

The coordinates of the iridium atoms were obtained from a Patterson map and the remaining nonhydrogen atoms were found with successive structure factor-Fourier calculations. After three cycles of full-matrix least squares, minimizing $\Sigma w(F_o^2$-

Table 2.1. Crystal Data for $[Ir_2(C_{10}H_{16}N_2)_4](B(C_6H_5)_4)_2 \cdot 2CH_3CN$.

Formula: $Ir_2C_{92}H_{110}N_{10}B_2$	Formula Wt.: 1761.99
a = 17.053(2) Å	Space Group $P2_1/n$ (#14)
b = 32.481(11) Å	
c = 17.616(5) Å	T: 22 °C
β = 115.59(2)°	
V = 8800(5) $Å^3$	λ MoKα = 0.71073 Å
μ = 32.56 cm^{-1}	d_{calc} = 1.329 g cm^{-3}
Crystal irregular, max. dim. ~0.4 mm	
F(000) = 3548 electrons	

$F_c^2)^2$, hydrogen atoms were introduced at calculated positions, assuming a C-H distance of 0.95 Å and staggered geometries. Each hydrogen atom was given an isotropic thermal parameter 10% greater than that of the carbon atom to which it was bonded. The least-squared converged (iridium atoms and methyl carbon atoms of the ligands anisotropic, the remaining atoms isotropic: 106 nonhydrogen atoms, 515 parameters, plus 104 hydrogen atoms) with $R(=\Sigma(F_o-F_c)/\Sigma F_o)$ of 0.062 for all reflections with $F_o^2 > 0$ and 0.050 for the reflections with $F_o^2 > 3\sigma(F_o^2)$. The goodness-of-fit, $[\Sigma w(F_o^2-F_c^2)^2/(n-p)]^{1/2}$, was 2.64. The final parameters are given in Table 2.2 and selected distances and angles in Table 2.3. The structure factors, hydrogen parameters and further distances and angles are given in Appendix 1.

A final difference Fourier map showed excursions of +1.00 and -1.12 electrons /Å^3 (e/Å^3) in the vicinity of the iridium atoms, two peaks of 1.15 and 0.97 e/Å^3 along the Ir-Ir vector, 3.2 Å from the Ir atoms, and several peaks of about 0.75 e/Å^3 in the vicinity of the acetonitrile molecules. The general noise level of the map was ±0.4 e/Å^3. The large excursions near the iridium atoms, as well as the two axial peaks, are caused by the inability to correct for absorption. The peaks near the acetonitrile molecules probably represent different orientations of partial solvent molecules, but they could not be interpreted in any chemically reasonable way. The rather high goodness-of-fit is the result of both of these factors.

The lack of an absorption correction has caused some of the carbon atoms to be mispositioned, particularly those bonded to iridium. The wide range of Ir-C distances (>0.1 Å) is surely not real but is a result of the least squares moving the carbon atoms to minimize the peaks around the iridium atoms caused by the absorption. This is also the reason that two of the carbon atoms, C11 and C31, have thermal parameters that are too small: the least squares is adjusting them so as to compensate as much as possible for the absorption effects.

Table 2.2. Final Parameters (x,y,z x 10^4).

Atom	x	y	z	B
Ir1	1252(0.4)	648(0.2)	1031(0.4)	338(2)*
Ir2	1457(0.4)	1628(0.2)	1084(0.4)	330(2)*
C1	−20(11)	660(5)	415(10)	3.6(4)
N1	−760(9)	660(4)	82(8)	3.8(3)
C2	−1695(10)	738(5)	−391(10)	2.9(4)
C3	−2182(10)	468(5)	−41(12)	674(62)*
C4	−1937(10)	611(5)	−1293(9)	621(59)*
C5	−1829(10)	1197(5)	−287(10)	3.7(4)
C6	−1689(10)	1338(5)	570(10)	3.4(4)
C7	−1284(10)	1767(5)	826(10)	3.4(4)
C8	−1790(10)	2105(5)	198(12)	724(63)*
C9	−1227(11)	1885(5)	1708(10)	650(56)*
N2	−389(8)	1757(4)	898(8)	3.3(3)
C10	306(10)	1704(5)	968(10)	3.5(4)
C11	1398(8)	629(4)	−28(9)	1.1(3)
N3	1518(8)	629(4)	−588(9)	3.9(3)
C12	1621(12)	663(6)	−1387(11)	4.0(4)
C13	2533(13)	598(7)	−1201(13)	962(69)*
C14	1050(15)	320(6)	−1978(12)	1141(88)*
C15	1269(11)	1087(6)	−1770(11)	4.9(4)
C16	348(11)	1183(6)	−1987(11)	5.1(5)
C17	160(11)	1616(6)	−1802(12)	4.2(4)
C18	455(11)	1949(5)	−2206(10)	593(59)*
C19	−773(10)	1676(6)	−1978(12)	866(68)*
N4	635(8)	1670(4)	−889(10)	4.3(3)
C20	965(10)	1657(5)	−180(12)	3.9(4)
C21	2495(11)	596(5)	1679(11)	4.1(4)
N5	3224(9)	562(4)	2058(8)	4.2(3)
C22	4201(11)	542(6)	2566(12)	4.6(5)
C23	4344(12)	485(7)	3497(11)	1060(84)*
C24	4542(11)	174(5)	2280(12)	839(70)*
C25	4561(11)	953(5)	2490(11)	4.8(4)
C26	4458(11)	1066(6)	1596(12)	5.5(5)
C27	4216(11)	1499(5)	1326(11)	4.2(4)
C28	4860(11)	1814(6)	1945(13)	989(73)*
C29	4140(13)	1567(6)	431(12)	971(64)*
N6	3346(9)	1577(4)	1291(8)	3.8(3)
C30	2633(10)	1599(5)	1206(10)	3.5(4)
C31	1060(8)	641(4)	2079(9)	0.9(3)
N7	929(8)	645(4)	2632(9)	3.3(3)
C32	761(10)	705(5)	3382(10)	2.5(4)
C33	1177(11)	350(5)	3973(10)	671(55)*
C34	−183(10)	714(6)	3110(11)	800(58)*
C35	1149(10)	1116(5)	3764(10)	4.3(4)

Atom	x	y	z	B
C36	2113(10)	1162(5)	4093(10)	4.7(4)
C37	2455(11)	1576(6)	3953(11)	4.4(4)
C38	3429(10)	1586(6)	4335(11)	887(70)*
C39	2041(13)	1924(6)	4206(12)	1021(83)*
N8	2163(8)	1619(4)	3021(10)	4.9(4)
C40	1866(10)	1632(5)	2322(11)	3.7(4)
B1	8189(11)	1149(6)	4764(12)	3.0(4)
C41	7796(10)	944(5)	3829(10)	3.1(4)
C42	7949(11)	1122(6)	3176(12)	4.8(4)
C43	7651(12)	940(6)	2366(12)	5.6(5)
C44	7254(11)	571(6)	2211(12)	5.5(5)
C45	7098(12)	376(6)	2834(13)	6.7(5)
C46	7371(11)	571(6)	3621(11)	4.8(4)
C51	7949(9)	1623(5)	4734(10)	3.2(4)
C52	8273(11)	1854(6)	5486(12)	5.8(5)
C53	8073(13)	2269(7)	5549(13)	7.4(6)
C54	7495(13)	2458(6)	4827(14)	7.4(5)
C55	7111(12)	2245(6)	4061(13)	6.9(5)
C56	7362(11)	1839(6)	4031(11)	5.1(4)
C61	7755(10)	932(5)	5329(10)	3.0(4)
C62	6868(12)	963(5)	5068(11)	5.1(5)
C63	6432(13)	825(6)	5539(14)	7.3(5)
C64	6926(12)	606(6)	6272(12)	5.9(5)
C65	7808(12)	562(6)	6576(12)	5.7(5)
C66	8221(10)	721(5)	6092(11)	4.5(4)
C71	9245(9)	1062(5)	5174(9)	3.0(4)
C72	9897(12)	1367(6)	5464(11)	5.6(5)
C73	10795(12)	1257(6)	5844(12)	6.3(5)
C74	10997(12)	865(6)	5934(12)	5.6(5)
C75	10424(12)	553(6)	5657(12)	5.9(5)
C76	9535(10)	660(5)	5269(10)	4.1(4)
B2	9643(11)	3681(5)	2539(11)	2.2(4)
C81	10406(9)	3388(5)	2499(9)	3.1(4)
C82	10348(10)	2973(5)	2411(10)	4.0(4)
C83	11047(14)	2737(7)	2423(13)	7.5(6)
C84	11804(12)	2904(6)	2494(12)	5.9(5)
C85	11883(11)	3314(6)	2570(11)	5.4(5)
C86	11197(11)	3553(5)	2611(10)	4.2(4)
C91	8837(9)	3393(5)	2464(10)	3.0(4)
C92	8576(10)	3340(5)	3108(11)	4.7(4)
C93	7879(11)	3086(5)	3004(12)	5.0(5)
C94	7426(11)	2861(5)	2293(12)	4.4(4)
C95	7650(11)	2920(5)	1650(11)	4.8(4)
C96	8330(10)	3176(5)	1734(11)	3.8(4)

Atom	x	y	z	B
C101	10039(9)	3924(5)	3435(10)	3.0(4)
C102	10591(10)	3715(5)	4174(11)	4.3(4)
C103	10848(11)	3908(6)	4978(12)	5.7(5)
C104	10581(12)	4290(6)	5002(13)	6.2(5)
C105	10050(14)	4518(7)	4331(15)	7.8(6)
C106	9775(11)	4310(6)	3513(12)	5.1(5)
C111	9277(9)	4017(5)	1764(10)	2.7(4)
C112	9691(10)	4137(5)	1256(10)	3.5(4)
C113	9359(11)	4449(5)	666(11)	4.5(4)
C114	8628(10)	4653(5)	526(10)	3.8(4)
C115	8171(10)	4536(5)	971(11)	4.1(4)
C116	8492(10)	4216(5)	1556(10)	3.2(4)
N9	5818(18)	2289(9)	265(18)	14.7(9)
C200	5212(22)	2497(10)	−279(21)	12.2(9)
C201	4554(19)	2675(9)	−915(19)	12.2(9)
N10	−174(18)	2691(9)	−956(20)	16.0(9)
C203	340(26)	2825(12)	−271(28)	16.3(12)
C204	881(19)	2990(9)	389(20)	12.0(9)

* $U_{eq} \times 10^4$

$$U_{eq} = \frac{1}{3} \sum_i \sum_j [U_{ij} (a_i^* a_j^*)(\vec{a}_i \vec{a}_j)]$$

Table 2.3. Selected Distances and Angles.

Atom	Atom	Distance (Å)
Ir1	Ir2	3.199(1)
Ir1	C1	1.962(17)
Ir1	C11	1.986(14)
Ir1	C21	1.932(18)
Ir1	C31	2.008(14)
Ir2	C10	1.900(17)
Ir2	C20	2.015(18)
Ir2	C30	1.924(17)
Ir2	C40	1.981(17)
C1	N1	1.14(2)
C11	N3	1.09(2)
C21	N5	1.13(2)
C31	N7	1.09(2)
C10	N2	1.15(2)
C20	N4	1.13(2)
C30	N6	1.16(2)
C40	N8	1.11(2)

Atom	Atom	Atom	Angle(Deg.)
Ir1	C1	N1	177.6(15)
Ir1	C11	N3	176.2(14)
Ir1	C21	N5	179.2(16)
Ir1	C31	N7	177.4(13)
Ir2	C10	N2	178.8(15)
Ir2	C20	N4	175.3(16)
Ir2	C30	N6	178.9(15)
Ir2	C40	N8	173.6(16)

Spectroscopic Measurements

All solvents were dried and degassed by standard methods.[5,6] Absorption spectra were recorded with a Cary 17 spectrophotometer. Spectra were obtained of solutions prepared on a high-vacuum line in a cell consisting of a 10 ml Pyrex bulb, a 1 cm pathlength quartz cell, and a Teflon vacuum valve.

Electronic Emission Spectroscopy

Electronic emission spectra were measured using an emission spectrophotometer constructed at CalTech that has been described previously.[7] Spectra recorded at ambient temperatures were obtained for solutions that were prepared on a high-vacuum line in a cell consisting of a 10 ml Pyrex bulb, a 1 cm pathlength quartz cell, and a Teflon vacuum valve. For the measurements at 77 K, solutions were prepared in the same manner in a glass NMR tube attached to a Teflon vacuum valve. Solvent was bulb-to-bulb distilled into the cell or tube containing the compound from the appropriate solvent storage flask. For the 77 K emission measurements, the NMR tubes were held in a liquid-nitrogen-filled quartz finger dewar.

Emission Lifetime Measurements

Emission lifetime measurements were conducted with a Nd:YAG pulsed laser system that has been described previously using 532 nm excitation.[8] The solutions for the measurements at ambient temperatures were prepared by the procedure used for the emission measurements. The solutions for 77 K lifetime measurements were prepared in NMR tubes by the same procedure. All emission intensity decays exhibited first-order kinetics over at least 3 half-lives. For the measurements at 77 K, the NMR tubes were held in a liquid-nitrogen-filled quartz finger dewar. The laser was operated at a low-power output to minimize local sample heating.

Resonance Raman Spectroscopy

Resonance Raman spectra were measured by Dr. Thomas Loehr at the Oregon Graduate Center and by Dr. R.F. Dallinger at Los Alamos National Laboratory. Time-resolved resonance Raman spectra were measured by Dr. R.F. Dallinger at Los Alamos National Laboratory.

Additional Measurements

Elemental analyses were obtained at the CalTech Analytical Laboratory.

Results and Discussion

Crystal Structure

The structure of $Ir_2(TMB)_4^{2+}$ is shown in Figure 2.1. The Ir-Ir distance of 3.119(1) Å is shorter than the metal-metal separation found for the analogous Rh(I) dimers ($Rh_2(CNC_6H_5)_8^{2+}$, 3.193(0) Å; $Rh_2b_4^{2+}$, 3.242(1) Å; $Rh_2(TMB)_4^{2+}$, 3.262(1) Å).[2,9] The shorter metal-metal separation may be indicative of a stronger metal-metal interaction (metal-metal bond) in $Ir_2(TMB)_4^{2+}$ in comparison to the Rh complexes.

The most striking feature of the structure is the twist of the two $Ir(CN)_4$ units (Figure 2.2). The four TMB ligands are arranged as a four-bladed propeller about the Ir-Ir axis, giving the two $Ir(CN)_4$ units a partially staggered conformation. The torsional angle, N-M-M-N, is 28(4)° (Table 2.4), similar to the torsion angle observed for $Rh_2(TMB)_4^{2+}$, 31°.[2] The pitch of the blade is 27(3)° as measured from C_β-Ir-Ir-C_β. A best-fit plane of the $Ir(CN)_4$ units shows a slight distortion (Table 2.5). Each Ir experiences a small pyramidal distortion with the metal displaced toward the center of the cation. For $Rh_2b_4^{2+}$, a similar pyramidal distortion is observed with all four CN groups displaced toward the center of the dimer.[2] A tetrahedral distortion about the Rh atom is observed for $Rh_2(TMB)_4^{2+}$ and $Rh_2(CNC_6H_5)_8^{2+}$.[2,9] The average bond lengths and angle for the $Ir(CN)_4$ units are unexceptional and compare well with other Ir(I) and Rh(I) isocyanide complexes.[2,10,11] The overall structure of the TMB ligand is quite similar to that observed in $Rh_2(TMB)_4(PF_6)_2{\cdot}2CH_3CN$.[2]

One of the interesting features of this structure is the arrangement of the cations in the unit cell. An ORTEP drawing of the unit cell, with the counter ions and solvent molecules removed for clarity, is given in Figure 2.3. The Ir-Ir vectors are aligned almost parallel to the b axis. Such an arrangement makes this crystal morphology ideally suited for polarized single-crystal spectroscopy.[12,13] However, the

Figure 2.1. View of the structure of $Ir_2(TMB)_4{}^{2+}$.

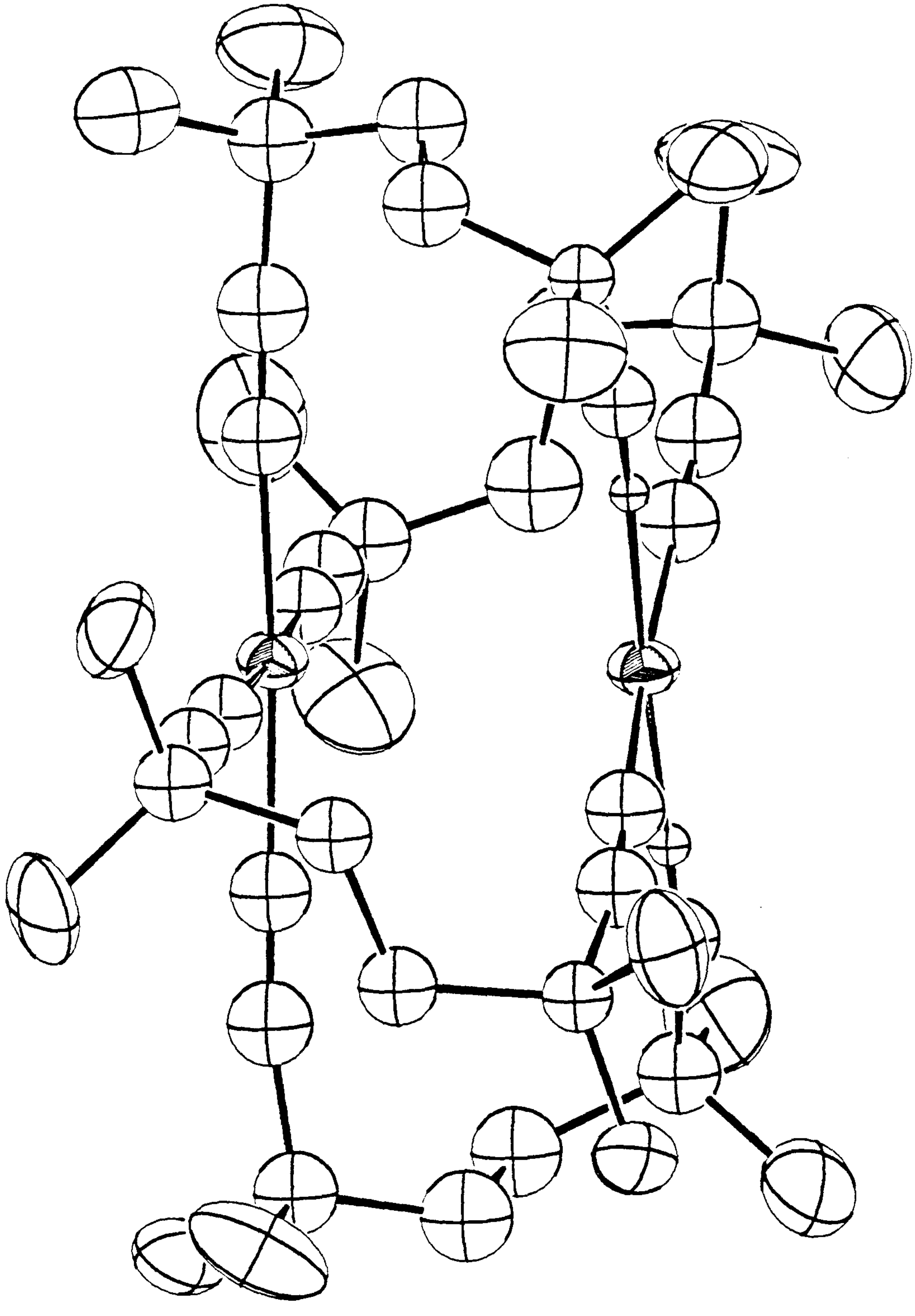

Figure 2.2. View of the structure of $Ir_2(TMB)_4^{2+}$ viewed down the Ir-Ir vector.

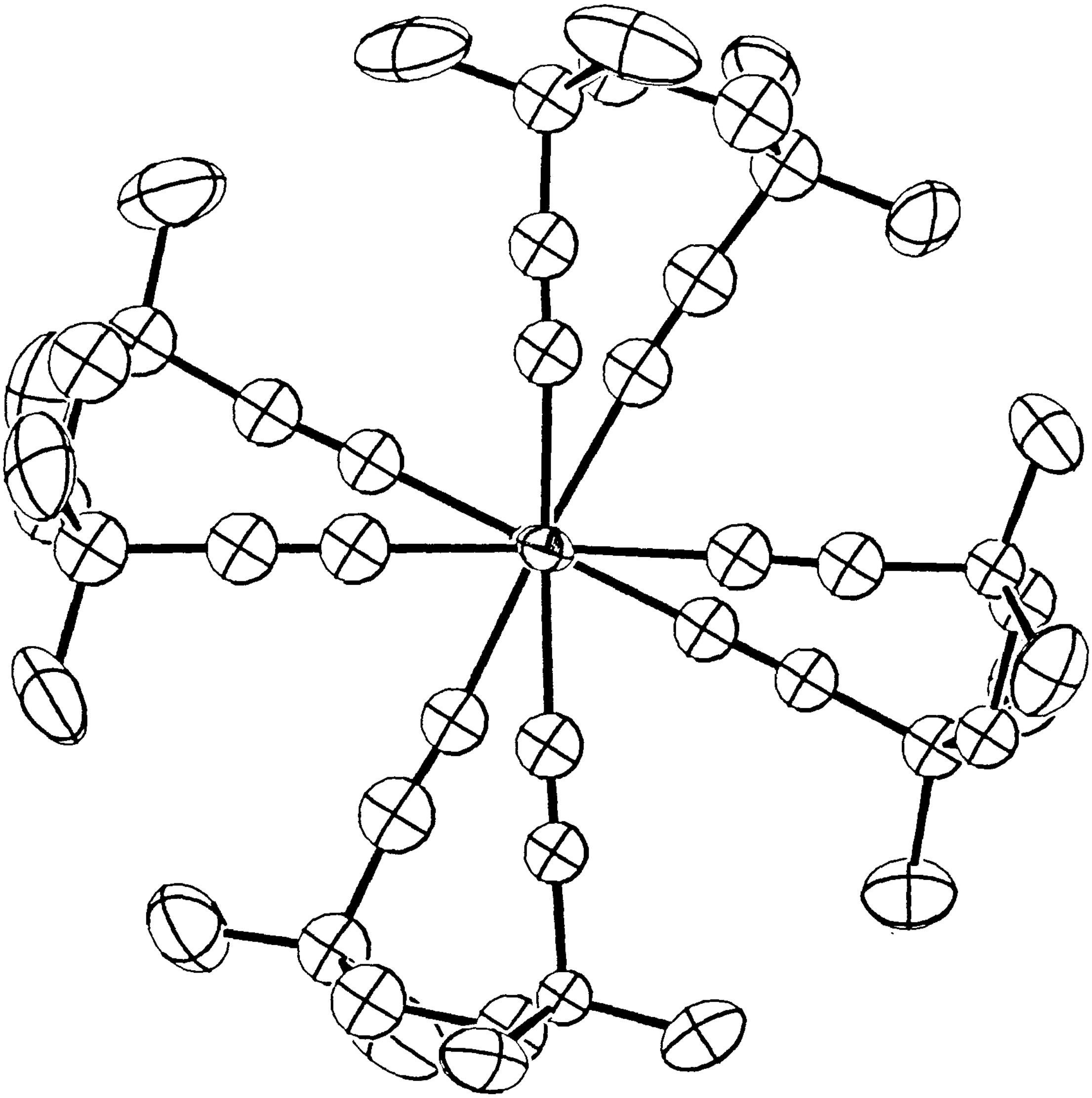

Table 2.4. Torsion Angles.

Atom	Atom	Atom	Atom	Angle (Deg.)
N1	Ir1	Ir2	N2	23.5(4)
N3	Ir1	Ir2	N4	31.6(4)
N5	Ir1	Ir2	N6	26.1(4)
N7	Ir1	Ir2	N8	29.7(4)
C2	Ir1	Ir2	C7	24.5(3)
C12	Ir1	Ir2	C17	32.6(3)
C22	Ir1	Ir2	C27	29.3(3)
C32	Ir1	Ir2	C37	27.3(3)

Table 2.5. Best plane fit of $Ir(CN)_4$ units.

Atom	Deviation (Å)	Atom	Deviation (Å)
Ir1	0.068	Ir2	-0.074
C1	0.004	C10	-0.005
N1	-0.055	N2	0.061
C11	0.018	C20	-0.033
N3	0.031	N4	-0.026
C21	0.001	C30	0.011
N5	-0.053	N6	0.048
C31	0.027	C40	-0.022
N7	0.028	N8	-0.034

Figure 2.3. View of the unit cell with $B(C_6H_5)_4^-$ and CH_3CN molecules removed.

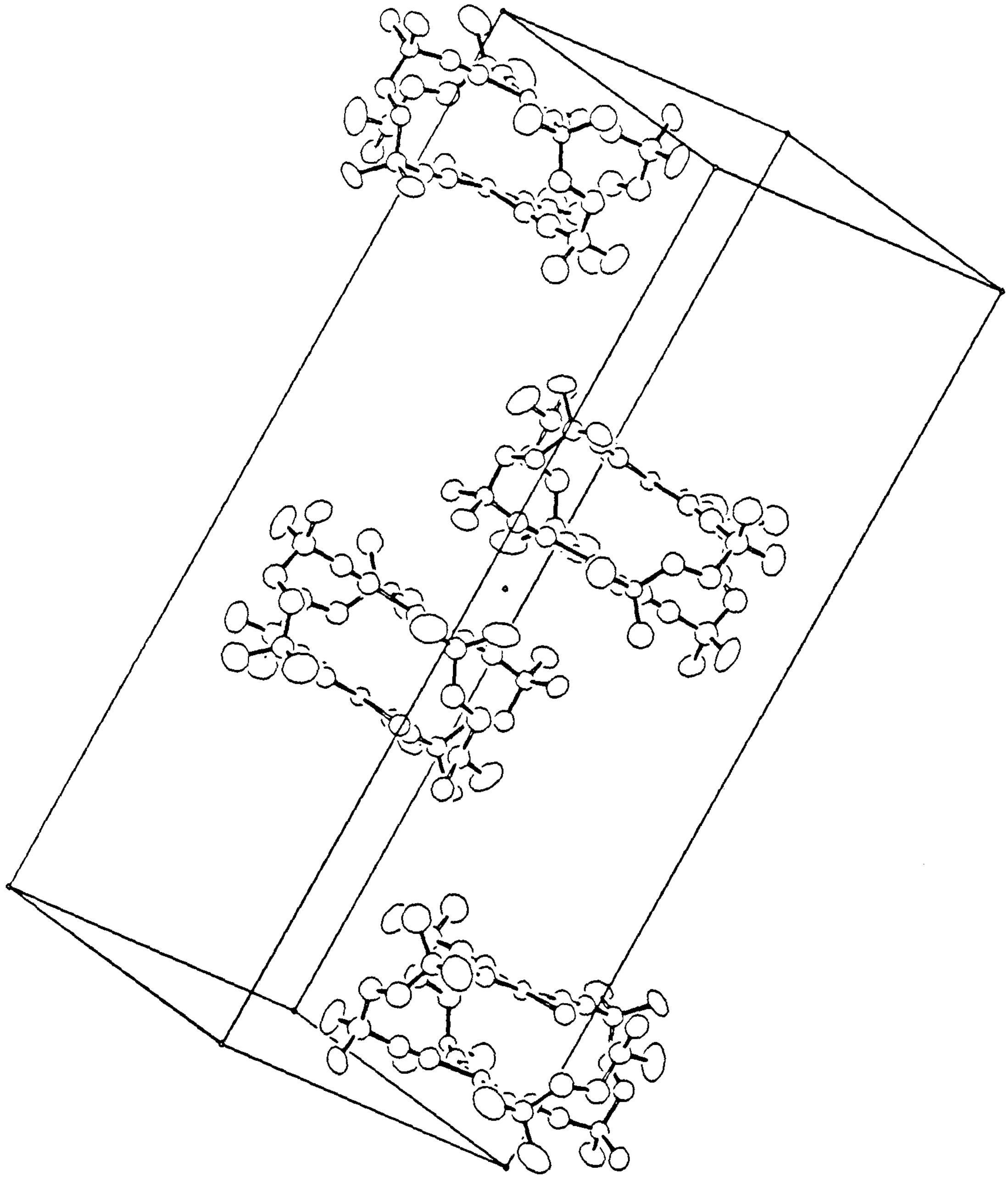

macroscopic features of the crystals (large chunky blue-black crystals, far too thick for spectroscopy) make such a study impractical.

Electronic Spectroscopy

A brief discussion of the spectroscopy and photophysics of $Ir_2(TMB)_4^{2+}$ has already been presented.[1] A detailed analysis of the optical absorption spectrum of $Ir_2(TMB)_4^{2+}$ is presented in Chapter 3.

The electronic absorption spectrum of $Ir_2(TMB)_4^{2+}$ is shown in Figure 2.4. In analogy to $Rh_2(TMB)_4^{2+}$,[14] the intense absorption centered at 625 nm (ε = 11200 M^{-1} cm^{-1}) is assigned to the $^1(d\sigma^* \rightarrow p\sigma)$ transition ($^1A_{1g} \rightarrow {}^1A_{2u}$). The intense features below 300 nm, having maxima at 318 nm (ε = 22000 $M^{-1}cm^{-1}$) and 372 nm (ε = 9750 $M^{-1}cm^{-1}$), are assigned to $d_{xz,yz} \rightarrow p_z$ transitions ($^1A_{1g} \rightarrow {}^1E_{1u}, {}^3E_{1u}$). To lower energy of the 625 nm band in both single crystal and concentrated solution, a feature centered at 820 nm (ε = 150 $M^{-1}cm^{-1}$) is observed (Figure 2.5). This feature is assigned to the $^3(d\sigma^* \rightarrow p\sigma)$ transition.

The electronic absorption spectrum of $Ir_2(TMB)_4^{2+}$ is summarized and compared to the spectra of $Ir(CN\text{-}t\text{-butyl})_4^+$ and $Rh_2(TMB)_4^{2+}$ in Table 2.6.[15] The large red shift of the $d_{z^2} \rightarrow p_z$ transition in going to the dimer has been understood to be a consequence of the smaller d-p gap inferred from the MO model. The greater width of the $A_{2u}(^1A_{2u})$ and $E_u(^3A_{2u})$ bands is a result of the greater metal-metal bonding in the excited state. Promotion of an electron from the $d\sigma^*$ orbital to the $p\sigma$ orbital results in a large molecular distortion, contraction along the metal-metal coordinate. While the $^1(d\sigma^* \rightarrow p\sigma)$ transition is shifted to the red of the monomer $d_{z^2} \rightarrow p_z$ transition, the $d\pi \rightarrow p\sigma$ transitions of the dimer have energies and widths almost coincident with the monomer transitions; this observation is general to d^8-d^8 complexes. Explanations for the dichotomy of transition types have been presented but none is very satisfying.[14] The VB model, as discussed in Chapter 3, does accommodate both transition types. In comparison

Figure 2.4. Electronic absorption spectrum of $[Ir_2(TMB)_4](B(C_6H_5)_4)_2$ in CH_3CN at 25 °C.

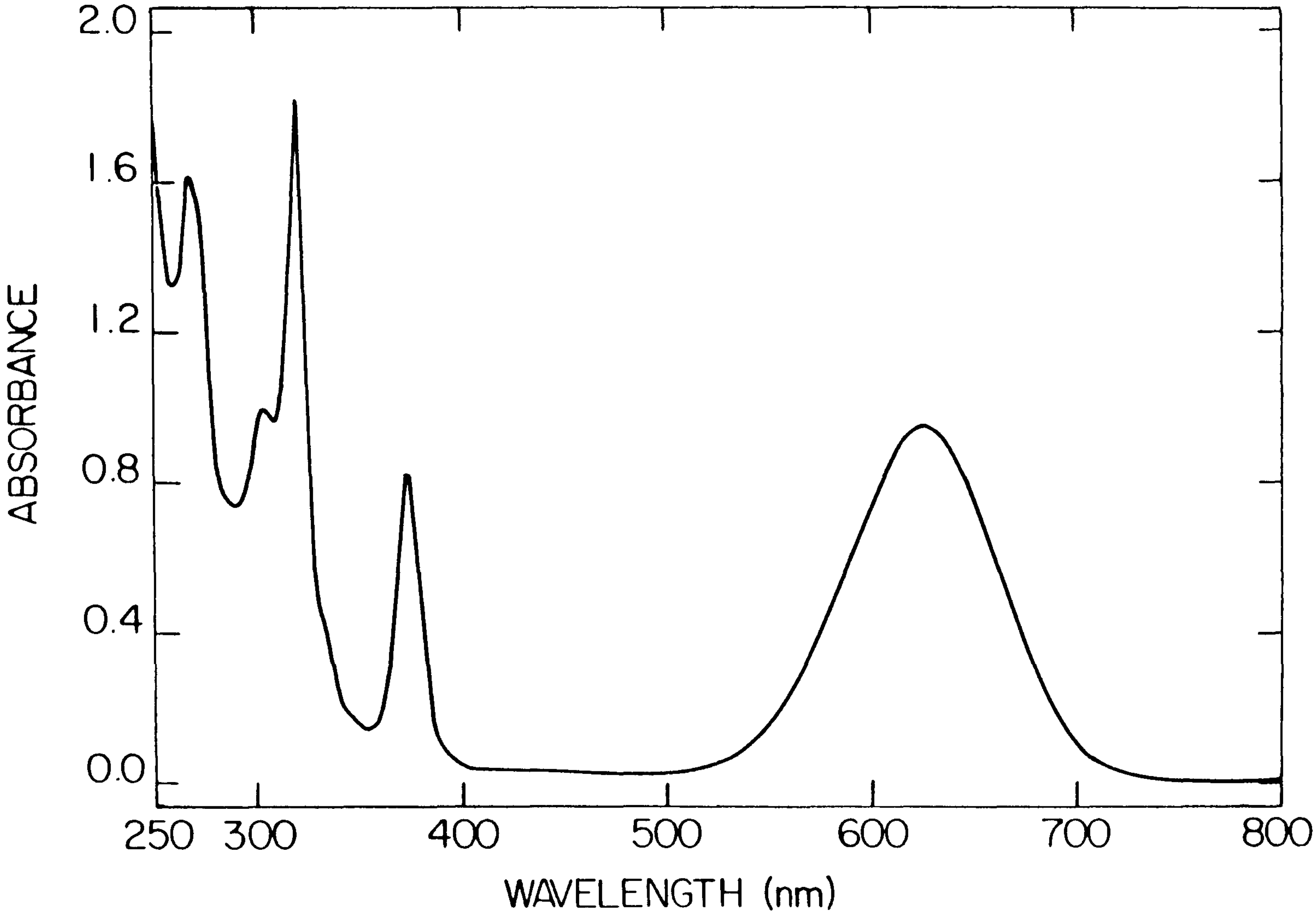
ABSORBANCE
2.0
1.6
1.2
0.8
0.4
0.0
250
300
400
500
600
700
800
WAVELENGTH (nm)

Figure 2.5. Electronic absorption spectrum of $[Ir_2(TMB)_4](B(C_6H_5)_4)_2$ in a glassy matrix of CH_3CH_2CN/2-MeTHF (1:2 volume ratio) at 77 K.

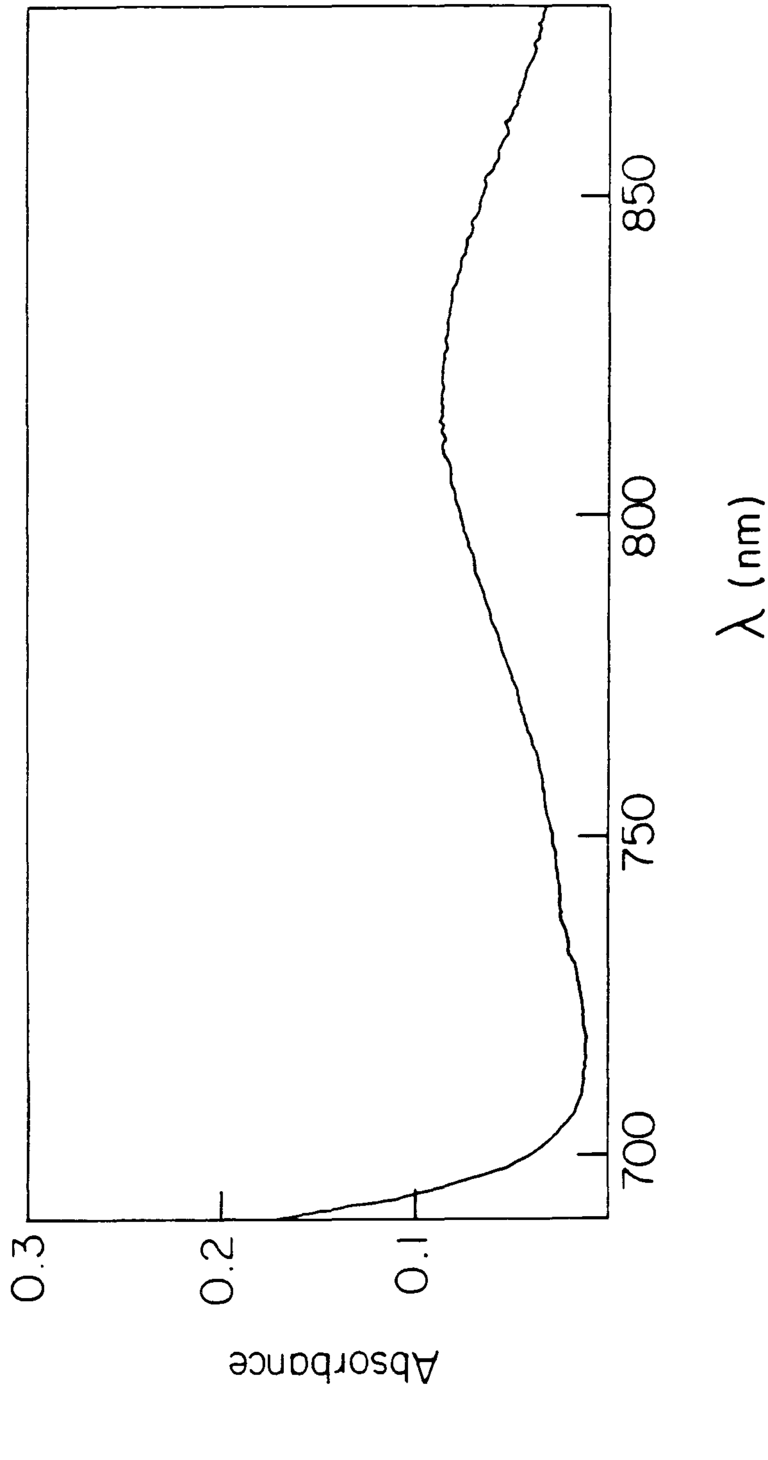

Absorbance
0.3
0.2
0.1
700
750
800
850
λ (nm)

Table 2.6. Absorption maxima for $[Ir_2(TMB)_4](B(C_6H_5)_4)_2$, [Ir(CN-*t*-butyl)$_4$]$BF_4$, and$[Rh_2(TMB)_4](PF_6)_2$ in CH_3CN at 25 °C.

$^1A_{1g} \rightarrow$	$Ir_2(TMB)_4^{2+}$	Ir(CN-*t*-butyl)$_4^+$	$Rh_2(TMB)_4^{2+}$
$^3A_{2u}$	820 nm	489 nm	a
$^1A_{2u}$	625	423	520
$^3E_u(E_u)$	372	373	342
$^3E_u(A_{2u})$	333	a	a
^1E_u	318	308	316
$^3B_{1u}$	305	291	290

a. Not observed.

to $Rh_2(TMB)_4^{2+}$, the $^1(d\sigma^* \rightarrow p\sigma)$ and $^3(d\pi \rightarrow p\sigma)$ for $Ir_2(TMB)_4^{2+}$ are red-shifted some 3000 cm^{-1}. The widths of all transitions are quite comparable, indicating that a similar molecular distortion is occurring for both complexes upon excitation.

Earlier works have correlated the energy of the d-p transition for binuclear d^8 complexes with the ground-state metal-metal separation.[16] Within the MO formalism, variation in the metal-metal separation will yield variation in the metal-metal interaction in the ground state. An increase in the metal-metal interaction in the ground state will serve to decrease the d-p gap, thereby shifting the $d\sigma^* \rightarrow p\sigma$ transition to the red. A blue shift in the transition energy is predicted for a decrease in the metal-metal interaction (Figure 2.6). This analysis has been extended to include variations in the metal.[16] A change in metal, Rh to Ir, generally yields a large red shift in the $^1(d\sigma^* \rightarrow p\sigma)$ transition. The variation in transition energy with metal has been presented as another example of the shift in energy of the $d_{z^2} \rightarrow p_z$ transition with change in metal-metal interaction, with the metal-metal interaction increased upon going from Rh to Ir.

The premise of the arguments for the shift in the $^1(d\sigma^* \rightarrow p\sigma)$ transition energy is that the ground-state metal-metal interaction, as described by the MO model, controls the electronic transitions; that is, the excited states are well described within the ground-state MO formalism.

As will be discussed in detail in Chapter 3, the electronic structure of binuclear d^8 complexes is more accurately described by a VB "weak-coupling" model. In this model, the ground state and various excited states are best described as weakly coupled monomers with the excitation localized on one center. For some states, it will be advantageous to increase the metal-metal one-electron interaction (shorten the metal-metal distance); this shortening of the metal-metal distance will result in an increased mixing of the covalent state with the higher-energy ionic state. This mixing will result in a lowering of the state energy relative to the weak coupling limit. Thus, unlike the ground-state MO model, the transition energies within the VB model are controlled by

Figure 2.6. MO diagram showing the effects on the energy of the dσ and pσ levels for a binuclear complex with an increase or a decrease in the metal-metal interaction.

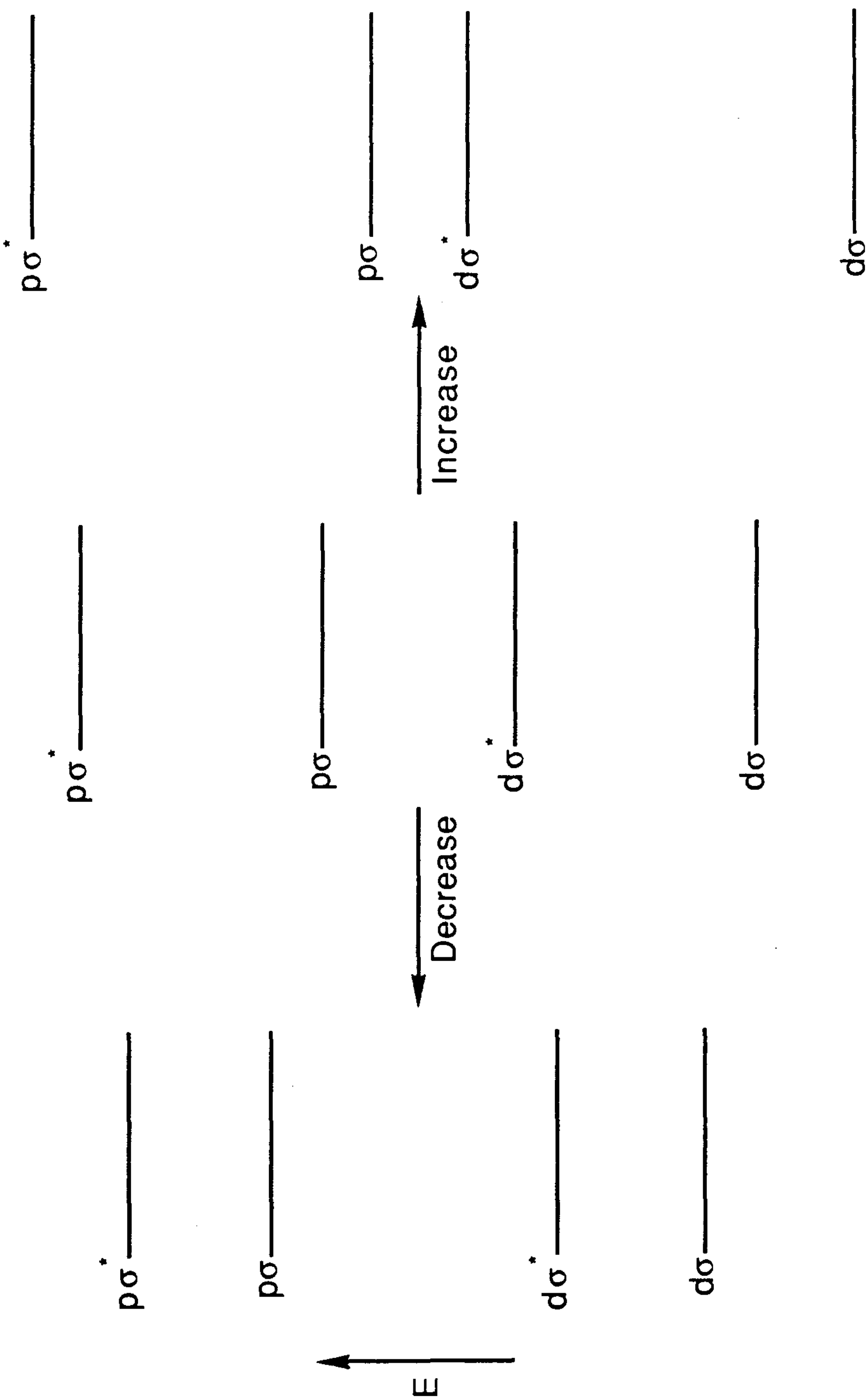
pσ*
pσ
dσ*
dσ
Increase
pσ*
pσ
dσ*
dσ
Decrease
pσ*
pσ
dσ*
dσ
E

excited-state properties, the amount of stabilization gained by increasing the metal-metal interaction.

Table 2.7 lists the $^1(d\sigma^* \rightarrow p\sigma)$ transition energies for several binuclear isocyanide complexes. The crystallographically determined metal-metal separations are tabulated along with the $^1(d_z{}^2 \rightarrow p_z)$ transition energies for the appropriate monomer model. For the series $Rh_2(TMB)_4{}^{2+}$, $Rh_2b_4{}^{2+}$, and $Rh_2(CNC_6H_5)_8{}^{2+}$, a decrease in the metal-metal separation and coincident bathochromic shift of the $d\sigma^* \rightarrow p\sigma$ transition is observed. However, when considering the shift from the corresponding $d_z{}^2 \rightarrow p_z$ monomer excitation, a comparable red shift is observed, a varying reference point. For the series of Rh(I) arylisocyanide complexes (L = CNC_6H_5, CN-*p*-C_6H_4F, and CN-*p*-$C_6H_4NO_2$), a systematic increase in the Rh-Rh distance is observed with a systematic **red shift** of the transition energy. A result contrary to the earlier reasoning, an increase in the metal-metal separation yields a decrease in metal-metal interaction and results in a blue shift of the $^1(d\sigma^* \rightarrow p\sigma)$ transition. Comparing $[Rh(2,6\text{-diMe-}4\text{-}BrC_6H_2NC)_3Cl]_2{}^{2+}$ to $Rh_2(CNC_6H_5)_8{}^{2+}$, a blue shift of only 640 cm^{-1} is observed for the $^1(d\sigma^* \rightarrow p\sigma)$ transition for an increase of 0.258 Å in the Rh-Rh separation, a surprisingly small change in energy for such a large variation in metal-metal distance. If one, instead, compares the energy of the $d\sigma^* \rightarrow p\sigma$ excitation to the monomer $d_z{}^2 \rightarrow p_z$ transition, a shift of ~6500 cm^{-1} is observed for all Rh(I) isocyanide complexes except $Rh_2b_4{}^{2+}$. Thus, comparisons of transition energies for a series of metal dimers can be misleading in that the absolute energies of the transitions may not be comparable. The true reference point for each complex (the monomer excitation) may vary through the series. For the binuclear Rh(I) complexes, while the metal-metal separation varies dramatically in the ground state, the shift in the energy of the $d_z{}^2 \rightarrow p_z$ transition is quite constant. The amount of stabilization in the $^1(d\sigma^* p\sigma)$ excited state is comparable through the series of Rh(I) complexes. For those systems for which Rh(II)-Rh(II) species are known (Table 2.8), it is observed that a comparable, short metal-metal

Table 2.7. $^1(d_{z^2} \rightarrow p_z)$ transition energies for d^8 complexes.

Metal Complex	$d_{z^2} \rightarrow p_z$, nm [a]	ΔE, cm^{-1} [b]	M-M, Å [c]	Ref.
$Rh(CN\text{-ethyl})_4^+$	380			17
$Rh_2b_4^{2+}$	553	8200	3.242(1)	2,18
$Rh(CN\text{-}t\text{-butyl})_4^+$	386			9
$Rh_2(TMB)_4^{2+}$	520	6700	3.262(1)	2
$Ir(CN\text{-}t\text{-butyl})_4^+$	423			15
$Ir_2(TMB)_4^{2+}$	625	7600	3.199(1)	
$Rh(CNC_6H_5)_4^+$	411			9
$Rh_2(CNC_6H_5)_8^{2+}$	568	6700	3.193(0)	9
$Rh(CN\text{-}p\text{-}FC_6H_4)_4^+$	d			
$[Rh(CN\text{-}p\text{-}FC_6H_4)_4]_2^{2+}$	597		3.207(2)	19
$Rh(CN\text{-}p\text{-}NO_2C_6H_4)_4^+$	d			
$[Rh(CN\text{-}p\text{-}NO_2C_6H_4)_4]_2^{2+}$	606		3.25(1)	19
$Rh(2,6\text{-diMe-4-}BrC_6H_2NC)_3Cl^+$	408			20
$[Rh(2,6\text{-diMe-4-}BrC_6H_2NC)_3Cl]_2^{2+}$	548	6300	3.451(2)	20

a. For mononuclear d^8 complexes, λ_{max} for the $^1(d_{z^2} \rightarrow p_z)$ transition. For binuclear d^8 complexes, λ_{max} for the $^1(d\sigma^* \rightarrow p\sigma)$ transition.

b. Red shift of the $^1(d_{z^2} \rightarrow p_z)$ transition in going from monomer to dimer. $\Delta E = E(^1(d_{z^2} \rightarrow p_z)) - E(^1(d\sigma^* \rightarrow p\sigma))$.

c. Crystallographically determined metal-metal separation.

d. Not known.

Table 2.8. Crystallographically determined metal-metal distances for Rh(I) and Rh(II) complexes.

d^8-d^8 complex	M-M, Å	Ref.	d^7-d^7 complex	M-M, Å	Ref.
$Rh_2b_4^{2+}$	3.242	2	$Rh_2b_4Cl_2^{2+}$	2.837	21
$Rh_2(TMB)_4^{2+}$	3.262	2	$Rh_2(TMB)_4Cl_2^{2+}$	2.770	22
$Rh_2(CNC_6H_5)_8^{2+}$	3.193	8			
$Rh_2(CN\text{-}p\text{-}CH_3C_6H_4)_8^{2+}$	a		$Rh_2(CN\text{-}p\text{-}CH_3C_6H_4)_8I_2^{2+}$	2.785	23

a. Not known.

separation can be accommodated for all the complexes. This observation implies that the ground-state potential surface is quite soft and can accommodate a large range of metal-metal separations without a significant change in energy. The excited state surface, possessing a formal, metal-metal single bond, allows for only a small variation in metal-metal separation.

For $Ir_2(TMB)_4^{2+}$, the $^1(d\sigma^* \rightarrow p\sigma)$ transition is to lower energy of the transition for $Rh_2(TMB)_4^{2+}$. However, the $d_{z^2} \rightarrow p_z$ transition for the Ir(I) monomer is also to lower energy of the Rh(I) monomer transition, a shift in reference point. In comparing the monomer-to-dimer shifts, the bathochromic shift observed for Ir(I) is larger than for Rh(I), 7600 cm^{-1} compared to 6700 cm^{-1}. The energy separation of the covalent and ionic states is less for Ir than for Rh, allowing for a greater mixing of the higher-energy states, yielding a greater stabilization of the $^1(d\sigma^* p\sigma)$ excited state.

Within the series of complexes discussed, $Rh_2b_4^{2+}$ appears to be an anomaly. The monomer-to-dimer shift of the $d_{z^2} \rightarrow p_z$ transition is much larger than that seen for analogous Rh(I) isocyanide complexes and is, in fact, larger than the shift observed for $Ir_2(TMB)_4^{2+}$. This surprising result can be understood if one reasons that the bridge ligand destabilizes the d^8-d^8 ground state in favor of the contracted single-bonded Rh complex. The spectral band widths and Stokes shift observed for $Rh_2b_4^{2+}$ are less than for $Rh_2(TMB)_4^{2+}$ and $Rh_2(CNC_6H_5)_8^{2+}$, indicating that the molecular distortion upon excitation is less.[2] This observation could be understood as a result of unfavorable ligand interactions at shorter Rh-Rh distances. The oxidation potential for $Rh_2b_4^{2+}$ is estimated to be 500 mV less positive of $Rh_2(TMB)_4^{2+}$, making the complex more easily oxidized than $Ir_2(TMB)_4^{2+}$.[24] This result indicates that the $Rh_2b_4^{2+}$ ground state is destabilized relative to the ground state of other binuclear d^8 complexes. Therefore, the shift of the $d_{z^2} \rightarrow p_z$ transition for $Rh_2b_4^{2+}$ is a combination of ground state and excited-state effects.

The important point of the above discussion is that the energy of the $d\sigma^* \rightarrow p\sigma$ transition is governed by the ability of the excited state, rather than being controlled by ground-state effects, to undergo a contraction along the metal-metal coordinate. Another way of describing the phenomenon is that at the weak coupling limit, the excited state appears as an excited monomer coupled to a ground-state monomer. Increasing the metal-metal interaction serves to delocalize the excitation over the entire complex, lowering the energy of the state (Figure 2.7). This concept appears to be general to the large class of binuclear metal complexes. For the series of complexes $Rh_2(CNR)_4(dppm)_2{}^{2+}$ (Table 2.9), the increased ability of the complex to accommodate a smaller Rh-Rh separation results in a systematic red shift of the $d\sigma^* \rightarrow p\sigma$ transition energy (the monomer reference point does not vary with variation in the alkyl isocyanide). One final point that should be emphasized is that only the shift in the $d_{z^2} \rightarrow p_z$ transition energy between monomer and dimer is comparable within a series of complexes. Comparison of absolute transition energies for a series of complexes can lead to erroneous results.

Photophysics

Excitation into the 625 nm band of $Ir_2(TMB)_4{}^{2+}$ at room temperature in fluid solution results in two emissions (Figure 2.8). The higher-energy band centered at 735 nm is quite short-lived (< 2 ns) and is assigned to the florescence ${}^1A_{2u} \rightarrow {}^1A_{1g}$. The second band centered at 1080 nm is assigned to the phosphorescence ${}^3A_{2u} \rightarrow {}^1A_{1g}$ with a temperature-independent lifetime of 210 ± 20 ns. No vibronic structure has been resolved in emission or absorption even at very low temperatures; therefore, the λ_{00} transition for the ${}^{1,3}A_{2u}$ states can be estimated only from either the overlap of the absorption and the emission spectra or by averaging the absorption and the emission maxima.[32] Either estimate places the λ_{00} transition for the ${}^3A_{2u}$ state at 940 nm and at

Figure 2.7. Qualitative valence bond state diagram for weak d/p interaction of two d^8 monomers. The energies of the $^1A_{2u}$ states are dependent on the amount of stabilization, contraction along the metal-metal coordinate.

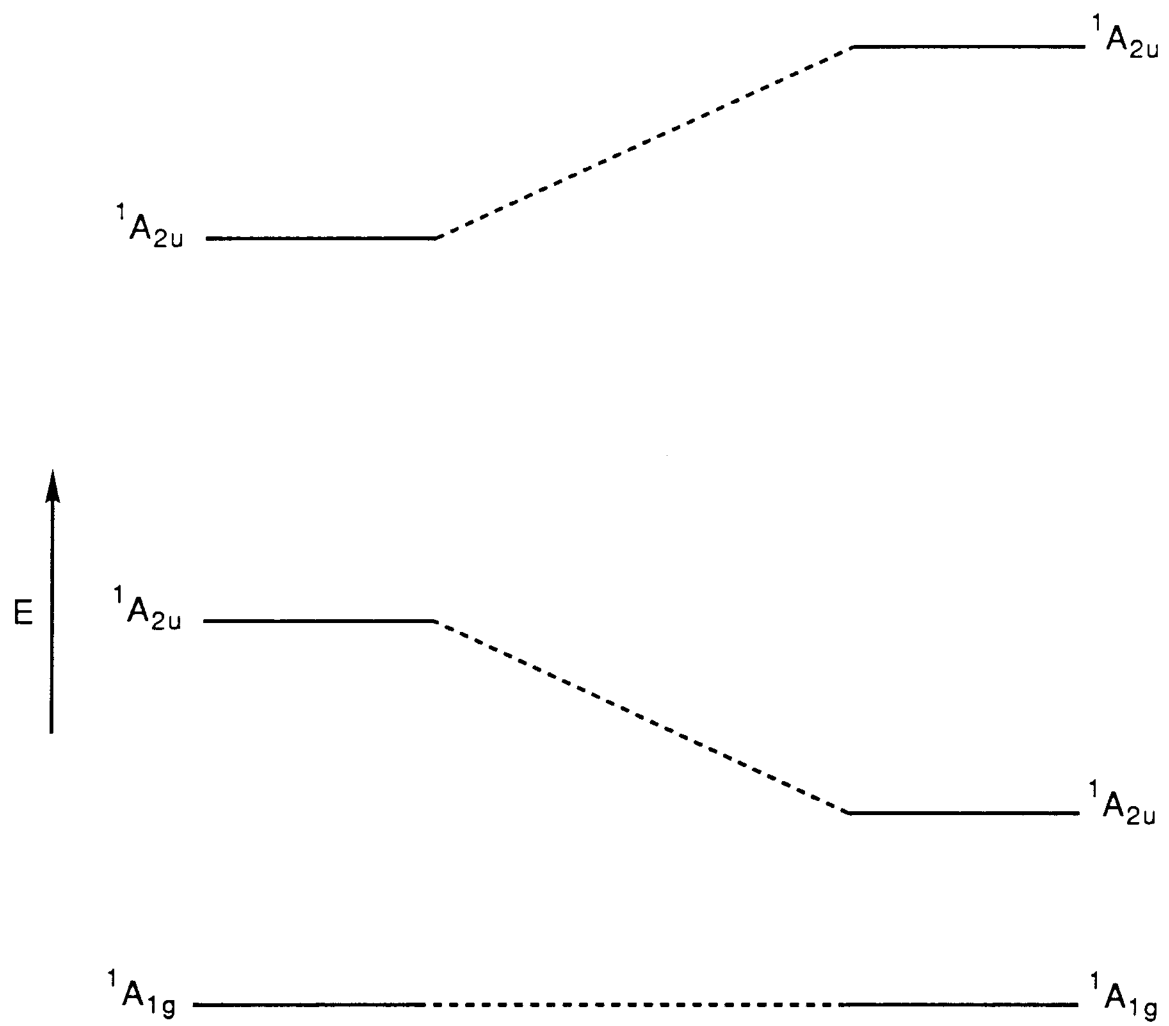
$^1A_{2u}$
$^1A_{2u}$
E
$^1A_{2u}$
$^1A_{2u}$
$^1A_{1g}$
$^1A_{1g}$

Table 2.9. $^1(d_{z^2} \rightarrow p_z)$ transition energies for d^8 complexes.

Metal Complex	$d_{z^2} \rightarrow p_z$, nm [a]	ΔE, cm^{-1} [b]	M-M, Å [c]	Ref.
$Rh(CO)Cl(P(C_6H_5)_3)$	367			30
$Rh_2(CO)_2Cl_2(dppm)_2$	442	4600	3.2386(5)	26, 27
$Rh(CO)Cl(As(C_6H_5)_3)$	356			25
$Rh_2(CO)_2Cl_2(dpam)_2$	466	6600	3.396(1)	26, 27
$Rh(CNCH_3)_2(P(C_6H_5)_3)^+$	458			29
$Rh_2(CN\text{-}t\text{-}butyl)_4(dppm)_2{}^{2+}$	523	2700	d	29
$Rh_2(CNC_6H_{11})_4(dppm)_2{}^{2+}$	550	3600	d	29
$Rh_2(CN\text{-}n\text{-}C_4H_9)_4(dppm)_2{}^{2+}$	560	4000	d	29
$Rh_2(CNCH_3)_4(dppm)_2{}^{2+}$	573	4400	d	29
$Rh_2(b)_2(dppm)_2{}^{2+}$	625	5800	d	30
$Rh_2(CNC_6H_5)_4(dppm)_2{}^{2+}$	606	e	d	31

a. For mononuclear d^8 complexes, λ_{max} for the $^1(d_{z^2} \rightarrow p_z)$ transition. For binuclear d^8 complexes, λ_{max} for the $^1(d\sigma^* \rightarrow p\sigma)$ transition.

b. Red shift of the $^1(d_{z^2} \rightarrow p_z)$ transition in going from monomer to dimer. $\Delta E = E(^1(d_{z^2} \rightarrow p_z)) - E(^1(d\sigma^* \rightarrow p\sigma))$.

c. Crystallographically determined metal-metal separation.

d. Not known.

e. Not comparable to alkyl isocyanide complexes that are due to shift in reference point. Spectral data for $Rh(CNC_6H_5)_2(P(C_6H_5)_3)_2{}^+$ not known.

Figure 2.8. Emission spectra of $[Ir_2(TMB)_4](B(C_6H_5)_4)_2$ in 2-MeTHF/Propionitrile at 298 K and 77 K. Taken from Reference 1.

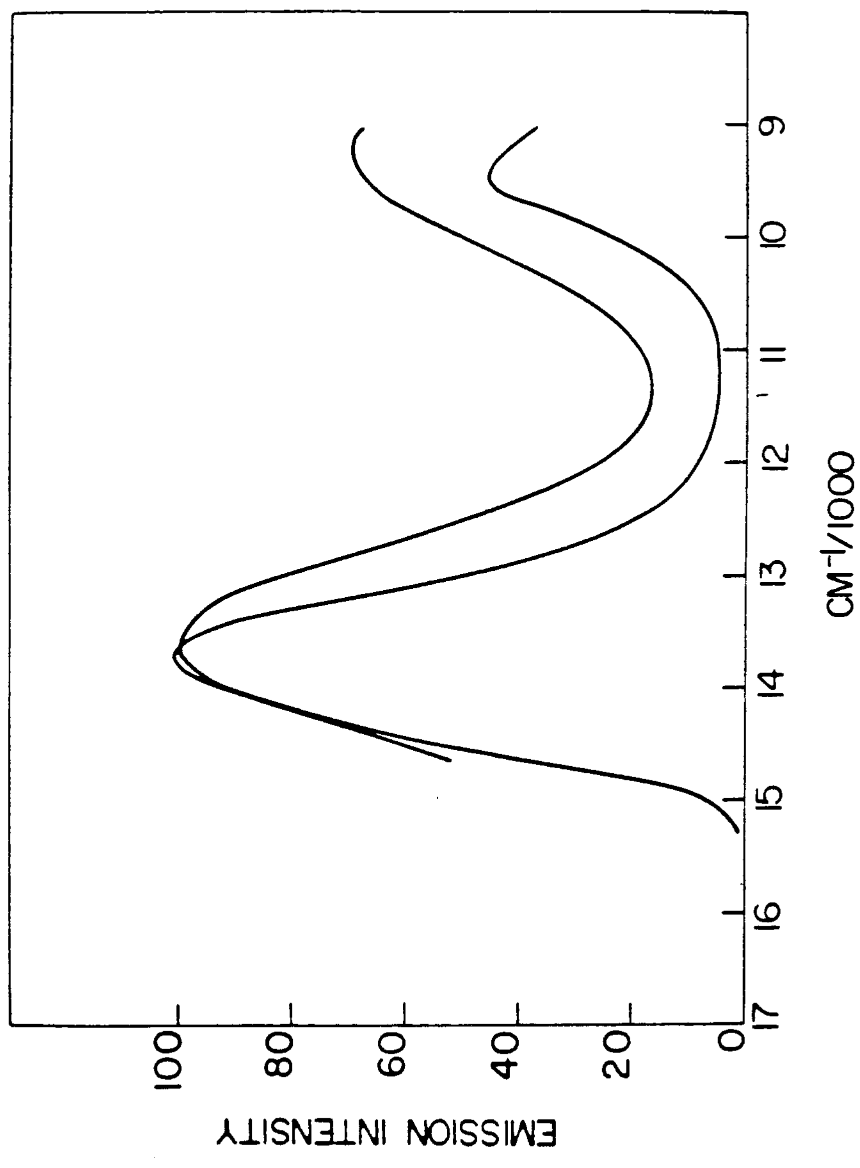
EMISSION INTENSITY
100
80
60
40
20
0
17
16
15
14
13
12
11
10
9
CM-1/1000

680 nm for the $^1A_{2u}$ state, 1.3 eV (30 kcal/mol) and 1.8 eV (42 kcal/mol) above the $^1A_{1g}$ ground state, respectively.

Table 2.10 summarizes the photophysical data for $Ir_2(TMB)_4^{2+}$ and compares these data to the analogous Rh(I) complexes. The Stokes shifts and emission band widths are comparable for the series of complexes, indicating a similar molecular distortion that accompanies the $d\sigma^* \rightarrow p\sigma$ excitation. From the emission lifetime (τ) and quantum yield data (Φ_{em}, emission quantum yield), the radiative rate (k_r) and nonradiative rate (k_{nr}) for the $^1A_{2u}$ and $^3A_{2u}$ states can be determined (Table 2.11). The nonradiative rate can be obtained, assuming that the nonradiative processes dominate the excited state deactivation.[3,34,37,38]

$$\tau = \frac{1}{(k_r + k_{nr})} \qquad 2.1$$

$$\tau \approx \frac{1}{k_{nr}} \qquad 2.2$$

From the measured quantum yields, the radiative rates can be estimated.

$$^1\Phi_{em} = \frac{^1k_r}{(^1k_r + {}^1k_{nr})} \qquad 2.3$$

$$^3\Phi_{em} = \Phi_{isc}\frac{^3k_r}{(^3k_r + {}^3k_{nr})} \qquad 2.4$$

For $Rh_2b_4^{2+}$, the Φ_{isc} (intersystem crossing quantum yield) has been estimated to be 0.8.[39] For those systems that lack good quantum yield data, the $^3A_{2u}$ state of $Rh_2(TMB)_4^{2+}$ and $Ir_2(TMB)_4^{2+}$, the Strickler-Berg equation can be used to estimate k_r.[37]

$$k_r = 2.88\times10^{-9}(n^2)\langle\upsilon^{-3}\rangle^{-1}(g_1/g_2)\int\varepsilon d\ln\upsilon \qquad 2.5$$

n - refractive index of the medium

Table 2.10. Photophysical data for $Ir_2(TMB)_4^{2+}$, $Rh_2(TMB)_4^{2+}$, and $Rh_2b_4^{2+}$.

	λ_{max}	τ		Φ_{em}		Stokes shift	Ref.
	nm	298 K	77 K	298 K	77 K	cm^{-1}	
$Ir_2(TMB)_4^{2+}$							1
$^1A_{2u}$	735	< 2 ns		2.5×10^{-3} [a]		2400	
$^3A_{2u}$	1080	210 ± 20 ns	200 ± 10 ns	10^{-3} [b]		2900	
$Rh_2(TMB)_4^{2+}$							2, 33, 34
$^1A_{2u}$	614	820 ± 20 ps		4.6×10^{-2} [c]		3200	
$^3A_{2u}$	740	25 ± 5 ns	20.5 μs	6×10^{-4} [d]	0.51 [c]		
$Rh_2b_4^{2+}$							2, 34, 35, 36
$^1A_{2u}$	656	1.3 ns		5.6×10^{-2} [c]	0.08 [c]	2800	
$^3A_{2u}$	810	8.5 ± 5 μs	12.5 μs	0.32 [c]	0.64	2600	

a. Error in determination ± 50%.

b. Error in determination ± 100%.

c. Error in determination ± 15%.

d. Estimate, $\Phi_{em}(298\ K)/\Phi_{em}(77\ K) = \tau(298\ K)/\tau(77\ K)$. Assumes Φ_{isc} and k_r to be temperature independent.

Table 2.11. Radiative rates (k_r) and nonradiative rates (k_{nr}) for the $^1A_{2u}$ and $^3A_{2u}$ excited states of $Ir_2(TMB)_4^{2+}$, $Rh_2(TMB)_4^{2+}$, and $Rh_2b_4^{2+}$.

$^1A_{2u}$ excited state

	$^1k_{nr}$		^1k_r	
	298 K	77 K	298 K	77K
$Ir_2(TMB)_4^{2+}$	9.5×10^9		2.3×10^7 [a]	
$Rh_2(TMB)_4^{2+}$	1.2×10^9	3.7×10^8	5.6×10^7	
			4.8×10^7 [a]	
$Rh_2b_4^{2+}$	7.7×10^8	5.4×10^8	4.3×10^7	

$^3A_{2u}$ excited state

	$^3k_{nr}$		^3k_r	
	298 K	77 K	298 K	77 K
$Ir_2(TMB)_4^{2+}$	4.8×10^6	5.0×10^6	4.8×10^3 [b]	
			9×10^4 [c]	
$Rh_2(TMB)_4^{2+}$	4.0×10^7	4.9×10^4	3.0×10^4	3.1×10^4
$Rh_2b_4^{2+}$	1.2×10^5	8.0×10^4	4.7×10^4	5.1×10^4

a. Calculated with Equation 2.6.

b. From the measure $^3\Phi_{em}$.

c. Calculated with Equation 2.6, using 77 K absorption data. This assumes that k_r is temperature-independent.

$<\upsilon^{-3}>$ - mean of the cube of the reciprocal of the emission frequency

g_1, g_2 - the degeneracies of the lower and upper states

υ - the emission maximum

$$k_r \approx 5\times10^{-9}\upsilon^2\varepsilon_{max}\Delta\nu \qquad 2.6$$

ε_{max} - extinction coefficient of the absorption band

$\Delta\nu$ - absorption band width (full width at half the maximum height)

The radiative rate for the series of complexes is found to be quite constant and temperature-independent. Similar radiative rates are expected for $Rh_2b_4^{2+}$ and $Rh_2(TMB)_4^{2+}$ but is somewhat surprising for $Ir_2(TMB)_4^{2+}$. One might have expected that the increased spin-orbit coupling for the third-row transition metal would have increased the radiative rate. This increase may be offset by the decrease in emission energy, which also accompanies the change in metal.

The nonradiative rates, unlike the radiative rates, vary through the series. The $^1k_{nr}$ changes because of the varying flexibility of the ligand system and the decreased energy gap through the series. For the $^3k_{nr}$, the expected linear relationship between $\ln k_{nr}$(77 K) and the emission energy (E_{em}) is observed.[40] At room temperature, the k_{nr} for $Rh_2(TMB)_4^{2+}$ increases dramatically, while for $Ir_2(TMB)_4^{2+}$ only a slight variation is observed. This marked temperature dependence of the nonradiative rate for $Rh_2(TMB)_4^{2+}$ has been studied previously.[34,41]

The earlier study of the temperature dependence of the $^3A_{2u}$ state discussed the nonradiative rate constants for the binuclear d^8 complexes within the framework of the strong-coupling model as described by Engleman and Jortner.[34] It was thought that the $^3(d\sigma^*p\sigma)$ excited state is thermally deactivated to a dd excited state, whose equilibrium geometry is D_{2d} distorted about the metal center, and that such a state would undergo a rapid nonradiative decay to the ground state. Such D_{2d} distortions are observed for certain dd excited states of d^8 square planar complexes. The $^3B_2$ and $^3B_1$ ligand field states having the configuration $(d_{z^2})^1(d_{x^2-y^2})^1$ are states that could couple to the $^3A_{2u}$ state. Ballhausen *et al.* have suggested that a similar configuration in d^8 monomers is unstable with respect to a D_{2d} distortion, which would result in intersection with the ground-state surface and account for the effective intersystem crossing.[42] That the $^3A_{2u}$ state of $Ir_2(TMB)_4^{2+}$ does not show a temperature-dependent lifetime is support of this analysis, since the ligand field states are thermally inaccessible. A recent NMR structural study of Rh and Ir isocyanide complexes proposed that rotation about the metal-metal axis contributes substantially to the deactivation of the $^3A_{2u}$ state, the rotation coupling the $^3A_{2u}$ state to intermediate dd states.[22] Again, for $Ir_2(TMB)_4^{2+}$, such states would be higher in energy; therefore, rotation about the metal-metal axis would not deactivate the $^3A_{2u}$ state.

There has been no direct measurement of the $^1A_{2u}$ excited-state lifetime for $Ir_2(TMB)_4^{2+}$. Two estimates of the $^1A_{2u}$ lifetime of $Ir_2(TMB)_4^{2+}$ can be made. If one assumes the radiative rates for $Rh_2(TMB)_4^{2+}$ and $Ir_2(TMB)_4^{2+}$ are the same, from the ratio of the $^1\Phi_{em}$, an estimate of 40 ps ($\tau = 1/k_{nr}$) is obtained. Using the calculated radiative rate, $^1\tau$ is estimated to be 100 ps. A $^1A_{2u}$ lifetime of 70 ± 30 ps is in line with other binuclear Ir(I) complexes.[3]

The transient absorption spectrum of $Ir_2(TMB)_4^{2+}$ has been measured previously (Figure 2.9).[1] The transient has a lifetime of 185 ± 15 ns, in good agreement with the lifetime obtained by measuring the decay of the phosphorescence. The decrease in absorbance at 625 nm is due to bleaching of the ground state, with the bands at 400 and 510 nm attributed to absorptions by the $^3A_2$ state. For $Rh_2b_4^{2+}$ and $Rh_2(TMB)_4^{2+}$, these absorptions have been assigned to $d\pi \rightarrow p\sigma$ and $d\sigma \rightarrow d\sigma^*$, respectively.[36]

Figure 2.9. Transient difference spectrum for $[Ir_2(TMB)_4](B(C_6H_5)_4)_2$ in CH_3CN at 25 °C. Taken from Reference 1.

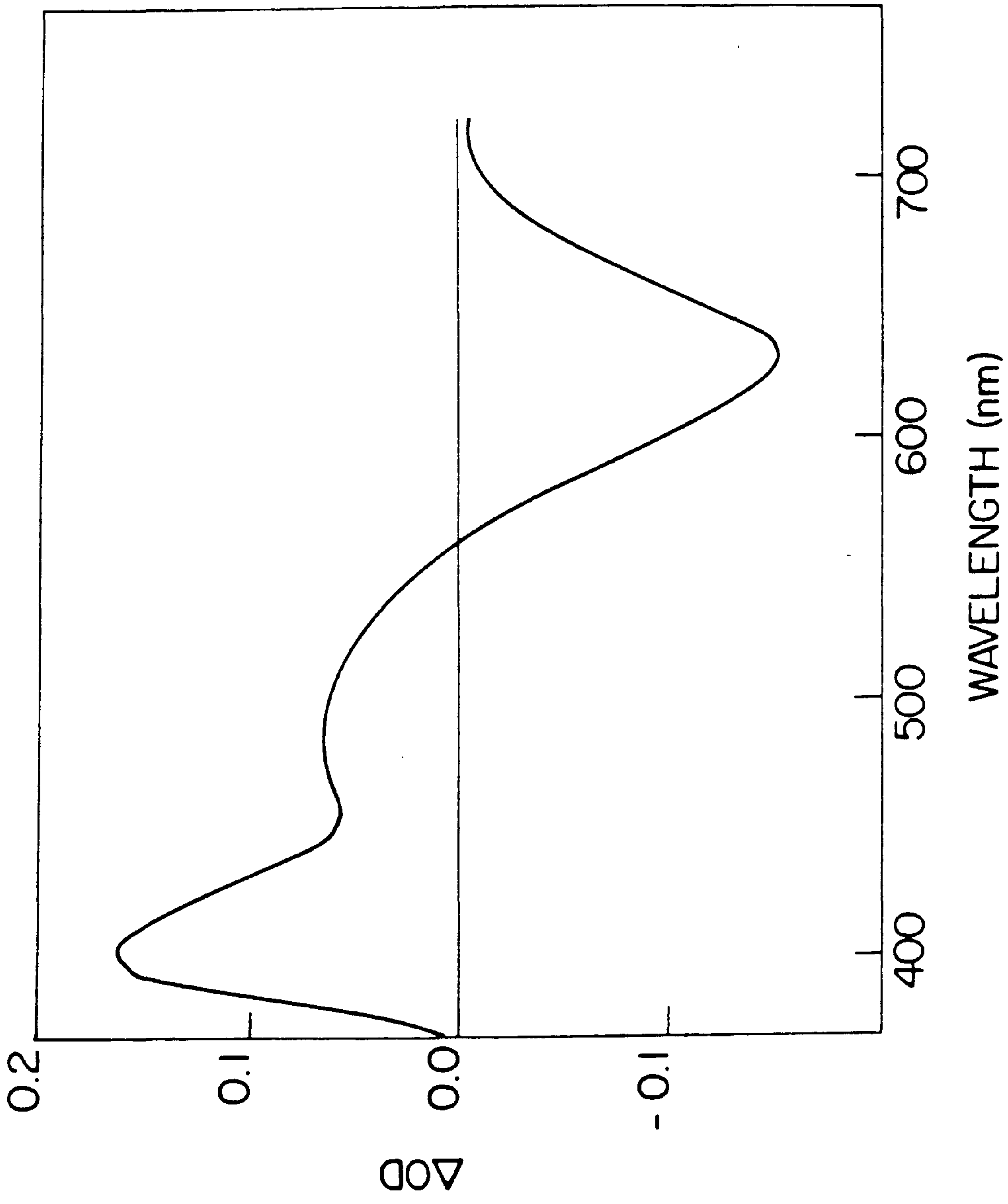

0.2
0.1
0.0
-0.1
ΔOD
400
500
600
700
WAVELENGTH (nm)

Vibrational Spectroscopy

The ground state of the binuclear d^8 complexes possesses only a weak metal-metal bonding interaction, with the $d\sigma^*p\sigma$ excited states possessing a formal metal-metal single bond. The metal-metal interactions in the ground and excited states of $Ir_2(TMB)_4^{2+}$ have been probed using resonance Raman spectroscopy. The spectra are shown in Figure 2.10. The low-frequency features for some of the spectra are poorly resolved because of Rayleigh scattering of the laser line. Other spectra show a substantial base-line slope because of emission from the fluorescent excited state. The ground state spectrum shows an intense peak at 53 cm^{-1} with a feature at 106 cm^{-1}, 2ν(Ir-Ir), which may be attributed to the first overtone of the 53 cm^{-1} vibration. The $^3A_2$ excited-state spectrum exhibits an intense peak at 132 cm^{-1}, with possibly a weak overtone at 264 cm^{-1}. These bands are assigned to the Ir-Ir stretching modes. For the excited-state spectrum, the assignment of the 132 cm^{-1} band to the excited state Ir-Ir vibration is supported by the dependence of the spectra on the per-pulse laser power. As the incident-per-pulse laser energy is varied from 2 to 5 mJ/pulse, the 132 cm^{-1} band increases in intensity as the 53 cm^{-1} intensity decreases (Figures 2.10e and 2.10f). Similar per-pulse laser-power dependence has been observed for $Rh_2b_4^{2+}$.[43] Upon excitation to the $^3A_{2u}$ excited state, there is a sixfold increase in the metal-metal restoring force (Table 2.12). This is in line with what is observed for other binuclear d^8 complexes.

It was stated earlier that the metal-metal interaction in $Ir_2(TMB)_4^{2+}$ is greater (stronger metal-metal bonding) than in the analogous Rh(I) complex. This is manifest in the vibrational data. The metal-metal restoring force for the $^1A_{1g}$ state increases by a factor of 1.9 in going from $Rh_2(TMB)_4^{2+}$ to $Ir_2(TMB)_4^{2+}$. The metal-metal bond strength in the $^3A_{2u}$ state of $Ir_2(TMB)_4^{2+}$ is also greater than in the Rh(I) dimers. The Rh-Rh bond strength in the $^3A_{2u}$ state of $Rh_2b_4^{2+}$ is estimated to be 42 kcal/mol.[14] The shorter metal-metal bond length calculated for $Ir_2(TMB)_4^{2+}$ and larger metal-metal

Figure 2.10. Resonance Raman spectra of $[Ir_2(TMB)_4](B(C_6H_5)_4)_2$: (a) CH_3CN solution, λ_{ex} = 568.2 nm; (b) CH_3CN solution, λ_{ex} = 647.1 nm; (c) K_2SO_4 pellet, λ_{ex} = 647.1 nm; (d) Time resolved, CH_3CN solution, λ_{ex} = 565 nm, 10 scans; (e) Time resolved, CH_3CN solution, λ_{ex} = 565 nm, 10 scans, 2 mJ/P; (f) Time resolved, λ_{ex} = 565 nm, 10 scans, 5 mJ/P.

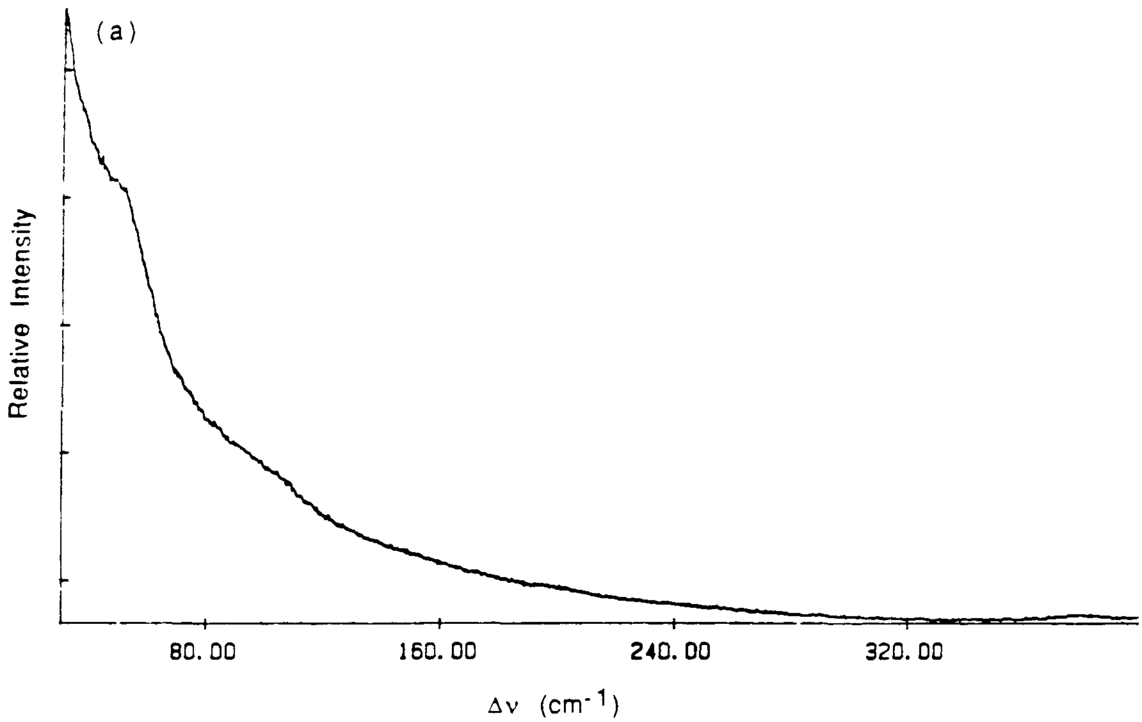
(a)
Relative Intensity
80.00
160.00
240.00
320.00
Δν (cm-1)

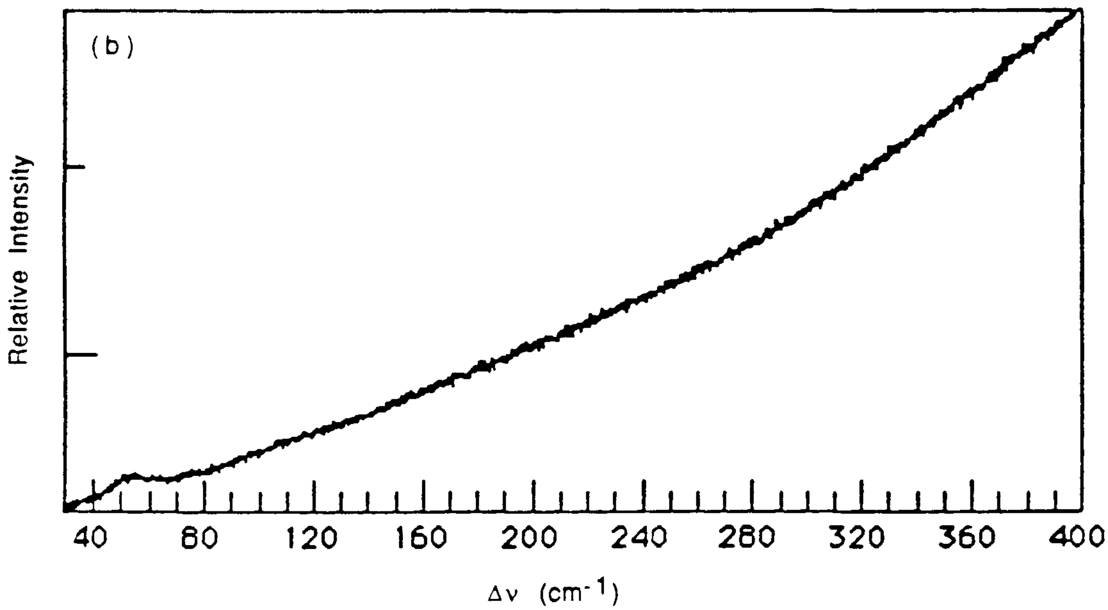
(b)
Relative Intensity
40
80
120
160
200
240
280
320
360
400
Δν (cm-1)

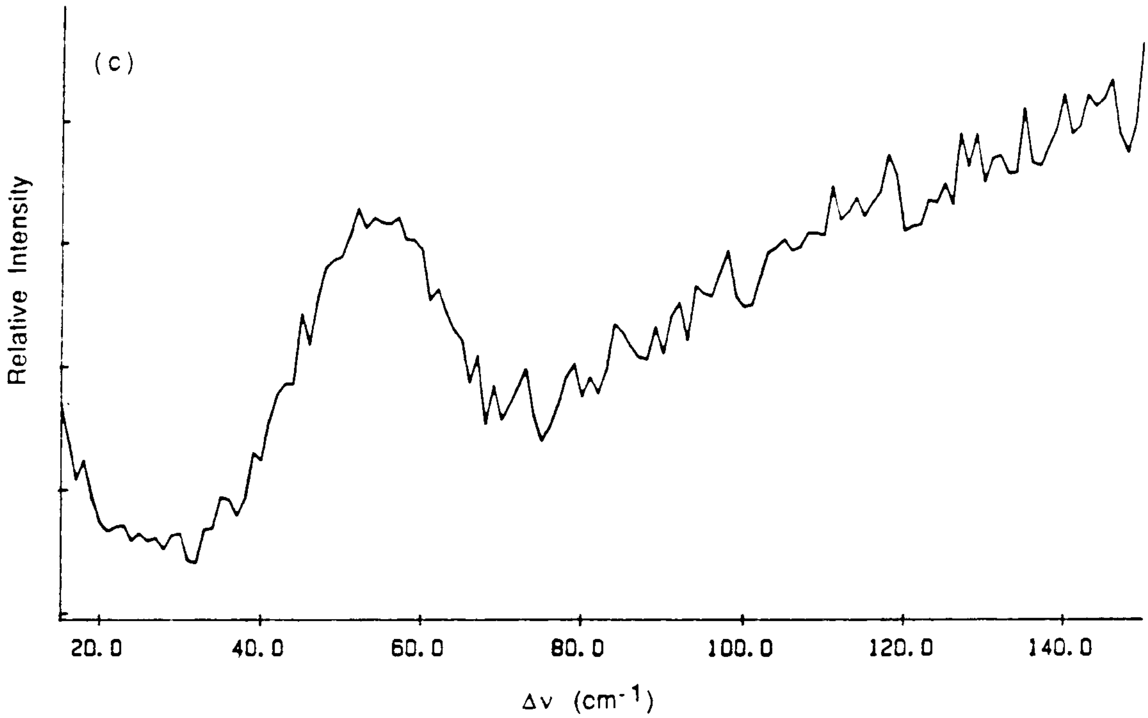
(c)
Relative Intensity
20.0
40.0
60.0
80.0
100.0
120.0
140.0
Δν (cm⁻¹)

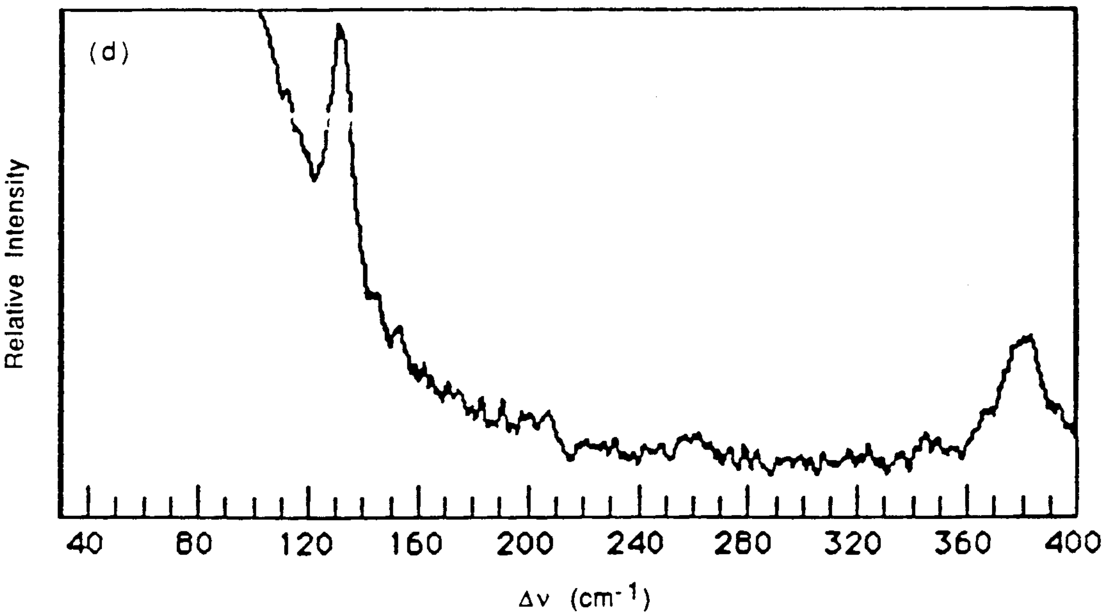
(d)
Relative Intensity
40
80
120
160
200
240
280
320
360
400
Δν (cm⁻¹)

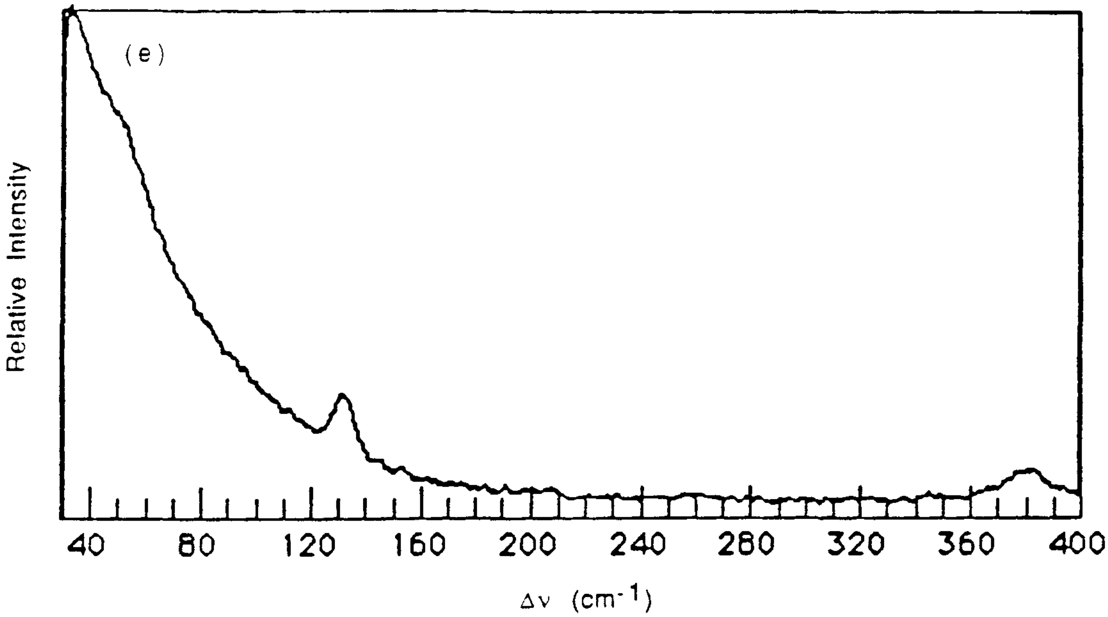
(e)
Relative Intensity
40
80
120
160
200
240
280
320
360
400
Δν (cm⁻¹)

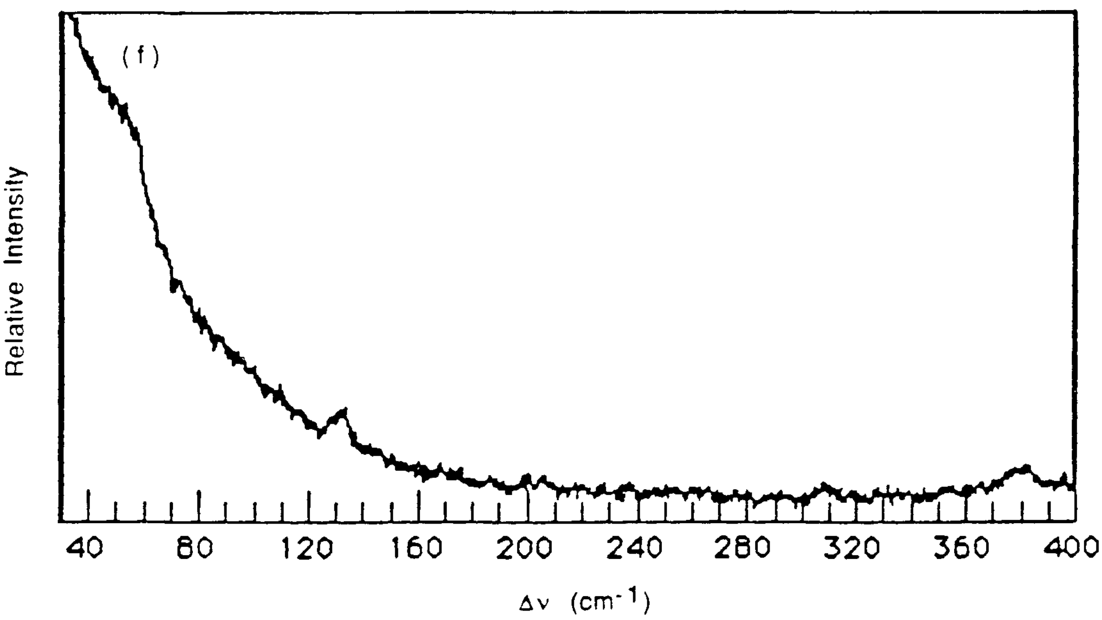
(f)
Relative Intensity
40
80
120
160
200
240
280
320
360
400
Δν (cm⁻¹)

Table 2.12. Observed metal-metal vibrational frequencies and calculated force constants. Observed metal-metal distances and calculated metal-metal distances using Woodruff's relationship.

	$^1A_{1g}$		$^3A_{2u}$		
	ν(M-M) cm^{-1}	F mdyne/Å	ν(M-M) cm^{-1}	F mdyne/Å	Ref.
$Rh_2b_4^{2+}$	79	0.19	144	0.63	43
$Rh_2(TMB)_4^{2+}$	55	0.09			44
$Ir_2(TMB)_4^{2+}$	53	0.16	132	0.99	

Metal-Metal Sepatation

	$^1A_{1g}$		$^3A_{2u}$	
	X-ray, Å	W.R, Å [a]	W.R., Å [a]	Δ, Å [b]
$Rh_2b_4^{2+}$	3.242(1)	3.17 [c]	2.96	0.28 [d]
$Rh_2(TMB)_4^{2+}$	3.262(1)	3.23		0.4
$Ir_2(TMB)_4^{2+}$	3.199(1)	3.23	2.87	0.33

a. Woodruff's relationship: Rh, $D = 1.83 + 1.45\exp(-F/2.53)$; Ir, $D = 2.01 + 1.31\exp(-F/2.36)$.[45]

b. Decrease in metal-metal separation upon excitation, $\Delta = W.R.(^1A_{1g}) - W.R.(^3A_{2u})$.

c. The large discrepency between the calculated and observed metal-metal distances is a consequence of ligand contribution to the observed vibrational frequency; using the crystallographically determined Rh-Rh distance $F_{calc} = 0.07$, $\nu_{calc} = 47$ cm^{-1}

d. Frank-Condon analysis yields $\Delta Q = 0.31$ Å.[14]

restoring force in the $^3A_{2u}$ excited state imply a stronger metal-metal interaction. While it is not necessarily the case that the increased force constant is an indication of a stronger bonding interaction, there is precedent in the literature for such a correlation within a series of analogous metal-metal bonded compounds.[46,47] Larger force constants for Ir in comparison to Rh have been observed for complexes that possess formal metal-metal single bonds.[44] The major distortion upon excitation is along the Ir-Ir coordinate; a contraction of 0.3 Å is expected.

References and Notes

1. Smith, T.P., Ph.D. Dissertation, California Institute of Technology, 1982.

2. Mann, K.R.; Thich, J.A.; Bell, R.A.; Coyle, C.L.; Gray, H.B. *Inorg. Chem.* **1980**, *19*, 2462-2468.

3. Marshall, J.L., Ph.D. Dissertation, California Institute of Technology, 1987.

4. *International Tables of X-ray Crystallography*; Kynoch Press: Birmingham, England, 1974; Vol. V, p.72.

5. Gordon, A.J.; Ford, R.A. *The Chemist's Companion*; John Wiley & Sons: New York, 1972.

6. Perrin, D.D.; Armarego, W.L.F.; Perrin, D.R. *Purification of Laboratory Chemicals*; Pergamon: Oxford, 1966.

7. Rice, S.F.; Gray, H.B. *J. Am. Chem. Soc.* **1983**, *105*, 4571-4575.

8. Nocera, D.G.; Winkler, J.R.; Yocom, K.M.; Bordignon, E.; Gray, H.B. *J. Am. Chem. Soc.* **1984**, *106*, 5145-5150.

9. Mann, K.R.; Lewis, N.S.; Williams, R.M.; Gray, H.B.; Gordon, J.G. II *Inorg. Chem.* **1978**, *17*, 828-834.

10. Goldberg, S.A.; Eisenberg, R. *Inorg. Chem.* **1976**, *15*, 58-63.

11. Churchhill, M.R.; Hutchinson, J.P. *Inorg. Chem.* **1979**, *18*, 2451-2454.

12. Ferguson, J. In *Electronic States of Inorganic Compounds: New Experimental Techniques*; Day, P., Ed.; D. Reidel: Boston, 1975; pp. 59-93.

13. Albrecht, A.C. *J. Mol. Spect.* **1961**, *6*, 84-108.

14. Rice, S.F.; Miskowski, V.M.; Gray, H.B. *Inorg. Chem.* **1988**, *27*, 4704-4708, and references therein.

15. Chapter 3.

16. Rodman, G.S.; Daws, C.A.; Mann, K.R. *Inorg. Chem.* **1988**, *27*, 3347-3353, and references therein.

17. Isci, H.; Mason, W.R. *Inorg. Chem.* **1975**, *14*, 913-918.

18. Lewis, N.S.; Mann, K.R.; Gordon, J.G. II; Gray, H.B. *J. Am. Chem. Soc.* **1976**, *98*, 7461-7463.

19. Endres, H.; Gottstein, N.; Keller, H.J.; Martin, R.; Rodemer, W.; Steiger, W. *Z. Naturforsch.* **1979**, *34B*, 827-833.

20. Yamamoto, Y.; Wakatsuki, Y.; Yamazaki, H. *Organometallics* **1983**, *2*, 1604-1607.

21. Mann, K.R.; Bell, R.A.; Gray, H.B. *Inorg. Chem.* **1979**, *18*, 2671-2673.

22. Maverick, A.W.; Smith, T.P.; Maverick, E.F.; Gray, H.B. *Inorg. Chem.* **1987**, *26*, 4336-4341.

23. Olmstead, M.M.; Balch, A.L. *J. Organomet. Chem.* **1978**, *148*, C15-C18.

24. Fukuzumi, S.; Hironaka, K.; Nishizawa, N.; Tanaka, T. *Bull. Chem. Soc. Jpn.* **1983**, *56*, 2220-2227.

25. Brady, R.; Flynn, B.R.; Geoffroy, G.L.; Gray, H.B.; Peone, J., Jr.; Vaska, L. *Inorg. Chem.* **1976**, *15*, 1485-1488.

26. Kenny, M.I.S.; Kenny, J.W. III; Crosby, G.A. *Organometallics* **1986**, *5*, 230-234.

27. Cowie, M.; Dwight, S.K. *Inorg. Chem.* **1980**, *19*, 2500-2507.

28. Mague, J.T. *Inorg. Chem.* **1969**, *8*, 1975-1981.

29. Balch, A.L. *J. Am. Chem. Soc.* **1976**, *98*, 8049-8054.

30. Yaneff, P.V.; Powell, J. *J. Organomet. Chem.* **1979**, *179*, 101-113.

31. Fordyce, W.A.; Crosby, G.A. *J. Am. Chem. Soc.* **1982**, *104*, 985-988.

32. Fox, L.S., Ph.D. Dissertation, California Institute of Technology, 1989.

33. Winkler, J.R.; Marshall, J.L.; Netzel, T.L.; Gray, H.B. *J. Am. Chem. Soc.* **1986**, *108*, 2263-2266.

34. Rice, S.F., Ph.D. Dissertation, California Institute of Technology, 1982.

35. Milder, S.J.; Goldbeck, R.A.; Kliger, D.S.; Gray, H.B. *J. Am. Chem. Soc.* **1980**, *102*, 6761-6764.

36. Milder, S.J.; Kliger, D.S.; Butler, L.G.; Gray, H.B. *J. Phys. Chem.* **1986**, *90*, 5567-5570.

37. Adamson, A.W.; Fleischauer, P.D., Eds., *Concepts of Inorganic Photochemistry*; John Wiley & Sons: New York, 1975.

38. Balzani, V.; Carassiti, V. *Photochemistry of Coordination Compounds*; Academic Press: New York, 1970.

39. Miskowski, V.M.; Nobinger, G.L.; Kliger, D.S.; Hammond, G.S.; Lewis, N.S.; Mann, K.R.; Gray, H.B. *J. Am. Chem. Soc.* **1978**, *100*, 485-488.

40. Caspar, J.V.; Meyer, T.J. *J. Phys. Chem.* **1983**, *87*, 952-957.

41. Rice, S.F.; Milder, S.J.; Gray, H.B.; Goldbeck, R.A.; Kliger, D.S. *Coord. Chem. Rev.* **1982**, *43*, 349-354.

42. Gray, H.B.; Ballhausen, C.J. *J. Am. Chem. Soc.* **1963**, *85*, 260-265.

43. Dallinger, R.F.; Miskowski, V.M.; Gray, H.B.; Woodruff, W.H. *J. Am. Chem. Soc.* **1981**, *103*, 1595-1596.

44. Miskowski, V.M.; Smith, T.P.; Loehr, T.M.; Gray, H.B. *J. Am. Chem. Soc.* **1985**, *107*, 7925-7934.

45. Woodruff's relationship is an empirical correlation of force constants and bond distances: Miskowski, V.M.; Dallinger, R.F.; Christoph, G.G.; Morris, D.E.; Spies, G.H.; Woodruff, W.H. *Inorg. Chem.* **1987**, *26*, 2127-2132.

46. Spiro, T.G. *Prog. Inorg. Chem.* **1970**, *11*, 1-51.

47. Nakamoto, K. *Infrared and Raman Spectra of Inorganic and Coordination Compounds*; John Wiley & Sons: New York, 1986.

Chapter 3

Detailed Study of the Electronic Spectrum of $Ir_2(TMB)_4^{2+}$

Introduction

The electronic spectra of face-to-face, metal-metal bonded d^8-d^8 complexes have been extensively discussed on the basis of a molecular orbital (MO) model.[1-10] In this picture, the metal-based d_{z^2} (filled) and p_z (empty) orbitals each interact strongly to produce pairs of bonding and antibonding orbitals. Configuration interaction between the empty and filled sets (which might be visualized alternatively as dative d-p bonding) provides the weak ground-state bond, while the lowest-energy singlet and triplet excited states, derived from the $d\sigma^* \rightarrow p\sigma$ one-electron transition, are strongly stabilized relative to their respective monomer $d_{z^2} \rightarrow p_z$ states.

While this picture accounts nicely for several important aspects of the metal-metal interaction, it has also been noted that several monomer $d \rightarrow p$ excitations are only slightly perturbed in the d^8-d^8 complexes.[1] This observation and the rather long metal-metal bonds (3.1 - 3.3 Å)[11,12] suggest that d^8-d^8 species should be examined from a valence bond (VB) "weak-coupling" viewpoint.

In addition to beginning such an examination, and to complement earlier investigations of rhodium complexes, ($Rh_2(TMB)_4^{2+}$; $Rh_2b_4^{2+}$, b = 1,3-diisocyanopropane), we undertook a detailed study of the electronic spectrum of $Ir_2(TMB)_4^{2+}$ (TMB = 2,5-diisocyano-2,5-dimethylhexane). A change in the metal from rhodium to iridium should perturb the electronic structure, thereby altering the characteristic d^8-d^8 electronic spectrum and allowing us to test key aspects of the MO and VB models. Electronic absorption and magnetic circular dichroism (MCD) spectra of $Rh_2(TMB)_4^{2+}$ and $Ir_2(TMB)_4^{2+}$ are reported along with polarized single-crystal absorption spectra of $[Ir_2(TMB)_4](B(C_6H_5)_4)_2 \cdot CH_3C_6H_5$.

Experimental

Synthesis

All synthetic procedures were carried out with standard Schlenk techniques unless otherwise specified. Tetrahydrofuran (THF) was distilled from CaH_2 prior to use. All other solvents were from freshly opened bottles with no further purification, except as noted. All solvents were Schlenk-degassed prior to use. Standard procedures were used to prepare 2,5-diisocyano-2,5-dimethylhexane (TMB),[11] $[Ir_2(TMB)_4](B(C_6H_5)_4)_2$,[13] $[Ir(COD)Cl]_2$ (COD = 1,5-cyclooctadiene),[14] $[Ir(COD)_2]BF_4$,[15] and $[Rh_2(TMB)_4](PF_6)_2$.[11] The literature preparation of the compound Ir(COD)(acac),[16] a precusor to $[Ir(COD)_2]BF_4$, was modified as noted below. All other chemicals were of reagent grade or comparable quality and were used as received. The ^1H NMR spectra were obtained on a 400-MHz JNM-GX400 FT NMR spectrometer. The IR spectra were taken on a Beckman IR 4240.

$[Ir_2(TMB)_4](PF_6)_2$

A filtered methanol solution of $NaPF_6$ was added to a stirred methanol solution of $[Ir_2(TMB)_4]Cl_2$ (prepared by the method of Reference 13). Immediate precipitation of a blue powder occurred. The solution was filtered and the blue material recrystallized by slow evaporation of a toluene/acetonitrile solution. Electronic absorption spectra of this compound were identical with that of the $B(C_6H_5)_4^-$ salt except for the absence of absorption that was due to the $B(C_6H_5)_4^-$ anion in the UV region.

Ir(COD)(acac)

A THF solution of Tl(acac) (acac = acetylacetone) was added with stirring to a THF solution of $[Ir(COD)Cl]_2$. Formation of a white precipitate, TlCl, occurred immediately. The solution was stirred for approximately 1 h to ensure complete reaction. THF was removed under vacuum, and pentane was added. The solution was filtered through a Celite plug to yield a clear, bright-yellow filtrate. The pentane was removed under vacuum to yield a bright-yellow crystalline material. The material was further purified by sublimation at 70-80 °C onto a water-cooled cold finger condenser (0 °C) at 10^{-5} to 10^{-6} torr. The final material was a bright-yellow powder. Calculated for Ir(COD)(acac): C, 39.09; H, 4.79. Found: C, 38.3; H, 4.6. NMR: δ($CDCl_3$, 20 °C); 1.60 (quartet, CH_2, 4H), 1.98 (singlet, CH_3, 6H), 2.23 (multiplet, CH_2, 4H), 3.93 (multiplet, CH=CH, 4H), 5.49 (singlet, CH, 1H). This preparative method appeared to yield a product that was less contaminated with chloride impurities than the literature preparation.

[Ir(CN-t-butyl)$_4$]BF$_4$

To a clear yellow CH_3CN solution of $[Ir(COD)_2]BF_4$ was added, via syringe, a large excess of *t*-butyl isocyanide (CN-*t*-butyl). A rapid color change from yellow to orange was observed. The solution was stirred for approximately 1 h. The solvent and volatiles were then removed under high vacuum, yielding an extremely air-sensitive bright-orange solid.

Acetonitrile in this preparation was distilled twice from CaH_2, degassed with a minimum of 5 freeze-pump-thaw cycles, and stored under vacuum over activated alumina. The *t*-butyl isocyanide was thoroughly degassed by 5 freeze-pump-thaw cycles. The reaction was done in a Vacuum Atmospheres inert atmosphere box to ensure oxygen exclusion. Earlier attempts to prepare the desired compound using standard Schlenk techniques yielded materials that appeared to be partially oxidized according to UV-Vis spectroscopic criteria. Attempts to prepare Ir(CN-*t*-butyl)$_4^+$ directly from $[Ir(COD)Cl]_2$ yielded material that did not give reproducible spectra. We infer some partial oxidation of the material enhanced by the presence of chloride ion. NMR: δ(CD_3CN, 20 °C); 1.49 (singlet, CH_3). IR: (Nujol mull, NaCl plates) 2190 cm^{-1} (ν(NC), vs).

X-ray Data Collection and Reduction for $[Ir_2(TMB)_4](B(C_6H_5)_4)_2 \cdot CH_3C_6H_5$

Crystal data are given in Table 3.1. The thin-flat plate crystal was of a form suited for spectroscopic measurements, but ill-suited for x-ray diffraction. It was glued on a glass fiber with the *c* axis approximately parallel to the fiber. The *b* axis is perpendicular to the plate. The crystal was much larger than the collimator; it was centered on a Nonius CAD-4 diffractometer equipped with graphite-monochromated MoKα radiation. Unit cell dimensions were obtained from the setting angles of 14 reflections with $8.4° < 2\theta < 10.1°$; the long *b* axis caused difficulties in indexing the reflections. A data set of 1654 reflections in $\pm$h,k,l out to 9° in 2θ was collected in a θ–2θ scan at 8° per min, and then a second set of 148 data with h and k = 0 or 1 was collected with an ω scan. The θ–2θ data near the *b* axis were deleted and the two data sets merged. The data were corrected for absorption, and Lorentz and polarization factors were applied. The four independent iridium atoms were located from the Patterson map and their positions refined with 6 cycles of least squares (Table 3.2). A subsequent Fourier map did not have sufficient resolution to locate the atoms of the TMB ligands, so refinement was terminated.

Calculations were done with programs of the CRYM Crystallographic Computing System and ORTEP. Scattering factors and corrections for anomalous scattering were taken from a standard reference.[17] The function minimized in least squares was $\Sigma w(F_o^2 - F_c^2)^2$, where $w = 1/\sigma^2(F_o^2)$. Variances of the individual reflections were assigned based on counting statistics plus an additional term, $(0.14)I^2$. Variances of the merged reflections were determined by standard propagation of error plus an additional term, $0.14 < I^2$. The absorption correction was done by Gaussian integration over an 8x8x8 grid. Transmission factors varied from 0.151 to 0.945.

Table 3.1. Crystal and Intensity Collection Data.

Formula: $Ir_2N_8C_{94}B_2H_{112}$	Formula Weight: 1772.03
Crystal Color: Green	Habit: flat plate
a = 17.678(8) Å	α = 90°
b = 55.03(4) Å	β = 110.54(8)°
c = 18.01(3) Å	γ = 90°
v =16408(8) $Å^3$	z = 8
d_{calc} = 1.435(1) g cm^{-3}	
λ = 0.71073 Å	T: room
Graphite monochromator	
Space group: $P2_1/c$	Absences: h0l, l = 2n+1; 0k0, k = 2n+1
Crystal size: 1.37 X 0.60 X 0.016 mm	μ = 34.88 cm^{-1}
CAD-4 Diffractometer	θ-2θ scan, ω scan
2θ range: 0-18°	Octants collected: ±h,k,l
Number of reflections measured: 1802	
Number of independent reflections: 1505	
Number with $F_0^2 > 0$: 1381	
Number with $F_0^2 > 3\sigma(F_0^2)$: 1052	
Goodness-of-fit for merging data: 1.51	

Table 3.2. Coordinates of the Iridium Atoms.

Atom	x	y	z
Ir1	0.4155(16)	0.1059(5)	0.0742(16)
Ir2	0.4828(15)	0.1168(5)	0.2580(16)
Ir3	0.9180(15)	0.1293(5)	0.5440(15)
Ir4	0.9659(15)	0.1447(5)	0.7277(16)

Spectroscopic Measurements

All solvents were dried and degassed by standard methods.[18,19] Absorption spectra presented in Figures 3.2 and 3.6-3.9 were recorded with a Cary 17 spectrophotometer. Absorption and MCD spectra presented in Figures 3.4 and 3.5 were determined simultaneously and synchronously along the same light path by means of a computer-controlled spectrometer described previously.[20] A field strength of 7.0 T was provided by a superconducting magnet system (Oxford instruments SM2-7, fitted with a bore tube held at room temperature). The $\Delta\varepsilon_M$ values are presented in units of M^{-1} cm^{-1} T^{-1}, where T is the magnetic field strength in Tesla units. All spectra were corrected for solvent blank. Single-crystal polarized absorption measurements employed dual Glan-Thompson, air-spaced calcite polarizers. Low-temperature absorption experiments were performed with two temperature-control systems: a quartz optical dewar of local design (77 K measurements); or a CTI-Cryogenics model 70 Cryodyne Cryocooler.

Propionitrile/2-methyl-THF (1:2 volume ratio) solutions for 77 K glassy matrix experiments were prepared on a high-vacuum line in an evacuable 1 cm pathlength quartz cuvette attached to a high-vacuum Teflon stopcock.

Absorption spectra at ~20 K were recorded of single crystals mounted on quartz flats. Crystal orientation was established with a polarizing microscope; the crystals transmitted light yellow-green and dark-blue light for polarization parallel to their two extinction directions determined between crossed polarizers. The former extinction was found to correspond to $\|a$ of the (010) crystal face. The extinctions were very sharp with white light, and are therefore inferred to be wavelength-independent in the visible region. The crystals were carefully masked with heat-conducting grease (fine copper powder suspended in vacuum grease) in order to provide good thermal contact with the cold station of the cryostat. The thickness of the $[Ir_2(TMB)_4](B(C_6H_5)_4)_2$ crystal whose spectra are given in Figures 3.7 and 3.8 was determined with a micrometer to be

21 μm. The thickness of the crystal whose spectra are shown in Figure 3.9 was not determined.

Results and Discussion

Crystal Structure of $[Ir_2(TMB)_4](B(C_6H_5)_2)_2 \cdot CH_3C_6H_5$

In the course of our studies, we required thin single crystals for spectroscopic purposes. The crystal structure of $[Ir_2(TMB)_4](B(C_6H_5)_4)_2 \cdot 2(CH_3CN)$, which had been determined previously,[12] revealed a cation orientation amenable to polarized spectroscopy, but crystals obtained from CH_3CN solution were chunky blue blocks, far too thick for spectroscopy. Attempts to grow thin crystals eventually yielded clusters of thin blue-green plates[21] by slow evaporation of toluene-acetonitrile solutions, from which high-quality spectroscopic data were obtained. X-ray examination of these crystals showed them not to be isomorphous with those of the structurally characterized material. NMR spectra showed that these crystals contained toluene ($n \approx 1$) instead of the acetonitrile of crystallization that was found in the previously characterized phase.[12,22]

The structure of this phase was partially determined, as described in the experimental section. The well-developed crystal face was (010); in Figure 3.1 we show a (010) view of the Ir-Ir units of the structure. The Ir_2 bond distances of the two independent Ir_2 units in this structure (3.16(4) and 3.23(4) Å) are, within their large esd's, equivalent to those found in the earlier study, 3.199(1) Å.[12] The Ir_2 units are all aligned nearly perpendicular to the *a* axis, which corresponds to an optical extinction, and lie very nearly in the (010) plane. Thus, our single-crystal polarized spectra should approximate molecular z and x,y spectra for the $\perp a$ and $\| a$ polarizations, respectively. It should be noted that for a monoclinic crystal face that does not contain the *b* axis, extinctions are not required to be parallel to a crystallographic axis, nor are they required to be wavelength-independent. However, both properties were found (within experimental error).

Figure 3.1. Projection of Ir-Ir units onto the (010) plane. Ir position indicated by o. The two metal atoms of a dimer unit are connected by a solid line.

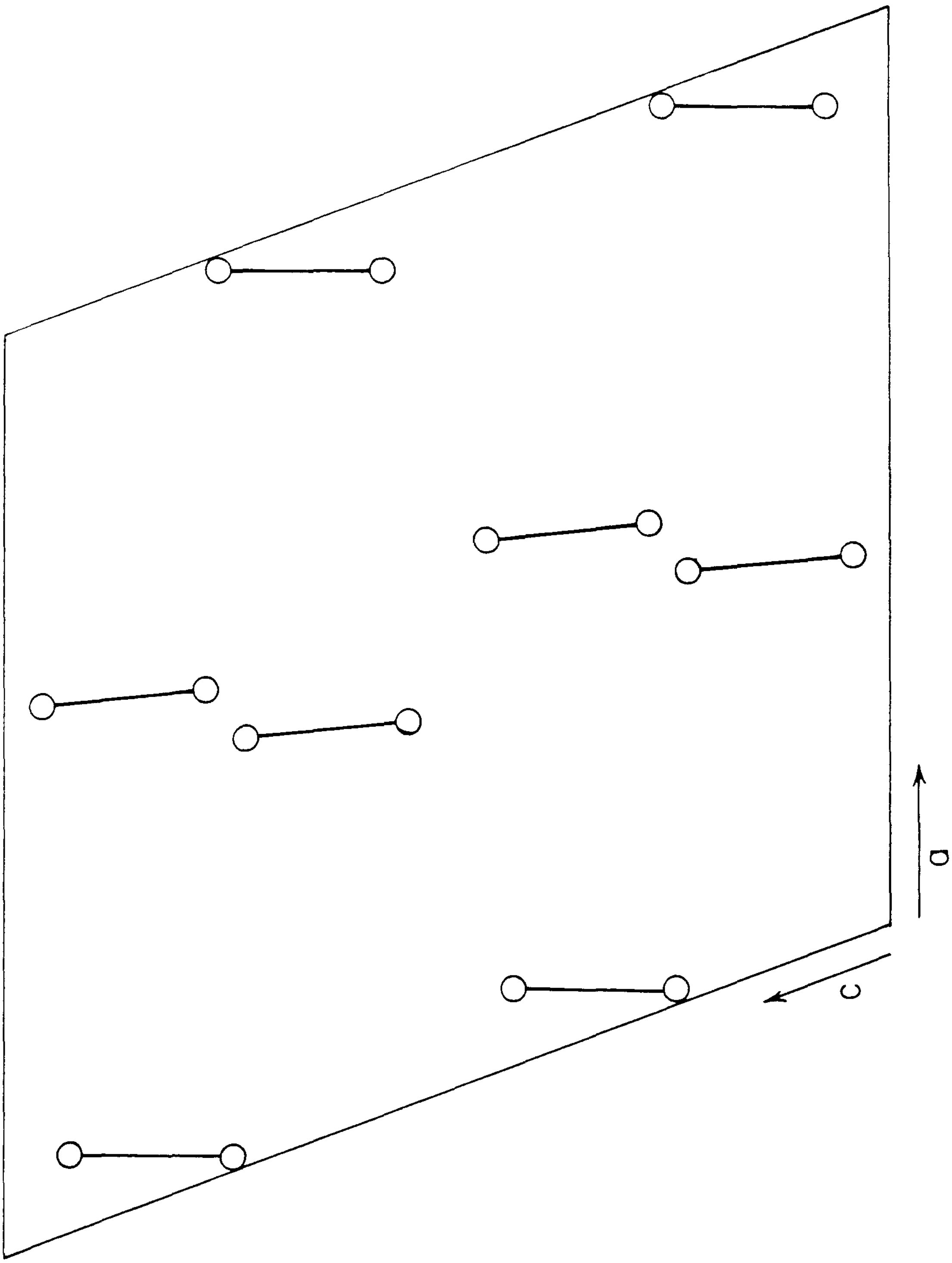
a
c

Electronic Spectrum of $Ir(CN\text{-}t\text{-}butyl)_4^+$

For comparison to binuclear Ir(I) complexes, it is important to have a reliable monomer electronic absorption spectrum. This apparently simple task proved to be difficult. We eventually obtained reproducible spectra for $Ir(CN\text{-}t\text{-}butyl)_4^+$, when a synthetic route (see the experimental section) was employed that rigorously excluded both halide and oxygen. The isolated BF_4^- salt is remarkably air-sensitive, instantaneously changing color from orange to blue-green upon exposure to trace contamination of air.

The probable explanation of this color change is the formation of partially oxidized oligomers, analogous to well-characterized rhodium species such as $Rh_4b_8^{6+}$, which have similar colors.[23,26]

Well-characterized Rh(I) isocyanide oligomeric systems, which are relatively air-insensitive, hence easier to handle, are thermally labile (because of very weak ground-state Rh-Rh bonding) but not photosensitive, since the excited states are strongly bound.[1,30,31] The similar spectroscopic properties of binuclear Rh(I) and Ir(I) isocyanide complexes that are documented here and elsewhere suggest that their thermal and photochemical properties would not be very different. In contrast, partially oxidized Rh(I) isocyanide oligomers are thermally much less labile (the Rh-Rh ground state is strongly bound) but undergo dissociative photochemistry.[23] Moreover, net photoreduction has been noted for Rh isocyanide systems.[13] With regard to authentic Ir(I) oligomers, we note that samples of $[Ir(CN\text{-}t\text{-}butyl)_4]BF_4$ during dissolution in CH_3CN show flashes of blue-green color near the dissolving crystals, the color disappearing with diffusion into the bulk solvent. This may represent Ir(I) oligomerization in very concentrated solutions,[27] as previously reported for Rh(I) isocyanides, including the *t*-butyl isocyanide complex.[31] We have not attempted to quantify this observation, however, because of the extreme difficulties involved in working with this compound.

The electronic absorption spectrum found for $[Ir(CN\text{-}t\text{-butyl})_4]BF_4$ in dilute solution is shown in Figure 3.2; data are summarized in Table 3.3. The observed bands are assigned to $d_{z^2} \rightarrow p_z$, $d_{xz,yz} \rightarrow p_z$, and $d_{xy} \rightarrow p_z$ excitations, as indicated by the extensive work of Mason and coworkers.[28,32,33] The features at 291 and 343 nm could each be assigned either to pure electronic transitions (Table 3.3) or to vibronic sidebands involving one quantum of ν(NC) built upon lower energy transitions. For the 291 nm feature, the vibronic assignment is excluded because the intensity is much too high relative to that seen for authentic ν(NC) sidebands in the present work (*vide infra*) as well as in a previous investigation.[1] The interpretation of the 343 nm feature is, however, ambiguous.

Our results are consistent with the conventional MO scheme for square-planar d^8 complexes containing π-backbonding ligands.[26,32-34] The filled d level ordering is $d_{z^2} > d_{xz,yz} > d_{xy}$, and no electronic transitions involving the empty $d_{x^2-y^2}$ orbital have been located experimentally. As usual for such complexes, the last point only suggests the probable energetic ordering $d_{x^2-y^2} > p_z$ (i.e., that the LUMO is p_z), since d-d transitions to $d_{x^2-y^2}$ are dipole-forbidden, and could be obscured by the intense (allowed) $d \rightarrow p$ absorptions.

Valence-Bond Model

Consider a dimer with no one-electron coupling of the two centers. For clarity, we consider only singlet states of a D_{4h} symmetry dimer. Low-lying molecular states involving $d_{z^2} \rightarrow p_z$ and $d_{xz,yz} \rightarrow p_z$ excitations are shown in Figure 3.3.

The single-center excitations are Davydov-coupled[35] in symmetric and antisymmetric fashion to yield, for the $^1A_{2u}$ ($d_{z^2} \rightarrow p_z$) monomer excited state, for example, $^1A_{1g}$ and $^1A_{2u}$ dimer states. The MO picture gives a total of four excited states correlating to $d_{z^2} \rightarrow p_z$ excitations. In the VB picture, the remaining two excited states are a $^1A_{1g}$, $^1A_{2u}$ pair corresponding to excitation of a d_{z^2} electron on one center into a p_z

Figure 3.2. Electronic absorption spectrum of $[Ir(CN\text{-}t\text{-}butyl)_4]BF_4$ in CH_3CN at 25 °C.

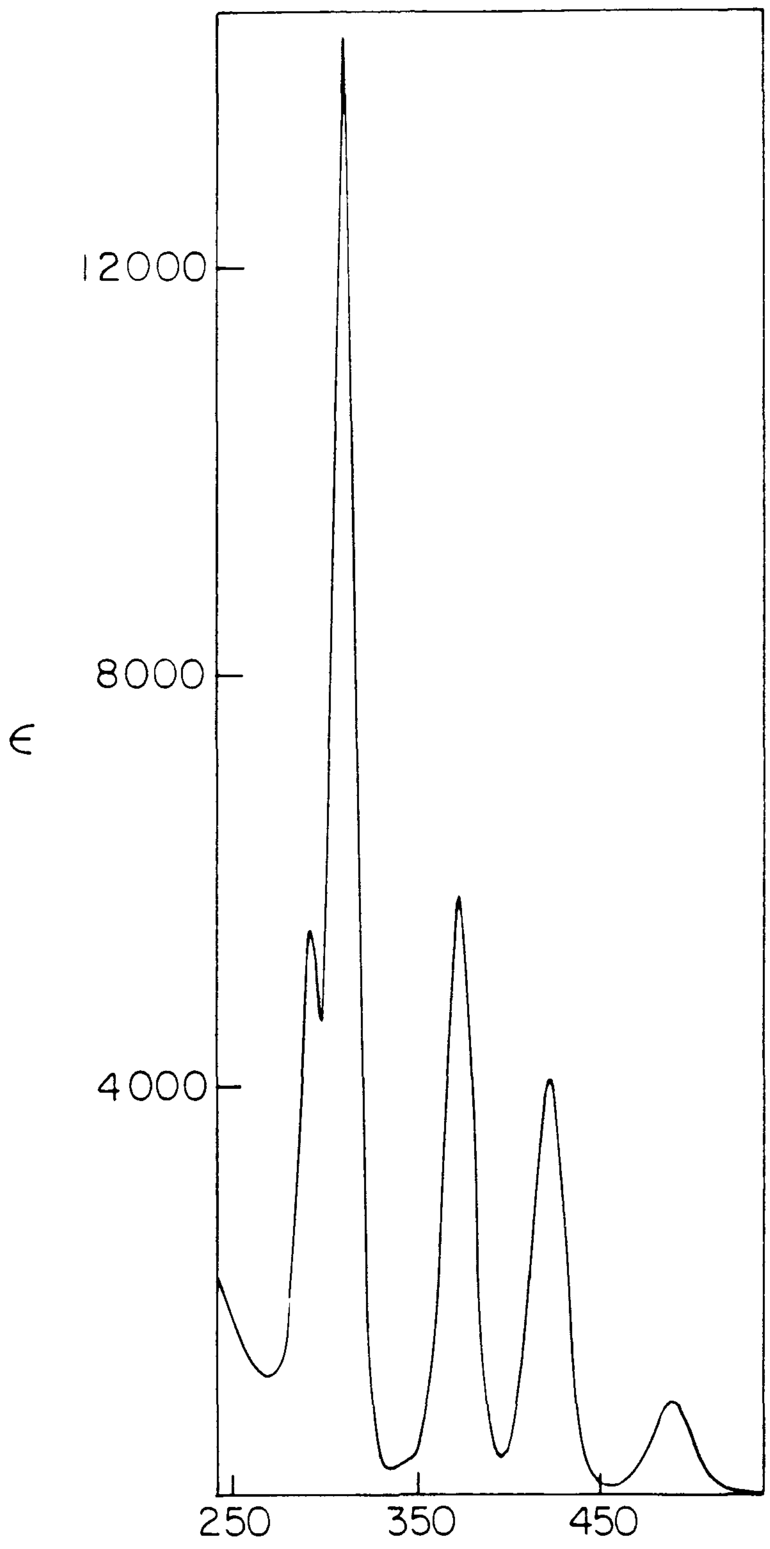
12000
8000
4000
ϵ
250
350
450
λ (nm)

Table 3.3. Absorption spectral data for $[Ir(CN\text{-}t\text{-}butyl)_4]BF_4$ measured in CH_3CN at 25 °C.

$^1A_{1g} \rightarrow$	λ_{max}, nm (ε, $M^{-1}cm^{-1}$)	fwhm, cm^{-1} [a]
$E_u(^3A_{2u})$, $d_{z^2} \rightarrow p_z$	489 (870)	1130
$A_{2u}(^1A_{2u})$, $d_{z^2} \rightarrow p_z$	423 (4100)	1120
$E_u(^3E_u)$, $d_{xz,yz} \rightarrow p_z$	373 (5900)	1300
$E_u(^1E_u)$, $d_{xz,yz} \rightarrow p_z$	308 (14500)	1360
$E_u(^3B_{1u})$, $d_{xy} \rightarrow p_z$	291 (5500)	b

a. fwhm - full width at half the maximum height.

b. Not measured.

Figure 3.3. Qualitative VB state diagram for weak d/p interaction of two Rh(I) or Ir(I) monomers. See text. Note that for the strong interaction case, state energies are implicitly for the equilibrium bond distance of each individual state.

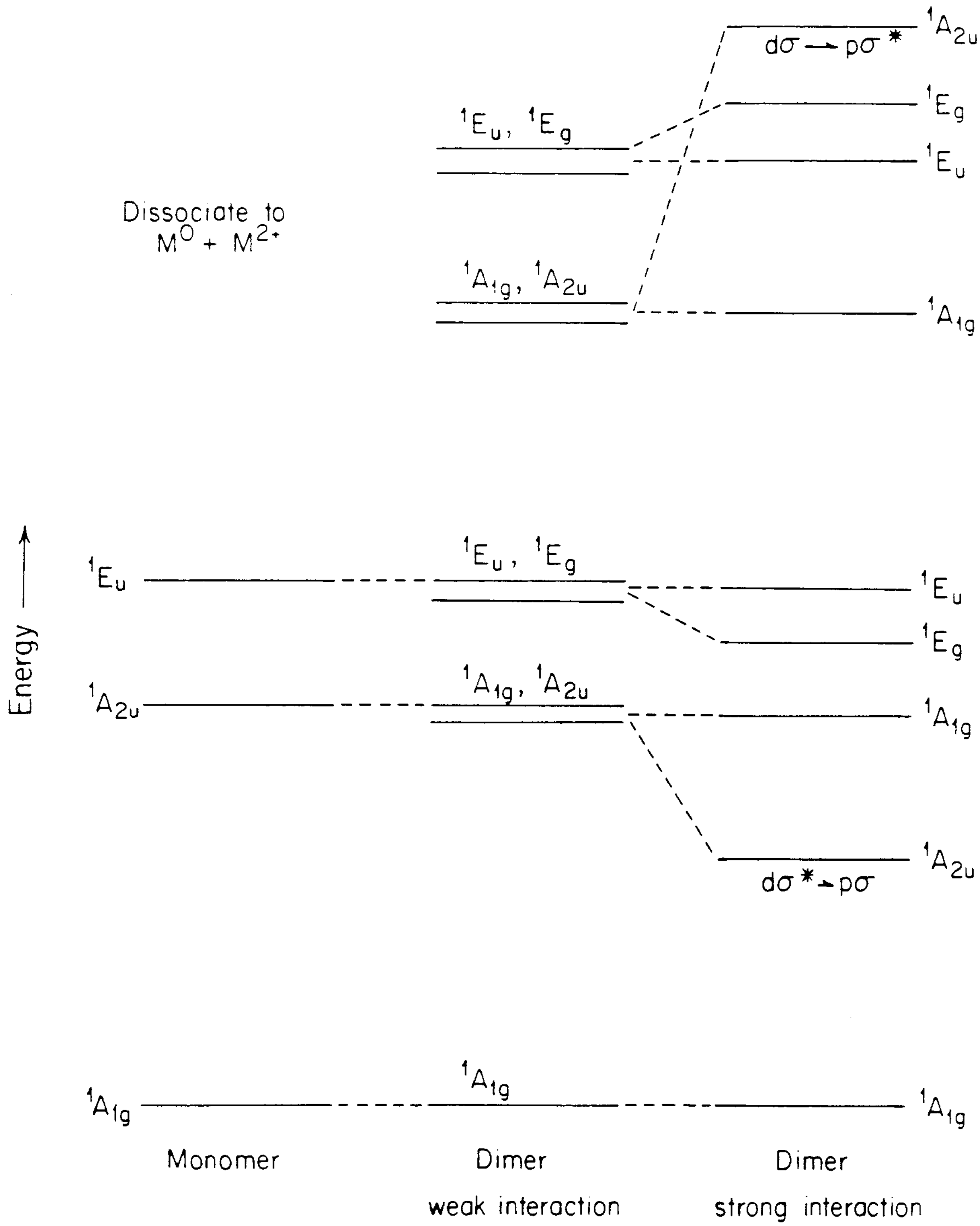

1A2u
dσ → pσ*
1Eg
1Eu, 1Eg
1Eu
Dissociate to
M0 + M2+
1A1g, 1A2u
1A1g
Energy
1Eu
1Eu, 1Eg
1Eu
1Eg
1A2u
1A1g, 1A2u
1A1g
1A2u
dσ* → pσ
1A1g
1A1g
1A1g
Monomer
Dimer
weak interaction
Dimer
strong interaction

orbital on the other center; thus, they are "ionic" states that must dissociate to M^{2+} plus M^0. As such, they must lie at much higher energy, *even for no metal-metal bonding.*

The energy of the metal-to-metal charge transfer states are dependent on the ease of ionization of the metal center and the ability of a single metal center to accommodate an additional electron. Such a transition should scale roughly as IP_d-EA_p. An estimate of the molecular IP_d-EA_p can be obtained by considering the atomic IP_d-EA_p. The atomic IP and EA calculated for Rh and Ir are listed in Table 3.4.[36]

$$(d_{z^2})^2 p_z^0 + (d_{z^2})^2 p_z^0 \rightarrow (d_{z^2})^2 p_z^1 + (d_{z^2})^1 p_z^0 \qquad 3.1$$

$$M^+ + M^+ \rightarrow M^{2+} + M^0 \qquad 3.2$$

The transition energies, as defined above, are listed in Table 3.4, corrected for the 1/R repulsion terms. The transition energies, as they stand, are not comparable to the molecular system, in that the molecular stabilization of the atomic charge transfer state (via delocalization of charge onto the ligands, in a simplistic viewpoint) has not been accounted for. An estimate of the molecular stabilization accompanying the metal-to-metal charge transfer can be obtained from earlier work on $Re_2Cl_8^{2-}$, a quadruply bonded ($\sigma^2\pi^4\delta^2$) metal dimer.[37] Similar to the binuclear d^8 complexes, the δ interaction is best viewed in the VB "weak-coupling" limit. Thus, the $^1(\delta \rightarrow \delta^*)$ transition is best described as a metal-to-metal charge-transfer (MMCT) transition. It can be shown that the energy separation of the $^3(\delta\delta^*)$ state, the lowest energy covalent excited state, and the $^1(\delta\delta^*)$ state, the lowest energy charge-transfer excited state, is 2K:[38]

$$K = 1/2[(aa|aa) - (aa|bb)], \qquad 3.3$$

Table 3.4. Metal-to-metal charge transfer transition energies.

	Calculated Atomic State Energies (hartrees)		
	s^0d^8	p^1d^8	s^0d^7
Ir	-103.51082	-103.54144	-102.83667
Rh	-108.36242	-108.47397	-107.73884

	IP (eV)	-EA (eV)
Ir	15.47	-3.19
Rh	16.97	-3.03

	$M^+ + M^+ \rightarrow M^{2+} + M^0$		
	IP-EA (eV)	(IP-EA) - 1/R (eV)	(IP-EA) - 1/R + MS (eV)[a]
Ir	12.8	8.3	5.7
			(45000 cm^{-1})
Rh	13.9	9.4	6.8
			(55000 cm^{-1})

a. M.S. - Molecular stabilization = 2.6 eV.

where (aa|aa) is the energy required to transfer a δ electron from metal center A to metal center B at infinite A-B distance. The (aa|bb) term is the electrostatic correction to finite R that we have already applied, as noted above. A value for the molecular stabilization of an MMCT state can be obtained by comparing the energy separation of the $^3(\delta\delta^*)$ and $^1(\delta\delta^*)$ excited states to the estimate, using atomic IP and EA values. For $Re_2Cl_8^{2-}$, the molecular stabilization of an MMCT state is 2.65 eV. This estimate is obtained using the experimentally observed $^1(\delta\delta^*)$ transition energy[39] (which is greater than, but very close to, the singlet-triplet energy separation) and the calculated energy separation using *ab initio* atomic energies.[40]

Using 2.6 eV as a rough estimate of the molecular stabilization of the charge-transfer state, an estimate of the MMCT state energy for the Ir(I) and Rh(I) complexes is obtained (Table 3.4). The transition energies are indicated to be in the UV with those of Ir lower than those of Rh. These estimates are upper limits to the transition energies. The calculated IP and EA for Ir and Rh may be in error because of correlation effects not accounted for in the calculations. However, the excitation in question does not require an increased pairing of electrons; therefore, energy differences (in particular, the predicted strong decrease in energy for Ir_2 versus Rh_2) may not have a large error associated with them. These are very crude estimates, and the crude agreement with experiment that will be evident later should be taken only to indicate that our assignments are not absurd.

The VB wave functions are equal mixtures of the two MO wavefunctions of the same symmetry. Thus, the two $^1A_{2u}$ wave functions are given by $d\sigma^*p\sigma \pm d\sigma p\sigma^*$, the plus combination corresponding to the lowest energy state. If we increase the metal-metal one-electron interaction (shorten the metal-metal distance), the two $^1A_{2u}$ states will mix in such a way as to resolve into the two MO wave functions, as indicated on the right-hand side of Figure 3.3.[41] The same thing should happen for the other d $\rightarrow$ p excited states if the metal-metal distance is decreased. However, there is much less reason for them to do so. Both the ^1E_u and $^1A_{1g}$ states are, at long distance, equal mixtures of bonding-bonding and antibonding-antibonding MO states; the $^1A_{1g}$ states, for example, are ($d\sigma^*p\sigma^* \pm d\sigma p\sigma$). Thus, bonding contributions tend to cancel out. It is difficult to predict the relative bonding-antibonding contributions, particularly since the various interactions ($d\sigma$-$d\sigma$, $d\sigma$-$p\sigma$, $p\sigma$-$p\sigma$, $d\pi$-$d\pi$, etc.) undoubtedly maximize stabilization at greatly different metal-metal distances. However, it is reasonable that much less stabilization would arise than for $^1A_{2u}$ ($d\sigma^* \rightarrow p\sigma$), and our experimental data (*vide infra*) support the idea that the ^1E_u and $^1A_{1g}$ excitations are nearly vertical. There is, moreover, an interesting comparison available in diatomic mercury, Hg_2, which in its ground state ($s\sigma^2 s\sigma^{*2}$) is an extremely weakly bound van der Waals molecule.[42-44] However, corresponding to the atomic $^1S \rightarrow {}^3P$ transition at 254 nm, Hg_2 shows two allowed transitions. One, $s\sigma^* \rightarrow p\sigma$, is to a strongly bound excited state, and is richly structured in $\nu(Hg_2)$ and red-shifted from the atomic line. The second, $(s\sigma/s\sigma^*) \rightarrow (p\pi/p\pi^*)$, is vertical, and is shifted from the atomic line by only 57 cm^{-1}. These two Hg_2 states are clearly analogous to the low-lying $^1A_{2u}$ and ^1E_u excited states of d^8-d^8 Rh_2 and Ir_2 species.

Finally, we consider the ^1E_g excited states. The VB wave functions of these states ($d\pi^*p\sigma \pm d\pi p\sigma^*$) indicate that the lowest ^1E_g should be stabilized by resolving into the antibonding-to-bonding $d\pi^*p\sigma$ wave function. However, it is unclear how much stabilization can actually be expected, since the $d\pi$ overlap will be very small except at very short metal-metal distances, which would be precluded by repulsive metal-metal and ligand-ligand interactions. We compromise in Figure 3.3 by suggesting a smaller stabilization than for $^1A_{2u}$.

The important points that emerge from this discussion are that, in contrast to a simple MO picture, a VB model readily accommodates both weakly and strongly perturbed monomer transitions, and that it identifies fully half of the dimer electronic excited states as ionic (MMCT); these ionic states should lie at considerably higher energy than the monomer excited states. Both of these points prove to be crucial to understanding the electronic spectra of d^8-d^8 complexes.

Solution Electronic Absorption and MCD Spectra

The electronic absorption and MCD spectra of $Rh_2(TMB)_4^{2+}$ are shown in Figure 3.4. The assignments have been discussed extensively elsewhere, with supporting single-crystal data,[1,11] and our present (entirely consistent) data are offered largely for comparisons with the Ir complex. The theory necessary for interpretation of the MCD spectrum has been given elsewhere.[3] In the following discussion, we will use D_{4h} symmetry labels. The symmetry of the TMB complexes is only D_4, because of significant torsion of the MC_4 units with respect to each other.[12] The effect of the lower symmetry is that D_{4h} g/u labels should be dropped. However, the only effect of the lower symmetry upon the states under consideration is that D_{4h} states of E_g symmetry become formally x,y-dipole-allowed, and these transitions are expected to be weak, since it depends upon low-symmetry-induced mixing of the D_{4h} E_u and E_g states. The low-energy feature (λ_{max} 517 nm) is assigned to the $d\sigma^* \rightarrow p\sigma$ singlet ($A_{1g}(^1A_{1g}) \rightarrow A_{2u}(^1A_{2u})$) transition. This band shows the expected -B term in the MCD spectrum.[45] The strong band centered at 314 nm is attributed to the $A_{1g}(^1A_{1g}) \rightarrow E_u(^1E_u)$ ($d\pi \rightarrow p\sigma$) excitation. This transition is to a degenerate excited state and the MCD band appears to be dominated by a +A term. A weak band (λ_{max} 340 nm) is observed to lower energy of the $E_u(^1E_u)$ band. From low-temperature, polarized single-crystal spectra, this band is deconvoluted into two features,[1] an x,y-polarized component assigned to the E_u component of the ^3E_u transition (λ_{max} 342 nm) and a z-polarized A_{2u} component (λ_{max} 335 nm). The E_u component of the ^3E_u state should have +A and +B terms associated with it and the A_{2u} state, a -B term. The two ^3E_u states appear to be resolved in the MCD spectrum. A slight $-\Delta\varepsilon$ is observed on the low-

Figure 3.4. Electronic absorption (lower curves) and MCD (upper curves) spectra of $[Rh_2(TMB)_4](PF_6)_2$ in CH_3CN at 25 °C. Note that the MCD scales in the regions 210 - 295 nm and 400 - 600 nm have been expanded fivefold; similarly, the absorptivity scale has been expanded fivefold in the 325 - 400 nm region. $\Delta\varepsilon$ has units of $(M\ cm\ T)^{-1}$.

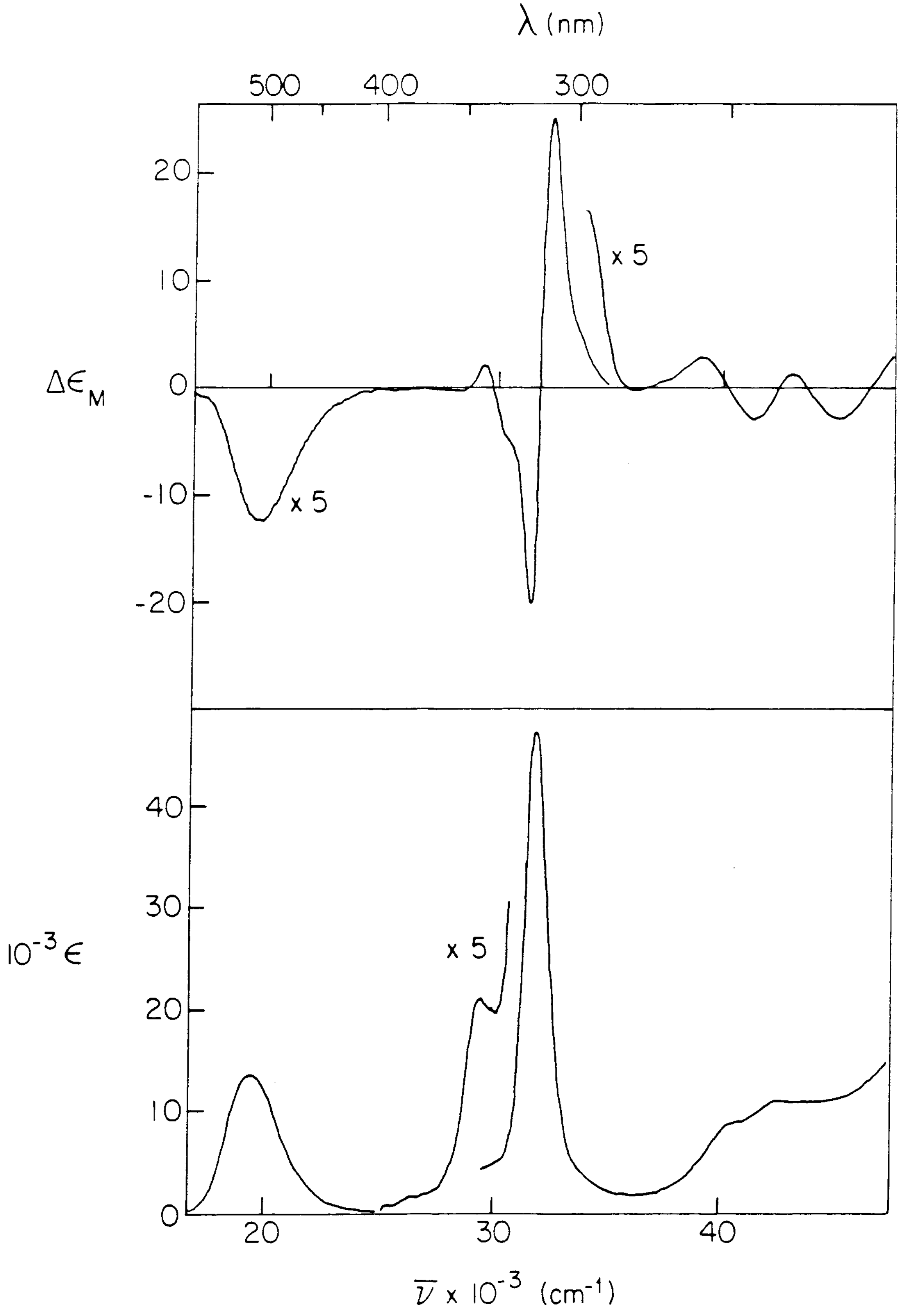
λ (nm)
500
400
300
20
10
0
-10
-20
Δε_M
x 5
x 5
40
30
20
10
0
10^-3 ε
x 5
20
30
40
ν̄ x 10^-3 (cm^-1)

energy side of the MCD band at 330 nm (~3.00 μm^{-1}), indicating a weak +A term; this transition is dominated by a +B term. Similarly, weak +A terms have been observed for analogous states of monomeric Rh(I) isocyanides.[28] To higher energy, a transition with a -B term is observed, consistent with the presence of an A_{2u} state. Several weak features are observed to higher energy of the $E_u(^1E_u)$ transition. The shoulder at 290 nm appears to have a +B term, consistent with an $E_u(^3B_{1u})$ $d_{xy} \rightarrow p\sigma$ assignment. However, this would also be consistent with the feature being a vibronic $E_u(^1E_u)$ + ν(NC) band, and the energy and low intensity of the band are reasonable for either assignment. The two bands above 250 nm (4.00 μm^{-1}) appear to possess A terms, indicating degenerate excited states, although the interpretation of the data for the higher-energy band is ambiguous. Emission polarization ratios of these bands measured for 77 K glassy solutions are also consistent with x,y-polarization, again most clearly for the lower-energy band.[46] These bands have not been reported in previous work (largely because they are obscured by anion absorption for $B(C_6H_5)_4^-$ salts), but we note here that similar features are seen in the spectra of all other binuclear Rh(I) isocyanide complexes that we have examined, whereas monomers such as Rh(CN-*t*-butyl)$_4^+$ show no resolved absorption in this region.[46] Assignments listed in Table 3.5 will be justified later.

The electronic absorption and MCD spectra of $[Ir_2(TMB)_4](PF_6)_2$ are shown in Figure 3.5. In analogy to $Rh_2(TMB)_4^{2+}$, the intense absorption centered at 625 nm (ε = 11,200 $M^{-1}cm^{-1}$) is assigned to the fully allowed $A_{1g}(^1A_{1g}) \rightarrow A_{2u}(^1A_{2u})$ ($d\sigma^* \rightarrow p\sigma$) excitation. This band shows the expected -B term in the MCD. The intense features below 300 nm, having maxima at 318 (ε = 22,000 $M^{-1}cm^{-1}$) and 372 nm (ε = 9750 $M^{-1}cm^{-1}$) are attributed to $d\pi \rightarrow p\sigma$ transitions to $E_u(^1E_u)$ and $E_u(^3E_u)$ states, respectively. The 318 nm absorption, while complicated by the overlap of the weaker bands to low and high energy, displays the expected +A term in the MCD. The $A_{1g}(^1A_{1g}) \rightarrow E_u(^3E_u)$ transition appears in the MCD as a skewed band because of the contribution of

Table 3.5. Absorption maxima for $Rh_2(TMB)_4^{2+}$ and $Ir_2(TMB)_4^{2+}$. The convention we adopt in this and the following table is that the previously adopted MO $d\sigma^* \rightarrow p\sigma$ assignments are retained for such excitations, but other transitions are labeled either as single-center excitations (e.g., $d_{xz,yz} \rightarrow p_z$) or MMCT.

$^1A_{1g} \rightarrow$	$[Rh_2(TMB)_4](PF_6)_2$ in CH_3CN (25 °C) λ_{max}, nm (ε, $M^{-1}cm^{-1}$) ν, $cm^{-1} \times 10^{-3}$	fwhm, cm^{-1} [a]	MCD ν, $cm^{-1} \times 10^{-3}$	MCD $\Delta\varepsilon_M$, $M^{-1}cm^{-1}T^{-1}$
$E_u(^3A_{2u})$, $d\sigma^* \rightarrow p\sigma$	b			
$^1A_{2u}$, $d\sigma^* \rightarrow p\sigma$	517 (13600)	2800	1.95	-2.45
	1.93			
			2.78	-0.076
$E_u(^3E_u)$, $d_{xz,yz} \rightarrow p_z$	340 (4200, sh)		2.87	0.0
	2.94		2.95	+2.38
$A_{2u}(^3E_u)$, $d_{xz,yz} \rightarrow p_z$	c		3.04 (sh)	-4.67
			3.15	-20.1
$E_u(^1E_u)$, $d_{xz,yz} \rightarrow p_z$	314 (47500)	1400	3.19	0.0
	3.18		3.24	+25.2
$E_u(^3B_{1u})$, $d_{xy} \rightarrow p_z$	290 (3500, sh)		~3.3 (sh)	~+5
and/or $E_u(^1E_u)$ + ν(CN)	3.45			
			3.91	+0.059
MMCT(?)	245 (8600, sh)		4.02	0.0
	4.08		4.14	-0.581
MMCT(?)	234 (10700, sh)		4.24	0.0
	4.27		4.30	+0.291
			4.51	-0.531

$^1A_{1g} \rightarrow$	$[Ir_2(TMB)_4](B(C_6H_5)_4)_2$ in CH_3CN (25 °C) λ_{max}, nm (ε, $M^{-1}cm^{-1}$) ν, cm^{-1} x 10^{-3}	fwhm, cm^{-1} [a]	MCD [d] ν, cm^{-1} x 10^{-3}	$\Delta\varepsilon_M$, $M^{-1}cm^{-1}T^{-1}$
$E_u(^3A_{2u})$, $d\sigma^* \rightarrow p\sigma$				
$^1A_{2u}$, $d\sigma^* \rightarrow p\sigma$	625 (11200)	2200	1.61	-1.26
	1.60			
			2.63	-0.118
$E_u(^3Eu)$, $d_{xz,yz} \rightarrow p_z$	372 (9750)	1000	2.66	0.0
	2.69		2.71	+6.25
+ ν(CN)	b			
$A_{2u}(^3E_u)$, $d_{xz,yz} \rightarrow p_z$	333 (4000, sh)		3.03	-12.0
	3.00			
			3.09 (sh)	-10.1
$E_u(^1E_u)$, $d_{xz,yz} \rightarrow p_z$	318 (22,000)	1300	3.13	0.0
	3.14		3.23	+8.98
$E_u(^3B_{1u})$, $d_{xy} \rightarrow p_z$	305 (9500, sh)		(obscured)	
	3.28			
MMCT			3.46	-1.05
$E_u(^3E_u)$, $d_{xz,yz} \rightarrow p_z$	~280 (8500, sh)		3.51	0.0
	~3.6		3.56	+0.23
			3.65	-1.34
$E_u(^1E_u)$, $d_{xz,yz} \rightarrow p_z$	268 (17000)	1500	3.69	0.0
	3.73		3.75	+3.49
			3.88	-1.94
"$d\sigma \rightarrow p\sigma^*$"	~210 (25000)		4.31	-1.20
	~4.7			

$[Ir_2(TMB)_4](B(C_6H_5)_4)_2$ in a glassy matrix of CH_3CH_2CN/2-MeTHF (77 K)

$^1A_{1g} \rightarrow$	λ_{max}, nm (ε, $M^{-1}cm^{-1}$)	fwhm, cm^{-1} [a]
$E_u(^3A_{2u})$, $d\sigma^* \rightarrow p\sigma$	520 (150)	1500
$^1A_{2u}$, $d\sigma^* \rightarrow p\sigma$	635 (25500)	1200
$E_u(^3Eu)$, $d_{xz,yz} \rightarrow p_z$	373 (17000)	650
+ ν(CN)	344 (1500, sh)	
$A_{2u}(^3E_u)$, $d_{xz,yz} \rightarrow p_z$	331 (5000)	700
$E_u(^1E_u)$, $d_{xz,yz} \rightarrow p_z$	320 (38000)	690
$E_u(^3B_{1u})$, $d_{xy} \rightarrow p_z$	304 (6000)	800
MMCT		
$E_u(^3E_u)$, $d_{xz,yz} \rightarrow p_z$	280 (11000, sh)	
$E_u(^1E_u)$, $d_{xz,yz} \rightarrow p_z$	268 (32000)	1000
"$d\sigma \rightarrow p\sigma^*$"	e	

a. fwhm = full width at half the maximum height.

b. Not observed.

c. Polarized single-crystal spectra resolve this band into two features: $E_u(^3E_u)$, λ_{max} 342 nm; $A_{2u}(^3E_u)$, λ_{max} 335 nm.

d. For PF_6^- salt.

e. Not determined because of anion absorption.

Figure 3.5. Electronic absorption (lower curve) and MCD (upper curves) spectra of $[Ir_2(TMB)_4](PF_6)_2$ in CH_3CN at 25 °C. Note that the MCD scale has been expanded fivefold in the 700 - 500 nm region. $\Delta\varepsilon$ has units of $(M\ cm\ T)^{-1}$.

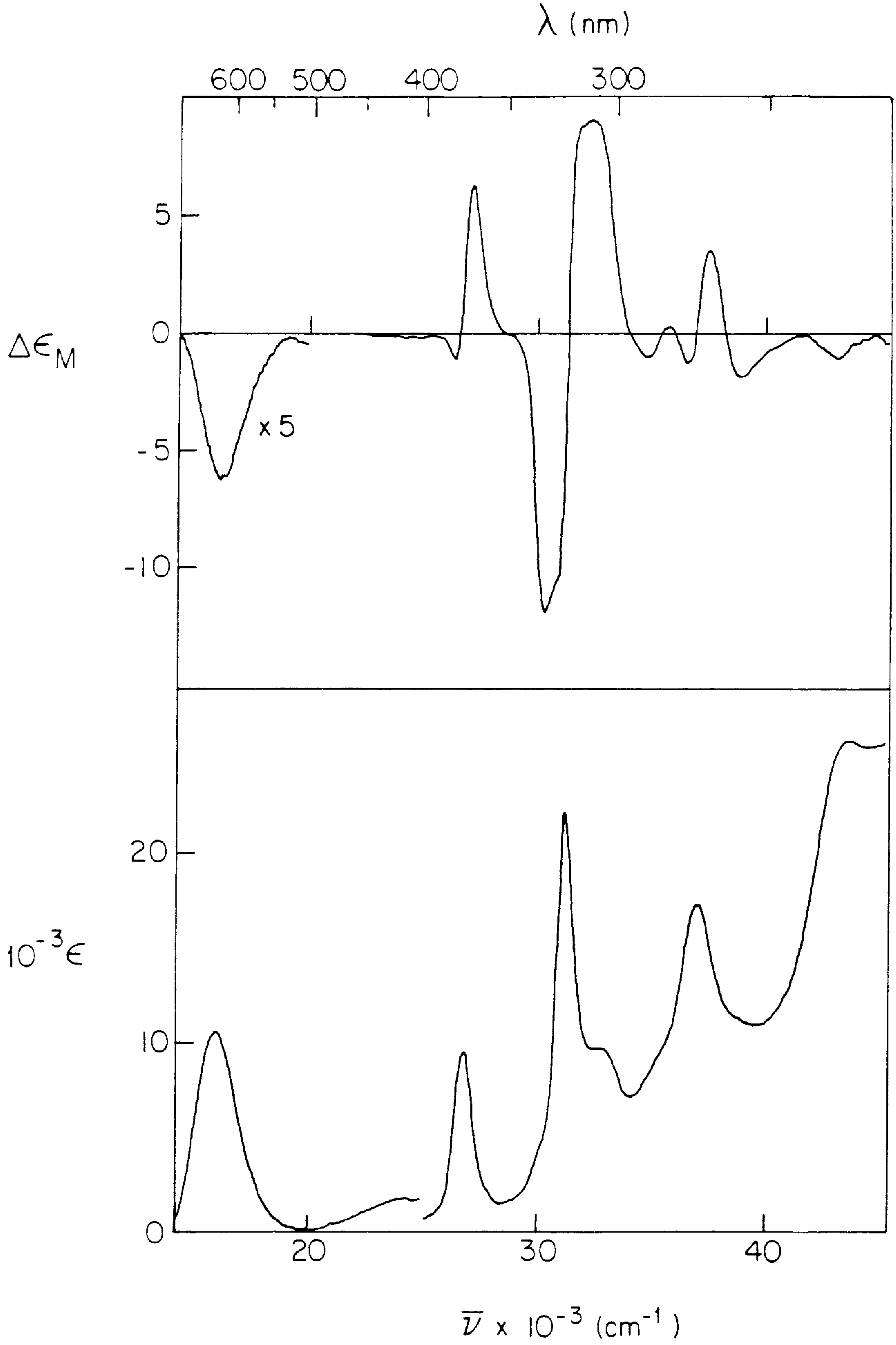
λ (nm)
600
500
400
300
5
0
-5
-10
ΔϵM
x 5
20
10
0
10⁻³ϵ
20
30
40
ν̄ x 10⁻³ (cm⁻¹)

the +A and +B terms. In comparison to $Rh_2(TMB)_4^{2+}$, there is a much larger +A term contributing to this transition. A feature centered at 820 nm is observed to lower energy of the 625 nm absorbance in both single crystals and concentrated solutions. The MCD of this band was not measured because of spectrometer limitations. This band is assigned to the $^3(d\sigma^* \rightarrow p\sigma)$ transition. To lower energy of the 372 nm band, a weak shoulder is observed. A similar weak feature is observed for $Rh_2(TMB)_4^{2+}$. Several features not well resolved for $Rh_2(TMB)_4^{2+}$ are observed for $Ir_2(TMB)_4^{2+}$. To both the high- and low-energy side of the 318 nm band, shoulders are observed (305 and 333 nm). The low-energy shoulder appears as a -B term in the MCD spectrum, consistent with an assignment to the $A_{2u}(^3E_u)$ transition. The shoulder to higher energy, although overlapped with the ^1E_u band, appears to be dominated by a +B term, perhaps with a small -A component, in accord with the $E_u(^3B_{1u})$ $d_{xy} \rightarrow p\sigma$ transition. In addition, bands to higher energy of 300 nm are resolved for both the $B(C_6H_5)_4^-$ and PF_6^- salts. Neither of these features has an analogue in monomer spectra. The two lower-energy bands exhibit +A terms in the MCD, indicating transitions to degenerate excited states. The highest-energy shoulder possesses a weak -B term and no A term, suggestive of a nondegenerate excited state. Assignments are listed in Table 3.5.

The energies and widths of the bands derived from the lowest-energy $d_{z^2} \rightarrow p_z$ excitation for $Ir_2(TMB)_4^{2+}$ are in stark contrast to the $d_{z^2} \rightarrow p_z$ absorption in the spectrum of Ir(CN-*t*-butyl)$_4^+$. The large red shift has been attributed to the smaller d-p gap in the dimer.[10] The greater widths of the $A_{2u}(^1A_{2u})$ and $E_u(^3A_{2u})$ bands are a consequence of the enhanced metal-metal bonding interaction in the $^{1,3}(d\sigma^*p\sigma)$ excited states. Promotion of an electron from $d\sigma^*$ to $p\sigma$ produces a large molecular distortion; this distortion is mainly a contraction along the metal-metal coordinate.[1]

In contrast to the $d\sigma^* \rightarrow p\sigma$ transition, features assigned to $d\pi \rightarrow p\sigma$ excitation have energies and widths very similar to those observed for the monomer, implying very little if any molecular distortion along the metal-metal coordinate. If one adheres strictly to the MO model for the binuclear complex, a shift in the dσ* → pσ transitions implies a shift in the dπ → pσ excitations, unless pσ/dσ and pσ/pσ bonding interactions are negligible,[1] which would contradict the ground-state bonding picture. Since a large shift is observed for the dσ* → pσ transitions and very little if any shift is seen for dπ → pσ, the VB model is preferred; according to VB, the low-energy dσ* → pσ transition is red-shifted from the monomer $d_{z^2} \rightarrow p_z$ because of a favorable metal-metal interaction at shorter distance, with the $^{1,3}E$ states only slightly shifted from their reference monomer energies.

The weak features observed to lower energy of the $A_{1g}(^1A_{1g}) \rightarrow E_u(^3E_u)$ transition have been the subject of much speculation. Arguments against assignment to transitions to $d_{x^2-y^2}$-derived levels (e.g., "ligand-field" excited states) have been presented, and other assignments have been suggested: $d_{xy} \rightarrow p_z$, dσ* → pσ*, and dσ → pσ.[1]

Figure 3.6 shows the low-temperature (77 K) absorption spectrum of $[Ir_2(TMB)_4](B(C_6H_5)_4)_2$. Upon cooling, the expected sharpening and red shift of $A_{1g}(^1A_{1g}) \rightarrow A_{2u}(^1A_{2u})$ (dσ* → pσ) are observed. The red shift of the maximum indicates that the effective vibrational frequency that is coupled to the electronic transition is higher in the excited state than in the ground state.[47]

The high-energy portion of the spectrum resolves impressively upon cooling. The bands assigned to dπ → pσ excitations sharpen but do not shift. The shoulders on each side of the 320 nm band are resolved into distinct features with widths similar to those of the intense dπ → pσ absorptions. A weak shoulder at 344 nm attributable to one quantum of ν(NC) (2260 cm^{-1}) is resolved. The similarity of the high-energy portion of the low-temperature absorption spectrum of $Ir_2(TMB)_4^{2+}$ to that of Ir(CN-*t*-butyl)$_4^+$ is remarkable.

Figure 3.6. Electronic absorption spectrum of $[Ir_2(TMB)_4](B(C_6H_5)_4)_2$ in a glassy matrix of CH_3CH_2CN/2-MeTHF (1:2 volume ratio) at 77 K.

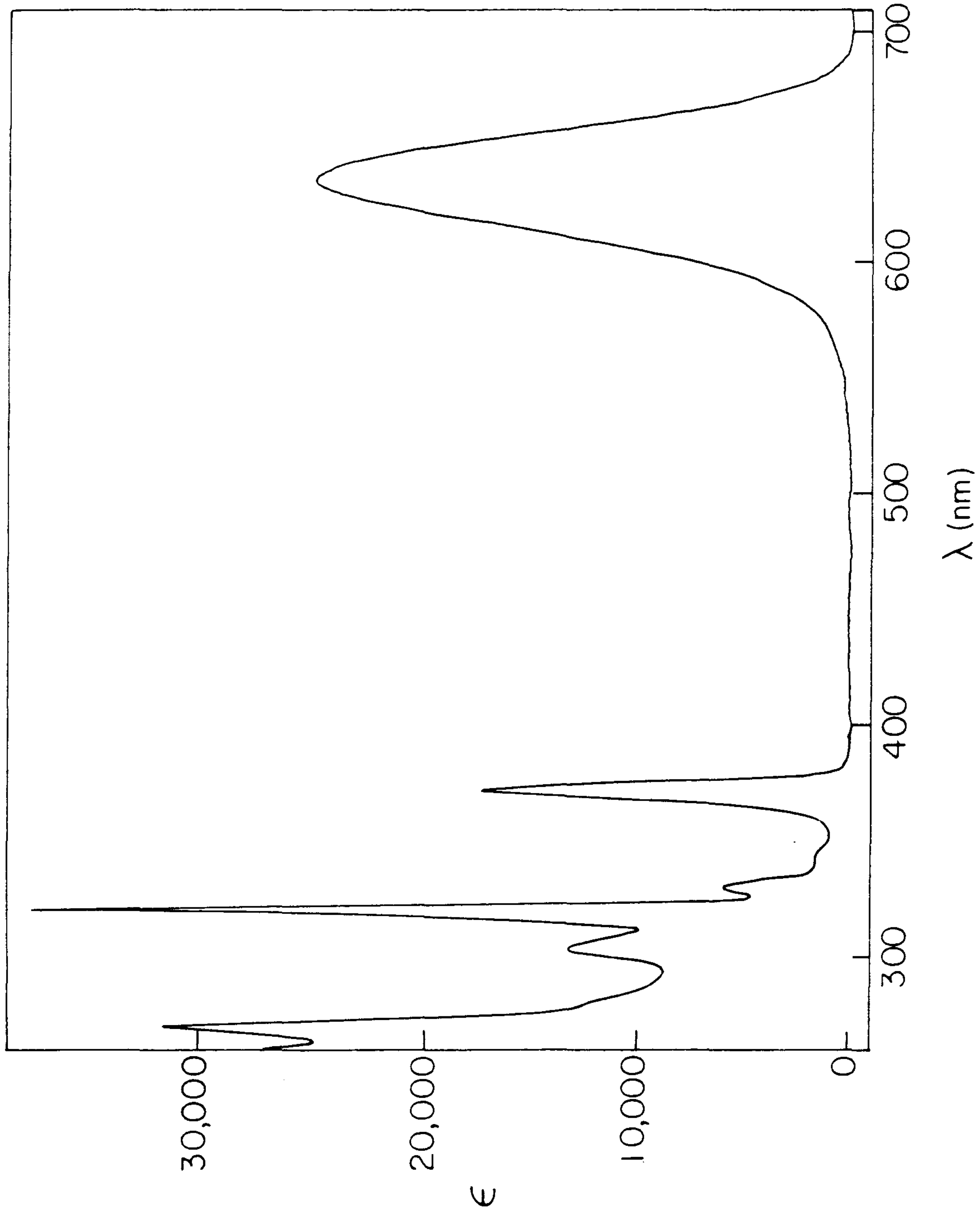

ε
30,000
20,000
10,000
0
300
400
500
600
700
λ (nm)

Single-Crystal Polarized Spectra of $[Ir_2(TMB)_4](B(C_6H_5)_4)_2 \cdot CH_3C_6H_5$

To verify the assignments of the solution and 77 K glass spectra, and to probe the nature of the weak transitions, single-crystal polarized spectra were measured. The room-temperature polarized single-crystal absorption spectra of $[Ir_2(TMB)_4](B(C_6H_5)_4)_2 \cdot CH_3C_6H_5$ are shown in Figure 3.7. Consistent with the earlier assignment, $A_{1g}(^1A_{1g}) \rightarrow A_{2u}(^1A_{2u})$ (λ_{max} 645 nm) shows the expected z-polarization. At lower energy is the x,y-polarized $A_{1g}(^1A_{1g}) \rightarrow E_u(^3A_{2u})$ band (λ_{max} 830 nm). These two features are the $d\sigma^* \rightarrow p\sigma$ transitions.

Upon cooling to 24 K, the spectrum sharpens and reveals additional features not resolved at room temperature (Figure 3.8). To the high-energy side of the $A_{2u}(^1A_{2u})$ band, a feature assignable to one quantum of ν(NC) (2100 cm^{-1}) is observed in both polarizations (λ_{max} 565 nm). (Modes of e_g and a_{1g} symmetries presumably lead to $\perp z$ and $\parallel z$ intensities, respectively.) This feature appears as a broad shoulder in the x,y-polarized room-temperature spectrum. The weak feature at 640 nm in the $\parallel a$ spectra at both room temperature and 24 K is interpreted in terms of a vibronically induced $\perp z$ intensity component of the transition to $A_{2u}(^1A_{2u})$, presumably involving low-frequency modes of e_g symmetry.[48] The observation that the intensity of this feature decreases significantly as the temperature is reduced to 24 K is consistent with the vibronic interpretation. The band assigned to the transition to $E_u(^3A_{2u})$ sharpens and red-shifts, as expected because of the higher-frequency metal-metal vibration in the excited state. Similar to the $A_{1g}(^1A_{1g}) \rightarrow E_u(^3A_{2u})$ band in the spectrum of $Rh_2(TMB)_4^{2+}$, but in contrast to $Rh_2b_4^{2+}$, no vibronic structure is resolved at 24 K.[1] The metal-metal vibration (which is known from a Raman study to have values for the Ir_2 compound of 55 and 132 cm^{-1} in the ground and $^3A_{2u}$ excited states, respectively)[12] is expected to be the primary promoting mode for this electronic transition. The absence of a resolved vibronic progression built on the electronic

Figure 3.7. Polarized single-crystal absorption spectra of $[Ir_2(TMB)_4](B(C_6H_5)_4)_2$ at 25 °C. The $\|a$ base line is vertically offset by 20 ε units.

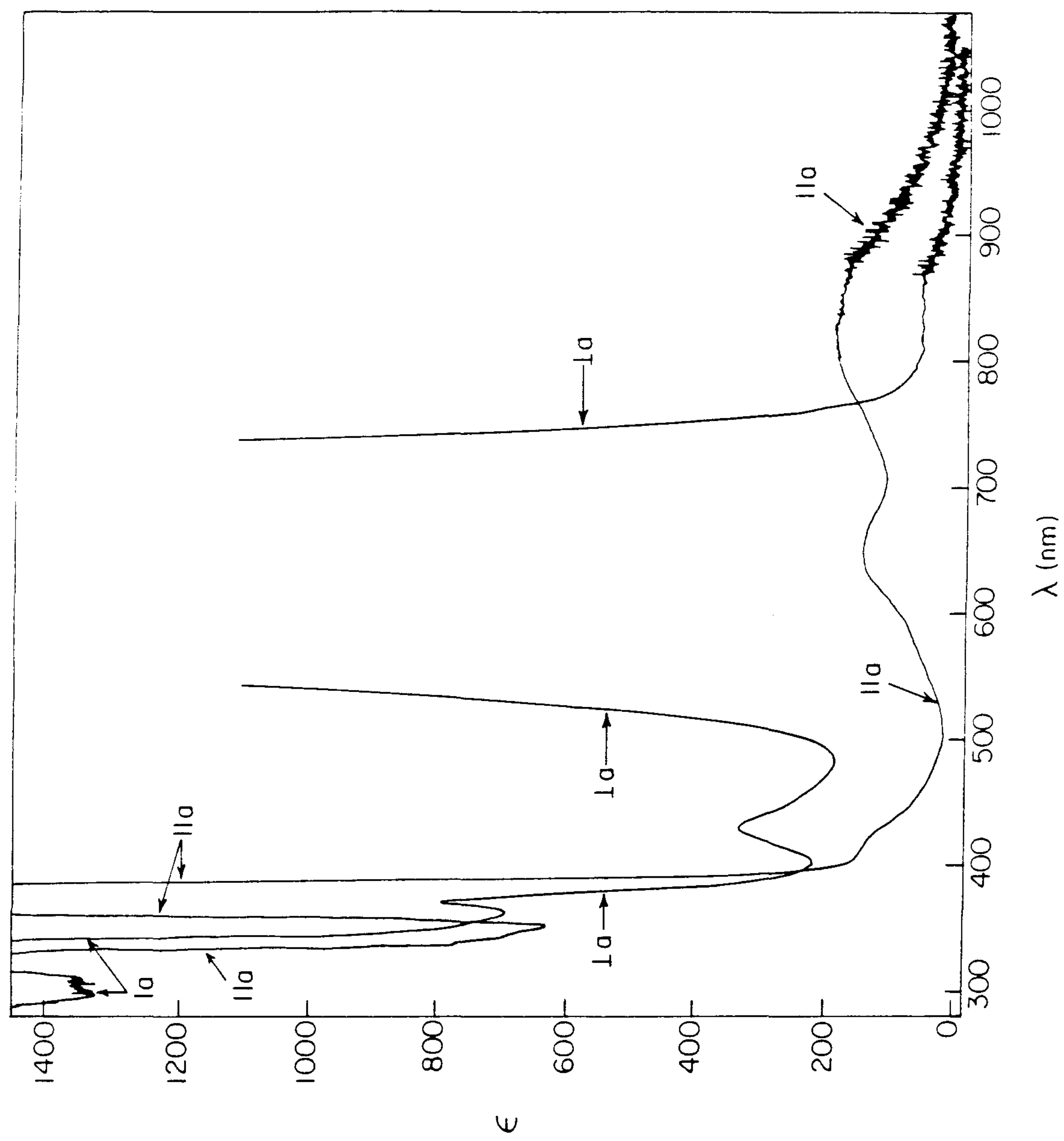
ε
λ (nm)
0
200
400
600
800
1000
1200
1400
300
400
500
600
700
800
900
1000
⊥a
∥a

Figure 3.8. Polarized single-crystal absorption spectra of $[Ir_2(TMB)_4](B(C_6H_5)_4)_2$ at 24 K. The $||a$ base line is vertically offset by 100 ε units.

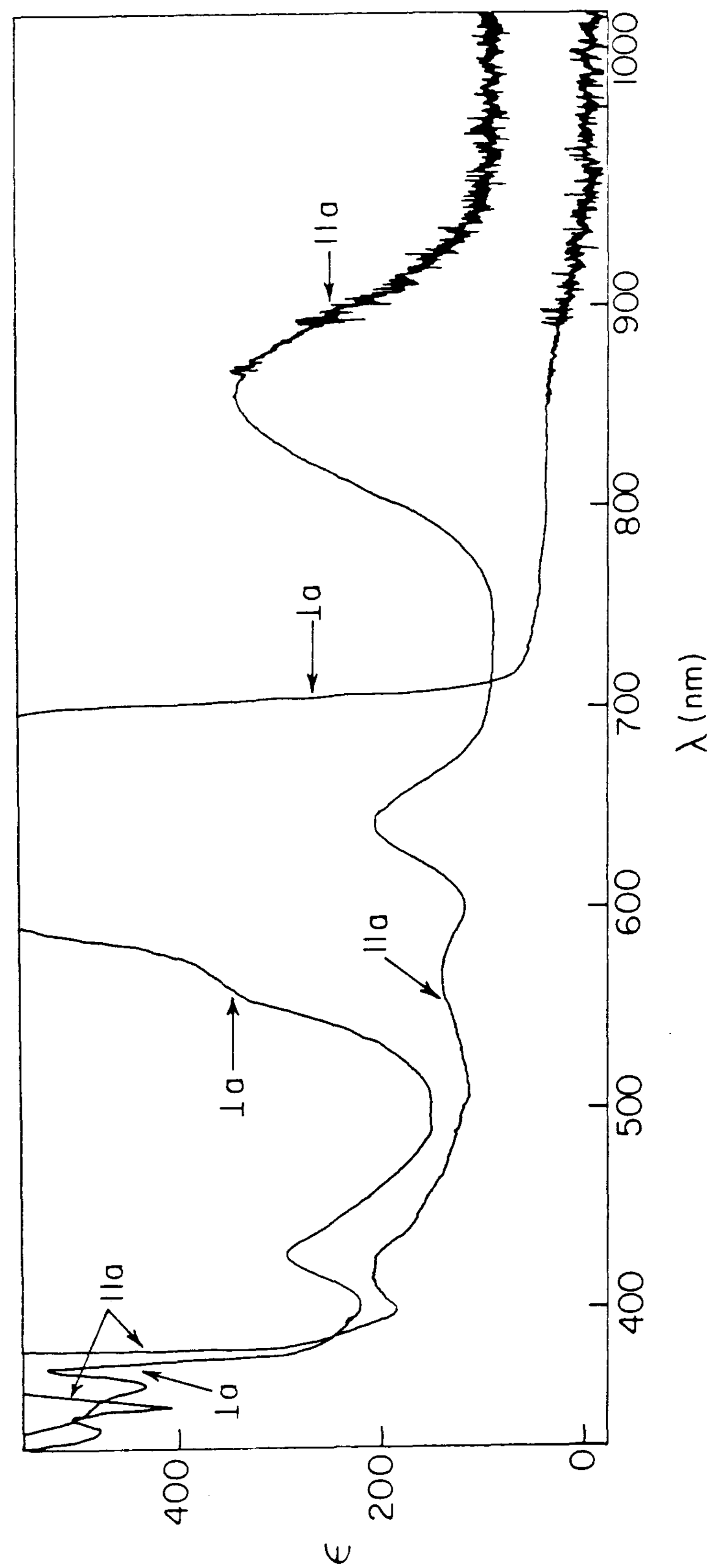
ε
λ (nm)
0
200
400
400
500
600
700
800
900
1000
∥a
⊥a
∥a
⊥a
∥a
⊥a

absorption band may be due to broadening attributable to vibronic coupling involving a low-energy ligand mode.

Several well-resolved bands are observed at higher energy than the $d\sigma^* \rightarrow p\sigma$ absorption. The intense feature at 371 nm displays x,y-polarization, as expected for the $A_{1g}(^1A_{1g}) \rightarrow E_u(^3E_u)$ system. The weak band at 344 nm, resolved in both room-temperature and 24 K spectra, is x,y-polarized; it represents one quantum of ν(NC) (1970 cm^{-1}) built on the transition to $E_u(^3E_u)$. The sharp band at 369 nm in the z-polarized spectrum is assigned to $A_{1g}(^1A_{1g}) \rightarrow E_u(^3E_u)$; it appears in this polarization because of the slight misalignment of the chromophore in the crystal. The shoulder to higher energy is assigned to one quantum of ν(NC), presumably an e_g mode in this polarization.

Unambiguous polarizations for the higher-energy transitions could not be obtained because available crystals were too thick to allow maxima to be measured in either polarization. Indirect polarizations can be obtained from the room-temperature spectra (Figure 3.7), which could be extended to higher optical density than the low-temperature spectra. The band at 328 nm appears to be z-polarized, since intensity in the ⊥a polarization goes off scale near 340 nm well before it does in the || a polarization, but then comes back on scale at ~318 nm. This polarization is consistent with the $A_{1g}(^1A_{1g}) \rightarrow A_{2u}(^3E_u)$ assignment. The intense band(s) to higher energy are similarly indicated to be x,y-polarized, since the absorption ⊥a remains on scale down to nearly 290 nm. These observations are consistent with our assignments of the intense solution bands at 318 and 305 nm as the x,y-polarized transitions $A_{1g}(^1A_{1g}) \rightarrow E_u(^1E_u)$ and $A_{1g}(^1A_{1g}) \rightarrow E_u(^3B_{1u})$.

Several weak features are resolved to lower energy of the $A_{1g}(^1A_{1g}) \rightarrow E_u(^3E_u)$ band. Low-temperature single-crystal spectra of a thicker crystal of $[Ir_2(TMB)_4](B(C_6H_5)_4)_2 \cdot CH_3C_6H_5$ are shown in Figure 3.9. The weak features in the 400- 500 nm region are better resolved and show distinct polarizations. Similar

Figure 3.9. Polarized single-crystal absorption spectra of a thicker crystal of $[Ir_2(TMB)_4](B(C_6H_5)_4)_2$ at 22 K.

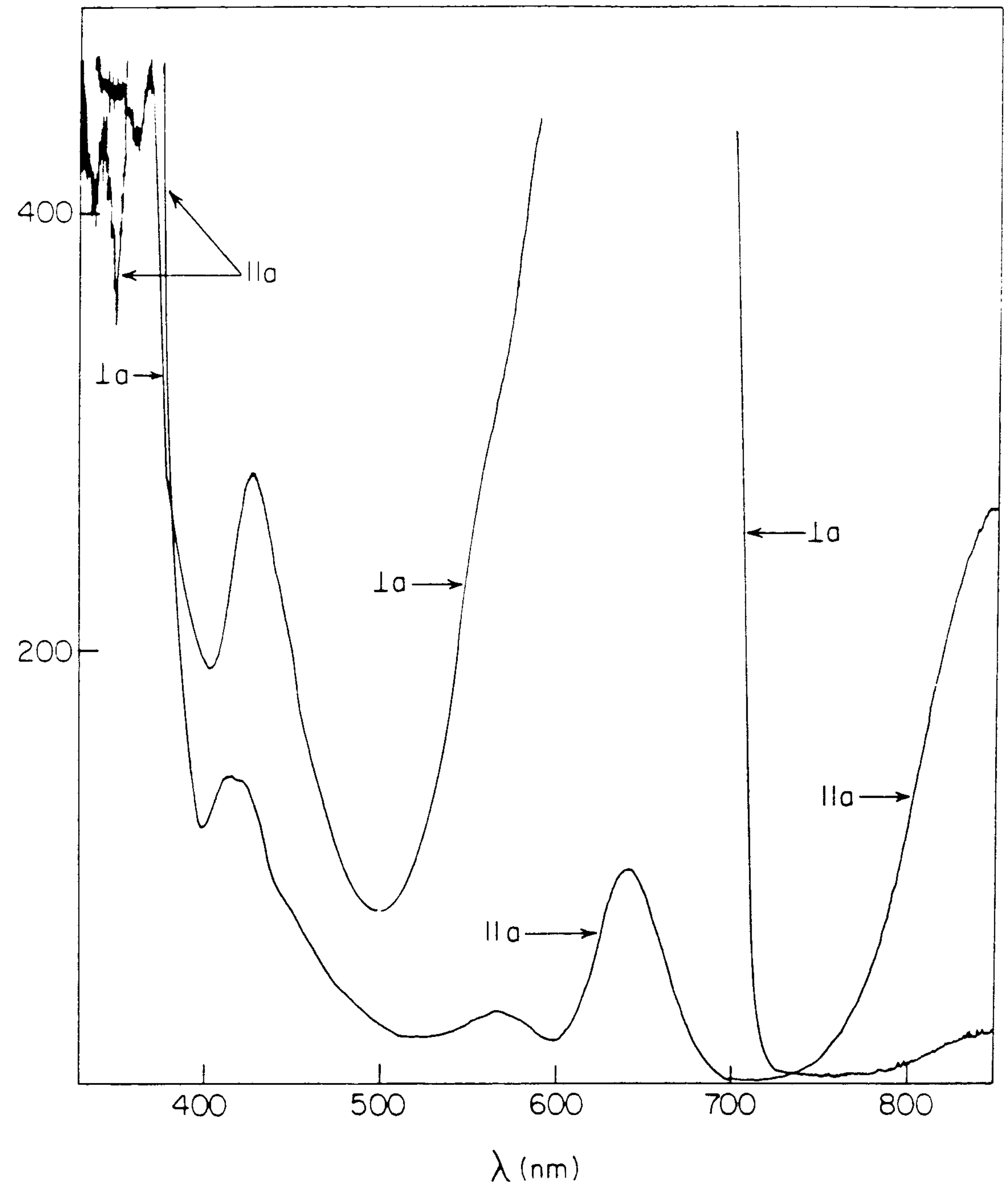
400
200
∈
400
500
600
700
800
λ (nm)
∥a
⊥a
⊥a
∥a
⊥a
∥a

features have been reported for the analogous Rh complex.[1] Because of drastic thermal narrowing of the intense bands to higher and lower energy (Figures 3.7 and 3.8), the temperature dependence of the intensity of these bands is obscured. The most intense band, which peaks at 428 nm, is predominantly z-polarized. In x,y-polarization, the shape of the absorption is reproducibly very different, and we infer additional weak shoulders ar 415 and 450 nm. The absorption maxima in the polarized single-crystal spectra of $[Ir_2(TMB)_4](B(C_6H_5)_4)_2$ are set out in Table 3.6.

Assignments

Many possible assignments have been considered for the weak features observed at lower energy than the $A_{1g}(^1A_{1g}) \rightarrow E_u(^3E_u)$ band. One initially attractive assignment, suggested for the Rh_2 complexes, was excitations into the $d\sigma^*$(Rh-C) orbitals derived from Rh($d_{x^2-y^2}$),[49] as excited states of this type have been postulated to be thermally accessible from $^3A_{2u}(d\sigma^* \rightarrow p\sigma)$.[50] However, the halfwidths of these bands are far too narrow for transitions to $d_{x^2-y^2}$-derived orbitals, because the excited state in question would be strongly distorted along ν(M-C) coordinates.

The $d_{xy} \rightarrow p_z$ transitions ($d\delta,\delta^* \rightarrow p\sigma$), which are dipole-forbidden for both mononuclear and binuclear d^8 complexes, were viewed as another attractive possibility for the weak features.[1] The assignment of the 291 nm band in the spectrum of [Ir(CN-*t*-butyl)$_4$]BF_4 to a transition to $E_u(^3B_{1g})$ (derived from $d_{xy} \rightarrow p_z$) indicates that it is not likely that the weak feature at 430 nm represents an analogous excitation. The $d_{xy} \rightarrow p_z$ transitions evidently are only weakly perturbed, as are the $d_{xz,yz} \rightarrow p_z$ excitations.

Another possibility has been suggested for the weak features. For $Rh_2b_4^{2+}$ and $Rh_2(TMB)_4^{2+}$, $d\sigma \rightarrow p\sigma$ and $d\sigma^* \rightarrow p\sigma^*$ excitations could be responsible for these bands.[1] (The relevant excited state, $d\sigma^*p\sigma^* + d\sigma p\sigma$, may not be strongly bound (*vide infra*) and therefore is best described as an excited monomer weakly coupled to a ground-state

Table 3.6. Absorption maxima for polarized single-crystal spectra of $[Ir_2(TMB)_4](B(C_6H_5)_4)_2$.

	at 25 °C			at 24 K		
$^1A_{1g} \rightarrow$	pol.	λ_{max}, nm (ε, $M^{-1}cm^{-1}$)	fwhm, cm^{-1}	pol.	λ_{max}, nm (ε, $M^{-1}cm^{-1}$)	fwhm, cm^{-1}
$E_u(^3A_{2u})$, $d\sigma^* \rightarrow p\sigma$	x,y	830 (180, $\parallel a$; 60, $\perp a$)	2200	x,y	855 (250, $\parallel a$; 40, $\perp a$)	1300
$^1A_{2u}$, $d\sigma^* \rightarrow p\sigma$	z	645 (140, $\parallel a$; $\perp a$ ^{a})		z	642 (110, $\parallel a$; $\perp a$ ^{a})	1100
+ ν(CN)	z; x,y	565		z; x,y	568 (50, $\parallel a$)	
a	x,y	~455 (40 sh, $\parallel a$)		x,y	~450 (65 sh, $\parallel a$)	
$^1A_{1g}$, $d\sigma/\sigma^* \rightarrow p\sigma/\sigma^*$	z > x,y	430 (~300, $\perp a$)	1400	z > x,y	428 (300, $\perp a$)	1500
a				x,y	415	
$E_u(^3E_u)$, $d_{xz,yz} \rightarrow p_z$	x,y	371		x,y	369	
+ ν(CN)	z; x,y	345 (sh)		z; x,y	344	
$A_{2u}(^3E_u)$, $d_{xz,yz} \rightarrow p_z$	z	~328				
$E_u(^1E_u)$, $d_{xz,yz} \rightarrow p_z$	x,y	>320				

a. Off-scale.

b. Not assigned, see text.

monomer.) Such an assignment is quite appealing for $Ir_2(TMB)_4^{2+}$. The spectral bandwidth (1500 cm^{-1}) is too great to correspond to a $d\pi \rightarrow p\sigma$ transition, but is similar to the bandwidths associated with $d_{z^2} \rightarrow p_z$ excitations. Such transitions are dipole-forbidden; hence, the absorptions should be weak, with intensities induced by vibronic or crystal site-symmetry couplings. An interesting consequence of such an assignment is the correspondence of the 430 nm band in the spectrum of $Ir_2(TMB)_4^{2+}$ to the $A_{1g}(^1A_{1g}) \rightarrow A_{2u}(^1A_{2u})$ ($d_{z^2} \rightarrow p_z$) absorption at 423 nm for Ir(CN-*t*-butyl)$_4^+$. A similar correspondence between dimer and monomer band positions has been noted previously for the $d\pi \rightarrow p_z$ and $d_{xy} \rightarrow p_z$ excitations.

Note that only one $^1A_{1g}(d_{z^2} \rightarrow p_z)$ transition is expected near 430 nm, since the other one (MO model) is to an ionic transition in the VB model (Figure 3.3).

Possible assignments for the additional weak features near 430 nm, as suggested by the VB model, are transitions to $^{1,3}E_g$ bound states arising from $d\pi/\pi^* \rightarrow p\sigma/\sigma^*$ excitations. Such features might be somewhat red-shifted from the monomer transitions (Figure 3.1) and have widths comparable to the bound $d\sigma^* \rightarrow p\sigma$ excitation. The low intensity would suggest spin-forbidden transitions, possibly $^3(d\pi/\pi^* \rightarrow p\sigma/\sigma^*)$.

If the $d\sigma/\sigma^* \rightarrow p\sigma/\sigma^*$ assignment is correct, a corresponding band should be observed for the analogous Rh complexes. Indeed, for $Rh_2(TMB)_4^{2+}$ and $Rh_2b_4^{2+}$, bands at 375 and 385 nm, respectively, are observed, each with the appropriate width and polarization.[46] (The $A_{2u}(^1A_{2u})$ transition for $Rh(CNEt)_4^+$ is observed at 380 nm.)[31]

In addition to accommodating both weakly and strongly perturbed monomer transitions, the VB model identifies fully half of the dimer electronic excited states as ionic (MMCT). Earlier, we placed the MMCT transitions for Ir(I) and Rh(I) at approximately 240 and 200 nm, respectively. The correspondence between the predicted MMCT transition energies and the broad features at 270 and 240 nm for $Ir_2(TMB)_4^{2+}$ and $Rh_2(TMB)_4^{2+}$, respectively, makes assignment of the observed bands to such transitions very attractive. The A-term behavior in the MCD spectrum suggests transitions to $^{1,3}E_u$ ($d_{xz,yz} \rightarrow p_z$) states. The peak separation observed for $Ir_2(TMB)_4^{2+}$ (2000 cm^{-1}) is consistent with the expected singlet-triplet state splitting. For the covalent $d_{xz,yz} \rightarrow p_z$ transition, peak separations of 1400 cm^{-1} ($A_{2u}(^3E_u)$) and 4500 cm^{-1} ($E_u(^3E_u)$) are observed. The large bandwidths are attributed to ligand distortions caused by the change in electron density around the metal. In analogy to $Ir_2(TMB)_4^{2+}$, the high-energy features for $Rh_2(TMB)_4^{2+}$ are tentatively assigned to MMCT ($d_{xz,yz} \rightarrow p_z$) transitions. While this is but one of the possible assignments (other possibilities are transitions to $d_{x^2-y^2}$ states, which would have to be from $d\pi/\pi^*$ levels in order to account for the A terms, or MLCT states), the large blue shift of the bands in going from Ir to Rh is consistent with the ionic nature of the transition, and is not obviously consistent with any other interpretation. In line with this discussion, the highest energy band for $Ir_2(TMB)_4^{2+}$, which shows a weak -B term, may be attributable to an ionic $^1A_{2u}$ state derived from a $d\sigma/\sigma^* \rightarrow p\sigma/\sigma^*$ transition (e.g., the $d\sigma \rightarrow p\sigma^*$ state of the MO limit).

We have not made any assignments to states derived from excitations to the $d_{x^2-y^2}$ orbital. Such transitions, which are formally allowed for the dimer and have been assigned[2] for d^8-d^8 $Pt_2(P_2O_5H_2)_4^{4-}$, are not expected to give rise to intense bands.

Conclusions

The MO model accounts for some of the important aspects of the metal-metal interaction in binuclear d^8 complexes, but it is unable to accommodate all of the observed spectral features. The VB "weak-coupling" model allows for dimer transitions that are highly perturbed from the monomer bands as well as monomer-like dimer excitations. The VB model also identifies half of the dimer electronic excited states as ionic, involving metal-to-metal charge transfer; these MMCT states do not correlate to any monomer states. With the VB model, we have been able to rationalize the energies and widths of the previously observed bands; in addition, we have arrived at plausible assignments for bands that were either not interpreted satisfactorily or not observed in earlier work. There is a striking similarity of our picture of the d^8-d^8 states to that derived from the spectroscopy of van der Waals molecules. The VB model does not change any of the MO-based interpretations of the thermal chemistry, photochemistry, or photophysics of these systems. What it does do is emphasize that weakly bound ground-state systems will show just a few strongly stabilized excited states that correlate to monomer states, and these are the only ones that MO theory describes correctly. The weakly perturbed monomer-like states, and, particularly, the ionic states, are better described by the VB model.

The VB model is applicable to the general class of dimeric systems in which the metals are nonbonded, in a formal sense, and can be viewed as weakly coupled (e.g., $[Ir(\mu\text{-}pz)(COD)]_2$,[51] binuclear d^8 A-frame; $Au_2(dmpm)_2{}^{2+}$,[52] binuclear d^{10} complex; $Pt_2(dppm)_3$,[53] binuclear d^{10} complex). In all of these cases, minimal perturbations of monomer states are expected except when collapse to a strongly bonded state can occur.

Acknowledgment. We thank Terry Smith, Steve Rice, Dave Brinza, Bill Goddard, and Woody Woodruff for early contributions to this work and for helpful discussions through the years. This research was supported by the Sun Company and by National Science Foundation Grant CHE84-19828.

References and Notes

1. Rice, S.F.; Miskowski, V.M.; Gray, H.B. *Inorg. Chem.*, 1988, 27, 4704-4708.

2. Stiegman, A.E.; Rice, S.F. Gray, H.B.; Miskowski, V.M. *Inorg. Chem.* **1987**, *26*, 1112-1116.

3. Isci, H.; Mason, W.R. *Inorg. Chem.* **1985**, *24*, 1761-1765.

4. Rodman, G.S.; Daves, C.A.; Mann, K.R. *Inorg. Chem.* **1988**, *27*, 3347-3353.

5. Milder, S.J.; Kliger, D.S. *J. Phys. Chem.* **1985**, *89*, 4170-4171.

6. Milder, S.J. *Inorg. Chem.* **1984**, *24*, 3376-3378.

7. Milder, S.J.; Kliger, D.S.; Butler, L.G.; Gray, H.B. *J. Phys. Chem.* **1986**, *90*, 5567-5570.

8. Winkler, J.R.; Marshall, J.L.; Netzel, T.L. Gray, H.B. *J. Am. Chem. Soc.* **1986**, *108*, 2263-2266.

9. Marshall, J.L.; Stiegman, A.E.; Gray, H.B. In *Excited States and Reactive Intermediates*; Lever, A.B.P., Ed.; ACS symposium Series 307; American Chemical Society: Washington, D.C., 1986; pp. 166-176.

10. Mann, K.R.; Gordon, J.G. II; Gray, H.B. *J. Am. Chem. Soc.* **1975**, *97*, 3553-3555.

11. Mann, K.R.; Thich, J.A.; Bell, R.A.; Coyle, C.L.; Gray, H.B. *Inorg. Chem.* **1980**, *19*, 2462-2468.

12. Smith, D.C., Ph.D. Dissertation, California Institute of Technology, 1989; Details of the Raman measurements (performed by Prof. R. Dallinger of Wabash College) will be published in a subsequent paper.

13. Miskowski, V.M.; Smith, T.P.; Loehr, T.M.; Gray, H.B. *J. Am. Chem. Soc.* **1985**, *107*, 7925-7934.

14. Herde, J.L.; Lambert, J.C.; Seroff, C.V. *Inorg. Synth.* **1974**, *15*, 18-20.

15. Green, M.; Kuc, T.A.; Taylor, S.H. *J. Chem. Soc. (A)* **1971**, 2334-2337.

16. Robinson, S.D.; Shaw, B.L. *J. Chem. Soc.* **1965**, 4997-5001.

17. *International Tables for X-ray Crystallography, Vol. IV*; Kynoch Press: Birmingham, England, 1974; p. 71, p. 149.

18. Gordon, A.J.; Ford, R.A. *The Chemist's Companion*; John Wiley & Sons: New York, 1972.

19. Perrin, D.D.; Armarego, W.L.F.; Perrin, D.R. *Purification of Laboratory Chemicals*; Pergamon: Oxford, 1966.

20. Mason, W.R. *Anal. Chem.* **1982**, *54*, 646-648.

21. The differences in color of the two phases is due to the high degree of orientation in the well-developed crystal face of the toluene solvate, one extinction ($\perp$ to the Ir_2 axis) transmitting yellow-green light (see Experimental Section). The crystals are air-stable *when dry* for days, but are air-oxidized (with notable surface degradation) upon longer exposure.

22. Determined from the ratio of the integrated intensities for toluene-CH_3 resonance and aromatic proton resonances, to the integrated intensities of the TMB resonances. A signal corresponding to the methyl resonance of the CH_3CN was not seen.

23. Miskowski, V.M.; Sigal, I.S.; Mann, K.R.; Gray, H.B.; Milder, S.J.; Hammond, G.S.; Ryason, P.R. *J. Am. Chem. Soc.* **1979**, *101*, 4383-4385.

24. Sigal, I.S.; Gray, H.B. *J. Am. Chem. Soc.* **1981**, *103*, 2220-2225.

25. Miskowski, V.M.; Gray, H.B. *Inorg Chem.* **1987**, *26*, 1108-1112.

26. Several earlier studies of Ir(I) isocyanide complexes probably encountered such species.[27-29] In particular, the study of Geoffroy *et al.*[29] in which blue species in solution could be photolyzed to generate monomeric Ir(I) isocyanide complexes probably represents photolysis of partially oxidized oligomers rather than photolysis of Ir(I) isocyanide oligomers.[29]

27. Kawakami, K.; Hoga, M.-A.; Tanaka, T. *J. Organomet. Chem.* **1973**, *60*, 363-373.

28. Isci, H.; Mason, W.R. *Inorg. Chem.* **1975**, *14*, 913-918.

29. Geoffroy, G.L.; Bradley, M.G.; Kenny, M.E. *Inorg. Chem.* **1978**, *17*, 777-779.

30. Miskowski, V.M.; Nobinger, G.L.; Kliger, D.S. Hammond, G.S.; Lewis, N.S.; Mann, K.R.; Gray, H.B. *J. Am. Chem. Soc.* **1978**, *100*, 485-488.

31. Mann, K.R.; Lewis, N.S.; Williams, R.M.; Gray, H.B.; Gordon, J.G., II *Inorg. Chem.* **1978**, *17*, 828-834.

32. Isci, H.; Mason, W.R. *Inorg. Chem.* **1975**, *14*, 905-912.

33. Geoffroy, G.L.; Isci, H.; Litrenti, J.; Mason, W.R. *Inorg. Chem.* **1977**, *16*, 1950-1955

34. Brady, R.; Flynn, B.R.; Geoffroy, G.L.; Gray, H.B.; Peone, J.,Jr.; Vaska, L. *Inorg. Chem.* **1976**, *15*, 1485-1488.

35. Craig, D.P.; Walmsley, S.H. *Excitons in Molecular Crystals*; Benjamin: New York, 1968.

36. Effective core potentials were utilized in which only the 19 outermost electrons of Rh and Ir are treated explicitly. See: Hay, P.J.; Wadt, W.R. *J. Chem. Phys.* **1985**, *82*, 299-310.

37. Smith, D.C.; Goddard,W.A. III *J. Am. Chem. Soc.* **1987**, *109*, 5580-5583.

38. Hopkins, M.D.; Gray, H.B.; Miskowski, V.M. *Polyhedron* **1987**, *6*, 705-714.

39. Cotton, F.A.; Walton, R.A. *Multiple Bonds Between Metal Atoms*; Wiley: New York, 1982.

40. The calculated Re atomic spectrum is fit to the observed atomic spectrum using a Condon-Shortley formalism. Corrections to the Condon-Shortley parameters were determined so as to fit the calculated spectrum to the observed spectrum. These parameters were then used to correct the energies of other calculated Re atomic states. The estimate of 2.65 eV is the difference between the observed $^1(\delta\delta^*)$ transition energy and the calculated value of 2K using the corrected atomic state energies. Using either the calculated $^3(\delta\delta^*)$ and $^1(\delta\delta^*)$ state splitting or calculated $^1(\delta\delta^*)$ transition energy would require using uncorrected atomic state energies and would not properly describe the ligand stabilization of the MMCT state.

41. The higher energy $^1A_{2u}$ state ("$d\sigma \rightarrow p\sigma^*$") obviously does not demand a shorter metal-metal bond. However, its extreme antibonding character mandates a higher energy, as supported by calculations on analogous states of Hg_2.

42. Morse, M.D. *Chem. Rev.* **1986**, *86*, 1049-1109.

43. Celestino, K.C.; Ermler, W.C. *J. Chem. Phys.* **1984**, *81*, 1872-1881.

44. van Zee, R.D.; Blankespoor, S.C.; Zwier, T.S. *J. Chem. Phys.* **1988**, *88*, 4650-4654, and references therein.

45. For a detailed description of MCD terms together with the theory and conventions in standard use, see: Piepho, S.B.; Schatz, P.N. *Group Theory in Spectroscopy with Application to Magnetic Circular Dichroism*; Wiley-Interscience: New York, 1983.

46. Miskowski, V.M., unpublished results.

47. Ballhausen, C.J. *Molecular Electronic Structures of Transition Metal Complexes*; McGraw-Hill: New York, 1979; pp. 132-135.

48. The intensity is too high, according to oriented gas calculations, to be attributable to the slight misorientation of the Ir_2 axes.

49. Rice, S.F., Ph.D. Dissertation, California Institute of Technology, 1982.

50. Rice, S.F.; Milder, S.J.; Gray, H.B.; Goldbeck, R.A.; Kliger, D.S. *Coord. Chem. Rev.* **1982**, *43*, 349-354.

51. Marshall, J.L.; Stobart, S.R.; Gray, H.B. *J. Am. Chem. Soc.* **1984**, *106*, 3027-3029.

52. Jaw, H.-R.C.; Savas, M.M.; Rogers, R.D.; Mason, W.R., to be submitted.

53. Harvey, P.D.; Gray, H.B. *J. Am. Chem. Soc.*, in press.

Chapter 4

Thermal Reactivity of $Ir_2(TMB)_4^{2+}$

Introduction

Binuclear d^8 complexes are known to undergo two-electron oxidative addition reactions similar to mononuclear d^8 complexes.[1-9] Unlike the mononuclear systems in which the metal is oxidized by two electrons,[10] the dimers undergo addition reactions in which the metals are oxidized by one electron with formation of a metal-metal single bond. Interest in the addition reactions of binuclear complexes arises from two sources. In an effort to characterize the excited-state chemistry of a system, it is necessary to understand the thermal ground-state reactivity. Second, it is thought that binuclear complexes are more attractive for activating organic molecules than mononuclear complexes because of the possibility of cooperative involvement of metal sites.[11-15]

While much effort has been expended toward understanding the various oxidative addition pathways for mononuclear systems, little is known for bimetallic complexes. Some general statements can be made by considering the electronic structure and the three-dimensional structure of these systems. Similar arguments for the orbital involvement in addition reactions can be made for the dimers as have been made for the mononuclear complexes.[10] This is not necessarily apparent within the MO formalism; however, within the VB model, where the ground state is best described as two weakly coupled monomers, this is more apparent. For some dimer complexes, the metals have been observed to react independently, mimicking the monomer reactivity.[16] One of the major considerations in the reactivity of bimetallic complexes is the influence of the three-dimensional structure on the reactivity. For a cage-like complex, concerted addition to one or both metal centers is unlikely. For an open A-frame complex, concerted additions to one or both metals are possible and have been observed.[16-20] One added feature that bimetallic systems possess, which may enhance their reactivity in comparison to monomers, is the formation of a metal-metal bond in the final product. It has been suggested that the increased enthalpy of reaction for oxidation addition may be attributed to formation of a metal-metal bond.[7]

Earlier work found that $Rh_2b_4^{2+}$, $Rh_2(TMB)_4^{2+}$, $Pt_2(P_2O_5H_2)_4^{4-}$, and [Ir(μ-pz)COD]$_2$ react with dihalides to yield the corresponding d^7-d^7 dimer, X-M-M-X.[1,2,9] $Pt_2(P_2O_5H_2)_4^{4-}$ and [Ir(μ-pz)COD]$_2$ were also found to react with CH_3I to yield CH_3-M-M-I.[2,9] It was found that $Ir_2(TMB)_4^{2+}$ reacts with dihalides (Cl_2, Br_2, I_2), CH_3I, HCl, and $CH_2(CN)_2$ to yield the corresponding d^7-d^7 complex, X-M-M-Y (X = Y, Cl_2, Br_2, I_2; X = I, Y = CH_3; X = Cl, Y = H; X = $CH(CN)_2$, Y = H).[3] Because of the greater reactivity expected for Ir and the interest in the photochemical reactivity of the excited states of $Ir_2(TMB)_4^{2+}$, extension of the thermal chemistry was pursued.

Experimental

Synthesis

All synthetic procedures were carried out with standard Schlenk techniques. All solvents were from freshly opened bottles with no further purification. All solvents were degassed prior to use. Standard procedures were used to prepare $[Ir_2(TMB)_4](B(C_6H_5)_4)_2$.[21] Methyl iodide was distilled prior to use. All other chemicals were of reagent grade or of comparable quality and were used as received. The ^1H NMR spectra were obtained on a 400 MHz JNM-GX400 FT NMR spectrometer.

$[Ir_2(TMB)_4(CH_3)I](B(C_6H_5)_4)_2$

To a CH_3CN solution of $[Ir_2(TMB)_4](B(C_6H_5)_4)_2$, a slight excess of freshly distilled CH_3I was added via syringe. The color of the solution changed immediately upon addition, from clear blue to clear yellow. The solution was stirred for 10 minutes. Solvent and excess CH_3I were removed under vacuum to yield an orange-yellow powder that was recrystallized from acetone to yield yellow crystalline material. A red-orange emission was observed from the recrystallized material at 77 K in the solid state. Calculated for $[Ir_2(TMB)_4(CH_3)I](B(C_6H_5)_4)_2$: C, 58.7; H, 5.9; N, 6.1. Calculated for $0.85[Ir_2(TMB)_4(CH_3)I](B(C_6H_5)_4)_2$ and $0.15[Ir_2(TMB)_4(I)_2](B(C_6H_5)_4)_2$: C, 58.1; H, 5.8; N, 6.1. Calculated for $[Ir_2(TMB)_4(CH_3)I](B(C_6H_5)_4)_2 \cdot 2CH_3COCH_3$: C, 58.9; H, 6.2; N, 5.8. Found: C, 58.8; H, 6.1; N, 5.7. Sample dried in vacuum: C, 58.3, H, 5.9; N, 6.1. ^1H NMR: δ(CD_3CN, 20 °C); 0.95 (singlet, CH_3, 3H), 1.53 (broad singlet, CH_2, 16H), 2.09 (singlet, CH_3, 48H), 6.83 (triplet-of-triplets, 8H), 6.98 (triplet, 16H), 7.25 (multiplet, 16H).

$[Ir_2(TMB)_4(CH_3CO)Cl](B(C_6H_5)_4)_2$

To a clear, blue acetonitrile solution of $[Ir_2(TMB)_4](B(C_6H_5)_4)_2$, 1.4 equivalents of acetylchloride was added via syringe. An immediate color change was observed, blue to yellow. The solution was stirred for 10 minutes. The final solution was a cloudy yellow. Solvent and excess acetylchloride were removed under vacuum to yield a light yellow powder. Attempts to recrystallize this material from acetone led to a rapid color change of the solution, yellow to blue-green.

NMR Tube Reactions

Acetonitrile-*d3* was freeze-pump-thaw degassed, stored under vacuum over activated alumina, and vacuum-transferred into the NMR tube. Cyclohexadienes were distilled from $NaBH_4$ under argon, freeze-pump-thaw degassed, stored under vacuum, and protected from light. 9,10-dihydroanthracene was recrystallized three times from absolute ethanol. A CD_3CN solution of $[Ir_2(TMB)_4](B(C_6H_5)_4)_2$ was prepared in a grease-free/vacuum-adapted NMR tube. To this tube was added the desired substrates. Gases (HCl and HI) were freeze-pump-thaw degassed or scrubbed (H_2) with the appropriate catalyst prior to addition. Liquids were either added via syringe in an inert atmosphere (R_3SnH and R_3SiH) or vacuum-transferred from an appropriate storage flask (1,4-cyclohexadiene and 1,3-cyclohexadiene). Solids ($CH_2(CN)_2$ and 9,10-dihydroanthracene) were added to crystalline $[Ir_2(TMB)_4](B(C_6H_5)_4)_2$ and the mixture dissolved in CD_3CN.

$[Ir_2(TMB)_4(C_6H_5C{\equiv}C)H](B(C_6H_5)_4)_2$

To the CD_3CN solution of $[Ir_2(TMB)_4](B(C_6H_5)_4)_2$ (0.005 g) was added via syringe an excess of phenylacetlyene. The solution was agitated at room temperature overnight. ^1H NMR: δ(CD_3CN, 20 °C); -10.79 (singlet, Ir-H), 1.52 (broad singlet, CH_3), 1.91 (broad singlet, CH_2), 6.83 (triplet), 6.98 (triplet), 7.26 (multiplet).

$[Ir_2(TMB)_4](B(C_6H_5)_4)_2$ + 9,10-dihydroanthracene

$[Ir_2(TMB)_4](B(C_6H_5)_4)_2$ and freshly recrystallized 9,10-dihydroanthracene were combined in a grease-free/vacuum-adapted NMR tube. Acetonitrile-d_3 was vacuum-transferred onto the solids. The NMR tube was wrapped in foil and placed in the dark at room temperature overnight to allow the solid material to dissolve. The NMR spectrum of the sample was measured after 12 hrs. The sample, wrapped in foil, was placed in an 80 °C oil bath for 20 hrs. ^1H NMR: $\delta(CD_3CN$, 20 °C); -10.62 (singlet, Ir-H); anthracene, 7.50 (multiplet, 4H), 8.05 (quartet, 4H), 8.50 (singlet, 2H).

Spectroscopic Measurements

All solvents were dried and degassed by standard methods.[22,23] Absorption spectra were recorded with a Cary 17 spectrophotometer, a Hewlett-Packard 8450A spectrophotometer, or a Shimadzu UV-260 spectrophotometer. Spectra were obtained of solutions prepared on a high-vacuum line in a cell consisting of a 10 ml Pyrex bulb, a 1 cm pathlength quartz cell, and a Teflon vacuum valve. Several spectra of the complexes that are air-stable in solution were measured, of samples prepared in the air in 1 cm pathlength quartz cuvettes. Substrates were introduced to $[Ir_2(TMB)_4](B(C_6H_5)_4)_2$ solutions as described for the NMR tube reactions.

Electrochemical Measurements

Cyclic voltametric measurements were conducted with a Princeton Applied Research (PAR) model 173 potentiostat/galvanostat, a model 175 universal programmer, and a model 179 digital coulometer. Cyclic voltammograms (CVs) were plotted on a Houston Instruments Omnigraphic 2000 x,y-recorder. Fast-sweep CVs were recorded on a Tektronix 5223 digitizing oscilloscope. The cell geometry used to measure the CVs is described elsewhere.[24] CVs were measured at a BAS Pt button working electrode, with a Pt wire auxiliary electrode, and a sodium saturated calomel electrode (SSCE) as the reference. Dichloromethane was distilled from CaH_2 under an atmosphere of argon, freeze-pump-thaw degassed, and stored under argon. Tetra-*n*-butyl ammonium hexafluorophosphate ($TBAPF_6$) was recrystallized 3 times from 95% ethanol. CVs of $[Ir_2(TMB)_4](B(C_6H_5)_4)_2$ were measured for dichloromethane solutions under argon that contained 0.1 M $TBAPF_6$ as the supporting electrolyte and 10^{-3} M compound.

Additional Measurements

Elemental analyses were obtained at the CalTech Analytical Laboratory.

Results and Discussion

Thermal Reactivity

Nonpolar and Low Polarity Reagents (H_2, C-H, Si-H, Sn-H)

As was noted by T.P. Smith, no reaction with H_2 is observed.[3] This is not surprising in that no reaction with H_2 has been observed for the mononuclear alkyl isocyanide complexes. This has been understood to be a result of the decrease in electron density at the metal because of the π acidity of the isocyanide ligands. If phosphine is exchanged for isocyanide, as in the complex $Rh_2(dppm)_2(CN\text{-}n\text{-hexyl})_4^{2+}$, slow thermal addition of H_2 is observed. In analogy to $[Ir(CO)Cl(dppm)]_2$,[16] H_2 addition is thought to proceed in a concerted fashion to one metal with rapid transfer of one hydride to the other metal center.

There are no known examples of concerted C-H addition to a binuclear d^8 complex. For $Ir_2(TMB)_4^{2+}$, preliminary results indicate that thermolysis with 9,10-dihydroanthracene in CD_3CN at 80 °C yields products that are derived from C-H bond cleavage. Figure 4.1 shows the growth with time of anthracene and a metal product independently characterized as $Ir_2(TMB)_4H_2^{2+}$. The most likely pathway to the observed products is a free-radical process. Over a 12 hr period a 78% yield of anthracene, based on starting metal concentration, is obtained. This is the first example of a thermal C-H bond cleavage reaction by a binuclear d^8 complex. There is no observable reaction with 1,4-cyclohexadiene or 1,3-cyclohexadiene at 25 or 80 °C.

For substrates described as carbon acids ($CH_2(CN)_2$, $pK_a \sim 11$; $C_6H_5C{\equiv}CH$, $pK_a \sim 18.5$),[25] reactions with $Ir_2(TMB)_4^{2+}$ are observed and yield products best represented as H-Ir-Ir-R. Earlier work by T.P. Smith suggested that the reaction of malononitrile was not an acid/base reaction in that acetyl acetone ($pK_a \sim 9$) and benzoic acid ($pK_a \sim 10.7$) did not show similar reactivity.[3] Rigorous exclusion of light did not alter the reaction with malononitrile. It was thought that the prior coordination of the CN groups to the iridium center may be necessary for reaction, although no evidence to

Figure 4.1. NMR spectra of $[Ir_2(TMB)_4](B(C_6H_5)_4)_2$ and 9,10-dihydroanthracene (a) prior to thermolysis, and (b) after 12 hrs thermolysis in 80 °C oil bath.

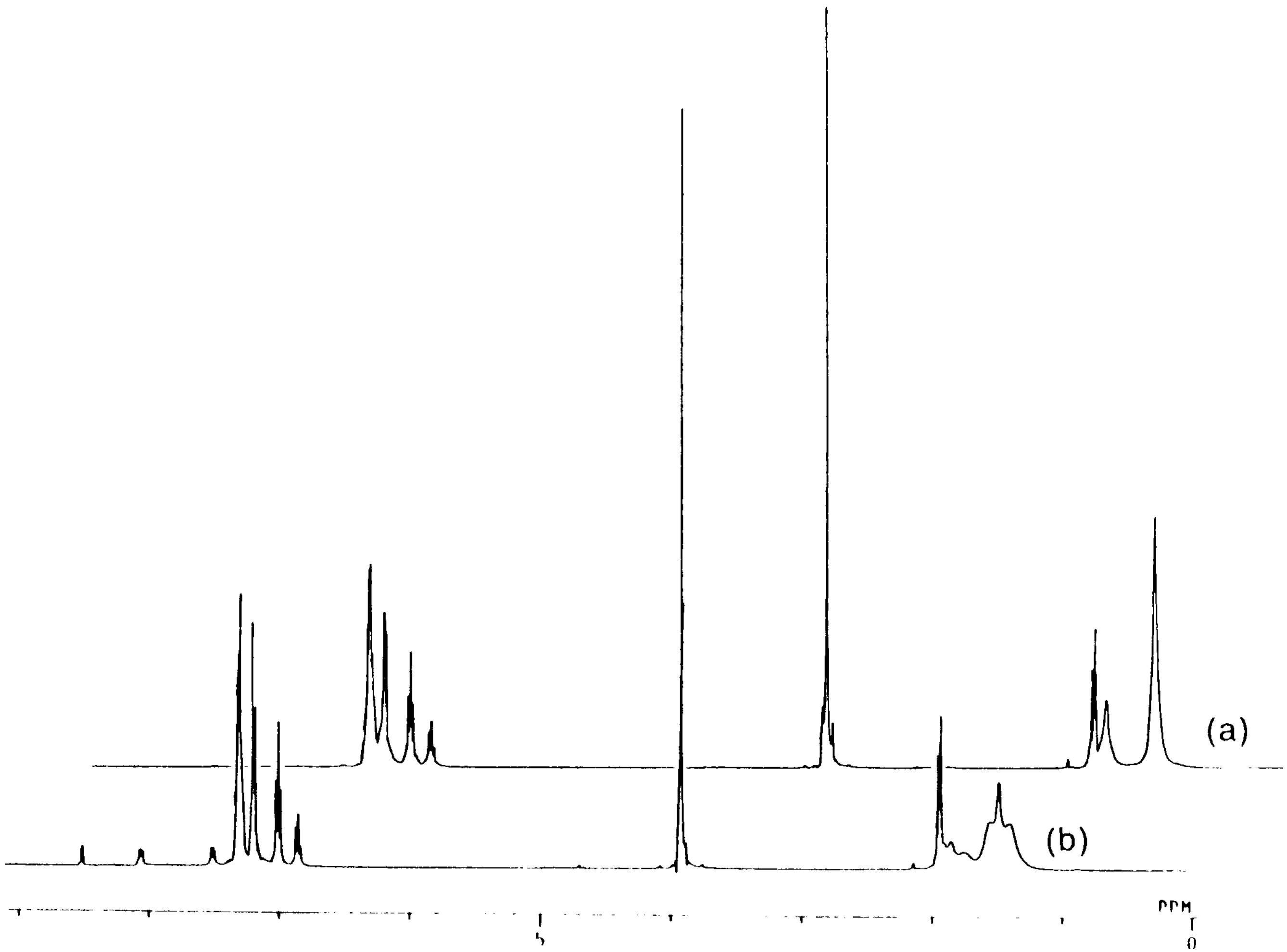

(a)
(b)
PPM
5
0

support this suggestion could be obtained. The lack of reactivity of acetyl acetone may be due to bad steric interactions with the methyl groups of the TMB ligand in the final product. Dimerization of benzoic acid or the instability of the final product are possible explanations of the lack of reactivity of this substrate.[26]

For $C_6H_5C{\equiv}CH$, a smooth reaction with $Ir_2(TMB)_4^{2+}$ is observed. Although the final product has not been isolated, the chemical shift of the Ir-H resonance and the nature of the aliphatic resonances lead to the suggestion that the product is H-Ir-Ir-$C{\equiv}CC_6H_5$. Similar to the reaction with malononitrile, the addition of phenylacetlyene is thought to be an acid/base process. Homolytic cleavage of the C-H bond of phenylacetylene seems unlikely ($D(C_6H_5C{\equiv}C\text{-}H)$ ~ 130 kcal/mol).[27]

Addition of acetylenes to Rh(I) and Ir(I) phosphine complexes has been recently studied.[28] It is suggested that these reactions rather than acid/base processes are concerted additions to the metal center. For $Ir_2(TMB)_4^{2+}$, such a concerted addition is not likely, and an acid/base pathway is preferred. It may, in fact, be the case that for the mononuclear Rh(I) and Ir(I) phosphine complexes, the true reaction pathway is acid/base.

For R_3SiH and R_3SnH, rapid thermal reactions with $Ir_2(TMB)_4^{2+}$ are observed. In the optical absorption spectrum, a rapid bleach of the binuclear d^8 spectrum is observed with growth of a spectrum that indicates oxidation of the metal complex, but not necessarily formation of a d^7-d^7 dimer complex. For $Pt_2(P_2O_5H_2)_4^{4-}$, no thermal reaction with R_3SiH or R_3SnH is observed.[29] The NMR spectra of the reaction mixtures do reveal formation of metal hydrides.

Electrophilic Reagents (X_2, RX, HX, CH_3COCl)

Previous work has shown that dihalides and mineral acids will add to $Ir_2(TMB)_4^{2+}$ oxidatively to yield the corresponding d^7-d^7 complex.[3] The only alkyl halide found to add thermally to $Ir_2(TMB)_4^{2+}$ is CH_3I. No thermal reaction is observed with CH_2Cl_2, $CHCl_3$, CCl_4, or $ClCH_2CH_2Cl$. Previous discussion of the CH_3I reaction had concluded that the reaction follows a free-radical pathway. For analogous mononuclear d^8 complexes, detailed studies have shown that the addition of CH_3I, unlike other alkyl halides, proceeds by an S_N2 pathway,[10] contrary to the result for $Ir_2(TMB)_4{}^{2+}$. Emphasized in the work on mononuclear complexes is the fine balance that exists between the concerted S_N2 pathway and the electron-transfer, free-radical pathway. For $Ir_2(TMB)_4{}^{2+}$, the balance may be swayed in favor of electron transfer.

Careful preparation and isolation of the addition products from the reaction of CH_3I and $Ir_2(TMB)_4{}^{2+}$ indicate that, unlike the earlier report, there is very little if any $Ir_2(TMB)_4I_2{}^{2+}$ (Ir_2I_2) contamination. The Ir_2I_2 by-product was used as evidence for a free-radical process. The UV-Vis spectrum of the isolated material (Figure 4.2) shows no evidence of Ir_2I_2 contamination. The NMR spectrum of the isolated product appears quite clean. Neglecting the large uncertainty in the integrated intensities of the NMR resonances, an estimate of ~15% Ir_2I_2 contamination is arrived at by comparing the ratio of Ir-CH_3 to TMB-CH_2. However, from the combustion data a 15% Ir_2I_2 impurity seems unlikely. Rather, the complex appears to be an acetone solvate. Thus, addition of CH_3I to $Ir_2(TMB)_4{}^{2+}$ appears to yield only $Ir_2(TMB)_4(CH_3)(I)^{2+}$.

These results do not distinguish between the possible pathways for addition of CH_3I. Alkyl halide addition to binuclear gold complexes is thought to proceed via an S_N2 pathway.[30,31] Another possibility is an inner-sphere electron-transfer pathway in which a solvent-caged radical pair is formed. This pathway would yield products that are the same as that from an S_N2 reaction. Evidence exists that suggests the addition of I_2 to $Rh_2b_4{}^{2+}$ follows an electron-transfer pathway.[32] No conclusion concerning the pathway of alkyl halide addition to $Ir_2(TMB)_4{}^{2+}$ is possible until more detailed experiments designed to test the various mechanism are done. Such experiments would be similar to those discussed for the mononuclear complexes.

Figure 4.2. Electronic absorption spectrum of $[Ir_2(TMB)_4(CH_3)I](B(C_6H_5)_4)_2$ in CH_3CN at 25 °C.

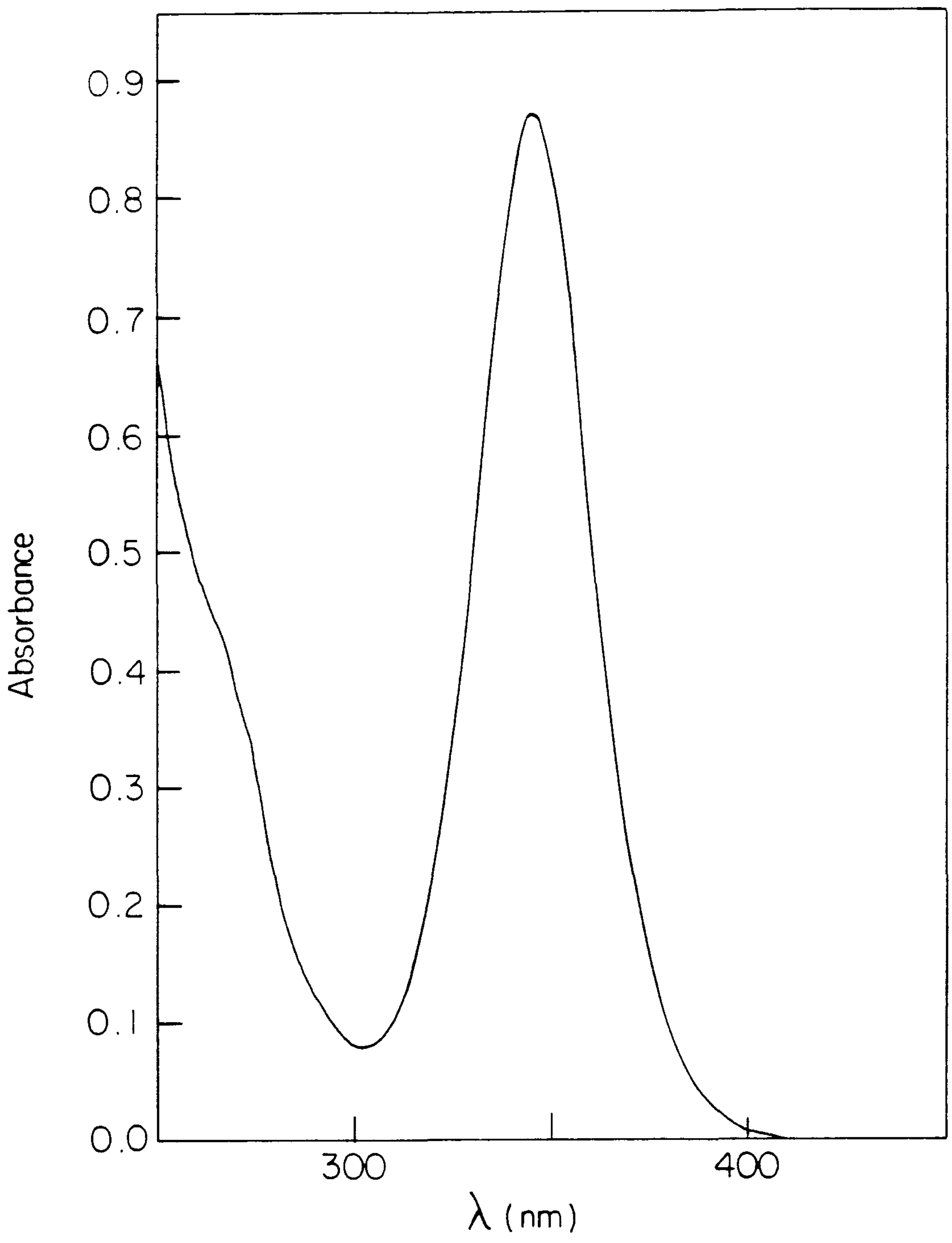
0.9
0.8
0.7
0.6
0.5
0.4
0.3
0.2
0.1
0.0
Absorbance
300
400
λ (nm)

Addition of acetylchloride to a solution of $Ir_2(TMB)_4^{2+}$ results in a rapid reaction with formation of a yellow material similar to that obtained from the reaction of CH_3I. The optical absorption spectrum of this material (Figure 4.3) indicates formation of a d^7-d^7 complex different from the previously prepared dichloride adduct and red-shifted from the spectrum expected for $Ir_2(TMB)_4(CH_3)(Cl)^{2+}$. The proposed product is $Ir_2(TMB)_4(CH_3CO)(Cl)^{2+}$. Attempts to recrystallize the material lead to rapid decomposition. For analogous mononuclear Ir(III) acyl complexes, decarbonylation occurs rapidly upon heating.[10] The yellow material is quite susceptible to decomposition, yielding blue-green materials upon heating, exposure to solvents such as acetone, and prolonged exposure to light.

Summary

The observed thermal reactivity for $Ir_2(TMB)_4^{2+}$ (Figure 4.4) conforms to the earlier expectations of net two-electron chemistry. While the details of the specific pathways for the various reactions are not known, the reactivity parallels that observed for the analogous mononuclear complexes. The reactivity of the monomers is controlled by the $(d_{z^2})^2$ configuration, with the reactivity of the dimer being dictated by the $(d\sigma^*)^2$ configuration, or more accurately, two weakly coupled $(d_{z^2})^2$ metal centers. In contrast to the monomers, the metal centers of the dimer are oxidized by only one electron with formation of a metal-metal single bond. No complications that were due to reactions involving the isocyanide ligand were observed.[33]

It will be shown in subsequent sections that the excited-state chemistry contrasts drastically to the ground-state chemistry. As stated earlier, the $^{1,3}(d\sigma^*p\sigma)$ excited states may be viewed as a diradical species, implying that the chemistry for such excited states will be one electron in nature, i.e., electron transfer and atom transfer, in contrast to the two-electron chemistry of the ground state. Free-radical reactions may occur for the ground state. These reactions involve oxidation of the metal complex,

Figure 4.3. Electronic absorption spectrum of $[Ir_2(TMB)_4(CH_3CO)Cl](B(C_6H_5)_4)_2$ in CH_3CN at 25 °C.

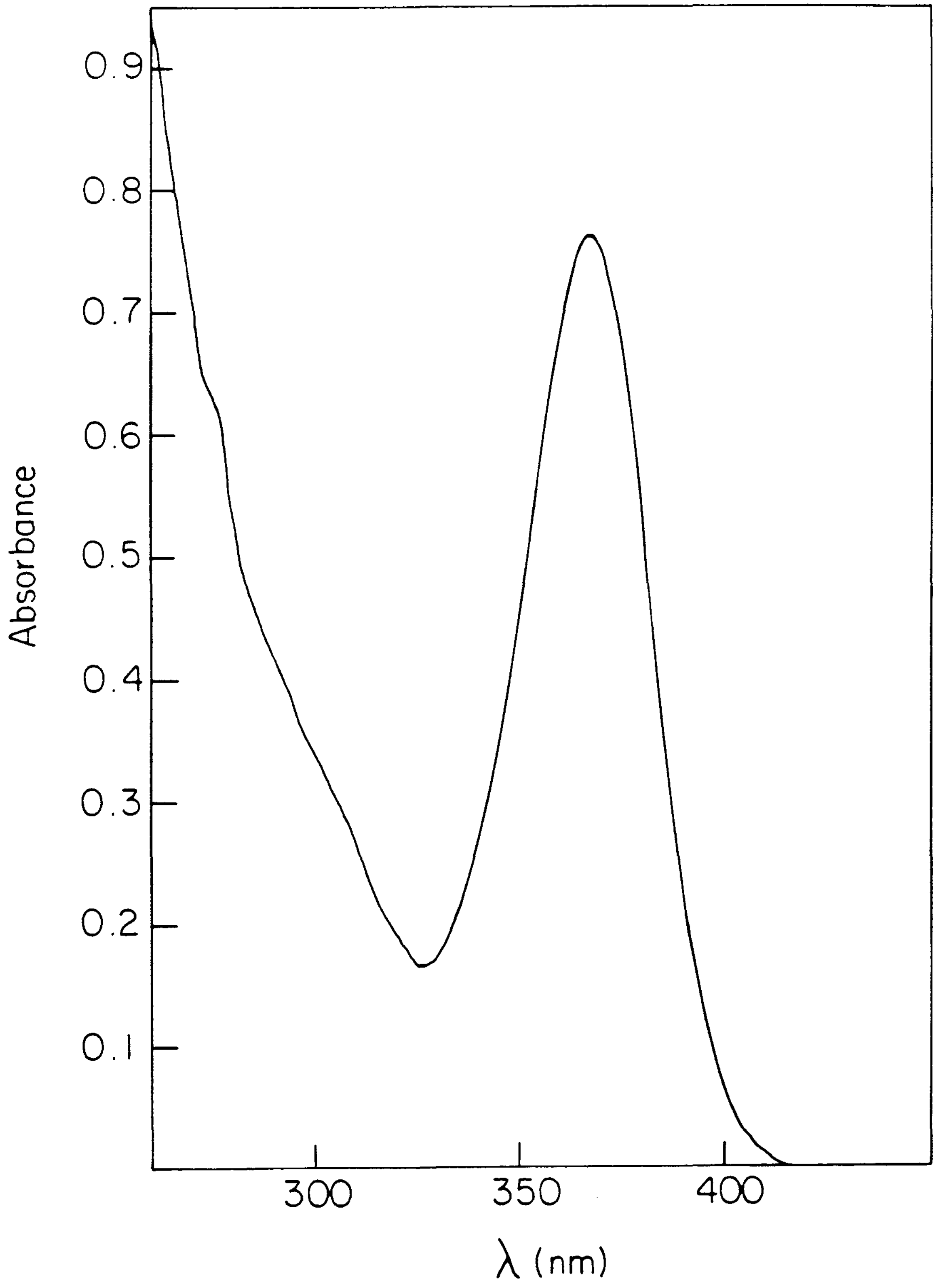
0.9
0.8
0.7
0.6
0.5
0.4
0.3
0.2
0.1
Absorbance
300
350
400
λ (nm)

Figure 4.4. Observed thermal reactions of $[Ir_2(TMB)_4](B(C_6H_5)_4)_2$.

$$Ir_2 \xrightarrow[CH_3CN]{X_2} X-Ir-Ir-X \qquad X = Cl, Br, I$$

$$Ir_2 \xrightarrow[CH_3CN]{RX} R-Ir-Ir-X \qquad RX = CH_3I, CH_3COCl$$

$$Ir_2 \xrightarrow[CH_3CN]{HX} H-Ir-Ir-X \qquad HX = HCl, HBr$$

$$Ir_2 \xrightarrow[CH_3CN]{HR} H-Ir-Ir-R \qquad HR = CH_2(CN)_2, HCCC_6H_5$$

generating a species whose electronic structure is similar to the triplet excited state, an oxidizing hole in the $d\sigma^*$ orbital. It will be shown that electrochemical oxidation of $Rh_2(TMB)_4^{2+}$ to generate $Rh_2(TMB)_4^{3+}$ in the presence of alkyl halides and H-atom donors results in reactions that parallel those observed for the $^3(d\sigma^*p\sigma)$ excited state.

Ir-H Chemical Shifts

In Table 4.1, the Ir-H chemical shifts for a series of d^7-d^7 complexes of $Ir_2(TMB)_4^{2+}$ are listed. The unique feature of these complexes is the extreme sensitivity of the chemical shift of the Ir-H resonance to the nature of the ancillary group. A possible explanation for this behavior comes from the theory of Buckingham and Stephen in which the mixing of low-lying, electronic excited states into the ground-state wave function determines the hydride chemical shift.[34,35] For complexes of the type YX_4MH, the paramagnetic shielding, σ^p, is predicted to be very sensitive to the anisotropy of the complex. This is borne out for the limited date in Table 4.1.

In the Buckingham model, the relative chemical shifts for complexes of the type YX_4MH are governed by the ligand-field strength of the ligand Y; as the ligand-field strength of Y increases, σ^p should decrease. Within the limited data set for H-Ir-Ir-Y, the expected shift of the hydride resonance with increasing ligand-field strength of Y is observed. Electronic coupling of groups trans to one another through a metal-metal bond is known;[36] however, the trend in hydride chemical shift for the d^7-d^7 complexes of $Ir_2(TMB)_4^{2+}$ is surprising, considering the complexity of the electronic coupling of the metal centers. Further studies are necessary to determine how well the Buckingham model describes these systems.

Electronic Spectra of d^7-d^7 Complexes of $Ir_2(TMB)_4^{2+}$

In Table 4.2, the optical absorption spectra for a series of d^7-d^7 complexes of $Ir_2(TMB)_4^{2+}$ are summarized. Figure 4.5 presents the spectra for several of these

Table 4.1. Ir-H Chemical Shifts.

H-Ir-Ir-X	δ (ppm)
H-Ir-Ir-Cl	-13.5
H-Ir-Ir-I	-13.1
H-Ir-Ir-$CH(CN)_2$	-11.9
H-Ir-Ir-$C \equiv CC_6H_5$	-10.8
H-Ir-Ir-H	-10.6

Table 4.2. Electronic absorption data for $Ir_2(TMB)_4XY^{2+}$ complexes.

	$d\sigma \rightarrow d\sigma^*$, nm ($\varepsilon$, M^{-1} cm^{-1})	"$d\pi$" $\rightarrow d\sigma^*$, nm (ε, M^{-1} cm^{-1})	Ref.
$Ir_2(TMB)_4Cl_2^{2+}$	275 (50520)	349 (5910)	4
$Ir_2(TMB)_4Br_2^{2+}$	297 (52569)	330 (4510)	4
$Ir_2(TMB)_4I_2^{2+}$	330 (49800)	375 (8110)	4
$Ir_2(TMB)_4(H)Cl^{2+}$	336	a	3
$Ir_2(TMB)_4(H)(CH(CN)_2)^{2+}$	330	a	b
$Ir_2(TMB)_4(CH_3)I^{2+}$	346	a	b
$Ir_2(TMB)_4(CH_3CO)Cl^{2+}$	366	a	b
$Ir_2(TMB)_4H_2^{2+}$	320	a	b

a. Not observed.

b. This work.

Figure 4.5. Electronic absorption spectra of (a) $[Ir_2(TMB)_4Cl_2](B(C_6H_5)_4)_2$ in CH_3CN, (b) $[Ir_2(TMB)_4I_2](B(C_6H_5)_4)_2$ in CH_3CN,
(c) $[Ir_2(TMB)_4(H)Cl](B(C_6H_5)_4)_2$ in CH_3CN,
(d) $[Ir_2(TMB)_4(CH_3)I](B(C_6H_5)_4)_2$ in CH_3CN,
(e) $[Ir_2(TMB)_4(CH_3CO)Cl](B(C_6H_5)_4)_2$ in CH_3CN, and
(f) $[Ir_2(TMB)_4H_2](B(C_6H_5)_4)_2$ in CH_3CN.

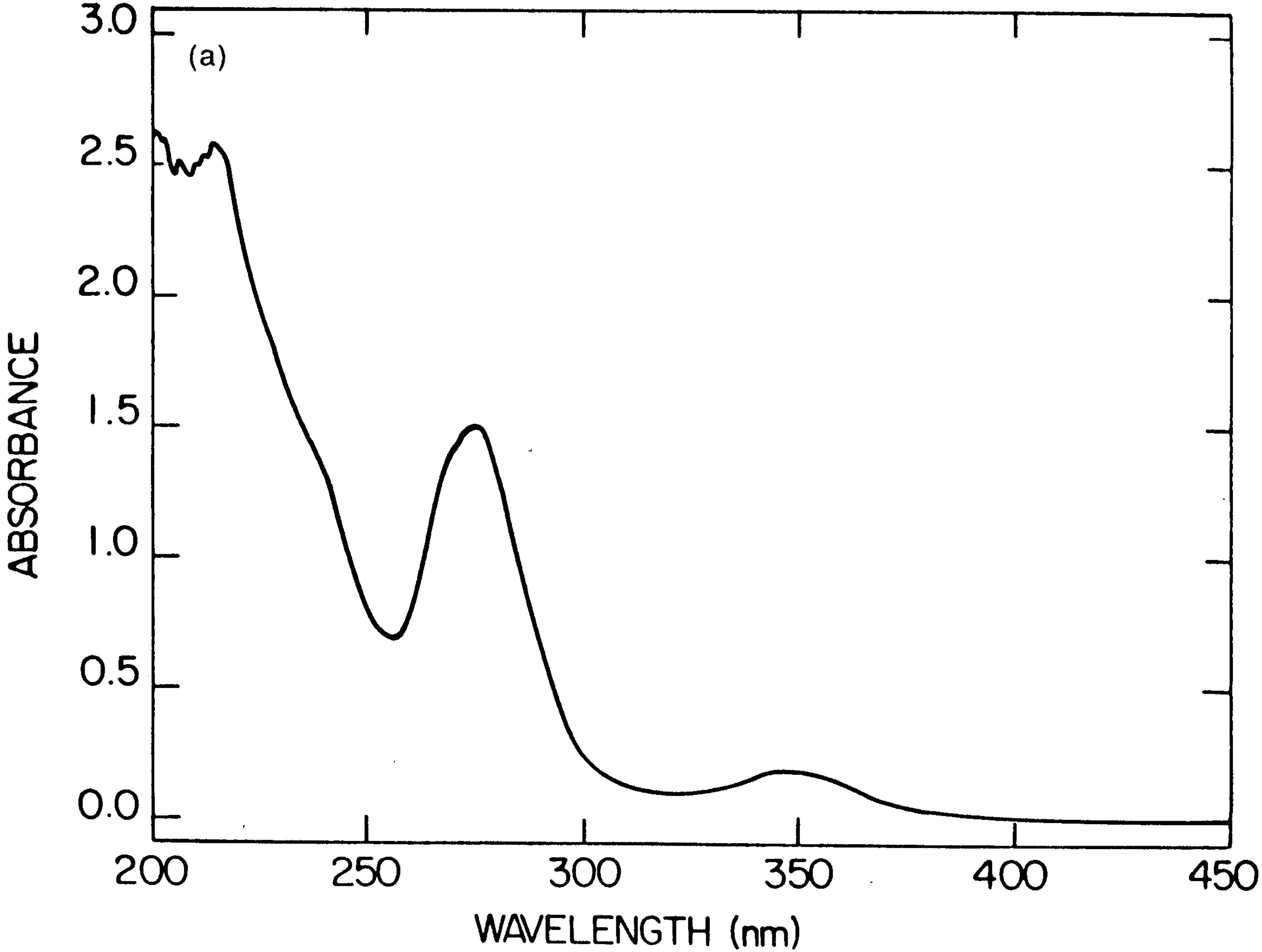
(a)
ABSORBANCE
3.0
2.5
2.0
1.5
1.0
0.5
0.0
200
250
300
350
400
450
WAVELENGTH (nm)

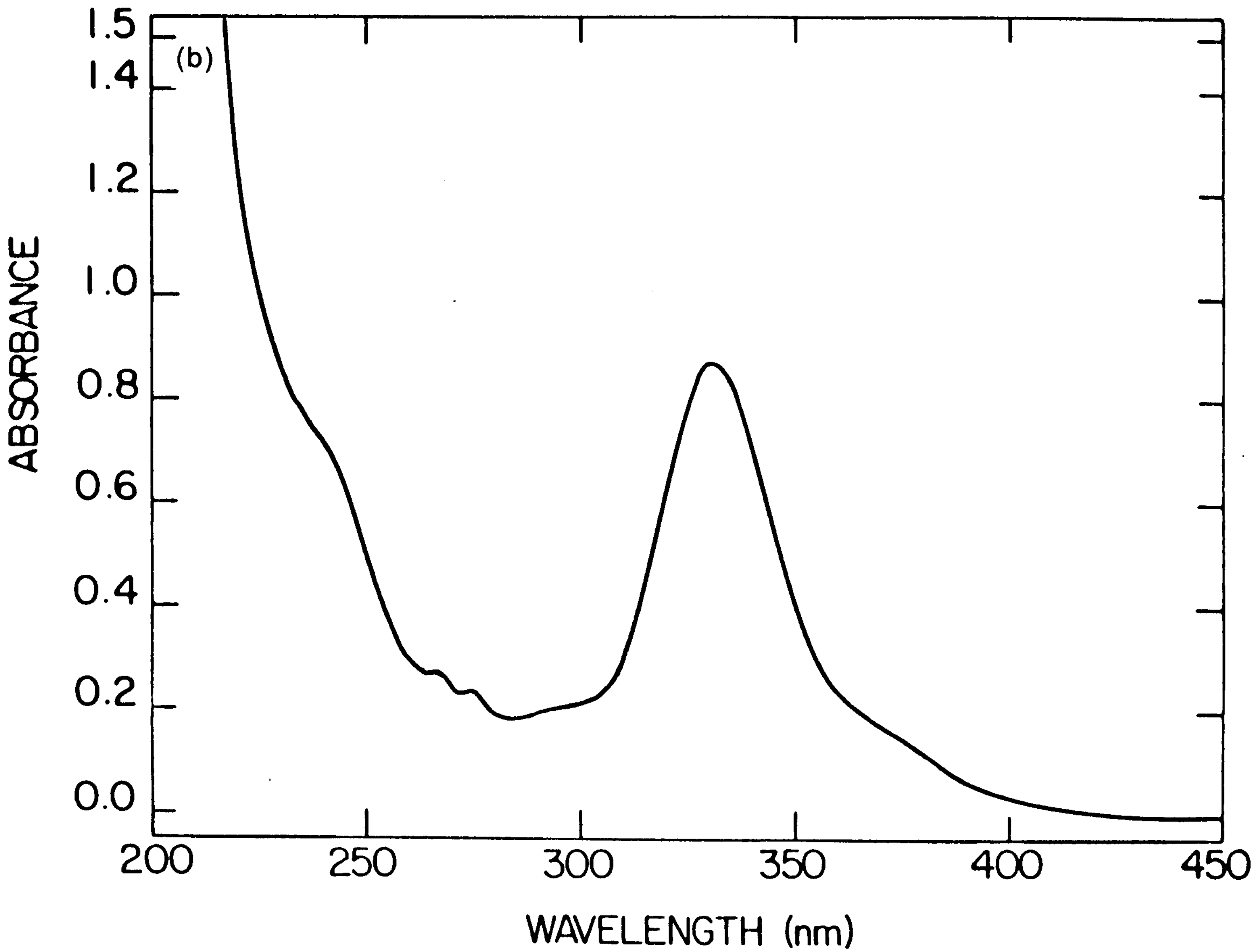
(b)
ABSORBANCE
1.5
1.4
1.2
1.0
0.8
0.6
0.4
0.2
0.0
200
250
300
350
400
450
WAVELENGTH (nm)

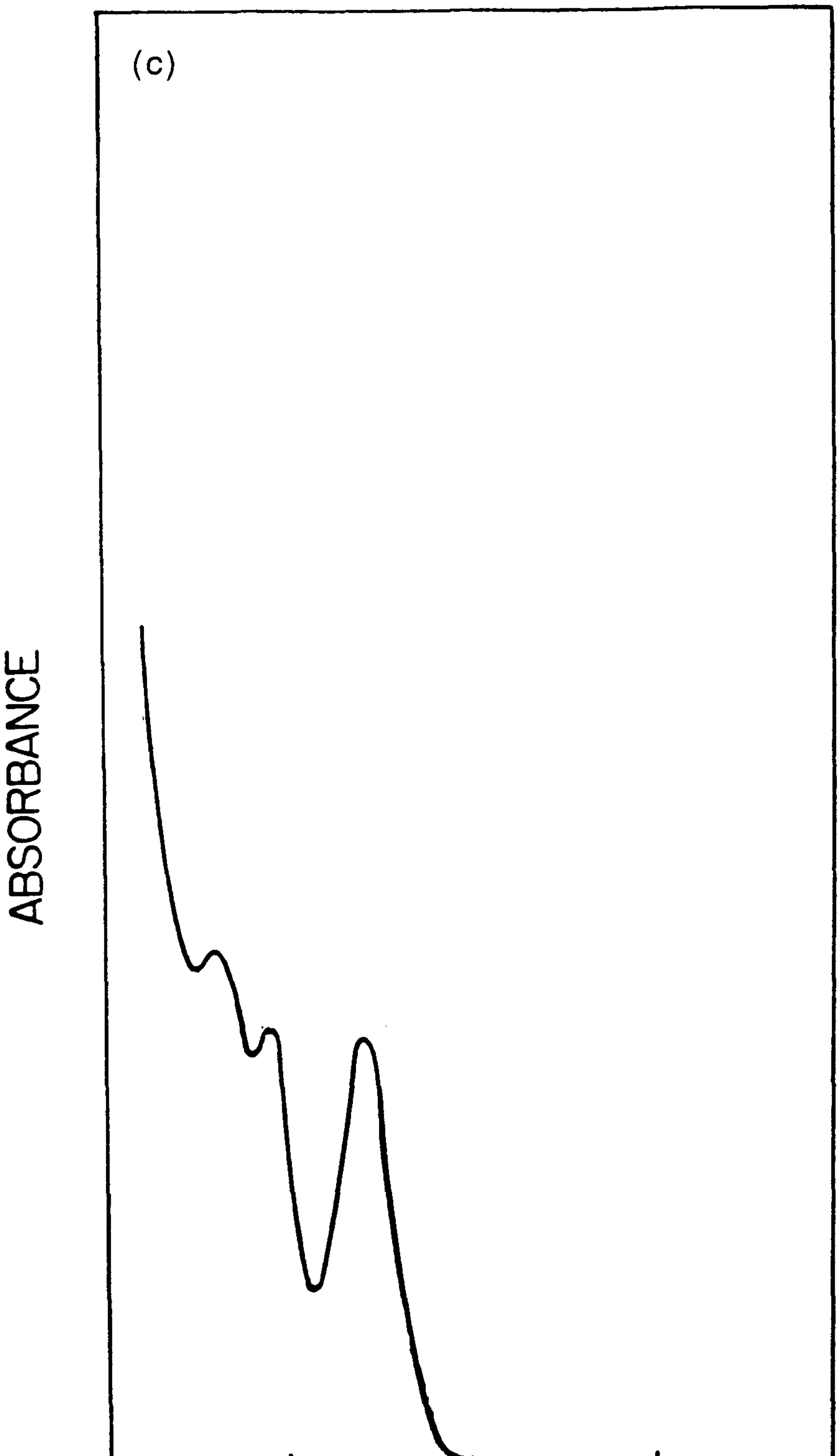
(c)
ABSORBANCE
300
400
500
WAVELENGTH (nm)

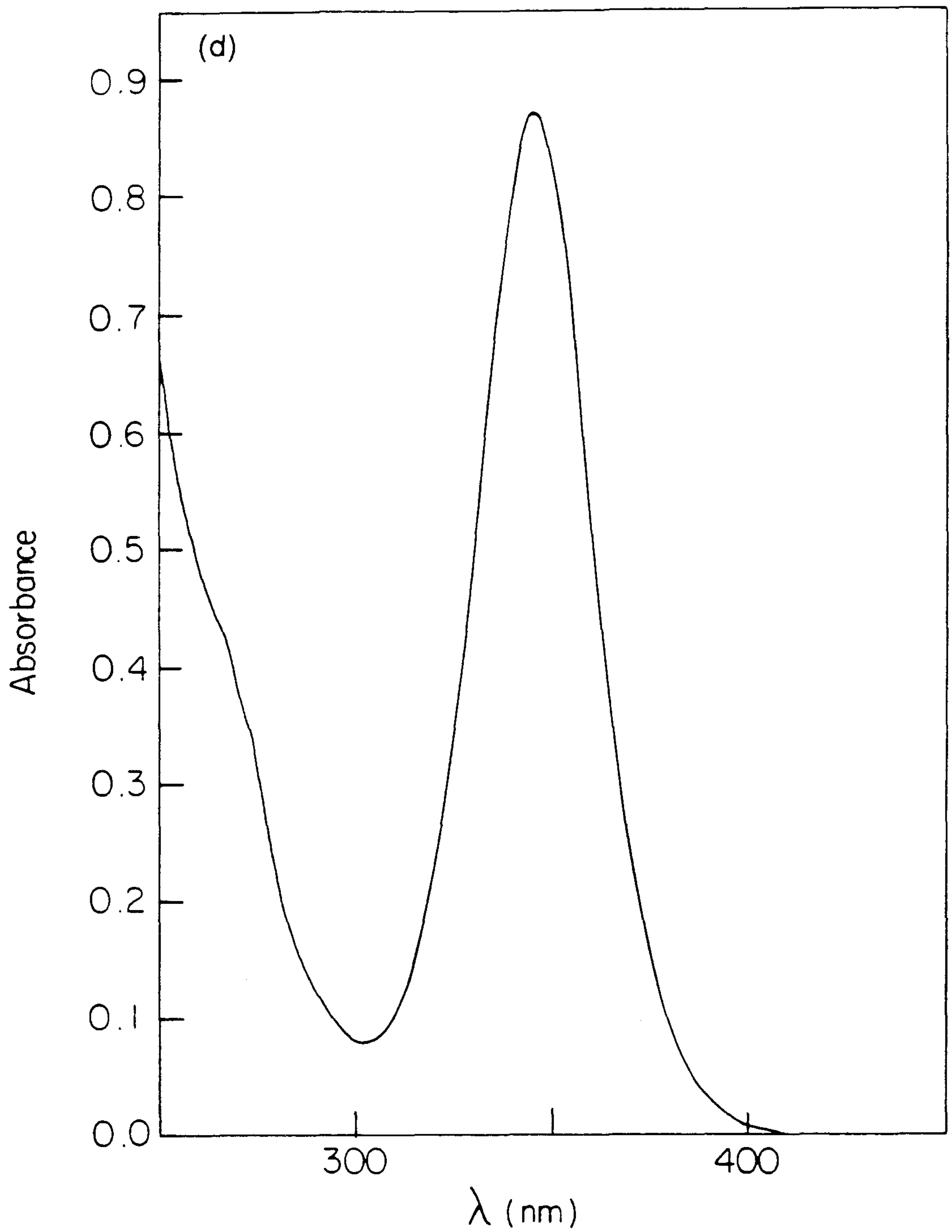
(d)
0.9
0.8
0.7
0.6
0.5
0.4
0.3
0.2
0.1
0.0
Absorbance
300
400
λ (nm)

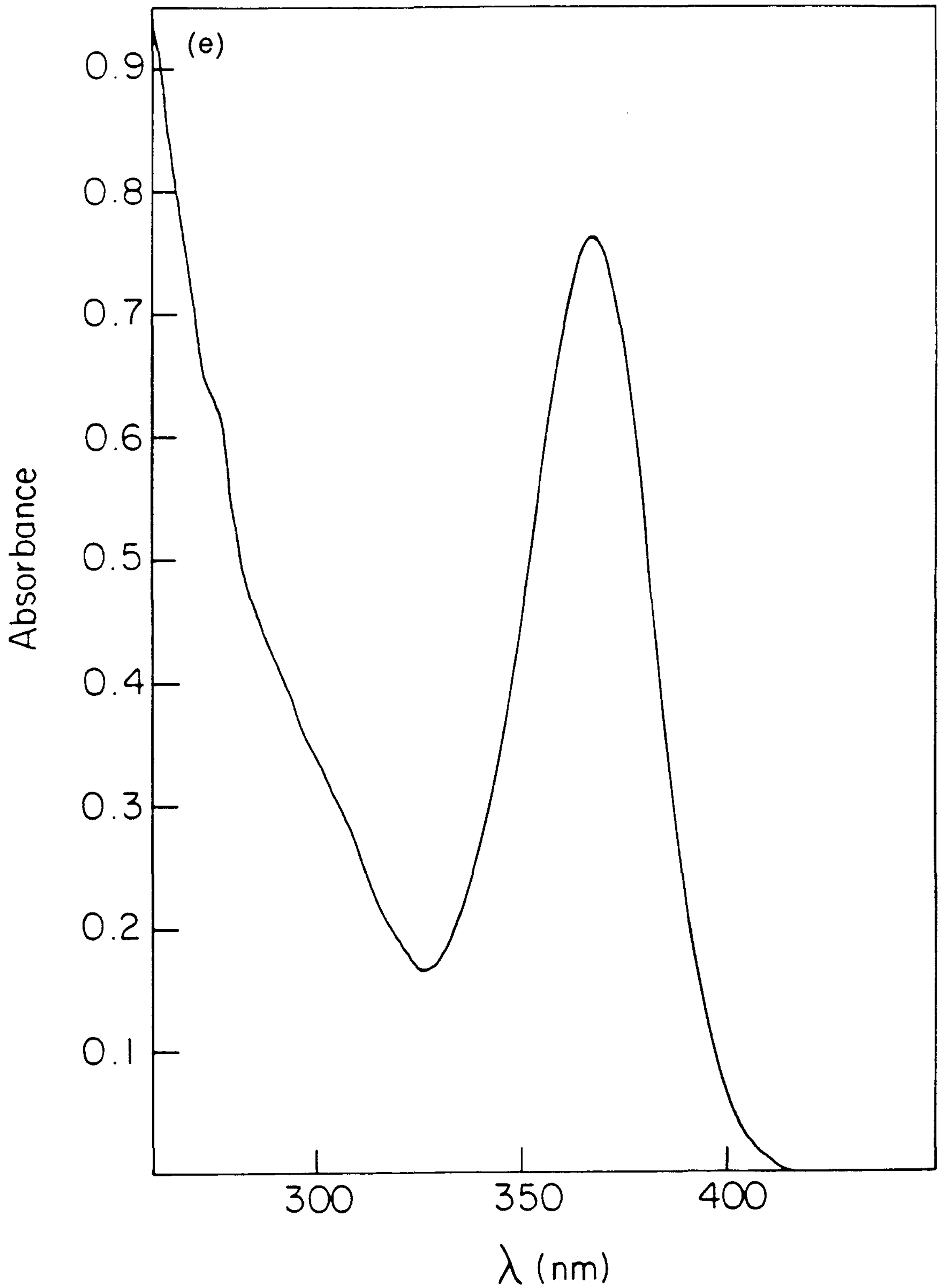
(e)
Absorbance
0.9
0.8
0.7
0.6
0.5
0.4
0.3
0.2
0.1
300
350
400
λ (nm)

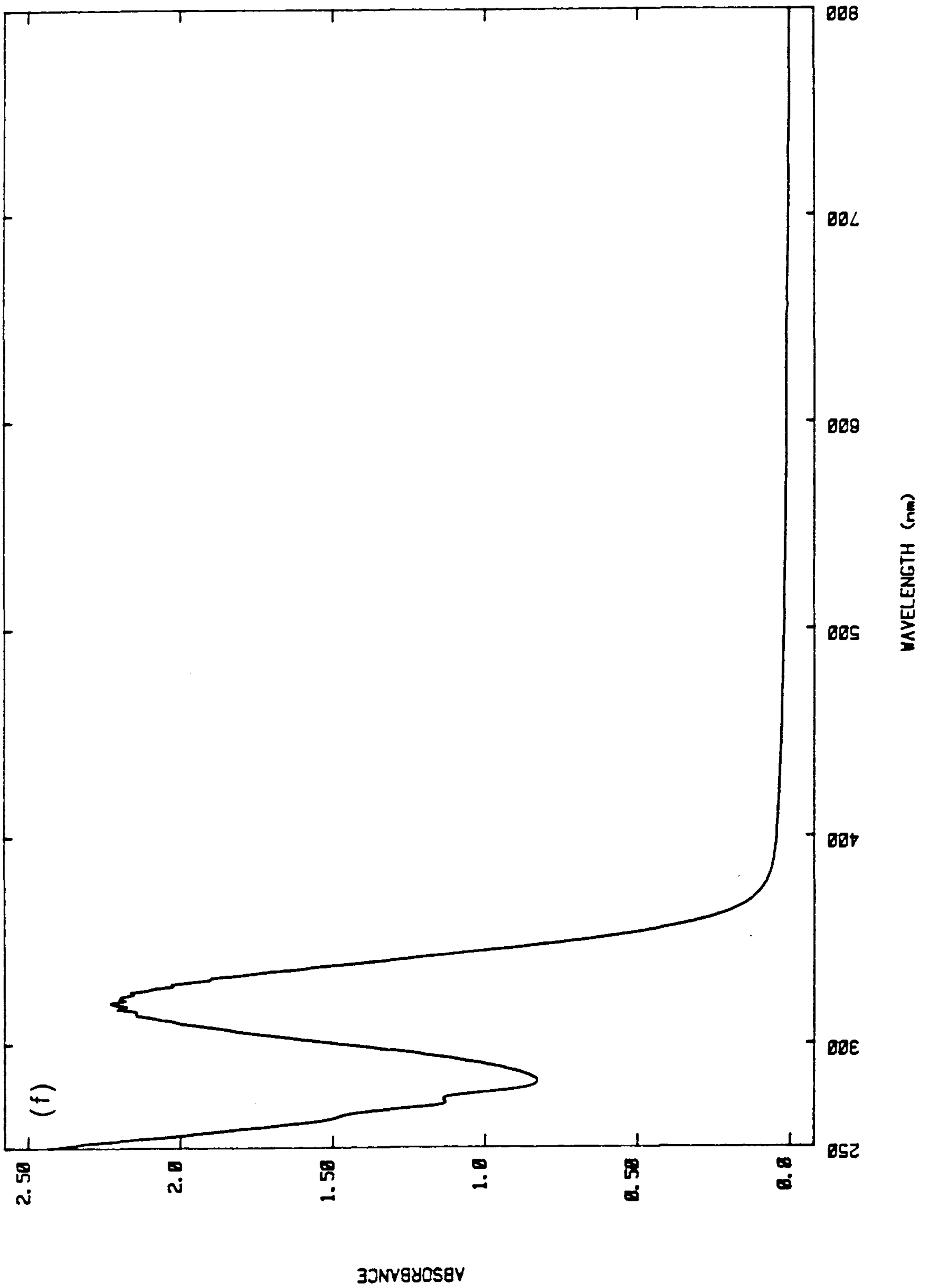
(f)
ABSORBANCE
2.50
2.0
1.50
1.0
0.50
0.0
WAVELENGTH (nm)
250
300
400
500
600
700
800

complexes. Earlier work on the dihalide adducts has assigned the intense high-energy feature to the $d\sigma \rightarrow d\sigma^*$ transition in analogy to $Mn_2(CO)_{10}$. The weak lower-energy feature is attributed to the "$d\pi$" $\rightarrow d\sigma^*$ transition.

Work on axially substituted $M_2(CO)_{10}$ complexes had suggested a correlation between the $d\sigma \rightarrow d\sigma^*$ transition energy and the metal-metal bond strength.[37,38] Additional work on the adducts of the binuclear d^8 complexes suggested a more reasonable explanation for the shift in the $d\sigma \rightarrow d\sigma^*$ energy involving mixing of the metal-metal $d\sigma \rightarrow d\sigma^*$ transition with axial ligand-to-metal charge transfer (LMCT).[4] This is indicated by the orbital mixing diagram in Figure 4.6. For the dihalides, a systematic red shift of the $d\sigma \rightarrow d\sigma^*$ transition is observed through the series Cl, Br, I, a shift with decreasing ionization potential of the axial ligand, an increase in the amount of axial LMCT mixing. Substitution of a hydride for a chloride, $Ir_2(TMB)_4(H)(Cl)^{2+}$, results in a dramatic red shift of the $d\sigma \rightarrow d\sigma^*$ transition, 6700 cm^{-1}. Within the model, this shift can be understood to arise from a significantly greater charge transfer contribution for H^- in comparison to Cl^-. The increased interaction of the hydride ligand with the σ-symmetry combination is evident in comparing the transition energy of Ir_2H_2. In comparison to Ir_2Cl_2, a 5200 cm^{-1} red shift of the $d\sigma \rightarrow d\sigma^*$ transition is observed. The large red shift of the $d\sigma \rightarrow d\sigma^*$ transition with introduction of a strong σ-donating ligand is general for the series of complexes listed in Table 4.2 and can be accounted for within the model presented earlier to describe the electronic structure of M_2^{4+} complexes with two σ-donor axial ligands.

A low-energy feature assignable to the "$d\pi$" $\rightarrow d\sigma^*$ transition is not observed for the hydride and alkyl substituted complexes. This transition may now be roughly isoenergetic with the $d\sigma \rightarrow d\sigma^*$ transition, with the large red shift observed for the latter. Also, the absence of π-symmetry electrons on the ligand may increase the energy of the "$d\pi$" $\rightarrow d\sigma^*$ transition because of the loss of π-CT mixing, a simultaneous blue shift of the "$d\pi$" $\rightarrow d\sigma^*$ transition and red shift of the $d\sigma \rightarrow d\sigma^*$ transition. For [Ir(μ-

Figure 4.6. Molecular orbital diagram for interaction of M_2^{4+} with two σ-donor axial ligands.

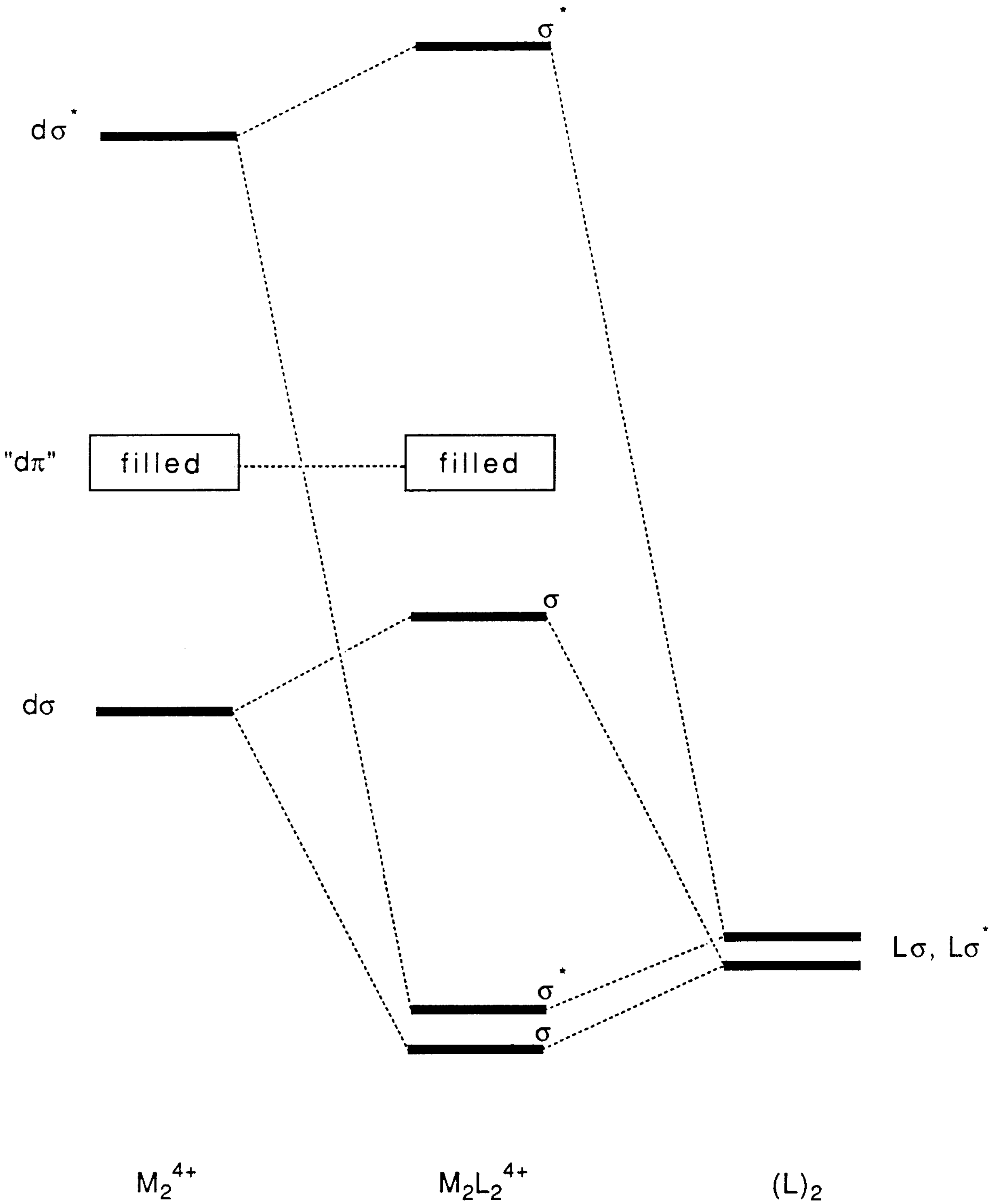

dσ*
"dπ"
filled
filled
dσ
σ*
σ
σ*
σ
Lσ, Lσ*
M2 4+
M2L2 4+
(L)2

pz)COD(X)]$_2$ complexes, it has been suggested that the d$\sigma \rightarrow$ pσ^* transition is to lower energy of the "dπ" $\rightarrow$ dσ^* transition.[39]

Electrochemistry

Little is known about the electrochemistry of Ir(I) isocyanide complexes. Much of the work in the literature has focused on Ir(I) phosphine complexes.[40-42] Earlier work on the $Ir_2(TMB)_4^{2+}/Ir_2(TMB)_4^{+}$ couple found a quasi-reversible reduction at -1.15 V (SCE) in CH_3CN.[3] This reduction was found to be complicated by follow-up chemistry, which was thought to involve interaction between dimer units. No reference to the oxidation of $Ir_2(TMB)_4^{2+}$ was made in this work.

The cyclic voltammogram (CV) of $[Ir_2(TMB)_4](B(C_6H_5)_4)_2$ in CH_2Cl_2 (0.1 M $TBAPF_6$) is shown in Figure 4.7. CH_2Cl_2 was chosen over CH_3CN as a solvent because earlier work had shown that the oxidation chemistry of binuclear d^8 complexes was complicated by ECE processes in coordinating solvents.[43] The wave at +0.95 V (SSCE) is associated with the oxidation of the $B(C_6H_5)_4^-$ counter ion. This observation was confirmed by independent study of $NaB(C_6H_5)_4$. The broad wave at +0.63 V (SSCE) is associated with the oxidation of $Ir_2(TMB)_4^{2+}$. This feature appears very irreversible on the electrochemical time scale with no reversible component observed up to scan rates of 100 V/s. The fast-sweep experiments are, however, not conclusive because of experimental difficulties. The value of the $Ir_2(TMB)_4^{2+}$ oxidation was found to vary 100 mV between experiments. The weak feature at -0.4 V (SSCE) is associated with the oxidation at +0.63 V. This observation was made by reversing the scan direction and by probing only the first oxidation wave. No features were observed in this region for $NaB(C_6H_5)_4$. The wave at -1.25 V (SSCE) is associated with the reduction of $Ir_2(TMB)_4^{2+}$. There was no change in the CV with variation in solvent (CH_2Cl_2 and $(CH_3)_2CO$).

Figure 4.7. Cyclic voltammogram of $[Ir_2(TMB)_4](B(C_6H_5)_4)_2$ (1 mM) in CH_3CN (0.1 M $TBAPF_6$).

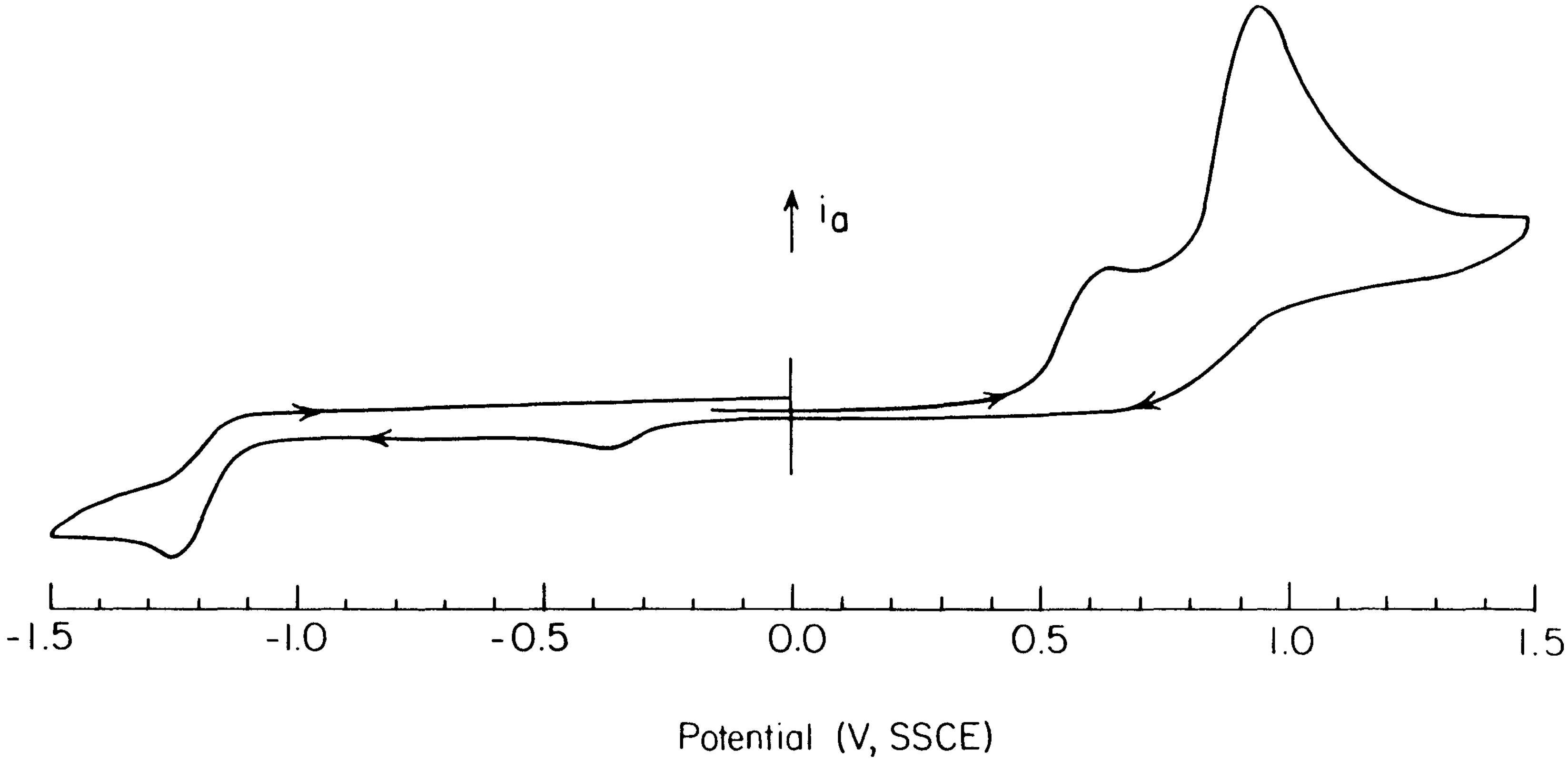

i_a
-1.5
-1.0
-0.5
0.0
0.5
1.0
1.5
Potential (V, SSCE)

A possible explanation as to why this couple is so irreversible is suggested by the work of Geiger.[44,45] The oxidation of $Ir_2(TMB)_4^{2+}$ will result in a contraction of the metal-metal distance. If the structural rearrangements between the reactants and the products are concerted with the actual electron transfer, an increased energy barrier to electron transfer is expected. If the reorganization energy is of moderate or large magnitude, a quasi-reversible or irreversible electrode reaction will be observed. Another more likely explanation for the irreversible electrochemistry observed for $Ir_2(TMB)_4^{2+}$ is a rapid associative chemical step following the initial oxidation.

$$Ir_2(TMB)_4^{2+} \rightarrow Ir_2(TMB)_4^{3+} + e^- \quad 4.1$$

$$Ir_2(TMB)_4^{3+} + Y \rightarrow Ir_2(TMB)_4^{3+}\bullet\bullet\bullet Y \quad 4.2$$

$$Ir_2(TMB)_4^{3+}\bullet\bullet\bullet Y \rightarrow Ir2(TMB)_4^{4+}\bullet\bullet\bullet Y + e^- \quad 4.3$$

The intermediate formed (Equation 4.2), being more easily oxidized than $Ir_2(TMB)_4^{2+}$, is rapidly oxidized (Equation 4.3), an ECE process. At present no information toward this end is available.

With knowledge of the ground-state thermodynamics and values for the excited-state energies, an estimate of the excited-state redox potentials can be made.[46,47]

$$E^0(M^+/^*M) = E^0(M^+/M) - E_{00}(M/^*M) \quad 4.4$$

$$E^0(^*M/M^-) = E^0(M/M^-) + E_{00}(M/^*M) \quad 4.5$$

Excited-state potentials can also be estimated from kinetic studies of electron-transfer quenching reactions involving a series of acceptors and/or donors with varying potentials.

Because of the irreversibility of the $Ir_2(TMB)_4^{3+}/Ir_2(TMB)_4^{2+}$ couple, attempts to estimate the excited-state reduction potentials are very problematic. Using an average value of the E_p(oxidation), a modified Latimer diagram can be completed, which describes the excited-state redox potentials (Figure 4.8). The $^1A_{2u}$ and $^3A_{2u}$ excited states are, as expected, much more powerful reductants and oxidants than the ground state. One of the major assumptions in this analysis is that the entropy changes associated with the redox processes and excitation are small compared to the enthalpy changes. The excited-state reduction potentials, because of the uncertainty of the $Ir_2(TMB)_4{}^{3+}/Ir_2(TMB)_4{}^{2+}$ couple, are only upper bounds of the true values. In comparison to other binuclear d^8 complexes, the excited-state reduction potential of $Ir_2(TMB)_4{}^{2+}$ is on the low end of the energy scale (Table 4.3 and Figure 4.9).

In subsequent sections, the ability of the $^3(d\sigma^*p\sigma)$ excited state of $Ir_2(TMB)_4{}^{2+}$ to carry out various chemical conversions will be studied. It will be found that while the excited state is a far superior reductant than the ground state, the photochemical reactions follow an atom-transfer pathway. This conclusion will be found to be general for binuclear d^8 complexes.

Figure 4.8. Modified Latimer diagrams for $Ir_2(TMB)_4^{2+}$ describing the reduction energies for the $^1(d\sigma^*p\sigma)$ and $^3(d\sigma^*p\sigma)$ excited states.

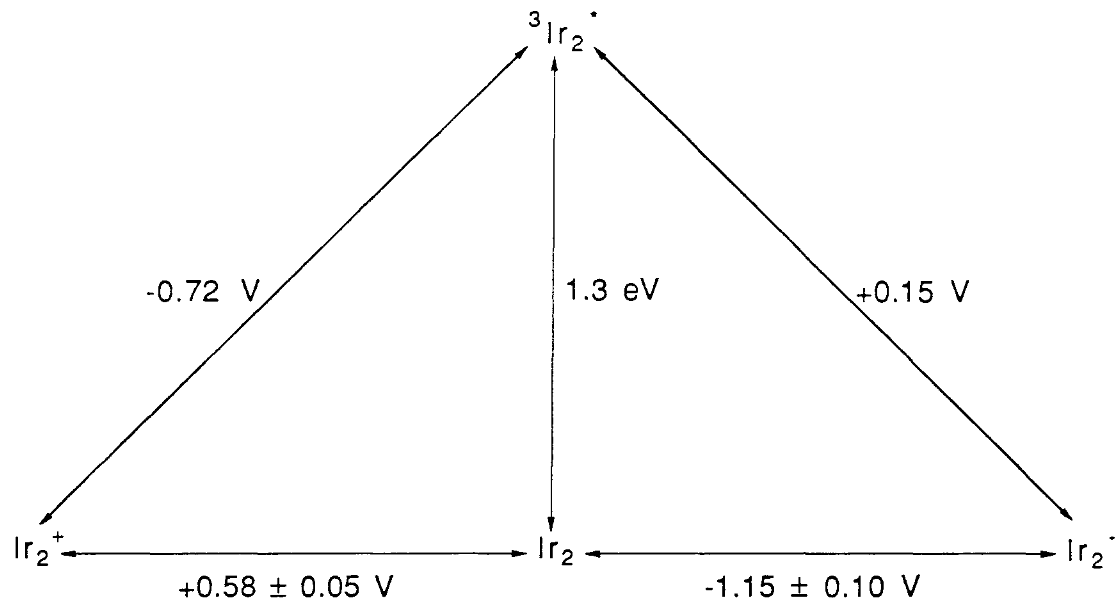
$^{3}Ir_2^{*}$
-0.72 V
1.3 eV
+0.15 V
Ir_2^{+}
Ir_2
Ir_2^{-}
+0.58 ± 0.05 V
-1.15 ± 0.10 V

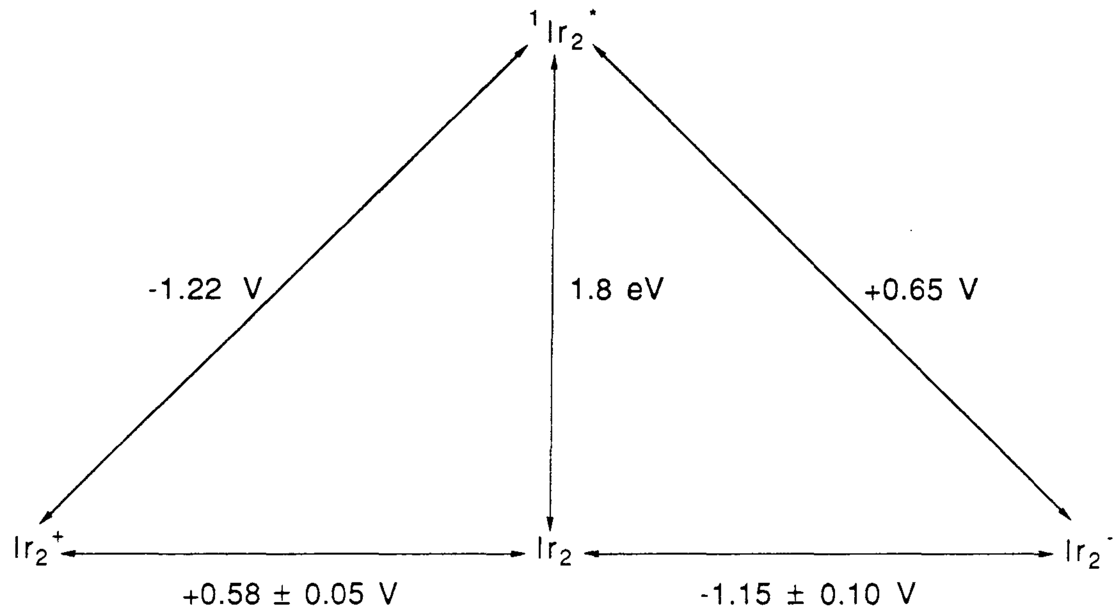
$^{1}Ir_2^{*}$
-1.22 V
1.8 eV
+0.65 V
Ir_2^{+}
Ir_2
Ir_2^{-}
+0.58 ± 0.05 V
-1.15 ± 0.10 V

Table 4.3. Excited state reduction potentials for binuclear d^8 complexes.

Metal Complex	$E^0(M_2^+/^3M_2^*)$, V (SSCE)	$E^0(M_2^+/^1M_2^*)$, V (SSCE)	Ref.
$Ir_2(TMB)_4^{2+}$	-0.72	-1.22	a
$Rh_2b_4^{2+}$	< -0.8	< -1.3	48
$Rh_2(TMB)_4^{2+}$	-1.03	-1.4	a
$[Ir(\mu\text{-}pz)COD]_2$	-1.75	-2.2	49
$Pt_2(P_2O_5H_2)_4^{4-}$	-2.24	< -2.7	49

a. This work.

Figure 4.9. Reduction potentials for the $^3(d\sigma^*p\sigma)$ excited state of binuclear d^8 complexes and alkyl halides.

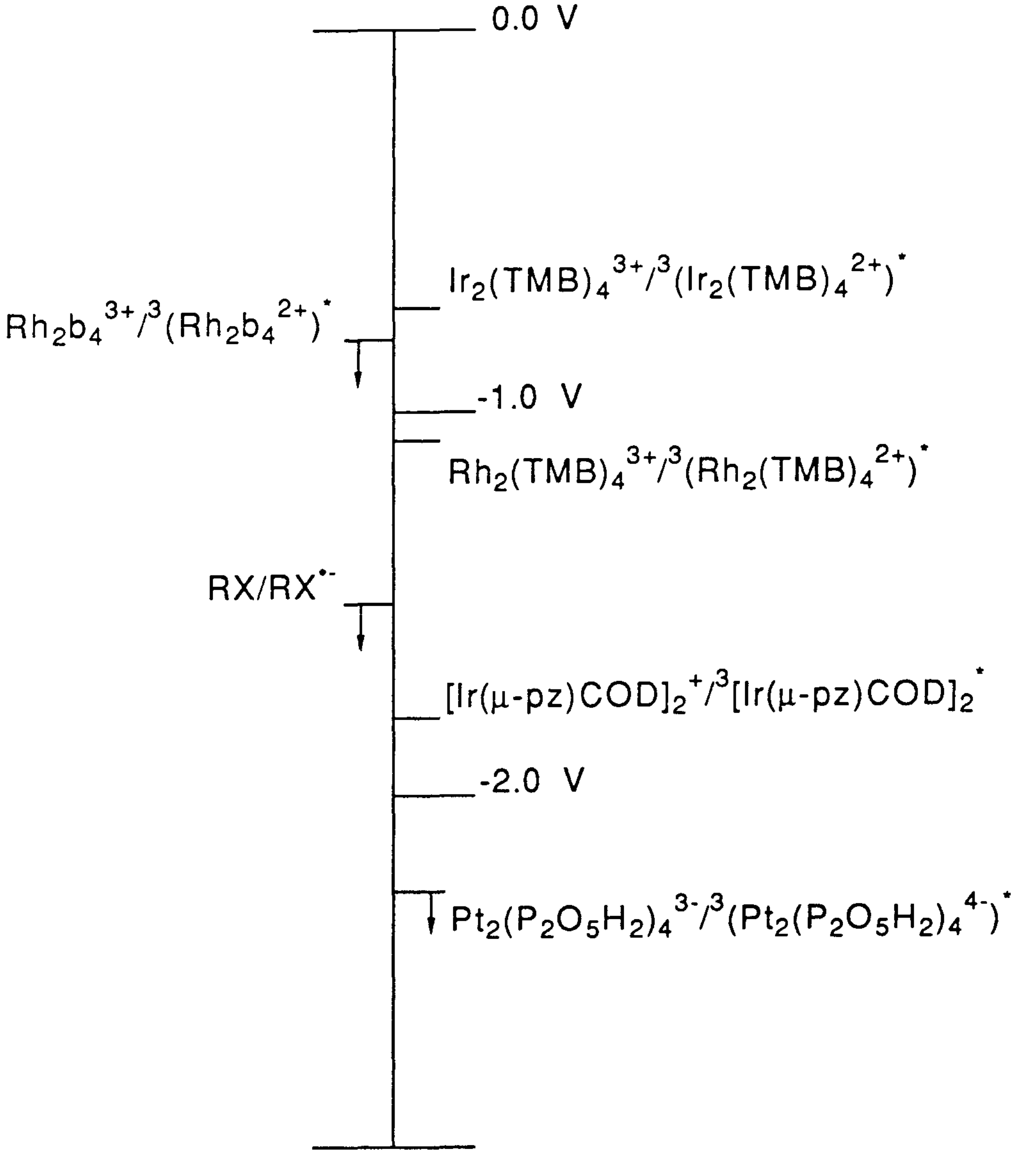
0.0 V
$Ir_2(TMB)_4{}^{3+}/{}^3(Ir_2(TMB)_4{}^{2+})^*$
$Rh_2b_4{}^{3+}/{}^3(Rh_2b_4{}^{2+})^*$
-1.0 V
$Rh_2(TMB)_4{}^{3+}/{}^3(Rh_2(TMB)_4{}^{2+})^*$
$RX/RX^{\bullet-}$
$[Ir(\mu\text{-}pz)COD]_2{}^+/{}^3[Ir(\mu\text{-}pz)COD]_2{}^*$
-2.0 V
$Pt_2(P_2O_5H_2)_4{}^{3-}/{}^3(Pt_2(P_2O_5H_2)_4{}^{4-})^*$

Photochemical and Electrocatalytic Reactions of Binuclear d^8 Complexes

Introduction

An electronic excited state of a metal complex is both a stronger reductant and a stronger oxidant than the ground state.[46] Excitation of an electron from a low-energy to a high-energy orbital reduces the ionization potential and increases the electron affinity of a molecule (Figure 4.10). Therefore, complexes with relatively long-lived excited states can participate in intermolecular electron-transfer reactions that are uphill for the corresponding ground-state species. Such excited-state electron-transfer reactions often play key roles in multistep schemes for the conversion of light to chemical energy.[50]

While electron-transfer processes are common in inorganic photochemistry, excited-state atom transfer is limited to a small class of inorganic complexes. For UO_2^{2+}, the diradical excited state (•U-O•) is active in alcohol oxidation.[51] The primary photoprocess is hydrogen-atom abstraction by the oxygen-centered radical. Photoaddition to a metal center via atom transfer has been observed for binuclear metal complexes such as $Re_2(CO)_{10}$.[52-55] The primary photoprocess is metal-metal bond homolysis. The photogenerated metal radical undergoes thermal atom-abstraction reactions. Until recently, atom transfer to a metal-localized excited state had not been observed.

Atom transfer to a metal complex is facilitated if localized electron or hole generation occurs at one or more open coordination sites. Binuclear d^8 complexes have been found to undergo photochemical atom transfer to one of the metal centers.[2,30,49,56] These complexes possess open coordination sites in addition to an electronic structure that localizes the electron (hole) necessary for atom transfer to the metal center.

The lowest energy optical transition for the binuclear systems is $d\sigma^* \rightarrow p\sigma$. This excitation results in formation of a formal metal-metal single bond in the excited state. The transition is metal-localized and can be viewed as movement of an electron from an

Figure 4.10. Schematic orbital diagram showing the decrease in the ionization potential and increase in the electron affinity upon excitation of a molecule.

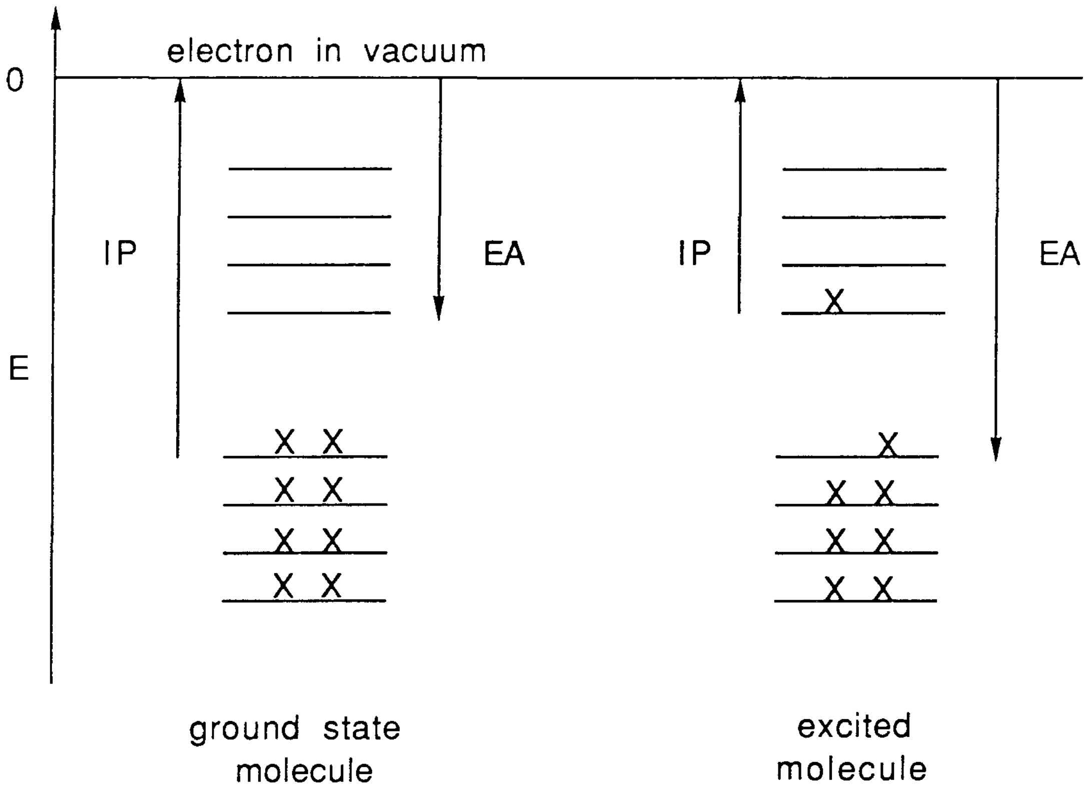
electron in vacuum
0
E
IP
EA
IP
EA
ground state
molecule
excited
molecule

orbital localized on the exterior of the M_2 unit (the $d\sigma^*$ orbital) to an orbital localized in the interior of the dimer cage (the $p\sigma$ orbital). The excitation results in hole formation localized on a metal center at an open coordination site (Figure 4.11). The lifetime of the $^3(d\sigma^*p\sigma)$ excited state, normally in between 100 ns and 10 μs, makes M_2 systems attractive for bimolecular photoprocesses.

The initial interest in these systems was stimulated by observations of their photochemical electron-transfer reactivity.[48,49] From spectroscopic and electrochemical studies, the $^3(d\sigma^*p\sigma)$ excited state is predicted to be a powerful reductant, with $E^0(M_2^+/^3M_2^*)$ estimated to range from -0.8 to -2.0 V vs SSCE in CH_3CN. That this state is a powerful reductant has been confirmed by investigation of the electron-transfer quenching of $^3M_2^*$ by a series of pyridinium acceptors with varying reduction potentials.[57] For several binuclear complexes, the excited-state reduction potential cannot be calculated accurately because of the irreversibility of the ground-state electrochemistry; but it can be estimated from bimolecular electron-transfer quenching experiments.

For systems that are powerful excited-state reductants, photoreduction of alkyl halides is observed.[49,58] This reaction was initially interpreted to be an outer-sphere electron transfer to form an alkyl halide radical anion, which rapidly decomposes to yield R· and X^-. Subsequent thermal reactions give the observed products, an $S_{RN}1$ mechanism (Figure 4.12). While such a mechanism, $S_{RN}1$, appears plausible for a metal complex with $E^0(M_2^+/^3M_2^*) < -1.5$ V (SSCE), it seems unlikely for complexes with $E^0(M_2^+/^3M_2^*) > -1.0$ V (SSCE). Reduction potentials for alkyl halides of interest are generally more negative than -1.5 V (SSCE).[59] Alkyl-halide photoreduction is observed for binuclear d^8 complexes whose excited-state reduction potentials are more positive than -1.0 V (SSCE) in CH_3CN.

An alternative pathway to outer-sphere electron transfer, which yields similar photoredox products with alkyl halides, is excited-state atom transfer (Figure 4.13).

Figure 4.11. Pictorial representation of the M_2-localized hole in a $^3(d\sigma^*p\sigma)$ state.

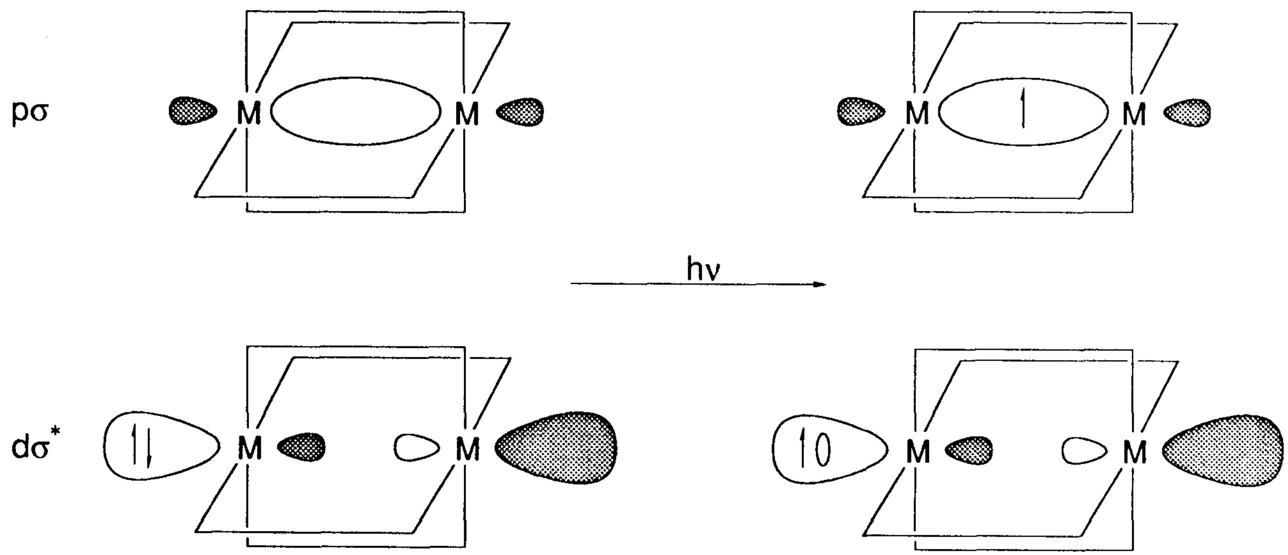
pσ
dσ*
M
M
hν

Figure 4.12. $S_{RN}1$ mechanistic scheme for halocarbon photooxidative addition to binuclear d^8 complexes.

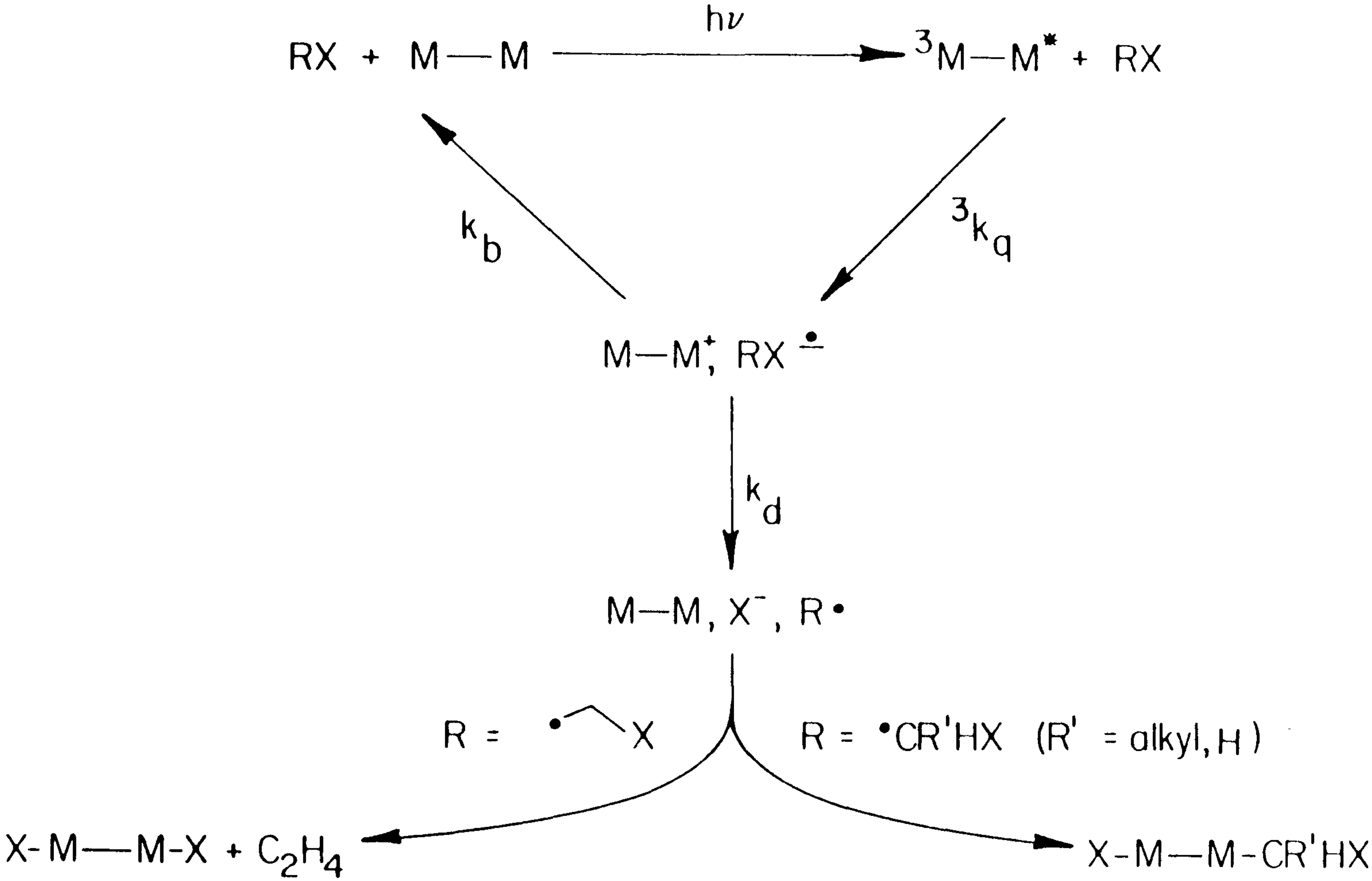
RX + M—M
hν
³M—M* + RX
³k_q
k_b
M—M⁺, RX⁻
k_d
M—M, X⁻, R•
R = •CR'HX (R' = alkyl, H)
X-M—M-X + C₂H₄
X-M—M-CR'HX

Figure 4.13. Atom-transfer mechanism for halocarbon photooxidative addition.

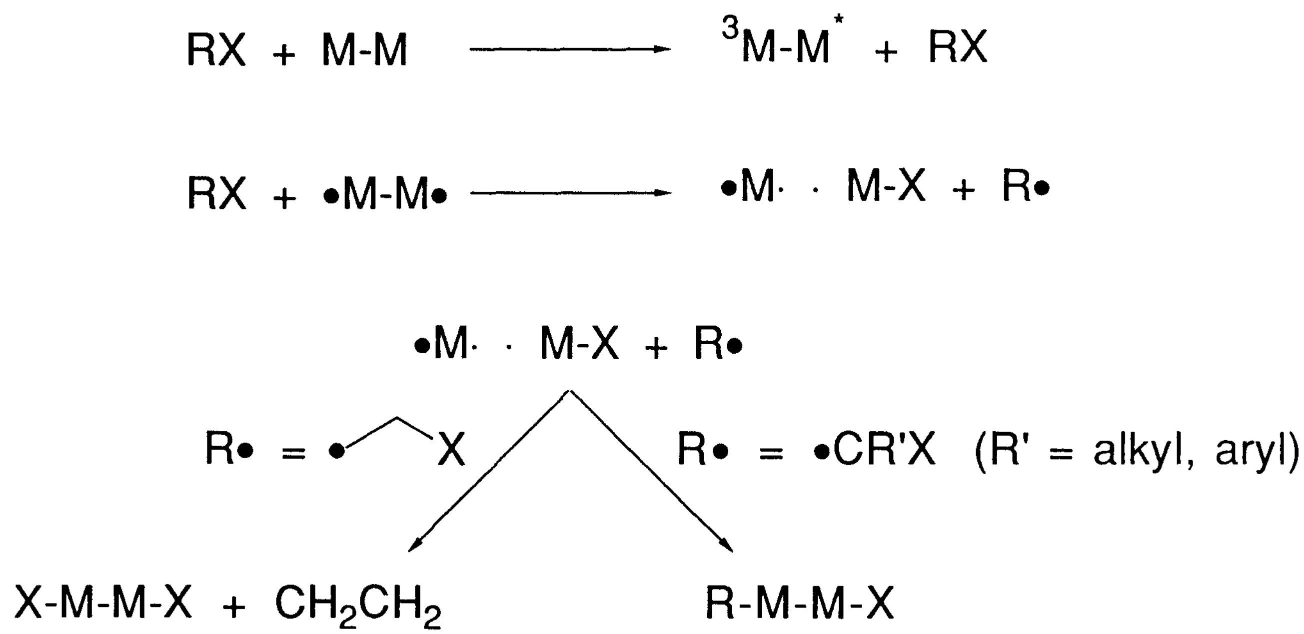
RX + M-M → ³M-M* + RX
RX + •M-M• → •M· · M-X + R•
•M· · M-X + R•
R• = •CH2CH2X
R• = •CR'X (R' = alkyl, aryl)
X-M-M-X + CH2CH2
R-M-M-X

Data obtained for $Pt_2(P_2O_5H_2)_4^{4-}$ indicate that alkyl and aryl halides react with the $^3(d\sigma^*p\sigma)$ excited state via halogen-atom transfer.[2]

Although the primary photoprocess for alkyl-halide photoreduction may not be atom transfer in all cases, $^3(d\sigma^*p\sigma)$ excited-state hydrogen-atom transfer has been established as the mechanism of the reactions between several binuclear d^8 complexes and a number of organic and organometallic substrates.[2,29,49,56] Initial work in this area focused on $Pt_2(P_2O_5H_2)_4^{4-}$, for which the catalytic conversion of isopropanol to acetone (Equation 4.6) had been first observed.[60]

$$Pt_2(P_2O_5H_2)_4^{4-} + (CH_3)_2CHOH \xrightarrow{h\nu} Pt_2(P_2O_5H_2)_4^{4-} + H_2 + (CH_3)_2CO \qquad 4.6$$

From detailed studies of this system, it was concluded that the primary photoprocess is abstraction of the α-hydrogen by the $^3Pt_2^*$ to form a monohydride species (directly observed by transient absorption spectroscopy for a number of substrates) and the organic radical (Equation 4.7), with the final photoproduct being Pt_2H_2 and acetone (Equation 4.8). The Pt_2H_2 complex has been characterized by NMR, UV-Vis, and IR (but has not been successfully isolated).[61]

$$^3Pt_2^* + (CH_3)_2CHOH \rightarrow Pt_2H + (CH_3)_2COH \qquad 4.7$$

$$Pt_2H + (CH_3)_2COH \rightarrow Pt_2H_2 + (CH_3)_2CO \qquad 4.8$$

The relatively long lifetime of the $^3(d\sigma^*p\sigma)$ excited state of $Ir_2(TMB)_4^{2+}$ in fluid solution suggests that it should be able to participate in bimolecular photochemical reactions. In light of the favorable absorption and emission properties of this complex, it is of interest to examine the possibility of the conversion of visible light to net chemical energy through a photochemical process, either electron transfer or atom transfer. The excited-state electron-transfer reactivity of $Ir_2(TMB)_4{}^{2+}$ with pyridinium acceptors is reported and analyzed in the context of classical Marcus theory for outer-sphere electron transfer. The photochemical reactions of $Ir_2(TMB)_4{}^{2+}$ with alkyl halides and hydrogen atom donors are reported.

Experimental

Synthesis

Pyridinium Hexafluorophosphates

All solvents were from freshly opened bottles with no further purification. All chemicals were of reagent grade or comparable quality and used as received. The ^1H NMR spectra were obtained on a 90 MHz EM-390 spectrometer. Elemental analyses were obtained at the Cal Tech Analytical Laboratory.

Several of the pyridinium hexafluorophosphates were prepared and recrystallized by Dr. Janet L. Marshall[39] and used as received. Methyl viologen di(hexafluorophosphate) was received from Dr. Miriam A. Heinrichs.

4-CN-N-Benzylpyridinium

A slight excess of benzyl bromide was added to an acetone solution of 4-CN-pyridine. After refluxing for 10 hrs, the solution was cooled to room temperature and the precipitated pyridinium halide was filtered off. The yellow powder was dissolved in a minimum of distilled water and metathesized with KPF_6. The precipitated pyridinium hexafluorophosphate was filtered off and recrystallized from acetone. Calculated for $C_{13}H_{11}NPF_6$: C, 45.9; H, 3.3; N, 8.2. Found: C, 45.8; H, 3.4; N, 8.4. ^1H NMR: δ (CD_3CN, 20 °C); 5.8 (singlet, 2H, CH_2), 7.5 (singlet, 5H, C_6H_5), 8.4 (multiplet, 2H, 3,5-H), 8.9 (doublet, 2H, 2,6-H).

3-CN-N-Methylpyridinium

A tenfold excess of methyl iodide was added to a stirred THF solution of 3-cyanopyridine. The solution was stirred for 48 hrs. The precipitated pyridinium iodide was filtered off and washed with THF. The yellow powder was dissolved in distilled water and metathesized with NH_4PF_6. The white precipitate was recrystallized from

H_2O/acetone/ethanol (2:1:1). Calculated for $C_7H_7N_2PF_6$: C, 31.8; H, 2.7; N, 10.6. Found: C, 32.0; H, 2.6; N, 10.6.

3-Carbomethoxy-N-Benzylpyridinium

A fivefold excess of benzyl chloride was combined with methyl nicotimate in a 1:1 ethanol/acetone solution. The solution was refluxed for 10 hrs. No solid material precipitated upon cooling to room temperature. The solvent was removed under vacuum, yielding a viscous oil. The oil was dissolved in a minimum of distilled water and metathesized with KPF_6. The white precipitate was recrystallized from methanol. Calculated for $C_{14}H_{14}NO_2PF_6$: C, 45.1; H, 3.8; N, 3.8. Found: C, 45.2; H, 3.8; N, 3.8. ^1H NMR: δ (CD_3CN, 20 °C); 3.9 (singlet, 3H, CH_3), 5.8 (singlet, 2H, CH_2), 7.5 (singlet, 5H, C_6H_5), 8.1 (triplet, 1H, 5-H), 8.9 (multiplet, 2H, 4,6-H), 9.3 (singlet, 1H, 2-H).

3-Carbomethoxy-N-Methylpyridinium

A tenfold excess of methyl iodide was added to a THF solution of methyl nicotimate. After stirring the solution overnight, the precipitated pyridinium iodide was filtered off and washed with THF. The yellow powder was dissolved in a minimum of distilled water and metathesized with NH_4PF_6. The white precipitate was recrystallized from H_2O/acetone/ethanol (2:1:1). Calculated for $C_8H_{10}NO_2PF_6$: C, 32.2; H, 3.4; N, 4.7. Found: C, 32.2; H, 3.1; N, 4.8. ^1H NMR: δ (CD_3CN, 20 °C); 4.0 (singlet, 3H, OCH_3), 4.4 (singlet, 3H, NCH_3), 8.1 (triplet, 1H, 5-H), 8.8 (multiplet, 2H, 4,6-H), 9.2 (singlet, 1H, 2-H).

Additional Compounds

Standard synthetic procedures were used to prepare $[Ir_2(TMB)_4](B(C_6H_5)_4)_2$,[62] $[Rh_2b_4](B(C_6H_5)_4)_2$,[63] and $[Rh_2(TMB)_4](PF_6)_2$.[64]

Physical Measurements

Materials

All solvents were purified, if necessary, degassed with a minimum of five freeze-pump-thaw cycles on a high-vacuum line, and bulb-to-bulb distilled into glass, round-bottomed storage flasks equipped with Teflon vacuum valves. Acetonitrile was used as received and stored over activated alumina. 1,2-Dichloroethane was distilled from CaH_2 and stored over activated molecular sieves. Dichloromethane was distilled from CaH_2 and stored under argon. The halocarbon solvents' storage flasks were wrapped in foil to prevent exposure to room light. 1,4-Cyclohexadiene was distilled from $NaBH_4$ under argon, freeze-pump-thaw degassed,and stored under vacuum, protected from light. Cyclohexene was distilled from either CaH_2 or Na, freeze-pump-thaw degassed, and stored under vacuum, protected from the light. 9,10-Dihydroanthracene was recrystallized three times from absolute ethanol. Cyclohexene-d_{10} was used as received. All other hydrocarbon quenchers were purified by standard methods,[22,23] freeze-pump-thaw degassed, and stored, protected from light, under vacuum or argon.

Tetra-*n*-butyl ammonium hexafluorophosphate was prepared from tetra-*n*-butyl ammonium iodide and ammonium hexafluorophosphate by addition of a hot, saturated, acetone solution of NH_4PF_6 to a hot, saturated, acetone solution of Bu_4NI. To this hot solution was added a large excess of distilled water. The solution was cooled and filtered. The precipitated Bu_4NPF_6 ($TBAPF_6$) was recrystallized three times from 95% ethanol.

Electrochemistry

Cyclic voltammograms (CVs) and constant potential bulk electrolysis were performed using a Princeton Applied Research (PAR) model 173 potentiostat/galvanostat, a model 175 universal programmer, and a model 179 digital coulometer. The CVs were plotted on a Houston Instruments Omnigraphic 2000 x,y-recorder. Volatile organics obtained from bulk electrolysis were analyzed on a Hewlett-Packard 5890A gas chromatograph. The UV-Vis spectra were measured on a Shimadzu UV-260 spectrophotometer.

Pyridinium Hexafluorophosphates

The cell geometry used to measure the CVs is described elsewhere.[24] CVs were measured at a BAS Pt button electrode, with a Pt wire auxiliary electrode, and a sodium saturated calomel electrode (SSCE) as the reference. CVs of the pyridinium hexafluorophosphates were measured for acetonitrile solutions under argon that contained 0.1 M $TBAPF_6$ as the supporting electrolyte and 10^{-3} M compound. Acetonitrile was obtained from a freshly opened bottle and was used as received.

$Rh_2(TMB)_4{}^{2+}$

The cell geometry used to measure the CVs for $[Rh_2(TMB)_4](PF_6)_2$ was similar to that used to measure the CVs of the pyridinium hexafluorophosphates. CVs were measured at either a BAS Pt button or a BAS glassy carbon electrode, with a Pt wire auxiliary electrode, and an SSCE as the reference. CVs were measured of dichloromethane solutions under argon that contained 0.1 M $TBAPF_6$ as supporting electrolyte and 10^{-3} M compound.

The Pt button electrode was prepared following the procedure described by Anson, *et al.*[65] The glassy carbon electrode was polished with 0.3 μm α-alumina slurry, sonicated in purified water for 15 mins, and rinsed with dichloromethane.

Constant potential bulk electrolysis experiments were done in an H-tube type cell at either a Pt basket or a pyrolytic graphite working electrode. The H-tube cell was modified to allow CVs to be measured of the solution in the compartment with the working electrode. CVs were measured at either a BAS Pt button or a BAS glassy carbon electrode. The auxiliary electrode was a Pt basket and was separated from the working electrode by a medium-porosity, sintered glass frit. Potentials were measured with respect to an SSCE. Measurements were made of dichloromethane solutions under argon, which contained 0.1 M $TBAPF_6$ as the supporting electrolyte and 10^{-3} M compound. Substrates were added to the electrolysis cell via syringe.

A twentyfold excess of 1,4-cyclohexadiene (or cyclohexene) was added to a dichloromethane solution of $[Rh_2(TMB)_4](PF_6)_2$ and $TBAPF_6$. The initial solution was clear, red. Exhaustive electrolysis yielded a clear, light-red solution. This solution was transferred to a round-bottom flask and the volatiles were vacuum-transferred to a second round-bottom flask. Benzene was identified as the electrolysis product by gas chromatography. Production of protons was confirmed from the CV of the final solution. This CV compared well to a CV of a dichloromethane solution of HBF_4. Extraction of the dichloromethane electrolysis solution with distilled water resulted in an increase in pH of the water phase. UV-Vis spectra of the electrolysis solution during the course of the reaction showed the slow appearance of $Rh_2(TMB)_4Cl_2^{2+}$ with loss of $Rh_2(TMB)_4^{2+}$. $Rh_2(TMB)_4Cl_2^{2+}$ was isolated as a yellow powder from the final electrolysis solution.

Electronic Emission Spectroscopy

Electronic emission spectra were measured using an emission spectrophotometer constructed at Cal Tech, which has been described previously.[66] Spectra recorded at ambient temperature were obtained for solutions that were prepared on a high-vacuum line in a cell consisting of a 10 ml Pyrex bulb, a 1 cm pathlength quartz cell, and a Teflon vacuum valve. Solvent was bulb-to-bulb distilled into the cell from the appropriate solvent storage flask.

Stern-Volmer Quenching

For the experiments with methyl viologen di(hexafluorophosphate) and the pyridinium hexafluorophosphate quenchers, acetonitrile solutions of $[Ir_2(TMB)_4](B(C_6H_5)_4)_2$ and $TBAPF_6$ (μ = 0.1 M) were prepared on a high-vacuum line in a two-compartment spectrophotometric cell consisting of a 1 cm pathlength square cuvette and a 10 ml bulb. Acetonitrile was vacuum-distilled from its storage flask to a calibrated volumetric cylinder, then to the evacuated cell containing the iridium complex and the electrolyte. Addition of solid quencher to one compartment of the cell was followed by re-evacuation of the cell to maintain the oxygen-free conditions of the experiment. Rate constants for the quenching of the triplet excited state of $Ir_2(TMB)_4^{2+}$ were determined by measuring its lifetime as a function of quencher concentration. The emission lifetime measurements were conducted with a Nd:YAG pulsed laser system that has been described previously, using 532 nm excitation.[67] All emission intensity decays exhibited first-order kinetics over at least three half-lives. Nonlinear-least-squares fits of $RT\ln(k_q')$ (k_q' = activation-controlled rate constant) versus $E^0(A^{+/0})$ using Equations 4.20 and 4.23 were accomplished using the program MARQUARDT.

Rate constants for the quenching of the triplet excited of $Ir_2(TMB)_4^{2+}$ with hydrogen-atom donors were determined by the same methods as described for the study using the pyridinium hexafluorophosphates. Acetonitrile solutions were prepared in a similar fashion except with no added electrolyte. The hydrocarbon quenchers were either added via syringe in an inert atmosphere and the solution freeze-pump-thaw degassed after each addition, or vacuum-transferred from an appropriate storage flask. At least two independently prepared lots of hydrocarbon quencher were used for each kinetic analysis. For cyclohexene, two different purification procedures were also used. Unlike the electron-transfer quenching, irreversible photochemical reactions were observed with some hydrocarbon quenchers. For these substrates, each data point required a separate sample to be prepared. Low laser powers along with a limited number of laser pulses (20 to 50) were used to minimize the amount of photoreaction. All emission-intensity decays exhibited first-order kinetics over at least three halflives.

Absorption spectra of the solutions were measured with a Hewlett-Packard 8450A spectrophotometer or a Shimadzu UV-260 spectrophotometer before and after the quenching experiments to insure that the quenching was reversible and that no reaction, either thermal or photochemical, was occurring between $Ir_2(TMB)_4^{2+}$ and the quenchers during the course of the experiments.

Steady-State Photolysis

Steady-state photolysis experiments were conducted on solutions prepared on a high-vacuum line in a two-compartment cell. Solvent was bulb-to-bulb distilled into the cell containing the metal complex from the appropriate storage flask followed by the addition of the reactant. Liquid reactants were bulb-to-bulb distilled into the cell, and solid reactants were added to one compartment of the cell, followed by re-evacuation of the cell to maintain oxygen-free conditions.

$[Ir_2(TMB)_4](B(C_6H_5)_4)_2$ in neat 1,2-dichloroethane was irradiated with λ_{ex} > 604 nm and showed formation of $Ir_2(TMB)_4Cl_2^{2+}$. Solutions kept in the dark showed no formation of the oxidative addition product. Solutions of $[Rh_2b_4](B(C_6H_5)_4)_2$ in neat 1,2-dichloroethane were irradiated with λ_{ex} > 500 nm and showed rapid formation of $Rh_2b_4Cl_2^{2+}$. Solutions kept in the dark showed no formation of the oxidative addition products. The d^7-d^7 complexes were identified by their absorption spectra; the organic products were not identified.

Acetonitrile solutions of $[Ir_2(TMB)_4](B(C_6H_5)_4)_2$ and the hydrogen-atom donors were photolyzed with λ_{ex} > 550 nm. The oxidative addition product was identified by its absorption spectrum and NMR spectrum. The organic products from the photoreaction of 9,10-dihydroanthracene and 1,4-cyclohexadiene were identified by their NMR spectra.

A 1000 W high-pressure Hg/Xe arc lamp equipped with Corning cut-off filters was used for the irradiations. Spectrophotometric monitoring of both photolysis and thermal-blank experiments was done with either a Hewlett-Packard 8450A spectrophotometer or a Shimadzu UV-260 spectrophotometer. ^{1}H NMR spectra were obtained on a 400 MHz JNM-GX400 FT NMR spectrometer.

Results and Discussion

Homogeneous Electron Transfer

Earlier work has shown that the $^3(d\sigma^*p\sigma)$ excited state of $Ir_2(TMB)_4^{2+}$ can be reductively quenched with *N,N,N',N'*-tetramethylphenylenediamine (TMPD), yielding $TMPD^{+\bullet}$ and presumably $Ir_2(TMB)_4^{+}$.[3] Kinetic data were not reported. Similar reductive quenching has been reported for $Rh_2(TMB)_4^{2+}$, $Rh_2b_4^{2+}$, and $Pt_2(P_2O_5H_2)_4^{4-}$ with spectroscopic characterization of the reduced products.[48] No discussion of the oxidative quenching of $Ir_2(TMB)_4^{2+}$ was presented in the earlier work.

It has been reported that $Ir_2(TMB)_4^{2+}$ undergoes a thermal reaction with *N,N'*-dimethyl-4,4'-pyridinium (MV^{2+}) or with chloranil.[3] No characterization of the final products was presented. Tetracyanoethylene and chloranil react thermally with $Ir_2(TMB)_4^{2+}$. The final products appear to be the one-electron reduced acceptors and the two-electron oxidized metal complex. Contrary to the earlier result, there is no thermal reaction between $MV(PF_6)_2$ and $Ir_2(TMB)_4^{2+}$.

While no thermal ground-state reaction with MV^{2+} is observed for $Ir_2(TMB)_4^{2+}$, MV^{2+} efficiently quenches the phosphorescence of the metal complex. Electron transfer is the expected quenching process with a net driving force for reaction of the $^3(d\sigma^*p\sigma)$ excited state of $Ir_2(TMB)_4^{2+}$ with MV^{2+} of 0.27 V ($E_{1/2}(MV^{2+}/MV^{+})$ = -0.45 V (SSCE)).[68] The triplet energy of MV^{2+} (3.10 eV)[69] is too high for energy-transfer quenching to be competitive with electron-transfer quenching of $^3(Ir_2^{2+})^*$, and energy transfer can be ruled out. Additional support for excited-state electron transfer is obtained from the measurement of the rate of the quenching reaction (Equation 4.9).

$$^3(Ir_2^{2+})^* + MV^{2+} \rightarrow Ir_2^{3+} + MV^{+} \qquad 4.9$$

The reaction obeys Stern-Volmer quenching kinetics;[70] the quenching rate constant is determined by measuring the change in the $^3(d\sigma^*p\sigma)$ excited state lifetime as a function of the concentration of MV^{2+}.

$$\frac{\tau_0}{\tau} = 1 + k_q\tau_0[Q] \qquad 4.10$$

A plot of τ_0/τ versus [Q], where τ_0 is the unquenched $^3(d\sigma^*p\sigma)$ lifetime and τ is the quenched $^3(d\sigma^*p\sigma)$ lifetime, yields a line of slope $k_q\tau_0$ (Figure 4.14). The measured rate constant for the quenching by MV^{2+} ($2.7 \pm 0.3 \times 10^8$ $M^{-1}s^{-1}$) is approximately two orders of magnitude below the calculated diffusion-limited rate constant in CH_3CN (k_d ~ 2×10^{10} $M^{-1}s^{-1}$).[71] Attempts to characterize the redox products from the photoreaction using conventional microsecond flash photolysis were unsuccessful, presumably because back electron transfer occurs too quickly.

A small change in the optical absorption spectrum of a CH_3CN solution of $Ir_2(TMB)_4^{2+}$ and MV^{2+} was observed over an extended period of irradiation. This change may be attributed to the formation of trace amounts of $MV^{+\bullet}$.[72] No significant build-up of products is observed since the rapid back reaction of the quenching products Ir_2^{3+} and $MV^{+\bullet}$ gives ground-state Ir_2^{2+} and MV^{2+}. Consequently, this photoinduced electron transfer does not lead to net chemistry.

The measured rate constant for electron-transfer quenching of $^3(Ir(TMB)_4^{2+})^*$ by MV^{2+} is compared to the measured rate constants for several related reactions in Table 4.4. The variation in the observed rates may be understood as a result of the increased driving force (more negative $\Delta G^{0\prime}$) for electron transfer through the series of complexes. Such an argument appears reasonable for the comparison to $Rh_2(TMB)_4^{2+}$ and $[Ir(\mu\text{-pz})COD]_2$. These systems should have comparable electronic and nuclear factors (for the same intermolecular separation) that determine the reaction rate; redox

Figure 4.14. Stern-Volmer plot for the oxidative quenching of the $^3(d\sigma^*p\sigma)$ excited state of $Ir_2(TMB)_4^{2+}$ by methyl viologen di(hexafluorophosphate) (0.1 M $TBAPF_6$, CH_3CN).

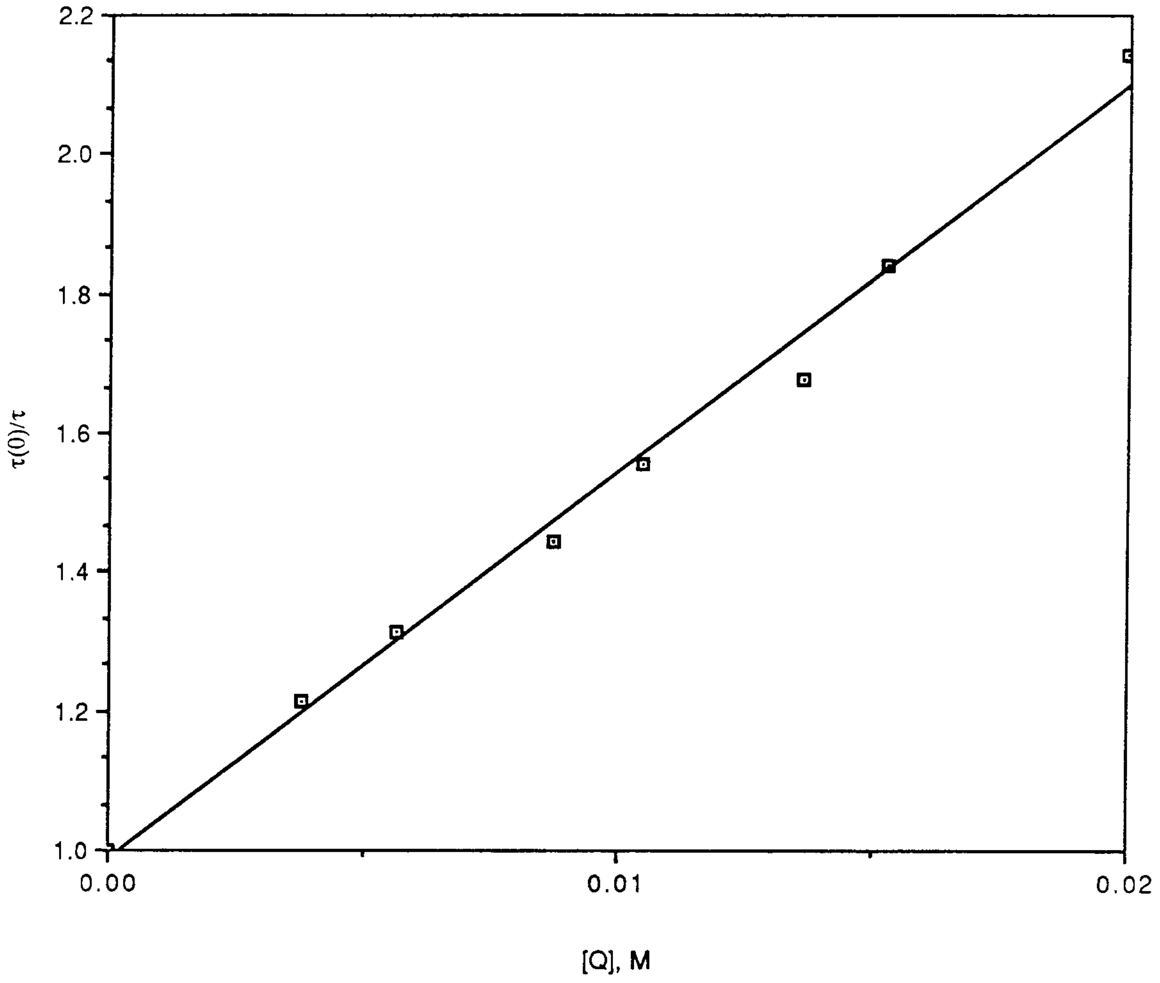
2.2
2.0
1.8
1.6
1.4
1.2
1.0
τ(0)/τ
0.00
0.01
0.02
[Q], M

Table 4.4. Measured rate constant for the reaction $^3M_2^* + MV^{2+} \rightarrow M_2^+ + MV^+$ or $M^* + MV^{2+} \rightarrow M^+ + MV^+$.

Metal Complex	k_q, $M^{-1}s^{-1}$	$E^0(M^+/M^*)$, V (SSCE)	Ref.
$Ir_2(TMB)_4^{2+}$	2.7×10^8	-0.72	a
$Ru(bpy)_3^{2+}$	2.4×10^9	-0.81	73
$Rh_2(TMB)_4^{2+}$	1.1×10^9	-1.25	48
$[Ir(\mu\text{-pz})COD]_2$	8.7×10^9	-1.75	39

a. This work.

orbitals are the same, and oxidation involves comparable contractions of the metal-metal distance. For $Ru(bpy)_3^{2+}$, the measured rate constant is an order of magnitude larger than that of $Ir_2(TMB)_4^{2+}$ and comparable to that for $Rh_2(TMB)_4^{2+}$. However, the driving force for the excited-state electron transfer for $Ru(bpy)_3^{2+}$ is comparable to that for $Ir_2(TMB)_4^{2+}$. Variations in factors other than driving force have a dramatic effect on the rate of reaction. The donor orbital for excited $Ru(bpy)_3^{2+}$ is located on one of the ligands,[74] which means that it is more accessible to the acceptor than the metal-localized orbital of the binuclear d^8 complexes. (In other words, the electron-transfer reaction for $Ir_2(TMB)_4^{2+}$ may be more nonadiabatic than that one for $Ru(bpy)_3^{2+}$.) To further understand the electron-transfer reactivity of the $^3(d\sigma^*p\sigma)$ excited state of $Ir_2(TMB)_4^{2+}$, a study of electron-transfer quenching by a series of pyridinium acceptors of variable reduction potential was undertaken. This study has allowed a better determination of the excited-state reduction potential ($M_2^{3+} + e^- \rightarrow {}^3(M_2^{2+})^*$); it has also elucidated the factors controlling the excited-state reactivity and has enabled comparisons of the electron-transfer reactivity of $Ir_2(TMB)_4^{2+}$ to be made with other inorganic systems.

Previous work has made available a series of pyridinium compounds that are well-suited for a systematic study.[57] The list of pyridinium quenchers and the measured $E_{1/2}(A^{+/0})$ or $E_{p,c}(A^{+/0})$ values for one-electron reductions of these acceptors is given in Table 4.5. Discussion of the possible complications of using a series of acceptors that are electrochemically irreversible is presented elsewhere.[39] No complications that are due to the dimerization of the pyridinium radical were observed.

Addition of the pyridiniums to an acetonitrile solution of $Ir_2(TMB)_4^{2+}$ does not alter the optical absorption spectrum of the metal complex. Emission spectra showed only quenching of the triplet excited state (Figure 4.15). No evidence for singlet

Table 4.5. Reduction Potentials of the Pyridinium Quenchers.

	Quencher[a]	$E(A^{+/0})$, V (SSCE)[b]
(1)	4-cyano-N-benzylpyridinium	-0.58
(2)	4-cyano-N-methylpyridinium	-0.65
(3)	4-carbomethoxy-N-methylpyridinium	-0.78
(4)	3-cyano-N-methylpridinium	-0.90
(5)	4-amido-N-ethylpyridinium	-0.93
(6)	3-carbomethoxy-N-benzylpyridinium	-0.96
(7)	3-carbomethoxy-N-methylpyridinium	-1.01
(8)	3-amido-N-benzylpyridinium	-1.04

a. All of the compounds are hexafluorophosphate salts.

b. For Pyridiniums 1-3, $E(A^{+/0}) = E_{1/2}(A^{+/0})$. For pyridiniums 4-8 the reductions are irreversible; therefore the values of $E(A^{+/0})$ are the cathodic peak potentials, $E_{p,c}(A^{+/0})$ measured at a scan rate of 200 mV/s. Both $E_{1/2}(A^{+/0})$ and $E_{p,c}(A^{+/0})$ were measured by cyclic voltammetry (0.1 M $TBAPF_6$) in acetonitrile solution.

Figure 4.15. (a) Emission spectrum of $[Ir_2(TMB)_4](B(C_6H_5)_4)_2$ in CH_3CN (0.1 M $TBAPF_6$). (b) Emission spectrum of $[Ir_2(TMB)_4](B(C_6H_5)_4)_2$ in CH_3CN (0.1 M $TBAPF_6$) with 4-CN-*N*-methylpyridinium.

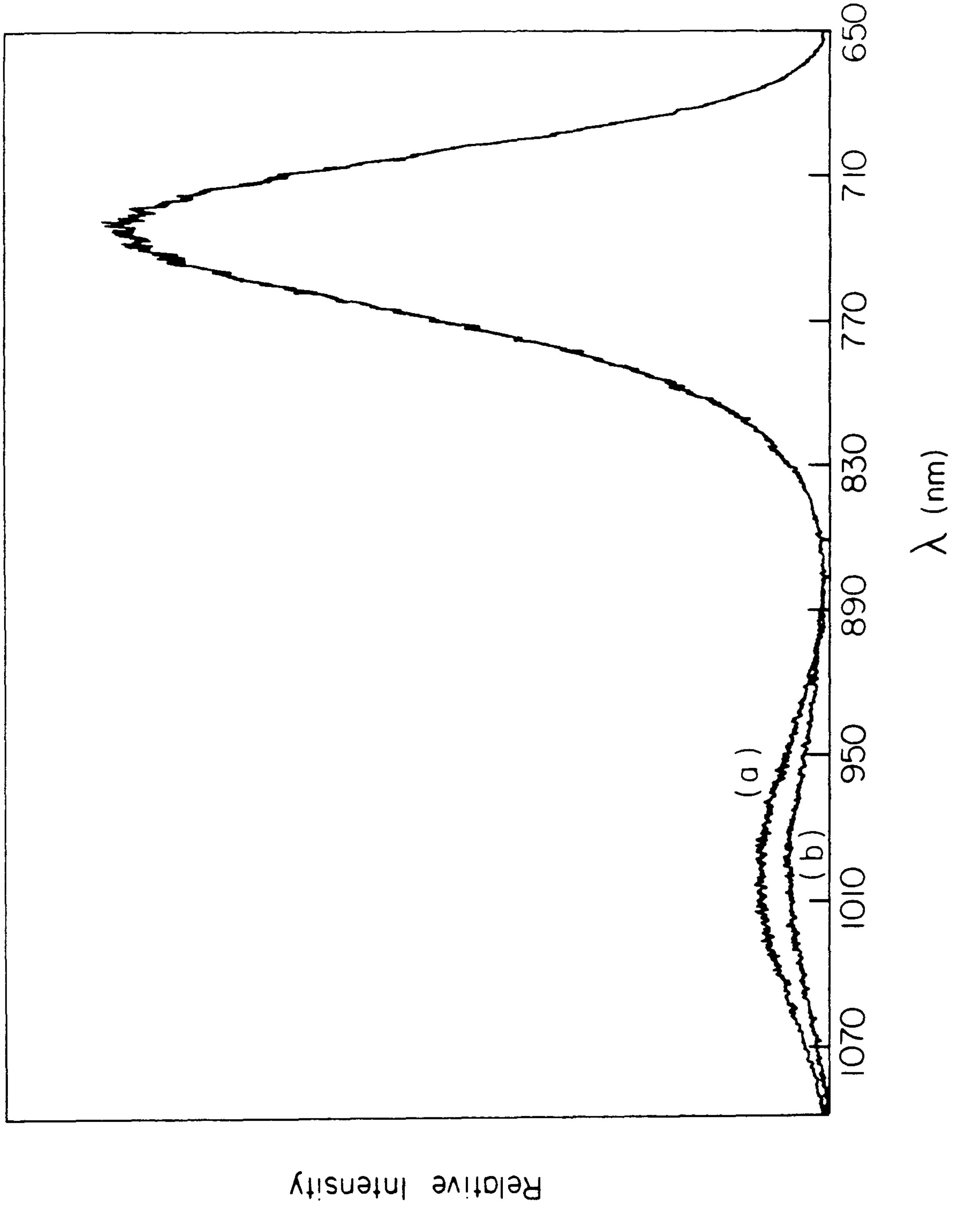
650
710
770
830
890
950
1010
1070
λ (nm)
Relative Intensity
(a)
(b)

reactivity was observed. Presumably, the singlet state does not react because of its short lifetime.

The kinetics of the excited state quenching of $Ir_2(TMB)_4^{2+}$ with the pyridinium acceptors was studied, using the same techniques as in the study of the quenching by MV^{2+}. All systems were found to obey Stern-Volmer kinetics over the quencher concentration range studied. A representative plot of the data for 4-CN-*N*-benzylpyridinium hexafluorophosphate is shown in Figure 4.16. The quenching rate constants, listed in Table 4.6, were obtained from the slopes of linear-least-squares fits to the data.

Excited-state electron transfer has been the subject of many reviews in the recent literature.[46,47,50,75-77] The general scheme presented to describe the kinetics is given in Figure 4.17. The quenching rate constant for the system is

$$k_q = \frac{k_d}{1 + \frac{k_{-d}}{k_e}\left(1 + \frac{k_{-e}}{k_{-e}(g)}\right)} . \tag{4.11}$$

For $k_{-e} << k_{-e}(g)$, the expression reduces to

$$k_q = \frac{k_d}{1 + \frac{k_{-d}}{k_e}} \tag{4.12}$$

$$\frac{1}{k_q} = \frac{1}{k_d} + \frac{1}{Kk_e} . \tag{4.13}$$

Correcting the observed rate constants for diffusion, one obtains the activation-controlled rate constant (k_q') for the bimolecular reaction

$$k_q' = Kk_e , \tag{4.14}$$

Figure 4.16. Stern-Volmer plot of oxidative quenching of the $^3(d\sigma^*p\sigma)$ excited state of $Ir_2(TMB)_4{}^{2+}$ by 4-CN-*N*-benzylpyridinium (0.1 M $TBAPF_6$, CH_3CN).

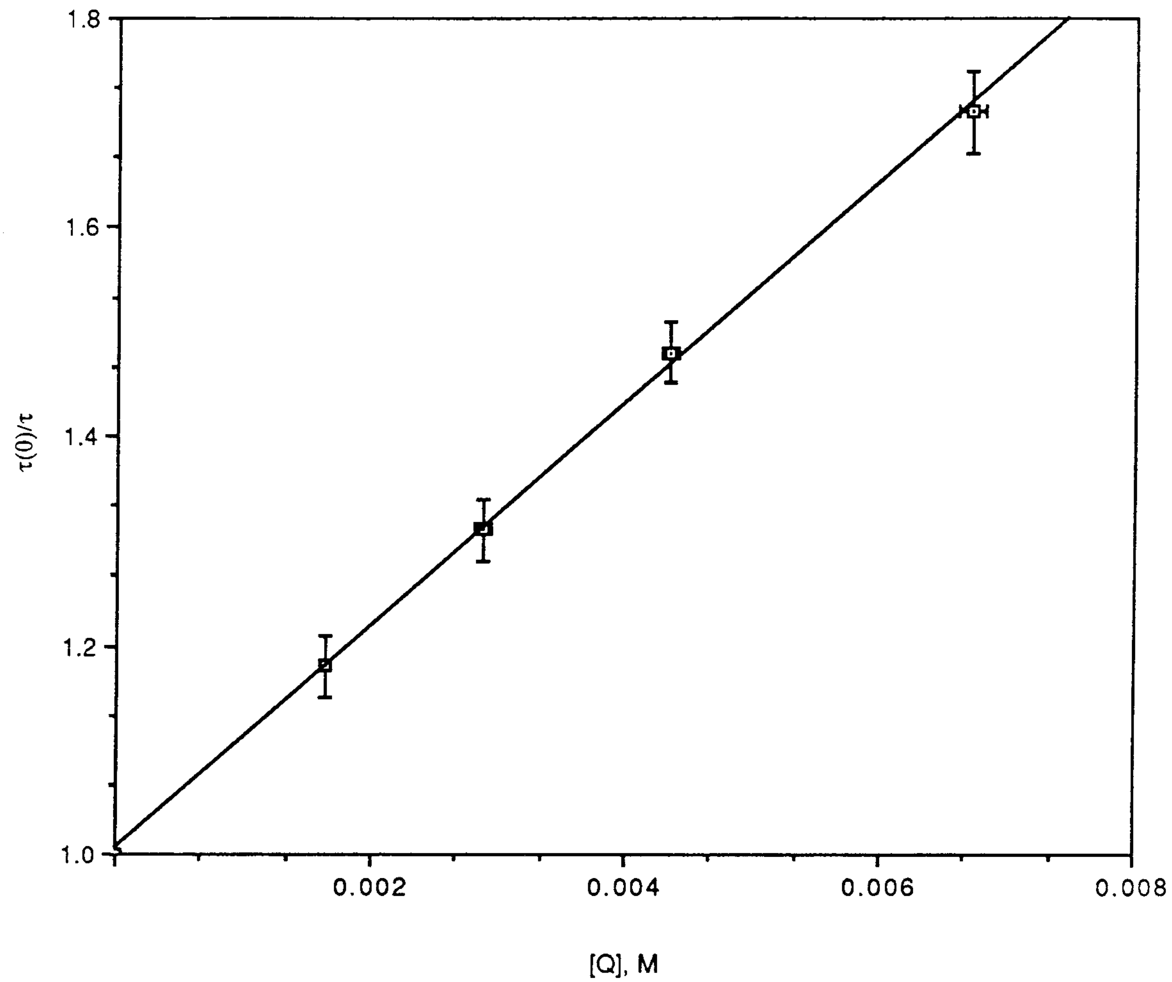
1.8
1.6
1.4
1.2
1.0
τ(0)/τ
0.002
0.004
0.006
0.008
[Q], M

Table 4.6. Rate constants for the electron-transfer quenching of $^3(Ir_2(TMB)_4{}^{2+})^*$ by pyridinium acceptors in acetonitrile solution.

Pyridinium Acceptors[a]	k_q, $M^{-1}s^{-1}$ [b]	k_q', $M^{-1}s^{-1}$ [c]
1	$4.9 \pm 0.5 \times 10^8$	$5.0 \pm 0.5 \times 10^8$
2	$4.5 \pm 0.4 \times 10^8$	$4.6 \pm 0.5 \times 10^8$
3	$3.3 \pm 0.3 \times 10^8$	$3.4 \pm 0.3 \times 10^8$
4	$3.2 \pm 0.3 \times 10^8$	$3.3 \pm 0.3 \times 10^8$
5	$1.9 \pm 0.2 \times 10^8$	$1.9 \pm 0.2 \times 10^8$
6	$2.8 \pm 0.3 \times 10^7$	$2.8 \pm 0.3 \times 10^7$
7	$9.6 \pm 1.0 \times 10^6$	$9.6 \pm 1.0 \times 10^6$
8	$4.6 \pm 0.5 \times 10^6$	$4.6 \pm 0.5 \times 10^6$

a. The acceptors are the pyridinium hexafluorophosphates listed in Table 4.5.

b. The measured quenching rate constants (k_q) are not corrected for diffusional effects.

c. The quenching rate constants (k_q') are corrected for diffusional effects as discussed in the text.

Figure 4.17. Kinetic scheme for the electron-transfer quenching of $^*M_2$ by pyridinium acceptors.

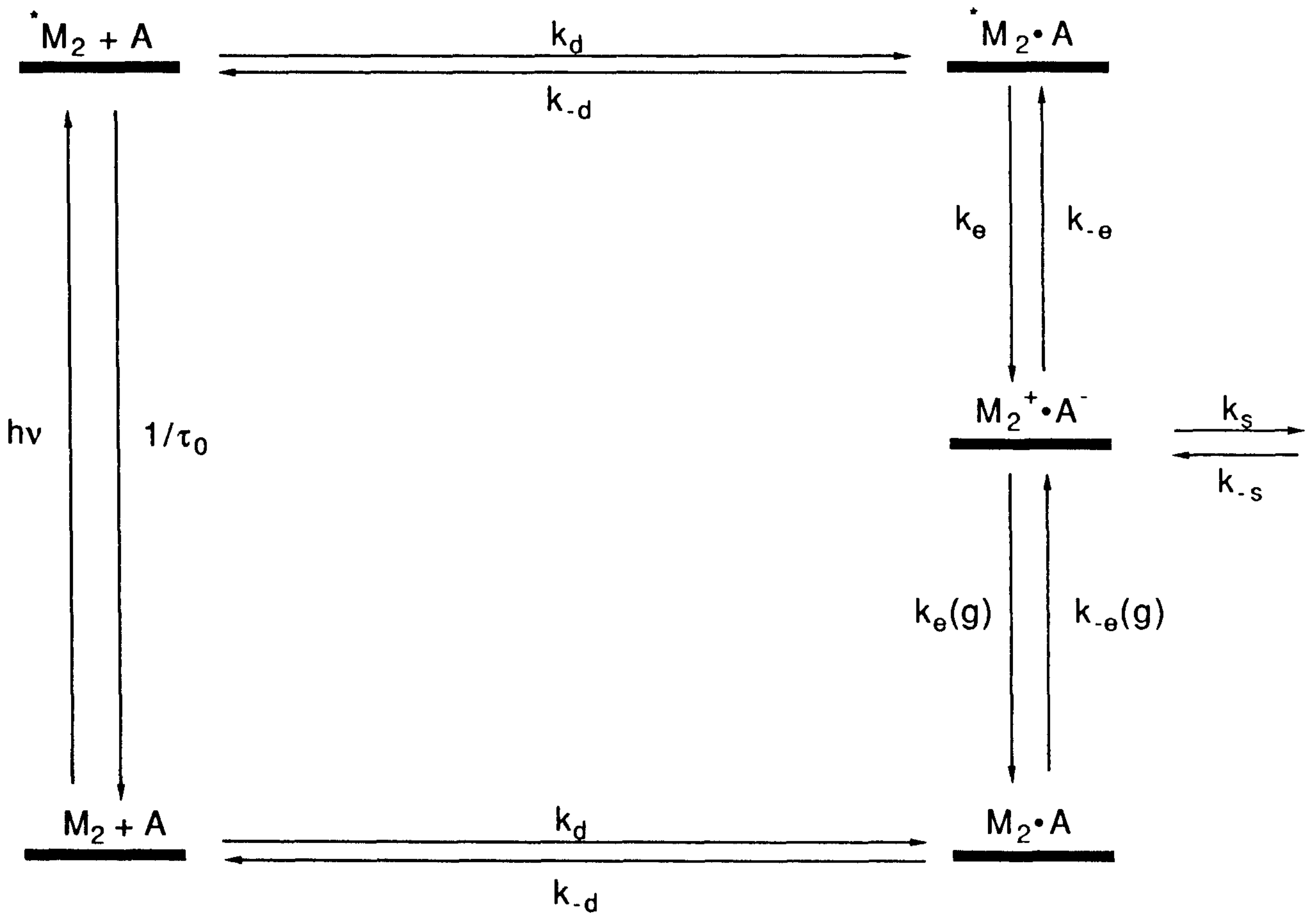
*M2 + A
kd
k-d
*M2•A
ke
k-e
hν
1/τ0
M2+•A-
ks
k-s
ke(g)
k-e(g)
M2 + A
kd
k-d
M2•A

where $K = \frac{k_d}{k_{-d}}$. From a classical approach, the rate constant for the electron-transfer step is

$$k_e = \kappa\nu\exp\left(\frac{-\Delta G^*}{RT}\right) , \qquad 4.15$$

where κ is the transmission coefficient or average probability for electron transfer per passage of the system through the intersection region, ν is the nuclear frequency, ΔG^* is the free energy of activation that is related to the reorganization energy of the system.

To analyze the kinetic data, it is necessary to adopt a relationship for ΔG^*. Several free-energy relationships, FERs, have been presented in the literature with the pros and cons of each formalism discussed in some detail.[50] Two FERs are used to analyze the bimolecular electron-transfer kinetics. From theoretical considerations, Marcus has suggested a relationship for ΔG^* in terms of $\Delta G^{0'}$, the standard free energy of the reaction, λ, the reorganization energy associated with the inner and outer coordination spheres, w_r and w_p, the work of bring reactants or products to the mean separation for reaction.[78]

$$\Delta G^* = \frac{\lambda}{4}\left(1 + \left(\frac{\Delta G^{0'}}{\lambda}\right)^2\right) \qquad 4.16$$

$$\Delta G^{0'} = \Delta G^0 + w_p - w_r \qquad 4.17$$

$$\Delta G^0 = E^0(Ir_2^{3+}/^3(Ir_2^{2+})^*) - E^0(A^{+/0}) - w_r \qquad 4.18$$

$$k_q' = K\kappa\nu\exp\left(\frac{\lambda}{4RT}\left(1 + \frac{\Delta G^{0'}}{\lambda}\right)^2\right) \qquad 4.19$$

$$RT\ln(k_q') = RT\ln(K\kappa\nu) + \frac{\lambda}{4}\left(1 + \frac{\Delta G^{0'}}{\lambda}\right)^2 . \qquad 4.20$$

Rehm and Weller, studying the fluorescence quenching of organic compounds, have suggested an empirical FER.[79]

$$\Delta G^{*} = \frac{\Delta G^{0'}}{2} + \left[\left(\frac{\Delta G^{0'}}{2}\right)^{2} + \left(\frac{\lambda}{4}\right)^{2}\right]^{1/2} \qquad 4.21$$

$$k_q' = K\kappa\nu\exp\left\{\frac{\Delta G^{0'}}{2RT} + \frac{1}{RT}\left[\left(\frac{\Delta G^{0'}}{2}\right)^{2} + \left(\frac{\lambda}{4}\right)^{2}\right]^{1/2}\right\} \qquad 4.22$$

$$RT\ln(k_q') = RT\ \ln(K\kappa\nu) + \frac{\Delta G^{0'}}{2} + \left[\left(\frac{\Delta G^{0'}}{2}\right)^{2} + \left(\frac{\lambda}{4}\right)^{2}\right]^{1/2} \qquad 4.23$$

Using either the Marcus or the Rehm-Weller expression, the rate of electron transfer can be analyzed as a function of the driving force of the reaction, $-\Delta G^{0}$. An analysis of $RT\ln(k_q')$ as a function of the ease of reduction of the pyridinium acceptor gives the excited-state reduction potential, the reorganization energy associated with the electron-transfer reaction, and the preexponential factor, assuming that the associative equilibrium constant can be estimated.[47,50,80]

The two FERs predict different behavior for the rate of electron transfer as a function of $\Delta G^{0'}$. The most pronounced difference occurs at high exoergicity. The Marcus relationship predicts that the reaction rate will reach a maximum for $\Delta G^{0'} = -\lambda$ and decrease for increasing exoergicity. For the Rehm-Weller empirical FER, the rate constant tends asymptotically to its maximum value with increasing exoergicity.

Rate constants corrected for the diffusional contribution are listed in Table 4.6. The diffusion-controlled rate constant can be calculated using the Debye-Smoluchowski equation[81]

$$k_d = \frac{4\pi N_0 \left(D_A + D_B\right) af}{1000} \qquad 4.24$$

N_0 = Avogadro's number.

a = distance of closest approach, $r_A + r_B$.

D_A, D_B = diffusion coefficient for the ions calculated, using the Stokes-Einstein equation,

where f is the integral

$$\left[a \int_a^{\infty} \exp\left(\frac{U}{k_b T}\right) \frac{dr}{r^2} \right]^{-1} . \qquad 4.25$$

$$U = \left(\frac{z_A z_B e^2}{D_s}\right)\left[\frac{\exp(Ka)}{(1 + Ka)}\right]\left(\frac{\exp(-Kr)}{r}\right)$$

r = distance of separation of the ions.

z_A, z_B = charge of the ions.

e = unit electron charge.

D_s = static dielectric of the medium.

$$K = \left[\frac{8\pi N_0 e^2 \mu}{1000 D_s k_b T}\right]^{1/2}$$

μ = ionic strength.

k_b = Boltzmann's constant.

T = temperature.

k_{-d} may be evaluated using the Eigen equation.[82]

$$k_{-d} = \left[\frac{3(D_A + D_B) f}{a^2}\right] \exp\left[\frac{b}{(1 + Ka)}\right] \qquad 4.26$$

$$b = \frac{z_A z_B e^2}{a D_s k_b T}$$

The equilibrium constant for association is then

$$\frac{k_d}{k_{-d}} = \left(\frac{4\pi a^3 N_0}{3000}\right) \exp\left[\frac{-b}{(1 + Ka)}\right] . \qquad 4.27$$

The equilibrium constant for association calculated for $Ir_2(TMB)_4^{2+}$ and the pyridinium quenchers is approximately 1 to 2 M^{-1}. See Appendix 2 for a numerical integration routine to evaluate f. Also included in Appendix 2 are the calculated constants for the various pyridinium acceptors.[83]

A plot of RTln(k_q') versus $E^0(A^{+/0})$ is shown in Figure 4.18. Two regions are observed; (i) an activated region that shows Arrhenius-type linear behavior, and (ii) a plateau region where the rate shows no change for a decrease in $E^0(A^{+/0})$. Lacking in these data is a region, predicted by both the Marcus and Rehm-Weller FERs, intermediate between (i) and (ii), where k_q' increases nonlinearly as $E^0(A^{+/0})$ decreases.

Within the Marcus formalism, a plot of RTln(k_q') versus $E^0(A^{+/0})$ should yield a line of slope 0.5 in the region where $\Delta G^{0'} << 2\lambda$.[73] A plot of the data with linear-least-squares fits to the activated region is shown in Figure 4.19. The slope is 0.7 ± 0.1. This poor agreement to the predicted value of 0.5 is not an indication that the Rehm-Weller formalism is a better description of the system.[50] Earlier work for $[Ir(\mu\text{-pz})COD]_2$ found excellent agreement between the experimentally determined slope (0.48) and the theoretical value of 0.5.[57] The uncertainty in the value of the slope determined for $Ir_2(TMB)_4^{2+}$ arises from the limited amount of data available in the activated region and the large uncertainty in $E^0(A^{+/0})$.

Figure 4.18. Plot of RTln(k_q') (V) versus $E^0(A^{+/0})$ (V) for the electron-transfer quenching of $^3(Ir_2(TMB)_4{}^{2+})^*$ by the pyridinium acceptors in Table 4.5 (μ = 0.1 M $TBAPF_6$, CH_3CN).

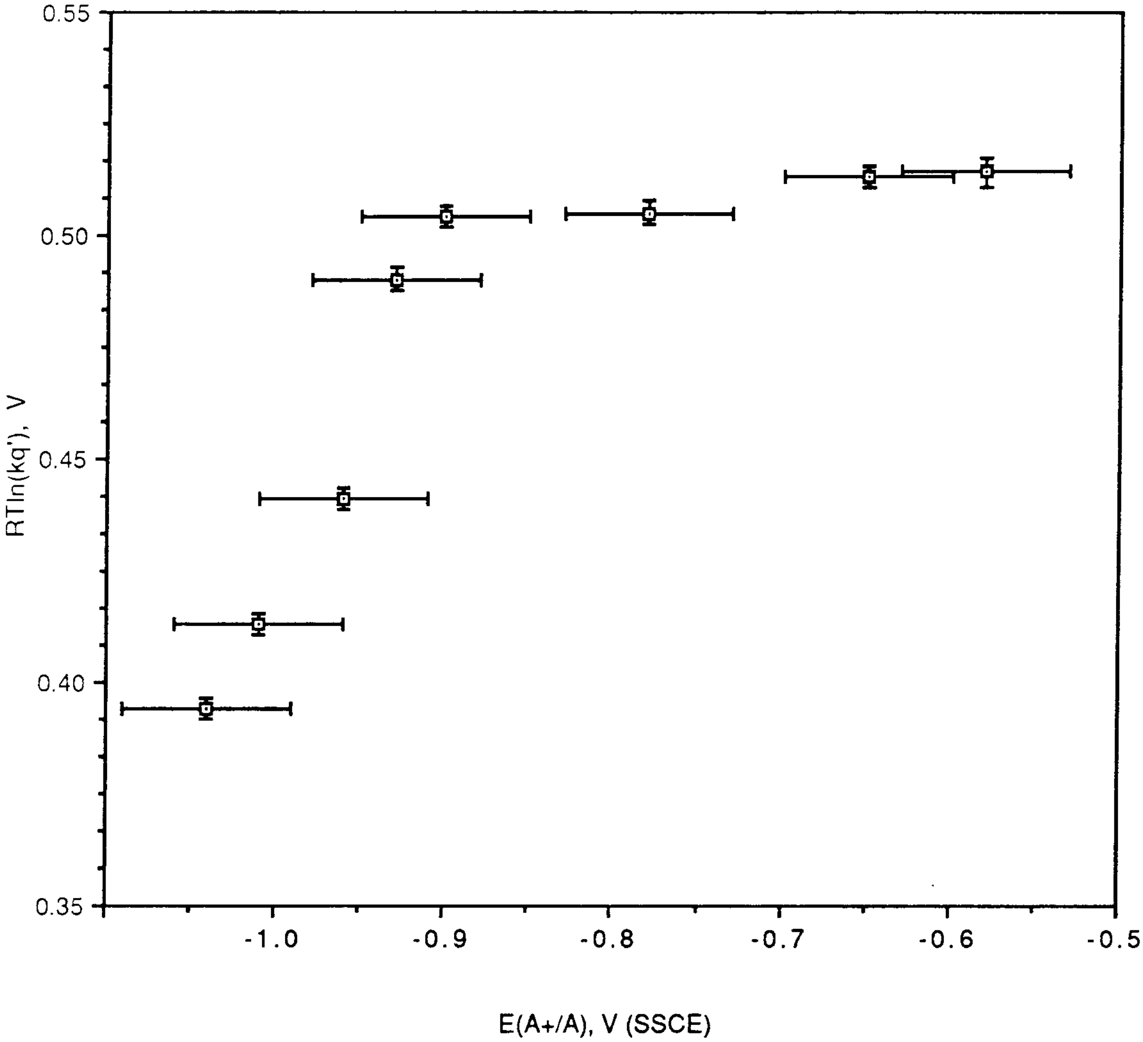
0.55
0.50
0.45
0.40
0.35
RTln(kq'), V
-1.0
-0.9
-0.8
-0.7
-0.6
-0.5
E(A+/A), V (SSCE)

Figure 4.19. Plot of RTln(k_q') (V) versus $E^0(A^{+/0})$ (V) for the electron-transfer quenching of $^3(Ir_2(TMB)_4{}^{2+})^*$ by the pyridinium acceptors in Table 4.5 (μ = 0.1 M $TBAPF_6$, CH_3CN). Diffusion-limited rate shown as the horizontal dashed line. Two linear fits to the activated region are shown.

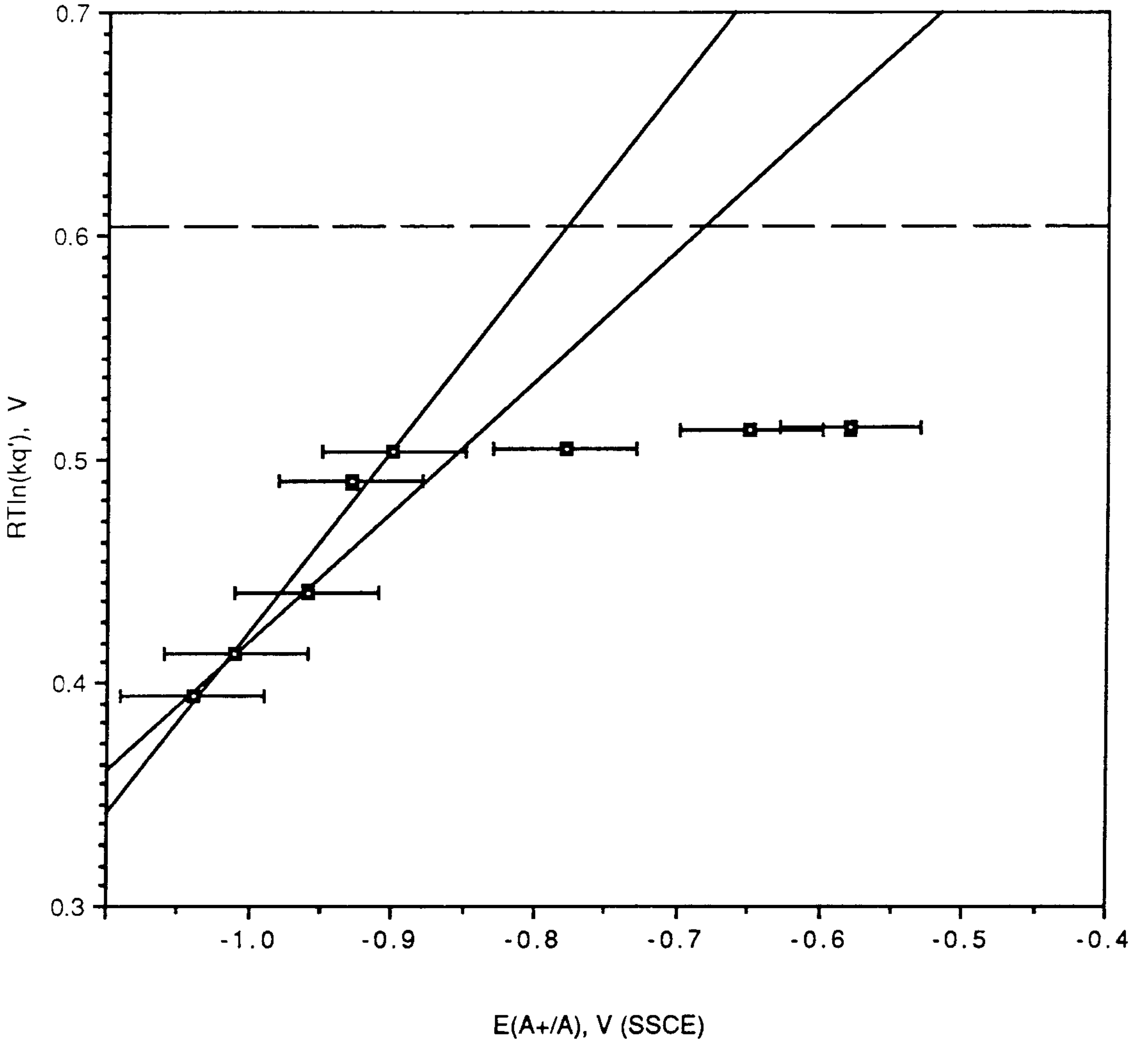
0.7
0.6
0.5
0.4
0.3
RTln(kq'), V
-1.0
-0.9
-0.8
-0.7
-0.6
-0.5
-0.4
E(A+/A), V (SSCE)

Three-parameter, nonlinear-least-squares fits of RTln(k_q') versus $E^0(A^{+/0})$ using Equations 4.20 and 4.23 are shown in Figure 4.20. The work term associated with bringing $Ir_2(TMB)_4^{2+}$ and a pyridinium acceptor together is 0.01 to 0.03 eV.[46] This contribution is neglected in the analysis of the electron-transfer rate data.

The fitted values for RTln(Kκν), $E^0(Ir_2^{3+}/^3(Ir_2^{2+})^*)$, and λ are listed in Table 4.7. The fitted values for the two FERs are almost identical with the largest variation observed for λ. It is satisfying to find that the fitted value of $E^0(Ir_2^{3+}/^3(Ir_2^{2+})^*)$ agrees with the earlier estimate of -0.72 V (SSCE). Variances of 200- 300 mV in reduction potentials are observed for other systems.[57] The surprising result from the nonlinear-least-squares fits is the low value for the reorganization energy (λ ~ 0.25 eV). Earlier studies for analogous binuclear systems found λ's of approximately 1 eV.[57,84] For small λ values, the intermediate curved region will decrease, and for very small values of λ, the intermediate range will be almost unnoticeable (Figure 4.21).[50] For [Ir(μ-pz)COD]$_2$, a broad, nonlinear region is observed (Figure 4.22). The curvature observed for $Ir_2(TMB)_4^{2+}$ is in stark contrast to that for [Ir(μ-pz)COD]$_2$ (Figure 4.22); however, this may be a consequence of the low limiting rate, not a small value of λ. In Figure 4.23, several two-parameter, nonlinear-least-squares fits to the data for $Ir_2(TMB)_4^{2+}$ are shown. The value of λ is fixed, and $E^0(Ir_2^{3+}/^3(Ir_2^{2+})^*)$ and RTln(κν) are optimized according to Equation 4.20. Reasonable fits to the observed data are obtained for λ from 0.5 to 0.8 eV (Table 4.8). Thus, the reorganization energy for the oxidative electron-transfer quenching of $^3(Ir_2(TMB)_4^{2+})^*$ by pyridinium acceptors may be comparable to that determined for other binuclear d^8 complexes. Also, for a large value of λ, the fitted Marcus curve does not show an artificial downward curvature at higher driving force as for λ ~ 0.2 eV.

The limiting rate observed for $Ir_2(TMB)_4^{2+}$ is approximately two orders of magnitude below the calculated diffusional rate constant. For the plateau region two limiting values are predicted. As $\Delta G^{0'} \rightarrow -\infty$,

Figure 4.20. Plot of RTln(k_q') (V) versus $E^0(A^{+/0})$ (V) for the electron-transfer quenching of $^3(Ir_2(TMB)_4{}^{2+})^*$ by the pyridinium acceptors in Table 4.5 (μ = 0.1 M $TBAPF_6$, CH_3CN). Three-parameter, nonlinear-least-squares fit using Marcus formalism (dashed curve) and Rehm-Weller (solid curve).

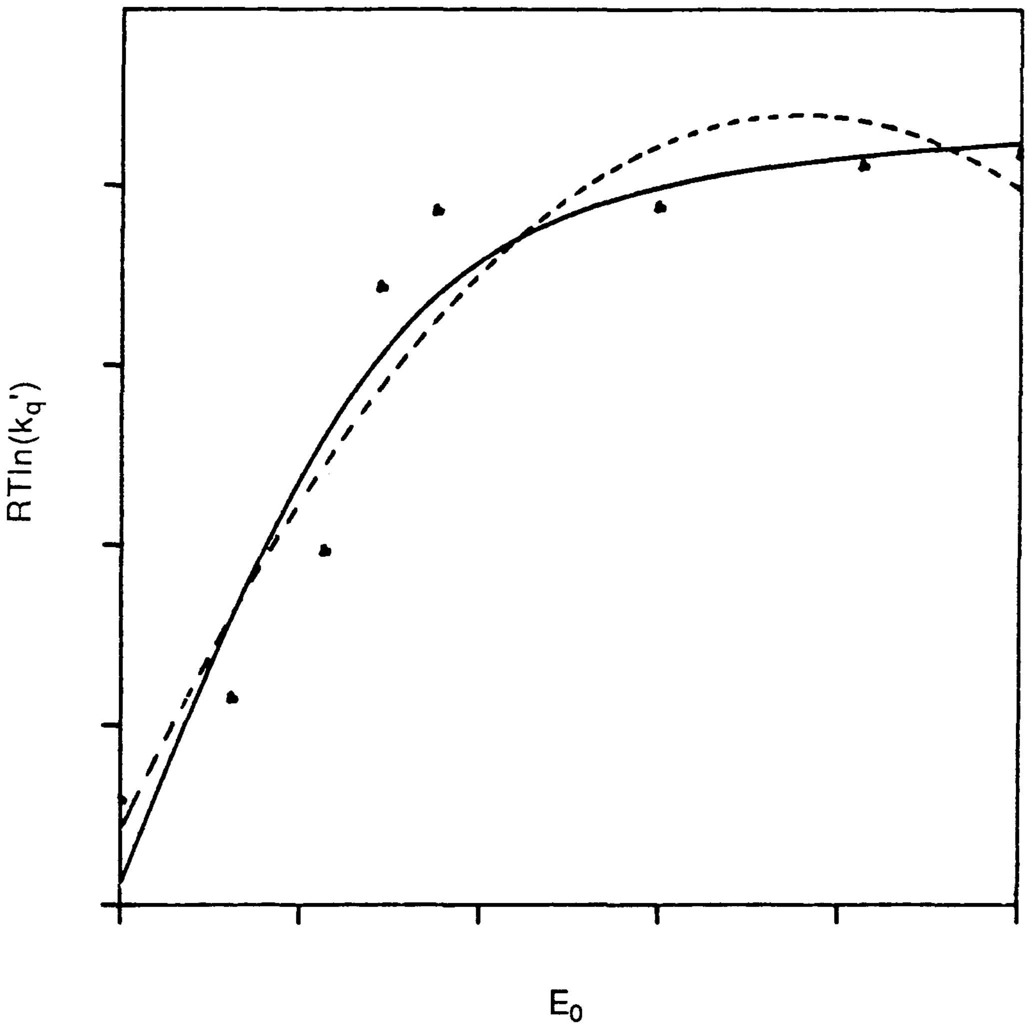
RTln(k_q')
E_0

Table 4.7. Values for RTln(Kκν), $E^0(Ir_2^{3+}/^3(Ir_2^{2+})^*)$, and λ for $Ir_2(TMB)_4^{2+}$ obtained from three-parameter, nonlinear-least-squares fits.

	Marcus	Rehm-Weller
RTln(Kκν), V (SSCE)	0.52	0.52
$E^0(Ir_2^{3+}/^3(Ir_2^{2+})^*)$, V (SSCE)	-0.95	-0.94
λ, eV	0.25	0.21

Figure 4.21. Influence of λ on $\log(k_q)$ versus ΔG plots.

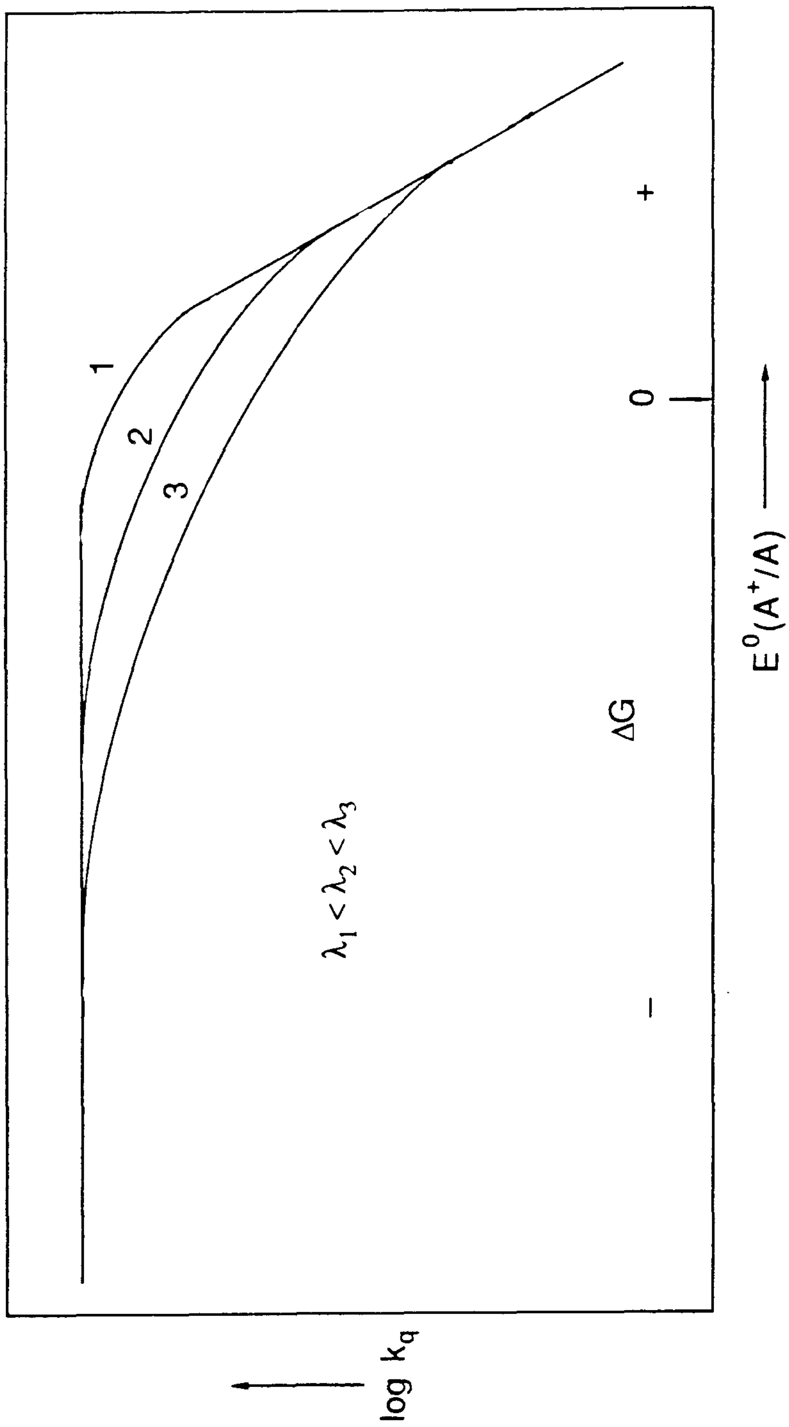
log k_q
$E^0(A^+/A)$
ΔG
$\lambda_1 < \lambda_2 < \lambda_3$
1
2
3
0
+
−

Figure 4.22. Plot of RTln(k_q') versus $E^0(A^{+/0})$ for the electron-transfer quenching of $^3[Ir(\mu\text{-}pz)COD]_2^*$ (curve a) and $^3(Ir_2(TMB)_4{}^{2+})^*$ (curve b) by the pyridinium acceptors. Diffusion-limited rate horizontal dashed line.

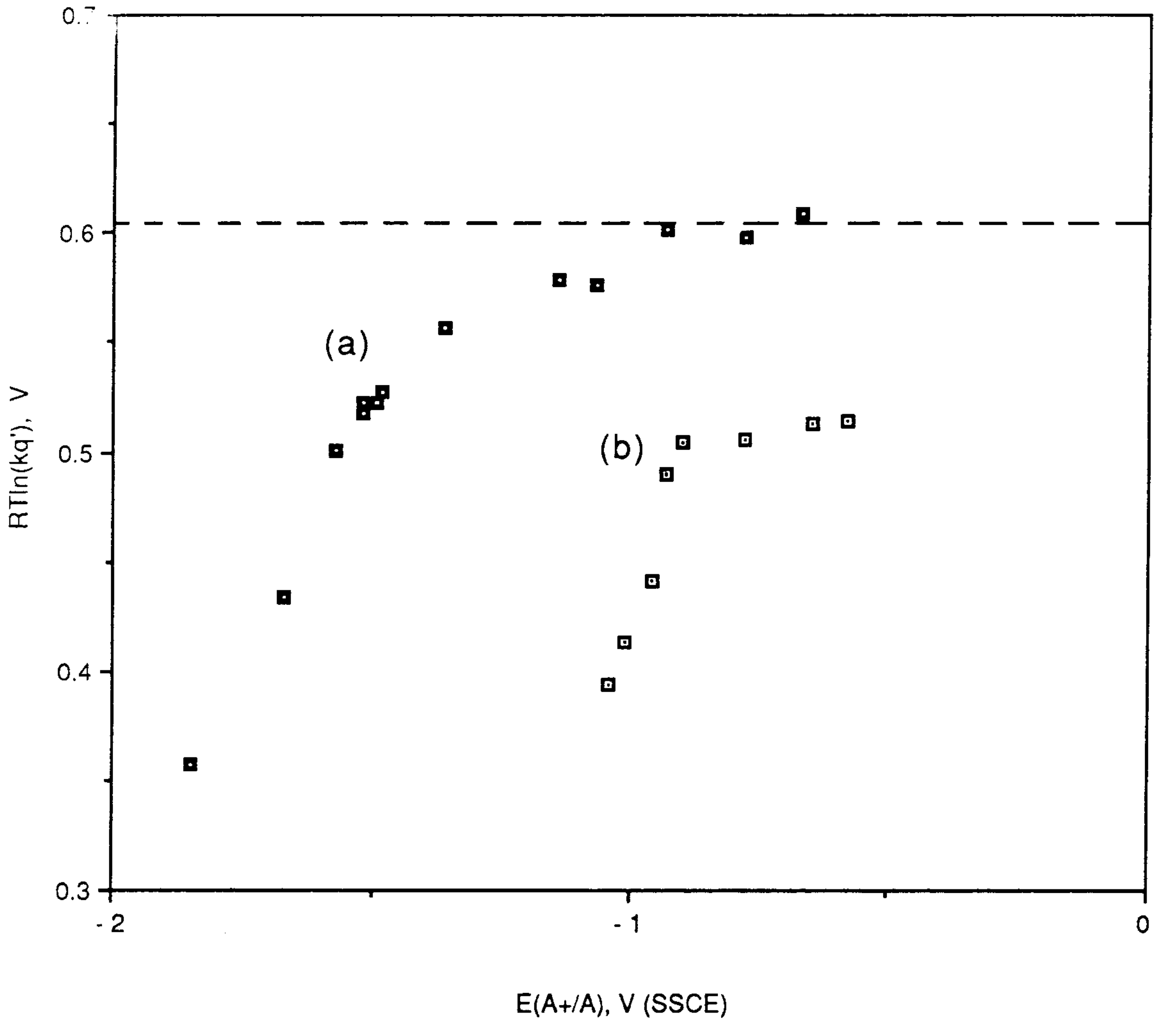
0.7
0.6
0.5
0.4
0.3
RTln(kq'), V
(a)
(b)
-2
-1
0
E(A+/A), V (SSCE)

Figure 4.23. Plot of RTln(k_q') (V) versus $E^0(A^{+/0})$ (V) for the electron-transfer quenching of $^3(Ir_2(TMB)_4{}^{2+})^*$ by the pyridinium acceptors in Table 4.5 (μ = 0.1 M $TBAPF_6$, CH_3CN). Two-parameter, nonlinear-least-squares fits using Marcus formalism for (a) λ = 0.5 eV, (b) λ = 0.6 eV, (c) λ = 0.7 eV, and (d) λ = 0.8 eV.

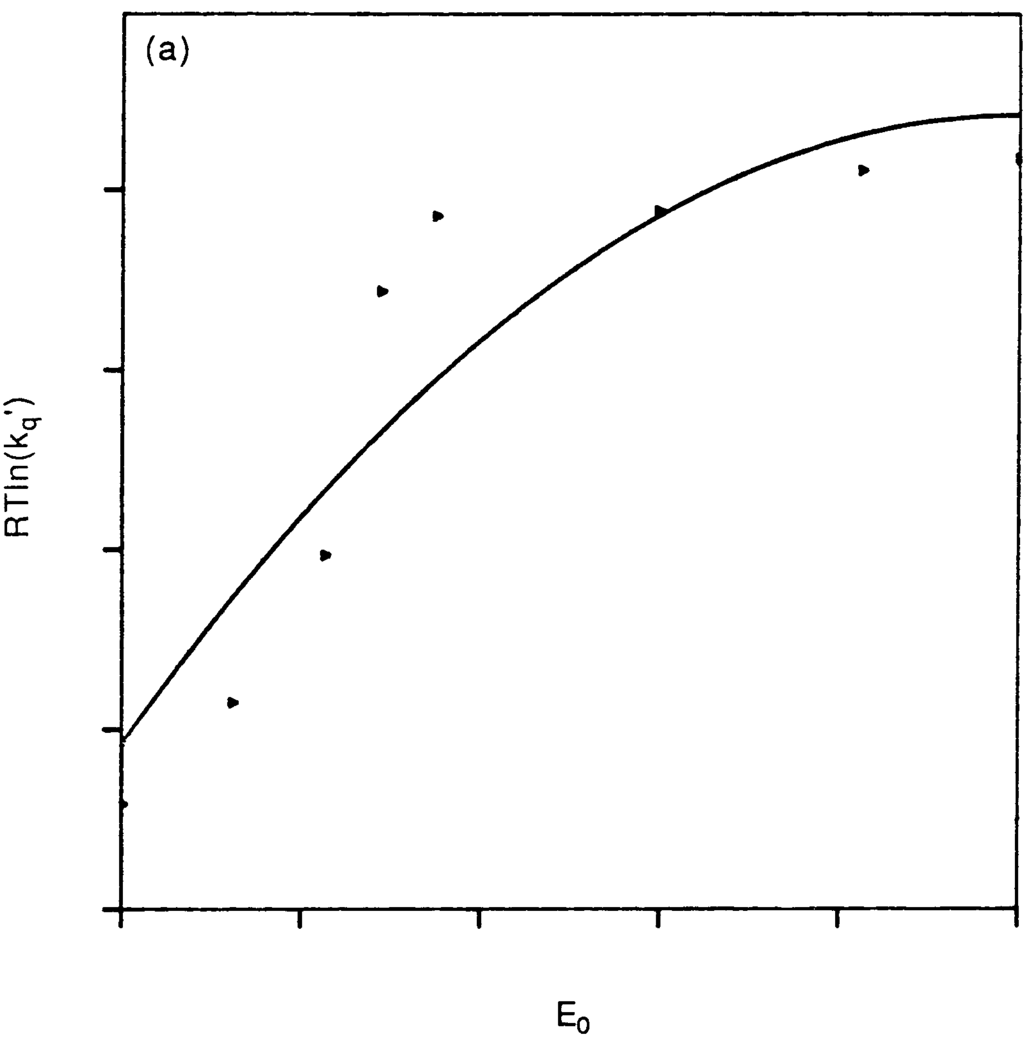
(a)
RTln(k_q')
E_0

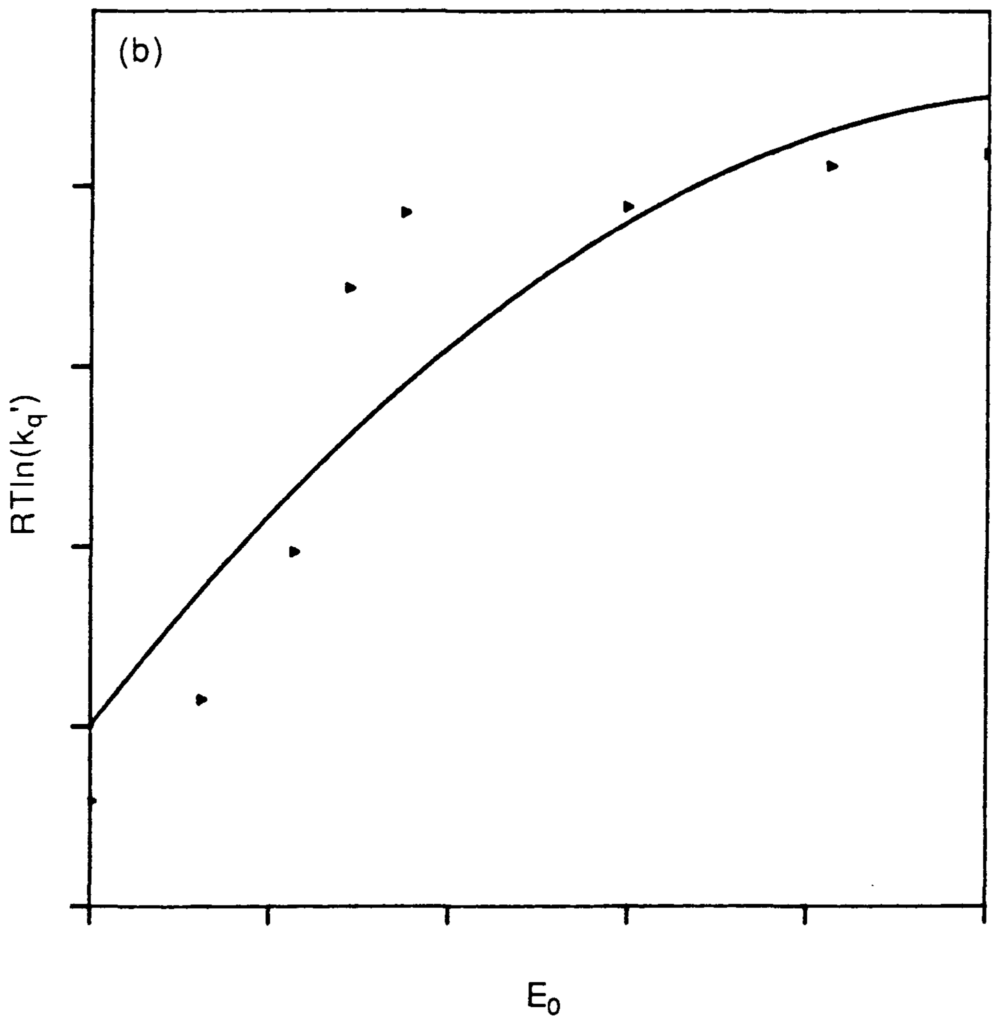
(b)
RTln(k_q')
E_0

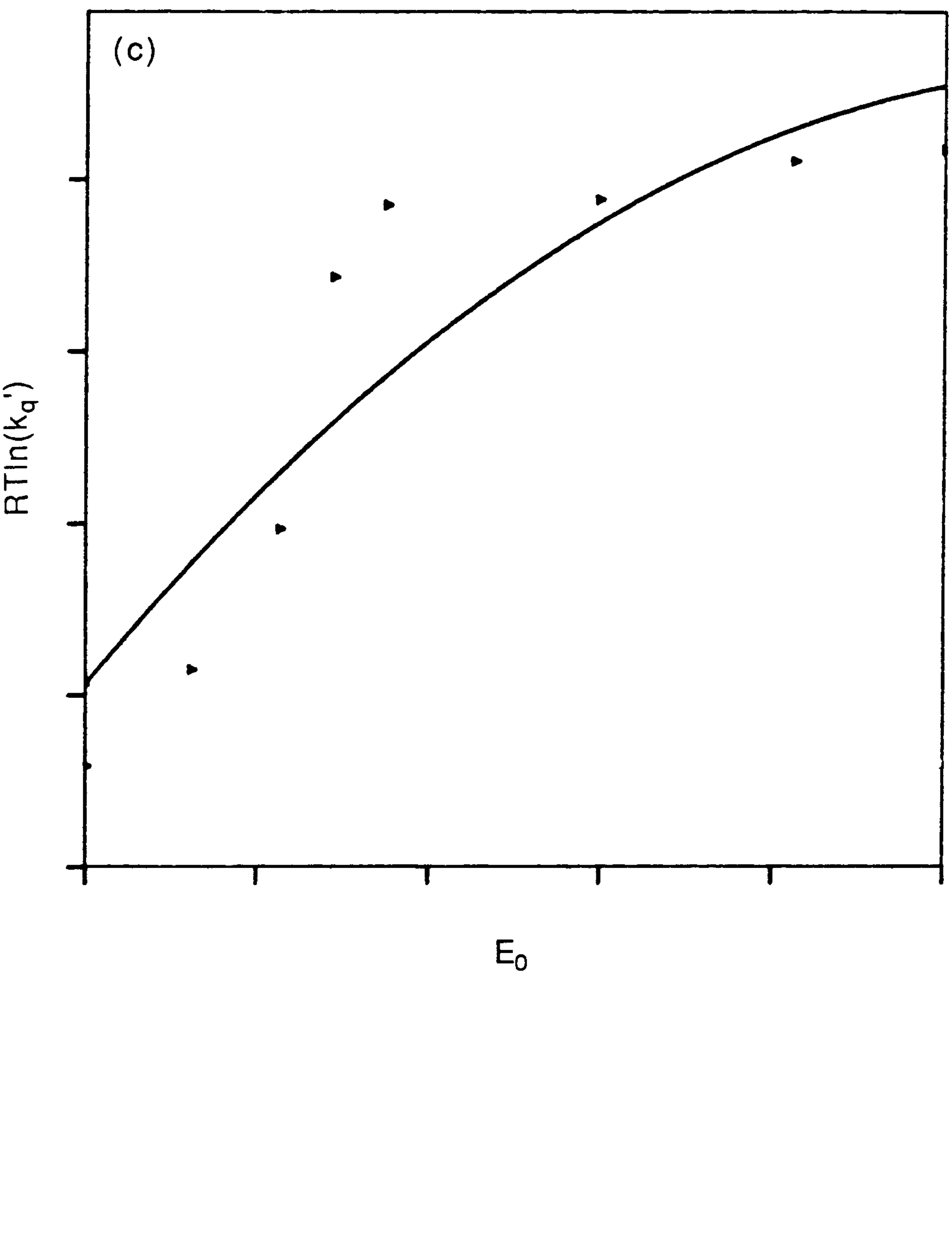
(c)
RTln(k_q')
E_0

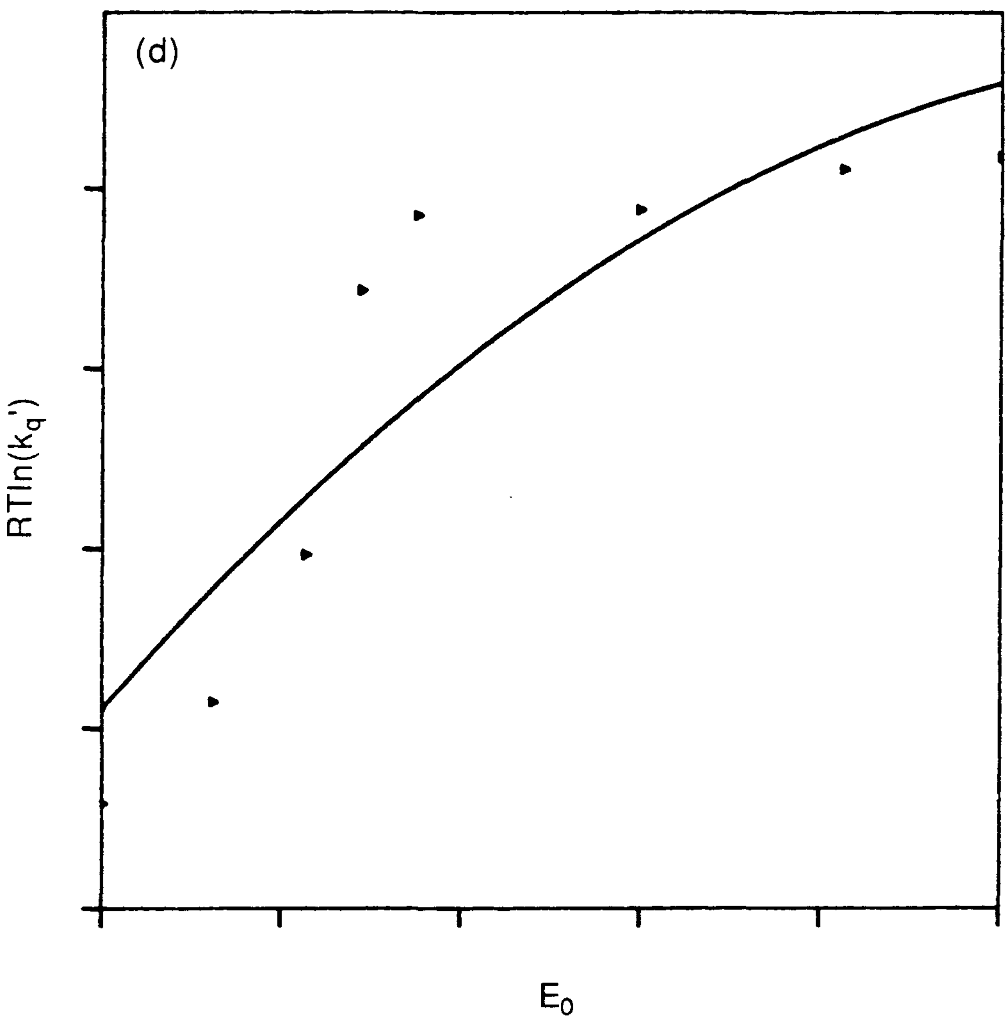
(d)
RTln(k_q')
E_0

Table 4.8. Values for RTln(Kκν) and $E^0(Ir_2{}^{3+}/{}^3(Ir_2{}^{2+})^*)$for $Ir_2(TMB)_4{}^{2+}$ obtained from two-parameter, nonlinear-least-squares fits to Marcus equation with fixed λ values.

λ, eV	RTln(Kκν), V (SSCE)	$E^0(Ir_2{}^{3+}/{}^3(Ir_2{}^{2+})^*)$, V (SSCE)
0.5	0.52	-1.08
0.6	0.53	-1.14
0.7	0.53	-1.19
0.8	0.53	-1.24

$$k_q = \frac{k_d \kappa \nu}{\left(\kappa \nu + k_{-d}\right)} \qquad 4.28$$

for $\kappa\nu > k_{-d}$

$$k_q = k_d$$

for $\kappa\nu < k_{-d}$

$$k_q = K\kappa\nu.$$

The limiting rate for $Ir_2(TMB)_4{}^{2+}$ is $K\kappa\nu$, indicating a highly nonadiabatic process, $\kappa \ll 1$.

A value for the nonadiabaticity of the electron-transfer reaction can be estimated from the value of $RT\ln(K\kappa\nu)$. The values of $RT\ln(K\kappa\nu)$ for $[Ir(\mu\text{-}pz)COD]_2$ determined for both the Marcus and Rehm-Weller FERs are listed in Table 4.9 (Figure 4.24). The electron-transfer reaction for $[Ir(\mu\text{-}pz)COD]_2$ is found to be nonadiabatic with $\kappa \approx 0.01$. A preexpotential factor of 5×10^8 s^{-1} is estimated for $Ir_2(TMB)_4{}^{2+}$, yielding a $\kappa \approx 0.0001$, indicative of a highly nonadiabatic process. The small values of κ may be understood in terms of the semiclassical Landau-Zener theory.[85] The probability of the reactants' being converted to products per single passage through the intersection region is given by

$$P_{if} = 1 - \exp\left[\frac{-4\pi^2 H_{if}{}^2}{h\nu \mid s_i - s_f \mid}\right], \qquad 4.29$$

where H_{if} is the electronic coupling matrix element between the initial reactant surface, and the final product surface. κ is given by

$$\kappa = \frac{2P_{if}}{\left(1 + P_{if}\right)}, \qquad 4.30$$

Table 4.9. Values for RTln(Kκν), $E^0(Ir_2^{3+}/^3(Ir_2^{2+})^*)$, and λ for [Ir(μ-pz)COD]$_2$ obtained from three-parameter, nonlinear-least-squares fits.

	Marcus	Rehm-Weller
RTln(Kκν), V (SSCE)	0.61	0.64
$E^0(Ir_2^{3+}/^3(Ir_2^{2+})^*)$, V (SSCE)	-1.84	-1.69
λ, eV	0.94	0.78

Figure 4.24. Plot of RTln(k_q') (V) versus $E^0(A^{+/0})$ (V) for the electron-transfer quenching of $^3[Ir(\mu\text{-pz})COD]_2^*$ by the pyridinium acceptors. Three-parameter, nonlinear-least-squares fit using Marcus formalism (dashed curve) and Rehm-Weller (solid curve).

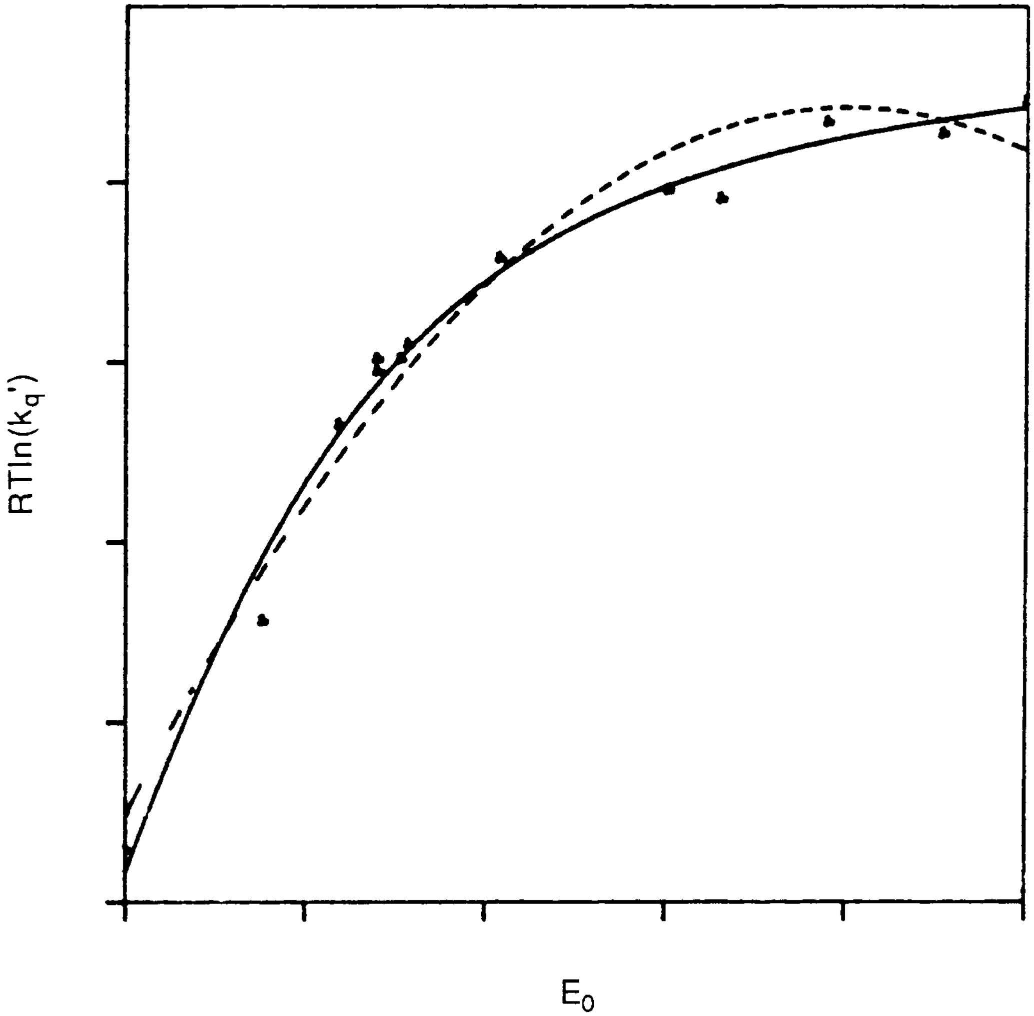
RTln(k$_q$')
E$_0$

For strong coupling between the initial and final states, κ is unity; when H_{if} is small (weak coupling), κ is also small. The origin of the small value of κ for $[Ir(\mu\text{-pz})COD]_2$ is not well understood. Weak electronic coupling might be expected for a donor and acceptor of like charge because of the Coulombic interaction that would keep them far apart, thus the very small value of κ observed for $Ir_2(TMB)_4^{2+}$.

An estimate of the donor-acceptor separation for the electron-transfer event can be obtained from the value of κ.[78] In the nonadiabatic region, $\kappa\nu$ is given by

$$\kappa\nu = 2\pi \frac{H_{ab}^2}{h\left(4\pi\lambda RT\right)^{1\backslash 2}} \quad . \qquad 4.31$$

H_{ab}^2 decreases exponentially with separation distance for many systems, and so $\kappa\nu$ can be written as

$$\kappa\nu = \nu_0 \exp\left[-\beta\left(r - r_0\right)\right] \quad , \qquad 4.32$$

where r_0 is the value of r at which $\kappa\nu$ equals some preassigned value. For bimolecular reactions r_0 is frequently assumed to correspond to close contact of the two reactants. Therefore, $r - r_0$ corresponds to the donor-acceptor separation. Assuming a β of 1.2 $Å^{-1}$, $r - r_0$ for the electron transfer reaction of $[Ir(\mu\text{-pz})COD]_2$ is approximately 4 Å. A closest contact ($r = r_0$) encounter complex is not formed for the reaction between $^3[Ir(\mu\text{-pz})COD]_2^*$ and a pyridinium acceptor. For $Ir_2(TMB)_4^{2+}$, $r - r_0$ is calculated to be ~8 Å, a reasonable value considering the unfavorable Coulombic interaction between $Ir_2(TMB)_4^{2+}$ and the pyridinium cation.

Alkyl-Halide Photoredox

Although the conversion of light to chemical energy via the electron transfer reaction of binuclear d^8 complexes is rather facile, the photochemical products return to starting materials because the back-electron-transfer reactions are very rapid. In order to utilize the strong reducing power of the $^3(d\sigma^*p\sigma)$ excited state, the nonproductive back electron transfer must be inhibited. The first approach taken was to intercept the d^8-d^7 complex. This species, possessing open coordination sites, might be trapped by Lewis bases. Photolysis of $[Ir(\mu\text{-pz})COD]_2$ with MV^{2+} in the presence of an excess of I^- did not yield $[Ir(\mu\text{-pz})COD(I)]_2$.[39] Stern-Volmer quenching of the excited state was observed with rapid, back-electron transfer to yield the starting materials. The back reaction between $Pt_2(P_2O_5H_2)_4^{3-}$ and A^- could be inhibited by axial ligand binding.[86] A fine balance between productive scavenging of $Pt_2(P_2O_5H_2)_4^{3-}$ and nonproductive back reaction to $Pt_2(P_2O_5H_2)_4^{4-}$ and A was found.

An alternative approach for inhibiting the back electron transfer is generation of a reduced acceptor, which is thermally unstable. The unimolecular decomposition of the reduced acceptor would compete with the bimolecular back-electron-transfer reaction.

Photolysis of the binuclear d^8 complexes in the presence of alkyl halides yields products that can be rationalized to occur from the thermal decomposition of the reduced alkyl halide: an excited-state electron-transfer reaction followed by dissociative decomposition of the alkyl halide radical anion, and rapid scavenging of the fragmentation products.[2,49,58,87,88] The back-electron-transfer reaction is inhibited by the decomposition of the alkyl halide radical anion. Photolysis of $Ir_2(TMB)_4^{2+}$ in 1,2-dichloroethane cleanly generates $Ir_2(TMB)_4Cl_2^{2+}$ (Figure 4.25). The presumed organic product is ethylene. Similarly for $Rh_2b_4^{2+}$, a clean photoredox reaction is observed with 1,2-dichloroethane for $\lambda_{ex} > 500$ nm (Figure 4.26). The inorganic product is $Rh_2b_4Cl_2^{2+}$.

Figure 4.25. Spectral changes upon irradiation of $[Ir_2(TMB)_4](B(C_6H_5)_4)_2$ in neat 1,2-dichloroethane, λ_{ex} > 604 nm.

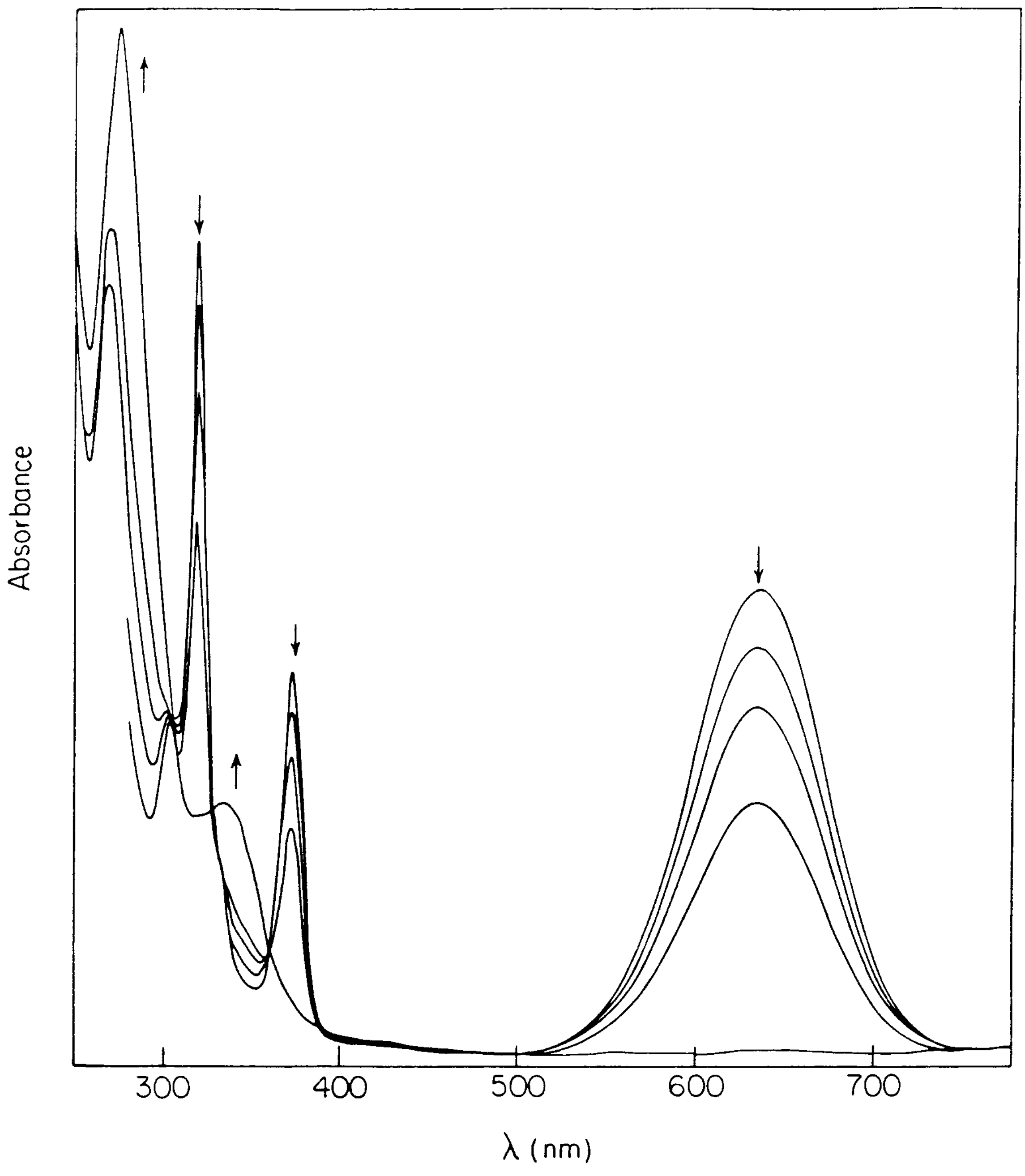
Absorbance
300
400
500
600
700
λ (nm)

Figure 4.26. Spectral changes upon irradiation of $[Rh_2b_4](B(C_6H_5)_4)_2$ in neat 1,2-dichloroethane, $\lambda_{ex} > 500$ nm.

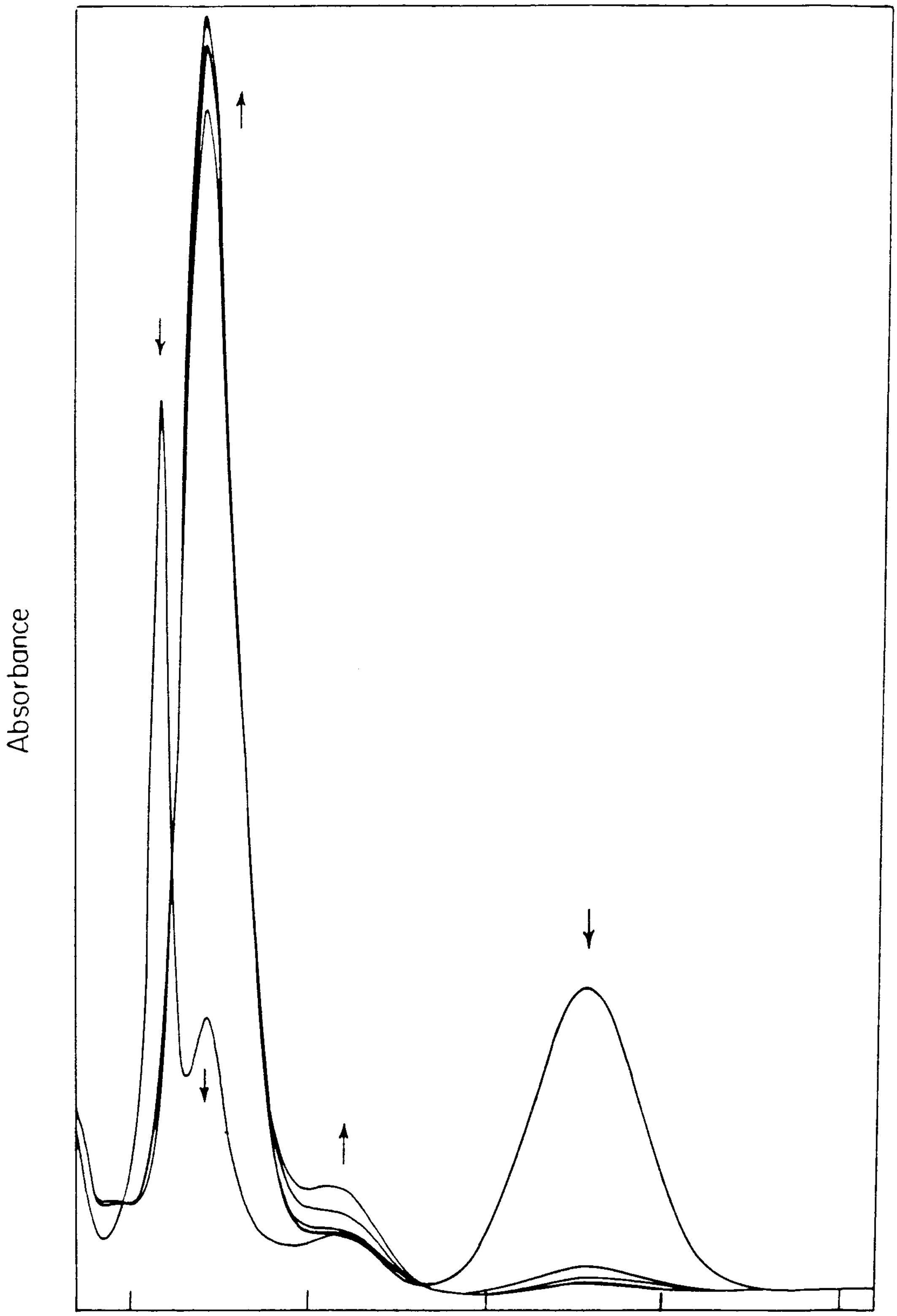
Absorbance
300
400
500
600
700
λ (nm)

An $S_{RN}1$ mechanism (Figure 4.12) has been proposed to explain the photoredox reaction of alkyl halides with binuclear d^8 complexes.[49] For $[Ir(\mu\text{-pz})COD]_2$ and $Pt_2(P_2O_5H_2)_4^{4-}$, whose excited-state reduction potentials are less than -1.5 V (SSCE), an outer-sphere electron-transfer reaction seems likely. Reduction potentials for alkyl halides of interest are generally more negative than -1.5 V (SSCE).[59] The quenching rate constant for the $^3(d\sigma^*p\sigma)$ excited state of $[Ir(\mu\text{-pz})COD]_2$ by 1,2-dichloroethane was found to agree with the rate expected for an outer-sphere electron-transfer reaction to an acceptor with a reduction potential of -2.0 V (SSCE).[58] However, an outer-sphere electron-transfer reaction seems unlikely for complexes with $E^0(M_2^+/^3M_2^*) > -1.0$ V (SSCE).

An alternate pathway to outer-sphere electron transfer, which yields similar photoredox products with alkyl halides, is excited-state atom transfer (Figure 4.13). Data obtained for $Pt_2(P_2O_5H_2)_4^{4-}$ indicate that alkyl and aryl halides react with the $^3(d\sigma^*p\sigma)$ excited state via halogen-atom transfer,[2] the $^3(d\sigma^*p\sigma)$ excited state abstracting the halide generating a d^8-d^7 monohalide species and an organic radical. An atom-transfer mechanism is favored for the photoredox reaction observed for $Ir_2(TMB)_4^{2+}$ and $Rh_2b_4^{2+}$ with 1,2-dichloroethane.

Earlier work had suggested that the photoreaction of $Rh_2b_4^{2+}$ with alkyl iodides proceeds by a radical chain mechanism initiated by an excited-state electron-transfer reaction.[88] An equivalent mechanism can be written with an atom-transfer initiation step. The photochemical reaction for $Rh_2b_4^{2+}$, unlike the reaction for $Ir_2(TMB)_4^{2+}$, is complete in a matter of minutes (rather than hours). The relative rates of the photoredox reaction for $Rh_2b_4^{2+}$ and $Ir_2(TMB)_4^{2+}$ can be understood from the varied lifetimes (and emission quantum yields) for the two complexes.[89]

The photoredox reaction for $Ir_2(TMB)_4^{2+}$ appears very clean for $\lambda_{ex} > 500$ nm. As λ_{ex} is decreased to 400 nm, secondary photolysis occurs. The most likely reaction is photochemical degradation of $Ir_2(TMB)_4Cl_2^{2+}$.[4] Higher-energy irradiation of $Rh_2b_4^{2+}$

in 1,2-dichloroethane results in very complex behavior (Figure 4.27). Rapid disappearance of $Rh_2b_4^{2+}$ with growth of $Rh_2b_4Cl_2^{2+}$ is observed with slower loss of $Rh_2b_4Cl_2^{2+}$ and appearance of bands attributable to oligomeric rhodium species.[90] The final solution is brown-orange. Removal of the solvent yields dark-purple material.

One concern for the photoreaction of $Rh_2b_4^{2+}$ is the possibility of oligomer reaction rather than dimer reaction. The photochemical generation of H_2 from HCl solutions of $Rh_2b_4^{2+}$ is thought to result from photochemical cleavage of $[Rh_2b_4Cl]_2^{4+}$.[91] Generation of mixed valence rhodium complexes followed by thermal electron transfer or atom transfer might explain the observed alkyl-halide photoreduction.

Atom transfer to the $^3(d\sigma^*p\sigma)$ excited state is the favored reaction mechanism for the alkyl-halide photoreduction reaction. While outer-sphere electron transfer appears plausible for a metal complex with $E^0(M_2^+/^3M_2^*) < -1.5$ V (SSCE), it seems unlikely for complexes with $E^0(M_2^+/^3M_2^*) > -1.0$ V (SSCE). One question remains to be answered. Why would systems, whose excited state reduction potentials are much less than -1.5 V (SSCE), react by an atom-transfer mechanism rather than by an outer-sphere electron-transfer pathway? One explanation may be obtained from the study of the electron-transfer quenching of binuclear d^8 complexes. The oxidative quenching of the $^3(d\sigma^*p\sigma)$ excited state is found to be quite nonadiabatic. In order to overcome the large nonadiabaticity, the metal complex coordinates the alkyl halide. Inner-sphere electron transfer coupled with C-X bond cleavage results in net halide-atom transfer to the metal complex.

Hydrogen-Atom Transfer

$Ir_2(TMB)_4^{2+}$ (Ir_2) is found to react photochemically with 9,10-dihydroanthracene and 1,4-cyclohexadiene. A representative electronic absorption spectrum of the photochemical reaction between $Ir_2(TMB)_4^{2+}$ and 9,10-

Figure 4.27. Spectral changes upon irradiation of $[Rh_2b_4](B(C_6H_5)_4)_2$ in neat 1,2-dichloroethane, $\lambda_{ex} > 400$ nm.

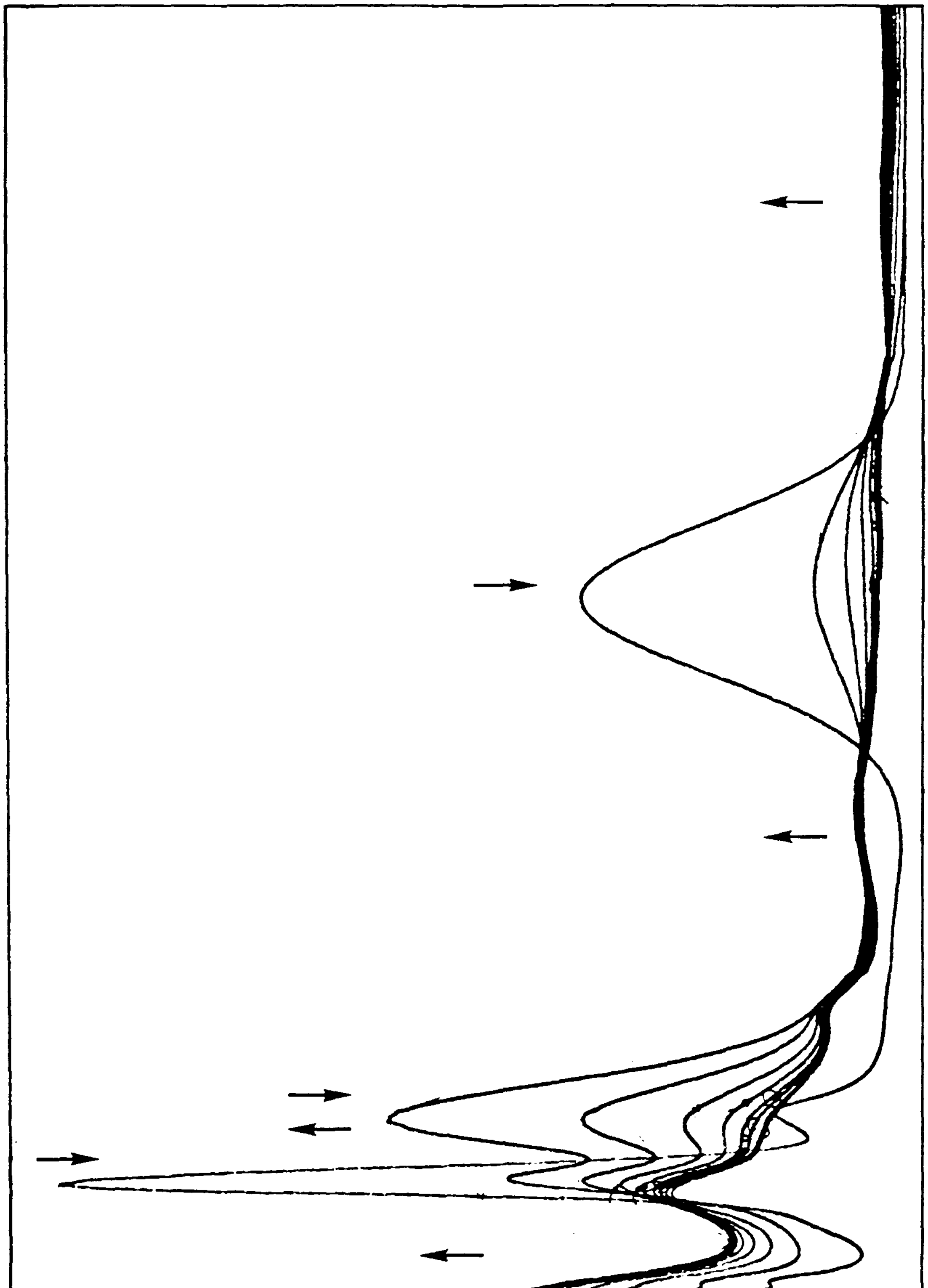

dihydroanthracene is shown in Figure 4.28. Rapid disappearance of the $^1(d\sigma^*p\sigma)$ band with growth of higher-energy transitions is observed, indicating the formation of anthracene. Growth of resonances assignable to anthracene and Ir-H are observed in the ^1H NMR (Figure 4.29). Isolation of the inorganic product from the reaction mixture yields a material whose electronic spectrum suggests the formation of a transdihydride d^7-d^7 adduct, $Ir_2(TMB)_4H_2^{2+}$ (Ir_2H_2). A moderate Ir-H stretch (1940 cm^{-1}) is observed in the IR, indicative of a terminal metal hydride. No appreciable thermal reaction with 9,10-dihydroanthracene is observed at room temperature; however, a reaction is observed at elevated temperatures. Anthracene and Ir-H resonances are observed in the ^1H NMR.

For 1,4-cyclohexadiene, no thermal reaction is observed, even at elevated temperatures. Photolysis of $Ir_2(TMB)_4^{2+}$ and 1,4-cyclohexadiene results in rapid disappearance of the d^8-d^8 metal complex. With no complication because of overlapping product spectra for the reaction with 1,4-cyclohexadiene, clean isosbestic conversion to the product spectrum is observed (Figure 4.30). Growth of resonances attributable to benzene and Ir-H are observed in the ^1H NMR (Figure 4.31).

No dark reaction is observed after partial photolysis for either 9,10-dihydroanthracene or 1,4-cyclohexadiene (no indication of a photoinitiated process).

The net photoreaction observed for $Ir_2(TMB)_4^{2+}$ with a number of hydrocarbon substrates is hydrogen-atom transfer to the metal center.

$$Ir_2 + RH_2 \xrightarrow{h\nu} Ir_2H_2 + R \qquad 4.33$$

No evidence of organic radical-coupling products ($(RH)_2$) or alkyl-hydride metal complexes (RH-Ir-Ir-H) is observed. The Ir_2H_2 complex has been isolated and characterized (see Chapter 5).

Figure 4.28. Spectral changes upon irradiation of an acetonitile solution of $[Ir_2(TMB)_4](B(C_6H_5)_4)_2$ and 9,10-dihydroanthracene.

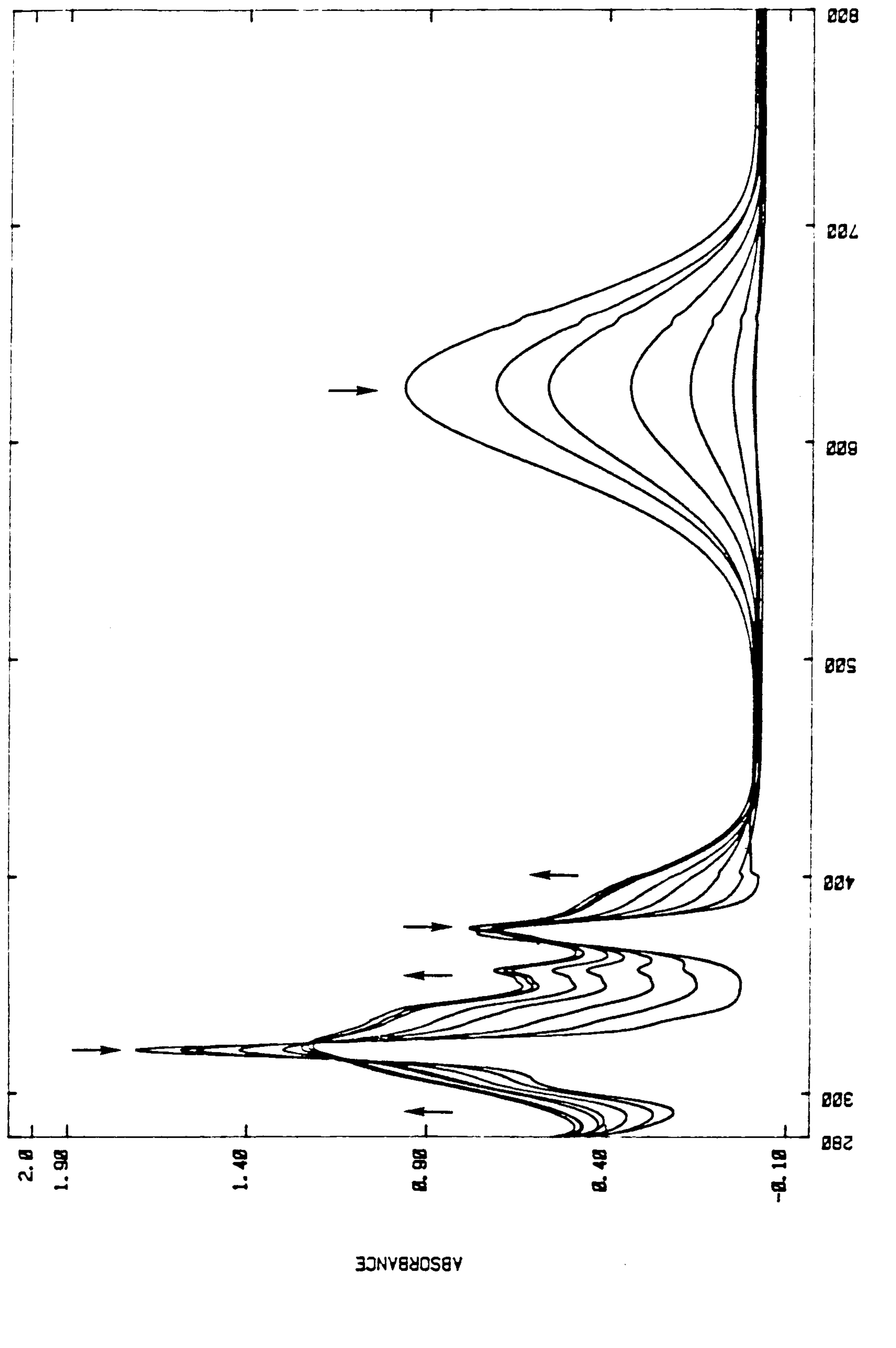
ABSORBANCE
2.0
1.90
1.40
0.90
0.40
-0.10
WAVELENGTH (nm)
280
300
400
500
600
700
800

Figure 4.29. NMR spectrum of an acetonitrile-d_3 photolysis solution of $[Ir_2(TMB)_4](B(C_6H_5)_4)_2$ and 9,10-dihydroanthracene.

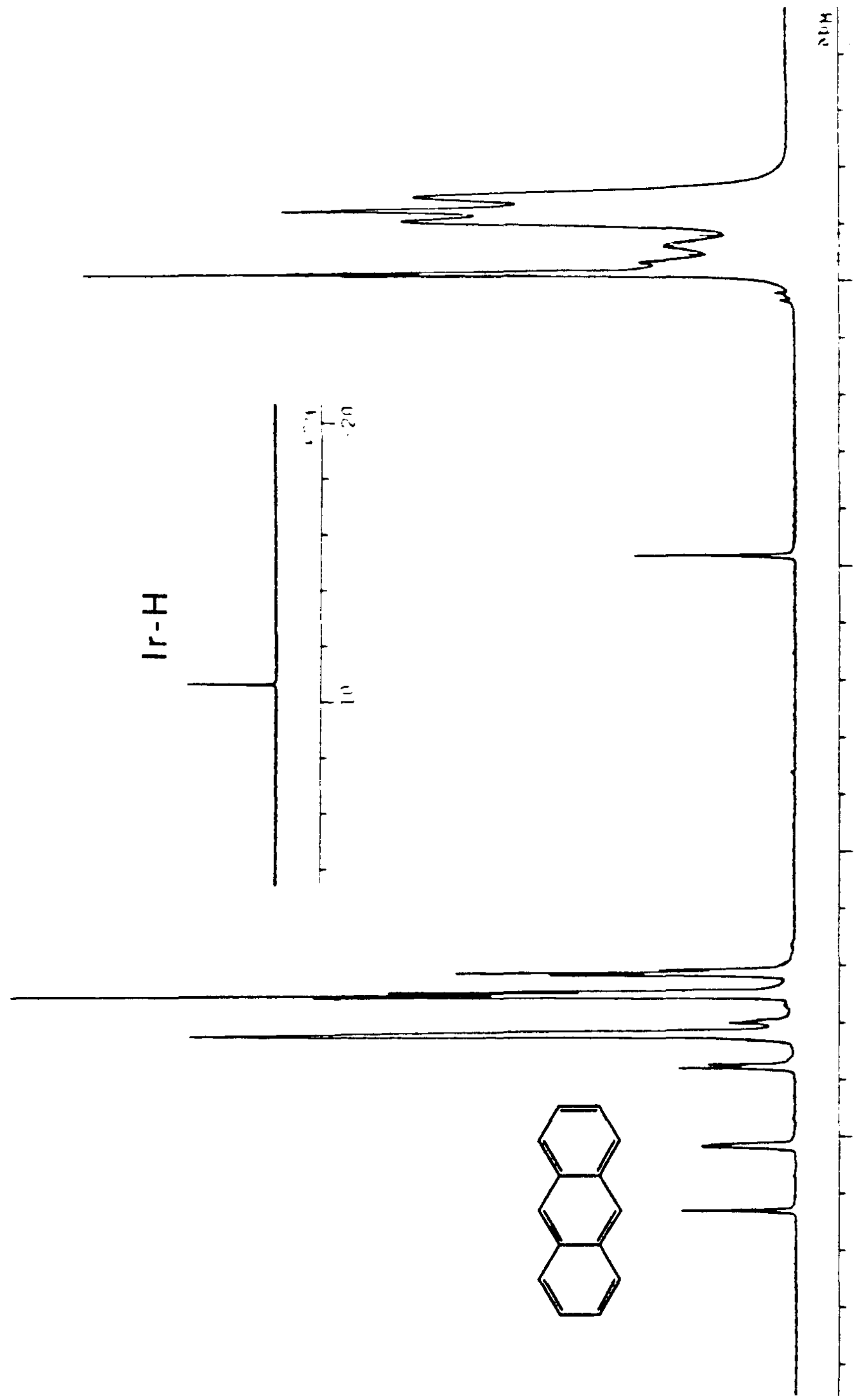
Ir-H

Figure 4.30. Spectral changes upon irradiation of an acetonitile solution of $[Ir_2(TMB)_4](B(C_6H_5)_4)_2$ and 1,4-cyclohexadiene.

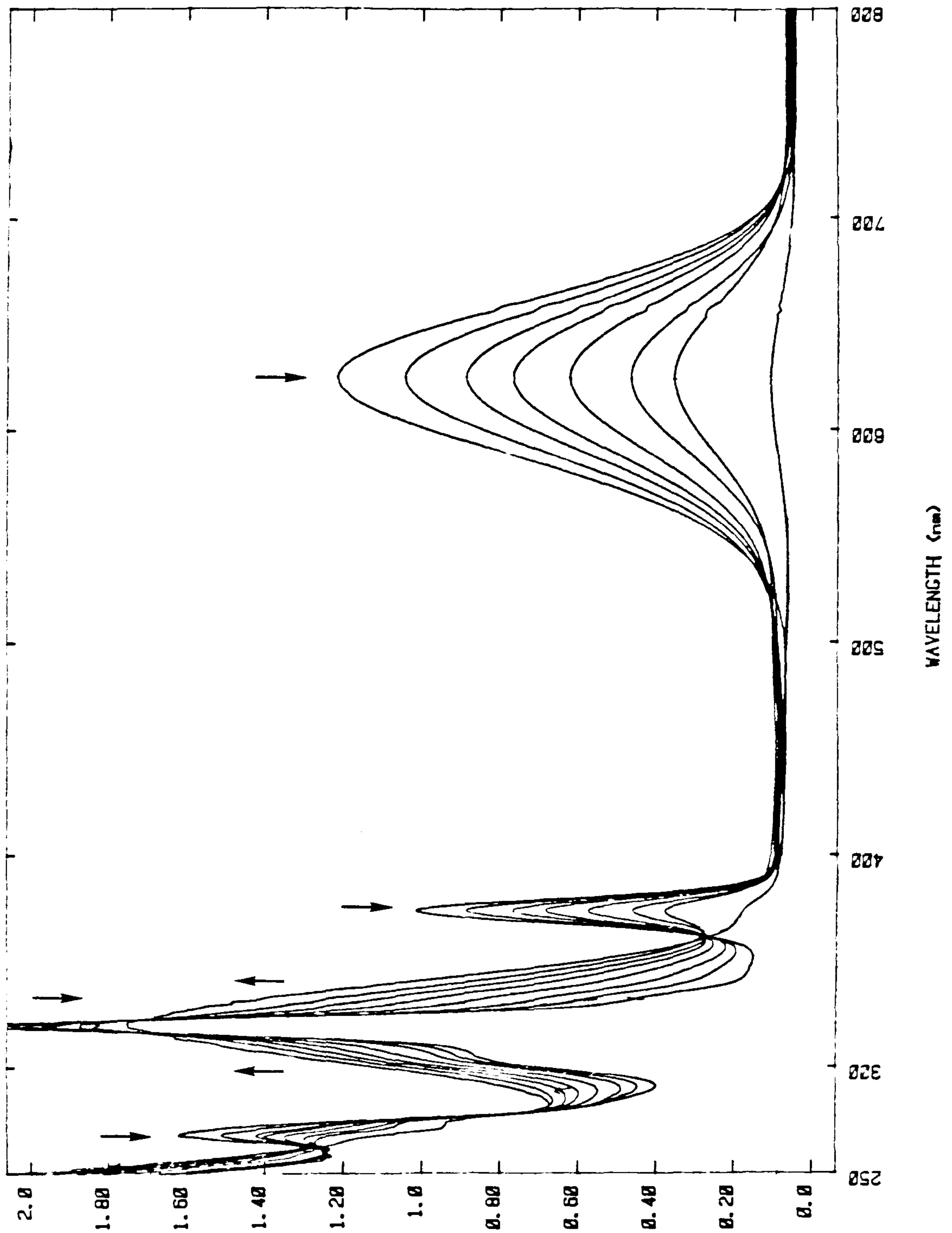
WAVELENGTH (nm)
250
320
400
500
600
700
800
2.0
1.80
1.60
1.40
1.20
1.0
0.80
0.60
0.40
0.20
0.0

Figure 4.31. NMR spectrum of an acetonitrile-d_3 photolysis solution of $[Ir_2(TMB)_4](B(C_6H_5)_4)_2$ and 1,4-cyclohexadiene.

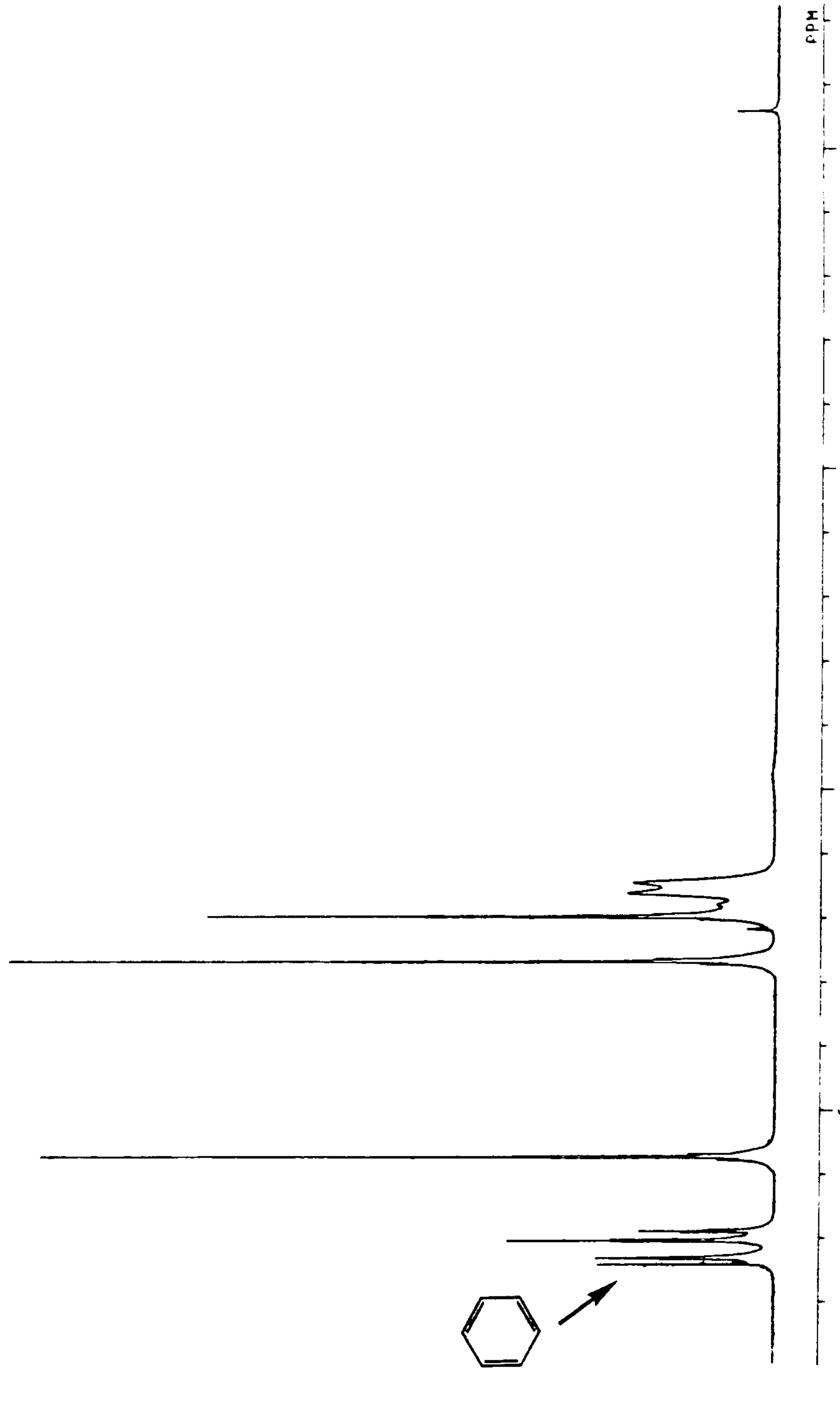
PPM
10
5
0
5

Table 4.10 lists a number of hydrocarbon substrates and their observed photochemical reactivity with Ir_2. The conclusions are based on conversion to Ir_2H_2. While conversion to Ir_2H_2 is not observed for all substrates, all but triphenylmethane quench the $^3(d\sigma^*p\sigma)$ excited state (*vide infra*). Photochemical conversion of the organic substrates may occur with no build-up of inorganic product. For $Pt_2(P_2O_5H_2)_4^{4-}$ (Pt_2), excited-state quenching by toluene and cumene is observed; steady-state photolysis (λ_{ex} 370 nm) produces H_2 and organic radical products (for toluene, bibenzyl; for cumene, 2,3-dimethyl-2,3-diphenylbutane) with no formation of Pt_2H_2.[92]

To better understand the hydrogen-atom transfer reactivity of the $^3(d\sigma^*p\sigma)$ excited state of $Ir_2(TMB)_4^{2+}$, a study of the hydrogen-transfer quenching by a series of hydrogen-atom donors with variable homolytic C-H bond strengths was undertaken. All systems were found to obey Stern-Volmer kinetics over the quencher concentration range studied. A plot of the data for the series of hydrogen-atom donors is shown in Figure 4.32. The quenching rate constants, listed in Table 4.11, were obtained from the slopes of linear-least-squares fits to the data.

Results for $^3Pt_2^*$ have been interpreted as supporting a hydrogen-abstraction pathway in which the H atom transfers via a linear Pt-H-E transition state with negligible charge transfer.[56] The reactivity of $^3Pt_2^*$ has been compared to that of the $n\pi^*$ excited states of ketones with similar triplet energies.[2] For $^3Ir_2^*$, a similar interpretation is possible; however, the analogy to the $n\pi^*$ excited states of ketones cannot be made in that the triplet energy for this complex is 30 kcal/mol compared to 60 kcal/mol for $^3Pt_2^*$.

If the photoreaction is truly an atom-transfer process, the observed rate in the absence of steric effects should track the homolytic C-H bond energies of the substrates. In a series of quenchers, the observed rate constant decreases with increasing C-H bond energy (Figure 4.33).[27] However, this trend is not general. For cyclohexene, whose

Table 4.10. Observed photochemical reactivity of hydorcarbons with $Ir_2(TMB)_4^{2+}$.

Substrate	D(C-H), kcal/mol[a]	Products
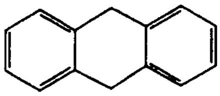	77	Ir_2H_2, 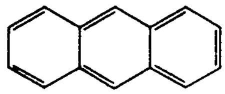
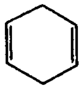	73	Ir_2H_2, 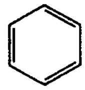
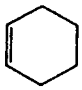	82	Ir_2H_2 [b]
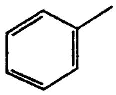	88	NR [c]
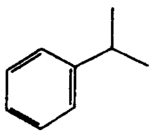	84.4	NR
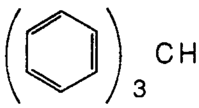	~75	NR

a. C-H bond dissociation energy, Reference 27.

b. Sluggish formation of Ir_2H_2.

c. No reaction, no observed formation of Ir_2H_2.

Figure 4.32. Stern-Volmer plot for hydrogen atom-transfer quenching of the $^3(d\sigma^* p\sigma)$ excited state of $Ir_2(TMB)_4^{2+}$ for a series of hydrocarbons.

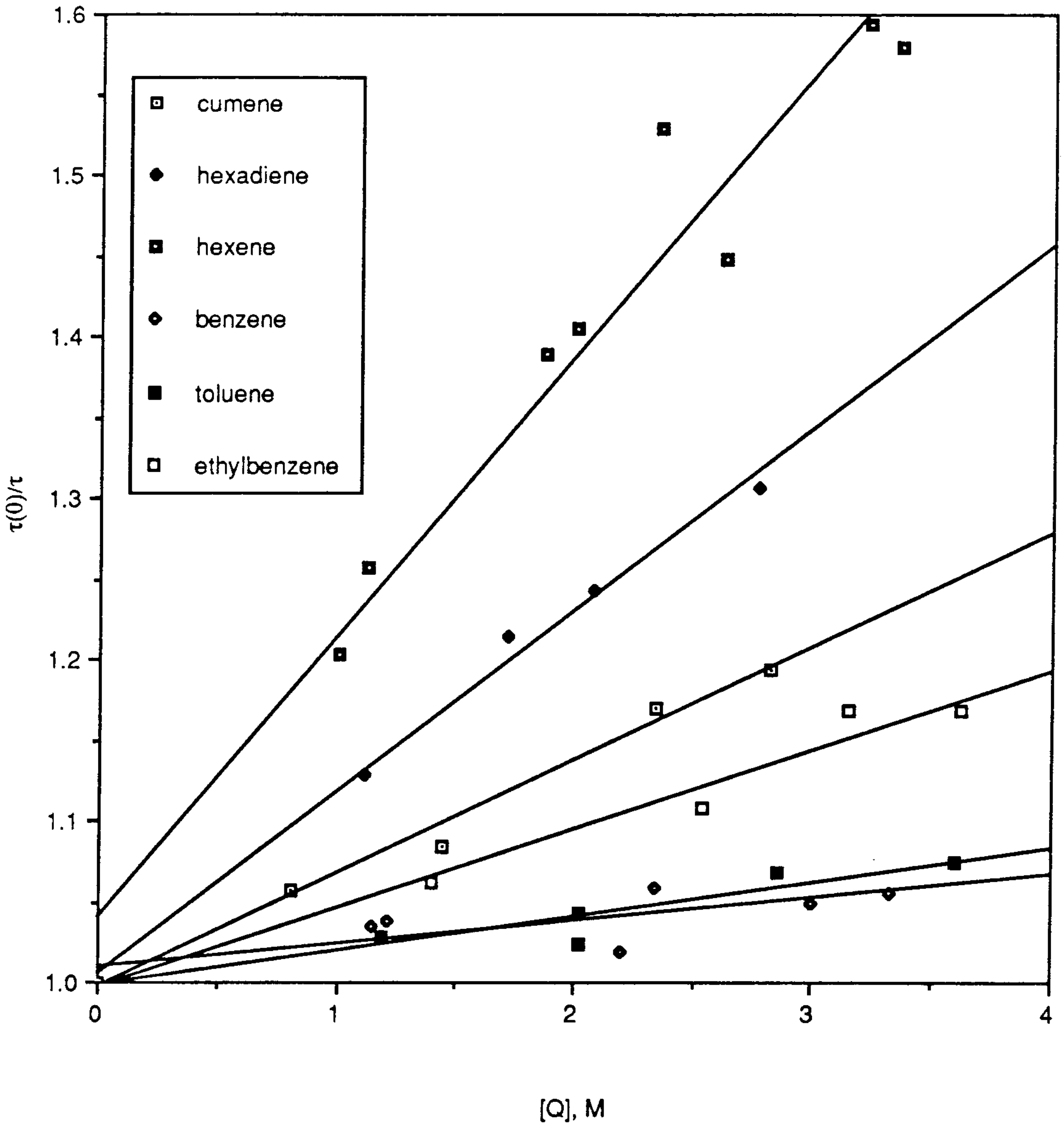
cumene
hexadiene
hexene
benzene
toluene
ethylbenzene
τ(0)/τ
[Q], M
1.6
1.5
1.4
1.3
1.2
1.1
1.0
0
1
2
3
4

Table 4.11. Stern-Volmer quenching rate constants for $Ir_2(TMB)_4^{2+}$ and $Pt_2(P_2O_5H_2)_4^{4-}$.

Substrate	BDE (kcal/mol)[a]	$^3Ir_2^*$ ($M^{-1}s^{-1}$)	$^3Pt_2^*$ ($M^{-1}s^{-1}$)
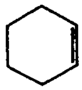	82 [b]	7.9×10^5 ($k_H/k_D > 3$)	1.2×10^6
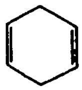	73 [b]	5.2×10^5	8.2×10^6
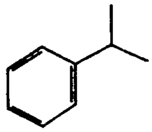	84.4 [b]	3.1×10^5	10^4
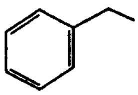	85.5 [b]	2.3×10^5	
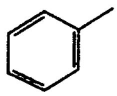	88.0 [b]	9.7×10^4	10^4
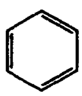		6.5×10^4	
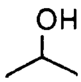	91.0 [b]		5×10^3
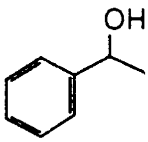	88		1.9×10^6 ($k_H/k_D = 4.6$)
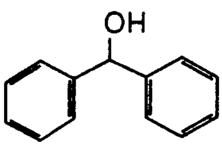	82		2×10^5
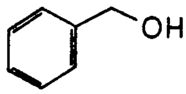	83		3×10^6
Et_3SiH	c	d	2.0×10^4
Bu_3SnH	c	d	1.2×10^7

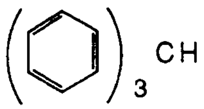	~75	$< 4 \times 10^5$	$< 2 \times 10^4$

a. C-H bond dissociation energy.

b. Reference 27.

c. The gas phase (298 K) E-H bond energies of $(CH_3)_3EH$ species have been reported: 90 (Si) and 74 kcal/mol (Sn). Jackson, R.A. *J. Organomet. Chem.* **1979**, *166*, 17-19.

d. Reacts upon mixing.

Figure 4.33. Plot of $\log(k_q)$ versus the C-H bond dissociation energy (D(C-H)) of the hydrogen atom-transfer quenching of $^3(Ir_2(TMB)_4{}^{2+})^*$ by the hydrocarbon substrates.

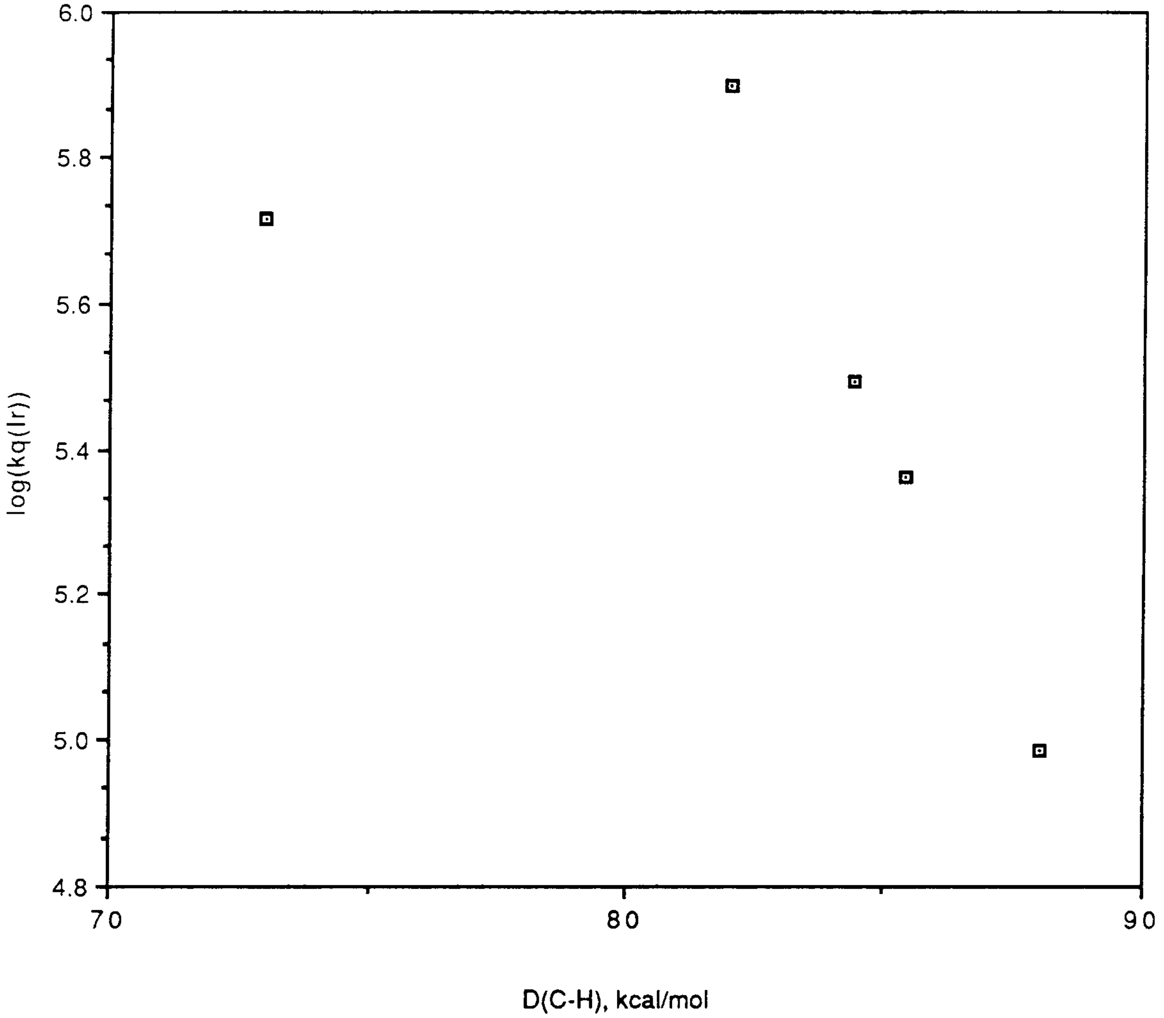
6.0
5.8
5.6
5.4
5.2
5.0
4.8
log(kq(Ir))
70
80
90
D(C-H), kcal/mol

homolytic C-H bond energy is ~10 kcal/mol greater than that of 1,4-cyclohexadiene, a larger rate constant is observed. However, steric arguments may be sufficient to reconcile the order of rates. Recent work has found the structure of 1,4-cyclohexadiene to be almost planar (Figure 4.34).[93] The structure of cyclohexene is a skewed boat (Figure 4.34).[94] For a linear M-H-C transition state, a much more unfavorable steric interaction is expected for the planar 1,4-cyclohexadiene. The angle defined by the M-H-C vector and the plane containing the allyl unit is much less for 1,4-cyclohexadiene than for cyclohexene.

The dihydride of $Ir_2(TMB)_4^{2+}$ (Ir_2H_2) has been characterized as the primary photoproduct. For some substrates (toluene and cumene), very little Ir_2H_2 product is observed. For cyclohexene, Ir_2H_2 appears slowly; either efficient Ir_2H_2 formation requires a rapid in-cage reaction of Ir_2H with the organic radical, or the factors that govern the second H atom-transfer reaction are unfavorable with either the substrates or the substrate radicals present.

An alternate explanation for the variation in quenching rates and chemical conversions is an alternative quenching mechanism. Both energy-transfer quenching and electron-transfer quenching can be ruled out.[95,96] The energies required for these processes are too great. An alternate mechanism, suggested for the photoreaction of $Pt_2(P_2O_5H_2)_4^{4-}$ with simple alkenes, is an inner-sphere process that involves formation of a diradical intermediate.[97]

$$^3M_2^* + RCH{=}CHR \rightarrow \bullet M_2\text{-}CHR\text{-}CHR\bullet \qquad 4.34$$

$$\bullet M_2\text{-}CHR\text{-}CHR\bullet \rightarrow M_2 + RCH{=}CHR \qquad 4.35$$

The second step in this mechanism involves the collapse of this intermediate back to the alkene and the ground-state metal complex. The rapid formation of Ir_2H_2 with 1,4-

Figure 4.34. (a) Stereoview of the X-ray structure of 1,4-cyclohexadiene. (b) Structure of cyclohexene; (i) stereo representation, (ii) conventional symbolism.

(a)

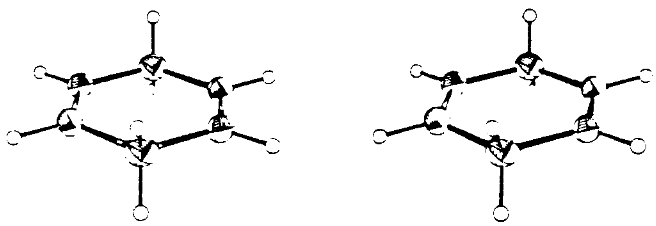

(b)

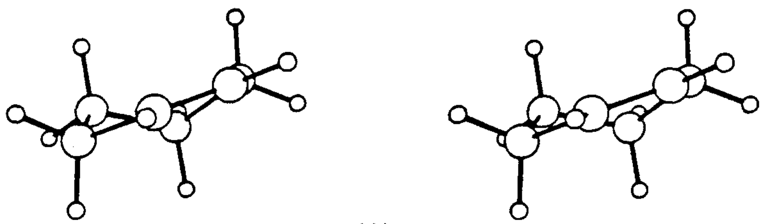

(i)

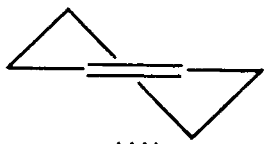

(ii)

cyclohexadiene and the large kinetic isotope effect observed for cyclohexene do not support such a mechanism.

From these data, the primary photoprocess from the $^3(d\sigma^*p\sigma)$ excited state is hydrogen-atom transfer:

$$^3M_2^* + R_3EH \rightarrow \bullet M_2H + R_3E\bullet \; . \qquad 4.36$$

Observation of a large kinetic isotope effect is supportive of an atom-transfer process for $^3Ir_2^*$. The monohydride species for $Ir_2(TMB)_4^{2+}$ has not been identified. The proposed pathway for formation of the observed products is

$$Ir_2 \rightarrow {}^3Ir_2^* \qquad 4.37$$

$$\bullet Ir \cdots Ir\bullet + RH_2 \rightarrow \bullet Ir \cdots Ir\text{-}H + RH\bullet \qquad 4.38$$

$$\bullet Ir_2H + RH\bullet \rightarrow Ir_2H_2 + R \qquad 4.39$$

$$\bullet Ir_2H + RH_2 \rightarrow Ir_2H_2 + RH\bullet \qquad 4.40$$

$$\bullet Ir_2H + \bullet Ir_2H \rightarrow Ir_2H_2 + Ir_2 \; . \qquad 4.41$$

The $^3(d\sigma^*p\sigma)$ excited state is written as •Ir···Ir• to emphasize the diradical-like structure.

The mechanism of radical atom abstraction has been extensively studied for many years and numerous reviews have appeared.[55] Three limiting atom abstraction mechanisms are defined by the timing of the various steps: M-Y bond making, R-Y bond cleavage, and electron transfer from M to Y. The three limiting mechanisms are shown in Figure 4.35. The timing of the electron-transfer event with respect to R-Y bond cleavage and M-Y bond formation becomes earlier in going from a to c.

Halogen-atom abstraction from alkyl halides has been extensively studied by Brown and coworkers.[98,99] They showed that the rate constant for

Figure 4.35. Possible limiting mechanism of atom transfer. (a) Heterolytic R-X bond cleavage and M-X bond formation followed by electron transfer. (b) Synchronous electron transfer, R-X bond cleavage, and M-X bond formation. (c) Electron transfer followed by $R\text{-}X^-$ heterolytic cleavage and M-X bond formation.

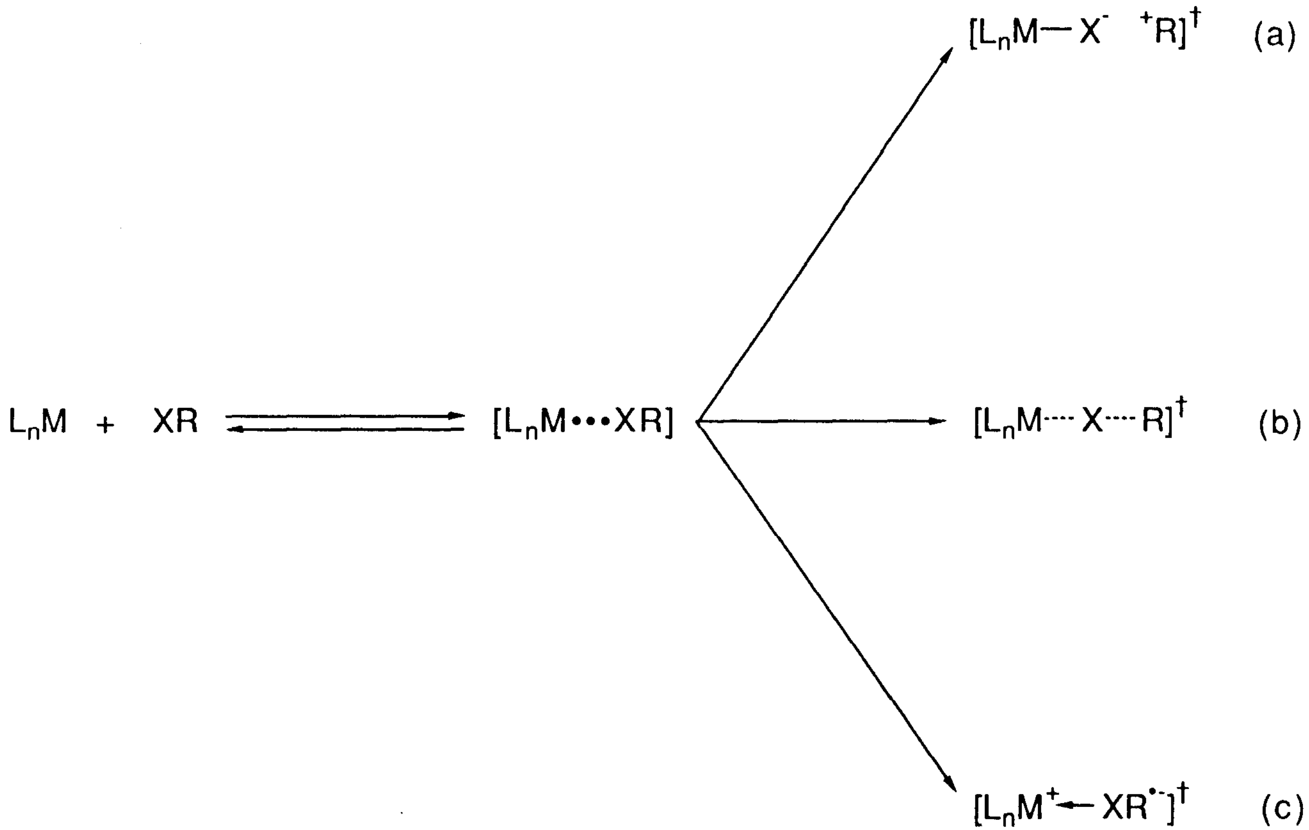
[LnM—X⁻ ⁺R]†
(a)
LnM + XR
[LnM•••XR]
[LnM····X····R]†
(b)
[LnM⁺←XR•⁻]†
(c)

$$\bullet Re(CO)_4L + RX \rightarrow Re(CO)_4LX + R\bullet \qquad 4.42$$

could be fit to the Marcus/Agmon-Levine equation, correlating the $E_{1/2}$ value for the halides and the rate constants for atom abstraction. The correlation between the rate constants and the C-X bond dissociation energy was not very good. That a Marcus/Agmon-Levine correlation exists between $E_{1/2}$ and the atom abstraction rates was interpreted as being consistent with some electron transfer, from the metal to the halogen-atom donor, in the transition state. Brown and coworkers were able to narrow down the possible pathways to b or c of Figure 4.35.

A limited correlation of the quenching rate constant with the C-H bond dissociation energy is observed for $Ir_2(TMB)_4^{2+}$ (Figure 4.33). Deviation from this correlation can be understood to be due to unfavorable steric interactions. If an atom-transfer mechanism with little to no charge development in the transition state is the preferred mechanism, correlation of the quenching rate constants for $Pt_2(P_2O_5H_2)_4^{4-}$ and the C-H bond dissociation energies is expected. The kinetic isotope effect observed for Bu_3SnH is interpreted to be in accord with hydrogen-atom transfer involving a linear Pt-H-Sn transition state with negligible charge transfer.[56]

A plot of the $\log(k_q)$ versus the C-H bond dissociation energy D(C-H) is given in Figure 4.36. While a limited correlation is observed for $Ir_2(TMB)_4^{2+}$, a very poor correlation is found for $Pt_2(P_2O_5H_2)_4^{4-}$. (A general downward drift in k_q is observed for increasing C-H bond energy.) This result may suggest an alternate quenching pathway for $Pt_2(P_2O_5H_2)_4^{4-}$. With the greater redox energy, electron transfer in the transition state may be important for the reaction of $^3Pt_2^*$. An alternative explanation for the observed behavior is a variation in the steric factors for the series of hydrogen atom donors.

Figure 4.36. Plot of $\log(k_q)$ versus the C-H bond dissociation energy (D(C-H)) of the hydrogen atom-transfer quenching of $^3M_2^*$ by the hydrocarbon substrates, $Ir_2(TMB)_4^{2+}$ open squares and $Pt_2(P_2O_5H_2)_4^{4-}$ solid diamonds.

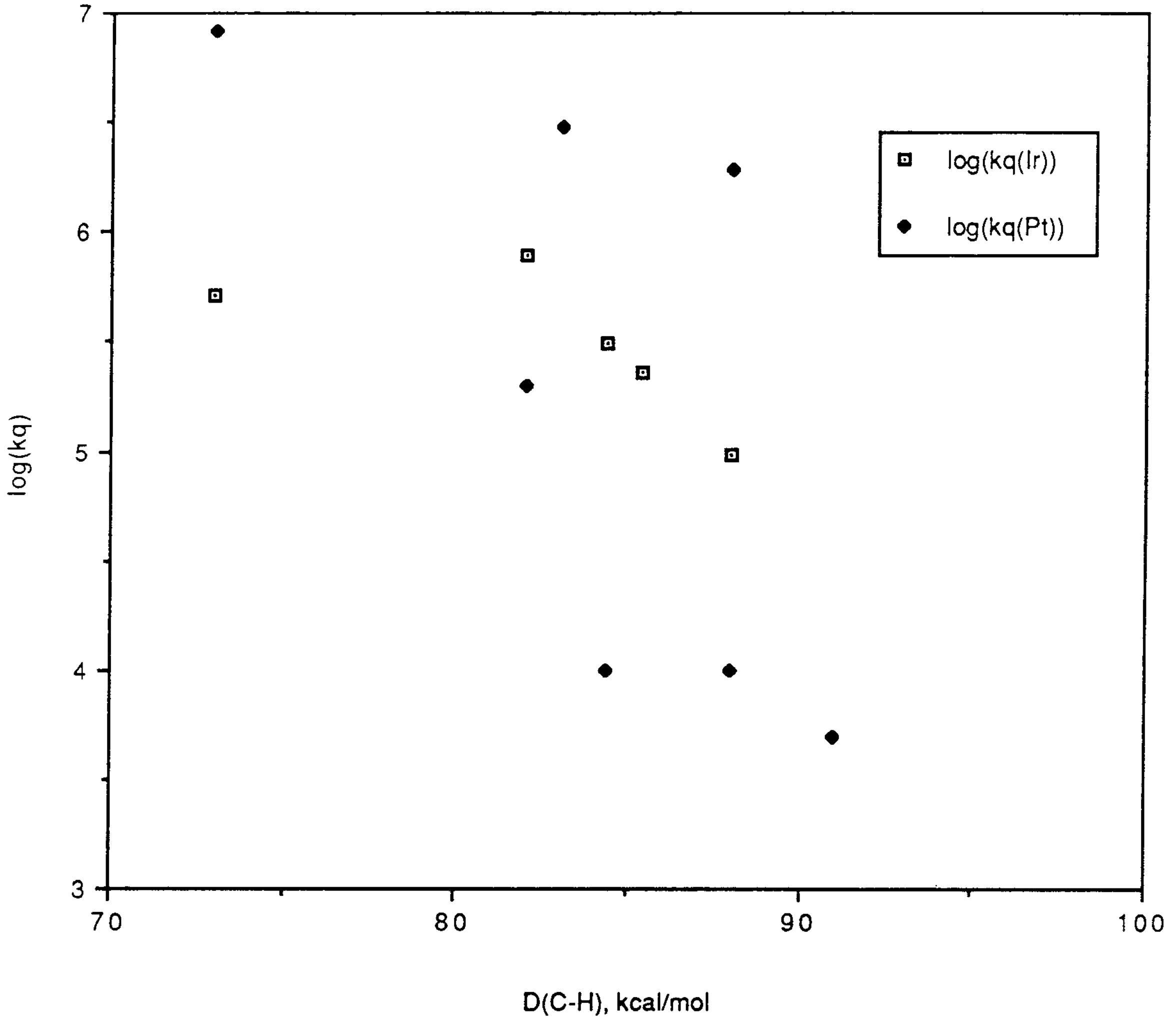

7
6
5
4
3
log(kq)
70
80
90
100
D(C-H), kcal/mol
log(kq(Ir))
log(kq(Pt))

In comparing rate constants for $^3Ir_2^*$ and $^3Pt_2^*$, some surprising trends emerge. For small substrates, such as 1,4-cyclohexadiene, the rate observed for $^3Pt_2^*$ is greater. This is expected and is due to the more energetic excited state. Assuming a M_2-H dissociation energy of 60 kcal/mol,[100] for both Ir and Pt,[101] the driving force for hydrogen-atom transfer is estimated to be roughly ($60 - D_{EH} + E_T$) 47 kcal/mol for Pt_2 and 17 kcal/mol for Ir_2. For cumene and possibly toluene, a larger rate is observed for $^3Ir_2^*$. These larger rates might be understood from the greater steric demands about the open axial site in $Pt_2(P_2O_5H_2)_4^{4-}$ in comparison to $Ir_2(TMB)_4^{2+}$.

For reactions where most of the reorganization comes from the bonds being broken and formed, rather than from all the other coordinates, the free energy of activation is controlled by the work terms for the process (w_r, w_p), and the steric (S^r, S^p) and statistical factors (s^r, s^p), which describe the orientation of the reactants and products.[102,103]

$$\Delta G^* \cong W^r \quad (-\Delta G^{0'} \geq \lambda) \qquad 4.43$$

$$\Delta G^* \cong \Delta G^{0'} + W^p \quad (\Delta G^{0'} \geq \lambda) \qquad 4.44$$

$$W^r = w^r - RT\ln(S^r s^r)$$

$$W^p = w^p - RT\ln(S^p s^p)$$

$S^{r/p}$, $s^{r/p}$ - steric and statistical factors that describe the orientation of the reactants and products, respectively.
$w^{r/p}$ - Coulombic and other work terms of the reactants and the products, respectively.

The poor correlation of the quenching rate of $Pt_2(P_2O_5H_2)_4^{4-}$ with the C-H bond dissociation energy can be understood as the result of variation in the steric factors of the reaction with variation of the substrate. Also, preassociation or favorable docking of the alcohol via hydrogen-bonding interactions with the $P_2O_5H_2^{2-}$ ligand may enhance the hydrogen-atom transfer process and may explain the increased quenching rate observed for alcohols in comparison to hydrocarbons with similar C-H bond dissociation energies. For $Pt_2(P_2O_5H_2)_4^{4-}$, the greater steric demands about the open axial site and the possible substrate and/or solvent hydrogen-bonding interactions with the pyrophosphite ligand increase the sensitivity of the reaction to variations in the substrate. For $Ir_2(TMB)_4^{2+}$, no preassociation or docking of the substrate is possible, and steric interactions alone discriminate between substrates.

The $^3(d\sigma^*p\sigma)$ excited state of the d^8-d^8 complexes has been shown to be involved in the photochemical hydrogen atom-transfer reaction. The atom-transfer reactivity of this state is attributed to the presence of a hole in the $d\sigma^*$ orbital, analogous to the $^3n\pi^*$ state of organic ketones. Interaction of the oxidizing hole with the electron pair of the C-H bond is the presumed pathway.

Electrocatalysis

If production of an oxidizing hole in the $d\sigma^*$ orbital is the important factor in the photochemical hydrogen-atom transfer reaction, then electrochemical generation of such a hole should produce a highly reactive intermediate that would mimic the initial step in the $^3(d\sigma^*p\sigma)$ photoreaction. Several of the binuclear d^8 complexes undergo reversible one-electron oxidations in noncoordinating solvents.[43,104,105] The complex $Rh_2(TMB)_4^{2+}$ possesses a quasi-reversible, one-electron oxidation at 0.74 V (SSCE). Electrochemical oxidation of $Rh_2(TMB)_4^{2+}$ in the presence of 1,4-cyclohexadiene exhibits an enhanced anodic current with loss of the cathodic wave, behavior indicative of an electrocatalytic process (Figure 4.37).[106] Bulk electrolysis of $Rh_2(TMB)_4^{2+}$ in an excess of 1,4-cyclohexadiene results in the formation of benzene and two protons (Equation 4.45).

$$C_6H_8 \rightarrow C_6H_6 + 2H^+ + 2e^- \quad (E^0 = 0.4 \text{ V NHE}) \qquad 4.45$$

Figure 4.37. Cyclic voltammograms of a dichloromethane solution (0.1 M $TBAPF_6$) of (a) $[Rh_2(TMB)_4](PF_6)_2$ (1 mM, i_a = 5 μA/cm) with (b) a twentyfold excess of 1,4-cyclohexadiene (i_a = 10 μA/cm).

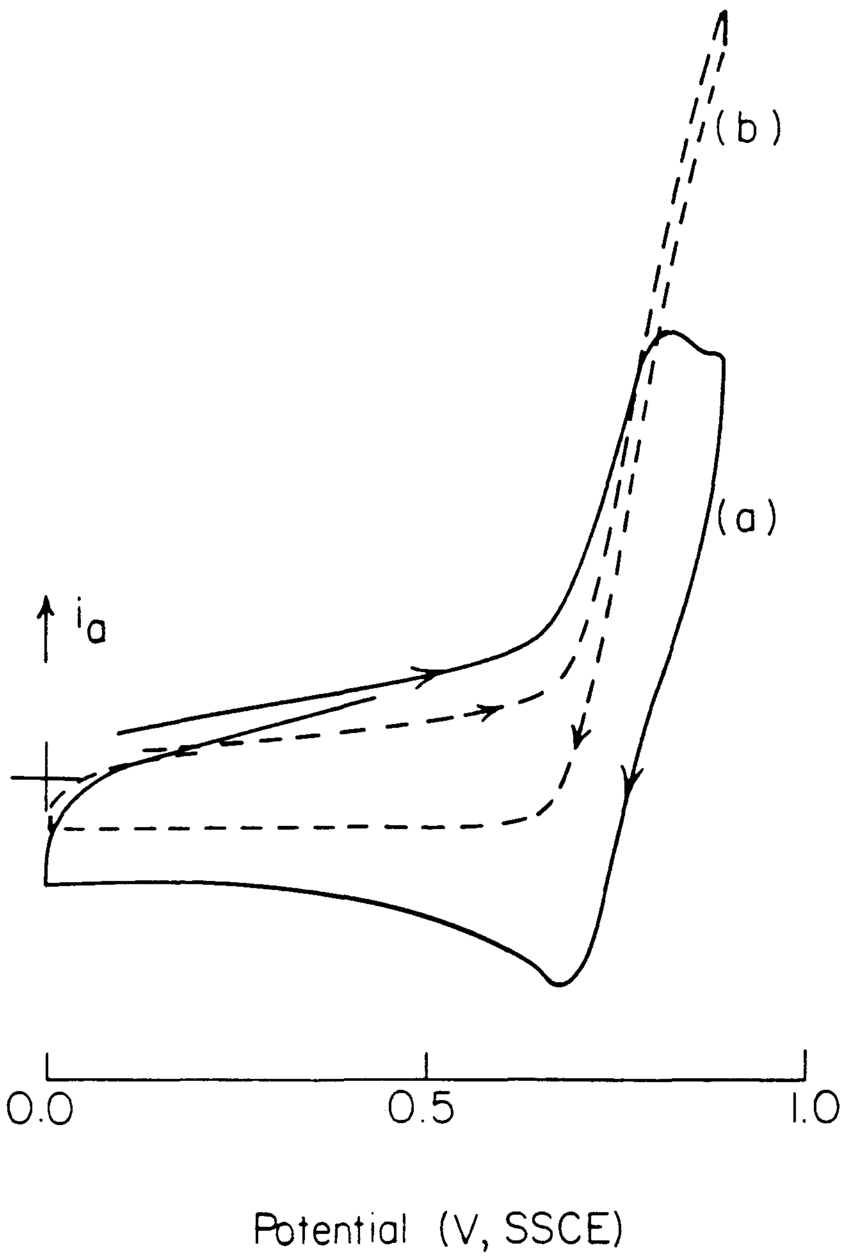
(b)
(a)
i_a
0.0
0.5
1.0
Potential (V, SSCE)

The maximum number of turnovers observed is limited by the amount of substrate relative to solvent. The complex $Rh_2(TMB)_4^{2+}$ is slowly lost because of a competitive reaction with CH_2Cl_2 to produce $Rh_2(TMB)_4Cl_2^{2+}$.

The pathway proposed to explain the observed oxidation of 1,4-cyclohexadiene is given in Figure 4.38. Oxidation $Rh_2(TMB)_4^{2+}$ generates the reactive d^8-d^7 complex, $Rh_2(TMB)_4^{3+}$. The metal complex abstracts a hydrogen atom from the organic substrate, generating a monohydride species and an organic radical. It is known that hydride complexes of $Rh_2(TMB)_4^{2+}$ are quite unstable.[3] (No reaction between $Rh_2(TMB)_4^{2+}$ and HCl is observed at room temperature, in the absence of air, suggesting that the equilibrium between the d^8-d^8 and d^7-d^7 adducts lies far to the side of the d^8-d^8 complex.) Therefore, the monohydride rapidly loses H^+, regenerating $Rh_2(TMB)_4^{2+}$. The cycle accounts for the generation of H^+ (identified electrochemically at a platinum button electrode and by the decrease in pH) and the observed electrocatalytic behavior of $Rh_2(TMB)_4^{2+}$.

The competitive reaction of $Rh_2(TMB)_4^{2+}$ with CH_2Cl_2 can also be accounted for with a pathway similar to that for the hydrogen-atom abstraction. The d^8-d^7 complex abstracts a halide atom, generating a monohalide species. The monohalide, rather than losing halide to regenerate $Rh_2(TMB)_4^{2+}$, reacts to yield $Rh_2(TMB)_4Cl_2^{2+}$.

This result demonstrates that highly reactive d^8-d^7 species can be generated electrochemically, and that complexes with an oxidizing hole in the $d\sigma^*$ orbital can participate in atom abstraction processes. This is the first direct example of chemistry for a d^8-d^7 complex.

The importance of this result is twofold. First, it demonstrates that the d^8-d^7 complex can be chemically intercepted. In constructing a system that can efficiently harvest light and store this energy in the form of a charge-separated state, some means of intercepting the charge-separated state is necessary. Systems using binuclear d^8

Figure 4.38. (a) Pictorial representation of an electrocatalytic cycle which regenerates the Rh_2^{2+} complex. (b) Atom-transfer pathway for electrochemical oxidation of 1,4-cyclohexadiene.

(a)

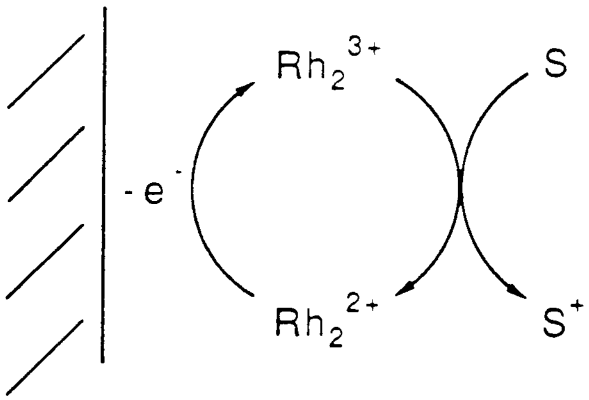

(b)

$$Rh_2^{2+} \rightleftharpoons Rh_2^{3+} + e^-$$

$$Rh_2^{3+} + C\text{-}H \longrightarrow Rh_2H^{3+} + C\bullet$$

$$Rh_2H^{3+} \longrightarrow Rh_2^{2+} + H^+$$

complexes covalently linked to pyridinium acceptors have been shown to yield charge-separated species upon excitation.[24] Excited-state electron transfer generates the one-electron oxidized metal complex and the one-electron reduced pyridinium. Intercepting the d^8-d^7 species of the charge-separated state would inhibit the back-electron-transfer step, creating a system where charge separation coupled with chemistry at the oxidized metal complex serves to harvest and store the photon energy (Figure 4.39). Second, the ability to generate reactive d^8-d^7 complexes electrochemically should make possible reactions with the most inert hydrocarbons. While the $^3(d\sigma^*p\sigma)$ excited state may possess a sufficient driving force for reaction with hydrocarbons with D(C-H) in excess of 100 kcal/mol, the expected rates for these reactions are orders of magnitude less than the lower limit for the observed rates for the $^3(d\sigma^*p\sigma)$ excited state. For $Pt_2(P_2O_5H_2)_4^{4-}$, the lower limit of the observed rates is 10^4 $M^{-1}s^{-1}$ for substrate with a D(C-H) of approximately 90 kcal/mol.[2] Electrochemically generated d^8-d^7 complexes may overcome the kinetic limitation of the ηs to μs $^3(d\sigma^*p\sigma)$ lifetime.

Figure 4.39. Pictorial representation of chemical step following charge separation to trap the charge-transfer state.

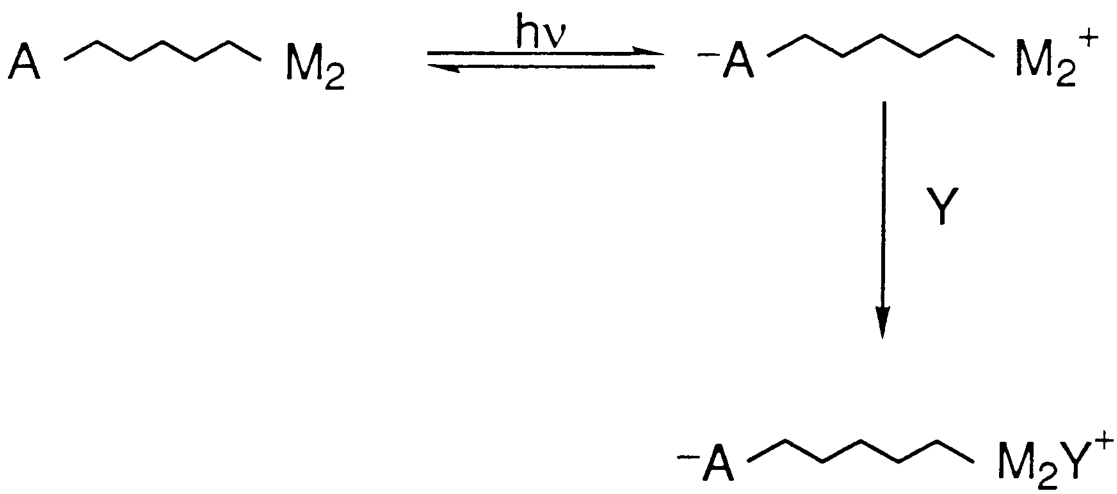
A
M2
hν
-A
M2+
Y
-A
M2Y+

References and Notes

1. Lewis, N.S.; Mann, K.R.; Gordon, J.G. II; Gray, H.B. *J. Am. Chem. Soc.* **1976**, *98*, 7461-7463.

2. Roundhill, D.M.; Gray, H.B.; Che, C.-M. *Accts. Chem. Res.*, in press.

3. Smith, T.P., Ph.D. Dissertation, California Institute of Technology. 1982.

4. Miskowski, V.M.; Smith, T.P.; Loehr, T.M.; Gray, H.B. *J. Am. Chem. Soc.* **1985**, *107*, 7925-7934.

5. Maverick, A.W.; Smith, T.P.; Maverick, E.F.; Gray, H.B. *Inorg. Chem.* **1987**, *26*, 4336-4341.

6. Olmstead, M.M.; Blach, A.L. *J. Organomet. Chem.* **1978**, *148*, C15-C18.

7. Mondal, J.U.; Young, K.G.; Blake, D.M. *J. Organomet. Chem.* **1982**, *240*, 447-451.

8. Balch, A.L. *J. Am. Chem. Soc.* **1976**, *98*, 8049-8054.

9. Coleman, A.W.; Eadie, D.T.; Stobart, S.R.; Zaworotho, M.J.; Atwood, J.L. *J. Am. Chem. Soc.* **1982**, *104*, 922-923.

10. Collman, J.P.; Hegedus, L.S.; Norton, J.R.; Finke, R.G. *Principles and Applications of Organotransition Metal Chemistry*; University Science Books: Mill Valley, California, 1987.

11. Poilblanc, R. *Inog. Chim. Acta.* **1982**, *62*, 75-78, and references therein.

12. Halpern, J. *Inorg. Chim. Acta.* **1982**, *62*, 31-37, and references therein.

13. Poilblanc, R. *Nouv. J. Chim.* **1978**, *2*, 145-150.

14. McCleverty, J.A. *Inorg. Chim. Acta.* **1982**, *62*, 67-73.

15. Chisholm, M.H. *ACS Symp. Ser.* **1980**, *155*, 17-39.

16. Sutherland, B.R.; Cowie, M. *Organometallics* **1984**, *3*, 1869-1878.

17. Mague, J.T.; DeVries, S.H. *Inorg. Chem.* **1982**, *2*, 1632-1638.

18. Mague, J.T. *Inorg. Chem.* **1983**, *22*, 1158-1162.

19. Bushnell, G.W.; Decker, M.J.; Eadie, D.T.; Stobart, S.R.; Vefghi, R.; Atwood, J.L.; Zaworotko, M.J. *Organometallics* **1985**, *4*, 2106-2111.

20. Stobart, S.R.; Coleman, A.W.; Harrison, D.G.; Atwood, J.L.; Zaworotko, M.J. *J. Am. Chem. Soc.*, submitted.

21. Chapter 2.

22. Gordon, A.J.; Ford, R.A. *The Chemist's Companion*; John-Wiley & Sons: New York, 1972.

23. Perrin, D.D.; Armarego, W.L.F.; Perrin, D.R. *Purification of Laboratory Chemicals*; Pergamon: Oxford, 1966.

24. Fox, L.S., Ph.D. Dissertation, California Institute of Technology, 1989.

25. Halpern, J.; Pribanic M. *Inorg. Chem.* **1970**, *9*, 2616-2618.

26. Reactions with phenol are of interest.

27. McMillen, D.F.; Golden, D.M. *Ann. Rev. Phys. Chem.* **1982**, *33*, 493-532.

28. Chan, D.M.T.; Marder, T.D.; Milstein, D.; Taylor, N.J. *J. Am. Chem. Soc.* **1987**, *109*, 6385-6388, and references therein.

29. Vlcek, A., Jr.; Gray, H.B. *Inorg. Chem.* **1987**, *26*, 1997-2001.

30. Schmidbaur, H.; Franke, R. *Inorg. Chim. Acta* **1975**, *13*, 85-89.

31. Fackler, J.P., Jr.; Murray, H.H.; Basil, J.D. *Organometallics* **1984**, *3*, 821-823.

32. Fukuzumi, S.; Nishizawa, N.; Tanaka, T. *Bull. Chem. Soc. Jpn.* **1982**, *55*, 2886-2891.

33. Isocyanide ligands provide the possibility of both insertion reactions and nucleophilic additions. Insertion of isocyanides into M-C bonds is now well established for many metal systems. In comparision to metal-carbonyl complexes, isonitrile insertion into metal-alkyls is more facile. Insertion into M-H bonds is known. Reaction of Pt_3(CN-*t*-butyl)$_6$ with either R_3SiH or R_3GeH yields formimidoyl species. There are also some examples of isocyanide insertion into metal-halide bonds. Nucleophilic addition of alcohols and amines to metal-isocyanides is well known. Such addition reactions have been observed for several binuclear d^8 complexes.

34. Buckingham, A.D.; Stephens, P.J. *J. Chem. Soc.* **1964**, 2747-2759.

35. Buckingham, A.D.; Stephens, P.J. *J. Chem. Soc.* **1964**, 4583-4587.

36. Felthouse, T.R.; Dong, T.-Y.; Hendrickson, D.N.; Shieh, H.-S.; Thompson, M.R. *J. Am. Chem. Soc.* **1986**, *108*, 8201-8214.

37. Jackson, R.A.; Poe, A. *Inorg. Chem.* **1978**, *17*, 997-1003.

38. Poe, A.; Jackson, R.A. *Inorg. Chem.* **1978**, *17*, 2330-2333.

39. Marshall, J.L., Ph.D. Dissertation, California Institute of Technology, 1987.

40. Pilloni, G.; Vecchi, E.; Martelli, M. *Electroanal. Chem. Interfac. Electrochem.* **1973**, *45*, 483-487.

41. Teo, B.-K.; Ginsberg, A.P.; Calabrese, J.C. *J. Am. Chem. Soc.* **1976**, *98*, 3027-3028.

42. Zotti, G.; Zecchin, S.; Pilloni, G. *J. Organometal. Chem.* **1983**, *246*, 61-71.

43. Womack, D.R.; Enlow, P.D.; Woods, C. *Inorg. Chem.* **1983**, *22*, 2653-2656.

44. Geiger, W.E. *Prog. Inorg. Chem.* **1985**, *33*, 275-352.

45. Gennett, T.; Geiger, W.E.; Willett, B.; Anson, F.C. *J. Electroanal. Chem.* **1987**, *222*, 151-160.

46. Balzani, V; Bolletta, F.; Gandolfi, M.T.; Maestri, M. *Top. Curr. Chem.* **1978**, *75*, 1-64.

47. Meyer, T.G. *Prog. Inorg. Chem.* **1983**, *30*, 389-440, and references therein.

48. Milder, S.J.; Goldbeck, R.A.; Kliger, D.S.; Gray, H.B. *J. Am. Chem. Soc.* **1980**, *102*, 6761-6764.

49. Marshall, J.L.; Stiegman, A.E.; Gray, H.B. In *Excited States and Reactive Intermediates*; Lever, A.B.P., Ed.; ACS Symp. Ser. 307; American Chemical Society: Washington, D.C., 1986; pp. 166-176.

50. Balzani, V. Scandola, F. In *Energy Resources through Photochemistry and Catalysis*; Gratzel, M., Ed.; Academic Press: New York, 1985; Chapter 1.

51. Bergamini, P.; Sostero, S.; Traverso, O. In *Fundamental and Technological Aspects of Organo-f-Element Chemistry*; Marks, T.J.; Fragala, I.L., Eds.; D. Reidel: Boston, 1985; pp. 361-385.

52. Stiegman, A.E.; Tyler, D.R. *Comm. Inorg. Chem.* **1986**, *5*, 215-245.

53. Hanckel, J.M.; Lee, K.-W.; Rushman, P.; Brown, T.L. *Inorg. Chem.* **1986**, *25*, 1852-1856.

54. Wayland, B.B.; Del Rossi, K.J. *J. Organomet. Chem.* **1984**, *276*, C27-C30.

55. Tyler, D.R. *Prog. Inorg. Chem.* **1988**, *36*, 125-194.

56. Vlcek, A., Jr.; Gray, H.B. *J. Am. Chem. Soc.* **1987**, *109*, 286-287.

57. Marshall, J.L.; Stobart, S.R.; Gray, H.B. *J. Am. Chem. Soc.* **1984**, *106*, 3027-3029.

58. Caspar, J.V.; Gray, H.B. *J. Am. Chem. Soc.* **1984**, *106*, 3029-3030.

59. Hawley, M.D. In *Encyclopedia of Electrochemistry of the Elements. Vol. XIV*; Bard, A.J., Ed.; Marcel Dekker: New York, 1980; pp. 1-135.

60. Roundhill, D.M. *J. Am. Chem. Soc.* **1985**, *107*, 4354-4356.

61. Harvey, E.L.; Stiegman, A.E.; Vlcek, A., Jr.; Gray, H.B. *J. Am. Chem. Soc.* **1987**, *109*, 5233-5235.

62. Chapter 2.

63. Miskowski, V.M.; Nobinger, G.L.; Kliger, D.S.; Hammond, G.S.; Lewis, N.S.; Mann, K.R.; Gray, H.B. *J. Am. Chem. Soc.* **1978**, *100*, 485-488.

64. Mann, K.R.; Thich, J.A.; Bell, R.A.; Coyle, C.G.; Gray, H.B. *Inorg. Chem.* **1980**, *19*, 2462-2468.

65. Che, C.-M.; Wong, K.-Y.; Anson, F.C. *J. Electroanal. Chem.* **1987**, *226*, 211-226.

66. Rice, S.F.; Gray, H.B. *J. Am. Chem. Soc.* **1983**, *105*, 4571-4575.

67. Nocera, D.G.; Winkler, J.R.; Yocum, K.M.; Bordignon, E.; Gray, H.B. *J. Am. Chem. Soc.* **1984**, *106*, 5145-5150.

68. Bock, C.R.; Meyer, T.J.; Whitten, D.G. *J. Am. Chem. Soc.* **1974**, *96*, 4710-4712.

69. Ledwith, A. *Accts. Chem. Res.* **1972**, *5*, 133-139.

70. Balzani, V.; Moggi, L.; Manfrin, M.F.; Bolletta, F.; Laurence, G.S. *Coord. Chem. Rev.* **1975**, *15*, 321-433.

71. Appendix 2.

72. Kosower, E.M.; Cotter, J.L. *J. Am. Chem. Soc.* **1964**, *86*, 5524-5527.

73. Bock, C.R.; Connor, J.A.; Gutierrez, A.R.; Meyer, T.J.; Whitten, D.G.; Sullivan, B.P.; Nagle, J.K. *J. Am. Chem. Soc.* **1979**, *101*, 4815-4824.

74. Kalyanasundaram, K. *Coord. Chem. Rev.* **1982**, *46*, 159-244.

75. Sutin, N.; Creutz, C. *J. Chem. Educ.* **1983**, *60*, 809-814.

76. Sutin, N. *Accts. Chem. Res.* **1982**, *15*, 275-282.

77. Sutin, N. *Prog. Inorg. Chem.* **1983**, *30*, 441-498.

78. Marcus, R.A.; Sutin, N. *Biochim. Biophys. Acta* **1985**, *811*, 265-322, and references therein.

79. Rehm, D.; Weller, A. *Isr. J. Chem.* **1970**, *8*, 259-271.

80. Sandrini, D; Maestri, M.; Belser, P.; Zelewsky, A. von; Balzani, V. *J. Phys. Chem.* **1985**, *89*, 3675-3679.

81. Debye, P. *Trans. Electrochem. Soc.* **1942**, *82*, 265-272.

82. Eigen, M. *Z. Physik. Chem. [N.F.]* **1954**, *1*, 176-200.

83. The pyridinum radii are calculated by averaging the van der Waals radii along the three molecular axes and they vary from 3.2 to 4.6 Å, r(MV^{2+}) = 7.8 Å, and r($Ir_2(TMB)_4{}^{2+}$) = 7.85 Å.

84. Heuer, W.B.; Totten, W.D.; Rodman, G.S.; Hebert, E.J.; Tracy, H.J.; Nagle, J.K. *J. Am. Chem. Soc.* **1984**, *106*, 1163-1164.

85. Brunshwig, B.S.; Logan, J.; Newton, M.D.; Sutin, N. *J. Am. Chem. Soc.* **1980**, *102*, 5798-5809.

86. Che, C.-M.; Cho, K.-R.; Chan, W.-S.; Gray, H.B. *Inorg. Chem.* **1986**, *25*, 4906-4909.

87. Che, C.-M.; Lu, W.-M. *J. Chem. Soc., Chem. Commun.* **1986**, 616-617.

88. Fukuzumi, S.; Nishizawa, N.; Tanaka, T. *Bull. Chem. Soc. Jpn.* **1983**, *56*, 709-714.

89. Chapter 2.

90. Sigal, I.S.; Gray, H.B. *J. Am. Chem. Soc.* **1981**, *103*, 2220-2225.

91. Miskowski, V.M.; Sigal, I.S.; Mann, K.R.; Gray, H.B.; Milder, S.J.; Hammond, G.S.; Ryason, P.R. *J. Am. Chem. Soc.* **1979**, *101*, 4383-4385.

92. Stiegman, A.E., unpublished results.

93. Jeffrey, G.A.; Buschmann, J.; Lehmann, C.W.; Luger, P. *J. Am. Chem. Soc.* **1988**, *110*, 7218-7219.

94. Streitwieser, A., Jr.; Heathcock, C.H. *Introduction to Organic Chemistry, 2nd Edition*; MacMillan: New York, 1981.

95. *Encyclopedia of Electrochemistry of the Elements*; Bard, A.J., Ed.; Marcel Dekker: New York, 1982.

96. Murov, S.L. *Handbook of Photochemistry*; Dekker: New York, 1973.

97. Roundhill, D.M.; Shen, Z.-P.; King, C.; Atherton, S.J. *J. Phys. Chem.* **1988**, *92*, 4088-4094.

98. Burke, M.R.; Brown, T.L. *J. Am. Chem. Soc.*, in press.

99. Lee, K.-W.; Brown, T.L. *J. Am. Chem. Soc.* **1987**, *109*, 3269-3275.

100. Pearson, R.G. *Chem. Rev.* **1985**, *85*, 41-49.

101. The M-H IR resonance is at higher energy for Ir than for Pt, leading to the conclusion that the M-H bond strength is larger for Ir than for Pt. (The reduced mass for the M-H system ($\mu = \frac{m_M m_H}{m_M + m_H}$ is approximately m_H.) The large Ir-H bond strength will increase the driving force for hydrogen-atom transfer to Ir_2

102. Marcus, R.A. *Proc. Symp. Chem. Physics Electrocatal.* **1984**, *84-12*, 169-186.

103. Marcus, R.A. *J. Phys. Chem.* **1968**, *72*, 891-899.

104. Enlow, P.D.; Woods, C. *Inorg. Chem.* **1985**, *24*, 1273-1274.

105. Boyd, D.C.; Matsch, P.A.; Mixa, M.M.; Mann, K.R. *Inorg. Chem.* **1986**, *25*, 3331-3333.

106. Bard, A.J.; Faulkner, L.R. *Electrochemical Methods: Fundamentals and Applications*; John Wiley & Sons: New York, 1980.

Chapter 5

Synthesis and Characterization of $Ir_2(TMB)_4H_2^{2+}$

Introduction

Hydrogen-atom transfer has been established as an important reaction pathway for the triplet $d\sigma^{*}p\sigma$ excited state of binuclear d^8 complexes.[1-4] Substrates that serve as hydrogen-atom donors include hydrocarbons (e.g., cyclohexene and 1,4-cyclohexadiene), alcohols with α(C-H) bonds, and triorganosilanes, -germanes, and -stannanes. Irradiation of the metal complex in the presence of these substrates produces complexes of the type M_2H_2. Earlier work has characterized the product formed with $Pt_2(P_2O_5H_2)_4^{4-}$ as the binuclear platinum(III) dihydride, $Pt_2(P_2O_5H_2)_4H_2^{4-}$ (Pt_2H_2).[5] In this chapter, the characterization of the dihydride of $Ir_2(TMB)_4^{2+}$ (Ir_2H_2) is reported. In addition to NMR, UV-Vis, IR, and Raman spectra, the complex has been characterized crystallographically. The reactivity of Ir_2H_2 is also reported.

Experimental

Synthesis

Standard Schlenk and high-vacuum techniques were used. Acetonitrile was used as received, freeze-pump-thaw degassed, and stored under vacuum over activated alumina. 1,4-Cyclohexadiene was distilled under argon from $NaBH_4$, freeze-pump-thaw degassed, and stored under vacuum. 9,10-Dihydroanthracene was recrystallized three times from absolute ethanol. Standard procedures were used to prepare $[Ir_2(TMB)_4](B(C_6H_5)_4)_2$.[6] The ^1H NMR spectra were obtained on a 400 MHz JNM-GX400 FT NMR spectrometer. The IR spectra were measured on a Beckman IR 4240. Absorption spectra were recorded with a Hewlett-Packard 8450A spectrophotometer or a Shimadzu UV-260 spectrophotometer. Elemental analyses were obtained from Galbraith Laboratories, Inc.

$[Ir_2(TMB)_4H_2](B(C_6H_5)_4)_2$

A twentyfold excess of 1,4-cyclohexadiene was added to an acetonitrile solution of $[Ir_2(TMB)_4](B(C_6H_5)_4)_2$ in an inert atmosphere. The solution was freeze-pump-thaw degassed three times and photolyzed for 2 hrs, using a 1000 W high-pressure Hg/Xe lamp equipped with a Corning cutoff filter (λ_{ex} > 550 nm). The final solution was a clear, light orange. The solvent was removed under vacuum, being careful to shield the material from light. An off-white powder was obtained. The solid was recrystallized from acetonitrile/toluene. Calculated for $Ir_2C_{95}H_{114}N_8B_2$: C,64.3; H, 6.5; N, 6.3. Found: C, 64.8, H, 6.8; N, 6.2. ^1H NMR: δ (CD_3CN, 20 °C); -10.6 (singlet, 1H, Ir-H), 1.4 (broad singlet singlet, CH_3), 1.6 (broad singlet, CH_3), 1.8 (broad singlet, CH_2), 6.9 (triplet, 8H), 7.04 (triplet, 16H), 7.33 (multiplet, 16H). IR (Nujol mull, NaCl plates): 1940 cm^{-1} (m), ν(Ir-H); 2160 cm^{-1}(s), ν(N≡C). UV-Vis (CH_3CN, 25 °C): 320 nm (ε = 17000 $M^{-1}cm^{-1}$)

A similar procedure was followed for the photolysis with 9,10-dihydroanthracene. The material obtained from the removal of the solvent contained the desired iridium complex, anthracene, and 9,10-dihydroanthracene. This material was washed with dry, degassed benzene to remove the organics. The remaining solid was dissolved in CH_3CN and filtered. The solvent was removed from the filtrate under vacuum, yielding a light blue-green powder.

Reactivity

Acetonitrile and acetonitrile-d_3 were used as received, freeze-pump-thaw degassed, and stored under vacuum over activated alumina. HCl was freeze-pump-thaw degassed prior to addition to the reaction vessel. Styrene was used as received, freeze-pump-thaw degassed, vacuum-transferred to a graduate cylinder, and a known volume of styrene vacuum transferred to the reaction vessel.

Thermal Stability of $Ir_2(TMB)_4H_2^{2+}$

A CH_3CN solution of Ir_2H_2 was prepared in a two-compartment cell consisting of a 10 ml bulb and a 1 cm pathlength square cuvette. The UV-Vis spectrum of the sample was measured. The cell was wrapped in foil to prevent exposure to light and immersed in an 80 °C oil bath. The UV-Vis spectrum was remeasured after 12 hrs. A 5% decrease in the intensity of the band at 320 nm was observed.

$Ir_2(TMB)_4H_2^{2+}$ + HCl

An atmosphere of HCl was introduced to an CH_3CN solution of Ir_2H_2 in a two-compartment cell. The UV-Vis spectrum of the sample was measured before and after the addition of HCl.

$Ir_2(TMB)_4H_2^{2+}$ + Styrene

An CH_3CN solution of Ir_2H_2 was prepared in a two-compartment cell. To this solution was added a large excess of styrene. A slow growth of $Ir_2(TMB)_4^{2+}$ was observed in the UV-Vis spectrum of the sample over a 24 hr period.

Two samples of Ir_2H_2 were prepared in vacuum-adapted NMR tubes. To one of these solutions was added a thirtyfold excess of styrene. Both tubes were stored in the dark at room temperature. NMR spectra were recorded every 24 hrs over a 7-day period.

No change was observed for the solution that did not contain styrene. For the sample with styrene, resonances for $Ir_2(TMB)_4^{2+}$ slowly grew into the spectrum with loss of the signals for $Ir_2(TMB)_4H_2^{2+}$. The sample that contained styrene was clear, dark-blue after 7 days. The NMR tube, which contained the styrene solution, was opened after 7 days, and the contents transferred to a round-bottom flask. The volatiles were vacuum-transferred to a new NMR tube. This solution was clear and colorless. A dark-blue material remained in the round-bottom flask. The NMR of the solvent, in addition to strong styrene resonances, contained two weak signals attributable to the ethyl group of ethyl benzene (δ (ppm): 1.2 (triplet, 3H, CH_3); 2.62 (quartet,2H, CH_2)). These resonances appeared in the NMR spectrum of the reaction mixture as the NMR spectrum of $Ir_2(TMB)_4^{2+}$ grew in.

$Ir_2(TMB)_4H_2^{2+}$ + hv

A CH_3CN solution of Ir_2H_2, prepared on a high-vacuum line in a two-compartment cell, was photolyzed using a 1000 W high-pressure Hg/Xe lamp equipped with Corning cut-off and band-pass filters. A set of filters was used, which yielded %T > 0.1% from 329 to 383 nm. The reaction was monitored by UV-Vis spectroscopy. Disappearance of the 320 nm band assigned to the $d\sigma \rightarrow d\sigma^*$ transition of Ir_2H_2 was observed with the growth of bands attributed to $Ir_2(TMB)_4^{2+}$ (λ_{max} 625 and 380 nm) and a new feature at 480 nm.

Raman Spectroscopy

Raman and resonance Raman spectra were measured by Dr. Thomas Loehr at the Oregon Graduate Center.

X-Ray Data Collection and Reduction for $[Ir_2(TMB)_4H_2](B(C_6H_5)_4)_2 \cdot CH_3C_6H_5$

Long, plate-like crystals were grown by slow evaporation of a toluene/acetonitrile solution; they appeared dichroic under a microscope with large, colorless faces and narrow, light-blue faces. A crystal was mounted in a capillary with a small amount of grease holding it in place, and was centered on a CAD-4 diffractometer equipped with graphite-monochromated MoKα radiation. Cell dimensions and an orientation matrix were obtained from the setting angles of 25 reflections with $15° < 2\vartheta < 25°$, and the intensity of reflections (±h,±k,l) was measured out to 2ϑ of 30°. Absences in the data for 0k0 with k odd identified the space group as either $P2_1$ or $P2_1/m$. The coordinate of the iridium atoms, obtained from a Patterson map, suggested $P2_1/m$. The remaining nonhydrogen atoms were found by successive structure factor-Fourier calculations; however, the resulting structure appeared to be disordered in several regions.

Before attempting to derive an ordered model in the space group $P2_1/m$, an oscillation photograph was taken, the axis of rotation being the needle axis, [2,0,-1].[7] This photograph showed weak, intermediate layer lines, which were interpreted in terms of a doubling of the *c* axis; none of these weak reflections had been noted by the CAD-4 diffractometer during the initial search. The crystal was remounted on a $P2_1$ diffractometer again equipped with MoKα radiation, and new cell dimensions were obtained. These were averaged with the cell dimensions determined by the CAD-4 (with the *c* axis doubled) to give the final values listed in Table 5.1. All reflections out to 2ϑ of 30° were measured twice (±h,±k,-l for 0° to 20°, ±h,±k,+l for 20° to 30°, and +h,+k,±l for h = 0, 1, 2 2ϑ from 30° to 40°). Absences in the data for 0k0, k=2n+1 and h0l, h+l=2n+1 identified the space group as $P2_1/c$, #14. The weakness of reflections with l odd is due to the fact that the iridium atoms lie very close to y = 0.25 and hence they plus many of the lighter atoms show a pseudotranslation of 1/2 along *c*.

Backgrounds were measured for each reflection at each end of scan; an average background as a function of 2ϑ was calculated and used to correct the measured counts. Absorption corrections were made, first on the basis of the correct value of μ (38 cm^{-1}) and later, on the basis of a revised value (32.5 cm^{-1}), which led to improved agreement between symmetry-related measurements. With this revised value, the goodness-of-fit for merging the 9434 measured intensities into 4692 independent reflections was 0.95; 3915 of these reflections had $F_o > 0$ and 2005 had $F_o^2 > 3\sigma(F_o^2)$. Variances of the

Table 5.1. Crystal data for $[Ir_2(C_{10}H_{16}N_2)_4H_2](B(C_6H_5)_4)_2 \cdot CH_3C_6H_5$.

Formula : $Ir_2N_8C_{95}B_2H_{114}$	Formula Weight: 1774.03
Crystal Color: Dichroic, colorless to light blue	Habit: flat plate
a = 10.54(2) Å	α = 90.0°
b = 31.02(4) Å	β = 91.57(3)°
c = 27.05(4) Å	γ = 90.0°
V = 8840(13) Å^3	Z = 4
d_{calc} = 1.333(2) gcm^{-3}	
λ = 0.71073 Å	
Graphite monochromator	
Space group: $P2_1/c$ (#14)	Absences: h0l, l = 2n+1; 0k0, k = 2n+1
Crystal size: 0.2 x 0.074 x 0.8 mm	μ = 32.5 cm^{-1}
	Transimission coefficients: 0.53 - 0.79

Number of data collected: 9434

Number of independent reflections: 4692

Number with $F_o^2 > 0$: 3915

Number with $F_o^2 > 3\sigma(F_o^2)$: 2005

Goodness-of-fit for 4692 measured intensities: 1.16

individual reflections were assigned, based on counting statistics plus an additional term, $0.14I^2$. Structure factors were taken from standard references.[8]

The earlier $P2_1/m$ model was converted to an ordered model in $P2_1/c$. After several cycles of full-matrix least squares, minimizing $\Sigma w(F_o^2 - F_c^2)^2$, hydrogen atoms were introduced at calculated positions (C-H = 0.95 Å). Each hydrogen was given an isotropic thermal parameter 10% greater than that of the carbon to which it was bonded. The hydrogens bound to iridium appeared on difference maps and were placed 1.6 Å from the iridium atoms. No parameters of the hydrogen atoms bound to iridium were further adjusted, nor were those of the toluene ring, which appeared as diffuse maxima in a late difference map. In the final refinement cycles, 411 parameters were adjusted: the coordinates of 100 atoms, the anisotropic thermal parameters of the Ir atoms, the isotropic thermal parameters for the 98 C, N, and B atoms (excluding the toluene), and a scale factor. The final goodness-of-fit, $[\Sigma w(F_o^2 - F_c^2)^2/(n - p)]^{1/2}$, was 1.16 for n = 4692 and p = 411; the R's were 0.118 for the 3915 reflections with $F_o^2 > 0$ and 0.045 for the 2005 reflections with $F_o^2 > 3\sigma(F_o^2)$. Final parameters are given in Table 5.2, bond lengths and angles in Table 5.3, anisotropic coefficients for the Ir atoms in Table A3.1, hydrogen coordinates in Table A3.2 and observed and calculated F's in Table A3.3.

Table 5.2. Final Parameters (x,y,z and U_{eq} x 10^4).

Atom	x	y	z	U_{eq} or B
IR1	45(.9)	2540(.5)	3276(.3)	298(4)
IR2	2126(.9)	2564(.4)	4010(.3)	321(4)
C1	1041(27)	2185(8)	2832(11)	4.4(8) *
N1	1679(21)	1998(6)	2560(8)	4.2(6) *
C2	2426(29)	1722(8)	2212(11)	3.9(7) *
C3	1959(31)	1263(9)	2278(12)	7.0(10)*
C4	2201(28)	1902(8)	1703(11)	6.5(9) *
C5	3767(28)	1757(8)	2425(10)	5.5(8) *
C6	4372(27)	2219(8)	2360(10)	5.5(8) *
C7	6060(28)	2041(8)	3037(11)	5.6(8) *
C8	5748(27)	2804(8)	2728(11)	5.8(8) *
C9	5154(25)	2375(9)	2835(10)	5.3(7) *
N2	4177(18)	2431(7)	3211(7)	4.0(5) *
C10	3395(21)	2523(10)	3504(8)	4.3(6) *
C11	712(25)	3059(8)	2980(10)	3.7(7) *
N3	1091(20)	3358(7)	2786(8)	4.0(6) *
C12	1861(28)	3716(8)	2531(11)	4.1(7) *
C13	2662(31)	3498(9)	2175(12)	6.6(9) *
C14	943(26)	4057(8)	2320(10)	5.1(8) *
C15	2691(25)	3900(8)	2975(10)	4.5(7) *
C16	1964(27)	4141(8)	3348(11)	5.4(8) *
C17	1451(30)	4253(8)	4248(12)	7.3(9) *
C18	3752(33)	4133(9)	4056(13)	7.2(10)*
C19	2270(33)	4042(9)	3897(12)	6.2(9) *
N4	2179(21)	3549(7)	3958(8)	3.9(6) *
C20	2108(30)	3184(9)	3990(12)	4.3(8) *
C21	−1073(30)	2858(8)	3713(11)	4.3(8) *
N5	−1749(25)	3060(7)	3938(9)	5.9(7) *
C22	−2584(33)	3295(10)	4303(13)	7.3(9) *
C23	−2512(31)	3763(9)	4129(13)	7.2(10)*
C24	−3944(35)	3099(10)	4246(13)	10.0(11)*
C25	−1953(29)	3200(9)	4790(12)	6.8(9) *
C26	−1930(31)	2755(9)	5017(12)	8.1(10)*
C27	−856(33)	2120(10)	5421(13)	9.2(11)*
C28	−245(34)	2862(10)	5661(14)	9.4(12)*
C29	−829(28)	2572(11)	5248(11)	7.0(8) *
N6	212(19)	2597(7)	4867(7)	5.0(5) *
C30	902(21)	2569(9)	4543(8)	4.7(7) *
C31	−494(24)	2024(8)	3553(9)	2.9(7) *
N7	−852(18)	1684(6)	3706(7)	2.9(5) *
C32	−1280(29)	1246(8)	3887(11)	4.8(7) *
C33	−2454(38)	1349(10)	4233(15)	9.6(12)*
C34	−1691(30)	986(9)	3459(12)	7.1(9) *
C35	−242(31)	1079(8)	4238(12)	6.9(9) *
C36	896(31)	939(8)	3927(11)	6.4(9) *

Atom	x	y	z	U_{eq} or B
C37	2340(30)	1006(9)	4747(13)	8.4(10)*
C38	3335(35)	938(9)	3933(13)	7.0(10)*
C39	2178(31)	1101(9)	4172(12)	6.2(9) *
N8	2215(21)	1589(7)	4132(8)	3.7(6) *
C40	2193(26)	1967(8)	4075(10)	2.4(7) *
B1	5694(38)	3954(11)	1047(14)	4.5(11)*
C111	6408(26)	3843(8)	1589(10)	2.9(6) *
C112	7483(34)	3555(9)	1634(13)	4.6(9) *
C113	8063(28)	3452(8)	2070(12)	4.6(8) *
C114	7623(30)	3657(9)	2508(11)	6.2(8) *
C115	6681(31)	3928(9)	2491(11)	5.8(8) *
C116	6001(28)	4023(8)	2034(13)	4.4(8) *
C121	6603(32)	4243(8)	717(12)	3.7(8) *
C122	7866(34)	4305(8)	784(11)	4.9(8) *
C123	8693(31)	4550(9)	470(12)	5.6(8) *
C124	8104(33)	4759(8)	79(12)	4.4(8) *
C125	6856(36)	4714(9)	−18(13)	5.0(9) *
C126	6154(31)	4475(8)	301(12)	3.9(8) *
C131	4358(26)	4240(8)	1134(9)	2.9(6) *
C132	4482(27)	4681(9)	1274(10)	5.5(8) *
C133	3281(32)	4917(9)	1354(11)	6.7(9) *
C134	2187(30)	4734(9)	1249(10)	5.8(8) *
C135	2098(28)	4319(9)	1080(10)	5.2(8) *
C136	3182(35)	4072(8)	1011(12)	4.7(8) *
C141	5330(27)	3495(8)	779(11)	3.9(8) *
C142	4743(27)	3159(9)	1031(10)	6.0(8) *
C143	4370(28)	2778(9)	803(12)	6.7(9) *
C144	4508(25)	2729(7)	320(11)	4.6(8) *
C145	5074(26)	3032(8)	68(10)	4.8(7) *
C146	5515(24)	3417(7)	273(10)	3.5(7) *
B2	6035(31)	1034(8)	1136(12)	1.5(8) *
C211	6778(28)	1462(8)	1358(10)	3.2(7) *
C212	7833(32)	1433(8)	1671(12)	4.5(9) *
C213	8508(26)	1788(8)	1908(9)	3.6(7) *
C214	8080(27)	2188(7)	1814(10)	3.7(7) *
C215	7025(26)	2236(7)	1514(9)	3.4(7) *
C216	6400(26)	1877(8)	1286(10)	4.4(8) *
C221	5911(24)	708(8)	1620(10)	3.1(7) *
C222	5828(29)	837(8)	2103(12)	4.8(9) *
C223	5575(27)	543(9)	2488(11)	6.0(8) *
C224	5358(28)	127(10)	2372(12)	6.5(9) *
C225	5403(26)	−21(8)	1905(11)	5.4(8) *
C226	5741(25)	264(8)	1548(10)	4.4(7) *
C231	6933(32)	788(8)	717(11)	3.9(8) *
C232	8270(30)	824(8)	648(11)	4.5(8) *

Atom	x	y	z	U_{eq} or B	
C233	8924(29)	582(9)	295(12)	5.3(8)	*
C234	8311(37)	327(9)	−19(13)	6.3(10)	*
C235	7023(38)	284(9)	10(13)	5.3(9)	*
C236	6293(30)	497(8)	363(12)	3.6(8)	*
C241	4666(27)	1131(7)	893(9)	2.7(6)	*
C242	4655(30)	1415(8)	481(11)	4.3(8)	*
C243	3409(32)	1502(8)	248(10)	5.3(8)	*
C244	2296(30)	1336(9)	419(12)	6.3(8)	*
C245	2303(32)	1064(9)	774(13)	6.5(9)	*
C246	3494(31)	958(7)	1041(11)	3.1(7)	*
CB1	1044	42	2523	4.0	*
CB2	1818	−12	2120	6.0	*
CB3	1335	59	1644	8.0	*
CB4	78	184	1571	10.0	*
CB5	−696	238	1974	8.0	*
CB6	−213	167	2450	6.0	*
CME	1579	−37	3051	12.0	*

[a] $U_{eq} = \frac{1}{3}\sum_i \sum_j [U_{ij}(a_i^* a_j^*)(\vec{a}_i \cdot \vec{a}_j)]$
*Isotropic displacement parameter, B

Table 5.3. Bond lengths and angles.

	Distance(Å)		Distance(Å)
IR1 -IR2	2.920(2)	C35 -C36	1.55(4)
IR1 -C1	1.96(3)	C36 -C39	1.57(4)
IR1 -C11	1.94(3)	C37 -C39	1.59(4)
IR1 -C21	1.96(3)	C38 -C39	1.49(5)
IR1 -C31	1.86(3)	C39 -N8	1.52(4)
IR2 -C10	1.94(3)	N8 -C40	1.18(3)
IR2 -C20	1.92(3)	B1 -C111	1.67(5)
IR2 -C30	1.96(3)	B1 -C121	1.60(5)
IR2 -C40	1.86(3)	B1 -C131	1.68(4)
C1 -N1	1.17(3)	B1 -C141	1.64(5)
N1 -C2	1.51(4)	C111-C112	1.45(4)
C2 -C3	1.52(4)	C111-C116	1.40(4)
C2 -C4	1.50(4)	C112-C113	1.35(4)
C2 -C5	1.51(4)	C113-C114	1.43(4)
C5 -C6	1.58(4)	C114-C115	1.30(4)
C6 -C9	1.58(4)	C115-C116	1.44(4)
C7 -C9	1.50(4)	C121-C122	1.35(4)
C8 -C9	1.50(4)	C121-C126	1.41(4)
C9 -N2	1.48(3)	C122-C123	1.45(4)
N2 -C10	1.19(3)	C123-C124	1.37(4)
C11 -N3	1.14(3)	C124-C125	1.34(5)
N3 -C12	1.55(3)	C125-C126	1.37(5)
C12 -C13	1.46(4)	C131-C132	1.42(4)
C12 -C14	1.53(4)	C131-C136	1.38(4)
C12 -C15	1.57(4)	C132-C133	1.48(4)
C15 -C16	1.49(4)	C133-C134	1.31(4)
C16 -C19	1.54(4)	C134-C135	1.37(4)
C17 -C19	1.46(4)	C135-C136	1.39(4)
C18 -C19	1.63(5)	C141-C142	1.40(4)
C19 -N4	1.54(4)	C141-C146	1.41(4)
N4 -C20	1.14(4)	C142-C143	1.39(4)
C21 -N5	1.14(4)	C143-C144	1.33(4)
N5 -C22	1.53(4)	C144-C145	1.31(4)
C22 -C23	1.53(5)	C145-C146	1.39(4)
C22 -C24	1.56(5)	B2 -C211	1.65(4)
C22 -C25	1.49(5)	B2 -C221	1.66(4)
C25 -C26	1.51(4)	B2 -C231	1.68(4)
C26 -C29	1.42(4)	B2 -C241	1.60(4)
C27 -C29	1.48(5)	C211-C212	1.38(4)
C28 -C29	1.55(5)	C211-C216	1.36(4)
C29 -N6	1.53(4)	C212-C213	1.45(4)
N6 -C30	1.16(3)	C213-C214	1.34(4)
C31 -N7	1.20(3)	C214-C215	1.37(4)
N7 -C32	1.52(3)	C215-C216	1.43(4)
C32 -C33	1.60(5)	C221-C222	1.37(4)
C32 -C34	1.47(4)	C221-C226	1.40(4)
C32 -C35	1.52(4)	C222-C223	1.41(4)

Distance(Å)	
C223–C224	1.35(4)
C224–C225	1.35(4)
C225–C226	1.36(4)
C231–C232	1.43(4)
C231–C236	1.47(4)
C232–C233	1.41(4)
C233–C234	1.32(5)
C234–C235	1.37(5)
C235–C236	1.41(5)
C241–C242	1.42(4)
C241–C246	1.42(4)
C242–C243	1.47(4)
C243–C244	1.37(4)
C244–C245	1.28(4)
C245–C246	1.47(4)
CB1– CB2	1.390(0)
CB1– CB6	1.390(0)
CB1– CME	1.541(0)
CB2– CB3	1.390(0)
CB3– CB4	1.390(0)
CB4– CB5	1.390(0)
CB5– CB6	1.390(0)

Angle(°)	
C11 –IR1 –C1	90.4(11)
C21 –IR1 –C1	174.9(11)
C31 –IR1 –C1	86.4(11)
C21 –IR1 –C11	93.6(11)
C31 –IR1 –C11	176.2(11)
C31 –IR1 –C21	89.6(11)
C20 –IR2 –C10	92.9(12)
C30 –IR2 –C10	175.9(10)
C40 –IR2 –C10	88.7(11)
C30 –IR2 –C20	90.4(11)
C40 –IR2 –C20	175.9(12)
C40 –IR2 –C30	87.8(11)
N1 –C1 –IR1	175.5(24)
C2 –N1 –C1	174.9(25)
C3 –C2 –N1	106.4(22)
C4 –C2 –N1	106.7(22)
C5 –C2 –N1	102.6(21)
C4 –C2 –C3	114.5(24)
C5 –C2 –C3	109.0(23)
C5 –C2 –C4	116.4(23)
C6 –C5 –C2	113.6(22)
C9 –C6 –C5	113.0(21)
C7 –C9 –C6	113.3(22)
C8 –C9 –C6	109.0(22)
N2 –C9 –C6	103.7(20)
C8 –C9 –C7	114.6(23)
N2 –C9 –C7	106.2(21)
N2 –C9 –C8	109.4(21)
C10 –N2 –C9	172.8(23)
N2 –C10 –IR2	169.7(22)
N3 –C11 –IR1	177.0(23)
C12 –N3 –C11	168.6(24)
C13 –C12 –N3	106.2(22)
C14 –C12 –N3	109.1(21)
C15 –C12 –N3	101.9(20)
C14 –C12 –C13	116.4(24)
C15 –C12 –C13	110.6(23)
C15 –C12 –C14	111.5(22)
C16 –C15 –C12	114.5(22)
C19 –C16 –C15	117.1(24)
C17 –C19 –C16	115.3(26)
C18 –C19 –C16	113.1(24)
N4 –C19 –C16	106.8(23)
C18 –C19 –C17	109.3(25)
N4 –C19 –C17	109.6(24)
N4 –C19 –C18	101.9(23)
C20 –N4 –C19	178.3(27)

	Angle(°)
N4 -C20 -IR2	174.8(26)
N5 -C21 -IR1	174.9(26)
C22 -N5 -C21	171.8(28)
C23 -C22 -N5	102.7(24)
C24 -C22 -N5	107.0(25)
C25 -C22 -N5	103.1(25)
C24 -C22 -C23	113.2(27)
C25 -C22 -C23	115.9(27)
C25 -C22 -C24	113.4(27)
C26 -C25 -C22	122.8(27)
C29 -C26 -C25	123.2(27)
C27 -C29 -C26	119.7(28)
C28 -C29 -C26	112.8(27)
N6 -C29 -C26	106.0(24)
C28 -C29 -C27	109.5(26)
N6 -C29 -C27	106.3(24)
N6 -C29 -C28	100.4(23)
C30 -N6 -C29	170.1(24)
N6 -C30 -IR2	175.6(22)
N7 -C31 -IR1	176.4(21)
C32 -N7 -C31	178.2(22)
C33 -C32 -N7	104.6(22)
C34 -C32 -N7	108.8(22)
C35 -C32 -N7	107.0(22)
C34 -C32 -C33	110.7(25)
C35 -C32 -C33	104.8(24)
C35 -C32 -C34	119.8(25)
C36 -C35 -C32	108.1(24)
C39 -C36 -C35	110.6(24)
C37 -C39 -C36	114.9(25)
C38 -C39 -C36	114.4(26)
N8 -C39 -C36	108.2(23)
C38 -C39 -C37	107.2(25)
N8 -C39 -C37	104.7(23)
N8 -C39 -C38	106.6(24)
C40 -N8 -C39	175.8(25)
N8 -C40 -IR2	177.6(23)
C121-B1 -C111	110.0(25)
C131-B1 -C111	110.1(24)
C141-B1 -C111	107.7(24)
C131-B1 -C121	107.4(25)
C141-B1 -C121	112.2(26)
C141-B1 -C131	109.4(24)
C112-C111-B1	122.4(24)
C116-C111-B1	122.1(24)
C116-C111-C112	115.4(25)
C113-C112-C111	123.8(28)

	Angle(°)
C114-C113-C112	117.8(27)
C115-C114-C113	121.4(28)
C116-C115-C114	121.6(28)
C115-C116-C111	119.8(26)
C122-C121-B1	127.4(28)
C126-C121-B1	122.6(27)
C126-C121-C122	110.0(27)
C123-C122-C121	127.0(28)
C124-C123-C122	115.6(28)
C125-C124-C123	121.4(30)
C126-C125-C124	118.5(31)
C125-C126-C121	127.3(29)
C132-C131-B1	118.1(23)
C136-C131-B1	121.2(24)
C136-C131-C132	120.1(25)
C133-C132-C131	116.2(24)
C134-C133-C132	120.3(27)
C135-C134-C133	122.1(28)
C136-C135-C134	120.9(27)
C135-C136-C131	119.8(27)
C142-C141-B1	122.3(25)
C146-C141-B1	122.7(25)
C146-C141-C142	114.9(25)
C143-C142-C141	122.9(26)
C144-C143-C142	119.8(27)
C145-C144-C143	119.6(26)
C146-C145-C144	124.0(25)
C145-C146-C141	118.7(23)
C221-B2 -C211	104.5(21)
C231-B2 -C211	109.9(22)
C241-B2 -C211	114.3(22)
C231-B2 -C221	108.3(21)
C241-B2 -C221	110.5(22)
C241-B2 -C231	109.2(22)
C212-C211-B2	122.6(24)
C216-C211-B2	125.3(24)
C216-C211-C212	112.0(25)
C213-C212-C211	126.8(27)
C214-C213-C212	117.3(25)
C215-C214-C213	118.5(24)
C216-C215-C214	122.0(23)
C215-C216-C211	123.3(24)
C222-C221-B2	125.6(24)
C226-C221-B2	120.1(22)
C226-C221-C222	114.0(24)
C223-C222-C221	122.2(27)
C224-C223-C222	118.6(27)

Angle(°)	
C225 -C224-C223	122.4(28)
C226 -C225-C224	117.5(26)
C225 -C226-C221	125.0(25)
C232 -C231-B2	128.9(25)
C236 -C231-B2	117.5(24)
C236 -C231-C232	113.5(25)
C233 -C232-C231	123.3(26)
C234 -C233-C232	121.1(29)
C235 -C234-C233	119.5(32)
C236 -C235-C234	123.7(31)
C235 -C236-C231	118.8(27)
C242 -C241-B2	115.3(23)
C246 -C241-B2	126.7(23)
C246 -C241-C242	118.0(24)
C243 -C242-C241	116.0(25)
C244 -C243-C242	123.4(27)
C245 -C244-C243	120.9(30)
C246 -C245-C244	120.4(29)
C245 -C246-C241	121.1(25)
CB6 - CB1- CB2	120.0(0)
CME- CB1- CB2	120.0(0)
CME- CB1- CB6	120.0(0)
CB3 - CB2- CB1	120.0(0)
CB4 - CB3- CB2	120.0(0)
CB5 - CB4- CB3	120.0(0)
CB6 - CB5- CB4	120.0(0)
CB5 - CB6- CB1	120.0(0)

Results and Discussion

Crystal Structure

$Ir_2(TMB)_4H_2^{2+}$ is the first example of a binuclear metal complex with a trans-dihydride (H-M-M-H) structure (Figure 5.1). The Ir-Ir separation is 2.920(2) Å, approximately 0.3 Å shorter than in the starting d^8 dimer (3.199(1) Å),[6] indicating formation of an Ir-Ir bond. This Ir-Ir separation is ~0.1 Å longer than that in the analogous $Ir_2(TMB)_4I_2^{2+}$,[9] presumably a result of two transhydride effects. The hydrogen-atom positions were not refined; electron density was observed ~1.6 Å away from each Ir atom and assigned to the hydrogen positions.

A comparison of the geometric parameters for $Ir_2(TMB)_4H_2^{2+}$ (Ir_2H_2), $Ir_2(TMB)_4^{2+}$ (Ir_2^{2+}),[6] $Ir_2(TMB)_4I_2^{2+}$ (Ir_2I_2),[9] $Rh_2(TMB)_4Cl_2^{2+}$ (Rh_2Cl_2),[9] and $Rh_2(TMB)_4^{2+}$ (Rh_2)[10] is given in Table 5.4. Comparison of the structure for Ir_2H_2 to the structure of $Ir_2(TMB)_4Cl_2^{2+}$ (Ir_2Cl_2) is preferred over the comparison to Ir_2I_2. However, the structure of the dichloride complex is not known.

The structural parameters observed for Ir_2H_2 compare well to those observed for Ir_2I_2. The geometry of the $Ir(CN)_4$ unit deviates only slightly from the idealized geometry (M-M-C, 90°; M-C-N, 180°) and compares well to those of Ir_2 and Ir_2I_2. The two $Ir(CN)_4$ planes are nearly parallel to one another with an angle of approximately 3° between the vectors normal to the planes and are twisted with respect to each other (Figure 5.2). The torsion angle, N-M-M'-N', is 28°, identical to that observed for Ir_2 and Ir_2I_2. A best-plane fit through the $Ir(CN)_4$ units shows a slight distortion about each metal center (Table 5.5), each experiencing a different distortion. Ir(1) experiences a tetrahedral distortion. The metal is displaced 0.05 Å toward the center of the dimer, away from the plane defined by the four isocyanide nitrogens. A pyramidal distortion is observed for Ir(2), displaced 0.11 Å away from the plane defined by the four isocyanide nitrogens, toward the center of the dimer.

Figure 5.1. View of the structure of $Ir_2(TMB)_4H_2^{2+}$.

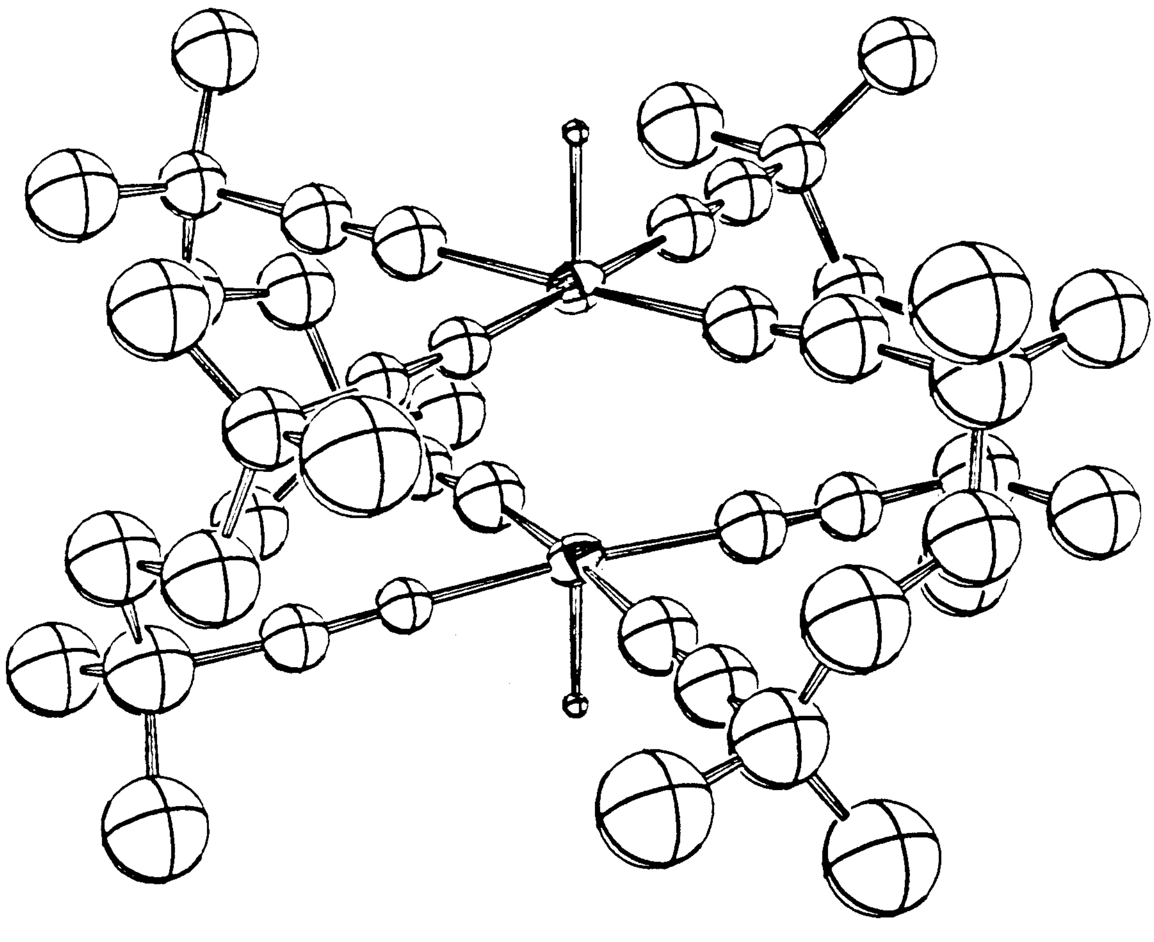

Table 5.4. Comparison of geometric parameters of Ir_2H_2 to other binuclear d^8 and d^7 complexes.

	Ir_2H_2 [a]	Ir_2I_2 [b]	Ir_2 [a]	Rh_2Cl_2 [b]	Rh_2 [c]
M-M	2.920(2) Å	2.803(4) Å	3.199(1) Å	2.773(2) Å	3.262(1) Å
M-X	1.6 Å	2.712(7) Å		2.425(6) Å	
M-C	1.92(1) Å	1.95(1) Å	1.96(1) Å	1.95(1) Å	1.92-1.98 Å
C-N	1.16(1) Å	1.16(2) Å	1.12(1) Å	1.15(1) Å	1.16 Å
ω	28.2(3)°	31(2)°	28.1(1)°	33.1(1)°	31°
C_β-C_γ-C_γ'-C_β'	136(1)°	130(2)°	141(1)°	137(2)°	
N•••N'	3.43(1) Å		3.68(1) Å		
M-M-C	91.0(3)°	90.12(5)°	91.7(2)°	90.7(4)°	
M-C-N	175.2(1)°	173(1)°	177.12(6)°	176(1)°	175°
displacement of M from plane of the 4 N	Ir(1) 0.05 Å Ir(2) 0.11 Å toward center	0.15 Å toward center of dimer of dimer	0.08 Å toward center of dimer	0.15 Å toward center of dimer	
dihedral angle of $M(CN)_4$ planes	179°		177°		

a. This work.

b. Reference 9.

c. Reference 10.

Figure 5.2. View of the structure of $Ir_2(TMB)_4H_2^{2+}$ viewed down the Ir-Ir vector.

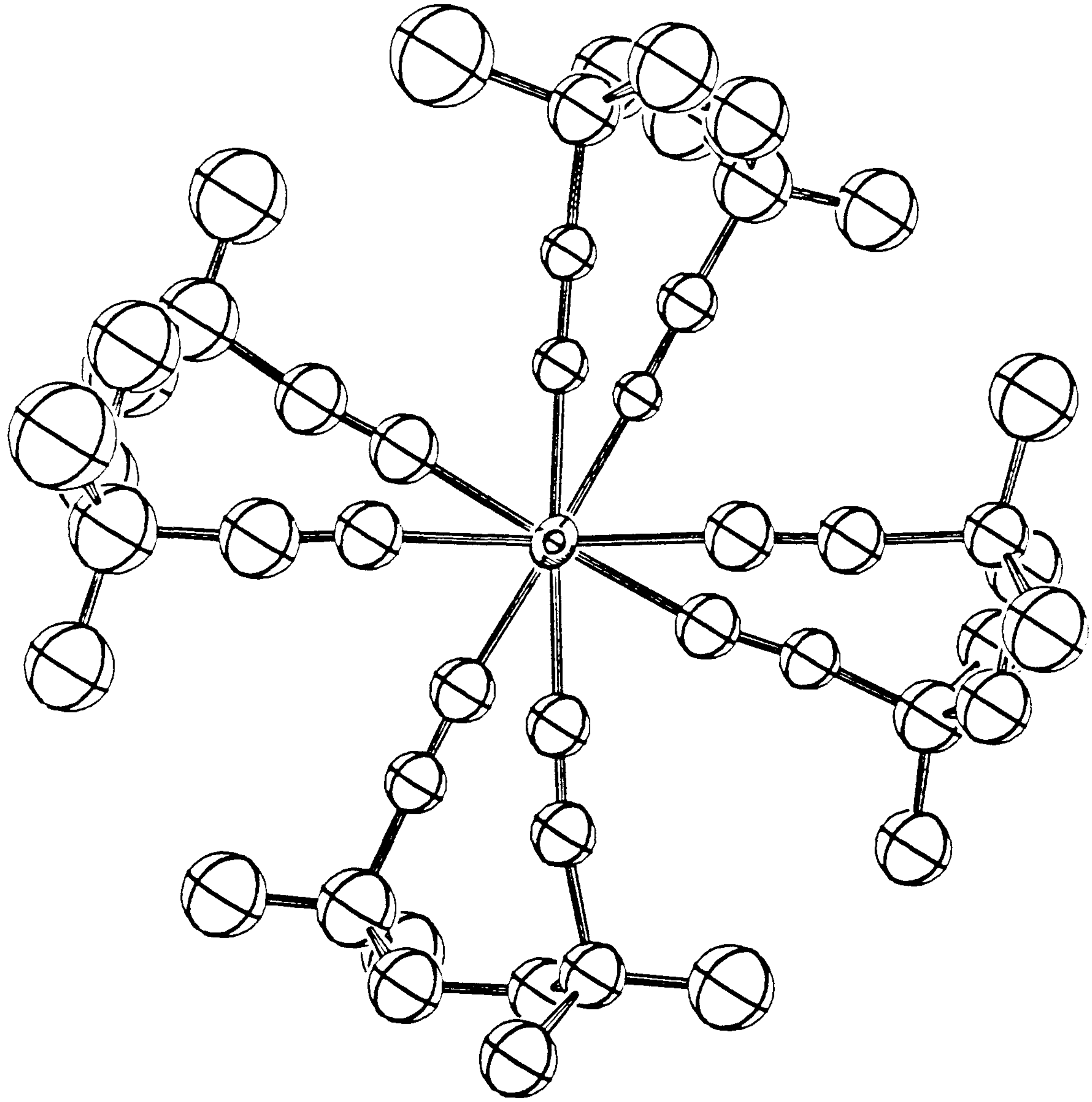

Table 5.5. Best plane fit of $Ir(CN)_4$ units.

Atom	Deviation, Å	Atom	Deviation, Å
Ir1	0.030	Ir2	-0.071
C1	-0.051	C10	-0.025
N1	-0.066	N2	0.023
C11	0.056	C20	-0.007
N3	0.033	N4	0.005
C21	-0.005	C30	-0.035
N5	-0.091	N6	0.030
C31	0.061	C40	-0.006
N7	0.034	N8	0.045

With the different metal-metal separations observed for the Ir complexes, some variation of geometric parameters is expected. No variation in the $Ir(CN)_4$ geometry is observed. A compression of the $Ir(CN)_4$ units toward one another is found (the N···N' separation decreases 0.25 Å from Ir_2 to Ir_2H_2) in addition to a slightly increased pyramidal distortion of the $Ir(CN)_4$ moieties. With a compression of the $Ir(CN)_4$ units, an increase in the torsion angle (N-M-M'-N') might be expected. However, no variation in the torsion angle is observed through the series of complexes; rather, a decrease in the C_β-C_γ-C_γ'-C_β' dihedral angle is found. A decrease in the metal-metal distance (increased metal-metal bonding interaction) results in a compression or kinking of the four-carbon atom backbone of the TMB ligand. The other geometric parameters of the TMB ligand compare well through the series of complexes.

Spectroscopy

The vibrational data for $Ir_2(TMB)_4H_2^{2+}$ are summarized in Tables 5.6 and 5.7. The IR spectrum in the region from 1800 cm^{-1} to 2400 cm^{-1} is shown in Figure 5.3. A moderate Ir-H absorption is observed at 1940 cm^{-1}, in line with the terminal metal hydride structure. This resonance is 100 cm^{-1} to higher energy of the Pt-H band for $Pt_2(P_2O_5H_2)_4H_2^{4-}$,[5] indicating a stronger metal hydrogen bond for iridium. The C≡N frequency for Ir_2H_2 has shifted 20 cm^{-1} to higher energy from that for Ir_2 (a 40 cm^{-1} shift to higher energy from the free ligand)[11] because of the increased σ donation from the isocyanide to the Ir(II) center. This increased σ donation reduces the σ antibonding contribution of the carbon lone pair to the C≡N bond.

Raman spectra for Ir_2H_2 are shown in Figure 5.4. Two low-energy bands are observed. The band at 38 cm^{-1} is a plasma line. Excitation at 647.1 nm (on resonance for Ir_2, see Chapter 2) results in a large enhancement of the 60 cm^{-1} band (Figure 5.4), identifying this resonance as the Ir-Ir frequency for Ir_2. Thus, a small amount of Ir_2 is present in the Ir_2H_2 material (hence the light-blue color of the crystals). The

Table 5.6. Infrared vibrational frequencies.

	ν(M-H), cm^{-1}	ν(N≡C), cm^{-1}
Ir_2H_2	1940	2160 [a]
Pt_2H_2 [b]	1840	
Ir_2		2140 [a]

a. Free ligand, 2120 cm^{-1}.

b. Reference 5.

Table 5.7. Raman vibrational frequencies.

	ν(M-M), cm^{-1}	k, mdyne/Å	k, mdyne/Å [a]	M-M, Å	
				X-ray	W.R. [a]
Ir_2H_2 [b]	136	1.05 [c]	0.86	2.920(2)	2.85
Ir_2I_2 [d]	116	2.09 [e]	1.18	2.803(4)	2.55
Ir_2Cl_2 [d]	140	1.56 [e]			2.69
Rh_2Cl_2 [d]	155	1.141 [e]	1.27	2.773(2)	2.82

a. Calculated using Woodruff's relationship, Reference 13.

b. This work.

c. Harmonic approximation.

d. Reference 12.

e. Determined from a force-field analysis, Reference 12.

Figure 5.3. Infrared spectrum of $[Ir_2(TMB)_4H_2\}(B(C_6H_5)_4)_2 \cdot CH_3C_6H_5$.

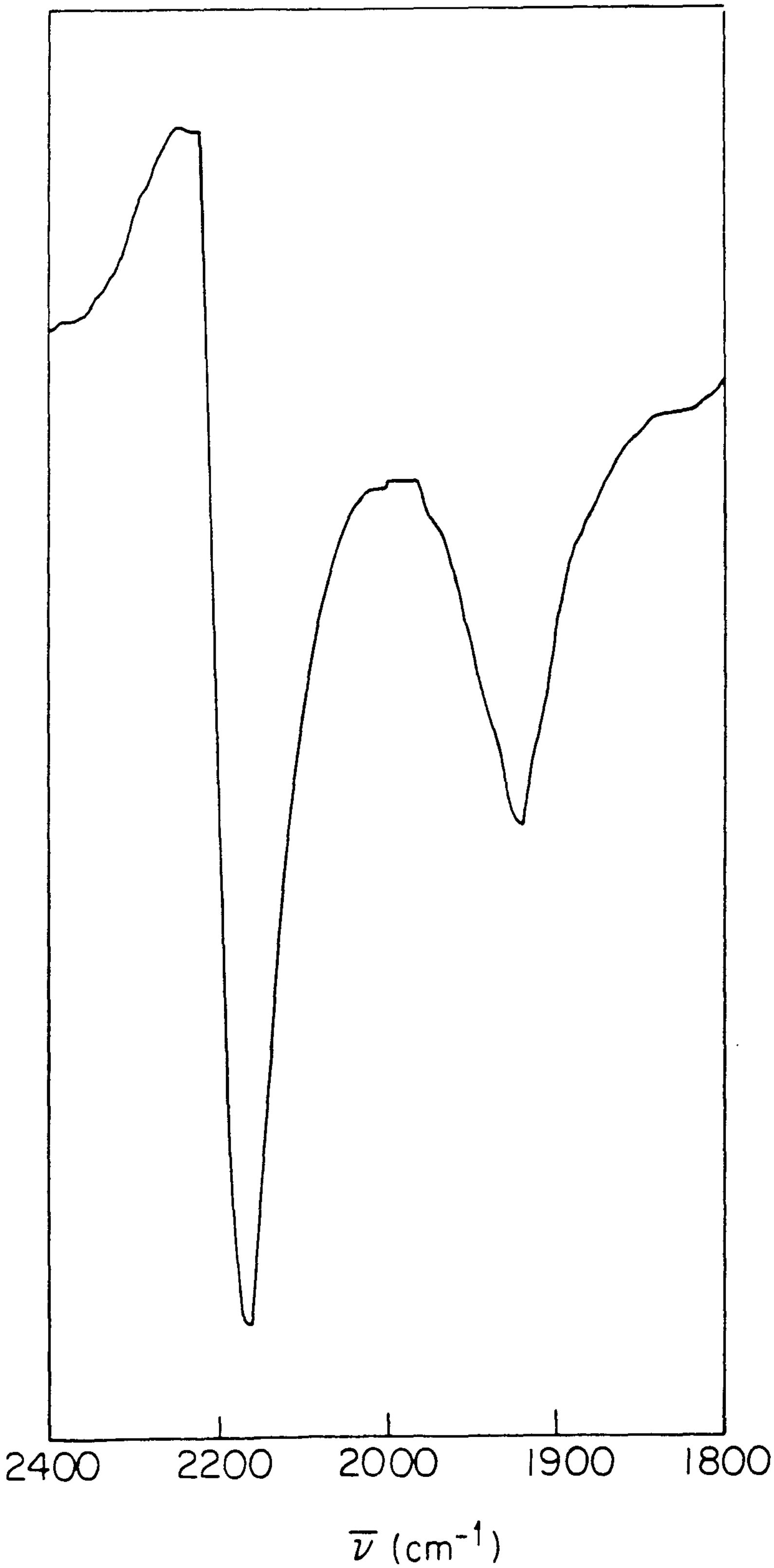
2400
2200
2000
1900
1800
$\overline{\nu}$ (cm^{-1})

Figure 5.4. Raman spectra of $[Ir_2(TMB)_4H_2](B(C_6H_5)_4)_2{\cdot}CH_3C_6H_5$: (a) Solid, 90 K, λ_{ex} = 488 nm; (b) Solid, 90 K, λ_{ex} = 647.1 nm.

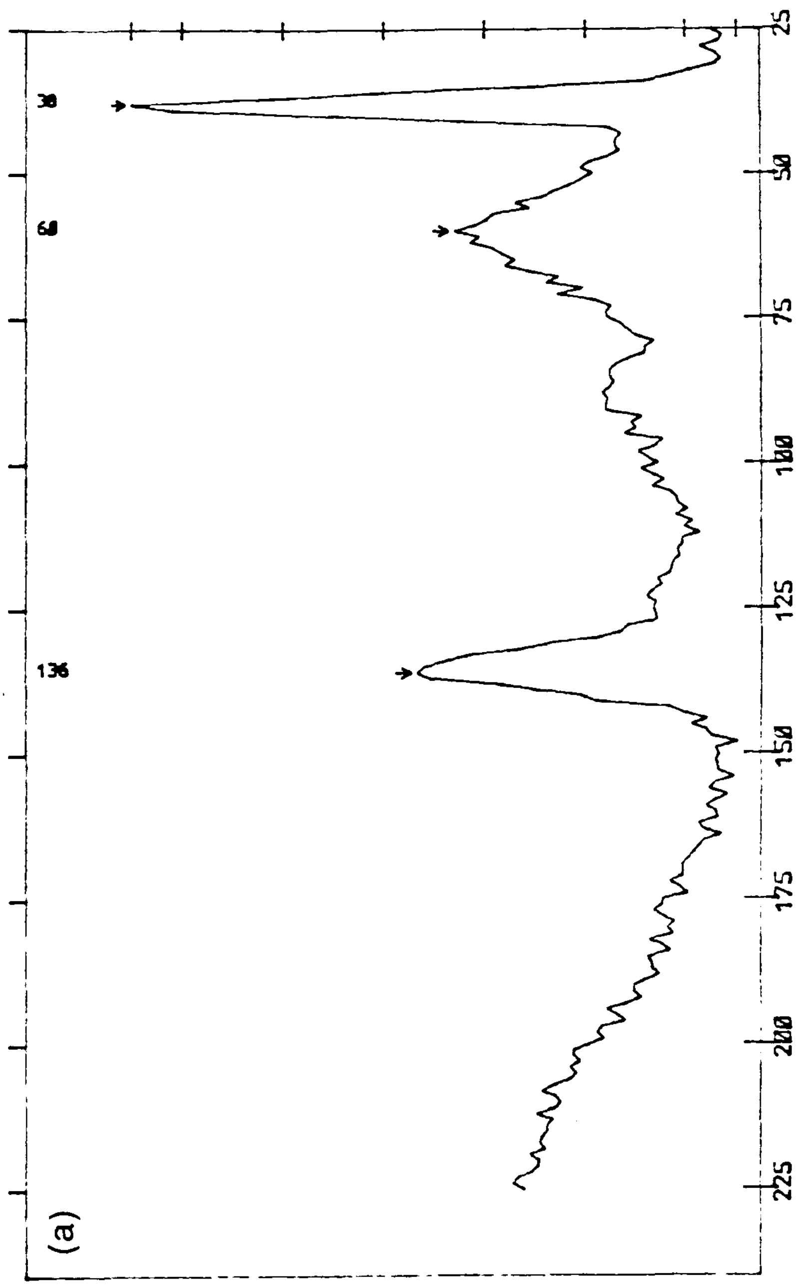
38
60
136
25
50
75
100
125
150
175
200
225
(a)

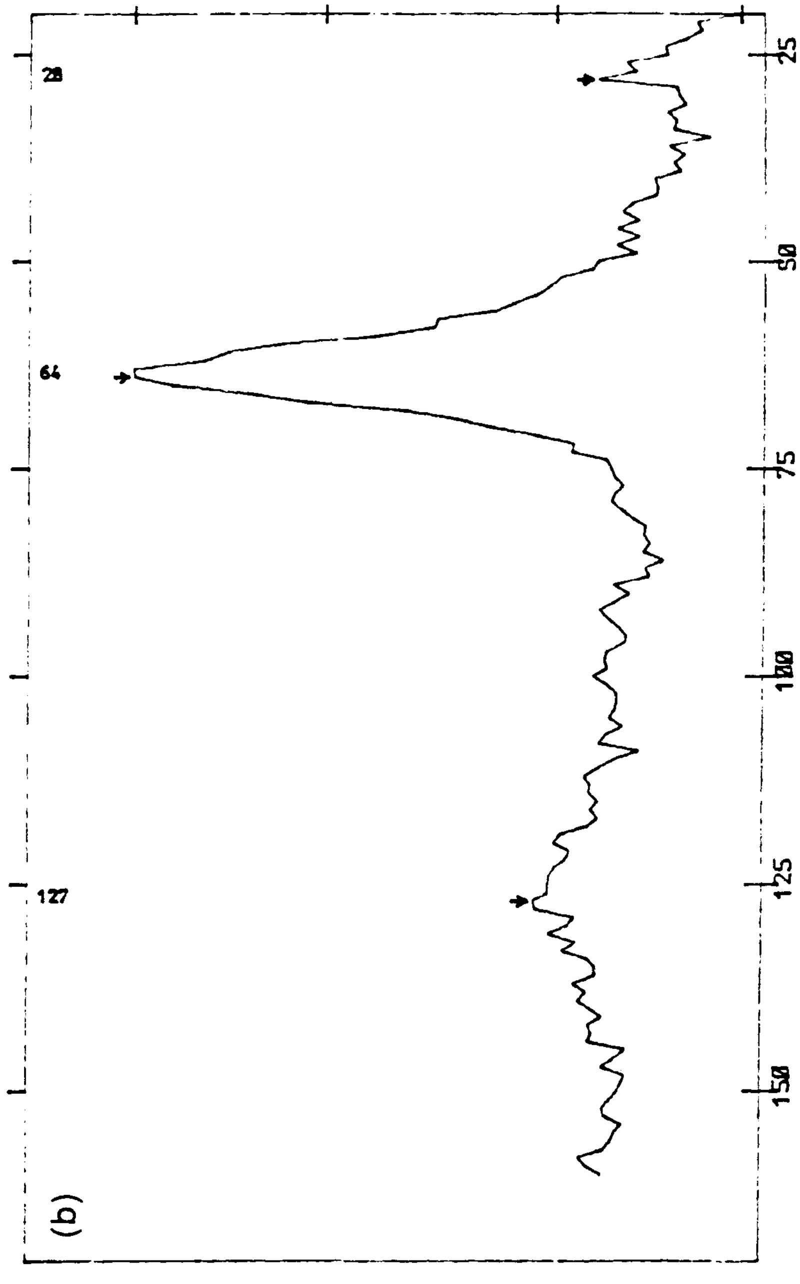
28
64
127
25
50
75
100
125
150
(b)

ratio of the concentration of Ir_2 to Ir_2H_2 (determined from optical absorption spectra) is 1/40. The band at 136 cm^{-1} is the Ir-Ir stretching frequency of Ir_2H_2.

While the Ir_2Cl_2 structure is not known, a comparison of the Ir-Ir interaction for Ir_2Cl_2 to that of Ir_2H_2 can be made using the Raman vibrational data.[12] A significantly larger Ir-Ir force constant is found for Ir_2Cl_2, indicating a stronger Ir-Ir interaction, and hence a smaller Ir-Ir separation. An estimate of the Ir-Ir distance for Ir_2Cl_2 can be obtained using Woodruff's correlation (Table 5.7).[13,14] A significantly shorter Ir-Ir distance, in comparison to Ir_2H_2, is calculated for Ir_2Cl_2. The longer Ir-Ir distance for Ir_2H_2 is a consequence of two transhydride effects.

The optical absorption spectrum of $[Ir_2(TMB)_4H_2](B(C_6H_5)_4)_2$ is shown in Figure 5.5. In analogy to other binuclear d^7-d^7 complexes, the broad feature (λ_{max} 320 nm, ε = 17000 $M^{-1}cm^{-1}$) is assigned to the $d\sigma \rightarrow d\sigma^*$ transition.[12] A weak absorption attributable to "$d\pi$" $\rightarrow d\sigma^*$ is not present in the spectrum. This band is presumably beneath the $d\sigma \rightarrow d\sigma^*$ band. The large red shift observed for the $d\sigma \rightarrow d\sigma^*$ transition from Ir_2Cl_2 to Ir_2H_2 is a result of the strong σ-donating character of the hydride ligand (a significantly greater charge-transfer contribution for H^- in comparison to Cl^-).

The ^1H NMR spectrum of $[Ir_2(TMB)_4H_2](B(C_6H_5)_4)_2 \cdot CH_3C_6H_5$ is shown in Figure 5.6. The Ir-H resonance is a sharp singlet at -10.6 ppm. The resonances attributed to the TMB methyls and methylenes are assigned to the broad features at 1.4, 1.6 and 1.8 ppm. The $B(C_6H_5)_4^-$ resonances are to lower field. One unique feature of this spectrum is the similarity of the TMB spectrum to that of the coalesced spectra for $Ir_2(TMB)_4^{2+}$ and $Ir_2(TMB)_4I_2^{2+}$.[15] While Ir_2H_2 is expected to be fluxional in solution at room temperature, the two types of methyl groups (one almost coplanar with the $Ir(CN)_4$ unit and the other projecting out over the $Ir(CN)_4$ plane, see Figure 5.1) are magnetically inequivalent and give rise to resonances at 1.4 and 1.6 ppm.

Figure 5.5. Electronic absorption spectrum of $[Ir_2(TMB)_4H_2](B(C_6H_5)_4)_2$ in CH_3CN at 25 °C.

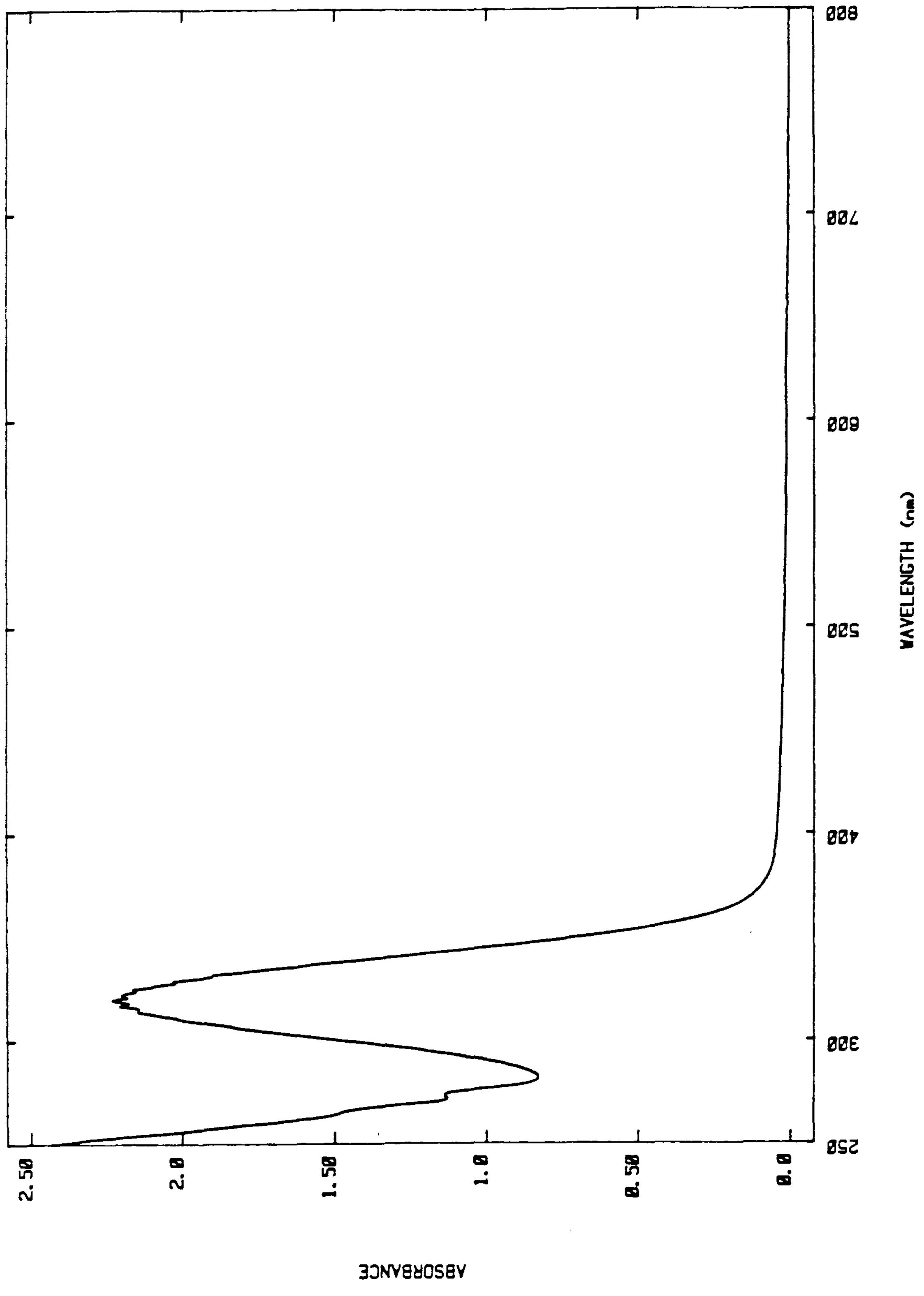
ABSORBANCE
2.50
2.0
1.50
1.0
0.50
0.0
WAVELENGTH (nm)
250
300
400
500
600
700
800

Figure 5.6. ^{1}H NMR spectrum of $[Ir_2(TMB)_4H_2](B(C_6H_5)_4)_2 \cdot CH_3C_6H_5$ in CD_3CN at 20 °C.

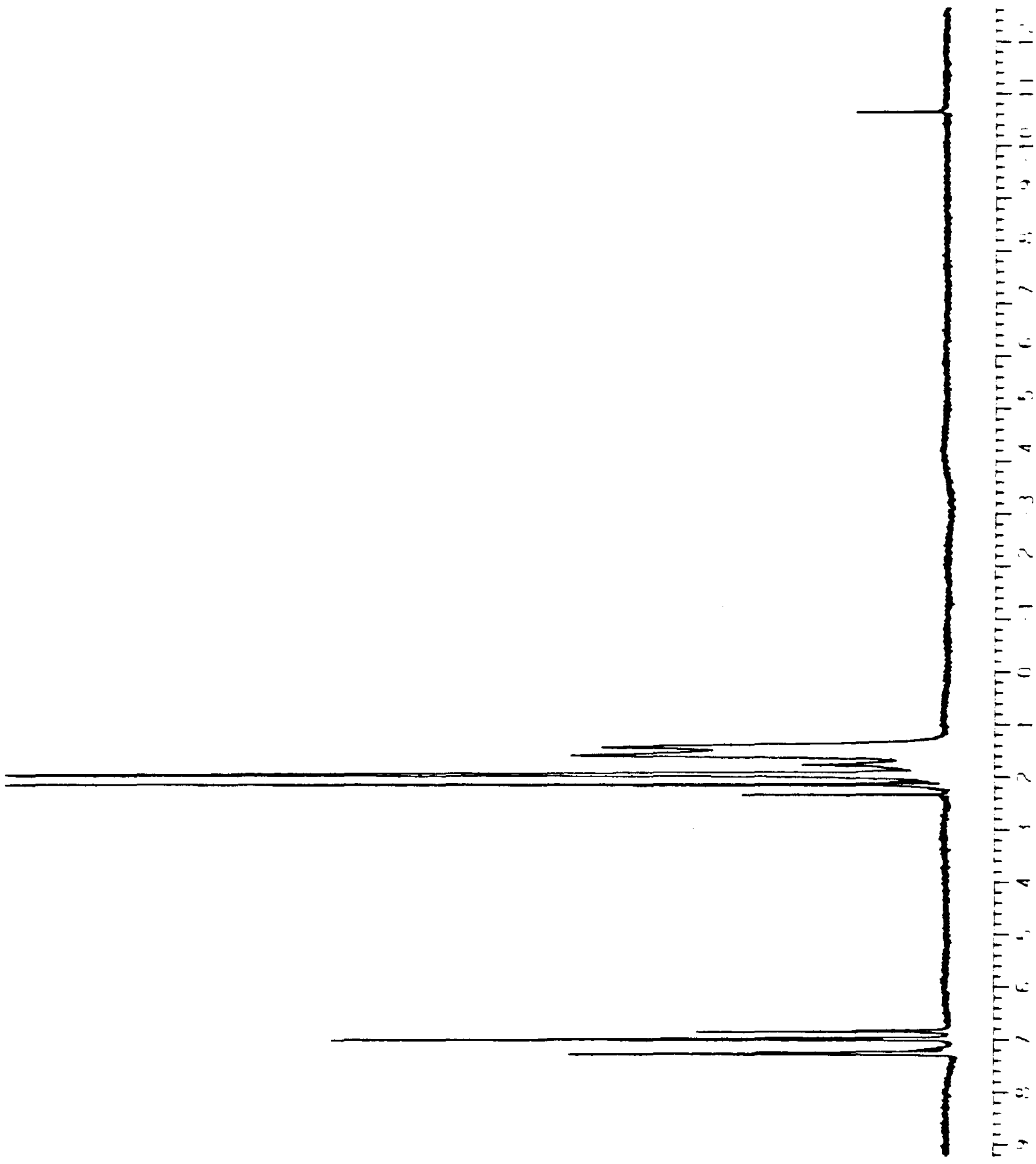

Reactivity

An exciting aspect of atom-transfer reactivity is the possibility of photocatalytic processes. The metal dihydrides formed in the initial photochemical hydrogen atom-transfer reaction may be turned over to produce H_2 and the d^8 -d^8 complex (M_2) or reacted with a substrate to effect hydrogenation (and again production of M_2).

Isolation and characterization of M_2H_2 afford an opportunity to explore its reactivity (Scheme 5.1). Some of this work has already been reported for $Pt_2(P_2O_5H_2)_4H_2^{4-}$ (Pt_2H_2).[1,5] Ir_2H_2 is found to be thermally quite stable. No significant decomposition of Ir_2H_2 is observed at 80 °C in CH_3CN over 12 hrs. Slow thermal decomposition of Pt_2H_2 is observed at room temperature. Both Pt_2H_2 and Ir_2H_2 react with HCl. Reaction of Ir_2H_2 yields $Ir_2(H)Cl$. For Pt_2H_2, reaction with HCl and DCl generates H_2 and HD, respectively. Pt_2H_2 photochemically eliminates H_2 to yield Pt_2. For Ir_2H_2, photolysis results in production of the starting Ir_2 complex. This reaction is not clean, and a large amount of decomposition of the iridium material is observed.

A potentially more useful reaction has been found. Reaction of Ir_2H_2 with styrene results in a slow, clean conversion to Ir_2 and ethylbenzene. The reaction may be related to the hydrogenation of alkenes by $Co(CN)_5^{3-}$, which involves a coordinatively saturated metal hydride that can effect hydrogen atom transfer to give a stable 1-electron reduced transition metal ion.[16] A similar reaction (transhydrogenation of cyclohexene and pentene with isopropanol) is observed for Pt_2.[17] Thus, combination of the photochemical hydrogen atom-transfer reaction with the hydrogenation step completes a catalytic cycle in which the Ir_2 complex functions as a photochemical two-hydrogen transfer reagent.

Scheme 5.1. Observed reactivity of $[Ir_2(TMB)_4H_2](B(C_6H_5)_4)_2$. Iridium containing by-product not characterized, "Ir".

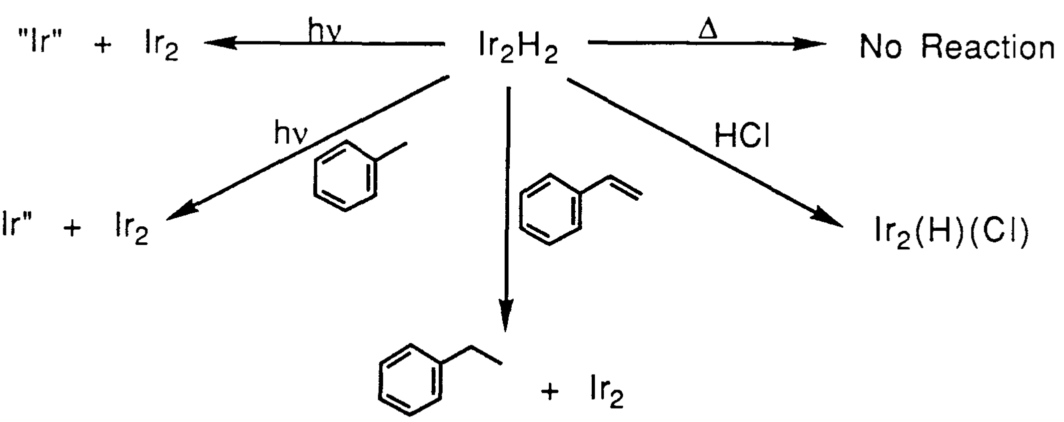
"Ir" + Ir2
hν
Ir2H2
Δ
No Reaction
hν
HCl
"Ir" + Ir2
Ir2(H)(Cl)
+ Ir2

References and Notes

1. Roundhill, D.M.; Gray, H.B.; Che, C.-M. *Accts. Chem. Res.*, in press.

2. Marshall, J.L.; Stiegman, A.E.; Gray, H.B. In *Excited States and Reactive Intermediates*; Lever, A.B.P., Ed.; ACS Symp. Ser. 307; American Chemical Society: Washington,. D.C., 1986; pp. 116-176.

3. Vlcek, A., Jr.; Gray, H.B. *J. Am. Chem. Soc.* **1987**, *109*, 286-287.

4. Vlcek, A., Jr.; Gray, H.B. *Inorg. Chem.* **1987**, *26*, 1997-2001.

5. Harvey, E.L.; Stiegman, A.E.; Vlcek, A., Jr.; Gray, H.B. *J. Am. Chem. Soc.* **1987**, *109*, 5233-5235.

6. Chapter 2.

7. Principal crystal faces [0,1,0] and [1,0,2].

8. *International Tables for X-ray Crystallogrphy,* Vol. IV; Kynoch Press: Birmingham, England, 1974.

9. Maverick, A.W.; Smith, T.P.; Maverick, E.F.; Gray, H.B. *Inorg. Chem.* **1987**, *26*, 4336-4341.

10. Mann, K.R.; Thich, J.A.; Bell, R.A.; Coyle, C.L.; Gray, H.B. *Inorg. Chem.* **1980**, *19*, 2462-2468.

11. An increase in the N≡C stretching frequency from the free ligand to Ir_2 is counter to the expected shift, if π-backbonding were an important part of the metal-isocyanide interaction. Therefore, the π-backbonding contributions to the metal-isocyanide interaction are negligible with σ donation from the isocyanide to the iridium center being the dominant bonding interaction leading to an increase in the N≡C frequency.

12. Miskowski, V.M.; Smith, T.P.; Loehr, T.M.; Gray, H.B. *J. Am. Chem. Soc.* **1985**, *107*, 7925-7934.

13. Miskowski, V.M.; Dallinger, R.F.; Christoph, G.G.; Morris, D.E.; Spies, G.H.; Woodruff, W.H. *Inorg. Chem.* **1987**, *26*, 2127-2132.

14. Poor agreement is found between the calculated and crystallographically determined Ir-Ir distances for Ir_2I_2. The significant mixing of the metal-halide vibration with the metal-metal vibration for Ir_2I_2 makes force-field analysis of this system quite difficult. The force constant for the Ir-Ir bond is not well determined. For Ir_2Cl_2 and Ir_2Br_2, the amount of mixing between the metal-halide mode and the metal-metal mode is much less, allowing force-field analyses to produce more reliable estimates of the Ir-Ir force constants. Therefore, better agreement between the calculated and the true Ir-Ir separations are expected. Good agreement is found between the calculated and crystallographically determined metal-metal distances for Rh_2Cl_2.

15.

	Chemical Shift [a]				
	$-CH_2-$ (fast)	$-CH_3$ (fast)	$-CH_3$ (slow)	T_C, °C	$\Delta G^{\dagger}$, kcal/mol
$Ir_2(TMB)_4^{2+}$ [b]	1.72	1.46	1.33, 1.58	15	14.6
$Ir_2(TMB)_4I_2^{2+}$ [b]	2.11	1.54	1.33, 1.63	-14	13.0

a. Given in δ (ppm) vs. TMS. "Fast" and "slow" refer to values determined in the fast-exchange and stopped-exchange limits, respectively.
b. In CD_3CN, see reference 9.

16. Kwiateh, J. *Catal. Rev.* **1967**, *1*, 37-72.

17. Che, C.-M.; Lee, W.-M. *J. Chem. Soc., Chem. Commun.* **1986**, 512-513.

Chapter 6

Ab Initio Calculations of $Re_2Cl_8^{2-}$

Introduction

The discovery of multiply bonded metal-metal dimers has provoked numerous studies aimed toward understanding the electronic structure and spectral properties of these systems. To begin to understand the nature of the quadruple metal-metal bond, one can analyze the d orbital interaction for a simple diatomic system M_2. Figure 6.1 shows the five nonzero overlaps between pairs of d orbitals when two metal atoms approach each other.

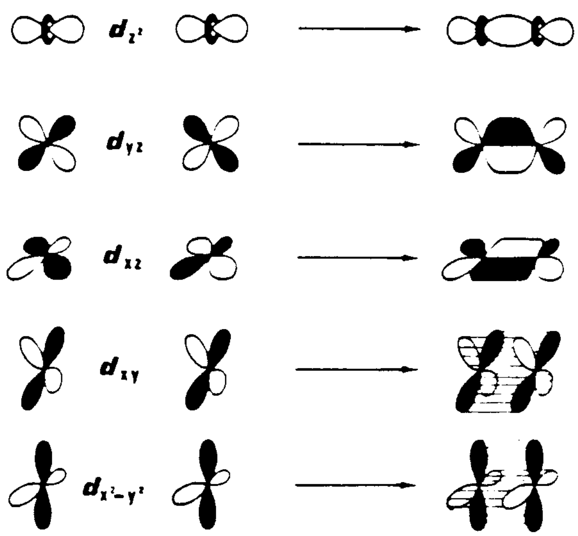

Figure 6.1. d-d overlaps between two metal atoms.

The positive overlap of the d_{z^2}, d_{xz}, and d_{yz} orbitals gives rise to the σ and π bonds, with the δ bonds being formed by the overlap of the d_{xy} and $d_{x^2-y^2}$ orbitals. The relative magnitudes of the orbital overlap are $\delta << \pi < \sigma$. Using the simple Huckel concept that the molecular orbital (MO) energy should be proportional to the orbital overlap, the following orbital energy ordering is predicted.

$$\sigma < \pi << \delta < \delta^* << \pi^* < \sigma^*$$

In order to explain the nonbridging eclipsed conformation and the observed diamagnetism of $Re_2Cl_8^{2-}$ Cotton proposed, based on the above MO scheme, that the ground-state configuration was $\sigma^2\pi^4\delta^2$. Because the $\delta_{x^2-y^2}$ orbitals of the metal are involved in the metal-ligand σ bonds, the $\delta_{x^2-y^2}$ and $\delta^*_{x^2-y^2}$ orbitals were assumed to be high in energy and unimportant in the description of the metal-metal bonds (see Figure 6.2). Using this MO scheme, estimates of the quadruple bond and δ bond strengths were made, as well as assignment of the optical absorption spectrum. However, the MO interpretation has been shown to be incorrect.[1]

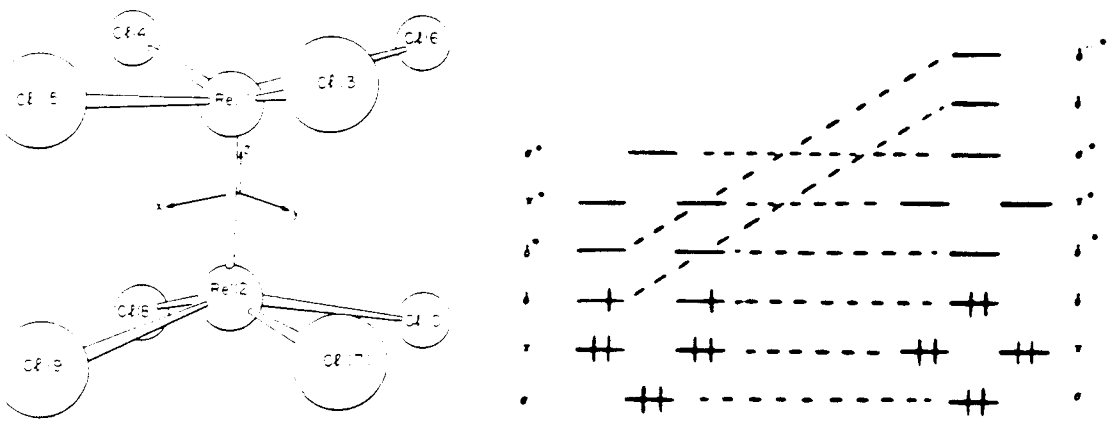

Figure 6.2. d orbitals for M_2 and M_2X_8.

In the MO formalism, a single configuration is used to describe the electronic structure of a molecule. For a singly bonded system such as H_2, the MO wave function is

$$\Psi_{MO} = \left[\varphi_\sigma(1)\varphi_\sigma(2)\right](\alpha\beta - \beta\alpha). \qquad 6.1$$

In terms of atomic orbitals, the MO wave function has an equal covalent and ionic contribution.

$$\varphi_\sigma = l + r \qquad 6.2$$

$$\Psi_{MO} = [l \;+\; r][l \;+\; r](\alpha\beta - \beta\alpha) \qquad 6.3$$

$$\Psi_{MO} = [(lr \;+\; rl) \;+\; (ll \;+\; rr)](\alpha\beta - \beta\alpha) \qquad 6.4$$

$$\psi_{cov} = lr + rl \qquad \psi_{ion} = ll + rr \qquad 6.5$$

The MO wave function for the ground state of H_2, while being bound at the equilibrium bond distance, is more than 2 eV above the exact energy. As the molecule is dissociated, the ground-state wave function should converge toward the covalent limit of two hydrogen atoms, lr + rl. At $R = \infty$, the MO wave function leads to an energy that is more than 8 eV above the correct dissociation limit. Since the MO wave function must have equal ionic and covalent contributions for all internuclear separations, it cannot correctly describe the long R region of the ground-state potential surface. This is a region of low orbital overlap that is best described by a covalent wave function.

For Re_2, with a metal-metal separation of 2.24 Å, the orbital overlaps are σ = 0.63, π = 0.53, and δ = 0.17. Because of the low δ orbital overlap, the wave function for the δ bond is required to be largely covalent. Therefore, an MO wave function will be an extremely inadequate description of the δ bond.

In order to correct for the deficiencies of the MO description, a wave function can be constructed using the exact wave functions at $R = \infty$ (i.e., the valence bond (VB) wave function). The VB wave function for H_2 is

$$\Psi_{VB} = [lr \;+\; rl](\alpha\beta - \beta\alpha). \qquad 6.6$$

This wave function is covalent for all internuclear distances and, while being only slightly better than the MO wave function at short R, correctly describes the long R region of the potential surface. Although dissociating to the correct limit, the VB wave function at R_e is ~1.5 eV above the exact energy of H_2.

Expressing the VB wave function for H_2 in terms of the MO wave functions, one sees that the correct description of the long R region requires a wave function that is made up of more than a single configuration.

$$\Psi_{MO} = [l\,r \;+\; r\,l](\alpha\beta - \beta\alpha) \qquad 6.7$$

$$\varphi_\sigma = l + r \qquad\qquad \varphi_\sigma^* = l - r \qquad 6.8$$

$$\varphi_\sigma\varphi_\sigma = (ll + rr) + (lr + rl) \qquad 6.9$$

$$\varphi_\sigma^*\varphi_\sigma^* = (ll + rr) - (lr + rl) \qquad 6.10$$

$$\Psi_{VB} = \left[\varphi_\sigma\varphi_\sigma - \varphi_\sigma^*\varphi_\sigma^*\right](\alpha\beta - \beta\alpha) \qquad 6.11$$

For the metal dimers, the VB wave function is a multiconfiguration description that correctly describes the weak coupling in the metal-metal bond.

A generalization to the VB description can be made by allowing the MO wave functions to optimize their contributions to the VB wave function. This generalization yields the generalized valence bond (GVB) wave function.

$$\Psi_{GVB} = \left[C_1(\varphi_\sigma\varphi_\sigma) - C_2(\varphi_\sigma^*\varphi_\sigma^*)\right](\alpha\beta - \beta\alpha) \qquad 6.12$$

A multiconfiguration description is necessary to represent adequately the ground state wave function for the quadruply bonded metal dimers. This level of theory, while providing the correct qualitative description of the quadruple bond, gives a very poor quantitative description of the metal dimer. Using an extensive *ab initio* wave function for $Mo_2Cl_8^{4-}$ and solving self-consistently for the $^1A_{2u}$ excited state ($\delta \rightarrow \delta^*$ transition), an excitation energy ~1.2 eV higher than the experimental assignment was obtained.[2] Such results have led some theoreticians to conclude that the earlier spectral assignments are incorrect.[2] Others, arguing that the errors are due to an inadequate description of the electron correlation, have corrected the calculated transition energies by subtracting from these values the difference in the theoretical estimate and experimental assignment for one well-characterized transition.[3]

Recently, it has been shown from studies on Cr_2 and Mo_2 that the large correlation error in the *ab initio* wave function results from a difficulty in describing the atomic electron affinities.[4,5] There exists an atomic correlation energy associate with a doubly occupied atomic orbital that is normally accounted for by doing double excitation out of a bond pair. For the hextuply bonded metal dimers, the number of configurations necessary to describe this atomic correlation is impractical. Reducing the size of the calculation to a manageable level leads to an energy for the doubly occupied atomic orbitals that is too high. However, by making a simple modification to the GVB methods, accurate ground-state properties could be determined.[5]

For the quadruply bonded metal dimers, an accurate description of the doubly occupied atomic orbitals, while being important in determining the ground-state properties, is imperative in the calculation of excitation energies. The importance of the intrapair correlation energy in the excited state is evident from the VB wave function for the $^1A_{2u}$ state.

$$\Psi(^1A_{2u}) = \left[\varphi_\delta\varphi_\delta + \varphi_\delta^*\varphi_\delta^*\right](\alpha\beta - \beta\alpha) \qquad 6.13$$

$$\varphi_\delta = l + r \qquad\qquad \varphi_\delta^* = l - r \qquad 6.14$$

$$\varphi_\delta\varphi_\delta^* = (l + r)(l - r) \qquad 6.15$$

$$\varphi_\delta^*\varphi_\delta = (l - r)(l + r) \qquad 6.16$$

$$\Psi(^1A_{2u}) = [l\,l - r\,r](\alpha\beta - \beta\alpha) \qquad 6.17$$

The $^1(\delta\delta^*)$ excited state is described by an ionic wave function, two electrons localized on the same atom. The correlation error associated with having two electrons in the same localized orbital is large, and to describe accurately the $^1(\delta\delta^*)$ state, it is necessary to include in the wave function the correct amount of correlation interaction to account for this correlation error. The $^1(\delta \rightarrow \delta^*)$ excitation energy is expected to have an error of 1-2 eV if a wave function is used that does not account for the intrapair correlation energy. A similar error is expected for any state that cannot be described by singly occupied orbitals on the metal centers.

For the *ab initio* calculations to date,[1-3] the level of correlation in the wave functions has not been sufficient to account for the intrapair correlation energy. Again, the size of the calculation necessary for an accurate description is impractical. However, the correlation neglected in the *ab initio* wave function can be accounted for by applying the modified generalized valence-bond (MGVB) method.

In addition to the *ab initio* calculations, many studies have been carried out using the extended Huckel and Xα scattered wave methods.[1] However, these methods are limited in their ability to describe accurately the multiply bonded metal dimers because of their MO formalisms and lack of correlation.

In order to determine accurate ground- and excited-state properties for quadruply bonded metal dimers, we have begun an *ab initio* study in which the ground and excited state wave functions are solved for self-consistently using the MGVB method. A detailed discussion of the results obtained from the *ab initio* study of the excited states for quadruply bonded metal dimers is presented elsewhere. In this chapter, the results of *ab initio* calculations of $Re_2Cl_8^{2-}$ are reported.

Calculational Details

Hartree-Fock (HF), generalized valence bond (GVB), configuration interaction (CI), multiconfiguration self-consistent field (MCSCF), and modified generalized valence bond (MGVB) calculations were carried out on all metal dimers of interest.

The general form of the ground-state HF wave function for the quadruply bonded metal dimers is

$$\Psi_{HF} = A\psi_{core}\left[\varphi_{a1g}(1)\alpha(1)\right]\left[\varphi_{a1g}(2)\beta(2)\right]\left[\varphi_{egx}(3)\alpha(3)\right]\left[\varphi_{egx}(4)\beta(4)\right]$$
$$\left[\varphi_{egy}(5)\alpha(5)\right]\left[\varphi_{egy}(6)\beta(6)\right]\left[\varphi_{b2g}(7)\alpha(7)\right]\left[\varphi_{b2g}(8)\beta(8)\right] , \quad 6.18$$

where A is the antisymmetrizer and ψ_{core} represents all the ligand and nonvalence metal electron pairs. The overall symmetry of the systems studied is D_{4h}, and the orbitals represented above are those that are equivalent to the σ, π, and δ metal-metal bonding orbitals.

$$\varphi_{a1g} \approx \sigma \quad 6.19$$

$$\varphi_{eg} \approx \pi \quad 6.20$$

$$\varphi_{b2g} \approx \delta \quad 6.21$$

In the GVB wave function, unlike the HF wave function where an electron pair is described by a pair of identical orbitals $\varphi_i(1)\varphi_i(2)$, each electron in a bond pair is allowed to have a different orbital $\varphi_i(1)\varphi_i'(2) + \varphi_i(2)\varphi_i'(1)$, and every orbital is optimized self-consistently. For the metal dimers, the $^1A_{1g}$ ground-state GVB-PP wave function has the form

$$\Psi_{GVB} = A\psi_{core}\left[\varphi_\sigma(1)\varphi_\sigma'(2) + \varphi_\sigma'(1)\varphi_\sigma(2)\right]\left[\varphi_{\pi x}(3)\varphi_{\pi x}'(4) + \varphi_{\pi x}'(3)\varphi_{\pi x}(4)\right]$$

$$\left[\varphi_{\pi y}(5)\varphi_{\pi y'}(6) + \varphi_{\pi y'}(5)\varphi_{\pi y}(6)\right]\left[\varphi_{\delta}(7)\varphi_{\delta'}(8) + \varphi_{\delta'}(7)\varphi_{\delta}(8)\right]\chi \qquad 6.22$$

$$<\varphi_i|\varphi_j> = \delta_{ij}, \quad <\varphi_i|\varphi_i'> = S_i\ , \qquad 6.23$$

where, again, A is the antisymmetrizer, ψ_{core} represents the closed-shell HF core and χ represents the spin function. This wave function describes the left-right static correlation in the two electron bonds. Where one electron is localized on the right, the other electron is more likely to be found on the left, thus relieving some of the electron-electron repulsion.

$$\varphi = l + \lambda r \qquad 6.24$$

$$\varphi' = r + \lambda l \qquad 6.25$$

In solving the GVB wave function, the GVB orbitals are cast in their orthogonal, natural orbital (NO) representation $c_1\varphi_{i1}(1)\varphi_{i1}(2) - c_2\varphi_{i2}(1)\varphi_{i2}(2)$ (plus and minus combination of the one-electron orbitals), where $<\varphi_{i1}|\varphi_{i2}> = 0$ and $c_1^2 + c_2^2 = 1$.

For the quadruple metal-metal bond, the NO's would be bonding and antibonding orbitals of the appropriate bond pairs.

$$\Psi_{GVB}^{NO} = A\psi_{core}\left[c_1(\varphi_\sigma)^2 - c_2(\varphi_\sigma^*)^2\right]\left[c_3(\varphi_{\pi x})^2 - c_4(\varphi_{\pi x}^*)^2\right]$$

$$\left[c_5(\varphi_{\pi y})^2 - c_6(\varphi_{\pi y}^*)^2\right]\left[c_7(\varphi_\delta)^2 - c_8(\varphi_\delta^*)^2\right]\chi \qquad 6.26$$

The designation given this wave function is GVB-PP(4/8), four bonds correlated with eight natural orbitals.

In the GVB-PP wave function, only a single spin-coupling (or valence bond structure) is allowed and the wave function is designated PP for perfect pairing. In the NO representation, this spin restriction leads only to configurations where the occupation for any given bond pair is {2,0} or {0,2}.

The GVB-PP wave function often provides an excellent description of saturated organic systems; however, for transition metal systems, singly occupied d orbitals on the same metal prefer to be high-spin coupled, and it is necessary to optimize the spin coupling of the GVB wave function.

Originally, the full GVB wave function was calculated using the form

$$A\varphi_a\varphi_b\cdots\varphi_z\chi , \qquad 6.27$$

where the orbitals $\varphi_a\cdots\varphi_z$ are all allowed to overlap and where the spin function χ is optimized.[6] Such calculations are too tedious for studies of large molecules, and a series of studies led to an abbreviated approach in which the GVB-PP wave function of (6.26) is generalized to allow the {1,1} configuration in each bond pair. The orbitals and CI coefficients of the resulting wave function are solved for using the GVB3 program.[4,7] This wave function does not correspond exactly to the full GVB wave function; however, it does allow a completely general description of the spin coupling and an unambiguous description of the two electrons in each bond pair, just as in GVB. The resulting wave function is denoted GVB-RCI in order to indicate the restricted coupling used.

In nontransition metal systems, the full GVB wave function can often be well approximated by using the GVB-PP orbital in the GVB-RCI wave function. However, for transition metal system, the orbitals in the GVB-RCI wave function must be optimized self-consistently. Calculations in which all the GVB occupied orbitals are used and general occupations are allowed are denoted as GVB-CI. This allows a more complete description of the resonance and the correlation effects.

Recently, it has been shown from studies on Cr_2 and Mo_2 that quite significant correlation errors result from difficulties in describing the atomic electron affinities.[4,8] With this insight, a simple modification to the GVB method was made that corrects certain Coulombic integrals so as to provide the correct atomic electron affinities.[4,5] This method, MGVB, when applied to the metal dimers gave accurate bond lengths and bond energies.

Modified Generalized Valence Bond Method

The MGVB method was developed by Goodgame and Goddard to account for the electron correlation missing in a GVB wave function.[4,5] Because of the importance of this method to the present investigation, a brief discussion is necessary.

In the long R limit, the homonuclear GVB wave function is covalent and has the form

$$\Psi_{GVB} = \left[\varphi_l(1)\varphi_r(2) + \varphi_r(1)\varphi_l(2)\right](\alpha\beta - \beta\alpha), \qquad 6.28$$

where φ_l and φ_r represent the one-electron orbitals localized on the left and right centers, respectively. As the internuclear distance is decreased, the one-electron orbitals delocalize and the GVB wave function has the form

$$\Psi_{GVB} = \left[\varphi_a(1)\varphi_b(2) + \varphi_b(1)\varphi_a(2)\right](\alpha\beta - \beta\alpha), \qquad 6.29$$

where the GVB orbitals can be thought of as consisting of optimized atomic orbitals (ignoring normalization),

$$\varphi_a = \varphi_l + \lambda\varphi_r \quad \text{and} \quad \varphi_b = \varphi_r + \lambda\varphi_l. \qquad 6.30$$

Expanding the GVB wave function in terms of these optimized atomic functions,

$$\Psi_{GVB} = \left(\varphi_l\varphi_r + \varphi_r\varphi_l\right) + \lambda\left(\varphi_l\varphi_l + \varphi_r\varphi_r\right) , \qquad 6.31$$

leads to a superposition of an ionic term (two electrons localized on the same center) and a covalent term (two electrons localized on different centers).

$$\Psi_{GVB} = C_c\psi_{cov} + C_i\psi_{ion} \qquad 6.32$$

Goodgame and Goddard postulated that the GVB wave function leads to an excellent description of the covalent terms, but the ionic terms, involving as they do doubly occupied orbitals, should be too high by ~1.3 eV.[5] They argued that the usual CI approach, in which one does double excitations out of each bond pair, is specifically correcting for the error in the ionic terms. They tested this hypothesis by carrying out calculations in which the one-center Coulomb integrals were modified so to have the effect of properly correcting the ionic terms at $R = \infty$.

There are several ways in which corrections for the error in the ionic terms can be determined. The simplest, used by Goodgame and Goddard in their first paper and referred to as MGVB/1,[5] corrects the limits so that the wave function ll or rr at $R = \infty$ has the correct energy relative to lr or rl, leading to

$$CC = IP^{(Exp\ -\ Calc)} - EA^{(Exp\ -\ Calc)} . \qquad 6.33$$

For the hextuply bonded metal dimers, the total error in the HF energy was

$$\delta E(s^0d^5) + \delta E(s^2d^5) - 2\delta E(s^1d^5) = \delta IP_s - \delta EA_s \qquad 6.34$$

$$\delta E(s^1d^4) + \delta E(s^1d^6) - 2\delta E(s^1d^5) = \delta IP_d - \delta EA_d \qquad 6.35$$

These correction values were then used to modify the s-s and d-d self-Coulomb terms while all other integrals were evaluated exactly.

In a new approach, MGVB/2, various one-center, one- and two-electron integrals are adjusted to fit the IP's, EA's and atomic-excitation energies. In MGVB/2, an energy expression based on the Condon and Shortley formalism is derived for various atom states. While the values of the one- and two-electron integrals in these energy expressions are dependent on the electron configuration of the atom, it has been shown that the correlation error expressed in terms of these integrals is relatively constant for a given ionic series and shows only minor fluctuation with changing ionicism. In other words, the correlation error in the HF energy appears to be constant.

MGVB/2 is an extension of the ideas developed in the earlier method. The corrections to the one- and two-electron Condon and Shortley parameters, obtained by fitting the difference between the calculated and experimental term energies with the parametric equations, are added to the appropriate integrals, while evaluating all integrals exactly. Now, instead of correcting only for the correlation error associated with placing two electrons in the same orbital, a spherical correction is applied that accounts not only for the correlation between electrons in the same orbital but also for the correlation of electrons in different orbitals.

Method of Correction

In applying the MGVB corrections, the following procedure is used:

(1) symmetric orthogonalization of the localized GVB orbitals;

(2) evaluate all integrals in terms of the localized orbitals and apply the appropriate corrections to the one-center integrals;

(3) transform these orbitals back to the GVB natural orbitals for use in a CI or an MCSCF calculation;

(4) recalculate the usual GVB-RCI wave function, using the modified integrals;

(5) in calculating the CI wave function of (4), the corrected integrals are used only for bond pairs in which bonding or antibonding GVB natural orbitals are doubly occupied, since only in this case is there static ionic character in the wave function.

References

1. Cotton, F.A.; Walton, R.A. *Multiple Bonds Between Metal Atoms*; Wiley: New York, 1982, and references therein.

2. Mathisen, K.B.; Walhgren, U.; Pettersson, L.G.M. *Chem. Phys. Lett.* **1984**, *104*, 336-342.

3. Hay, P.J. *J. Am. Chem. Soc.* **1982**, *104*, 7007-7017.

4. Goodgame, M.M., Ph.D. Dissertation, California Institute of Technology, 1983.

5. Goodgame, M.M.; Goddard, W.A. III *Phys Rev. Lett.* **1985**, *54*, 661-664.

6. Goddard, W.A. III; Ladner, R.C. *J. Am. Chem. Soc.* **1971**, *93*, 6750-6756.

7. Bobrowicz, F.W., Ph.D. Dissertation, California Institute of Technology, 1974.

8. Goodgame, M.M.; Goddard, W.A. III *Phys Rev. Lett.* **1982**, *48*, 135-138.

9. Crosswhite, H.M.; Crosswhite, H. *J. Optic. Soc. Am. B* **1984**, *1*, 246-254.

10. Hansen, J.E.; Raassen, A.J.J. *Physica* **1981**, *111C*, 76-101, and references therein.

11. Shadmi, Y. *Phys. Rev.* **1965**, *139*, A43-A47, and references therein.

Reprinted from the Journal of the American Chemical Society, 1987, *109*, 5580.

Bond Energy and Other Properties of the Re–Re Quadruple Bond

David C. Smith and William A. Goddard III*

Contribution No. 7558 from the Arthur Amos Noyes Laboratory of Chemical Physics, California Institute of Technology, Pasadena, California 91125. *Received February 18, 1987*

Abstract: Using generalized valence bond (GVB) methods designed for obtaining accurate bond energies, we predict an Re–Re quadruple bond strength of 85 ± 5 kcal/mol for $Re_2Cl_8^{2-}$. This is much less than early estimates of 370 kcal/mol and somewhat lower than estimates (124 to 150 kcal/mol) based on Birge–Sponer extrapolation but is in reasonable agreement with a recent thermochemical study (97 ± 12 kcal/mol). We obtain a rotational barrier of 3.0 kcal/mol and a singlet–triplet excitation energy of 3100 cm^{-1}, and we conclude that the intrinsic strength of the δ bond is 6 ± 3 kcal/mol.

Since their discovery in 1965, quadruply bonded metal dimers have provoked numerous theoretical and experimental studies. A particularly controversial issue has been the strength of the quadruple bond and, in particular, the contribution of the δ bond to the observed structure of the unbridged dimers.[1-4] We here report the results of ab initio calculations of $Re_2Cl_8^{2-}$ designed to provide accurate bond energies and torsion barriers as well as accurate shapes for the potential curves. These studies use the generalized valence bond (GVB) approach in which electron correlations are included for all eight electrons available for the quadruple bond, while solving self-consistently for all orbitals.[5,6]

We use the modified-GVB (M–GVB) approach of Goodgame and Goddard.[7] They pointed out that ab initio descriptions of multiple bonds in transition metals lead to substantial errors in the bond energy due to an inadequate treatment of the electron correlations in the ionic part of the wave function describing the bond.

$$\psi^{GVB} = \psi_{cov} + \lambda\psi_{ionic} = [\phi_l(1)\phi_r(2) + \phi_r(1)\phi_l(2)] + \lambda[\phi_l(1)\phi_l(2) + \phi_r(1)\phi_r(2)]$$

In GVB, electron correlation in the covalent part of the wave

(1) Cotton, F. A.; Walton, R. A. *Multiple Bonds Between Metal Atoms*; Wiley: New York, 1982; and references therein.
(2) Cotton, F. A.; Walton, R. A. *Struct. Bonding* **1985**, *62*, 1–49.
(3) Mathisen, K. B.; Wahlgren, U.; Pettersson, L. G. M. *Chem. Phys. Lett.* **1984**, *104*, 336–342 and references therein.
(4) Hay, P. J. *J. Am. Chem. Soc.* **1982**, *104*, 7007–7017 and references therein.
(5) Goddard, W. A., III; Ladner, R. C. *J. Am. Chem. Soc.* **1971**, 93, 6750–6756.
(6) Bobrowicz, F. W.; Goddard, W. A., III In *Modern Theoretical Chemistry: Methods of Electronic Structure Theory*; Schaefer, H. F., III, Plenum: New York, 1977; Vol. 3, Chapter 4, pp 79–127.

0002-7863/87/1509-5580$01.50/0

Table II. Comparison of Calculated Spectroscopic Constants for the $^1A_{1g}$ and $^3A_{2u}$ States at the M-GVB-RCI Level

	$^1A_{1g}$	$^3A_{2u}$^{a}	diff
bond length (Å)	2.26	2.30	+0.04
Re–Re force constant (mdyn/Å)	4.65	4.67	+0.02
vibrational frequency (cm^{-1})	293	293	0.0
bond energy (kcal/mol)	85.0	76.5	−8.5

^{a}Optimization of eclipsed rotomer neglecting relaxation of $ReCl_4$ fragments from their ground-state structure.

neutralized by counter charges (e.g., K^+), and in calculating bond energies it is necessary to include the effects of these counter charges (the Coulomb energy for two charges at 2.24 Å is 150 kcal/mol!). In order to ameliorate this problem, fractional charges (leading to a net charge of 0 on each fragment) are placed at positions extrapolated from the crystallographic positions of the counterions. The charges are placed so as to maintain the overall symmetry of the system and to be invariant under a 45° rotation of the $ReCl_4^-$ units.[10] The rotational invariance allows for a comparison of the properties of the eclipsed and staggered geometries. The results for the Re–Re bond distance optimization are shown in Figure 3 and in Tables I and II.[11]

The bond energy for the Re–Re quadruple bond calculated at the M-GVB level is 85.0 kcal/mol, the first ab initio estimate of the energy of a quadruple metal–metal bond. Similar calculations on Mo_2 and Cr_2 lead to bond energies within 5 kcal/mol of experiment, and we believe that similar accuracy can be expected in the Re–Re quadruple bond studies, leading to D_e(Re$\overset{4}{-}$Re) = 85 ± 5 kcal/mol. A more conservative estimate of the uncertainty, perhaps, ±10 kcal/mol, would be warranted given the lack of comparable theoretical and experimental studies on other systems. Experimental values for the bond energy of the quadruple bond have been quite difficult to obtain. Early estimates have ranged as high as 370 kcal/mol.[1] Birge–Sponer extrapolations using the harmonic stretching frequency and the anharmonicity constant determined from resonance Raman measurements suggest an Re–Re bond energy of 152 ± 19 kcal/mol for $Re_2Cl_8^{2-}$ and 139 ± 24 kcal/mol for $Re_2Br_8^{2-}$.[12] Such Birge–Sponer extrapolations for multiple bonds are fraught with peril and could easily lead to errors of 50–70 kcal/mol.[13] A more reliable thermochemical study places the Re–Re bond energy for $Cs_2Re_2Br_8$ at 97 ± 12 kcal/mol,[14] this estimate depending on empirically based assumptions in order to estimate the Re–Br bond energy. Given the various experimental uncertainties, we believe that the theoretical value of 85 kcal/mol is the best current estimate of the bond energy. Early extended Hückel calculations placed the quadruple bond in $Re_2Cl_8^{2-}$ at 370 kcal/mol.[1] Recent theoretical work with the Hartree–Fock–Slater transition-state method has estimated the Re–Re triple bond energy in $Re_2Cl_4(PH_3)_4$ to be 134 kcal/mol.[15] Generally, these latter methods lead to an overestimate of the bond energy by 1 to 2 eV,[16] suggesting $D_e \approx$ 90 to 110 kcal/mol, in line with the GVB results.

Given a total bond energy of 85 kcal/mol, the question is how strong is the δ-bond? One way to establish this is by the singlet–triplet gap at the eclipsed geometry (calculated at 3100 cm^{-1} = 0.38 eV = 8.8 kcal/mol), suggesting a δ bond strength of 4.5–9.0 kcal/mol (this estimate ignores spin-coupling with the other orbitals of the bond). A second approach is to use the rotational barrier at the ground-state equilibrium bond distance. The energy difference between the eclipsed and staggered geometries involves opposing energy contributions. Rotating from eclipsed to staggered changes the overlap, i.e., the δ bond goes to zero so that bonding is lost. Simultaneously electrostatic and steric interactions between Cl's bonded to opposite Re's are relieved. With this competitive effect in the total energy, one can only obtain bounds to the pure δ contribution to the bonding. The calculations give a direct barrier of 3.0 kcal/mol,[17a] a lower bound on the strength of the δ bond. The calculated barrier for the triplet state (favoring staggered) of 3.0 kcal/mol[17b] should be an upper limit on the steric barrier, suggesting an upper limit on the δ bond of 6.0 kcal/mol. From the above analysis, a reasonable estimate of the δ bond strength is 6 ± 3 kcal/mol, which is weak compared with σ and π bonds but sufficiently large to explain the ubiquity of the eclipsed geometry for d^4–d^4 metal dimers.

There are not experimental estimates of the δ bond strength; however, from dynamic NMR studies of meso-substituted molybdenum porphyrin dimers, the activation energy for rotation about the quadruple metal–metal bond has been estimated to be 10.1 ± 0.5 kcal/mol.[18] This is larger than the value calculated for $Re_2Cl_8^{2-}$, perhaps because steric interactions (which reduce the barrier) are smaller in the porphyrin. From measured δ → δ* splittings in odd-electron complexes [e.g., $Mo_2(SO_4)_4^{3-}$ and $Tc_2Cl_8^{3-}$], Trogler and Gray have estimated the δ bond energy to be 9–10 kcal/mol.[19]

Early self-consistent-field (SCF) calculations found the ground state of the staggered conformation to be a triplet, about 60 kcal/mol lower than the singlet ground state of the eclipsed geometry. Addition of CI reduced the difference between eclipsed and staggered geometries to 4 kcal/mol, yet still favored the triplet state of the staggered conformation.[20] Other recent ab initio calculations find the ground state for the eclipsed and staggered geometries to be a singlet with essentially no barrier between the two rotomers.[21]

The M-GVB calculations lead to an Re–Re bond distance of 2.26 Å, in excellent agreement with the experimental value of 2.24 Å. This is consistent with the results on Mo_2 where M-GVB leads to an error of −0.01 Å.[7] We calculate a metal–metal stretching force constant of 4.6 mdyn/Å, and using a valence force field,[22] we obtain a metal–metal stretching frequency of 293 cm^{-1}.[23] This can be compared with the vibrational frequency for $(n\text{-}Bu_4N)_2[Re_2Cl_8]$ (determined from resonance Raman) of 275 cm^{-1}.[24]

Summarizing, our calculations (i) provide the first prediction based on ab initio studies of an eclipsed ground state for a

(10) An average metal–ion distance of 4.3 Å was maintained (determined from the X-ray diffraction data). Charges of +0.125 were placed in the same plane as defined by the four Cl's of each $ReCl_4$ unit. The charges were placed at 22.5° off of the Re–Cl vector. The validity of this approach is supported by the small effect on excitation energies and rotational barriers where use of the counterions (i) increases the $^3(\delta\rightarrow\delta^*)$ excitation energy by 10 cm^{-1} for the eclipsed conformation and less than 10 cm^{-1} for the staggered conformation and (ii) decreases the rotational barrier by 0.5 kcal/mol.

(11) The calculations lead to a slight barrier in the potential curves as the neutral $ReCl_4$ fragments are brought together. This barrier is 0.45 kcal/mol (at 4.18 Å) for GVB-RCI and 0.13 kcal/mol (at 4.92 Å) for M-GVB. This occurs because the nonplanar $ReCl_4$ fragments are kept at a fixed nonplanar geometry as the fragments are separated, leading to a small dipole moment and hence a slight repulsive interaction at large R.

(12) Trogler, W. C.; Cowman, C. D.; Gray, H. B.; Cotton, F. A. *J. Am. Chem. Soc.* **1977**, *99*, 2993–2996.

(13) Gaydon, A. G. *Dissociation Energies and Spectra of Diatomic Molecules*; Chapman and Hall: London, 1968; see Chapter 5.

(14) Morss, L. R.; Porcja, R. J.; Nicoletti, J. W.; San Filippo, J.; Jenkins, H. D. B. *J. Am. Chem. Soc.* **1980**, *102*, 1923–1927.

(15) Ziegler, T. *J. Am. Chem. Soc.* **1984**, *106*, 5901–5908.

(16) Messmer, R. P. *J. Vac. Sci. Technol. A.* **1984**, *2*, 899–904.

(17) (a) The ground-state rotational barrier calculated for $Re_2Cl_8^{2-}$ is 3.3 kcal/mol, while the ground-state rotational barrier calculated for $Re_2Cl_8^{2-}$ with counterions is 2.8 kcal/mol. (b) The triplet barrier calculated for $Re_2Cl_8^{2-}$ is 3.0 kcal/mol, while the triplet barrier calculated for $Re_2Cl_8^{2-}$ with counterions is 3.4 kcal/mol.

(18) Collman, J. P.; Woo, L. K. *Proc. Natl. Acad. Sci. U.S.A.* **1984**, *81*, 2592–2596.

(19) Trogler, W. C.; Gray, H. B. *Acc. Chem. Res.* **1978**, *11*, 232–239.

(20) Bernard, M. *J. Am. Chem. Soc.* **1978**, *100*, 2354–2362.

(21) (a) At the GVB-CI level there is less than 1 kcal/mol difference between the staggered and eclipsed forms of $Re_2Cl_8^{2-}$; see ref 4. (b) The staggered form of $Mo_2Cl_8^{4-}$ was found to be 3 kcal/mol *more* stable than the eclipsed form at the CAS-SCF level: Strömberg, A.; Pettersson, L. G. M.; Wahlgren, U. *Chem. Phys. Lett.* **1985**, *118*, 389–394.

(22) Bratton, W. K.; Cotton, F. A.; Debeau, M.; Walton, R. A. *J. Coord. Chem.* **1971**, *1*, 121–131.

(23) Details and further analysis of the force field calculations will be published later. These calculations were carried out with BIOGRAF/IV (from Biodesign, Inc.).

(24) Clark, R. J. H.; Stead, M. J. *Inorg. Chem.* **1983**, *22*, 1214–1220.

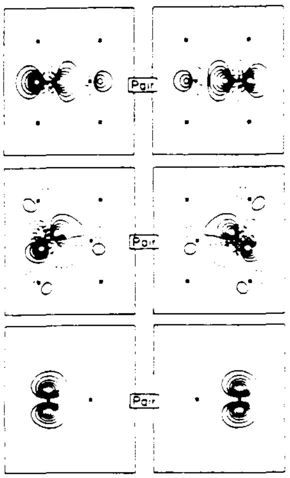

Figure 1. GVB orbitals involved in the σ, π, and δ bonds of $Re_2Cl_8^{2-}$ (reading top to bottom). Spacing between contours is 0.05 au. Negative contours are denoted by dashed lines; asterisks denote position of nuclei. The σ and π orbitals are plotted in the *xz* plane; the δ orbitals are plotted in a plane rotated 45° from the *xz* plane.

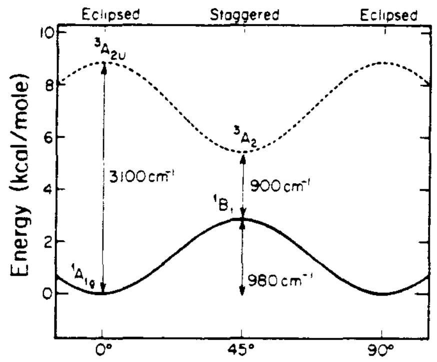

Figure 2. Energy profile for the ground state and $^3(\delta\delta^*)$ excited state of $Re_2Cl_8^{2-}$ as a function of dihedral angle. The $^3(\delta \rightarrow \delta^*)$ excitation energy was calculated for φ of 0° and 45°. The plot assumes a periodic energy function with the energies at φ of 0° and 45° as the minimum and maximum of the function for the ground state and the maximum and minimum of the function for the $^3(\delta\delta^*)$ excited state.

function is well described, but the ionic terms are forced to use doubly occupied orbitals. Because of the spatial compactness of the d orbitals, there are substantial electron correlations in such doubly occupied orbitals, leading to large errors in certain atomic electron affinities and ionization potentials. In M–GVB, this correlation error of the atom is built into the atomic Coulomb integrals, but calculations are otherwise as in normal GVB.[7] The electron correlations imbedded in M–GVB would have been included in normal GVB wave functions by suitably high-level excitations (CI) and hence with M–GVB we cannot go *beyond* GVB-level calculations (since some electron correlation effects would be double corrected). M–GVB has been successfully applied in studying the sextuple bonds of Mo_2 and Cr_2, where an accurate description of bond energies (D_e) and bond distances (R_e) was obtained.[7] Thus, for Mo_2, D_e^{calcd} = 90.9 kcal/mol, D_e^{exptl} = 97 ± 5 kcal/mol, R_e^{calcd} = 1.92 Å, R_e^{exptl} = 1.93 Å; and for Cr_2, D_e^{calcd} = 42.9 kcal/mol, D_e^{exptl} = 46 ± 7 kcal/mol, R_e^{calcd} = 1.61 Å, R_e^{exptl} = 1.68 Å. The current studies involve exactly the same approach as in these earlier studies except that we now utilize effective core

(7) Goodgame, M. M.; Goddard, W. A., III, *Phys. Rev. Lett.* **1985**, *54*, 661–664.

Table I. Comparison of Calculated and Experimental Spectroscopic Constants

	GVB-PP[a]	GVB-RCI[b]	M–GVB-RCI	exptl
bond length (Å)	2.37	2.36	2.26	2.24[c]
Re–Re force constant (mdyn/Å)	2.75	2.48	4.64	
vibrational frequency[d] (cm^{-1})	247	240	293	275[e]
bond energy (kcal/mol)	g	25.8	85.0	(97 ± 12)[f]
rotational barrier (kcal/mol)	−1.6	0.1	2.8	

[a] For a description of GVB-PP wave functions, see ref 6. [b] CI wave function similar to that described in Table Ia of Moss, B. J.; Goddard, W. A., III *J. Chem. Phys.* **1975**, *63*, 3523–3531. [c] Based on X-ray diffraction study of $K_4[Re_2Cl_8]\cdot 2H_2O$; ref 9. [d] The calculated Re–Re bond length and force constants were used with an earlier determined valence force field in the vibrational analysis; ref 22. [e] Based on solid-state resonance Raman study of $(n\text{-}Bu_4N)_2[Re_2Cl_8]$; ref 24. [f] Based on thermochemical study of $Cs_2Re_2Br_8$; ref 14. [g] Keeping a constant spin coupling, GVB-PP leads to a dissociation error of 55.5 kcal/mol.

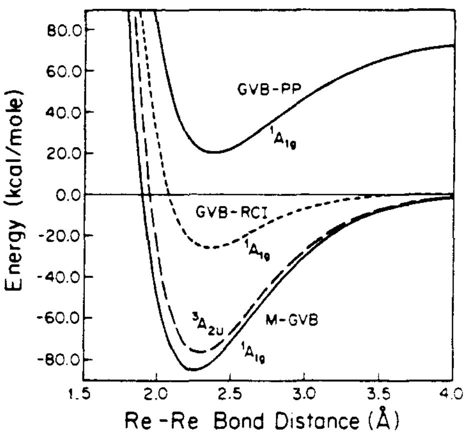

Figure 3. Calculated potential curves for $Re_2Cl_8^{2-}$.

potentials (ECP) so that only the 15 outermost electrons (5s,5p,6s,5d) of each Re are treated explicitly; however, the potentials describe the effects of core electrons including the dominant relativistic effects.[8]

The GVB orbitals of the singlet ground state ($^1A_{1g}$) are shown in Figure 1 where we see that four electrons in dσ, $d\pi_x$, $d\pi_y$, and $d\delta_{xy}$ orbitals on each Re are spin-paired to form the quadruple bond. Uncoupling the spins of the two electrons in δ orbitals leads to the lowest triplet state ($^3A_{2u}$). Rotating one $ReCl_4$ group about the bond by 45° leads (see Figure 2) to essentially identical bonding in the σ, π_x, and π_y orbitals, but the δ bond is broken with the result that the singlet and triplet states (denoted as $^1B_1$ and $^3A_2$) are nearly degenerate. Some indications of the relative strengths of these bonds are given by the overlaps in the GVB orbitals, S_σ = 0.68, S_π = 0.54, S_δ = 0.12 for the eclipsed configurations, but S_σ = 0.68, S_π = 0.53, and S_δ = 0.0 for the staggered. As the bond is stretched, the overlaps of the GVB orbitals decrease continuously to zero, leading to a smooth description of bond dissociation (molecular orbital based schemes often lead to the wrong dissociation limit, complicating predictions of bond energies).

In these calculations the geometry of each $(ReCl_4)^-$ fragment was fixed as that in the crystal,[9] and the Re–Re bond distance was optimized. An important issue here for bond energies concerns the charges. In crystals and solution, the charge of $Re_2Cl_8^{2-}$ is

(8) Hay, P. J.; Wadt, W. R. *J. Chem. Phys.* **1985**, *82*, 299–310.
(9) Cotton, F. A.; Harris, C. B. *Inorg. Chem.* **1965**, *4*, 330–333.

quadruply bonded metal dimer, (ii) predict an Re–Re quadruple bond energy of 85 ± 5 kcal/mol—the first direct estimate of the strength of this prototypical quadruple bond, and (iii) suggest that the δ bond energy is 6 ± 3 kcal/mol.

Acknowledgment. We acknowledge Dr. Siddharth Dasgupta for his contributions in the vibrational analysis. This work was partially supported by grants from the Sun Co. and from National Science Foundation (No. CHE83-18041).

Appendix 1

Table A1.1. Hydrogen Coordinates x 10^4.

Atom	x	y	z	B
H3A	−2119	180	−103	5.8
H3B	−1996	521	555	5.8
H3C	−2813	523	−303	5.8
H4A	−1871	319	−1353	4.8
H4B	−2547	673	−1669	4.8
H4C	−1595	752	−1522	4.8
H8A	−1515	2369	356	5.7
H8B	−1812	2047	−363	5.7
H8C	−2378	2131	112	5.7
H9A	−986	2147	1873	5.0
H9B	−1790	1874	1707	5.0
H9C	−864	1685	2121	5.0
H13A	2745	325	−970	8.1
H13B	2647	621	−1696	8.1
H13C	2912	792	−797	8.1
H14A	1224	39	−1778	8.3
H14B	441	339	−2060	8.3
H14C	1011	326	−2547	8.3
H18A	332	2219	−2078	5.1
H18B	1084	1936	−2034	5.1
H18C	194	1926	−2820	5.1
H19A	−883	1960	−1866	7.2
H19B	−1164	1625	−2559	7.2
H19C	−941	1503	−1637	7.2
H23A	4104	207	3565	8.0
H23B	4925	484	3896	8.0
H23C	4016	678	3652	8.0
H24A	4288	−85	2344	6.9
H24B	4411	193	1686	6.9
H24C	5165	140	2578	6.9
H28A	4675	2095	1755	7.1
H28B	4872	1791	2495	7.1
H28C	5436	1784	2001	7.1
H29A	3955	1841	224	7.6
H29B	4623	1493	348	7.6
H29C	3644	1388	21	7.6
H33A	936	88	3735	5.0
H33B	1801	332	4133	5.0
H33C	1127	372	4502	5.0
H34A	−455	459	2873	6.4
H34B	−337	780	3565	6.4
H34C	−446	925	2685	6.4
H38A	3641	1845	4263	7.0
H38B	3673	1527	4934	7.0
H38C	3637	1377	4083	7.0
H39A	2252	2193	4120	7.7
H39B	1424	1931	3908	7.7
H39C	2177	1920	4807	7.7

Atom	x	y	z	B
H5A	−2417	1285	−686	4.2
H5B	−1439	1357	−444	4.2
H6A	−1306	1133	975	3.9
H6B	−2234	1319	625	3.9
H15A	1380	1128	−2268	5.3
H15B	1628	1296	−1371	5.3
H16A	165	987	−1679	5.7
H16B	10	1116	−2581	5.7
H25A	5176	971	2871	5.3
H25B	4275	1168	2655	5.3
H26A	4004	882	1194	6.0
H26B	4985	988	1540	6.0
H35A	997	1184	4224	4.8
H35B	897	1327	3347	4.8
H36A	2330	948	3835	4.8
H36B	2400	1092	4701	4.8
H42	8254	1384	3283	5.5
H43	7720	1077	1909	6.1
H44	7081	433	1659	6.1
H45	6805	98	2738	7.3
H46	7212	436	4039	5.1
H52	8697	1716	5999	6.1
H53	8315	2421	6078	7.7
H54	7344	2746	4833	7.3
H55	6701	2400	3560	6.9
H56	7119	1694	3487	5.2
H62	6513	1072	4514	5.7
H63	5826	872	5378	7.5
H64	6648	487	6607	6.0
H65	8137	412	7117	6.0
H66	8855	689	6305	4.7
H72	9714	1659	5405	5.9
H73	11257	1468	6042	7.0
H74	11618	785	6216	6.2
H75	10631	253	5743	6.6
H76	9085	430	5053	4.5
H82	9803	2838	2336	4.6
H83	10994	2430	2387	8.4
H84	12280	2730	2494	6.4
H85	12412	3442	2612	5.8
H86	11293	3862	2722	4.5
H92	8885	3490	3639	5.2
H93	7692	3067	3471	5.3
H94	6970	2667	2254	5.1
H95	7306	2774	1107	5.2
H96	8478	3215	1239	4.5
H102	10825	3439	4138	4.8
H103	11213	3758	5507	6.1

Atom	x	y	z	B
H104	10802	4415	5560	6.9
H105	9846	4803	4381	9.0
H106	9392	4470	2984	5.8
H112	10233	4000	1325	3.8
H113	9682	4530	340	5.0
H114	8422	4880	126	4.3
H115	7631	4681	892	4.7
H116	8137	4128	1849	3.4

Table A1.2. Anisotropic Thermal Parameters x 10^4.

Atom	U_{11}	U_{22}	U_{33}	U_{12}	U_{13}	U_{23}
IR1	374(5)	410(5)	229(5)	58(4)	128(4)	−8(4)
IR2	384(5)	388(5)	236(5)	28(4)	150(4)	18(4)
C3	584(126)	472(140)	1055(173)	−10(105)	437(125)	136(124)
C4	656(130)	571(140)	435(112)	116(110)	46(96)	−26(103)
C8	698(126)	444(130)	983(164)	308(103)	319(119)	124(117)
C9	926(148)	466(129)	659(132)	−9(108)	438(116)	−139(104)
C13	1439(165)	939(199)	904(180)	346(150)	880(145)	6(154)
C14	2151(217)	687(149)	601(148)	242(150)	609(148)	134(126)
C18	628(133)	638(146)	458(131)	−137(112)	182(110)	116(112)
C19	562(119)	1413(193)	745(169)	138(125)	398(116)	555(149)
C23	693(143)	1553(214)	551(133)	−30(138)	−92(110)	118(132)
C24	604(135)	664(148)	1007(172)	332(113)	119(125)	−33(126)
C28	534(126)	896(163)	1462(182)	−139(116)	359(126)	80(140)
C29	1175(175)	1143(177)	932(165)	157(144)	772(144)	212(141)
C33	837(136)	745(129)	489(131)	−58(107)	340(110)	32(110)
C34	694(122)	1118(189)	784(146)	−72(120)	505(109)	58(135)
C38	711(124)	1161(184)	611(149)	−301(123)	118(110)	102(139)
C39	1343(169)	861(164)	590(167)	160(133)	164(138)	−45(131)

Table A1.3. More Distances and Angles.

	Distance(Å)		Distance(Å)
N1 -C2	1.47(2)	C52 -C53	1.41(3)
C2 -C3	1.51(3)	C53 -C54	1.37(3)
C2 -C4	1.52(2)	C54 -C55	1.40(3)
C2 -C5	1.53(2)	C55 -C56	1.40(3)
C5 -C6	1.49(2)	C61 -C62	1.38(3)
C6 -C7	1.53(2)	C61 -C66	1.41(2)
C7 -C8	1.53(3)	C62 -C63	1.40(3)
C7 -C9	1.56(2)	C63 -C64	1.39(3)
C7 -N2	1.48(2)	C64 -C65	1.37(3)
N3 -C12	1.50(2)	C65 -C66	1.42(3)
C12 -C13	1.46(3)	C71 -C72	1.41(3)
C12 -C14	1.55(3)	C71 -C76	1.38(2)
C12 -C15	1.54(3)	C72 -C73	1.43(3)
C15 -C16	1.48(3)	C73 -C74	1.31(3)
C16 -C17	1.51(3)	C74 -C75	1.34(3)
C17 -C18	1.50(3)	C75 -C76	1.41(3)
C17 -C19	1.50(3)	B2 -C81	1.64(3)
C17 -N4	1.47(2)	B2 -C91	1.62(3)
N5 -C22	1.51(2)	B2 -C101	1.63(3)
C22 -C23	1.56(3)	B2 -C111	1.65(2)
C22 -C24	1.51(3)	C81 -C82	1.35(2)
C22 -C25	1.50(3)	C81 -C86	1.38(2)
C25 -C26	1.55(3)	C82 -C83	1.41(3)
C26 -C27	1.48(3)	C83 -C84	1.35(3)
C27 -C28	1.55(3)	C84 -C85	1.34(3)
C27 -C29	1.54(3)	C85 -C86	1.43(3)
C27 -N6	1.48(2)	C91 -C92	1.40(2)
N7 -C32	1.48(2)	C91 -C96	1.39(2)
C32 -C33	1.51(2)	C92 -C93	1.39(3)
C32 -C34	1.47(3)	C93 -C94	1.37(3)
C32 -C35	1.51(2)	C94 -C95	1.36(3)
C35 -C36	1.50(3)	C95 -C96	1.38(3)
C36 -C37	1.53(3)	C101-C102	1.41(2)
C37 -C38	1.50(3)	C101-C106	1.36(3)
C38 -C39	2.53(3)	C102-C103	1.43(3)
C37 -C39	1.50(3)	C103-C104	1.33(3)
C37 -N8	1.50(3)	C104-C105	1.36(3)
B1 -C41	1.63(3)	C105-C106	1.47(3)
B1 -C51	1.59(3)	C111-C112	1.41(2)
B1 -C61	1.64(3)	C111-C116	1.39(2)
B1 -C71	1.65(3)	C112-C113	1.39(3)
C41 -C42	1.41(3)	C113-C114	1.34(3)
C41 -C46	1.38(3)	C114-C115	1.38(2)
C42 -C43	1.42(3)	C115-C116	1.40(2)
C43 -C44	1.34(3)	N9 -C200	1.26(5)
C44 -C45	1.39(3)	C200-C201	1.33(5)
C45 -C46	1.41(3)	N10 -C203	1.22(5)
C51 -C52	1.41(3)	C203-C204	1.25(6)
C51 -C56	1.40(3)		

Angle(°)		Angle(°)	
C1 -IR1 -C11	92.2(6)	C23 -C22 -C25	108.4(15)
C1 -IR1 -C21	175.5(7)	C24 -C22 -C25	116.3(16)
C1 -IR1 -C31	85.9(6)	C22 -C25 -C26	115.5(15)
C11 -IR1 -C21	90.1(7)	C25 -C26 -C27	116.4(16)
C11 -IR1 -C31	176.8(6)	C26 -C27 -C28	112.7(15)
C21 -IR1 -C31	91.6(7)	C26 -C27 -C29	110.6(16)
C10 -IR2 -C20	87.5(7)	C28 -C27 -C29	110.2(15)
C10 -IR2 -C30	175.4(7)	C26 -C27 -N6	108.1(15)
C10 -IR2 -C40	88.5(7)	C28 -C27 -N6	108.0(14)
C20 -IR2 -C30	92.4(7)	C29 -C27 -N6	107.0(15)
C20 -IR2 -C40	175.3(7)	C27 -N6 -C30	172.4(16)
C30 -IR2 -C40	91.3(7)	C31 -N7 -C32	173.0(16)
C1 -N1 -C2	169.5(17)	N7 -C32 -C33	107.4(13)
N1 -C2 -C3	108.9(14)	N7 -C32 -C34	108.6(14)
N1 -C2 -C4	106.6(13)	C33 -C32 -C34	111.1(14)
C3 -C2 -C4	108.6(14)	N7 -C32 -C35	107.3(13)
N1 -C2 -C5	106.4(13)	C33 -C32 -C35	112.6(14)
C3 -C2 -C5	112.4(14)	C34 -C32 -C35	109.6(14)
C4 -C2 -C5	113.8(14)	C32 -C35 -C36	117.1(15)
C2 -C5 -C6	116.8(14)	C35 -C36 -C37	117.1(15)
C5 -C6 -C7	115.4(14)	C36 -C37 -C38	111.8(16)
C6 -C7 -C8	113.4(14)	C36 -C37 -C39	110.8(16)
C6 -C7 -C9	109.9(13)	C38 -C37 -C39	115.1(17)
C8 -C7 -C9	108.4(14)	C36 -C37 -N8	106.7(15)
C6 -C7 -N2	108.9(13)	C38 -C37 -N8	105.6(15)
C8 -C7 -N2	108.5(13)	C39 -C37 -N8	106.3(15)
C9 -C7 -N2	107.6(13)	C37 -N8 -C40	172.5(18)
C7 -N2 -C10	172.5(16)	C41 -B1 -C51	112.1(14)
C11 -N3 -C12	174.5(17)	C41 -B1 -C61	110.0(14)
N3 -C12 -C13	109.0(16)	C41 -B1 -C71	105.5(14)
N3 -C12 -C14	106.7(15)	C51 -B1 -C61	105.1(14)
C13 -C12 -C14	110.2(17)	C51 -B1 -C71	113.5(14)
N3 -C12 -C15	107.2(15)	C61 -B1 -C71	110.8(14)
C13 -C12 -C15	113.8(16)	B1 -C41 -C42	121.1(15)
C14 -C12 -C15	109.7(16)	B1 -C41 -C46	124.7(15)
C12 -C15 -C16	118.0(16)	C46 -C41 -C42	113.9(16)
C15 -C16 -C17	116.2(16)	C41 -C42 -C43	122.5(17)
C16 -C17 -C18	115.1(16)	C42 -C43 -C44	120.3(18)
C16 -C17 -C19	112.5(16)	C43 -C44 -C45	119.9(19)
C18 -C17 -C19	110.6(16)	C44 -C45 -C46	118.5(19)
C16 -C17 -N4	106.4(15)	C45 -C46 -C41	124.8(17)
C18 -C17 -N4	107.1(15)	B1 -C51 -C52	119.6(15)
C19 -C17 -N4	104.3(15)	B1 -C51 -C56	126.2(15)
C17 -N4 -C20	170.2(18)	C56 -C51 -C52	113.9(16)
C21 -N5 -C22	176.6(17)	C51 -C52 -C53	125.0(18)
N5 -C22 -C23	105.1(15)	C52 -C53 -C54	117.2(20)
N5 -C22 -C24	108.6(15)	C53 -C54 -C55	121.5(20)
C23 -C22 -C24	110.4(16)	C54 -C55 -C56	118.6(19)
N5 -C22 -C25	107.5(15)	C55 -C56 -C51	123.7(17)

	Angle(°)
B1 -C61 -C62	119.1(15)
B1 -C61 -C66	125.0(15)
C66 -C61 -C62	115.9(16)
C61 -C62 -C63	124.3(18)
C62 -C63 -C64	116.5(19)
C63 -C64 -C65	122.6(19)
C64 -C65 -C66	118.3(18)
C65 -C66 -C61	122.0(16)
B1 -C71 -C72	125.4(15)
B1 -C71 -C76	118.8(15)
C76 -C71 -C72	115.8(15)
C71 -C72 -C73	120.8(17)
C72 -C73 -C74	118.3(19)
C73 -C74 -C75	125.2(20)
C74 -C75 -C76	116.8(18)
C75 -C76 -C71	123.0(17)
C81 -B2 -C91	108.8(13)
C81 -B2 -C101	108.6(13)
C81 -B2 -C111	112.0(13)
C91 -B2 -C101	110.0(13)
C91 -B2 -C111	108.1(13)
C101-B2 -C111	109.4(13)
B2 -C81 -C82	124.3(15)
B2 -C81 -C86	120.7(14)
C86 -C81 -C82	114.9(15)
C81 -C82 -C83	121.2(17)
C82 -C83 -C84	123.4(20)
C83 -C84 -C85	117.2(19)
C84 -C85 -C86	119.7(18)
C85 -C86 -C81	123.3(16)
B2 -C91 -C92	124.2(15)
B2 -C91 -C96	122.3(15)
C96 -C91 -C92	113.5(15)
C91 -C92 -C93	121.3(16)
C92 -C93 -C94	123.5(18)
C93 -C94 -C95	116.0(17)
C94 -C95 -C96	121.4(17)
C95 -C96 -C91	124.1(16)
B2 -C101-C102	119.7(15)
B2 -C101-C106	121.9(15)
C106-C101-C102	117.9(16)
C101-C102-C103	120.1(16)
C102-C103-C104	118.4(18)
C103-C104-C105	126.1(21)
C104-C105-C106	114.5(20)
C105-C106-C101	122.9(18)
B2 -C111-C112	126.4(14)
B2 -C111-C116	120.4(14)
C116-C111-C112	113.2(14)

	Angle(°)
C111-C112-C113	121.5(16)
C112-C113-C114	123.1(17)
C113-C114-C115	118.1(16)
C114-C115-C116	119.2(16)
C115-C116-C111	124.6(15)
N9 -C200-C201	172.6(37)
N10 -C203-C204	174.3(46)

Table A1.4. Structure Factors.

The columns contain, in order k, $10F_o$, $10F_c$, and $10[(F_o^2-F_c^2)/\sigma(F_o^2)]$.

-14 k 4

0	1621	1556	19
1	292	304	-1
2	335	239	11
3	707	668	9
4	734	710	5

-14 k 5

1	660	700	-9
2	766	728	9
3	1134	1070	18
4	1320	1296	7
5	357	331	3
6	486	531	-8

-14 k 6

0	472	500	-5
1	1010	1021	-3
2	1061	1046	4
3	641	680	-9
4	458	449	1
5	404	244	20
6	1452	1387	18

-14 k 7

1	1195	1226	-9
2	1746	1622	35
3	677	641	8
4	714	621	20
5	933	905	7
6	-218	117	-13

-14 k 8

0	584	609	-5
1	269	367	-12
2	720	709	2
3	728	745	-4
4	-108	30	-2
5	1524	1548	-7

-14 k 9

1	1334	1354	-5
2	855	836	5
3	581	555	5

-13 k 1

0	610	651	-9
1	697	700	0
2	833	800	8
3	243	308	-7
4	-237	140	-17
5	238	566	-56
6	964	988	-6

-13 k 2

1	1025	1098	-22
2	590	615	-5
3	244	292	-5
4	1064	975	25
5	174	122	3
6	524	508	3
7	-77	303	-21
8	881	864	5

-13 k 3

0	1467	1412	17
1	-194	28	-9
2	-167	115	-9
3	851	884	-9
4	652	709	-14
5	1351	1253	29
6	369	394	-3
7	-84	138	-5
8	595	592	0
9	538	549	-2
10	520	560	-8

-13 k 4

1	-233	130	-17
2	849	864	-4
3	1145	1075	21
4	1139	1097	12
5	778	776	0
6	861	815	12
7	942	839	30
8	307	236	8
9	973	1018	-13
10	1118	1068	14
11	245	163	6

-13 k 5

0	555	515	8
1	1538	1545	-2
2	1211	1160	15
3	851	925	-21
4	389	530	-28
5	424	412	2
6	1346	1343	0
7	947	977	-9
8	1174	1201	-8
9	285	209	7
10	619	523	19
11	1937	1870	19

-13 k 6

1	1228	1277	-15
2	1058	1066	-2
3	741	754	-3
4	868	873	-1
5	655	651	0
6	438	293	21
7	1733	1693	12
8	1281	1299	-5
9	1424	1509	-26
10	1230	1165	18
11	307	138	15

-13 k 7

0	1808	1848	-12
1	245	47	13
2	546	510	7
3	703	769	-17
4	447	483	-6
5	1324	1333	-2
6	-95	18	-2
7	309	260	5
8	1311	1366	-17
9	430	415	2
10	1096	1047	13
11	265	192	6

-13 k 8

1	1333	1332	0
2	594	608	-3
3	1107	1082	7
4	1382	1309	21
5	-288	1	-20
6	480	475	0
7	127	99	1
8	408	375	5
9	1198	1173	7
10	675	708	-7

-13 k 9

0	-257	248	-30
1	830	784	12
2	777	776	0
3	905	1023	-34
4	618	701	-20
5	763	780	-4
6	1517	1541	-7
7	803	937	-36
8	493	359	21
9	660	665	0

-13 k 10

1	943	900	12
2	1693	1693	0
3	572	596	-5
4	-276	178	-24
5	323	436	-17
6	390	348	5
7	1251	1246	1
8	593	614	-4

-13 k 11

0	1509	1533	-7
1	954	1029	-22
2	790	761	7
3	281	239	4
4	206	196	0
5	1395	1372	6

-12 k 1

1	1129	1119	2
2	465	596	-29
3	529	646	-28
4	1236	1209	8
5	135	203	-5
6	508	543	-7
7	436	464	-5
8	977	964	3
9	1489	1512	-7
10	231	268	-4
11	283	248	3
12	159	7	5

-12 k 2

0	973	979	-1
1	-72	185	-10
2	271	325	-7
3	1213	1153	18
4	332	368	-5
5	1690	1626	20
6	928	967	-11
7	285	386	-15
8	918	879	11
9	730	677	13
10	1077	1009	19
11	1031	1096	-20
12	1132	1167	-10
13	940	882	15

-12 k 3

1	62	39	0
2	1538	1677	-48
3	1080	1121	-13
4	560	619	-14
5	406	496	-18
6	773	809	-10
7	1408	1358	15
8	383	352	5
9	608	607	0
10	1412	1355	17
11	336	432	-15
12	1150	1131	5
13	588	531	11
14	397	391	0

-12 k 4

0	660	581	20
1	1666	1695	-9
2	1038	997	13
3	858	881	-7
4	335	318	2
5	357	413	-9
6	1585	1553	10
7	1418	1402	5
8	957	861	27
9	342	355	-1
10	220	34	11
11	2019	1963	16
12	514	497	3
13	501	498	0
14	408	430	-3

-12 k 5

1	1578	1586	-2
2	1034	1072	-12
3	245	140	10
4	1358	1318	13
5	537	410	25
6	421	405	3
7	1002	973	9
8	1521	1488	10
9	1968	1978	-3
10	1007	935	21
11	139	82	2
12	348	235	14
13	1333	1277	16
14	1510	1475	10
15	936	883	13

-12 k 6

0	2687	2757	-20
1	400	217	27
2	425	284	23
3	711	796	-25
4	1055	1027	8
5	1585	1634	-16
6	177	26	7
7	87	158	-4
8	1175	1161	4
9	809	755	14
10	903	882	6
11	164	64	5
12	1268	1320	-16
13	1471	1400	21
14	200	353	-18
15	575	513	12

-12 k 7

1	710	564	37
2	1075	1073	0
3	1555	1495	19
4	1898	1849	15
5	522	560	-8
6	1195	1148	14
7	628	683	-14
8	476	556	-17
9	1272	1285	-4
10	1033	954	22
11	258	347	-11
12	1349	1276	21
13	1118	1098	5
14	517	619	-21

-12 k 8

0	670	640	8
1	1117	1170	-17
2	526	535	-2
3	972	1036	-20
4	573	521	11
5	-183	34	-8
6	925	909	4
7	1522	1466	17
8	179	199	-1
9	420	376	7
10	180	166	1
11	2099	2170	-21
12	615	606	1
13	291	241	5
14	598	596	0

-12 k 9

1	1038	1058	-6
2	2048	2055	-1
3	832	847	-4
4	568	600	-7
5	392	572	-37
6	135	108	1
7	1361	1344	5
8	1281	1274	2
9	844	868	-7
10	1497	1484	3
11	637	620	3
12	1125	1035	24
13	332	362	-4

-12 k 10

0	2412	2428	-4
1	1264	1213	15
2	703	719	-4
3	326	308	2
4	422	432	-1
5	1432	1436	-1
6	573	577	0
7	1099	1154	-16
8	1715	1720	-1
9	263	300	-4
10	1111	1126	-4
11	778	878	-26

-12 k 11

1	1880	1892	-3
2	609	459	29
3	1331	1329	0
4	1632	1606	7
5	92	34	1
6	828	832	0
7	349	111	22
8	227	107	8
9	2073	2153	-23

-12 k 12

0	1592	1680	-26
1	914	919	-1
2	614	634	-4
3	966	967	0
4	724	764	-9
5	484	489	0
6	1461	1484	-6

-11 k 1

0	1814	1867	-18
1	923	841	26
2	366	490	-27
3	1369	1347	7
4	923	1006	-28
5	794	787	2
6	1320	1447	-45
7	343	450	-20
8	610	548	14
9	645	603	10
10	1072	1065	1
11	1580	1500	24
12	1421	1332	27
13	1115	997	33
14	-177	231	-19
15	-237	219	-24

-11 k 2

1	339	238	16
2	1976	1989	-4
3	1565	1531	11
4	601	599	0
5	822	819	1
6	948	983	-11
7	1455	1459	-1
8	667	698	-8
9	679	676	0
10	1874	1762	34
11	581	510	15
12	1491	1459	9
13	463	416	8
14	-205	61	-11
15	1551	1445	31
16	143	197	-4

-11 k 3

0	1284	1277	2
1	1777	1713	21
2	1401	1407	-2
3	753	692	19
4	-113	80	-5
5	1122	1057	22
6	1642	1690	-16
7	1073	1190	-42
8	1223	1241	-6
9	-99	26	-2
10	527	482	9
11	2031	1964	20
12	522	363	29
13	676	596	19
14	1107	1033	21
15	738	734	0
16	1734	1611	35
17	775	726	11

-11 k 4

1	2137	2127	3
2	1466	1418	17
3	819	853	-12
4	1556	1587	-10
5	-110	184	-13
6	653	639	3
7	630	556	19
8	1081	1142	-21
9	2080	2117	-12
10	966	992	-8
11	248	19	15
12	34	29	0
13	1362	1306	17
14	1500	1458	13
15	384	318	9
16	751	760	-2
17	1035	915	32

-11 k 5

0	3209	3123	21
1	621	564	15
2	429	329	19
3	666	647	5
4	1102	1085	5
5	1884	1852	10
6	971	939	10
7	-166	178	-16
8	1508	1608	-35
9	486	501	-3
10	1565	1578	-4
11	645	604	10
12	2017	1906	32
13	1516	1451	20
14	647	725	-19
15	59	106	-1
16	159	343	-20
17	997	959	11

-11 k 6

1	914	847	21
2	1672	1638	11
3	1660	1648	4
4	1478	1464	5
5	831	814	5
6	1017	1082	-22
7	800	814	-4
8	439	443	0
9	1606	1672	-22
10	1270	1303	-11
11	380	347	5
12	1434	1431	1
13	1075	1032	12
14	652	703	-12
15	1100	1120	-6
16	-278	193	-26
17	406	259	19

-11 k 7

0	343	176	23
1	2030	1945	27
2	1239	1190	17
3	1900	1876	7
4	403	371	6
5	-166	5	-8
6	1526	1491	12
7	784	733	15
8	555	524	7
9	232	207	2
10	306	20	23
11	2056	2021	10
12	958	869	26
13	320	352	-4
14	674	704	-7
15	-62	151	-6
16	1214	1274	-18
17	322	317	0

-11 k 8

1	1553	1533	7
2	1612	1613	0
3	354	442	-18
4	1259	1258	0
5	649	635	3
6	192	181	1
7	1448	1423	8
8	1585	1569	5
9	1440	1411	9
10	1281	1272	2
11	322	293	4
12	785	793	-2
13	943	1000	-16
14	1004	989	4
15	914	912	0
16	504	546	-8

-11 k 9

0	2373	2279	27
1	1200	1162	12
2	516	528	-2
3	172	126	3
4	860	941	-26
5	1482	1455	8
6	-172	205	-19
7	600	638	-9
8	1812	1818	-1
9	298	248	6
10	1507	1470	11
11	739	687	12
12	1263	1303	-12
13	1136	1194	-17
14	688	744	-13
15	327	379	-7

-11 k 10

1	1676	1632	14
2	1208	1152	18
3	1314	1270	14
4	1721	1674	14
5	205	143	5
6	754	795	-11
7	377	276	14
8	566	483	17
9	1972	2009	-11
10	612	561	11
11	-78	41	-1
12	1251	1231	5
13	1464	1498	-10
14	903	914	-2

-11 k 11

0	1473	1435	11
1	1460	1451	3
2	667	683	-4
3	1791	1808	-5
4	839	945	-30
5	397	393	0
6	1181	1189	-2
7	813	844	-8
8	366	371	0
9	454	572	-23
10	475	494	-3
11	2096	2128	-9
12	1114	1166	-15

-11 k 12

1	510	427	15
2	2129	2120	2
3	666	667	0
4	198	206	0
5	645	646	0
6	294	304	-1
7	1108	1057	14
8	1340	1333	1
9	404	98	29
10	1651	1628	6

-11 k 13

0	1272	1290	-5
1	1244	1233	3
2	418	416	0
3	313	374	-8
4	-226	136	-15
5	914	909	1
6	-256	215	-23

-10 k 1

1	529	378	36
2	1967	1930	12
3	1642	1682	-14
4	400	405	0

5	470	518	-12
6	219	231	-1
7	1423	1415	2
8	889	942	-18
9	358	363	0
10	1668	1679	-3
11	877	933	-18
12	1519	1590	-24
13	209	185	2
14	850	904	-16
15	1683	1563	36
16	-232	18	-13
17	495	440	10
18	288	140	13

-10 k 2

0	1534	1489	16
1	1956	1874	27
2	1055	1016	14
3	531	629	-30
4	141	282	-19
5	996	1086	-34
6	1169	1179	-3
7	1162	1153	3
8	1221	1283	-23
9	242	219	3
10	564	640	-21
11	1544	1550	-2
12	268	326	-8
13	713	796	-24
14	1385	1300	26
15	422	468	-8
16	929	850	24
17	835	818	4
18	624	460	32
19	1279	1180	28

-10 k 3

1	2609	2551	17
2	912	868	15
3	1067	962	38
4	2167	2215	-16
5	481	466	3
6	336	384	-10
7	265	254	1
8	1376	1388	-4
9	2037	2042	-1
10	709	763	-17
11	-103	150	-9
12	222	197	2
13	1365	1372	-2
14	1292	1274	5
15	-128	152	-9
16	551	538	2
17	918	840	22
18	659	615	10
19	961	841	31

-10 k 4

0	2940	2996	-15
1	689	508	53
2	702	653	16
3	1514	1415	35
4	1315	1351	-13
5	1140	1118	8
6	1844	1835	3
7	190	64	9
8	1419	1537	-45
9	639	488	39
10	2028	2044	-5
11	875	900	-8
12	1706	1822	-40
13	771	858	-27
14	-39	267	-18
15	-155	5	-6
16	644	652	-1
17	576	532	9
18	1698	1699	0
19	741	580	35

-10 k 5

1	961	775	63
2	1959	1920	13
3	2147	1984	52
4	980	1029	-18
5	776	710	23
6	926	964	-13
7	1179	1245	-25
8	763	810	-15
9	1096	1025	24
10	1739	1826	-30
11	533	554	-5
12	1558	1618	-20
13	729	679	13
14	216	166	4
15	1325	1314	3
16	121	134	0
17	74	79	0
18	512	539	-5
19	622	574	10

-10 k 6

0	579	586	-2
1	1922	1896	9
2	1226	1160	24
3	1124	1142	-7
4	490	448	10
5	-218	34	-16
6	1875	1864	3
7	1420	1454	-12
8	707	763	-18
9	469	469	0
10	571	505	16
11	2438	2623	-57
12	276	210	8
13	-222	358	-46
14	1179	1087	28
15	436	407	5
16	1088	1102	-4
17	424	387	6
18	-212	84	-11
19	1402	1333	20

-10 k 7

1	2019	2041	-7
2	1843	1867	-8
3	135	11	5
4	614	605	2
5	573	634	-18
6	46	90	-1
7	1275	1255	7
8	1560	1471	30
9	2287	2174	34
10	1656	1543	37
11	-69	115	-5
12	799	787	4
13	1045	1112	-21
14	1307	1213	28
15	828	919	-26
16	618	657	-9
17	1309	1311	0
18	274	88	14
19	542	552	-1

-10 k 8

0	3080	3057	6
1	574	470	27
2	393	416	-5
3	657	641	4
4	647	685	-11
5	1303	1320	-6
6	192	148	4
7	429	375	11
8	1982	1929	17
9	520	408	24
10	1679	1677	0
11	159	166	0
12	1350	1328	7
13	1275	1257	5
14	1067	1095	-8
15	533	515	3
16	385	376	1
17	1066	1038	7
18	1360	1309	14

-10 k 9

1	1647	1614	11
2	1206	1166	13
3	1265	1249	5
4	1274	1298	-8
5	309	275	5
6	832	809	7
7	228	305	-11
8	312	114	22
9	2053	2004	15
10	1196	1220	-8
11	488	386	18
12	1318	1331	-4
13	1423	1384	11
14	534	548	-3
15	651	742	-22
16	83	62	0
17	440	413	4

-10 k 10

0	596	701	-30
1	1604	1668	-22
2	898	891	2
3	1689	1730	-13
4	713	755	-13
5	378	331	8
6	1330	1293	12
7	1391	1411	-6
8	276	159	12
9	365	386	-3
10	764	642	30
11	2437	2451	-3
12	1229	1158	20
13	422	418	0
14	356	366	-1
15	333	366	-4
16	824	835	-2

-10 k 11

1	900	852	14
2	1719	1736	-5
3	670	571	24
4	173	257	-9
5	157	298	-15
6	489	560	-15
7	1218	1166	15
8	1103	1141	-11
9	833	839	-1
10	1796	1811	-4
11	377	159	23
12	1340	1347	-2
13	303	393	-12
14	657	716	-13

-10 k 12

0	1875	1880	-1
1	774	864	-25
2	645	734	-22
3	-202	69	-11
4	427	433	-1
5	1052	1037	4
6	289	336	-6
7	806	811	-1
8	1547	1526	6
9	-96	94	-4
10	1172	1231	-17
11	1162	1139	6
12	1019	915	26

-10 k 13

1	1394	1459	-19
2	212	275	-6
3	952	1007	-15
4	885	894	-2
5	245	191	4
6	358	401	-6
7	-204	78	-10
8	403	367	5
9	1942	1939	0

-10 k 14

0	1451	1512	-18
1	788	806	-4
2	-262	200	-23
3	927	987	-16

-9 k 1

0	739	637	36
1	1272	1268	1
2	715	677	13
3	365	404	-9
4	-173	131	-18
5	928	908	7
6	471	442	7
7	1253	1316	-25
8	1076	1140	-24
9	-69	106	-5
10	1126	1107	6
11	1700	1807	-39
12	393	461	-15
13	204	316	-16
14	779	848	-22
15	-173	254	-24
16	803	782	6
17	709	711	0
18	808	708	25
19	1026	941	23
20	183	150	2

-9 k 2

1	1825	1793	11
2	271	301	-6
3	541	640	-35
4	1321	1345	-9
5	-176	160	-22
6	925	944	-7
7	725	721	1
8	922	924	0
9	2557	2681	-38
10	-78	155	-10
11	-226	1	-17
12	450	477	-6
13	1575	1740	-61
14	1063	1165	-36
15	-259	128	-23
16	647	627	5
17	739	694	11
18	1021	967	16
19	816	728	22
20	425	331	14
21	1386	1269	33

-9 k 3

0	3219	3157	16
1	1019	1046	-11
2	450	417	9
3	1982	2018	-12
4	1532	1576	-17
5	1054	1044	4
6	1169	1247	-31
7	1177	1136	16
8	1341	1444	-41
9	724	764	-14
10	1760	1733	9
11	1675	1709	-12
12	1858	1853	1
13	654	646	2
14	-190	160	-18
15	365	401	-7
16	510	575	-15
17	244	130	10
18	1817	1746	21
19	1415	1351	19
20	351	298	7
21	1154	1068	24

-9 k 4

1	457	277	42
2	2052	2028	8
3	1512	1477	13
4	1143	1068	29
5	1054	994	23
6	1148	1156	-3
7	1109	1062	17
8	1187	1215	-11
9	829	818	3
10	2522	2708	-59
11	692	679	4
12	2625	2638	-3
13	685	707	-6
14	566	706	-41
15	1535	1582	-16
16	-107	200	-13
17	-71	86	-3
18	696	543	34
19	810	764	12
20	2245	2067	49
21	759	687	17

-9 k 5

0	957	879	29
1	1681	1675	2
2	296	205	15
3	1272	1332	-24
4	257	251	1
5	295	330	-7
6	901	991	-36
7	1986	1990	-1
8	935	939	-1
9	429	319	23
10	344	309	6
11	2668	2760	-27
12	386	287	18
13	266	282	-2
14	695	762	-20
15	-246	247	-34
16	1124	1270	-50
17	731	738	-1
18	406	430	-4
19	1503	1444	17
20	360	212	17
21	1191	1067	34

-9 k 6

1	2334	2356	-8
2	703	712	-5
3	410	448	-14
4	927	917	5
5	1160	1173	-6
6	57	157	-10
7	876	885	-4
8	1046	1008	19
9	2067	2055	5
10	736	726	4
11	131	72	3
12	188	313	-17
13	1215	1382	-62
14	1330	1407	-27
15	860	988	-41
16	467	208	38
17	1096	1155	-18
18	349	420	-11
19	782	817	-9
20	756	608	33
21	1580	1559	6

-9 k 7

0	3213	3201	3
1	257	129	17
2	319	339	-4
3	1212	1207	1
4	871	886	-5
5	1846	1799	16
6	417	372	10
7	-92	78	-5
8	1555	1615	-22
9	118	256	-16
10	1745	1696	16
11	631	582	13
12	1727	1734	-2
13	1078	1069	3
14	627	632	-1
15	188	258	-8
16	89	213	-9
17	645	621	5
18	1561	1484	23
19	349	396	-7
20	456	475	-3

-9 k 8

1	1191	1148	16
2	1925	1848	26
3	1771	1713	20
4	1064	1119	-21
5	-205	178	-26
6	1466	1374	32
7	883	854	9
8	146	145	0
9	2074	2052	7
10	1812	1711	33
11	455	426	6
12	1636	1602	11
13	1609	1558	16
14	92	228	-11
15	726	696	7
16	-332	134	-32
17	551	626	-17
18	775	756	4
19	945	900	11

-9 k 9

0	646	580	19
1	1810	1837	-9
2	813	766	16
3	1160	1243	-31
4	410	455	-10
5	-198	61	-13
6	962	1027	-23
7	1985	2007	-7
8	286	189	12
9	322	378	-10
10	260	6	18
11	2553	2517	10
12	597	525	17
13	409	493	-16
14	327	363	-5
15	-212	39	-11
16	982	1025	-12
17	109	286	-15
18	342	226	13

-9 k 10

1	1761	1718	14
2	2476	2440	10
3	333	255	12
4	52	379	-41
5	684	698	-4
6	337	311	4
7	1138	1144	-2
8	1354	1433	-27
9	1336	1310	8
10	2166	2148	5
11	464	296	27
12	1169	1248	-25
13	780	792	-3
14	1238	1200	11
15	767	732	8
16	805	859	-14
17	929	875	14

-9 k 11

0	3232	3230	0
1	1261	1153	35
2	470	442	6
3	-198	24	-11
4	727	733	-1
5	1187	1144	13
6	-221	51	-14
7	698	716	-5
8	2033	1979	16
9	379	316	9
10	1746	1768	-6
11	823	793	8
12	1069	1116	-14
13	986	977	2
14	1206	1202	0
15	494	480	2

-9 k 12

1	1899	1890	2
2	412	442	-5
3	1214	1236	-6
4	723	728	-1
5	-140	116	-8
6	672	681	-2
7	302	287	1
8	70	136	-3
9	2344	2362	-5
10	607	587	4
11	446	418	4
12	583	546	7
13	1434	1411	6

-9 k 13

0	1852	1939	-27
1	1021	1104	-25
2	217	253	-3
3	1085	1126	-12
4	896	876	6
5	-392	116	-41
6	844	836	1
7	837	856	-5
8	650	641	2
9	146	267	-10
10	949	946	0
11	1784	1774	2

-9 k 14

1	369	346	3
2	2169	2253	-24
3	382	518	-23
4	193	197	0
5	30	302	-18
6	51	290	-16

-8 k 1

1	1911	1854	20
2	254	255	0
3	723	787	-26
4	1417	1508	-38
5	388	431	-12
6	775	777	0
7	368	405	-9
8	961	975	-5
9	2571	2566	1
10	583	641	-19
11	235	332	-18
12	369	438	-16
13	1685	1846	-60
14	1022	1095	-27
15	-162	345	-44
16	162	340	-25
17	993	1128	-47
18	947	880	19
19	1103	936	47
20	-61	121	-4
21	1476	1337	40
22	643	586	12

-8 k 2

0	1777	1780	0
1	1429	1436	-2
2	549	453	30
3	754	707	18
4	368	507	-44
5	221	62	17
6	1704	1846	-57
7	934	941	-2
8	986	989	-1
9	985	952	12
10	1798	1886	-33
11	1524	1476	18
12	1717	1781	-24
13	806	837	-11
14	-292	32	-29
15	-326	1	-35
16	866	964	-34
17	546	575	-7
18	1354	1262	28
19	1458	1411	14
20	175	54	6
21	1015	815	52
22	1315	1239	22

-8 k 3

1	406	120	53
2	4260	4202	12
3	1521	1455	26
4	172	255	-13
5	1008	1036	-12
6	653	657	-1
7	1238	1297	-25
8	1261	1314	-21
9	806	867	-25
10	2493	2637	-46
11	885	911	-9
12	2083	2153	-24
13	511	560	-14
14	832	959	-46

15	1187	1302	-43
16	533	701	-49
17	647	669	-6
18	653	748	-26
19	907	679	59
20	2477	2369	29
21	685	506	38
22	117	244	-10

-8 k 4

0	2443	2398	14
1	1852	1715	50
2	1460	1396	26
3	1576	1535	16
4	189	322	-26
5	1606	1534	28
6	958	990	-13
7	1163	1204	-17
8	1944	1930	4
9	381	318	14
10	824	867	-16
11	2276	2423	-50
12	221	310	-15
13	740	716	8
14	1005	1058	-19
15	615	701	-26
16	901	960	-20
17	970	1020	-17
18	857	814	12
19	1661	1618	13
20	345	226	14
21	1077	989	25
22	1195	1093	28

-8 k 5

1	2593	2492	31
2	1713	1645	26
3	317	240	15
4	1243	1237	2
5	-161	152	-19
6	546	545	0
7	1710	1734	-9
8	564	531	10
9	2741	2865	-37
10	527	587	-19
11	331	119	29
12	-271	18	-26
13	1841	1958	-41
14	1258	1320	-22
15	678	834	-56
16	722	806	-26
17	1055	1176	-42
18	342	326	2
19	904	818	23
20	1037	1002	10
21	1558	1513	13
22	672	615	12

-8 k 6

0	3813	3704	30
1	643	641	1
2	198	52	20
3	925	931	-3
4	1098	1086	6
5	1720	1713	3
6	851	820	16
7	150	51	10
8	1800	1779	9
9	176	182	-1
10	1824	1899	-35
11	858	824	16
12	1342	1391	-24
13	1088	1160	-36
14	611	664	-22
15	298	360	-15
16	-271	38	-31
17	540	560	-6
18	1825	1716	33
19	718	705	3
20	509	383	22
21	672	578	20
22	1778	1820	-12

-8 k 7

1	1274	1252	8
2	2634	2512	36
3	1123	1101	8
4	1731	1672	21
5	22	155	-8
6	1188	1149	15
7	310	285	5
8	1219	1191	10
9	1550	1456	33
10	2314	2223	28
11	196	93	9
12	2147	2120	8
13	1332	1296	12
14	37	185	-9
15	842	796	15
16	-249	49	-18
17	146	241	-9
18	802	864	-17
19	947	857	24
20	2001	1996	1
21	838	784	13

-8 k 8

0	275	45	25
1	2677	2661	4
2	985	943	16
3	1399	1382	6
4	-143	101	-11
5	596	481	33
6	1403	1369	13
7	1993	2011	-6
8	489	481	2
9	606	623	-5
10	144	71	4
11	3135	3086	12
12	586	475	27
13	183	150	3
14	611	661	-14
15	250	298	-6
16	1090	1102	-3
17	762	721	10
18	269	1	16
19	1807	1732	22
20	361	81	24

-8 k 9

1	1859	1925	-23
2	2766	2723	12
3	-137	126	-12
4	618	621	-1
5	669	583	25
6	357	380	-5
7	935	967	-11
8	1450	1451	0
9	2046	2012	10
10	1749	1720	9
11	427	511	-19
12	1375	1360	4
13	1342	1333	3
14	1169	1137	10
15	959	972	-3
16	547	612	-15
17	906	900	1
18	161	53	5
19	-110	237	-14

-8 k 10

0	2980	3062	-22
1	598	573	7
2	320	315	0
3	304	281	3
4	1168	1220	-19
5	1178	1127	17
6	676	700	-7
7	445	425	4
8	1944	2005	-20
9	346	258	13
10	1921	1882	12
11	597	564	8
12	1670	1681	-3
13	648	642	1
14	739	681	14
15	195	408	-29
16	266	368	-13
17	-159	225	-16
18	1617	1562	15

-8 k 11

1	2453	2359	27
2	1471	1411	20
3	1678	1674	1
4	1232	1243	-3
5	-304	39	-28
6	566	571	-1
7	-297	3	-26
8	137	81	3
9	2513	2474	11
10	1055	1042	3
11	447	391	9
12	974	939	9
13	1731	1729	0
14	176	283	-10
15	399	571	-33
16	96	35	1
17	653	659	-1

-8 k 12

0	1191	1188	1
1	1639	1701	-21
2	692	599	24
3	1358	1355	0
4	447	544	-22
5	292	429	-24
6	1164	1120	13
7	879	885	-1
8	445	441	0
9	277	374	-14
10	749	764	-3
11	2180	2178	0
12	960	995	-9
13	316	229	9
14	-173	28	-6

-8 k 13

1	405	384	3
2	2317	2368	-14
3	95	186	-5
4	248	330	-10
5	-228	95	-14
6	441	537	-18
7	632	698	-15
8	1698	1644	16
9	400	315	11
10	1834	1856	-6
11	236	18	11
12	1269	1231	10

-8 k 14

0	2087	2051	10
1	1310	1371	-18
2	468	486	-3
3	429	537	-20
4	260	446	-26
5	793	817	-6
6	230	147	6
7	941	1049	-33
8	1407	1421	-4

-7 k 1

0	3630	3549	20
1	1723	1680	17
2	877	833	18
3	2066	2095	-10
4	1530	1586	-23
5	1462	1473	-4
6	1290	1350	-26
7	1940	2090	-58
8	872	928	-23
9	317	367	-12
10	593	608	-5
11	2946	2980	-9
12	1927	1958	-11
13	1004	1080	-30
14	-214	109	-20
15	152	219	-7
16	1065	1232	-64
17	109	175	-5
18	1154	1271	-43
19	1427	1532	-36
20	351	193	19
21	1280	1110	50
22	1481	1409	21
23	505	379	21

-7 k 2

1	533	473	21
2	4712	4633	15
3	1351	1371	-8
4	536	566	-11
5	343	499	-50
6	130	91	3
7	1462	1487	-10
8	1556	1596	-16
9	221	99	15
10	2491	2587	-31
11	518	507	3
12	1697	1830	-52
13	163	153	1
14	1111	1157	-18
15	1233	1300	-26
16	664	695	-9
17	206	339	-21
18	454	568	-29
19	184	123	4
20	2575	2374	54
21	210	208	0
22	-301	18	-22
23	549	487	12

-7 k 3

0	2704	2614	28
1	3245	3185	16
2	989	939	22
3	861	880	-8
4	376	461	-27
5	1296	1298	-1
6	-147	7	-9
7	1710	1765	-22
8	2009	2049	-14
9	210	111	12
10	1308	1394	-36
11	2520	2534	-4
12	689	789	-38
13	931	972	-16

14	1057	1075	-7
15	558	677	-37
16	278	439	-34
17	998	1136	-51
18	1115	1164	-17
19	1324	1461	-49
20	12	30	0
21	1058	892	46
22	1516	1384	39
23	1664	1568	28

-7 k 4

1	3336	3188	39
2	1025	1053	-12
3	1642	1636	2
4	2429	2361	22
5	-207	265	-49
6	264	316	-11
7	376	420	-12
8	1501	1490	4
9	3523	3584	-15
10	1139	1232	-39
11	500	372	34
12	218	34	16
13	1969	2059	-32
14	776	935	-68
15	-284	69	-29
16	583	672	-27
17	1106	1151	-16
18	470	544	-18
19	920	936	-5
20	684	661	6
21	1775	1575	58
22	857	786	18
23	1191	1118	20

-7 k 5

0	3085	2896	52
1	1339	1239	42
2	338	65	42
3	2035	2052	-6
4	1321	1325	-1
5	863	798	26
6	956	966	-4
7	1157	1222	-28
8	1442	1397	17
9	936	964	-11
10	2047	2082	-12
11	1481	1533	-20
12	1182	1240	-23
13	1378	1429	-20
14	601	702	-34
15	502	578	-21
16	-312	147	-38
17	466	502	-8
18	1404	1439	-12
19	1061	1164	-34
20	408	175	30
21	1151	1081	20
22	1516	1359	45
23	224	223	0

-7 k 6

1	848	806	23
2	2922	2811	38
3	1593	1603	-4
4	1033	1133	-61
5	720	767	-26
6	1333	1331	1
7	1086	1039	25
8	779	776	1
9	1701	1663	18
10	2573	2574	0
11	263	127	25
12	1879	1961	-38
13	920	992	-37
14	271	352	-21
15	856	845	5
16	58	220	-18
17	-167	225	-32
18	605	721	-46
19	715	665	12
20	2165	2065	28
21	918	895	6
22	-120	38	-3
23	142	44	3

-7 k 7

0	475	497	-7
1	2296	2130	54
2	968	920	19
3	1651	1667	-6
4	239	315	-16
5	1065	996	27
6	1176	1140	14
7	1954	1949	1
8	676	651	8
9	132	349	-38
10	745	732	5
11	3089	3023	29
12	-42	1	0
13	-166	193	-21
14	473	564	-24
15	64	297	-25
16	936	936	0
17	747	742	1
18	283	104	16
19	2060	1930	38
20	260	140	10
21	1389	1469	-25
22	353	253	12

-7 k 8

1	2284	2271	4
2	1722	1727	-2
3	1213	1176	14
4	-154	30	-9
5	294	360	-15
6	97	163	-6
7	770	774	-1
8	1246	1222	9
9	2158	2145	4
10	1578	1576	0
11	325	263	10
12	950	960	-3
13	1420	1361	20
14	1236	1262	-9
15	439	439	0
16	488	456	7
17	1237	1264	-8
18	-171	70	-8
19	628	618	2
20	944	987	-12
21	1558	1596	-11

-7 k 9

0	3712	3825	-27
1	206	206	0
2	223	111	13
3	383	419	-9
4	1280	1278	0
5	1109	1193	-33
6	553	476	21
7	604	603	0
8	2170	2209	-12
9	353	291	11
10	2124	2072	16
11	402	167	35
12	2009	1990	6
13	780	776	1
14	878	871	2
15	365	467	-20
16	68	85	0
17	594	546	10
18	2216	2168	13
19	287	9	17
20	365	118	23

-7 k 10

1	2109	2107	0
2	1640	1630	3
3	1058	1074	-5
4	1518	1436	28
5	-197	123	-18
6	693	644	15
7	-236	23	-18
8	571	526	11
9	2142	2220	-25
10	1678	1555	40
11	450	384	13
12	1859	1861	0
13	1729	1674	17
14	-112	94	-5
15	682	721	-10
16	-159	230	-18
17	589	640	-11
18	866	783	20
19	892	852	10

-7 k 11

0	661	598	17
1	2073	2142	-22
2	249	166	9
3	1601	1525	25
4	502	556	-14
5	-275	198	-36
6	517	549	-8
7	1878	1830	15
8	-139	2	-5
9	503	421	17
10	870	801	21
11	2750	2714	9
12	491	445	8
13	423	474	-9
14	-171	70	-8
15	-184	108	-10
16	89	208	-7
17	185	309	-12

-7 k 12

1	1199	1070	41
2	2353	2305	14
3	189	302	-14
4	-192	282	-32
5	506	467	8
6	491	600	-27
7	930	875	18
8	1343	1311	10
9	1464	1384	24
10	2130	2076	15
11	155	191	-2
12	1495	1441	16
13	861	891	-8
14	1138	1117	6
15	931	863	17

-7 k 13

0	2531	2569	-10
1	812	858	-12
2	490	637	-34
3	-280	133	-24
4	535	611	-17
5	782	763	5
6	132	168	-2
7	1023	941	22
8	1761	1743	5
9	260	49	13
10	1872	1853	5
11	1270	1257	3
12	1073	1054	5

-7 k 14

1	1771	1898	-39
2	823	793	7
3	853	960	-33
4	833	741	22
5	92	134	-2
6	472	482	-1
7	499	517	-3
8	306	123	15
9	1153	2302	-12

-6 k 1

1	1203	1064	62
2	2286	2317	-11
3	194	122	11
4	1231	1176	25
5	337	371	-10
6	938	991	-25
7	793	736	24
8	2004	2136	-51
9	805	827	-9
10	1984	2045	-23
11	176	15	12
12	1693	1794	-40
13	624	684	-23
14	747	794	-17
15	540	552	-3
16	397	573	-50
17	443	658	-65
18	316	268	7
19	181	175	0
20	2338	2412	-22
21	484	508	-5
22	319	229	11
23	835	779	14
24	1040	925	33

-6 k 2

0	3634	3477	39
1	2805	2677	39
2	355	107	52
3	560	522	15
4	1485	1487	-1
5	1757	1798	-17
6	412	399	4
7	3120	3250	-37
8	2087	2125	-14
9	218	157	9
10	1742	1749	-2
11	2865	3016	-46
12	1700	1831	-53
13	856	848	3
14	945	917	10
15	169	390	-43
16	305	431	-28
17	1097	1227	-51
18	1612	1607	1
19	1117	1283	-63
20	268	313	-6
21	666	589	19
22	1731	1658	22
23	1533	1501	9
24	229	195	3

-6 k 3

1	3111	2945	47
2	-162	25	-14

3	1582	1528	23
4	1786	1684	41
5	-130	155	-20
6	1009	1054	-21
7	576	554	8
8	458	449	2
9	3445	3632	-50
10	448	523	-25
11	669	529	49
12	750	852	-42
13	1975	2098	-45
14	491	583	-30
15	556	614	-18
16	403	593	-56
17	1204	1375	-67
18	718	814	-33
19	1418	1504	-31
20	-286	17	-23
21	1996	1941	16
22	681	620	14
23	1129	1047	23
24	-261	159	-21

-6 k 4

0	4421	4141	58
1	1615	1525	38
2	424	260	46
3	1796	1666	52
4	1349	1282	29
5	1508	1485	10
6	-185	34	-16
7	1631	1695	-27
8	2204	2163	14
9	906	926	-8
10	1635	1756	-50
11	2497	2512	-5
12	2066	2181	-41
13	629	621	2
14	633	717	-30
15	-274	18	-28
16	-229	28	-18
17	-208	13	-14
18	1394	1506	-41
19	1152	1235	-30
20	316	361	-7
21	1427	1234	58
22	1622	1516	32
23	624	646	-5
24	115	103	0

-6 k 5

1	967	870	43
2	2705	2594	34
3	1052	1013	17
4	120	162	-5
5	885	910	-11
6	1155	1157	0
7	723	688	13
8	1258	1286	-12
9	1284	1266	7
10	2787	2876	-27
11	868	797	26
12	2268	2460	-67
13	460	464	-1
14	-198	193	-28
15	806	887	-30
16	73	438	-58
17	-298	76	-30
18	787	888	-33
19	510	510	0
20	2283	2502	-69
21	735	619	28
22	207	106	7
23	-183	7	-7
24	962	981	-5

-6 k 6

0	1345	1249	54
1	2206	2171	15
2	822	759	37
3	2267	2244	10
4	864	866	-1
5	324	232	30
6	-117	240	-43
7	1111	1138	-16
8	1174	1234	-34
9	582	528	25
10	953	935	9
11	3521	3564	-12
12	581	543	17
13	251	283	-8
14	716	833	-60
15	791	883	-47
16	781	810	-13
17	602	670	-27
18	631	730	-41
19	1688	1690	-1
20	448	350	17
21	1184	1169	4
22	1020	840	47
23	1073	992	22
24	438	434	0

-6 k 7

1	3145	3082	17
2	1477	1409	27
3	1265	1203	26
4	1403	1269	53
5	105	189	-10
6	-184	172	-27
7	1236	1227	3
8	1704	1602	37
9	3046	2976	19
10	1006	970	13
11	516	422	25
12	497	533	-10
13	1991	1901	29
14	1190	1248	-22
15	-194	180	-22
16	-94	376	-45
17	1062	1091	-10
18	121	64	2
19	1218	1229	-3
20	970	883	24
21	1691	1555	40
22	535	519	3
23	1469	1408	17

-6 k 8

0	3394	3373	5
1	176	167	1
2	223	291	-13
3	735	823	-36
4	1382	1349	13
5	1065	1044	8
6	1133	1087	18
7	186	118	7
8	2217	2197	6
9	228	52	17
10	1785	1842	-21
11	675	647	9
12	1901	1882	6
13	778	754	7
14	810	790	6
15	-247	8	-19
16	-289	78	-27
17	770	659	30
18	1939	1813	37
19	450	346	17
20	659	661	0
21	271	1	15
22	2298	2162	36

-6 k 9

1	1115	1144	-11
2	1662	1708	-17
3	1378	1349	11
4	180	29	11
5	202	317	-21
6	1074	1072	0
7	447	490	-12
8	1073	1074	0
9	2087	2051	11
10	1772	1772	0
11	-165	103	-12
12	1735	1703	10
13	1533	1488	15
14	79	221	-12
15	162	337	-23
16	321	414	-17
17	691	769	-21
18	413	395	3
19	686	505	38
20	1983	1950	9
21	1292	1242	14

-6 k 10

0	356	274	16
1	2173	2183	-3
2	552	515	10
3	2030	2041	-3
4	145	248	-13
5	550	564	-3
6	867	825	14
7	2618	2569	14
8	234	209	3
9	516	525	-2
10	415	317	18
11	3541	3450	21
12	319	204	15
13	319	276	6
14	-234	226	-29
15	-180	191	-17
16	642	651	-2
17	707	784	-20
18	407	499	-16
19	1757	1725	9

-6 k 11

1	1979	1904	24
2	2562	2501	17
3	-247	21	-19
4	-104	114	-7
5	496	480	4
6	773	785	-3
7	1332	1244	29
8	888	900	-3
9	1946	1897	15
10	2200	2178	6
11	587	481	24
12	1153	1204	-16
13	1045	1039	1
14	679	659	5
15	963	1006	-12
16	674	712	-9
17	1349	1303	13
18	264	252	1

-6 k 12

0	3928	3833	20
1	519	439	17
2	748	740	2
3	-35	6	0
4	1159	1143	5
5	179	210	-3
6	370	288	13
7	739	733	1
8	2440	2348	26
9	472	302	28
10	2332	2200	36
11	873	717	39
12	1554	1486	20
13	308	230	8
14	1369	1349	5
15	-381	112	-36
16	751	659	20

-6 k 13

1	1802	1920	-37
2	410	502	-18
3	1238	1252	-4
4	-45	222	-12
5	-368	17	-35
6	694	767	-19
7	85	92	0
8	749	652	23
9	2492	2461	8
10	917	856	15
11	438	444	0
12	977	936	11
13	1828	1841	-3

-6 k 14

0	1545	1550	-1
1	1769	1739	8
2	95	29	1
3	1822	1796	7
4	262	442	-26
5	-52	200	-9
6	121	362	-24
7	455	654	-41
8	797	796	0
9	310	394	-11

-5 k 1

0	4371	4312	13
1	1393	1327	31
2	452	345	39
3	1126	1148	-10
4	894	936	-21
5	1425	1514	-43
6	-44	275	-41
7	781	881	-50
8	3163	3347	-54
9	240	384	-38
10	2121	2172	-19
11	1557	1512	18
12	1587	1708	-51
13	661	671	-4
14	1144	1290	-64
15	241	350	-23
16	698	750	-20
17	907	994	-34
18	1659	1756	-35
19	799	821	-8
20	220	332	-17
21	838	732	31
22	2037	1923	34
23	1168	1090	23
24	230	425	-28
25	375	405	-4

-5 k 2

1	1616	1504	49
2	259	319	-18
3	746	792	-24
4	1090	1031	29
5	386	446	-22
6	242	312	-18

7	468	495	-10
8	172	168	0
9	4018	4133	-27
10	1491	1583	-40
11	296	263	7
12	668	681	-5
13	2843	3063	-68
14	565	555	3
15	745	820	-30
16	109	87	1
17	1102	1121	-7
18	563	531	9
19	1574	1619	-16
20	686	683	0
21	1935	2046	-37
22	346	158	22
23	1145	1055	26
24	-292	162	-27
25	508	650	-31
-5	k	3	
0	2668	2532	44
1	2128	2001	48
2	475	468	2
3	653	594	27
4	534	483	20
5	-58	133	-11
6	1756	1783	-11
7	1289	1356	-32
8	2092	2117	-9
9	326	287	9
10	2139	2238	-36
11	2453	2598	-49
12	2723	2893	-53
13	489	472	5
14	368	431	-17
15	745	729	5
16	453	586	-41
17	467	499	-8
18	1328	1423	-36
19	1651	1705	-19
20	445	527	-20
21	1105	1205	-35
22	1596	1469	39
23	1068	1034	10
24	509	583	-15
25	-279	231	-30
-5	k	4	
1	1188	1102	41
2	2678	2593	27
3	85	89	0
4	-119	194	-27
5	266	411	-46
6	-127	193	-27
7	1019	935	38
8	1174	1244	-33
9	226	42	20
10	2053	2125	-27
11	1049	1067	-7
12	1088	1116	-11
13	150	46	7
14	415	540	-38
15	977	1009	-12
16	245	391	-30
17	489	552	-17
18	677	667	3
19	340	403	-12
20	2223	2252	-9
21	335	328	1
22	180	222	-4
23	209	120	6
24	1068	989	22
25	134	229	-7
-5	k	5	
0	1066	963	48
1	2539	2333	67
2	1166	1159	3
3	1569	1526	18
4	655	670	-6
5	258	379	-34
6	480	536	-21
7	1050	1023	11
8	873	951	-35
9	366	357	2
10	899	940	-17
11	2396	2353	14
12	757	756	0
13	92	20	3
14	1016	1060	-17
15	532	672	-47
16	-191	199	-26
17	-245	138	-26
18	891	1046	-56
19	1476	1501	-9
20	-198	16	-10
21	1018	973	13
22	1463	1466	-1
23	1035	1030	1
24	315	268	5
25	-217	370	-40
-5	k	6	
1	3248	3108	45
2	444	251	81
3	897	798	60
4	1267	1230	21
5	456	383	34
6	801	765	21
7	675	645	16
8	864	878	-7
9	3867	3928	-17
10	565	540	11
11	560	533	12
12	265	101	30
13	2313	2423	-46
14	633	667	-16
15	-221	3	-25
16	528	596	-28
17	1298	1357	-28
18	276	259	3
19	1444	1463	-8
20	894	906	-5
21	2013	2022	-2
22	496	338	26
23	988	908	21
24	701	721	-4
-5	k	7	
0	6130	5886	38
1	1067	947	53
2	667	488	70
3	767	678	38
4	1500	1376	50
5	325	530	-66
6	473	453	6
7	844	765	31
8	3266	3135	34
9	211	124	11
10	2265	2199	21
11	1147	1245	-40
12	1748	1764	-5
13	368	436	-17
14	628	649	-6
15	-263	74	-25
16	290	373	-15
17	136	215	-8
18	2092	2020	22
19	1047	1045	0
20	593	467	26
21	852	827	6
22	1840	1803	10
23	408	395	2
-5	k	8	
1	865	829	14
2	3795	3670	29
3	1292	1255	14
4	1274	1170	41
5	778	768	3
6	951	980	-11
7	297	309	-2
8	909	859	19
9	1965	1933	11
10	2868	2772	27
11	330	152	27
12	2448	2364	25
13	918	867	17
14	-245	4	-19
15	575	561	3
16	305	320	-2
17	438	434	0
18	785	737	13
19	1102	1108	-1
20	2497	2432	17
21	692	626	15
22	559	487	13
-5	k	9	
0	523	464	17
1	2579	2695	-36
2	130	72	4
3	2139	2070	23
4	-148	13	-8
5	-210	111	-22
6	-187	103	-17
7	2070	2046	8
8	605	586	6
9	622	592	9
10	685	727	-14
11	4042	3928	24
12	589	407	43
13	372	314	10
14	927	962	-11
15	529	521	1
16	664	731	-19
17	710	776	-18
18	98	136	-2
19	2231	2216	4
20	569	483	16
21	1538	1532	1
-5	k	10	
1	3362	3304	23
2	2536	2473	18
3	825	815	3
4	433	338	21
5	439	385	12
6	750	756	-1
7	1181	1107	26
8	1083	1072	3
9	2907	2842	17
10	1757	1714	14
11	576	480	23
12	1317	1291	9
13	1335	1336	0
14	550	529	4
15	472	535	-13
16	272	317	-5
17	1317	1300	5
18	522	473	9
19	922	868	14
20	1383	1384	0
-5	k	11	
0	4280	4317	-7
1	629	543	23
2	959	925	11
3	-30	186	-11
4	1286	1336	-18
5	815	782	11
6	-162	93	-10
7	300	104	21
8	2741	2667	20
9	296	213	11
10	2123	2115	2
11	575	430	31
12	1766	1765	0
13	519	470	10
14	1042	1124	-25
15	390	506	-21
16	817	817	0
17	277	292	-1
18	1720	1734	-3
-5	k	12	
1	2377	2352	7
2	1955	1949	1
3	1346	1379	-11
4	714	798	-26
5	237	208	3
6	380	381	0
7	367	367	0
8	629	584	11
9	2381	2341	11
10	1212	1177	10
11	263	76	14
12	1310	1140	48
13	1812	1761	15
14	213	43	9
15	-245	112	-16
16	506	527	-4
-5	k	13	
0	306	444	-23
1	1436	1480	-14
2	-108	181	-10
3	931	1028	-30
4	-291	176	-29
5	77	271	-15
6	496	458	7
7	1555	1540	4
8	295	220	8
9	415	340	11
10	793	731	15
11	2726	2626	25
12	558	504	10
13	-92	68	-2
-5	k	14	
1	-79	130	-5
2	1917	2019	-31
3	-248	40	-14
4	83	216	-8
5	320	417	-14
6	540	522	3
7	-82	137	-5
8	1082	1150	-19
9	400	421	-3
-4	k	1	
1	4621	4508	23
2	1449	1526	-39
3	3388	3443	-15
4	1379	1274	50
5	1409	1426	-8
6	991	1084	-51
7	513	514	0

8	437	422	5
9	3584	3760	-46
10	304	399	-29
11	-170	53	-14
12	1618	1627	-3
13	2487	2526	-12
14	1309	1357	-20
15	473	523	-16
16	161	172	-1
17	1303	1412	-44
18	524	686	-55
19	1292	1409	-45
20	1234	1354	-45
21	1828	1898	-24
22	296	334	-5
23	1207	1177	9
24	345	360	-2
25	515	462	10
26	-129	267	-19

-4 k 2

0	2848	2733	36
1	5293	5090	37
2	515	419	39
3	2624	2569	18
4	2884	2852	10
5	-138	175	-26
6	1438	1424	7
7	2034	2036	0
8	1008	1005	1
9	354	286	19
10	159	65	10
11	3426	3654	-62
12	1392	1565	-80
13	-79	139	-10
14	-100	32	-4
15	200	363	-35
16	774	812	-14
17	615	694	-28
18	1171	1259	-35
19	2012	2131	-41
20	242	205	4
21	1216	1217	0
22	1447	1511	-22
23	1040	1097	-18
24	435	457	-4
25	-264	37	-17
26	-302	110	-24

-4 k 3

1	338	321	5
2	4801	4623	35
3	1435	1393	20
4	1367	1354	6
5	108	181	-11
6	189	162	4
7	481	418	24
8	1931	1978	-19
9	815	795	8
10	2501	2590	-30
11	128	145	-2
12	1963	2024	-23
13	-157	161	-21
14	1025	1087	-26
15	453	505	-16
16	625	682	-21
17	-107	283	-33
18	512	466	12
19	532	543	-3
20	2553	2653	-30
21	-34	3	0
22	76	171	-5
23	505	539	-7
24	993	972	6
25	-206	217	-20
26	-246	14	-13

-4 k 4

0	3695	3500	48
1	3635	3394	60
2	155	143	1
3	386	254	39
4	191	185	1
5	181	191	-1
6	581	561	8
7	1415	1353	28
8	1089	1191	-51
9	176	44	13
10	528	566	-14
11	1719	1752	-13
12	778	683	36
13	202	65	14
14	636	783	-59
15	-269	236	-52
16	475	550	-23
17	810	845	-12
18	617	733	-38
19	1236	1291	-20
20	168	289	-15
21	937	965	-9
22	1578	1396	55
23	1040	1080	-12
24	261	346	-11
25	-390	84	-39

-4 k 5

1	2738	2528	65
2	496	468	11
3	1397	1320	35
4	143	182	-6
5	-127	177	-24
6	224	372	-41
7	985	964	9
8	436	451	-5
9	3654	3768	-29
10	180	92	9
11	373	290	20
12	162	95	6
13	2269	2467	-70
14	-196	183	-28
15	393	371	5
16	-32	324	-36
17	1467	1650	-72
18	518	550	-8
19	1321	1465	-54
20	-236	22	-16
21	1645	1790	-50
22	427	258	25
23	1219	1209	3
24	-216	63	-11
25	-363	69	-32

-4 k 6

0	3406	3352	17
1	1197	1046	89
2	795	698	60
3	2997	2897	35
4	870	879	-6
5	592	530	35
6	330	218	39
7	1093	1097	-2
8	2423	2469	-18
9	765	724	22
10	2816	2764	18
11	2662	2764	-39
12	1832	1803	13
13	852	891	-21
14	977	1071	-51
15	155	273	-24
16	-246	55	-31
17	-244	0	-27
18	1669	1752	-38
19	1272	1230	19
20	233	118	14
21	1240	1198	13
22	1743	1629	34
23	254	78	12
24	-183	68	-8

-4 k 7

1	1371	1340	14
2	3569	3497	18
3	971	852	53
4	1364	1234	55
5	407	35	73
6	1485	1448	14
7	192	111	10
8	1609	1492	45
9	942	918	9
10	3010	2912	27
11	315	280	7
12	2411	2407	1
13	866	859	2
14	-177	75	-13
15	380	448	-16
16	243	307	-10
17	582	589	-1
18	1163	1133	10
19	801	764	11
20	2756	2682	19
21	929	818	30
22	290	140	14
23	445	389	9
24	1346	1253	26

-4 k 8

0	2102	2035	23
1	3179	3101	21
2	919	862	23
3	2873	2740	38
4	1030	978	21
5	108	155	-5
6	749	719	11
7	1866	1869	-1
8	582	627	-15
9	595	579	5
10	1340	1310	11
11	3538	3500	9
12	314	284	5
13	762	697	20
14	670	692	-6
15	289	182	14
16	620	590	8
17	446	381	13
18	1199	1196	0
19	2314	2268	13
20	346	132	22
21	1391	1357	10
22	1151	1159	-2
23	892	913	-5

-4 k 9

1	2389	2501	-37
2	899	981	-33
3	328	426	-25
4	-139	90	-10
5	447	569	-39
6	-229	26	-21
7	906	901	1
8	1392	1360	11
9	3175	3113	16
10	1537	1534	0
11	249	99	16
12	1377	1292	29
13	2113	2057	17
14	718	702	4
15	-197	151	-18
16	24	89	-2
17	1063	1013	14
18	76	211	-9
19	1300	1254	13
20	1225	1248	-7
21	1406	1390	4

-4 k 10

0	4347	4283	13
1	346	29	38
2	1005	993	4
3	575	563	3
4	1352	1353	0
5	546	537	2
6	290	46	25
7	411	354	12
8	2576	2465	32
9	412	263	27
10	2182	2056	39
11	497	500	0
12	1659	1629	10
13	500	476	5
14	1066	1077	-3
15	207	339	-17
16	474	547	-15
17	-247	110	-17
18	2027	1986	11
19	267	219	4
20	465	380	13

-4 k 11

1	1870	1888	-6
2	2099	2087	3
3	882	860	7
4	313	443	-27
5	-134	56	-6
6	527	525	0
7	310	386	-14
8	607	645	-10
9	2302	2331	-8
10	1599	1602	0
11	354	152	25
12	1319	1315	1
13	1474	1399	23
14	456	580	-26
15	-69	163	-7
16	259	383	-16
17	947	988	-11
18	416	366	7

-4 k 12

0	1011	932	25
1	2207	2163	13
2	335	115	25
3	1774	1647	40
4	578	638	-16
5	-314	83	-31
6	-60	14	-1
7	1766	1690	24
8	199	238	-4
9	487	360	22
10	454	258	29
11	3285	3271	3
12	485	428	10
13	419	473	-9
14	-145	4	-4
15	307	440	-19
16	-244	14	-12

-4 k 13

1	1183	1190	-2
2	1626	1767	-46
3	253	393	-20

4	-337	196	-38
5	147	316	-17
6	743	753	-2
7	98	257	-12
8	1020	1073	-15
9	1103	1095	2
10	1568	1587	-5
11	311	123	16
12	1178	1150	8
13	787	846	-14

-4 k 14

0	2205	2343	-40
1	557	624	-14
2	370	310	8
3	210	293	-8
4	273	459	-27
5	198	320	-13
6	-383	216	-44
7	350	297	6
8	1560	1603	-12

-3 k 1

0	2315	2262	20
1	3810	3781	7
2	474	578	-56
3	950	950	0
4	1212	1279	-38
5	2700	2842	-49
6	514	632	-55
7	3354	3466	-31
8	972	994	-11
9	812	812	0
10	1739	1715	9
11	3000	3094	-28
12	1086	1131	-21
13	-89	203	-22
14	-157	196	-27
15	618	642	-8
16	-206	17	-18
17	961	1001	-16
18	682	692	-3
19	2213	2289	-25
20	410	395	3
21	1870	1955	-29
22	896	766	39
23	1548	1420	40
24	432	537	-22
25	373	345	4
26	-304	59	-23

-3 k 2

1	770	700	40
2	2017	1962	23
3	452	521	-33
4	3507	3716	-58
5	1885	1991	-48
6	668	758	-45
7	348	444	-35
8	2433	2621	-69
9	956	995	-20
10	3265	3406	-40
11	375	395	-6
12	2444	2475	-10
13	1272	1273	0
14	2002	2078	-28
15	208	320	-23
16	245	419	-43
17	-192	81	-17
18	345	92	35
19	443	360	19
20	2308	2275	10
21	430	212	36
22	476	461	3
23	835	733	28
24	885	801	24
25	75	365	-29
26	628	687	-14

-3 k 3

0	2478	2313	58
1	563	524	18
2	404	466	-28
3	2108	2104	2
4	988	905	43
5	-383	88	-84
6	616	715	-49
7	2089	2131	-16
8	2460	2636	-64
9	-159	70	-15
10	1716	1750	-14
11	1221	1336	-55
12	1701	1708	-3
13	539	614	-28
14	639	780	-59
15	361	320	9
16	700	735	-13
17	697	701	-1
18	1519	1538	-7
19	722	696	8
20	636	656	-6
21	706	712	-1
22	1892	1972	-26
23	734	619	29
24	415	479	-12
25	78	160	-4
26	62	8	0

-3 k 4

1	5021	4572	83
2	2157	2030	48
3	795	787	3
4	1455	1402	25
5	1307	1363	-28
6	887	925	-20
7	1496	1414	37
8	513	551	-15
9	3217	3367	-43
10	503	489	5
11	597	607	-3
12	533	548	-5
13	1836	2034	-80
14	355	474	-34
15	535	626	-34
16	116	222	-13
17	1357	1388	-12
18	508	542	-10
19	1402	1422	-7
20	475	461	3
21	1928	2043	-39
22	159	85	4
23	1548	1478	21
24	358	353	0
25	96	246	-11
26	471	474	0

-3 k 5

0	3380	3072	81
1	1335	1250	40
2	228	147	15
3	752	710	20
4	1243	1298	-27
5	137	209	-12
6	602	747	-69
7	1375	1370	2
8	1873	1998	-52
9	706	675	13
10	2715	2764	-15
11	3093	3335	-71
12	1582	1588	-2
13	280	288	-1
14	1144	1252	-46
15	-56	229	-21
16	-277	70	-31
17	-260	16	-24
18	1781	1927	-53
19	1520	1660	-52
20	-214	60	-14
21	1241	1302	-21
22	1893	1778	34
23	526	667	-34
24	-78	15	-1
25	332	459	-20

-3 k 6

1	499	365	63
2	3964	3815	41
3	400	216	71
4	2122	2022	45
5	222	48	34
6	1502	1530	-15
7	411	374	16
8	1269	1227	23
9	787	771	9
10	3447	3524	-24
11	646	569	38
12	2776	2902	-46
13	612	621	-4
14	282	382	-32
15	-180	259	-52
16	283	361	-22
17	-241	158	-39
18	961	1062	-50
19	191	10	14
20	2708	2831	-44
21	362	35	30
22	221	24	11
23	211	68	8
24	1036	1012	6
25	-144	103	-6

-3 k 7

0	3821	3754	16
1	2499	2477	7
2	1171	1040	58
3	2774	2644	39
4	387	142	61
5	1378	1304	31
6	1373	1237	56
7	1510	1499	4
8	2494	2354	44
9	819	779	16
10	968	983	-6
11	3538	3511	6
12	695	678	6
13	282	166	17
14	659	686	-9
15	-108	256	-25
16	660	669	-2
17	569	624	-15
18	1495	1451	14
19	2168	2116	16
20	317	54	22
21	1967	1887	23
22	1094	1022	20
23	1112	1064	15
24	609	645	-8

-3 k 8

1	4184	4033	32
2	2215	2032	61
3	1023	994	12
4	335	345	-2
5	1042	1020	9
6	-208	29	-18
7	1249	1183	26
8	461	434	7
9	3967	3862	23
10	1006	941	24
11	113	31	4
12	1145	1052	34
13	2670	2593	22
14	685	635	15
15	672	737	-20
16	-239	114	-21
17	1541	1542	0
18	410	402	1
19	1369	1279	28
20	1547	1436	33
21	2364	2216	40
22	429	288	19
23	1395	1413	-5

-3 k 9

0	1811	1936	-47
1	418	469	-15
2	287	343	-12
3	453	423	8
4	445	485	-11
5	625	543	29
6	694	684	3
7	764	788	-8
8	2291	2238	17
9	148	45	6
10	2337	2322	4
11	870	859	3
12	1875	1805	23
13	423	421	0
14	1143	1086	19
15	-250	93	-21
16	-266	205	-32
17	412	409	0
18	1851	1894	-13
19	621	581	8
20	542	541	0
21	465	492	-4

-3 k 10

1	1725	1634	32
2	1636	1704	-25
3	685	686	0
4	170	112	5
5	-170	80	-12
6	1016	1038	-8
7	239	319	-13
8	884	871	4
9	1785	1739	15
10	1555	1604	-17
11	170	183	-1
12	1029	1110	-28
13	1185	1217	-10
14	463	496	-7
15	-277	59	-20
16	132	204	-5
17	583	593	-2
18	171	292	-12
19	804	755	12
20	1546	1495	14

-3 k 11

0	507	374	29
1	2105	2024	25
2	308	270	6
3	1840	1821	6
4	198	141	5
5	-259	125	-26
6	-148	35	-6
7	2006	1942	20
8	162	101	4
9	298	122	19

10	432	406	5
11	3155	3061	23
12	149	49	4
13	252	275	-2
14	-116	123	-6
15	-163	61	-7
16	-109	342	-28
17	1016	982	9
18	410	227	22

-3 k 12

1	1243	1299	-19
2	1991	1888	31
3	843	846	0
4	487	597	-27
5	-197	69	-12
6	705	688	4
7	615	571	11
8	1015	860	43
9	1889	1858	9
10	2196	2131	18
11	379	282	13
12	1711	1721	-3
13	1565	1536	8
14	529	586	-11
15	-170	68	-7

-3 k 13

0	2365	2545	-53
1	502	595	-20
2	148	226	-6
3	-260	220	-28
4	357	449	-15
5	-198	185	-17
6	-131	311	-26
7	351	357	0
8	1718	1796	-24
9	473	386	14
10	1651	1744	-28
11	450	375	11
12	1014	1083	-20

-3 k 14

1	1589	1687	-30
2	1155	1264	-32
3	635	735	-23
4	-346	65	-28
5	541	546	-1
6	253	186	5
7	-339	60	-26

-2 k 1

1	2687	2621	23
2	4915	5066	-30
3	1303	1445	-89
4	400	499	-51
5	-275	126	-59
6	185	378	-61
7	906	915	-5
8	2734	2904	-58
9	3280	3433	-44
10	3015	3052	-11
11	1273	1305	-15
12	2405	2415	-3
13	1621	1628	-2
14	1326	1290	15
15	286	409	-33
16	1651	1712	-24
17	1354	1409	-22
18	423	89	55
19	628	559	21
20	2886	3069	-53
21	1492	1517	-9
22	239	21	16
23	871	886	-4
24	1285	1274	3
25	-313	42	-25
26	520	508	2
27	368	223	17

-2 k 2

0	2316	1841	171
1	581	459	69
2	452	653	-132
3	371	515	-76
4	310	459	-66
5	467	629	-87
6	159	377	-64
7	578	595	-7
8	3229	3429	-59
9	285	328	-13
10	3776	3909	-33
11	1871	1906	-14
12	2372	2372	0
13	-211	138	-30
14	2106	2231	-47
15	58	290	-33
16	522	524	0
17	461	596	-45
18	2465	2552	-28
19	755	778	-8
20	590	476	30
21	690	637	15
22	2320	2376	-17
23	596	601	-1
24	156	62	5
25	-44	285	-19
26	525	623	-21
27	-297	203	-29

-2 k 3

1	3726	3535	48
2	490	456	15
3	329	368	-14
4	1643	1694	-24
5	-231	298	-82
6	932	986	-28
7	2104	2152	-19
8	344	450	-41
9	3267	3546	-81
10	924	887	17
11	202	42	18
12	1005	1097	-43
13	2253	2394	-51
14	77	166	-8
15	-189	95	-18
16	-200	176	-29
17	1301	1379	-32
18	470	452	4
19	1081	1229	-59
20	592	527	17
21	1723	1791	-23
22	250	155	10
23	1512	1470	13
24	287	286	0
25	142	302	-16
26	240	105	10

-2 k 4

0	4529	4220	64
1	3057	2889	49
2	1149	1017	67
3	4565	4410	32
4	1349	1364	-7
5	293	237	13
6	210	185	5
7	2195	2256	-23
8	2048	2209	-65
9	663	712	-23
10	1395	1393	1
11	3278	3552	-78
12	1489	1530	-17
13	1167	1166	0
14	1315	1388	-31
15	314	393	-19
16	297	445	-38
17	-126	330	-46
18	1115	1131	-6
19	2561	2654	-28
20	-44	105	-3
21	1770	1786	-5
22	1697	1813	-40
23	1267	1177	28
24	255	342	-11
25	273	255	2
26	-167	99	-8

-2 k 5

1	879	802	38
2	2935	2772	49
3	686	663	10
4	-50	85	-5
5	-174	159	-30
6	1507	1563	-25
7	901	912	-5
8	1342	1405	-29
9	787	852	-29
10	3689	3895	-52
11	299	215	16
12	2665	2863	-64
13	229	206	3
14	1501	1684	-76
15	352	555	-61
16	303	567	-75
17	-117	245	-25
18	594	674	-25
19	-118	53	-5
20	2714	2878	-48
21	189	28	9
22	130	170	-3
23	114	270	-14
24	843	879	-9
25	346	334	1

-2 k 6

0	3867	3732	38
1	3592	3380	63
2	831	811	12
3	2096	2018	36
4	274	146	38
5	636	645	-5
6	713	681	19
7	2476	2468	3
8	2270	2217	22
9	442	389	21
10	2291	2334	-18
11	2866	3054	-69
12	784	818	-18
13	400	423	-9
14	503	581	-35
15	-114	278	-46
16	586	633	-21
17	221	288	-14
18	1431	1466	-16
19	1942	2032	-39
20	-119	68	-7
21	1623	1541	25
22	1294	1119	51
23	1413	1366	14
24	-205	72	-10
25	545	562	-3

-2 k 7

1	3349	3247	27
2	1022	935	39
3	1479	1339	58
4	589	465	48
5	951	756	81
6	135	188	-6
7	-98	123	-10
8	284	303	-4
9	4109	4021	19
10	749	685	25
11	167	159	0
12	513	565	-16
13	1821	1811	3
14	199	313	-19
15	99	136	-2
16	220	334	-19
17	1437	1492	-19
18	216	141	7
19	1567	1437	41
20	415	280	21
21	2364	2328	10
22	333	34	23
23	1189	1195	-1
24	560	481	14

-2 k 8

0	4586	4465	24
1	2044	1978	23
2	490	483	2
3	195	236	-7
4	1484	1395	35
5	444	459	-4
6	-49	18	-1
7	1740	1699	15
8	2754	2751	0
9	698	780	-32
10	2655	2538	34
11	1433	1396	14
12	2339	2258	25
13	407	402	1
14	1252	1241	3
15	-291	29	-28
16	-160	130	-12
17	457	348	21
18	2236	2125	33
19	1096	1034	18
20	293	177	12
21	606	458	29
22	2084	2039	13

-2 k 9

1	1050	1107	-23
2	2594	2632	-11
3	854	790	23
4	425	378	11
5	477	377	26
6	502	496	1
7	487	435	14
8	1512	1473	14
9	1700	1640	21
10	3071	2963	28
11	259	18	20
12	2035	1949	27
13	1058	1043	5
14	912	861	16
15	-277	197	-34
16	318	339	-3
17	352	350	0
18	600	692	-22
19	1069	1108	-12
20	2277	2226	14
21	769	664	23

-2 k 10

0	791	703	29
1	2579	2493	25

2	377	290	17
3	1994	1971	7
4	318	166	22
5	251	394	-29
6	91	151	-4
7	1816	1825	-3
8	762	754	2
9	321	372	-9
10	358	209	22
11	2832	2830	0
12	491	476	3
13	-235	4	-15
14	-225	42	-14
15	279	321	-5
16	311	295	2
17	644	703	-14
18	560	535	5
19	1729	1731	0

-2 k 11

1	2728	2582	40
2	2140	2020	37
3	1800	1676	40
4	297	374	-14
5	-157	36	-7
6	259	317	-9
7	109	139	-2
8	691	654	10
9	2578	2586	-2
10	1462	1439	7
11	320	155	18
12	1330	1308	6
13	1452	1368	25
14	559	616	-12
15	295	166	12
16	-110	302	-22
17	1192	1229	-10

-2 k 12

0	3814	3845	-6
1	368	163	26
2	503	501	0
3	180	95	6
4	1449	1525	-25
5	-230	158	-21
6	325	358	-5
7	159	46	5
8	2076	2046	8
9	357	115	24
10	2138	2118	6
11	351	249	12
12	1929	1858	20
13	345	311	4
14	890	947	-15

-2 k 13

1	1728	1856	-40
2	1172	1290	-37
3	459	614	-33
4	328	246	9
5	-42	213	-10
6	576	653	-17
7	589	490	19
8	602	658	-12
9	1983	1980	0
10	1202	1231	-8
11	129	114	0

-2 k 14

0	590	554	7
1	1394	1537	-43
2	211	258	-4
3	802	867	-16
4	257	182	6

-1 k 1

0	6017	5725	47
1	550	535	9
2	583	566	11
3	235	326	-41
4	1559	1543	8
5	-359	105	-106
6	1683	1772	-44
7	378	446	-28
8	5204	5249	-8
9	33	24	0
10	4413	4483	-15
11	1448	1463	-7
12	3599	3472	32
13	948	965	-8
14	2136	2157	-7
15	110	137	-2
16	343	311	7
17	748	753	-1
18	3066	3181	-32
19	570	491	23
20	1059	659	122
21	861	882	-7
22	2834	2973	-40
23	297	127	18
24	139	38	4
25	142	115	1
26	479	598	-25
27	154	56	4

-1 k 2

1	5054	4787	51
2	3188	3060	38
3	2298	2372	-30
4	-292	188	-87
5	88	341	-65
6	987	1048	-35
7	204	334	-36
8	263	22	31
9	4162	4326	-38
10	1868	1737	53
11	391	46	66
12	1632	1689	-25
13	2857	2981	-38
14	326	152	32
15	192	257	-11
16	461	408	15
17	1441	1451	-3
18	1113	1089	9
19	1775	1779	-1
20	1514	1493	7
21	1991	2049	-19
22	255	123	13
23	884	935	-16
24	233	171	6
25	-270	7	-18
26	-217	8	-11
27	1100	1134	-10

-1 k 3

0	2198	2019	70
1	2605	2428	61
2	864	843	12
3	4351	4221	28
4	1489	1541	-26
5	1666	1678	-5
6	-191	290	-63
7	3264	3424	-46
8	1280	1322	-21
9	281	91	34
10	778	653	55
11	2807	2955	-47
12	1070	1083	-6
13	549	540	3
14	967	1004	-16
15	898	923	-10
16	-212	32	-19
17	604	589	5
18	887	772	40
19	2316	2385	-22
20	453	216	42
21	1658	1662	-1
22	1596	1547	16
23	1036	1022	4
24	-257	82	-18
25	-276	227	-31
26	121	270	-12

-1 k 4

1	1522	1463	28
2	8569	8110	52
3	1854	1811	18
4	270	341	-18
5	924	943	-10
6	478	603	-59
7	127	263	-27
8	1516	1511	2
9	444	497	-20
10	2843	3089	-79
11	253	420	-47
12	2227	2322	-34
13	784	844	-25
14	1118	1264	-65
15	-73	183	-15
16	737	750	-4
17	226	307	-14
18	488	520	-9
19	215	303	-13
20	2973	3048	-20
21	584	562	5
22	326	314	1
23	187	5	8
24	1302	1228	22
25	104	161	-3
26	-202	176	-16

-1 k 5

0	3202	3017	52
1	2103	2029	28
2	1099	966	64
3	423	389	12
4	807	753	26
5	-181	17	-18
6	640	642	-1
7	2145	2201	-21
8	2372	2482	-39
9	368	309	16
10	3254	3437	-51
11	3240	3419	-50
12	2063	2216	-57
13	854	803	20
14	687	763	-29
15	717	810	-35
16	278	364	-18
17	500	567	-19
18	2159	2340	-61
19	1577	1578	0
20	392	428	-7
21	1009	1132	-42
22	1951	1869	25
23	959	925	9
24	-269	70	-18
25	170	35	5

-1 k 6

1	3522	3343	54
2	359	168	66
3	2728	2635	35
4	1312	1231	47
5	290	9	58
6	478	401	38
7	1137	1079	33
8	252	120	31
9	3733	3829	-28
10	348	272	24
11	1128	1169	-22
12	410	386	8
13	2371	2519	-61
14	335	380	-15
15	373	535	-64
16	-242	80	-32
17	1327	1387	-29
18	208	264	-10
19	1142	1190	-23
20	119	169	-5
21	1781	1702	24
22	367	283	12
23	1082	1032	14
24	174	98	4

-1 k 7

0	4880	4811	13
1	3305	3121	48
2	651	487	65
3	1904	1732	63
4	1793	1661	50
5	1643	1581	24
6	1165	1100	27
7	1710	1702	2
8	1885	1916	-11
9	550	468	25
10	2142	2029	37
11	2864	2767	27
12	1886	1790	33
13	203	68	12
14	642	636	1
15	-262	86	-26
16	-138	70	-7
17	1110	1072	13
18	2088	2053	10
19	1624	1571	17
20	500	362	25
21	1177	1166	3
22	2659	2545	30
23	926	822	26

-1 k 8

1	1365	1309	22
2	3439	3441	0
3	651	635	5
4	559	400	46
5	88	8	3
6	194	77	11
7	412	462	-14
8	2031	1965	22
9	770	715	21
10	2973	2921	14
11	401	309	19
12	2293	2355	-19
13	1023	973	17
14	1365	1236	44
15	46	268	-20
16	503	524	-5
17	-237	155	-23
18	779	816	-10
19	195	242	-4
20	2474	2401	20
21	332	276	7
22	568	493	14

-1 k 9

0	2379	2359	6
1	2316	2371	-18
2	105	156	-4

3	1991	2031	-14
4	708	696	4
5	-278	30	-31
6	624	582	13
7	2248	2182	21
8	1268	1262	2
9	597	593	1
10	994	881	38
11	3245	3285	-10
12	895	830	21
13	-80	130	-6
14	-71	99	-4
15	95	103	0
16	-252	34	-16
17	249	255	0
18	1055	1053	0
19	1782	1788	-1
20	113	169	-3
21	1266	1224	11

-1 k 10

1	3247	3239	2
2	1865	1830	12
3	2213	2112	31
4	180	122	5
5	404	406	0
6	492	592	-27
7	277	229	7
8	941	876	21
9	3325	3305	4
10	1071	1084	-4
11	70	135	-3
12	1038	1048	-3
13	1894	1897	-1
14	-52	74	-2
15	556	699	-35
16	-68	79	-2
17	1069	1037	9
18	434	401	5
19	1387	1373	4

-1 k 11

0	3701	3652	11
1	354	223	19
2	331	404	-14
3	228	73	12
4	1520	1509	3
5	232	286	-7
6	738	762	-7
7	614	585	7
8	2209	2129	24
9	215	3	11
10	2181	2160	6
11	719	548	39
12	2123	1989	38
13	344	387	-6
14	843	815	7
15	-300	9	-20
16	-226	186	-18

-1 k 12

1	1392	1386	1
2	1611	1715	-34
3	298	373	-11
4	-82	346	-30
5	-293	144	-27
6	557	658	-24
7	655	663	-1
8	1060	1072	-3
9	1946	1981	-10
10	1775	1753	6
11	276	78	14
12	1237	1230	2
13	1155	1132	6

-1 k 13

0	347	3	24
1	2424	2496	-20
2	399	356	6
3	1438	1516	-24
4	184	233	-4
5	122	302	-16
6	213	310	-10
7	1711	1816	-32
8	505	411	15
9	545	481	11

0 k 0

2	1271	1444	-125
4	6061	6040	3
6	1393	1403	-5
8	8892	8707	20
10	5596	5406	32
12	3432	3228	53
14	1161	1308	-71
16	885	858	11
18	4554	4551	0
20	1058	552	146
22	3552	3611	-14
24	486	428	11
26	486	627	-31

0 k 1

1	3130	2971	48
2	2252	2252	0
3	1847	1954	-54
4	1291	1400	-69
5	-295	91	-71
6	649	603	24
7	467	530	-30
8	2237	2160	29
9	5593	5588	0
10	2937	2669	79
11	551	195	103
12	1701	1701	0
13	2816	2725	27
14	935	877	25
15	845	903	-25
16	1114	1135	-8
17	2048	2148	-36
18	860	680	63
19	1567	1506	22
20	2107	2093	4
21	2517	2606	-27
22	566	396	39
23	1281	1380	-35
24	689	592	24
25	-216	10	-11
26	-347	94	-32
27	901	811	24

0 k 2

0	1982	1746	102
1	3396	3132	73
2	150	163	-3
3	2498	2543	-17
4	-293	296	-121
5	285	367	-29
6	1611	1716	-52
7	3303	3314	-3
8	302	61	41
9	1702	1671	13
10	1535	1340	84
11	4936	4844	17
12	693	488	80
13	268	261	1
14	403	430	-8
15	813	821	-3
16	743	663	30
17	569	602	-11
18	543	409	37
19	2215	2116	32
20	512	476	9
21	1544	1518	9
22	547	452	22
23	884	856	8
24	-255	24	-17
25	-211	149	-16
26	-298	13	-21
27	557	492	12

0 k 3

1	1661	1601	29
2	4545	4294	52
3	2466	2362	37
4	5138	5228	-17
5	672	765	-50
6	217	462	-70
7	1179	1255	-40
8	2215	2222	-2
9	1888	1937	-20
10	2116	2126	-3
11	829	819	4
12	1942	1933	3
13	626	607	7
14	1617	1687	-29
15	807	832	-10
16	955	956	0
17	742	664	27
18	214	252	-6
19	876	970	-35
20	2804	2847	-12
21	767	704	19
22	301	326	-4
23	791	846	-17
24	1439	1398	12
25	-200	109	-12
26	-321	78	-26

0 k 4

0	3777	3394	92
1	2183	1950	86
2	1402	1372	14
3	2908	2774	41
4	2055	2063	-3
5	-111	190	-27
6	575	631	-26
7	1397	1433	-17
8	3009	3163	-47
9	233	257	-5
10	2588	2842	-87
11	2084	2186	-38
12	2407	2574	-58
13	110	259	-22
14	775	781	-2
15	-202	195	-31
16	225	350	-25
17	211	165	5
18	2026	1993	10
19	1293	1195	34
20	600	640	-11
21	604	640	-10
22	1932	1853	24
23	668	678	-2
24	-284	88	-22
25	141	283	-13
26	-224	17	-11

0 k 5

1	1823	1646	71
2	1592	1474	51
3	1714	1609	44
4	1174	1090	39
5	284	298	-3
6	-207	72	-24
7	312	368	-16
8	935	946	-5
9	3685	3964	-71
10	101	11	4
11	449	505	-18
12	504	440	19
13	2718	2838	-37
14	249	277	-5
15	-154	211	-25
16	-84	174	-13
17	1145	1180	-13
18	331	358	-5
19	1469	1513	-15
20	453	401	10
21	2044	2173	-42
22	394	220	23
23	1140	1013	36
24	335	314	2
25	52	177	-6

0 k 6

0	3890	3786	28
1	2254	2190	27
2	574	435	73
3	1321	1297	14
4	698	617	49
5	1778	1701	38
6	1550	1541	4
7	1974	1977	-1
8	1764	1801	-18
9	173	86	12
10	2333	2374	-17
11	3043	3186	-49
12	1130	1197	-37
13	627	622	2
14	936	957	-10
15	191	390	-54
16	-266	14	-34
17	684	807	-60
18	1256	1267	-5
19	1631	1637	-2
20	575	604	-10
21	1314	1215	30
22	1130	987	40
23	1640	1628	3
24	160	209	-3

0 k 7

1	423	325	25
2	4477	4319	32
3	289	180	20
4	662	724	-26
5	297	345	-12
6	1002	992	4
7	172	121	5
8	1617	1607	3
9	416	368	12
10	3260	3194	17
11	559	462	28
12	1376	1401	-9
13	88	59	1
14	1141	1158	-6
15	213	364	-26
16	1114	1125	-3
17	153	327	-23
18	430	491	-13
19	258	261	0
20	2537	2476	16
21	296	17	19
22	-152	44	-5
23	-151	18	-5

0 k 8

0	2934	3024	-26

1	1547	1601	-21
2	357	208	29
3	2072	2045	9
4	1064	978	33
5	383	444	-17
6	-121	35	-6
7	1484	1540	-21
8	1382	1316	24
9	522	487	9
10	1587	1548	14
11	3443	3386	13
12	1744	1687	19
13	402	379	5
14	894	910	-5
15	-191	7	-10
16	581	548	8
17	271	325	-8
18	1511	1458	16
19	2314	2258	15
20	257	107	11
21	1507	1421	25
22	1474	1509	-10

0 k 9

1	2871	2833	10
2	1299	1321	-8
3	1464	1433	11
4	260	333	-14
5	196	304	-18
6	733	774	-14
7	516	452	16
8	357	86	34
9	3772	3756	3
10	1120	1099	7
11	227	96	12
12	894	879	4
13	2090	2121	-10
14	265	192	8
15	-332	111	-33
16	-232	142	-18
17	1220	1262	-13
18	691	712	-5
19	1202	1202	0
20	703	725	-5

0 k 10

0	3162	3211	-12
1	1141	1064	26
2	285	357	-13
3	503	377	28
4	998	919	26
5	705	686	5
6	502	490	2
7	681	677	1
8	2063	2121	-18
9	241	9	15
10	1809	1790	6
11	1252	1243	2
12	1688	1649	12
13	336	277	8
14	270	352	-11
15	594	682	-21
16	266	373	-14
17	674	705	-7
18	1793	1778	4

0 k 11

1	1389	1336	17
2	2691	2654	10
3	189	193	0
4	179	311	-17
5	-317	12	-29
6	670	682	-3
7	835	835	0
8	1552	1467	26
9	1574	1592	-5
10	1879	1831	14
11	-122	10	-3
12	1841	1785	16
13	753	739	3
14	818	799	4
15	232	316	-9

0 k 12

0	179	83	5
1	1473	1539	-21
2	19	40	0
3	1652	1761	-34
4	-93	95	-4
5	373	374	0
6	228	462	-35
7	1441	1495	-16
8	-61	18	0
9	847	765	20
10	551	463	16
11	2710	2720	-2
12	421	401	3

0 k 13

1	1019	1192	-52
2	1308	1371	-18
3	697	822	-31
4	735	751	-3
5	165	385	-24
6	969	1013	-11

1 k 0

1	3083	3139	-20
2	3757	3820	-19
3	1173	1227	-45
4	-259	236	-143
5	799	807	-7
6	1057	1087	-23
7	907	997	-72
8	4057	3955	28
9	4304	4298	1
10	3816	3654	46
11	652	423	122
12	2413	2411	0
13	1691	1689	1
14	1025	1018	4
15	963	941	12
16	587	527	29
17	2208	2266	-25
18	602	183	132
19	718	559	74
20	3163	3057	33
21	2362	2359	1
22	502	101	85
23	1288	1271	7
24	1483	1421	26
25	-147	17	-7
26	245	281	-6
27	478	415	15

1 k 1

0	384	335	24
1	4610	4681	-15
2	541	28	175
3	3058	2931	39
4	1175	1183	-4
5	-153	227	-47
6	407	304	37
7	2382	2304	28
8	2044	1988	22
9	2101	2062	15
10	1556	1237	132
11	6496	6350	21
12	408	181	56
13	291	38	34
14	446	365	23
15	685	682	0
16	232	308	-16
17	869	838	12
18	503	191	65
19	3042	2951	24
20	659	378	71
21	2222	2216	1
22	605	441	39
23	1169	1224	-19
24	-101	50	-3
25	242	401	-23
26	398	374	3
27	689	684	1

1 k 2

1	701	725	-15
2	991	998	-4
3	348	405	-23
4	364	132	60
5	-315	30	-62
6	961	1042	-45
7	120	192	-10
8	3013	2860	45
9	2118	1980	52
10	2778	2655	38
11	205	268	-14
12	2811	2708	31
13	1698	1699	0
14	-219	94	-25
15	495	566	-27
16	515	528	-4
17	415	281	30
18	927	926	0
19	1036	1017	6
20	2271	2183	27
21	1159	1144	5
22	90	1	2
23	556	577	-5
24	641	589	12
25	474	593	-26
26	-175	106	-9

1 k 3

0	5630	5464	28
1	524	271	89
2	773	20	210
3	577	552	11
4	2124	2168	-18
5	606	573	14
6	887	935	-26
7	483	413	27
8	2219	2229	-3
9	1178	1150	13
10	2067	1992	28
11	272	118	25
12	2240	2284	-15
13	999	1019	-9
14	377	381	-1
15	430	369	16
16	-139	135	-14
17	-99	195	-17
18	1934	1912	7
19	410	361	10
20	163	264	-12
21	298	76	22
22	2297	2328	-9
23	380	63	32
24	134	50	3
25	-214	45	-11
26	-320	128	-27

1 k 4

1	3139	3036	29
2	1721	1616	45
3	1565	1498	30
4	355	302	16
5	526	646	-59
6	-257	44	-38
7	-127	52	-9
8	842	896	-26
9	3573	3611	-9
10	684	720	-15
11	197	1	15
12	697	702	-2
13	2184	2100	28
14	966	1060	-39
15	280	250	5
16	484	494	-2
17	1457	1372	31
18	774	789	-5
19	1216	1206	3
20	956	1095	-50
21	1945	1965	-6
22	372	293	12
23	1135	1009	37
24	788	842	-14
25	257	446	-28

1 k 5

0	2888	2771	35
1	2435	2294	48
2	101	160	-7
3	1752	1698	22
4	864	887	-11
5	-229	106	-32
6	-70	196	-20
7	1517	1633	-51
8	1998	2157	-62
9	1458	1511	-22
10	641	692	-20
11	3457	3615	-41
12	1662	1729	-26
13	104	66	2
14	656	628	9
15	812	876	-24
16	661	660	0
17	370	478	-25
18	1010	1028	-6
19	2027	2101	-24
20	423	469	-9
21	1300	1273	8
22	950	943	2
23	949	882	18
24	443	392	8
25	-260	213	-25

1 k 6

1	668	558	62
2	4097	3918	47
3	1372	1290	45
4	931	838	54
5	727	683	24
6	1381	1441	-33
7	319	323	-1
8	1882	1952	-33
9	581	595	-7
10	2667	2734	-25
11	136	34	9
12	1945	1999	-24
13	739	770	-16
14	437	489	-20
15	330	388	-17
16	946	992	-22
17	349	361	-3
18	540	530	3
19	547	540	2
20	3020	2909	28
21	312	57	21
22	59	86	0

23	-125	51	-4
1 k 7			
0	3287	3258	7
1	2013	1946	23
2	-77	95	-6
3	1103	1148	-19
4	931	858	28
5	194	231	-6
6	1300	1216	33
7	1697	1679	6
8	1602	1556	17
9	347	489	-39
10	2057	2063	-1
11	2113	2051	20
12	1401	1351	18
13	516	531	-4
14	797	762	11
15	117	84	1
16	-96	41	-3
17	155	180	-2
18	1458	1432	8
19	1734	1706	8
20	350	277	9
21	890	924	-9
22	1703	1660	12
1 k 8			
1	2188	2284	-33
2	1038	983	21
3	429	474	-12
4	927	918	3
5	-259	26	-26
6	442	440	0
7	1042	1010	12
8	449	349	23
9	3230	3221	2
10	847	701	48
11	134	16	5
12	260	409	-28
13	1844	1916	-24
14	119	256	-14
15	-190	26	-10
16	-257	31	-17
17	1291	1310	-6
18	176	356	-22
19	1346	1311	10
20	423	273	20
21	1543	1540	0
1 k 9			
0	2408	2502	-30
1	1683	1670	4
2	287	329	-8
3	482	486	-1
4	648	615	10
5	860	784	25
6	-43	11	0
7	1170	1161	3
8	2108	2052	17
9	159	113	3
10	2026	1964	19
11	1669	1642	9
12	1434	1376	19
13	486	402	17
14	1102	1226	-41
15	440	531	-18
16	534	595	-13
17	431	434	0
18	1561	1567	-2
19	814	803	2
1 k 10			
1	1602	1566	12
2	2741	2685	15
3	88	80	0
4	-171	169	-17
5	441	477	-8
6	652	669	-4
7	1122	1121	0
8	1317	1350	-11
9	852	900	-16
10	2185	2207	-6
11	315	54	21
12	1796	1772	7
13	541	452	17
14	683	667	3
15	297	441	-22
16	536	591	-11
17	518	534	-3
1 k 11			
0	962	835	37
1	1183	1244	-20
2	-152	80	-8
3	1458	1553	-31
4	553	565	-2
5	459	523	-13
6	131	270	-13
7	1082	1068	4
8	372	370	0
9	496	422	13
10	552	477	14
11	2359	2426	-19
12	609	539	14
13	417	388	4
14	104	151	-2
1 k 12			
1	1772	1857	-26
2	1215	1265	-15
3	906	1072	-52
4	1093	1079	3
5	-237	238	-25
6	815	827	-3
7	-188	172	-14
8	248	72	11
9	1666	1710	-13
10	1355	1361	-1
2 k 0			
0	807	907	-98
1	2960	2906	20
2	367	475	-85
3	2460	2474	-6
4	-341	107	-130
5	948	1050	-84
6	679	720	-31
7	1711	1648	35
8	1218	1169	31
9	665	611	35
10	847	670	109
11	4000	3909	25
12	158	72	13
13	991	930	36
14	154	59	12
15	386	406	-8
16	635	657	-12
17	595	542	24
18	734	660	36
19	2927	2913	4
20	506	361	48
21	2086	2049	15
22	448	275	45
23	1536	1571	-16
24	438	430	2
25	568	482	25
26	-221	97	-19
27	610	609	0
2 k 1			
1	1440	1469	-16
2	1798	1672	57
3	620	707	-52
4	2121	2033	35
5	320	438	-47
6	3065	2921	42
7	888	935	-25
8	926	564	155
9	3969	3813	36
10	3013	2905	31
11	603	604	0
12	2663	2542	38
13	2295	2283	4
14	253	263	-2
15	647	619	10
16	479	495	-5
17	939	1022	-35
18	1304	1372	-27
19	1024	967	21
20	2291	2253	12
21	1860	1769	30
22	276	184	11
23	736	802	-27
24	604	608	-1
25	488	433	10
26	428	594	-34
2 k 2			
0	3001	3101	-31
1	62	17	2
2	768	424	147
3	1392	1277	56
4	1755	1700	24
5	-258	106	-35
6	356	343	4
7	91	168	-11
8	2219	2052	60
9	1463	1384	35
10	2195	2023	61
11	492	314	53
12	2584	2530	17
13	415	400	4
14	1474	1391	33
15	387	450	-18
16	-162	56	-11
17	452	445	2
18	1963	1868	32
19	419	208	37
20	394	386	1
21	439	251	33
22	2412	2360	15
23	582	554	6
24	-285	128	-25
25	-331	31	-27
26	-54	272	-17
2 k 3			
1	3557	3676	-32
2	2075	2213	-57
3	740	787	-24
4	-86	185	-23
5	671	665	3
6	200	244	-10
7	1497	1404	41
8	773	681	40
9	2127	1981	52
10	1494	1381	47
11	806	733	31
12	699	647	19
13	823	725	37
14	699	699	0
15	148	293	-24
16	-230	26	-21
17	1201	1286	-34
18	232	101	13
19	1276	1265	4
20	1280	1230	17
21	1723	1694	9
22	472	419	10
23	1131	1187	-17
24	430	329	16
25	-161	19	-6
2 k 4			
0	1049	809	106
1	1267	1303	-17
2	451	532	-34
3	1308	1340	-15
4	577	675	-45
5	792	825	-16
6	1112	1038	34
7	1487	1479	3
8	539	193	87
9	209	312	-22
10	265	203	11
11	2629	2538	28
12	909	812	37
13	445	470	-7
14	349	373	-5
15	128	319	-30
16	132	21	5
17	878	877	0
18	300	300	0
19	1869	1788	26
20	439	182	39
21	1334	1203	41
22	752	609	35
23	1260	1185	22
24	-212	96	-12
25	-206	16	-9
2 k 5			
1	1063	1025	17
2	3189	3123	18
3	1649	1629	8
4	-140	185	-24
5	-193	250	-45
6	1969	1825	52
7	615	651	-13
8	2243	2160	28
9	903	835	27
10	2999	2982	4
11	466	459	1
12	3001	3000	0
13	1310	1314	-1
14	229	88	14
15	600	678	-25
16	56	120	-3
17	92	2	2
18	688	741	-16
19	564	539	6
20	2518	2392	34
21	957	933	7
22	329	40	23
23	-159	59	-6
24	861	821	10
2 k 6			
0	3344	3363	-6
1	2083	2091	-3
2	412	419	-2
3	1729	1715	7
4	1024	1070	-20
5	911	796	45
6	502	547	-15
7	861	851	4
8	1999	1936	22
9	1140	1089	20

10	1858	1752	37
11	1688	1576	40
12	1744	1712	11
13	865	740	41
14	531	563	-9
15	47	168	-8
16	61	337	-33
17	-162	61	-8
18	1685	1647	12
19	1056	1024	10
20	225	301	-9
21	908	795	30
22	1656	1644	3
23	210	206	0

2 k 7

1	2795	2779	4
2	546	512	10
3	552	649	-35
4	998	992	2
5	1001	970	11
6	310	315	-1
7	776	796	-7
8	233	19	18
9	3313	3234	20
10	501	491	2
11	178	184	0
12	528	528	0
13	2089	1984	33
14	873	811	19
15	336	422	-17
16	50	31	0
17	1430	1447	-5
18	141	204	-5
19	1486	1477	2
20	193	191	0
21	1856	1739	33

2 k 8

0	2481	2546	-20
1	2007	2041	-11
2	474	442	8
3	926	890	13
4	778	843	-23
5	628	676	-17
6	505	523	-5
7	1299	1329	-10
8	1787	1794	-2
9	122	48	3
10	1125	1129	-1
11	2205	2174	9
12	1312	1260	17
13	106	93	0
14	1259	1259	0
15	112	114	0
16	635	663	-6
17	658	780	-32
18	1016	957	17
19	1275	1328	-16
20	263	307	-5

2 k 9

1	657	674	-5
2	3013	2993	5
3	326	363	-7
4	321	402	-16
5	-219	101	-18
6	631	649	-5
7	701	773	-24
8	1304	1317	-4
9	702	668	9
10	2271	2337	-20
11	429	377	10
12	1917	1979	-19
13	260	406	-22
14	443	468	-4
15	597	782	-47
16	290	440	-23
17	19	242	-12
18	643	613	6

2 k 10

0	1837	1838	0
1	1782	1868	-28
2	183	187	0
3	2203	2206	0
4	722	723	0
5	411	508	-21
6	706	688	4
7	1232	1271	-12
8	690	727	-9
9	227	241	-1
10	903	820	22
11	2328	2419	-26
12	737	753	-3
13	351	522	-30
14	-285	136	-22
15	-98	140	-6

2 k 11

1	1600	1717	-37
2	934	935	0
3	615	752	-35
4	1169	1162	2
5	-306	11	-22
6	-46	361	-30
7	246	286	-4
8	-78	19	-1
9	1984	1972	3
10	648	656	-1
11	-14	18	0
12	1131	1088	11

2 k 12

0	2075	2207	-38
1	103	147	-2
2	253	334	-9
3	182	253	-6
4	314	591	-49
5	358	580	-40
6	-296	71	-20

3 k 0

1	4530	4598	-17
2	4545	4689	-36
3	1872	1890	-10
4	4264	4269	-1
5	1025	1027	-1
6	1177	1212	-23
7	1034	1073	-27
8	1539	1457	47
9	2257	2211	20
10	2134	2126	4
11	290	206	26
12	1671	1668	1
13	1660	1693	-17
14	-184	16	-21
15	-198	28	-25
16	657	682	-13
17	1486	1484	1
18	573	566	2
19	1350	1313	18
20	1649	1659	-4
21	2022	2061	-16
22	425	412	4
23	1326	1255	30
24	453	322	31
25	277	296	-3
26	-279	176	-36

3 k 1

0	7485	7910	-58
1	2262	2227	13
2	2412	2226	66
3	-107	39	-7
4	1016	993	12
5	1206	1140	33
6	1308	1245	31
7	339	424	-32
8	3686	3544	35
9	324	18	49
10	3608	3272	82
11	196	1	17
12	1401	1313	37
13	1581	1479	41
14	2168	2191	-7
15	28	182	-13
16	1010	1027	-7
17	531	494	11
18	2207	2128	25
19	194	11	12
20	334	317	3
21	387	368	3
22	2409	2380	8
23	387	206	24
24	349	539	-37
25	211	333	-14
26	555	585	-6

3 k 2

1	2883	2962	-25
2	2570	2514	19
3	1141	1129	5
4	-86	72	-7
5	780	712	33
6	196	176	3
7	1466	1363	46
8	682	585	40
9	3107	2912	54
10	2335	2187	50
11	712	677	13
12	1025	996	12
13	2098	2041	20
14	1165	1158	3
15	1179	1111	27
16	453	414	10
17	1286	1232	20
18	569	536	9
19	973	917	19
20	1709	1774	-23
21	1461	1368	31
22	399	116	33
23	1249	1101	44
24	690	732	-10
25	-125	43	-4

3 k 3

0	505	342	57
1	1752	1872	-53
2	401	454	-20
3	1607	1661	-24
4	388	421	-11
5	96	76	1
6	180	180	0
7	1524	1425	41
8	611	91	121
9	504	461	14
10	945	877	28
11	3086	2891	53
12	657	262	104
13	344	374	-7
14	511	559	-15
15	432	468	-10
16	264	332	-13
17	694	792	-34
18	-143	27	-6
19	1806	1780	9
20	350	110	28
21	1578	1514	21
22	458	445	2
23	1421	1400	6
24	184	151	2
25	-303	156	-26

3 k 4

1	1233	1256	-10
2	2584	2721	-46
3	1082	1157	-36
4	897	898	0
5	7	217	-21
6	690	638	20
7	79	259	-25
8	220	158	9
9	1862	1760	37
10	2540	2371	52
11	966	926	16
12	2522	2427	29
13	1360	1270	34
14	680	589	30
15	864	857	2
16	254	243	1
17	355	464	-24
18	821	734	26
19	752	744	2
20	2218	2250	-10
21	899	801	28
22	367	226	18
23	414	481	-12
24	767	772	-1

3 k 5

0	3088	3142	-15
1	502	547	-15
2	-264	56	-31
3	1185	1246	-27
4	1181	1283	-46
5	594	646	-21
6	1283	1265	7
7	122	198	-9
8	2154	2036	40
9	390	314	17
10	2658	2580	23
11	1911	1791	41
12	1413	1355	21
13	682	646	12
14	671	649	7
15	248	268	-2
16	-153	94	-9
17	192	266	-9
18	2099	2135	-11
19	889	825	19
20	344	315	4
21	1029	963	20
22	1881	1797	24
23	222	164	4

3 k 6

1	2716	2624	27
2	626	642	-6
3	1098	1121	-9
4	538	530	2
5	355	346	2
6	717	701	5
7	750	754	-1
8	858	850	2
9	3016	2979	10
10	490	418	18
11	150	3	7
12	296	308	-2

13	2156	2167	-3
14	889	919	-10
15	535	560	-6
16	460	486	-6
17	1078	1068	3
18	395	347	8
19	900	768	35
20	719	629	21
21	1909	1799	31
22	518	492	4

3 k 7

0	2380	2324	17
1	1468	1506	-15
2	1456	1401	20
3	1182	1214	-12
4	172	267	-14
5	385	458	-19
6	752	667	29
7	1489	1518	-10
8	1400	1379	7
9	228	92	13
10	1597	1508	30
11	2318	2253	20
12	563	511	13
13	-106	172	-12
14	846	883	-12
15	186	164	1
16	218	338	-16
17	914	976	-18
18	928	848	21
19	1267	1270	0
20	341	138	19

3 k 8

1	323	199	19
2	3407	3429	-5
3	656	702	-14
4	450	518	-17
5	524	615	-26
6	909	931	-7
7	726	694	9
8	1142	1216	-26
9	242	101	13
10	2788	2767	5
11	432	483	-11
12	1954	1940	4
13	-84	24	-1
14	534	600	-15
15	1156	1138	5
16	114	209	-7
17	490	485	1
18	714	803	-22

3 k 9

0	2124	2069	17
1	1608	1596	3
2	350	252	15
3	1714	1709	1
4	667	671	-1
5	619	734	-34
6	928	911	5
7	1381	1347	11
8	899	916	-5
9	609	602	1
10	1195	1265	-22
11	2194	2189	1
12	1241	1243	0
13	795	820	-6
14	-224	43	-11
15	-92	186	-9
16	495	528	-6

3 k 10

1	1561	1607	-14
2	255	336	-11
3	773	865	-28
4	678	813	-37
5	-262	113	-20
6	169	444	-39
7	-206	110	-13
8	130	214	-6
9	2372	2466	-27
10	428	418	1
11	-144	166	-10
12	766	800	-8
13	1725	1790	-19

3 k 11

0	2210	2291	-23
1	1032	1046	-4
2	322	454	-21
3	-121	98	-5
4	410	468	-10
5	872	925	-14
6	232	223	0
7	434	572	-26
8	1727	1723	1
9	92	26	1

4 k 0

0	3658	3604	16
1	-223	128	-46
2	1405	1377	17
3	179	180	0
4	2067	2069	0
5	648	650	-1
6	979	977	1
7	837	853	-11
8	2748	2701	18
9	276	191	26
10	2819	2864	-17
11	1349	1345	2
12	2265	2297	-13
13	1035	1036	0
14	1467	1498	-17
15	420	547	-59
16	442	565	-57
17	1081	1109	-15
18	1933	1864	30
19	323	342	-5
20	836	887	-24
21	526	476	17
22	2373	2433	-23
23	292	188	16
24	321	429	-25
25	-156	231	-25
26	-206	20	-13

4 k 1

1	1359	1275	41
2	1912	1826	35
3	788	730	29
4	688	603	39
5	1400	1442	-20
6	952	911	20
7	1457	1409	21
8	1925	1765	61
9	2024	2002	8
10	2724	2496	69
11	485	479	2
12	1869	1843	10
13	2381	2355	8
14	505	416	26
15	1246	1247	0
16	240	221	3
17	1240	1307	-26
18	328	337	-1
19	861	868	-2
20	2384	2301	25
21	1189	1216	-9
22	345	156	22
23	1118	1174	-17
24	905	989	-25
25	545	710	-39

4 k 2

0	949	798	70
1	2556	2633	-26
2	682	742	-29
3	2262	2294	-11
4	809	790	9
5	590	568	9
6	1188	1203	-6
7	2126	2081	16
8	1261	1145	49
9	1564	1479	34
10	363	320	11
11	4315	4151	34
12	1219	1039	70
13	500	438	18
14	732	675	20
15	-156	28	-9
16	868	896	-10
17	228	84	14
18	236	218	2
19	2142	2054	27
20	469	158	47
21	1846	1814	13
22	87	95	0
23	869	799	18
24	572	505	13
25	733	839	-27

4 k 3

1	1636	1736	-44
2	2187	2240	-19
3	1780	1779	0
4	1071	1110	-18
5	859	776	35
6	1080	1043	16
7	200	91	13
8	2109	1974	47
9	2348	2182	54
10	2209	1991	72
11	261	52	24
12	2127	2016	37
13	1288	1257	12
14	477	365	28
15	624	703	-27
16	420	509	-23
17	614	613	0
18	468	371	20
19	992	857	42
20	1916	1814	32
21	1347	1297	15
22	386	424	-6
23	369	181	21
24	639	591	10

4 k 4

0	3166	3427	-76
1	246	312	-15
2	452	488	-11
3	1117	1176	-26
4	1425	1483	-25
5	1239	1206	13
6	1052	1000	21
7	487	322	43
8	2577	2384	58
9	389	217	35
10	2728	2534	56
11	759	689	24
12	2370	2319	16
13	705	651	17
14	804	846	-14
15	88	115	-1
16	88	9	2
17	364	359	1
18	1764	1636	41
19	541	478	18
20	514	463	10
21	554	354	35
22	2143	1976	46
23	237	228	0

4 k 5

1	2381	2483	-34
2	1749	1812	-25
3	815	897	-34
4	266	343	-17
5	-153	206	-26
6	-205	59	-18
7	1044	974	27
8	976	886	34
9	2741	2552	54
10	1098	1067	11
11	428	354	17
12	333	131	27
13	1679	1705	-9
14	1174	1160	5
15	381	355	4
16	628	609	5
17	1246	1144	32
18	568	558	2
19	851	750	26
20	986	913	22
21	1204	1209	-1
22	299	320	-2

4 k 6

0	2046	1949	33
1	2562	2475	26
2	1093	1071	8
3	1437	1355	31
4	499	449	14
5	518	593	-24
6	970	900	26
7	1891	1831	20
8	1349	1234	41
9	584	517	18
10	1317	1272	16
11	2855	2758	26
12	462	452	2
13	-214	17	-14
14	1063	962	32
15	385	436	-10
16	1020	928	28
17	714	744	-7
18	867	784	22
19	1836	1803	9
20	102	210	-7
21	1258	1197	17

4 k 7

1	599	521	22
2	2421	2469	-15
3	1053	1024	10
4	987	988	0
5	311	371	-12
6	1197	1154	15
7	740	756	-5
8	1199	1222	-8
9	726	698	8
10	2380	2303	22
11	161	205	-4
12	1825	1740	27
13	443	474	-6
14	398	408	-1

15	992	976	4
16	422	564	-29
17	-236	18	-13
18	598	564	7
19	668	618	10

4 k 8

0	1990	1918	23
1	879	851	9
2	453	403	10
3	1431	1441	-3
4	682	703	-6
5	877	872	1
6	1279	1293	-4
7	672	743	-21
8	1222	1279	-19
9	764	744	5
10	1434	1457	-7
11	1940	1878	18
12	1345	1354	-2
13	769	816	-12
14	407	479	-13
15	-210	18	-10
16	-84	253	-15
17	-155	192	-13

4 k 9

1	2302	2354	-15
2	257	93	14
3	1312	1310	0
4	1034	1084	-16
5	-244	47	-16
6	667	715	-12
7	327	508	-34
8	603	562	9
9	2411	2416	-1
10	328	224	12
11	-247	75	-15
12	459	500	-7
13	1664	1670	-1
14	819	762	14

4 k 10

0	1755	1786	-9
1	994	1021	-8
2	787	845	-15
3	-191	31	-8
4	-138	446	-49
5	809	821	-3
6	514	570	-11
7	971	956	4
8	1479	1447	9
9	-227	131	-15
10	1088	1182	-27

4 k 11

1	782	836	-13
2	1473	1649	-54
3	460	508	-8

5 k 0

1	1936	1925	5
2	3190	3181	2
3	1255	1250	2
4	502	511	-5
5	-209	40	-36
6	1047	1019	18
7	2125	2107	8
8	2173	2176	-1
9	2163	2126	16
10	3179	3230	-17
11	275	42	42
12	2228	2242	-6
13	455	436	8
14	1244	1185	31
15	1063	1029	18
16	1135	1105	15
17	1120	1125	-2
18	390	404	-4
19	258	202	10
20	2360	2401	-16
21	764	705	24
22	127	161	-3
23	977	905	28
24	1139	1099	16
25	683	665	5

5 k 1

0	1241	1130	51
1	2140	2095	17
2	701	652	22
3	2853	2817	11
4	442	439	1
5	1707	1625	33
6	360	343	5
7	1982	1999	-6
8	393	130	53
9	622	606	6
10	432	343	25
11	4411	4256	32
12	468	175	62
13	1385	1420	-14
14	-247	17	22
15	-141	69	-9
16	1037	974	23
17	228	142	9
18	574	470	26
19	2594	2566	8
20	378	102	33
21	1773	1799	-8
22	293	174	12
23	741	699	10
24	794	830	-9

5 k 2

1	2353	2454	-36
2	2606	2642	-11
3	1759	1762	-1
4	1832	1836	-1
5	771	795	-10
6	1297	1307	-4
7	130	179	-6
8	267	214	9
9	3238	3081	41
10	2002	1815	65
11	362	257	22
12	1903	1849	19
13	1553	1500	20
14	658	675	-5
15	193	120	7
16	-124	279	-30
17	846	832	5
18	1011	974	12
19	952	886	21
20	1715	1684	10
21	1704	1753	-15
22	680	558	27
23	620	731	-27
24	336	469	-21

5 k 3

0	4440	4734	-64
1	402	346	15
2	576	644	-26
3	449	585	-50
4	1178	1219	-18
5	1640	1590	20
6	276	231	8
7	275	53	27
8	2962	2794	47
9	926	855	27
10	1965	1840	43
11	329	78	35
12	2364	2248	36
13	1130	1098	12
14	732	595	44
15	719	644	23
16	94	185	-7
17	1108	1123	-5
18	2105	2098	2
19	456	387	13
20	459	312	24
21	202	148	4
22	2122	2080	11
23	651	584	14

5 k 4

1	2282	2360	-26
2	1729	1865	-55
3	619	664	-16
4	1539	1566	-11
5	468	498	-9
6	304	364	-14
7	853	854	0
8	1547	1519	10
9	1832	1711	42
10	1187	1136	19
11	302	47	28
12	973	901	25
13	1449	1406	15
14	1001	972	10
15	164	127	3
16	640	557	21
17	990	950	12
18	-169	7	-7
19	965	994	-9
20	1127	1085	12
21	1466	1386	23
22	650	538	23

5 k 5

0	536	558	-7
1	2007	2197	-70
2	606	677	-26
3	1190	1250	-24
4	-169	91	-14
5	801	757	15
6	1156	1126	11
7	1831	1783	16
8	922	917	1
9	395	218	31
10	485	324	34
11	2893	2729	44
12	159	61	6
13	72	10	1
14	976	918	18
15	307	310	0
16	1038	997	12
17	388	442	-9
18	-49	128	-4
19	1757	1643	33
20	349	188	17
21	1398	1273	35

5 k 6

1	267	301	-6
2	2237	2257	-6
3	1467	1443	8
4	512	512	0
5	792	814	-7
6	1240	1141	35
7	1017	950	23
8	891	941	-17
9	1275	1225	17
10	1861	1877	-5
11	421	456	-7
12	1781	1652	41
13	1023	986	11
14	323	361	-6
15	943	958	-4
16	-214	137	-15
17	-363	119	-36
18	-96	230	-13
19	688	606	17

5 k 7

0	2706	2693	3
1	638	731	-29
2	155	42	6
3	1350	1321	10
4	1155	1212	-20
5	1188	1200	-4
6	860	853	2
7	407	318	16
8	1301	1294	2
9	398	439	-8
10	1555	1503	17
11	1469	1423	14
12	1656	1588	21
13	1116	1024	27
14	351	378	-4
15	-88	263	-17
16	384	304	11
17	399	289	14

5 k 8

1	2071	2066	1
2	342	395	-9
3	1063	1030	10
4	1304	1302	0
5	-101	207	-14
6	142	289	-15
7	587	542	10
8	892	837	15
9	2329	2330	0
10	427	352	12
11	-154	36	-5
12	353	345	1
13	1461	1475	-4
14	954	995	-11

5 k 9

0	1750	1750	0
1	1475	1396	24
2	803	836	-9
3	793	834	-11
4	-98	290	-21
5	789	800	-2
6	522	640	-26
7	1046	1102	-17
8	1601	1630	-9
9	270	8	15
10	1183	1189	-1
11	1806	1783	6

5 k 10

1	330	419	-13
2	2022	2132	-32
3	930	973	-11
4	764	736	6
5	212	300	-9
6	487	616	-25

6 k 0

0	1268	1228	24
1	2430	2418	4

2	855	903	-31
3	4070	4122	-14
4	991	992	0
5	1937	1919	8
6	1649	1665	-8
7	697	735	-22
8	729	649	43
9	1021	1000	12
10	805	819	-8
11	2987	3000	-4
12	1411	1414	-1
13	951	949	1
14	-201	141	-33
15	-148	133	-20
16	546	584	-16
17	-246	13	-28
18	663	635	11
19	1916	1918	0
20	738	591	52
21	1692	1618	30
22	818	748	25
23	356	323	6
24	930	865	24

6 k 1

1	2774	2839	-20
2	2188	2161	9
3	1780	1685	37
4	2641	2659	-5
5	83	187	-12
6	1783	1747	14
7	204	175	4
8	334	176	30
9	2749	2581	49
10	1815	1777	14
11	607	456	46
12	1998	1949	17
13	1703	1741	-14
14	1273	1245	10
15	440	487	-12
16	287	222	9
17	1024	958	22
18	1179	1202	-8
19	1666	1600	22
20	1580	1569	3
21	1971	1974	-1
22	733	740	-1
23	929	935	-1

6 k 2

0	4290	4500	-47
1	546	551	-1
2	544	614	-26
3	321	376	-14
4	1213	1172	17
5	1379	1384	-1
6	-125	13	-6
7	643	641	0
8	2579	2501	24
9	659	524	43
10	2411	2344	21
11	450	219	47
12	1596	1556	14
13	1272	1212	22
14	1694	1695	0
15	209	195	1
16	368	391	-4
17	487	467	4
18	1863	1717	46
19	297	139	16
20	460	399	11
21	573	540	7
22	1920	1789	37
23	421	287	18

6 k 3

1	1149	1303	-69
2	2043	2141	-36
3	571	600	-10
4	928	941	-5
5	554	607	-18
6	-129	187	-20
7	731	744	-5
8	1662	1519	52
9	2007	1871	46
10	1911	1860	18
11	757	741	5
12	1241	1091	52
13	1051	967	29
14	1278	1208	24
15	1125	1094	10
16	573	595	-5
17	933	907	7
18	-210	122	-15
19	246	134	9
20	1877	1772	31
21	894	768	32
22	289	406	-16

6 k 4

0	310	316	-1
1	2177	2314	-48
2	551	581	-10
3	1345	1380	-13
4	-175	33	-11
5	186	313	-22
6	1168	1088	30
7	1623	1563	21
8	585	479	29
9	486	390	22
10	282	174	14
11	2819	2675	39
12	857	772	26
13	-209	88	-15
14	1000	891	34
15	511	536	-5
16	1230	1203	8
17	899	897	0
18	213	335	-15
19	1501	1467	10
20	376	68	27

6 k 5

1	978	1064	-33
2	2166	2359	-67
3	1353	1438	-33
4	772	885	-41
5	-135	124	-10
6	659	666	-2
7	879	886	-2
8	643	584	16
9	1351	1330	7
10	2027	1987	12
11	460	353	21
12	1927	1869	18
13	1091	1005	27
14	-60	80	-2
15	952	918	9
16	161	163	0
17	433	386	7
18	925	901	6
19	627	525	20

6 k 6

0	2541	2499	12
1	326	302	4
2	-255	28	-21
3	841	718	37
4	925	880	15
5	1376	1291	29
6	856	858	0
7	-157	26	-7
8	1644	1563	26
9	310	260	7
10	1833	1737	30
11	888	821	20
12	1472	1398	22
13	1056	1006	14
14	466	479	-2
15	-207	11	-10
16	-259	215	-26
17	1092	1066	7

6 k 7

1	2156	2118	11
2	808	729	23
3	688	665	6
4	1308	1294	4
5	-121	219	-17
6	448	417	5
7	960	942	5
8	1141	1105	11
9	2159	2204	-13
10	767	719	12
11	148	119	1
12	260	275	-1
13	1532	1418	33
14	1072	1118	-13
15	364	361	0

6 k 8

0	2073	1985	25
1	1863	1758	31
2	1007	954	15
3	1175	1225	-15
4	245	269	-2
5	756	794	-10
6	751	739	3
7	1121	1166	-13
8	1289	1291	0
9	-135	58	-4
10	976	982	-1
11	1815	1787	8
12	181	247	-5

6 k 9

1	388	339	7
2	2090	2217	-37
3	1228	1291	-18
4	532	566	-6
5	909	1012	-29
6	657	762	-25
7	1144	1154	-2

7 k 0

1	2254	2265	-4
2	1459	1431	15
3	924	988	-39
4	1782	1741	20
5	183	271	-23
6	1100	1077	13
7	352	409	-22
8	597	545	24
9	2920	2953	-11
10	834	665	83
11	287	269	5
12	1605	1617	-6
13	1734	1761	-12
14	905	931	-12
15	-142	246	-37
16	523	570	-18
17	1099	1101	0
18	881	870	4
19	1117	1105	5
20	1338	1266	30
21	1493	1454	16
22	290	206	12
23	907	948	-15

7 k 1

0	4192	4279	-19
1	1291	1236	22
2	1198	1172	11
3	-75	86	-5
4	1759	1763	-1
5	1463	1352	43
6	915	915	0
7	1260	1200	24
8	2010	1966	15
9	560	536	7
10	2209	2083	41
11	995	897	36
12	1664	1621	15
13	1101	1049	19
14	1525	1544	-7
15	666	530	37
16	983	1023	-14
17	1292	1264	9
18	1462	1383	25
19	545	507	8
20	582	695	-28
21	155	164	0
22	1804	1823	-5

7 k 2

1	1127	1200	-31
2	2098	2150	-18
3	-164	9	-10
4	938	898	15
5	454	553	-31
6	424	409	3
7	1540	1572	-12
8	1825	1750	26
9	1761	1781	-7
10	2277	2206	22
11	500	426	18
12	1294	1273	7
13	1462	1385	27
14	1335	1221	39
15	1814	1795	6
16	954	897	17
17	1013	1065	-16
18	379	347	5
19	177	18	7
20	2241	2237	0
21	817	909	-25

7 k 3

0	166	79	7
1	1540	1647	-42
2	1013	1079	-27
3	1612	1697	-33
4	578	556	6
5	59	215	-15
6	1305	1310	-1
7	1543	1562	-7
8	499	471	7
9	647	633	4
10	380	293	16
11	2870	2714	42
12	824	733	27
13	-169	63	-9
14	364	361	0
15	53	115	-2
16	460	433	5
17	468	538	-14
18	252	14	14
19	1738	1646	27
20	265	240	2

7 k 4

1	1091	1173	-31
2	1310	1449	-54
3	1517	1552	-12
4	1114	1156	-15
5	542	551	-2
6	731	845	-39
7	829	726	32
8	599	587	3
9	1869	1878	-3
10	1312	1258	18
11	205	2	11
12	1588	1587	0
13	1223	1184	17
14	493	432	11
15	935	920	4
16	-234	11	-13
17	159	266	-10
18	891	847	11
19	1345	1209	38

7 k 5

0	2935	3078	-40
1	106	14	3
2	-313	79	-33
3	1025	1052	-9
4	1082	1151	-24
5	1536	1559	-8
6	615	676	-17
7	-261	164	-28
8	1676	1610	21
9	573	579	-1
10	1525	1422	33
11	213	38	10
12	1855	1845	3
13	1215	1085	38
14	625	552	16
15	-129	316	-26
16	195	270	-7
17	692	698	-1

7 k 6

1	1956	1975	-6
2	1153	1162	-3
3	-193	77	-12
4	749	709	11
5	483	511	-6
6	150	302	-17
7	1112	1065	14
8	909	855	16
9	2098	2147	-14
10	840	742	25
11	266	89	13
12	-135	95	-6
13	1158	1196	-11
14	1132	1073	16
15	774	636	30

7 k 7

0	813	837	-6
1	1800	1781	6
2	1029	956	21
3	851	761	23
4	183	228	-4
5	633	639	-1
6	1139	1128	3
7	1497	1450	14
8	793	740	13
9	-189	116	-11
10	707	630	17
11	1955	1939	4
12	484	360	19

7 k 8

1	273	141	11
2	1811	1834	-6
3	891	846	11
4	447	561	-22
5	714	777	-15
6	908	940	-8
7	988	1005	-4

8 k 0

0	2081	2177	-43
1	852	840	6
2	669	657	6
3	101	52	4
4	333	438	-41
5	1545	1568	-12
6	321	365	-15
7	997	1044	-26
8	1847	1877	-14
9	251	120	23
10	1694	1714	-9
11	1183	1229	-24
12	1085	1187	-54
13	905	949	-21
14	1068	1115	-23
15	357	422	-19
16	595	584	4
17	1498	1476	9
18	1048	977	29
19	424	295	28
20	339	250	16
21	914	916	0

8 k 1

1	1960	2083	-46
2	2743	2831	-27
3	751	762	-4
4	322	230	17
5	633	641	-2
6	1042	1077	-13
7	2182	2163	6
8	1642	1561	29
9	1615	1493	43
10	2651	2557	27
11	501	433	16
12	1571	1525	16
13	374	234	22
14	493	445	11
15	1498	1402	32
16	565	492	16
17	1410	1414	-1
18	742	677	16
19	596	566	6
20	1823	1659	47

8 k 2

0	1015	1012	1
1	1327	1344	-6
2	1126	1154	-10
3	1772	1856	-31
4	927	962	-13
5	944	987	-16
6	1476	1440	13
7	1566	1477	31
8	258	191	8
9	693	657	12
10	619	459	40
11	2961	2929	8
12	1085	890	61
13	797	712	24
14	370	284	13
15	137	290	-16
16	1254	1248	1
17	148	235	-7
18	931	943	-3
19	1730	1743	-3

8 k 3

1	1818	1858	-14
2	1249	1316	-25
3	1462	1454	2
4	1829	1885	-20
5	-155	162	-16
6	1215	1277	-23
7	302	249	8
8	330	311	3
9	2291	2242	15
10	1126	1097	9
11	624	611	3
12	1774	1645	41
13	1506	1416	28
14	866	929	-21
15	738	669	17
16	194	24	8
17	302	260	5
18	911	908	0

8 k 4

0	3092	3145	-14
1	408	320	16
2	96	223	-11
3	840	880	-12
4	1008	1096	-31
5	1183	1104	26
6	146	270	-14
7	599	640	-11
8	1736	1657	25
9	619	659	-10
10	1107	957	44
11	-196	105	-12
12	1332	1280	16
13	757	645	27
14	268	409	-20
15	293	298	0
16	49	197	-7

8 k 5

1	1140	1241	-35
2	1393	1533	-49
3	-98	354	-34
4	764	901	-41
5	253	262	-1
6	-162	145	-12
7	1188	1131	17
8	1311	1290	6
9	1464	1463	0
10	955	893	17
11	588	583	1
12	521	545	-4
13	1014	917	26
14	1270	1236	9

8 k 6

0	259	362	-14
1	1109	1150	-12
2	1216	1173	13
3	662	698	-8
4	-286	37	-20
5	230	281	-5
6	1584	1536	14
7	1329	1258	21
8	619	669	-11
9	262	304	-5
10	76	8	1
11	2097	2109	-3

8 k 7

1	426	489	-11
2	1696	1697	0
3	1360	1239	35
4	441	467	-4
5	296	249	5
6	414	537	-22
7	977	912	19

9 k 0

1	1441	1373	34
2	2994	2994	0
3	1124	1120	2
4	244	57	27
5	1206	1232	-13
6	610	686	-35
7	1395	1331	31
8	969	1009	-21
9	474	357	37
10	1703	1663	18
11	233	249	-3
12	1384	1471	-43
13	-158	118	-16
14	779	809	-12
15	1138	1057	33
16	567	557	3
17	596	456	40
18	319	261	10
19	268	103	18

9 k 1

0	949	891	20
1	1653	1696	-16
2	804	835	-11
3	2410	2405	1
4	1125	1080	16
5	1182	1200	-6
6	1590	1640	-18
7	878	858	7
8	289	251	6
9	811	799	4
10	539	419	28
11	2410	2320	26
12	1280	1243	12
13	1106	1133	-8
14	575	687	-28
15	315	134	18
16	1458	1456	0
17	392	455	-11
18	664	548	24

9 k 2

1	1616	1707	-33
2	1166	1265	-37
3	1040	987	18
4	2433	2459	-7
5	334	267	11
6	1291	1384	-34
7	258	339	-13
8	718	593	34
9	1965	1941	7
10	1181	1225	-15
11	337	314	3
12	1452	1532	-26
13	1452	1400	16
14	1061	1062	0
15	298	217	9
16	454	355	16
17	565	644	-17

9 k 3

0	2243	2332	-28
1	829	889	-19
2	375	333	7
3	251	433	-34

4	752	746	1
5	1700	1752	-18
6	203	39	10
7	686	661	6
8	1325	1296	9
9	600	559	9
10	1652	1637	4
11	632	510	26
12	1096	1032	18
13	1296	1290	1
14	1184	1184	0
15	318	425	-16

9 k 4

1	1255	1245	3
2	1576	1568	2
3	228	198	3
4	833	789	12
5	599	625	-6
6	-138	95	-7
7	995	916	22
8	1322	1265	17
9	884	851	10
10	1427	1449	-7
11	270	326	-7
12	766	784	-4
13	444	327	17

9 k 5

0	200	65	8
1	1161	1135	8
2	767	765	0
3	821	894	-20
4	256	347	-12
5	103	268	-14
6	1328	1311	5
7	807	767	10
8	429	571	-28
9	-266	53	-17
10	-181	41	-7

9 k 6

1	743	775	-8
2	762	720	10
3	1436	1433	0
4	651	610	8
5	372	416	-6
6	680	669	2

10 k 0

0	1627	1660	-15
1	1249	1288	-19
2	686	686	0
3	1735	1735	0

4	812	849	-18
5	1169	1087	39
6	1419	1441	-10
7	853	774	35
8	655	679	-10
9	374	343	7
10	892	921	-13
11	1721	1648	30
12	1548	1508	17
13	1313	1222	38
14	-186	18	-12
15	349	361	-2
16	825	802	8
17	194	137	5

10 k 1

1	1654	1755	-36
2	487	541	-13
3	1092	1091	0
4	1927	1958	-10
5	-213	38	-14
6	799	804	-1
7	84	147	-4
8	845	850	-1
9	2133	2097	10
10	588	514	16
11	319	244	9
12	1360	1290	21
13	1394	1392	0
14	1197	1171	7
15	394	99	29
16	999	949	14

10 k 2

0	1963	2087	-41
1	1051	1031	6
2	831	887	-19
3	-123	124	-8
4	328	389	-10
5	1580	1591	-3
6	678	656	5
7	986	840	43
8	1867	1868	0
9	496	468	5
10	1722	1694	8
11	782	522	57
12	1042	1049	-2
13	1285	1339	-16
14	1127	1256	-39

10 k 3

1	1013	1092	-25
2	1711	1683	8
3	258	363	-15
4	786	741	13

5	602	683	-20
6	61	8	0
7	1209	1203	1
8	1180	1207	-8
9	589	581	1
10	1249	1258	-2
11	353	304	6
12	889	904	-4

10 k 4

0	636	570	14
1	974	964	2
2	904	917	-3
3	904	985	-23
4	675	661	3
5	-207	77	-11
6	1427	1451	-7
7	1039	1072	-9
8	111	38	2
9	221	135	6

10 k 5

1	701	786	-21
2	489	479	1
3	1253	1245	2
4	803	748	13

11 k 0

1	1288	1322	-16
2	216	261	-7
3	659	719	-25
4	1574	1592	-8
5	-161	16	-9
6	542	409	38
7	306	342	-7
8	1020	1017	1
9	1834	1750	33
10	162	6	8
11	306	209	15
12	376	333	9
13	988	942	18
14	1230	1198	12

11 k 1

0	1718	1750	-10
1	1017	1057	-12
2	526	626	-24
3	-170	232	-21
4	57	137	-3
5	1602	1582	6
6	714	660	13
7	1051	987	18
8	1312	1403	-29
9	450	345	17

10	742	841	-27
11	1048	1040	2
12	345	336	1

11 k 2

1	762	773	-2
2	1415	1460	-14
3	1166	1222	-17
4	644	623	5
5	763	755	2
6	215	330	-14
7	1394	1455	-19
8	1468	1462	1
9	719	797	-20
10	1560	1547	3

11 k 3

0	718	625	21
1	1072	1142	-21
2	977	1008	-9
3	1123	1172	-14
4	735	765	-7
5	580	666	-19
6	1299	1266	9
7	584	574	2

12 k 0

0	1177	1129	20
1	964	949	6
2	748	759	-3
3	-229	39	-18
4	-262	21	-24
5	1050	1052	0
6	744	636	36
7	875	895	-7
8	1060	987	28
9	258	216	6
10	538	496	11

12 k 1

1	275	339	-8
2	1449	1429	6
3	1140	1105	10
4	-102	303	-23
5	682	692	-2
6	321	370	-7
7	1216	1103	31

12 k 2

0	870	803	17
1	729	733	0
2	910	900	2

Appendix 2

```
C PROGRAM DIFFAN
C
      OPTIONS/G_FLOATING
      PARAMETER (LW=1000,LIW=LW/8+2)
      IMPLICIT DOUBLE PRECISION (A-H,O-Z)
      INTEGER IW(LIW)
      DIMENSION W(LW)
      EXTERNAL F,D01AJF
      COMMON/CONST/AK,C,KOUNT
      READ(5,101) IZA,IZB,X1,SI,T,RA,RB,OBSK,DA,DB,N
  101 FORMAT(2I4,F4.2,E10.4,F6.2,2F4.2,E9.3,2E10.4,I5)
      TK = 273.15 + T
      AB = RA + RB
      IF (X1.EQ.0) X1 = AB
      DIEL = EXP(3.69031 - 0.00430493*T)
      ETA = EXP(885.636/TK - 4.03662)
      AID = SI/(DIEL*TK)
      AK = 50.2900016*SQRT(AID)
      TB = IZA*IZB*167102.4/(DIEL*TK)
      BB = TB/X1
      CHK = ABS(IZA*IZB)
      IF (CHK.GT.0) GO TO 1
      RESULT = 1.0/X1
      GO TO 2
    1 DC = EXP(AK*X1)/(1.0 + AK*X1)
      C = TB*DC
      EPSABS = 0.0
      EPSREL = 1.0E-5
      A = X1
      B = N*X1
      KOUNT = 0
      IFAIL = -1
      CALL D01AJF(F,A,B,EPSABS,EPSREL,RESULT,ABSERR,W,LW,IW,LIW,IFAIL)
      IF (IFAIL .NE. 0) THEN
         WRITE(6,1001) IFAIL
 1001    FORMAT(' D01AJF FAILED. IFAIL = ',I2)
         STOP
      END IF
    2 FF = 1.0/(RESULT*X1)
      PDC = 7.3246393*TK/(ETA*10.0**8)
      DAA = PDC/RA
      IF (DA.GT.0) GO TO 3
      DA = DAA
    3 DBB = PDC/RB
      IF (DB.GT.0) GO TO 4
      DB = DBB
    4 DK = 75.675251*AB*FF*(DA + DB)*10.0**12
      DHF = EXP(BB/(1.0 + X1*AK))
      BDK = 3.0*(DA + DB)*FF*DHF*10.0**16/AB/AB
      EQK00 = 0.0025225083*AB*AB*AB
      EQK = EQK00/DHF
      EQK0 = EQK00/EXP(BB)
      ACTK = BDK/(DK/OBSK - 1.0)
      ACT1 = 1.0/(1.0/OBSK - 1.0/DK)
      WRITE(6,103) IZA,IZB,T,SI,X1,RA,RB,OBSK,DA,DB
  103 FORMAT(5X,'CHARGE ON ION A = ',I4,/5X'CHARGE ON ION B = ',I4,
     */5X,'TEMPERATURE (DEG. CELCIUS) = ',F6.2,/5X,'IONIC STRENGTH
     *(MOLES/LITER) = ',E10.4,/5X,'A-B SEPERATION DISTANE (A) = ',F5.2,
     */5X,'RADIUS OF ION A (A) = ',F5.2,/5X,'RADIUS OF ION B (A) = ',
     *F5.2,/5X,'OBSERVED RATE CONSTANT (1/Msec) = ',E9.3,/5X,'DIFFUSION
     *CONSTANT FOR ION A (CM2/SEC) = ',E10.4,/5X,'DIFFUSION CONSTANT
     *FOR ION B (CM2/SEC) = ',E10.4)
      WRITE(6,104)
  104 FORMAT(//3X,'THE CALCULATED PARAMETERS:')
```

```
      WRITE(6,105)DIEL,ETA,BB,AK,FF,DHF,DAA,DBB
  105 FORMAT(5X,'DIELETRIC CONSTANT OF CH3CN = ',F6.3,/5X,'VISCOSITY OF
     *CH3CN =',F7.4,/5X,'DEBYE-HUCKEL PARAMETER, B , = ',E12.6,/5X,'DEBYE-
     *HUCKEL PARAMETER, KAPPA (A-1), = ',E12.5,/5X,'DEBYE CHARGE-IONIC ATMOS
     *PHERE PARAMETER, F, = ',E12.6,/5X,'EIGEN-FUOSS k-d IONIC
     *PARAMETER = ',E12.6,/5X,'THE CALCULATED DIFFUSION COEFFICIENT OF
     *ION A (CM2/SEC) = ',E10.4,/5X,'THE CALCULATED DIFFUSION COEFFICIENT
     *OF ION B (CM2/SEC) = ',E10.4)
      WRITE(6,106)
  106 FORMAT(//3X,'THE CALCULATED RESULTS ARE:')
      WRITE(6,107)DK,BDK,EQK,EQK0,ACTK,ACT1
  107 FORMAT(5X,'DIFFUSION CONTROLLED RATE,(1/Msec) = ',E10.4,/5X,'DISSOCIA
     *TION RATE (1/SEC) = ',E10.4,/5X,'EQUILIBRIUM CONSTANT (MOLES/LITER)
     *= ',E10.4,/5X,'EQUILIBRIUM CONSTANT AT ZERO IONIC STRENGTH (MOLES/LITER)
     *= ',E10.4,/5X,'ACTIVATED 1ST ORDER RATE CONSTANT (1/SEC) = ',E10.4,
     */5X,'ACTIVATED 2ND ORDER RATE CONSTANT (1/Msec) = ',E10.4)
      WRITE(6,108)RESULT,KOUNT,IFAIL,ABSERR,IW(1)
  108 FORMAT(/5X,'RESULT = ',F10.4,5X,'KOUNT = ',I4,5X,'IFIAL = ',I4,
     */5X,'ABSERR = ',E10.4,5X,'IW(1) = ',I4)
      END
      REAL*8 FUNCTION F(X)
      IMPLICIT DOUBLE PRECISION (A-H,O-Z)
      COMMON/CONST/AK,C,KOUNT
      INTEGER KOUNT
      KOUNT = KOUNT + 1
      F = EXP(C/(X*EXP(AK*X)))/(X**2)
      RETURN
      END
```

Results for 4-cyano-N-methylpyridinium.

```
CHARGE ON ION A =     1
CHARGE ON ION B =     2
TEMPERATURE (DEG. CELCIUS) =  22.ØØ
IONIC STRENGTH (MOLES/LITER) = Ø.1ØØØE+ØØ
A-B SEPERATION DISTANE (A) = 11.19
RADIUS OF ION A (A) =  3.34
RADIUS OF ION B (A) =  7.85
OBSERVED RATE CONSTANT (1/Msec) = Ø.45ØE+Ø9
DIFFUSION CONSTANT FOR ION A (CM2/SEC) = Ø.1824E-Ø4
DIFFUSION CONSTANT FOR ION B (CM2/SEC) = Ø.776ØE-Ø5
UPPER BOUND OF INTEGRATION,N*X1, N =   1ØØ

THE CALCULATED PARAMETERS:
  DIELETRIC CONSTANT OF CH3CN = 36.438
  VISCOSITY OF CH3CN = Ø.3549
  DEBYE-HUCKEL PARAMETER, B , = Ø.2777Ø9E+Ø1
  DEBYE-HUCKEL PARAMETER, KAPPA (A-1), =  Ø.15335E+ØØ
  DEBYE CHARGE-IONIC ATMOSPHERE PARAMETER, F, = Ø.75Ø328E+ØØ
  EIGEN-FUOSS k-d IONIC PARAMETER = Ø.278Ø12E+Ø1
  THE CALCULATED DIFFUSION COEFFICIENT OF ION A (CM2/SEC) = Ø.1824E-Ø4
  THE CALCULATED DIFFUSION COEFFICIENT OF ION B (CM2/SEC) = Ø.776ØE-Ø5

THE CALCULATED RESULTS ARE:
  DIFFUSION CONTROLLED RATE,(1/Msec) = Ø.1652E+11
  DISSOCIATION RATE (1/SEC) = Ø.1299E+11
  EQUILIBRIUM CONSTANT (MOLES/LITER) = Ø.1271E+Ø1
  EQUILIBRIUM CONSTANT AT ZERO IONIC STRENGTH (MOLES/LITER) = Ø.2199E+ØØ
  ACTIVATED 1ST ORDER RATE CONSTANT (1/SEC) = Ø.3639E+Ø9
  ACTIVATED 2ND ORDER RATE CONSTANT (1/Msec) = Ø.4626E+Ø9

  RESULT = .119101994     KOUNT =  273     IFIAL =    Ø
  ABSERR = Ø.572ØE-Ø9     IW(1) =   28
```

Results for 4-carbomethoxy-N-methylpyridinium.

```
  CHARGE ON ION A =     1
  CHARGE ON ION B =     2
  TEMPERATURE (DEG. CELCIUS) =  22.00
  IONIC STRENGTH (MOLES/LITER) = 0.1000E+00
  A-B SEPERATION DISTANE (A) = 11.72
  RADIUS OF ION A (A) =  3.87
  RADIUS OF ION B (A) =  7.85
  OBSERVED RATE CONSTANT (1/Msec) = 0.330E+09
  DIFFUSION CONSTANT FOR ION A (CM2/SEC) = 0.1574E-04
  DIFFUSION CONSTANT FOR ION B (CM2/SEC) = 0.7760E-05
  UPPER BOUND OF INTEGRATION,N*X1, N =   100


THE CALCULATED PARAMETERS:
  DIELETRIC CONSTANT OF CH3CN = 36.438
  VISCOSITY OF CH3CN = 0.3549
  DEBYE-HUCKEL PARAMETER, B , = 0.265150E+01
  DEBYE-HUCKEL PARAMETER, KAPPA (A-1), =  0.15335E+00
  DEBYE CHARGE-IONIC ATMOSPHERE PARAMETER, F, = 0.773665E+00
  EIGEN-FUOSS k-d IONIC PARAMETER = 0.258026E+01
  THE CALCULATED DIFFUSION COEFFICIENT OF ION A (CM2/SEC) = 0.1574E-04
  THE CALCULATED DIFFUSION COEFFICIENT OF ION B (CM2/SEC) = 0.7760E-05


THE CALCULATED RESULTS ARE:
  DIFFUSION CONTROLLED RATE,(1/Msec) = 0.1613E+11
  DISSOCIATION RATE (1/SEC) = 0.1025E+11
  EQUILIBRIUM CONSTANT (MOLES/LITER) = 0.1574E+01
  EQUILIBRIUM CONSTANT AT ZERO IONIC STRENGTH (MOLES/LITER) = 0.2865E+00
  ACTIVATED 1ST ORDER RATE CONSTANT (1/SEC) = 0.2141E+09
  ACTIVATED 2ND ORDER RATE CONSTANT (1/Msec) = 0.3369E+09

  RESULT = .110285706     KOUNT =  273     IFIAL =    0
  ABSERR = 0.4390E-09     IW(1) =   28
```

Results for 3-carbomethoxy-N-benzylpyridinium.

```
CHARGE ON ION A =     1
CHARGE ON ION B =     2
TEMPERATURE (DEG. CELCIUS) =  22.00
IONIC STRENGTH (MOLES/LITER) = 0.1000E+00
A-B SEPERATION DISTANE (A) = 12.49
RADIUS OF ION A (A) =  4.64
RADIUS OF ION B (A) =  7.85
OBSERVED RATE CONSTANT (1/Msec) = 0.280E+08
DIFFUSION CONSTANT FOR ION A (CM2/SEC) = 0.1313E-04
DIFFUSION CONSTANT FOR ION B (CM2/SEC) = 0.7760E-05
UPPER BOUND OF INTEGRATION,N*X1, N =   100

THE CALCULATED PARAMETERS:
 DIELETRIC CONSTANT OF CH3CN = 36.438
 VISCOSITY OF CH3CN = 0.3549
 DEBYE-HUCKEL PARAMETER, B , = 0.248804E+01
 DEBYE-HUCKEL PARAMETER, KAPPA (A-1), =  0.15335E+00
 DEBYE CHARGE-IONIC ATMOSPHERE PARAMETER, F, = 0.802966E+00
 EIGEN-FUOSS k-d IONIC PARAMETER = 0.234768E+01
 THE CALCULATED DIFFUSION COEFFICIENT OF ION A (CM2/SEC) = 0.1313E-04
 THE CALCULATED DIFFUSION COEFFICIENT OF ION B (CM2/SEC) = 0.7760E-05

THE CALCULATED RESULTS ARE:
 DIFFUSION CONTROLLED RATE,(1/Msec) = 0.1585E+11
 DISSOCIATION RATE (1/SEC) = 0.7573E+10
 EQUILIBRIUM CONSTANT (MOLES/LITER) = 0.2094E+01
 EQUILIBRIUM CONSTANT AT ZERO IONIC STRENGTH (MOLES/LITER) = 0.4083E+00
 ACTIVATED 1ST ORDER RATE CONSTANT (1/SEC) = 0.1340E+08
 ACTIVATED 2ND ORDER RATE CONSTANT (1/Msec) = 0.2805E+08

 RESULT = .099710350      KOUNT =  273     IFIAL =    0
 ABSERR = 0.3123E-09      IW(1) =   28
```

Appendix 3

Table A3.1. U_{ij}'s, Ir atoms.

Atom	U_{11}	U_{22}	U_{33}	U_{12}	U_{13}	U_{23}
IR1	275(9)	371(9)	250(8)	−12(9)	42(7)	−19(8)
IR2	346(10)	366(9)	251(8)	−42(10)	21(7)	6(8)

The form of the displacement factor is:
$\exp -2\pi^2(U_{11}h^2a^{*2} + U_{22}k^2b^{*2} + U_{33}\ell^2c^{*2} + 2U_{12}hka^*b^* + 2U_{13}h\ell a^*c^* + 2U_{23}k\ell b^*c^*)$

Table A3.2. Hydrogen coordinates.

x, y and $z \times 10^4$

Atom	x	y	z	B
H1	−1095	2527	2873	5.0
H2	3266	2577	4413	5.0
H3A	2411	1074	2073	6.0
H3B	2135	1180	2620	6.0
H3C	1087	1247	2213	6.0
H4A	2651	1741	1469	6.0
H4B	1319	1897	1621	6.0
H4C	2489	2195	1698	6.0
H5A	4288	1554	2262	6.0
H5B	3754	1694	2766	6.0
H6A	3704	2418	2290	6.0
H6B	4920	2209	2086	6.0
H7A	6701	1994	2801	6.0
H7B	6416	2133	3338	6.0
H7C	5600	1779	3079	6.0
H8A	6370	2766	2480	6.0
H8B	5102	2994	2596	6.0
H8C	6119	2921	3013	6.0
H13A	3152	3707	2011	6.0
H13B	3205	3301	2346	6.0
H13C	2139	3348	1942	6.0
H14A	1425	4277	2167	6.0
H14B	386	3928	2085	6.0
H14C	478	4179	2581	6.0
H15A	3296	4092	2841	6.0
H15B	3103	3669	3136	6.0
H16A	1106	4087	3287	6.0
H16B	2149	4440	3297	6.0
H17A	1553	4563	4208	6.0
H17B	635	4172	4202	6.0
H17C	1778	4185	4575	6.0
H18A	3871	4435	4025	6.0
H18B	3845	4045	4384	6.0
H18C	4247	3980	3842	6.0
H23A	−2994	3941	4336	6.0
H23B	−1635	3853	4154	6.0
H23C	−2798	3785	3799	6.0
H24A	−4483	3244	4470	6.0
H24B	−4246	3144	3918	6.0
H24C	−3906	2804	4322	6.0
H25A	−2383	3376	5026	6.0
H25B	−1112	3289	4768	6.0
H26A	−2160	2564	4757	6.0
H26B	−2546	2753	5262	6.0
H27A	−1507	2088	5654	6.0

Atom	x	y	z	U_{eq} or B
H27B	−1035	1934	5145	6.0
H27C	−63	2049	5566	6.0
H28A	−837	2879	5921	6.0
H28B	521	2750	5769	6.0
H28C	−144	3146	5525	6.0
H33A	−2779	1088	4370	6.0
H33B	−2179	1531	4504	6.0
H33C	−3108	1491	4052	6.0
H34A	−1937	708	3573	6.0
H34B	−2355	1122	3290	6.0
H34C	−979	951	3248	6.0
H35A	−529	838	4420	6.0
H35B	36	1298	4461	6.0
H36A	823	1047	3609	6.0
H36B	935	628	3921	6.0
H37A	2337	696	4782	6.0
H37B	3116	1116	4857	6.0
H37C	1652	1124	4902	6.0
H38A	3349	625	3951	6.0
H38B	3330	1016	3594	6.0
H38C	4075	1043	4095	6.0
H112	7761	3434	1331	4.0
H113	8737	3251	2072	5.0
H114	8060	3590	2811	6.0
H115	6445	4055	2791	5.0
H116	5295	4211	2042	4.0
H122	8269	4182	1075	4.0
H123	9585	4570	534	5.0
H124	8589	4930	−139	6.0
H125	6451	4855	−290	5.0
H126	5271	4456	230	4.0
H132	5279	4820	1319	4.0
H133	3274	5205	1477	5.0
H134	1425	4896	1286	6.0
H135	1276	4202	1022	5.0
H136	3099	3790	875	4.0
H142	4567	3189	1378	4.0
H143	3976	2553	975	5.0
H144	4267	2468	152	6.0
H145	5186	2992	−278	5.0
H146	5926	3627	80	4.0
H212	8123	1149	1744	4.0
H213	9252	1736	2111	5.0
H214	8497	2429	1965	6.0
H215	6714	2522	1453	5.0

Atom	x	y	z	U_{eq} or B
H216	5673	1934	1074	4.0
H222	5927	1133	2187	4.0
H223	5564	629	2824	5.0
H224	5155	−70	2628	6.0
H225	5243	−316	1826	5.0
H226	5864	155	1222	4.0
H232	8726	1031	839	4.0
H233	9826	610	296	5.0
H234	8807	169	−248	6.0
H235	6614	116	−245	5.0
H236	5405	440	381	4.0
H242	5423	1546	380	4.0
H243	3404	1666	−52	5.0
H244	1530	1440	275	6.0
H245	1521	941	865	5.0
H246	3463	761	1313	4.0

Table A3.3. Structure Factors.

The columns contain, in order k, $10F_o$, $10F_c$, and $10[(F_o^2-F_c^2)/\sigma(F_o^2)]$.

Di-iridium complex.

-7 k 1

1	586	-125	11
2	558	52	10
3	-323	239	-5
4	362	-255	2
5	549	-417	4
6	-529	-160	-11
7	-245	148	-3
8	465	23	8
9	728	-642	4

-7 k 2

0	2035	-1881	12
1	109	-368	-4
2	2017	2050	-3
3	-559	145	-11
4	1949	-1954	0
5	271	-310	0
6	1567	1567	0
7	127	133	0
8	1651	-1512	14
9	-288	82	-3

-7 k 3

1	714	-45	17
2	599	332	8
3	514	227	7
4	-489	7	-8
5	258	-240	0
6	363	-487	-3
7	-58	433	-7
8	912	783	8

-7 k 4

0	1193	1274	-4
1	3027	-2990	5
2	845	-1005	-9
3	2496	2540	-5
4	1087	925	10
5	2482	-2375	14
6	909	-676	13
7	2446	2357	12
8	579	557	0

-7 k 5

1	546	117	9
2	-405	-46	-5
3	-358	-455	-11
4	651	383	9
5	232	297	-1
6	-535	-198	-11
7	523	-560	-1

-7 k 6

0	3070	3021	5
1	1472	1577	-9
2	2723	-2820	-13
3	1259	-1135	9
4	2882	2805	11
5	1607	1489	11
6	2782	-2762	2

-7 k 7

1	-345	110	-4
2	-306	151	-3
3	587	240	9
4	-202	-204	-2
5	622	591	1

-7 k 8

0	1680	-1795	-7
1	2628	2709	-10
2	1876	1869	0
3	2377	-2352	3

-6 k 1

1	166	250	-1
2	-146	192	-2
3	462	-288	5
4	797	82	26
5	569	-202	12
6	903	855	3
7	-79	330	-5
8	870	-929	-4
9	600	-621	-1
10	638	711	-4
11	-272	350	-8
12	828	-999	-12
13	647	-57	17
14	1251	1265	-1

-6 k 2

0	3242	-3268	-3
1	1360	1396	-3
2	3386	3344	7
3	1415	-1344	7
4	2616	-2658	-6
5	1716	1703	1
6	2997	3001	0
7	1644	-1648	0
8	3297	-3157	24
9	1738	1706	4
10	2651	2549	16
11	966	-1270	-27
12	2226	-2310	-12
13	1193	1306	-11
14	2244	2267	-3

-6 k 3

1	-511	-169	-11
2	761	-453	14
3	583	657	-3
4	339	251	2
5	751	-607	8
6	-234	-283	-5
7	186	251	-1
8	775	547	12
9	894	-626	17
10	-237	-263	-5
11	1096	1051	3
12	-476	486	-19
13	1238	-1133	9

-6 k 4

0	1445	-1477	-2
1	3700	-3690	1
2	1625	1484	15
3	2810	2822	-1
4	1098	-1250	-14
5	3125	-3108	2
6	1403	1300	11
7	3269	3257	2
8	845	-1039	-15
9	3131	-2978	25
10	700	738	-2
11	3133	3129	0
12	1015	-1089	-6
13	2609	-2678	-10

-6 k 5

1	278	150	2
2	589	-228	11
3	-534	-213	-13
4	518	453	2
5	-609	40	-15
6	1000	-783	15
7	390	-381	0
8	941	890	3
9	491	387	3
10	509	-651	-6
11	711	-309	17
12	1066	1044	1
13	645	598	2

-6 k 6

0	3447	3606	-18
1	-90	-802	-23
2	3118	-2972	22
3	596	487	4
4	2624	2687	-10
5	654	-358	12
6	2188	-2064	18
7	-215	460	-10
8	2750	2835	-14
9	-82	-500	-10
10	2408	-2283	18
11	-509	310	-15
12	2131	2371	-36

-6 k 7

1	425	66	6
2	-802	130	-24
3	567	-522	1
4	-461	140	-9
5	432	437	0
6	483	303	6
7	791	-294	22
8	718	-228	19
9	491	542	-2
10	695	649	2
11	731	-693	2

-6 k 8

0	1014	619	14
1	2346	2174	22
2	483	-608	-5
3	1572	-1486	9
4	387	26	5
5	1614	1697	-10
6	267	252	0
7	1742	-1644	12
8	454	19	8
9	1755	1768	-1
10	277	127	2
11	1465	-1423	4

-6 k 9

1	-339	-58	-3
2	-237	151	-2
3	260	201	1
4	-185	-47	-1
5	-343	-268	-7
6	217	167	0
7	-469	99	-9
8	-693	-168	-21
9	289	-100	3
10	475	284	5

-6 k 10

0	-856	-221	-17
1	-548	267	-12
2	578	193	10
3	-538	112	-10
4	-347	28	-4
5	386	-3	5
6	723	545	8
7	688	61	19
8	484	-221	7

-6 k 11

1	-151	40	0
2	480	-147	7
3	-151	-13	0
4	606	-138	13
5	-253	126	-3
6	-72	376	-5
7	433	57	7

-6 k 12

0	-455	-34	-4
1	1456	1448	0
2	-209	218	-3
3	1354	-1235	10
4	739	-83	20

-5 k 1

1	531	-416	4
2	-398	127	-8
3	1319	-1310	1
4	628	-654	-1
5	373	223	4
6	242	163	1
7	329	-481	-6
8	765	-692	5
9	605	345	12
10	1004	1058	-5
11	342	-572	-10
12	1415	-1435	-2
13	721	607	7
14	1310	1139	18
15	848	-866	-1
16	1393	-1272	13
17	683	718	-2

-5 k 2

0	1474	-1352	10
1	3690	3768	-14
2	1524	1319	24
3	3631	-3634	0
4	1578	-1587	-1
5	3906	3829	14
6	1278	1202	9
7	3071	-3070	0
8	1840	-1816	3
9	3386	3324	11
10	1282	1223	6
11	2632	-2708	-13
12	1454	-1202	29
13	2466	2384	14
14	702	816	-7
15	2267	-2317	-7
16	689	-914	-14
17	2506	2466	6

-5 k 3

1	310	114	3
2	870	620	18
3	384	114	6
4	642	524	6
5	588	-412	9
6	-668	255	-26
7	1135	1029	11
8	-271	-219	-6
9	377	-552	-8
10	364	168	5
11	1177	1053	12
12	828	-581	16
13	1274	-1267	0

14	570	649	-4
15	1181	1189	0
16	-36	-473	-9

-5 k 4

0	2415	-2352	7
1	1024	-1036	-1
2	3015	2986	5
3	1786	1760	3
4	2508	-2447	10
5	1718	-1632	12
6	2141	1926	35
7	1398	1289	13
8	1720	-1710	1
9	1444	-1384	7
10	1799	1884	-13
11	1236	1299	-7
12	2028	-2064	-5
13	1011	-920	7
14	1998	2008	-1
15	1171	1240	-6
16	1348	-1282	6

-5 k 5

1	-239	-11	-2
2	350	-480	-4
3	567	61	15
4	449	234	7
5	414	-332	3
6	435	360	3
7	128	-47	0
8	391	334	2
9	-415	-208	-11
10	612	-526	4
11	-423	-122	-9
12	600	357	11
13	99	-179	-1
14	1188	-941	22
15	703	644	3
16	422	789	-18

-5 k 6

0	510	798	-10
1	928	-1027	-7
2	736	-618	7
3	1168	1152	1
4	660	661	0
5	610	-356	12
6	1375	-1315	7
7	984	890	8
8	938	939	0
9	816	-697	8
10	1140	-966	17
11	1064	996	6
12	713	985	-20
13	703	-513	10
14	421	-611	-8
15	309	311	0

-5 k 7

1	-368	330	-10
2	473	-462	0
3	243	-358	-3
4	321	-276	1
5	124	76	0
6	248	132	2
7	-551	-247	-18
8	-198	377	-8
9	673	-659	0
10	312	-564	-10
11	458	586	-6
12	732	304	20
13	-504	-116	-12
14	-413	-136	-8
15	94	-137	0

-5 k 8

0	708	-894	-7
1	-340	-522	-15
2	781	592	11
3	362	323	1
4	492	-410	3
5	-141	1	-1
6	695	367	16
7	273	-102	3
8	487	-525	-1
9	-211	-112	-2
10	414	375	1
11	315	-70	4
12	520	-845	-19
13	-403	-91	-7
14	501	115	10

-5 k 9

1	553	-22	12
2	481	25	9
3	619	-337	12
4	-386	-152	-8
5	360	69	6
6	-425	-259	-11
7	164	38	1
8	107	304	-3
9	531	765	-13
10	651	-333	14
11	718	-147	21
12	616	446	7
13	567	479	3
14	562	-524	1

-5 k 10

0	1901	2004	-8
1	1175	-1097	6
2	2213	-2175	5
3	432	737	-15
4	2092	2126	-5
5	1214	-1336	-13
6	1368	-1344	2
7	1840	1766	10
8	1245	1360	-12
9	1170	-1138	3
10	1781	-1749	4
11	1400	1231	17
12	1326	1445	-13
13	1146	-1226	-7

-5 k 11

1	368	-307	1
2	-174	500	-11
3	373	-304	2
4	125	242	-1
5	595	527	3
6	254	229	0
7	680	-698	-1
8	-499	-6	-11
9	558	550	0
10	-98	396	-7
11	966	-881	6
12	-192	-232	-3

-5 k 12

0	1296	1358	-3
1	2998	2776	32
2	1714	-1702	1
3	3435	-3374	10
4	1680	1761	-10
5	2665	2687	-3
6	1494	-1420	8
7	2599	-2552	7
8	1284	1252	3
9	2093	2173	-11
10	1538	-1518	2

-5 k 13

1	-572	37	-12
2	-525	77	-11
3	-205	202	-3
4	475	-15	9
5	-516	-175	-12
6	455	554	-4
7	-420	135	-8
8	703	-832	-8
9	340	-192	3

-5 k 14

0	3805	-3845	-4
1	1561	1542	1
2	3326	3298	4
3	1071	-931	11
4	2858	-2851	1
5	1028	895	10
6	2409	2467	-9
7	1268	-1279	-1

-5 k 15

1	-545	-208	-12
2	-314	-2	-4
3	723	601	6

-4 k 1

1	77	6	0
2	472	273	7
3	919	855	7
4	725	-797	-7
5	667	-567	8
6	941	976	-4
7	688	-707	-2
8	579	-85	20
9	1250	1150	15
10	-306	-16	-5
11	1174	-1284	-14
12	-455	-205	-14
13	1163	1095	7
14	301	126	3
15	1191	-1249	-6
16	456	-257	6
17	1490	1451	4
18	423	517	-4
19	1483	-1470	1

-4 k 2

0	1459	1504	-3
1	1948	1911	5
2	1319	-1117	23
3	2191	-2235	-8
4	436	-316	5
5	2046	1936	20
6	486	-25	10
7	2392	-2371	4
8	907	700	13
9	2196	2190	1
10	-162	299	-6
11	1804	-1827	-3
12	864	1011	-14
13	2136	2133	0
14	634	-379	13
15	2237	-2242	0
16	341	-150	4
17	1595	1504	11
18	562	46	14
19	1477	-1445	3

-4 k 3

1	-316	-199	-6
2	-541	80	-15
3	-263	229	-6
4	185	3	2
5	547	474	4
6	357	-115	7
7	530	-418	6
8	214	-494	-12
9	612	-392	13
10	-487	310	-19
11	-577	-126	-20
12	668	-450	13
13	-66	401	-8
14	1244	1347	-12
15	670	-30	22
16	968	-1064	-8
17	520	-416	4
18	474	538	-2
19	663	-414	11

-4 k 4

0	1254	-973	19
1	1464	1373	11
2	471	581	-6
3	498	-428	3
4	1143	-1091	6
5	325	-398	-3
6	415	518	-5
7	1149	1239	-12
8	-398	-170	-11
9	236	264	0
10	859	913	-5
11	604	-669	-4
12	363	-452	-3
13	421	-366	2
14	487	120	11
15	390	399	0
16	763	-451	17
17	623	-600	1
18	-392	383	-13

-4 k 5

1	705	-561	8
2	567	-553	0
3	337	428	-3
4	588	-631	-3
5	225	718	-27
6	-296	27	-5
7	365	-353	0
8	691	-662	2
9	-233	346	-10
10	670	462	13
11	-347	152	-8
12	775	-726	3
13	-588	-81	-18
14	-328	186	-7
15	233	251	0
16	544	-468	3
17	551	88	13
18	-285	368	-9

-4 k 6

0	816	-680	6
1	2130	2089	6
2	631	524	6
3	723	-781	-4
4	-389	-17	-9
5	1747	1685	10
6	695	-697	0
7	1420	-1398	3
8	167	-466	-10
9	1388	1370	2

10	-256	0	-3
11	1090	-1077	1
12	681	615	4
13	1104	924	18
14	-397	-64	-7
15	1329	-1329	0
16	330	-192	3
17	884	758	8
18	456	-608	-7

-4 k 7

1	663	-501	9
2	-622	-186	-22
3	589	-388	11
4	294	80	4
5	432	-373	2
6	479	577	-5
7	375	514	-6
8	-453	150	-13
9	714	-597	8
10	384	353	1
11	776	723	4
12	368	-641	-14
13	499	-438	2
14	678	646	2
15	716	672	2
16	600	-494	5
17	1015	-892	10

-4 k 8

0	3577	-3522	7
1	746	-715	2
2	3691	3604	16
3	641	720	-5
4	1827	-1791	6
5	807	529	20
6	2717	2842	-25
7	22	401	-8
8	3324	-3326	0
9	415	-518	-5
10	2462	2497	-6
11	-377	26	-7
12	2425	-2469	-7
13	-382	-190	-8
14	2443	2420	3
15	568	-85	14
16	1787	-1752	4
17	434	-259	5

-4 k 9

1	481	297	6
2	380	-32	7
3	458	680	-13
4	479	225	9
5	1311	-1256	7
6	315	-183	3
7	1037	810	22
8	857	880	-2
9	-498	-56	-13
10	1449	-1467	-2
11	716	647	4
12	1122	1134	-1
13	744	-757	0
14	1289	-1284	0
15	617	597	1
16	1194	1185	0

-4 k 10

0	528	551	0
1	2966	-2958	1
2	822	-819	0
3	3619	3674	-10
4	482	753	-17
5	3198	-3371	-35
6	480	-634	-9
7	2724	2732	-1
8	753	661	6
9	3782	-3830	-8
10	797	-649	10
11	3320	3296	4
12	651	745	-6
13	3040	-3046	-1
14	1092	-988	9
15	2409	2457	-7

-4 k 11

1	290	-321	0
2	633	718	-5
3	385	-464	-3
4	-363	-42	-7
5	771	591	12
6	532	-549	0
7	1134	-1177	-4
8	-438	106	-10
9	1210	1292	-9
10	594	-40	17
11	1341	-1378	-4
12	210	373	-4
13	1418	1344	8
14	767	-674	5

-4 k 12

0	4863	4731	15
1	1456	1469	-1
2	3945	-3986	-7
3	1421	-1463	-5
4	3092	3130	-7
5	1407	1541	-17
6	3112	-3086	4
7	729	-895	-12
8	3525	3446	14
9	1762	1806	-6
10	3086	-3151	-11
11	1504	-1606	-12
12	2542	2501	6
13	1045	1042	0

-4 k 13

1	511	213	10
2	291	348	-1
3	352	-182	4
4	440	-520	-3
5	-370	318	-11
6	750	564	11
7	-464	-109	-10
8	799	-548	15
9	533	458	3
10	902	988	-6
11	516	-347	6
12	1150	-1195	-4

-4 k 14

0	664	-916	-11
1	2759	2821	-11
2	1769	1862	-13
3	2660	-2739	-14
4	1723	-1677	6
5	2515	2569	-9
6	1310	1497	-22
7	2562	-2503	9
8	1410	-1548	-16
9	2428	2426	0
10	1145	1191	-4
11	1978	-2190	-30

-4 k 15

1	627	-730	-6
2	-521	-213	-14
3	644	497	7
4	-240	90	-2
5	300	-323	0
6	-449	129	-9
7	375	317	1
8	-660	-230	-21
9	615	-708	-5

-4 k 16

0	1054	-1300	-12
1	900	-924	-1
2	1629	1665	-4
3	522	626	-5
4	928	-1071	-11
5	1076	-1157	-7
6	1072	1063	0

-4 k 17

1	395	-123	5
2	-543	122	-12

-3 k 1

1	1061	-956	10
2	430	275	6
3	339	-82	7
4	472	-176	14
5	-182	337	-11
6	1186	-1192	-1
7	424	-293	5
8	463	-270	9
9	775	712	7
10	388	30	12
11	1137	-1088	8
12	549	603	-4
13	779	735	4
14	417	-636	-13
15	326	-548	-10
16	566	-148	16
17	-347	44	-6
18	417	-536	-5
19	300	131	3
20	889	736	11

-3 k 2

0	-266	-88	-2
1	185	-556	-14
2	177	-436	-8
3	-542	54	-17
4	319	62	5
5	746	560	14
6	940	857	6
7	-268	78	-4
8	-220	-129	-4
9	528	246	14
10	-375	322	-16
11	214	144	1
12	485	-249	10
13	-97	377	-9
14	1248	1237	1
15	-439	-66	-11
16	516	-425	4
17	133	429	-8
18	277	428	-5
19	501	152	10
20	-304	-265	-7

-3 k 3

1	708	390	17
2	525	-343	8
3	-355	-64	-7
4	963	935	3
5	479	511	-1
6	1198	-1121	10
7	315	404	-4
8	813	704	10
9	166	92	1
10	676	-607	5
11	-309	143	-7
12	109	617	-21
13	-556	186	-20
14	-393	-163	-10
15	302	162	3
16	757	573	13
17	409	-87	8
18	706	-418	15
19	360	-26	6
20	644	488	7

-3 k 4

0	884	1005	-7
1	1620	-1558	9
2	1399	-1183	29
3	1716	1595	20
4	1609	1516	15
5	2153	-2173	-4
6	1325	-1101	22
7	1591	1527	11
8	915	777	15
9	1464	-1348	19
10	1232	-1068	22
11	1964	1976	-2
12	1678	1737	-10
13	993	-828	16
14	1515	-1591	-11
15	1312	1474	-21
16	843	949	-9
17	1321	-1412	-11
18	910	-945	-2
19	1149	1173	-2
20	-342	172	-6

-3 k 5

1	724	-594	8
2	366	182	5
3	287	-391	-4
4	657	-625	2
5	969	1075	-13
6	859	734	12
7	713	-691	2
8	788	-790	0
9	695	621	6
10	259	80	3
11	734	-871	-12
12	548	-245	14
13	1036	985	5
14	793	177	34
15	990	-1037	-4
16	-213	171	-3
17	978	807	14
18	-552	-141	-15
19	961	-1162	-18
20	538	-547	0

-3 k 6

0	1483	1308	14
1	4149	3947	39
2	2433	-2550	-25
3	3572	-3593	-4
4	2452	2415	8
5	2000	1944	11
6	2890	-2916	-6
7	2778	-2871	-21
8	3140	3057	18
9	3381	3374	1
10	1977	-2112	-26
11	1811	-1941	-23
12	1239	1219	2

Di-iridium complex. Page 4

13	2080	2121	-7
14	1670	-1651	2
15	1779	-1805	-4
16	1884	1898	-2
17	1533	1490	5
18	1581	-1525	7
19	1710	-1743	-4

-3 k 7

1	-370	371	-15
2	810	715	8
3	320	-145	5
4	1155	-1048	14
5	923	-894	3
6	728	722	0
7	822	745	7
8	1350	-1339	1
9	532	-379	8
10	1190	1340	-20
11	354	326	1
12	1311	-1292	2
13	206	-417	-7
14	1430	1447	-2
15	501	287	8
16	1655	-1599	7
17	663	-270	17
18	1780	1872	-12
19	-364	281	-9

-3 k 8

0	4140	-3960	25
1	2584	2562	4
2	4301	4382	-26
3	2950	-2911	8
4	4496	-4385	22
5	2452	2520	-14
6	4086	4212	-26
7	2070	-2007	12
8	2661	-2681	-4
9	1934	2103	-31
10	3303	3399	-19
11	1635	-1658	-3
12	2027	-1971	9
13	1826	1914	-14
14	2867	2881	-2
15	1601	-1462	18
16	2975	-2968	1
17	1436	1453	-1
18	2170	2233	-9

-3 k 9

1	378	235	5
2	527	-581	-3
3	-517	173	-19
4	541	422	7
5	309	-348	-1
6	-220	-385	-12
7	588	678	-6
8	219	452	-9
9	982	-970	1
10	425	-463	-1
11	1617	1684	-10
12	-209	10	-2
13	1262	-1263	0
14	838	-655	13
15	1819	1840	-3
16	520	405	4
17	1679	-1674	0
18	714	-260	19

-3 k 10

0	2819	-2876	-8
1	4547	-4574	-5
2	2032	2022	1
3	4007	3967	8
4	1942	-2021	-15
5	2098	-2277	-36
6	826	677	12
7	3815	3771	8
8	1104	-1126	-2
9	3139	-3236	-19
10	1647	1528	17
11	3087	3052	6
12	1360	-1339	2
13	2992	-2937	10
14	1187	1075	11
15	2711	2569	23
16	1313	-1369	-6
17	1949	-1975	-3

-3 k 11

1	263	-57	3
2	514	-607	-6
3	356	-50	7
4	703	813	-9
5	641	-402	14
6	810	-828	-1
7	438	61	10
8	451	332	5
9	572	151	16
10	713	-470	14
11	-580	-342	-23
12	923	888	3
13	614	390	10
14	1330	-1295	3
15	330	-149	3
16	1254	1191	6

-3 k 12

0	2384	2412	-3
1	-62	86	0
2	2507	-2555	-9
3	535	841	-23
4	2505	2551	-9
5	-209	-336	-8
6	2017	-2160	-25
7	-360	624	-27
8	2770	2760	1
9	304	-445	-5
10	2619	-2607	2
11	176	466	-8
12	2376	2346	4
13	423	-497	-3
14	2075	-2039	5
15	722	617	6

-3 k 13

1	-511	-152	-13
2	158	261	-2
3	630	-634	0
4	414	-264	5
5	993	928	6
6	372	-46	7
7	276	-278	0
8	701	-161	23
9	571	287	11
10	227	238	0
11	-534	-174	-14
12	-588	-243	-18
13	722	918	-13
14	881	76	34

-3 k 14

0	-216	904	-22
1	1209	967	21
2	683	-614	4
3	913	-981	-6
4	590	375	10
5	1219	1337	-13
6	295	79	3
7	780	-861	-6
8	-242	117	-3
9	1336	1204	14
10	-524	323	-17
11	817	-918	-7
12	658	-235	16
13	806	585	12

-3 k 15

1	431	-119	6
2	508	269	8
3	-180	-284	-5
4	451	238	7
5	-491	73	-11
6	-224	120	-3
7	497	307	7
8	572	-303	10
9	-414	130	-8
10	-653	-14	-19
11	326	-441	-3
12	-263	-43	-3

-3 k 16

0	306	670	-8
1	684	359	12
2	710	-737	-1
3	-532	209	-14
4	863	556	19
5	224	54	2
6	-219	-539	-15
7	482	158	9
8	686	438	11
9	-419	-102	-8
10	-97	-415	-7

-3 k 17

1	-508	-224	-10
2	332	-284	1
3	-154	278	-4
4	505	-14	10
5	-366	28	-5
6	673	551	6
7	-664	-39	-18

-3 k 18

0	-560	-173	-7
1	2225	2127	11
2	87	416	-5
3	1983	-1866	13
4	-647	-236	-18

-2 k 1

1	311	19	7
2	530	-475	4
3	3480	3529	-14
4	1298	-1296	0
5	682	742	-7
6	846	937	-13
7	981	1135	-21
8	995	-1010	-2
9	535	-82	22
10	313	-116	6
11	577	503	6
12	-185	-185	-5
13	443	-393	3
14	72	222	-2
15	1894	1913	-3
16	719	-711	0
17	895	-891	0
18	498	511	0
19	1000	1041	-4
20	751	-881	-9
21	904	-733	12

-2 k 2

0	3706	-3724	-3
1	1543	-1512	6
2	2209	2121	22
3	1296	-1335	-7
4	5141	-5107	6
5	320	292	1
6	3174	3174	0
7	330	94	6
8	2157	-2236	-17
9	929	960	-3
10	2536	2503	7
11	1587	-1673	-16
12	2888	-2914	-5
13	319	331	0
14	2182	2228	-9
15	-290	-453	-17
16	1410	-1461	-7
17	534	535	0
18	2010	2024	-2
19	320	-282	1
20	1038	-1112	-7
21	-208	252	-4

-2 k 3

1	424	-644	-17
2	800	-797	0
3	828	-952	-17
4	243	343	-4
5	646	-679	-3
6	960	-788	20
7	670	-746	-7
8	215	360	-5
9	505	-353	8
10	-195	359	-11
11	966	780	21
12	618	720	-8
13	1248	-1315	-9
14	969	-1019	-5
15	512	29	15
16	1070	1117	-5
17	795	-841	-3
18	1485	-1472	1
19	666	702	-2
20	1276	1267	0
21	930	-756	12

-2 k 4

0	623	391	9
1	7240	-6985	37
2	1152	-1136	2
3	6942	6988	-7
4	558	533	1
5	2651	-2620	7
6	502	120	11
7	2824	2789	8
8	498	-578	-5
9	5194	-5184	2
10	540	-443	6
11	4401	4346	11
12	93	388	-9
13	2923	-3004	-17
14	435	587	-9
15	3076	3083	-1
16	-288	8	-4
17	2628	-2514	21
18	-350	42	-6
19	2313	2312	0
20	392	298	2
21	2053	-2092	-5

-2 k 5

1	633	63	27
2	683	-830	-15
3	242	66	3
4	606	673	-5
5	-181	376	-11
6	1042	-984	7
7	456	-228	10
8	-227	479	-18
9	1044	1128	-11
10	1193	-1236	-6
11	1057	-1116	-8
12	1066	1048	2
13	1007	987	2
14	696	-720	-2
15	1557	-1455	15
16	1488	1344	19
17	1338	1270	8
18	1496	-1390	13
19	1433	-1360	8
20	1279	1064	21
21	1562	1635	-9

-2 k 6

0	3165	3007	23
1	693	515	14
2	3130	-3202	-17
3	866	-857	1
4	2987	3023	-8
5	1003	784	24
6	5278	-5319	-7
7	871	-872	0
8	4364	4332	6
9	606	755	-13
10	4151	-4133	3
11	675	-786	-10
12	4374	4390	-3
13	724	768	-3
14	3378	-3460	-17
15	636	-845	-16
16	3754	3715	7
17	755	833	-5
18	3030	-3022	1
19	536	-597	-3
20	2442	2483	-6

-2 k 7

1	345	142	6
2	1259	1214	6
3	658	762	-9
4	-302	-356	-14
5	573	-558	1
6	576	638	-4
7	-387	116	-11
8	1399	-1399	0
9	1147	1254	-15
10	1507	1540	-5
11	583	-632	-3
12	819	-911	-9
13	498	591	-5
14	1533	1592	-9
15	1535	-1477	8
16	1310	-1177	15
17	1441	1419	2
18	1309	1485	-20
19	1107	-1074	3
20	1386	-1371	1

-2 k 8

0	111	-164	0
1	4568	4507	12
2	644	550	7
3	4025	-4068	-9
4	1471	-1319	25
5	2661	2724	-14
6	1587	1750	-31
7	3855	-3828	5
8	2312	-2193	24
9	4214	4241	-5
10	1163	1166	0
11	2165	-2217	-9
12	865	-795	6
13	2386	2403	-3
14	848	1040	-18
15	2730	-2668	11
16	951	-845	9
17	2180	2230	-8
18	1310	1354	-4
19	2120	-2174	-8
20	639	-860	-9

-2 k 9

1	-464	-100	-13
2	-207	189	-5
3	453	725	-20
4	670	-580	7
5	-158	208	-4
6	860	-874	-1
7	-392	26	-10
8	370	-296	3
9	-273	-541	-22
10	214	400	-6
11	905	733	16
12	970	-938	3
13	943	-938	0
14	712	618	6
15	1165	1038	13
16	1062	-910	13
17	931	-1230	-27
18	804	828	-1
19	890	881	0
20	-257	-600	-11
21	1186	-1025	10

-2 k 10

0	2901	-2809	12
1	1290	-1246	5
2	1882	1724	29
3	521	205	15
4	3088	-3073	3
5	1926	-1863	12
6	1742	1749	-1
7	1502	1505	0
8	2088	-2132	-8
9	577	-731	-11
10	2195	2160	6
11	641	707	-4
12	1810	-1902	-15
13	1036	-1124	-9
14	1445	1319	15
15	1073	969	9
16	1065	-907	13
17	969	-1174	-19
18	1055	1127	-6
19	865	690	7
20	602	-862	-10
21	776	-597	6

-2 k 11

1	217	123	1
2	815	-745	6
3	211	-168	1
4	729	700	2
5	723	-719	0
6	-261	-119	-5
7	249	67	3
8	265	-140	3
9	-540	5	-16
10	550	-220	14
11	886	670	18
12	313	254	1
13	298	-456	-5
14	580	-465	5
15	188	410	-6
16	516	559	-2
17	413	-448	-1
18	717	-33	14
19	-677	334	-15
20	771	425	10
21	756	-579	6

-2 k 12

0	827	-1173	-21
1	1087	-950	13
2	-416	47	-9
3	417	466	-2
4	776	734	3
5	477	68	12
6	308	63	5
7	542	632	-5
8	409	359	2
9	-188	128	-2
10	235	-362	-4
11	591	377	10
12	-314	352	-11
13	-333	-323	-10
14	-25	-364	-6
15	388	455	-2
16	535	551	0
17	-353	120	-6
18	-149	181	-1
19	-636	302	-13
20	-219	545	-8
21	274	-42	1

-2 k 13

1	243	-29	2
2	-596	15	-18
3	391	170	6
4	741	-438	19
5	384	157	6
6	179	323	-4
7	528	19	15
8	371	79	6
9	652	-451	11
10	772	-404	22
11	590	666	-4
12	451	200	7
13	-483	-316	-15
14	281	-16	3
15	633	338	12
16	445	403	1
17	774	-378	12
18	0	-495	-6
19	502	148	6
20	660	522	4
21	-455	-450	-10

-2 k 14

0	1227	-1232	0
1	908	-920	0
2	696	877	-13
3	815	788	2
4	1179	-1202	-2
5	486	-711	-13
6	795	839	-3
7	369	394	0
8	1115	-1139	-2
9	739	-817	-5
10	1342	1222	13
11	624	396	10
12	1082	-1309	-23
13	886	-665	15
14	779	840	-4
15	974	729	12
16	974	-514	18
17	-456	-369	-9
18	379	292	1
19	-352	297	-5
20	-681	-446	-17
21	200	-680	-10

-2 k 15

1	622	-99	15
2	-266	385	-9
3	-347	-294	-9
4	-191	-122	-2
5	-385	268	-10
6	514	-705	-11
7	310	140	3
8	1005	836	14
9	429	307	4
10	849	-813	2
11	684	-404	13
12	799	682	7
13	753	503	13
14	-276	-735	-17
15	-150	-347	-4
16	877	713	6
17	-744	341	-17
18	558	-1009	-17
19	545	-729	-6
20	767	863	-3
21	-390	214	-4

-2 k 16

0	2230	2300	-6
1	1793	-1917	-14
2	2347	-2309	5
3	1862	1735	16
4	1602	1646	-5
5	1648	-1573	9
6	1776	-1709	9
7	1518	1435	9
8	1510	1650	-17
9	1925	-1878	6
10	1702	-1667	4
11	1455	1554	-11
12	1786	1870	-11
13	1303	-1313	0
14	1364	-1149	13
15	1235	1299	-4
16	1076	1077	0
17	614	-757	-4
18	645	-1082	-17
19	-518	635	-16
20	1136	1170	-1
21	1031	-692	14

-2 k 17

1	620	-139	12
2	77	349	-4
3	-570	-180	-13
4	-25	77	0
5	938	660	18
6	497	-159	9
7	538	-335	7
8	341	-121	4
9	980	1190	-18
10	364	150	4
11	935	-1117	-9
12	-185	-459	-6
13	1354	1062	18
14	380	373	0
15	787	-1070	-12
16	374	-296	1
17	1050	1166	-6
18	164	192	0
19	793	-913	-5
20	-317	-392	-6

21	1164	1190	-1

-2 k 18

0	1547	1453	6
1	2934	3021	-12
2	2155	-2109	5
3	2723	-2646	11
4	1399	1358	4
5	2706	2740	-5
6	1628	-1687	-6
7	2700	-2628	10
8	1826	1584	19
9	2322	2313	0
10	1336	-1506	-11
11	2170	-2209	-3
12	1443	1427	1
13	2429	2420	0
14	1218	-1319	-6
15	1976	-1853	10
16	1382	1280	6
17	1611	1598	0
18	672	-1044	-14
19	934	-1115	-8
20	659	955	-11

-2 k 19

1	386	-166	3
2	371	545	-5
3	486	-47	5
4	-298	-286	-5
5	578	-367	4
6	654	560	2
7	-594	359	-12
8	455	-658	-5
9	750	-431	9
10	721	864	-5
11	194	250	0
12	774	-995	-9
13	427	-489	-1
14	958	1002	-2
15	330	230	1
16	1090	-1067	1
17	-359	-423	-7
18	1541	1206	20
19	-369	268	-5

-2 k 20

0	2815	-2610	17
1	1363	1454	-5
2	2795	2936	-13
3	1484	-1528	-2
4	2807	-2718	8
5	1330	1197	7
6	2551	2663	-10
7	933	-1233	-14
8	2875	-2568	29
9	1421	1483	-4
10	2889	2773	12
11	1056	-960	4
12	2221	-2186	3
13	993	790	8
14	1840	1966	-10
15	811	-838	-1
16	1646	-1440	13
17	1040	729	12
18	1693	1648	3

-2 k 21

1	-561	93	-6
2	125	-596	-7
3	212	414	-2
4	-639	216	-9
5	835	-120	14
6	515	-85	5
7	-424	564	-11
8	-287	138	-2
9	934	-782	6
10	-457	-208	-5
11	1155	950	9
12	-413	120	-4
13	647	-555	2
14	-641	-450	-15
15	972	783	7
16	247	226	0

-2 k 22

0	-793	-819	-23
1	2540	-2447	7
2	647	506	3
3	1978	1919	4
4	353	-820	-11
5	2103	-2108	0
6	864	276	14
7	1756	1936	-13
8	296	-292	0
9	1538	-1750	-15
10	321	498	-3
11	1508	1559	-3
12	587	-484	2
13	1641	-1685	-3
14	512	489	0
15	1730	1565	11

-2 k 23

1	-620	25	-7
2	-133	175	-1
3	-848	-232	-15
4	804	225	12
5	853	-209	14
6	-767	-200	-13
7	886	84	17
8	483	480	0
9	-432	-41	-4
10	249	-662	-8
11	-697	-132	-11
12	-218	575	-8
13	-800	37	-15

-2 k 24

0	1066	893	6
1	0	170	0
2	1494	-1354	7
3	-751	163	-11
4	1348	1217	6
5	-682	69	-9
6	1430	-1065	17
7	-775	37	-13
8	-834	790	-28
9	-738	-54	-12
10	1213	-968	11

-2 k 25

1	619	325	5
2	245	-88	0
3	1021	-166	19
4	876	49	14
5	448	374	1
6	-483	249	-6

-1 k 1

1	361	-399	-4
2	-143	150	-7
3	553	-706	-32
4	384	-105	20
5	1997	1979	6
6	394	-280	8
7	-614	-172	-33
8	765	-586	21
9	643	585	5
10	815	813	0
11	228	-99	3
12	2612	-2628	-4
13	-216	62	-4
14	1402	1489	-17
15	336	153	5
16	1586	-1609	-3
17	336	519	-8
18	1731	1701	4
19	-540	182	-16
20	2075	-2061	2
21	581	86	15
22	1918	1924	0
23	-445	-92	-5
24	1665	-1740	-6
25	552	199	7
26	1821	1661	12
27	0	23	0
28	1747	-1601	11
29	1030	-31	27

-1 k 2

0	5472	-5731	-44
1	5037	5056	-4
2	3464	3553	-21
3	2028	-1988	12
4	2210	-2141	20
5	2149	2116	9
6	3177	3217	-10
7	5379	-5483	-20
8	2863	-2861	0
9	2405	2430	-5
10	3660	3633	6
11	2887	-2919	-7
12	3469	-3531	-14
13	2636	2650	-3
14	2095	2096	0
15	1926	-1870	10
16	1551	-1695	-23
17	1590	1641	-8
18	2447	2330	21
19	2108	-2066	7
20	2093	-2170	-12
21	1846	1837	1
22	1466	1440	3
23	148	-1078	-31
24	1062	-960	5
25	247	713	-11
26	698	705	0
27	883	-987	-4
28	814	-815	0
29	909	875	1

-1 k 3

1	337	-455	-8
2	2082	-2113	-10
3	46	-377	-11
4	453	404	4
5	1372	-1453	-18
6	772	356	38
7	638	460	14
8	1103	937	23
9	1719	-1736	-3
10	1166	1098	9
11	1654	1568	15
12	-143	-292	-7
13	1938	-2012	-15
14	218	-422	-8
15	1550	1584	-5
16	955	983	-3
17	1789	-1769	3
18	499	-207	10
19	2321	2313	1
20	184	151	0
21	2016	-2011	0
22	529	-94	12
23	1359	1469	-7
24	324	212	1
25	1496	-1551	-3
26	-568	-541	-15
27	1806	1463	24
28	-291	169	-2
29	1822	-1571	18

-1 k 4

0	2411	-2399	2
1	2977	-2960	5
2	2721	2699	6
3	3235	3251	-4
4	3434	-3461	-6
5	6732	-6799	-10
6	3181	3177	1
7	2864	2904	-9
8	766	-652	10
9	2650	-2711	-10
10	2472	2412	13
11	2949	2919	6
12	2154	-2088	14
13	3630	-3625	1
14	1279	1299	-2
15	2321	2314	1
16	1627	-1531	15
17	2332	-2301	5
18	1174	1192	-2
19	2395	2379	2
20	1607	-1544	8
21	1727	-1682	6
22	1078	1104	-1
23	1476	1556	-6
24	1391	-1157	16
25	1373	-1409	-2
26	933	711	9
27	1184	1160	1
28	774	-306	13
29	559	-683	-3

-1 k 5

1	2264	2299	-9
2	643	759	-14
3	2287	-2192	25
4	309	342	-1
5	531	701	-15
6	1072	-954	16
7	235	195	1
8	1945	2009	-13
9	-342	324	-14
10	1629	-1577	9
11	-166	-12	-1
12	2325	2356	-6
13	521	-486	2
14	1727	-1811	-15
15	622	-580	2
16	1561	1580	-2
17	328	562	-11
18	1727	-1679	7
19	450	-195	8
20	1640	1689	-6
21	375	290	2
22	1600	-1502	8
23	935	-523	16
24	1454	1260	13
25	-111	173	-1
26	931	-994	-3
27	673	-388	7
28	1347	1245	6
29	534	403	3

-1 k 6

0	2904	3084	-30

1	4684	-4563	25
2	5236	-5050	36
3	1462	1352	21
4	2462	2528	-16
5	1916	-1975	-12
6	2634	-2548	20
7	671	593	6
8	3574	3581	-1
9	1329	-1368	-6
10	2952	-2950	1
11	712	-40	34
12	2797	2851	-12
13	1543	-1646	-17
14	2426	-2482	-11
15	672	772	-8
16	1924	1989	-11
17	611	-454	8
18	1905	-1902	0
19	612	683	-4
20	1810	1727	11
21	793	-556	14
22	1124	-984	8
23	-468	449	-12
24	831	813	0
25	-390	-208	-5
26	1153	-1128	1
27	624	609	0
28	1132	1071	3

-1 k 7

1	874	755	11
2	467	-365	5
3	582	573	0
4	434	-467	-2
5	455	305	7
6	525	55	18
7	-352	303	-14
8	325	-181	4
9	690	745	-5
10	486	-206	13
11	1045	-1101	-7
12	441	174	10
13	1116	1016	12
14	261	171	2
15	949	-944	0
16	-238	294	-7
17	1338	1094	28
18	103	-35	0
19	984	-1108	-11
20	440	-309	4
21	1334	1193	10
22	-449	-16	-6
23	668	-863	-8
24	384	-332	1
25	736	858	-4
26	-519	476	-12
27	606	-732	-4
28	364	-105	3

-1 k 8

0	658	-408	8
1	1990	1980	1
2	699	-796	-8
3	1276	-1164	16
4	406	326	3
5	1850	1844	1
6	565	227	17
7	1482	-1461	3
8	362	464	-5
9	1198	1036	22
10	-173	16	-2
11	2298	-2259	8
12	1063	1062	0
13	1030	1017	1
14	423	77	10
15	749	-756	0
16	-499	71	-13
17	1234	1181	6
18	334	-268	1
19	1086	-996	8
20	654	173	17
21	789	643	6
22	-441	-148	-6
23	599	-786	-7
24	-317	112	-3
25	979	844	6
26	-524	185	-7
27	738	-471	8
28	830	-217	15

-1 k 9

1	-278	27	-4
2	-542	-74	-17
3	484	-685	-13
4	609	-683	-6
5	-188	277	-7
6	-258	-355	-12
7	310	-226	3
8	-405	292	-17
9	334	-334	0
10	-277	296	-10
11	402	-392	0
12	593	-636	-3
13	-360	-222	-10
14	991	765	21
15	-411	118	-9
16	592	-720	-8
17	-517	-29	-13
18	-606	352	-22
19	198	-455	-7
20	780	-436	12
21	529	277	6
22	-593	82	-10
23	-110	-61	0
24	467	66	5
25	306	140	1
26	-118	39	0
27	-540	-30	-7

-1 k 10

0	1350	1053	23
1	1695	1586	16
2	-329	-328	-12
3	632	615	1
4	824	611	18
5	452	-436	0
6	253	145	2
7	336	346	0
8	-208	238	-6
9	488	-690	-14
10	1519	-1403	17
11	312	-248	2
12	348	599	-13
13	589	-144	18
14	614	354	13
15	308	423	-4
16	-175	242	-4
17	896	-772	9
18	214	-247	0
19	-346	135	-6
20	672	-632	1
21	-284	-134	-2
22	452	-142	5
23	673	576	3
24	842	25	20
25	673	-243	10
26	-610	130	-9
27	-623	370	-12

-1 k 11

1	233	111	2
2	-257	-64	-4
3	472	-443	1
4	617	-416	12
5	623	429	12
6	223	388	-6
7	953	-896	6
8	621	-777	-12
9	342	281	2
10	494	779	-20
11	450	-399	2
12	-499	4	-13
13	754	575	12
14	590	638	-2
15	-258	-358	-9
16	495	26	11
17	544	-367	7
18	-474	290	-13
19	-723	-311	-18
20	1062	-635	21
21	288	483	-4
22	1168	1041	7
23	643	18	11
24	201	-567	-7
25	-777	75	-15
26	-1012	353	-28

-1 k 12

0	718	-477	9
1	2482	2509	-4
2	468	423	2
3	2751	-2690	12
4	-282	297	-9
5	1984	1986	0
6	927	-711	19
7	2301	-2188	21
8	-397	284	-13
9	1049	935	12
10	-83	-191	-2
11	1936	-1881	9
12	290	383	-3
13	1823	1829	0
14	361	196	4
15	2009	-2050	-6
16	610	292	13
17	766	975	-15
18	793	-765	1
19	1446	-1502	-4
20	473	241	4
21	1183	1210	-1
22	-629	-238	-12
23	653	-552	3
24	-1060	321	-32
25	841	885	-1
26	-548	-57	-7

-1 k 13

1	-323	357	-10
2	-360	-29	-6
3	687	2	24
4	226	377	-4
5	408	-347	2
6	-80	440	-11
7	1348	1429	-11
8	-327	-507	-19
9	939	-691	20
10	448	184	8
11	1133	1053	8
12	633	-311	15
13	1066	-1047	1
14	722	589	8
15	1156	978	16
16	598	-813	-12
17	960	-1006	-2
18	1149	1008	8
19	1186	1079	6
20	584	-602	0
21	901	-715	8
22	875	434	15
23	732	673	2
24	845	-617	9
25	761	-590	5

-1 k 14

0	3376	-3347	3
1	630	-408	10
2	3349	3294	9
3	-457	-341	-15
4	3609	-3594	2
5	508	-427	3
6	3120	3129	-1
7	-356	248	-9
8	3156	-3144	2
9	678	197	21
10	3185	3152	5
11	535	257	10
12	2404	-2508	-17
13	657	-370	13
14	2043	1948	13
15	485	-569	-3
16	1945	-2240	-29
17	729	-509	8
18	2323	2310	1
19	506	421	2
20	1341	-1478	-9
21	-280	402	-6
22	1454	1656	-15
23	-571	-105	-9
24	1267	-1246	1
25	-847	82	-17

-1 k 15

1	497	470	1
2	922	-546	23
3	264	73	2
4	806	886	-6
5	-23	-362	-6
6	508	-530	-1
7	621	294	14
8	226	584	-13
9	508	-402	4
10	1106	-1184	-7
11	706	654	3
12	1286	1188	9
13	930	-892	2
14	696	-989	-20
15	515	710	-6
16	1187	1168	1
17	705	-888	-7
18	1050	-933	6
19	617	833	-8
20	1302	1332	-1
21	719	-1005	-12
22	1200	-1180	1
23	1096	740	16
24	578	803	-7

-1 k 16

0	827	784	1
1	4098	-4154	-9
2	1127	-788	24
3	3466	3342	20
4	920	758	11
5	3309	-3210	16
6	732	-630	6
7	3260	3231	5
8	851	936	-6
9	2930	-2993	-10
10	643	-640	0
11	3002	2989	2
12	377	310	1
13	3026	-3131	-12

14	281	-555	-6
15	2265	2316	-5
16	579	229	7
17	2201	-2164	3
18	253	-138	1
19	2080	1908	15
20	350	345	0
21	1592	-1494	7
22	-695	-151	-13
23	1377	1405	-1

-1 k 17

1	512	68	9
2	-205	-481	-10
3	-729	-281	-23
4	621	84	15
5	564	41	13
6	738	-519	11
7	778	-849	-4
8	584	391	7
9	518	663	-6
10	514	-400	4
11	870	-861	0
12	1021	531	21
13	1242	1151	5
14	816	-925	-5
15	1154	-1097	3
16	682	612	2
17	1273	937	18
18	554	-487	1
19	1226	-1200	1
20	492	631	-4
21	1182	1009	9
22	-551	-797	-23

-1 k 18

0	3634	3417	23
1	907	1095	-12
2	3109	-3231	-18
3	965	-1031	-4
4	3140	2922	32
5	981	929	3
6	2575	-2517	8
7	732	-649	4
8	2762	2763	0
9	942	741	8
10	2986	-2937	5
11	1378	-1471	-6
12	2218	2206	1
13	635	779	-5
14	2356	-2309	4
15	588	-679	-2
16	1425	1667	-17
17	931	699	10
18	1494	-1403	6
19	688	-490	6
20	1638	1594	3
21	710	458	7

-1 k 19

1	-92	-123	0
2	-187	386	-5
3	-319	-213	-5
4	139	-511	-8
5	471	649	-7
6	-588	364	-12
7	-247	-203	-2
8	575	-542	0
9	893	442	15
10	588	784	-7
11	-500	-128	-7
12	478	-385	2
13	-812	204	-18
14	1258	1095	9
15	706	-479	7
16	1038	-1001	1
17	915	786	5
18	-362	834	-21
19	-441	-577	-13
20	786	-935	-6

-1 k 20

0	823	-930	-4
1	2190	2071	9
2	697	792	-3
3	1538	-1649	-7
4	-262	-361	-4
5	2002	1823	14
6	1409	1343	4
7	2058	-2069	0
8	949	-1071	-6
9	943	1105	-8
10	716	641	2
11	1855	-1799	4
12	1130	-869	13
13	1577	1399	12
14	755	855	-4
15	1544	-1325	15
16	-269	-416	-6
17	1368	1446	-5
18	427	588	-4
19	1083	-1107	-1

-1 k 21

1	882	-330	14
2	-415	-9	-3
3	301	292	0
4	-499	-90	-6
5	-813	-100	-16
6	-504	332	-9
7	968	387	19
8	0	-122	0
9	667	-361	8
10	579	298	6
11	605	556	1
12	892	-463	14
13	0	-601	-9
14	121	363	-3
15	122	334	-2
16	445	-358	1
17	808	-507	10

-1 k 22

0	1035	-707	11
1	-563	-234	-7
2	365	774	-9
3	336	426	-1
4	1112	-993	5
5	721	-608	3
6	274	197	0
7	-440	206	-5
8	1339	-1043	16
9	740	-552	6
10	844	387	14
11	122	395	-3
12	918	-367	17
13	740	-333	11
14	805	504	10
15	560	230	6

-1 k 23

1	702	-122	9
2	957	-4	18
3	-628	356	-10
4	-182	114	-1
5	675	-102	10
6	633	23	9
7	642	-8	9
8	-452	33	-4
9	639	27	10
10	452	-70	5
11	453	72	5
12	-454	-42	-5
13	537	-253	5

-1 k 24

0	-272	-85	-1
1	-638	197	-9
2	471	496	0
3	944	-746	7
4	638	-226	7
5	573	206	6
6	433	210	3
7	-649	-216	-11
8	224	-94	1
9	658	223	9
10	774	293	12
11	-447	-146	-5

-1 k 25

1	-836	57	-15
2	935	221	16
3	416	40	3
4	137	113	0
5	754	-83	12
6	711	-145	11
7	299	144	1
8	-691	-94	-11

0 k 0

4	4256	4087	41
6	5549	-5769	-43
8	5814	5773	7
10	2630	-2588	9
12	5376	5261	21
14	3846	-3765	16
16	2711	2795	-17
18	3297	-3175	23
20	2752	2819	-12
22	2134	-2224	-13
24	1352	1541	-14
26	1573	-1434	10
28	1172	1409	-15

0 k 1

3	1177	-1217	-18
4	318	424	-14
5	1344	1377	-11
6	985	-877	23
7	871	-965	-17
8	636	-656	-2
9	949	985	-5
10	421	435	-1
11	1226	-1202	4
12	1688	-1616	16
13	1493	1501	-1
14	1179	1253	-13
15	1159	-1264	-17
16	1278	-1249	3
17	1453	1582	-19
18	931	1018	-9
19	1826	-1876	-7
20	1658	-1561	13
21	1552	1670	-15
22	1155	1255	-10
23	1111	-1009	8
24	1460	-1439	2
25	1294	949	28
26	1319	1136	16
27	1099	-962	10
28	1053	-1000	4
29	1496	1074	37

0 k 2

0	726	-657	15
1	5166	5080	18
2	692	880	-57
3	6809	-6906	-16
4	1230	-1076	40
5	3653	3663	-2
6	1175	-1062	22
7	5750	-5790	-7
8	1811	-1819	-1
9	3387	3403	-3
10	859	-1038	-22
11	3786	-3813	-5
12	962	-1096	-17
13	3847	3812	7
14	-77	-35	0
15	3988	-4082	-19
16	677	-811	-11
17	2617	2642	-5
18	-494	-8	-13
19	2811	-2811	0
20	440	-409	1
21	2374	2272	16
22	340	208	3
23	1980	-2030	-7
24	812	-581	13
25	2077	1970	13
26	676	470	9
27	782	-1048	-18
28	590	-328	9
29	508	611	-4

0 k 3

1	903	-698	33
2	280	-450	-17
3	-78	111	-2
4	930	-959	-6
5	1621	-1655	-9
6	4440	4440	0
7	876	841	4
8	315	-325	0
9	1194	-1248	-8
10	544	342	12
11	288	346	-2
12	1178	-1238	-9
13	725	-708	1
14	1307	1125	26
15	484	632	-10
16	593	-712	-9
17	798	-933	-12
18	2004	1951	9
19	1242	1042	21
20	1174	-1155	2
21	814	-952	-10
22	449	711	-13
23	861	895	-2
24	1036	-863	13
25	601	-728	-6
26	1014	833	13
27	936	654	17
28	725	-676	2
29	915	-665	14

0 k 4

0	3009	-3053	-9
1	920	-830	15
2	2751	2725	7
3	1608	1575	9
4	830	-797	5
5	3056	-3120	-17
6	4233	4235	0
7	1608	1552	11
8	2066	-2068	0
9	-322	-310	-13
10	1170	1140	4

11	1144	1190	-6
12	2939	-2886	12
13	493	270	11
14	2232	2178	10
15	566	658	-6
16	1652	-1722	-11
17	256	-359	-3
18	2073	2095	-3
19	851	878	-2
20	1508	-1453	6
21	964	-792	13
22	1284	1291	0
23	699	725	-1
24	675	-757	-4
25	525	-625	-4
26	432	656	-9
27	215	379	-3
28	915	-898	1
29	861	-448	20

0 k 5

1	1571	1603	-7
2	274	419	-9
3	718	754	-4
4	888	-856	4
5	-69	344	-9
6	-210	368	-13
7	855	770	9
8	-416	99	-12
9	961	-870	10
10	803	-819	-1
11	524	526	0
12	-615	248	-30
13	-263	-74	-4
14	381	-185	7
15	360	538	-9
16	627	276	18
17	274	-167	2
18	672	-544	8
19	179	331	-3
20	501	394	4
21	1083	-989	8
22	461	-563	-4
23	673	772	-5
24	674	418	11
25	452	-429	0
26	383	-595	-8
27	738	571	8
28	403	322	2
29	-404	-394	-12

0 k 6

0	1938	-1871	9
1	2260	-2189	16
2	353	-337	0
3	-286	-197	-9
4	3933	3985	-12
5	-217	-192	-6
6	544	637	-7
7	480	401	4
8	1061	1019	5
9	829	-788	4
10	1653	-1661	-1
11	1352	1291	9
12	379	220	6
13	464	162	12
14	537	-805	-21
15	382	188	6
16	463	322	6
17	420	-5	9
18	833	-828	0
19	614	512	5
20	574	448	5
21	436	-142	7
22	972	-586	25
23	240	93	2
24	-106	280	-3
25	379	-550	-6
26	-492	-460	-18
27	-164	-11	-1
28	344	453	-3
29	747	-29	21

0 k 7

1	809	-914	-10
2	1011	-1014	0
3	-52	-42	0
4	438	-202	10
5	-86	46	0
6	355	-223	5
7	560	-239	17
8	455	322	6
9	516	-415	6
10	-314	-261	-11
11	1053	-929	15
12	674	830	-14
13	581	486	6
14	51	-259	-3
15	118	142	0
16	118	-316	-4
17	498	-492	0
18	225	-512	-10
19	607	337	12
20	172	708	-21
21	297	138	3
22	563	-120	12
23	225	-115	1
24	489	185	8
25	-398	-340	-10
26	327	146	3
27	163	336	-3
28	281	256	0

0 k 8

0	404	16	5
1	2146	-2156	-1
2	1903	1809	16
3	968	1012	-5
4	517	-474	2
5	-350	-143	-9
6	2010	2017	-1
7	992	-836	17
8	939	-922	2
9	1510	-1467	7
10	1347	1258	13
11	-399	150	-11
12	1363	-1283	11
13	876	957	-8
14	-175	294	-6
15	-92	249	-3
16	951	-1029	-7
17	-497	-185	-14
18	513	543	-1
19	-134	144	-1
20	697	-780	-5
21	-235	-151	-3
22	571	570	0
23	269	-201	1
24	851	-714	8
25	-506	239	-12
26	574	197	11
27	404	-348	1
28	898	-548	19

0 k 9

1	667	-774	-7
2	803	-807	0
3	644	-646	0
4	570	275	14
5	365	259	4
6	827	-728	9
7	207	345	-5
8	90	41	0
9	449	421	1
10	160	104	0
11	-221	-454	-15
12	1103	1050	6
13	413	-240	6
14	606	-745	-10
15	544	-452	4
16	359	456	-3
17	61	510	-12
18	903	-966	-5
19	181	175	0
20	934	888	3
21	-199	235	-4
22	1162	-1178	-1
23	746	-74	22
24	1047	726	21
25	-283	95	-3
26	793	-704	5
27	228	-56	1
28	827	694	7

0 k 10

0	3077	3060	2
1	2668	-2647	4
2	2027	-2061	-5
3	1552	1555	0
4	1236	1170	9
5	2485	-2413	15
6	1953	-2021	-13
7	1925	1849	14
8	1395	1300	14
9	2746	-2848	-22
10	681	-621	4
11	2292	2259	6
12	1929	1896	5
13	2117	-2132	-2
14	1980	-1960	3
15	2040	1964	12
16	711	718	0
17	1568	-1541	3
18	1173	-1096	7
19	1607	1629	-2
20	893	844	3
21	1436	-1363	7
22	727	-722	0
23	815	861	-3
24	-211	263	-4
25	984	-919	4
26	-525	-201	-12
27	657	661	0

0 k 11

1	-259	194	-5
2	656	699	-3
3	-427	204	-12
4	421	-365	2
5	846	825	2
6	1139	1067	8
7	1183	-1137	6
8	387	76	8
9	1260	1190	9
10	-271	188	-6
11	931	-893	3
12	630	308	16
13	1018	959	5
14	435	428	0
15	1600	-1566	4
16	360	171	4
17	1176	1376	-21
18	270	151	2
19	1207	-1327	-11
20	-205	-9	-1
21	1386	1368	1
22	683	368	12
23	1210	-1211	0
24	-228	-257	-4
25	1310	1313	0
26	359	7	5
27	1138	-1110	2

0 k 12

0	3746	3768	-3
1	3018	3151	-25
2	2600	-2529	12
3	2699	-2578	23
4	2479	2523	-8
5	2544	2539	0
6	3057	-2959	19
7	2767	-2682	16
8	2797	2954	-31
9	2552	2667	-22
10	2029	-1881	25
11	1993	-2083	-15
12	1914	1974	-9
13	2133	2187	-8
14	1919	-1972	-8
15	1715	-1666	6
16	1939	1981	-6
17	2033	2102	-10
18	1950	-1857	12
19	1603	-1542	6
20	918	1142	-17
21	939	1018	-5
22	1435	-1473	-3
23	955	-979	-1
24	954	918	2
25	972	779	12
26	895	-709	11

0 k 13

1	186	326	-3
2	377	507	-5
3	542	548	0
4	666	-748	-5
5	326	62	5
6	387	367	0
7	495	-279	9
8	1047	-1141	-10
9	404	-195	6
10	902	868	3
11	247	137	2
12	1591	-1570	2
13	-398	227	-10
14	1335	1336	0
15	-486	-161	-11
16	1393	-1401	0
17	385	-54	6
18	1744	1776	-4
19	-598	-81	-15
20	1837	-1949	-13
21	984	-659	20
22	1236	1242	0
23	-145	501	-10
24	1551	-1327	22
25	-555	-75	-12

0 k 14

0	3523	-3493	3
1	2192	2312	-18
2	3185	3087	17
3	2282	-2210	11
4	2793	-2867	-13
5	2328	2324	0
6	3344	3334	1
7	2007	-2004	0
8	2932	-2904	5
9	1852	1877	-3
10	2695	2678	3
11	2007	-1958	7

12	2396	-2346	8
13	2007	1942	9
14	2416	2347	10
15	1524	-1562	-4
16	2458	-2549	-14
17	1416	1492	-8
18	1657	1763	-12
19	1463	-1565	-10
20	1869	-2024	-19
21	761	889	-7
22	799	926	-8
23	963	-904	3
24	1236	-1028	16
25	1064	804	17

0 k 15

1	512	-493	0
2	-249	-64	-2
3	568	279	10
4	405	-325	2
5	800	-888	-6
6	-146	-25	-1
7	599	273	13
8	829	487	21
9	937	-752	14
10	382	-472	-3
11	1138	1262	-12
12	361	84	5
13	1299	-1293	0
14	665	-157	17
15	1364	1196	16
16	765	225	21
17	1390	-1332	5
18	588	-139	12
19	1357	1409	-5
20	133	215	-1
21	1280	-1253	2
22	470	-110	8
23	1349	1310	3
24	594	371	7

0 k 16

0	2076	-1998	7
1	2487	-2607	-17
2	1820	1911	-11
3	2841	2839	0
4	538	-788	-13
5	2735	-2764	-4
6	1851	1850	0
7	2666	2666	0
8	1522	-1375	16
9	2616	-2593	3
10	1507	1571	-7
11	2518	2621	-16
12	1467	-1325	15
13	2199	-2186	1
14	984	983	0
15	1517	1624	-11
16	666	-796	-7
17	1757	-1802	-5
18	378	492	-3
19	1658	1647	1
20	671	-956	-17
21	1361	-1261	9
22	462	539	-2
23	1297	1212	7

0 k 17

1	588	56	12
2	-160	-297	-4
3	803	-589	10
4	579	598	0
5	399	356	1
6	765	-468	15
7	-343	-159	-5
8	427	617	-7
9	-245	220	-4
10	-587	-300	-18
11	-293	-177	-4
12	-209	707	-21
13	-424	346	-11
14	787	-915	-8
15	583	-254	10
16	1300	1039	22
17	266	12	2
18	1003	-791	14
19	170	128	0
20	971	904	4
21	-79	186	-1
22	973	-1008	-2

0 k 18

0	1679	1517	11
1	854	-710	7
2	1603	-1581	2
3	866	802	3
4	1697	1525	18
5	716	-703	0
6	1955	-1957	0
7	812	389	20
8	1511	1495	1
9	334	-253	1
10	1410	-1427	-1
11	-444	352	-12
12	1415	1499	-8
13	-461	-468	-16
14	1349	-1337	1
15	-660	146	-17
16	988	840	10
17	652	-555	4
18	1408	-1364	4
19	371	334	0
20	649	692	-2
21	-327	-170	-5

0 k 19

1	-353	156	-4
2	-228	69	-1
3	-365	-6	-4
4	157	-65	0
5	-629	302	-17
6	-554	399	-16
7	-583	-90	-13
8	-597	337	-17
9	-655	206	-17
10	319	-155	2
11	429	-255	4
12	-433	76	-7
13	-279	543	-14
14	239	-26	2
15	522	-559	-1
16	706	240	16
17	-253	321	-6
18	-406	-161	-7
19	819	-433	18
20	-497	139	-10

0 k 20

0	562	262	7
1	373	278	2
2	-472	151	-8
3	503	-473	0
4	-328	146	-4
5	593	380	7
6	-433	33	-6
7	148	-271	-1
8	157	186	0
9	690	536	6
10	847	463	18
11	-616	-241	-15
12	180	-322	-2
13	323	234	1
14	-443	-158	-8
15	265	-401	-3
16	382	26	5
17	-565	20	-12
18	672	-195	15
19	379	-111	4

0 k 21

1	770	40	18
2	521	423	2
3	-363	-130	-4
4	-308	-318	-6
5	-508	59	-8
6	381	-357	0
7	536	98	9
8	-330	77	-4
9	-597	269	-14
10	578	-108	11
11	541	-716	-7
12	402	77	5
13	309	435	-3
14	172	-256	-1
15	563	-426	5
16	530	-182	9
17	763	437	14

0 k 22

0	771	596	7
1	-299	91	-2
2	1327	-1343	-1
3	545	169	8
4	1361	1349	0
5	-881	-127	-26
6	-310	-586	-14
7	739	238	16
8	1033	954	5
9	-719	-54	-18
10	1112	-1075	2
11	448	26	7
12	768	534	10
13	421	-427	0
14	780	-830	-2
15	632	102	14
16	1199	518	29

0 k 23

1	631	5	12
2	405	-41	4
3	269	-117	1
4	-432	-21	-5
5	-425	-246	-7
6	879	419	18
7	-533	-220	-10
8	-653	-303	-17
9	-276	257	-4
10	911	346	24
11	-204	-216	-3
12	502	-320	5
13	-454	193	-8
14	644	546	4

0 k 24

0	-179	184	-1
1	2257	2128	14
2	-365	309	-6
3	1843	-1783	5
4	295	-102	2
5	1993	2115	-12
6	-237	267	-4
7	1636	-1729	-8
8	215	80	1
9	1483	1642	-14
10	405	-98	5
11	1744	-1822	-7

0 k 25

1	467	-54	6
2	-766	28	-18
3	-86	390	-4
4	-572	17	-9
5	-605	-282	-13
6	-713	189	-17
7	98	285	-2
8	-426	-378	-10

0 k 26

0	2039	-2052	-1
1	-412	-365	-8

1 k 0

0	2606	2581	8
1	2699	-2626	27
2	3604	-3715	-36
3	2553	2543	3
4	4157	4124	9
5	1721	-1760	-14
6	2453	-2518	-23
7	4309	4288	5
8	3252	3209	12
9	1462	-1490	-7
10	2362	-2331	9
11	2573	2553	5
12	2467	2489	-6
13	2959	-2939	5
14	2364	-2292	19
15	1845	1876	-5
16	2286	2338	-10
17	1474	-1471	0
18	1982	-1869	18
19	1480	1579	-13
20	1579	1544	4
21	1293	-1285	0
22	1697	-1528	20
23	819	762	2
24	1452	1595	-11
25	1047	-876	8
26	1079	-1287	-11
27	768	414	10
28	375	706	-9
29	-121	-218	-1

1 k 1

1	762	765	0
2	241	-216	1
3	205	63	5
4	436	-331	11
5	992	1025	-7
6	1457	1517	-17
7	2235	-2214	6
8	453	-455	0
9	254	436	-10
10	801	-684	13
11	1642	-1652	-2
12	302	-293	0
13	2148	2153	-1
14	-347	18	-9
15	1592	-1572	3
16	383	-240	5
17	939	1046	-11
18	-330	75	-6
19	2071	-1978	15
20	-598	-119	-18
21	1377	1251	14
22	-232	-50	-2
23	1169	-1295	-8
24	304	-86	2

25	1200	1062	7
26	-453	-30	-5
27	970	-1053	-3
28	712	44	13
29	909	867	1

1 k 2

0	3145	3344	-46
1	5268	5108	32
2	2111	-2064	14
3	516	-436	8
4	1731	1833	-29
5	2133	2184	-14
6	4620	-4630	-2
7	539	-488	4
8	998	969	3
9	1250	1393	-24
10	1926	-1968	-8
11	1438	-1325	19
12	1792	1638	28
13	1872	1892	-3
14	436	-774	-25
15	1611	-1634	-3
16	438	408	1
17	1335	1253	10
18	-288	-642	-26
19	784	-876	-7
20	653	528	7
21	870	764	7
22	307	-338	0
23	1205	-1188	1
24	-978	37	-28
25	913	620	11
26	494	-37	6
27	1033	-539	19
28	-412	331	-6
29	996	484	18

1 k 3

2	627	-668	-5
3	-230	309	-15
4	296	173	5
5	494	439	4
6	502	-526	-2
7	888	-885	0
8	636	-675	-3
9	675	497	13
10	-427	465	-30
11	372	-475	-5
12	380	422	-2
13	1420	1401	3
14	228	28	3
15	-370	-151	-9
16	872	-802	6
17	111	401	-8
18	224	358	-4
19	394	-525	-5
20	337	-430	-3
21	-343	309	-9
22	708	592	6
23	-940	0	-26
24	-767	-429	-20
25	157	108	0
26	-322	456	-7
27	649	-100	10
28	547	-424	2
29	244	229	0

1 k 4

0	447	412	1
1	499	665	-15
2	1519	1467	11
3	1162	1049	20
4	986	906	12
5	2102	2129	-6
6	1259	-1163	16
7	230	298	-2
8	636	-682	-2
9	1182	1160	3
10	457	256	9
11	-442	-140	-14
12	1056	779	34
13	1077	1098	-2
14	306	-236	2
15	493	246	11
16	298	242	1
17	326	-186	4
18	178	-320	-3
19	149	-83	0
20	-437	52	-9
21	-710	-89	-23
22	-254	-50	-2
23	803	514	10
24	723	-28	13
25	-432	-405	-9
26	627	287	7
27	331	232	1
28	-786	-34	-15
29	490	-251	4

1 k 5

1	1356	-1308	8
2	283	-358	-3
3	369	316	2
4	665	589	7
5	407	-444	-2
6	216	91	2
7	600	-462	9
8	113	127	0
9	91	-147	0
10	545	523	1
11	223	-222	0
12	1118	-986	17
13	-463	-176	-15
14	449	654	-13
15	444	-453	0
16	881	-906	-2
17	622	710	-6
18	613	703	-5
19	311	-472	-6
20	690	-805	-7
21	-229	519	-14
22	-455	289	-8
23	-339	-577	-12
24	-711	-121	-13
25	551	592	-1
26	-257	418	-5
27	992	-677	13
28	1029	-464	20
29	-729	154	-13

1 k 6

0	2040	1971	9
1	3059	3078	-4
2	-316	104	-7
3	1829	-1811	3
4	1877	1712	32
5	1911	1911	0
6	1620	-1725	-19
7	1792	-1760	6
8	545	-162	17
9	2693	2696	0
10	-55	-306	-6
11	2017	-2079	-13
12	878	810	7
13	1606	1644	-6
14	930	-848	8
15	780	-821	-3
16	-317	378	-13
17	138	660	-22
18	-462	-193	-13
19	1196	-1139	5
20	686	344	15
21	788	856	-4
22	-236	-542	-10
23	858	-527	13
24	664	527	4
25	734	450	8
26	715	-489	6
27	-556	-434	-12
28	776	362	12

1 k 7

1	709	-60	26
2	586	559	1
3	178	375	-6
4	-195	-122	-3
5	-125	-301	-6
6	879	802	7
7	414	-571	-9
8	313	-455	-7
9	811	603	19
10	997	1021	-3
11	801	681	10
12	1016	-910	12
13	1079	-1137	-7
14	845	740	9
15	953	828	11
16	658	-654	0
17	598	-712	-7
18	1083	942	13
19	1144	1203	-5
20	820	-1030	-16
21	666	-925	-12
22	723	759	-1
23	1145	965	10
24	866	-978	-5
25	767	-677	3
26	891	596	10
27	534	810	-8
28	-211	-766	-15

1 k 8

0	3968	-3797	25
1	553	110	14
2	3513	3455	12
3	1596	-1438	24
4	3745	-3691	11
5	947	869	8
6	2815	2885	-15
7	507	-292	11
8	2413	-2373	8
9	1687	1615	13
10	2295	2315	-4
11	422	-283	6
12	3176	-3209	-6
13	636	311	18
14	2871	2854	3
15	951	-766	16
16	2079	-2003	12
17	-579	268	-20
18	2218	2119	15
19	498	-479	0
20	1829	-1796	4
21	942	483	19
22	1607	1559	3
23	156	-411	-3
24	696	-970	-11
25	-283	145	-2
26	843	854	0
27	418	-357	1
28	1226	-897	16

1 k 9

1	-385	40	-7
2	771	563	14
3	800	816	-1
4	804	830	-2
5	-179	44	-2
6	-250	-125	-5
7	887	834	5
8	-321	191	-9
9	1492	-1423	10
10	423	-572	-8
11	553	777	-16
12	1049	1102	-6
13	1110	-1121	-1
14	973	-1093	-12
15	812	979	-14
16	1377	1430	-6
17	1000	-982	1
18	1470	-1408	7
19	997	1074	-6
20	644	868	-9
21	887	-956	-3
22	1001	-1005	0
23	865	672	8
24	1198	1235	-2
25	522	-801	-9
26	1447	-1289	9
27	1041	878	7

1 k 10

0	1504	-1417	8
1	3868	-4017	-29
2	140	-298	-3
3	2896	2878	3
4	596	133	20
5	4085	-4145	-12
6	465	466	0
7	5430	5435	0
8	-430	37	-11
9	3296	-3290	1
10	579	-612	-2
11	4062	4069	-1
12	514	-651	-8
13	2927	-2898	5
14	538	-548	0
15	2871	2896	-4
16	218	28	2
17	2361	-2280	12
18	748	442	16
19	2440	2359	12
20	-280	56	-2
21	2117	-2144	-2
22	-221	168	-2
23	1437	1519	-5
24	644	-426	5
25	923	-1135	-10
26	-553	2	-7
27	1383	1138	13

1 k 11

1	908	642	20
2	-158	141	-2
3	1602	-1598	0
4	1208	-987	25
5	1369	1395	-3
6	871	-669	17
7	1062	-1030	3
8	399	539	-7
9	746	800	-4
10	758	-631	9
11	1271	-1151	14
12	1291	1198	11
13	562	698	-8
14	1105	-1115	-1
15	1075	-1097	-2
16	462	844	-22
17	1443	1266	19
18	1215	-1177	3
19	1201	-1263	-4

20	870	1149	-14
21	1161	1325	-11
22	656	-979	-13
23	1065	-1329	-15
24	-438	789	-20
25	1050	1041	0
26	701	-684	0

1 k 12

0	4510	4609	-13
1	446	599	-7
2	3627	-3553	13
3	-288	241	-7
4	3901	3803	18
5	437	531	-4
6	3729	-3618	21
7	1139	-1022	12
8	4096	4142	-8
9	1030	975	5
10	3083	-3018	12
11	506	-204	11
12	3251	3292	-7
13	97	437	-8
14	3044	-3053	-1
15	547	-251	10
16	2237	2327	-13
17	598	358	10
18	2176	-2113	6
19	939	-327	21
20	2420	2303	12
21	-112	22	0
22	1386	-1292	5
23	-308	-152	-3
24	723	1222	-22
25	-814	-62	-16
26	1250	-1358	-6

1 k 13

1	280	-435	-4
2	323	-5	4
3	566	328	10
4	653	-565	5
5	471	-78	10
6	-610	257	-22
7	189	-45	1
8	150	-608	-17
9	-416	404	-17
10	1311	1090	24
11	1205	-1196	1
12	697	-990	-22
13	1097	1195	-9
14	1213	1052	15
15	119	-707	-20
16	967	-1099	-10
17	941	952	0
18	889	836	2
19	1099	-759	17
20	936	-1028	-4
21	1106	813	14
22	1257	870	19
23	205	-365	-2
24	1073	-959	5
25	-536	678	-17

1 k 14

0	-680	-274	-16
1	3706	3772	-11
2	775	834	-4
3	2550	-2380	27
4	762	-837	-5
5	2976	2922	9
6	625	601	1
7	2490	-2483	1
8	354	-946	-36
9	2210	2218	-1
10	327	386	-1
11	2043	-2269	-34
12	602	-685	-4
13	2270	2290	-3
14	567	746	-9
15	1335	-1379	-4
16	852	-800	2
17	1929	1845	7
18	935	777	7
19	1558	-1532	1
20	411	-441	0
21	636	1081	-19
22	204	161	0
23	1292	-1189	6
24	-122	-374	-3

1 k 15

1	261	-332	-1
2	-117	139	-1
3	-291	569	-17
4	460	-194	7
5	-657	-138	-19
6	-196	26	-1
7	575	-334	9
8	190	125	0
9	420	-49	7
10	662	388	12
11	393	299	2
12	503	-311	6
13	542	-526	0
14	877	881	0
15	416	678	-8
16	831	-491	12
17	1229	-1054	10
18	850	897	-2
19	677	533	4
20	386	-735	-10
21	932	-447	17
22	208	192	0
23	-534	685	-18
24	305	-445	-2

1 k 16

0	831	-716	4
1	539	302	7
2	1151	1201	-4
3	-235	507	-12
4	1245	-1351	-10
5	715	-696	1
6	828	725	6
7	630	686	-3
8	1199	-1146	4
9	916	-702	14
10	985	968	1
11	671	435	10
12	868	-781	5
13	470	-232	4
14	779	864	-3
15	1126	780	17
16	916	-821	4
17	879	-619	10
18	631	685	-1
19	827	289	15
20	291	-870	-17
21	-693	-503	-19
22	-506	331	-9
23	-891	278	-22

1 k 17

1	431	-235	4
2	-226	-198	-3
3	380	154	4
4	85	131	0
5	-423	50	-6
6	113	-57	0
7	606	224	12
8	192	-296	-2
9	-260	-71	-2
10	716	-56	20
11	-308	176	-3
12	-269	39	-2
13	-637	-532	-18
14	-537	-187	-8
15	-689	480	-18
16	794	128	15
17	201	-397	-3
18	-874	-70	-20
19	746	136	13
20	-514	34	-7
21	389	-381	0
22	637	-56	10

1 k 18

0	-892	-391	-23
1	192	9	1
2	314	376	-1
3	-606	-434	-19
4	-681	-187	-18
5	-156	244	-3
6	-452	82	-8
7	261	-125	1
8	827	4	26
9	679	633	1
10	354	-10	3
11	-477	8	-6
12	531	14	7
13	-748	222	-15
14	814	332	13
15	201	-187	0
16	895	16	21
17	119	243	-1
18	120	-37	0
19	-518	-140	-7
20	-821	114	-18
21	453	289	3

1 k 19

1	226	49	1
2	540	-401	4
3	-492	-29	-8
4	767	339	16
5	808	-337	13
6	-760	32	-14
7	-383	471	-9
8	199	21	0
9	701	-232	11
10	-663	-366	-14
11	666	794	-4
12	-824	53	-17
13	870	-523	12
14	529	45	7
15	266	530	-5
16	-713	217	-14
17	711	-498	6
18	-493	-68	-6
19	572	551	0
20	456	201	4

1 k 20

0	1503	-1230	16
1	1311	-1112	10
2	1369	1278	5
3	878	1203	-14
4	1196	-1194	0
5	380	-736	-9
6	942	1150	-9
7	429	794	-10
8	1030	-941	4
9	-356	-771	-17
10	952	1038	-3
11	925	1008	-3
12	1181	-1065	6
13	467	-431	0
14	1291	1139	9
15	765	655	3
16	741	-1034	-12
17	330	-610	-6
18	378	615	-6

1 k 21

1	767	-171	12
2	-660	-63	-9
3	-810	-169	-15
4	-451	72	-4
5	-541	-230	-7
6	-855	-268	-18
7	0	-232	-1
8	785	706	2
9	300	124	1
10	841	-651	6
11	777	-108	13
12	750	546	6
13	-277	-29	-1
14	432	-720	-8
15	699	-142	11
16	537	769	-7
17	-404	199	-5

1 k 22

0	1859	1833	1
1	1761	-1858	-6
2	1717	-1767	-3
3	1118	1346	-11
4	1381	1630	-14
5	1000	-1428	-20
6	1358	-1513	-9
7	1477	1500	-1
8	1676	1505	10
9	1503	-1447	3
10	1562	-1343	14
11	1683	1649	2
12	1430	1308	7
13	1503	-1327	10
14	1427	-1325	6
15	1196	1092	5

1 k 23

1	680	65	9
2	-586	188	-7
3	1183	-262	28
4	-618	-124	-8
5	527	594	-1
6	-571	-167	-8
7	-1043	-363	-26
8	-520	24	-6
9	649	837	-6
10	-224	525	-7
11	802	-757	1
12	583	-290	5
13	1080	1050	1

1 k 24

0	1081	1302	-10
1	2313	1967	26
2	1695	-1682	0
3	1966	-1905	4
4	1730	1638	5
5	1799	1743	3
6	981	-1150	-7
7	1925	-1733	13
8	1565	1445	7
9	2060	1894	12
10	1267	-1266	0
11	1905	-1717	13

1 k 25

1	-476	-191	-5
2	-584	216	-8
3	965	94	19
4	-677	-302	-11
5	555	-181	5
6	339	518	-3
7	-632	141	-9

2 k 0

0	2029	-2076	-11
1	1570	-1469	26
2	997	-983	3
3	574	-241	34
4	4126	4124	0
5	1039	-1146	-24
6	952	-1014	-12
7	1212	1084	26
8	-167	2	-2
9	407	-383	1
10	240	-171	2
11	714	586	15
12	514	366	12
13	619	-545	7
14	617	-458	10
15	886	772	10
16	277	464	-8
17	741	-874	-11
18	227	-57	2
19	453	684	-12
20	611	556	2
21	616	-806	-11

2 k 1

1	688	-698	-1
2	932	-932	0
3	305	300	0
4	1002	-900	17
5	2106	-2046	17
6	476	-430	3
7	673	222	35
8	405	-333	4
9	-203	-361	-13
10	1008	-946	9
11	182	41	2
12	-501	339	-31
13	335	-283	2
14	455	-691	-16
15	831	-706	11
16	500	131	13
17	495	66	13
18	825	-917	-8
19	250	39	3
20	-468	395	-17
21	442	-421	0

2 k 2

0	1971	-1971	0
1	584	378	14
2	1491	-1415	14
3	130	101	0
4	1675	-1641	7
5	615	451	12
6	1644	1503	26
7	420	-320	5
8	1102	-1116	-1
9	1120	-1034	11
10	506	232	13
11	288	458	-8
12	1180	-1217	-5
13	747	-748	0
14	1189	1196	-1
15	772	570	16
16	781	-717	5
17	152	-3	1
18	591	719	-8
19	494	-16	12
20	549	-302	9
21	-264	44	-3

2 k 3

1	-206	-168	-4
2	1376	1415	-6
3	-509	-282	-23
4	477	377	5
5	873	-895	-2
6	770	-786	-1
7	-347	-40	-8
8	1508	1582	-13
9	446	210	10
10	657	-697	-3
11	-212	-92	-3
12	-482	113	-16
13	-337	265	-11
14	314	4	6
15	342	400	-2
16	997	1060	-6
17	757	455	19
18	809	-827	-1
19	351	-120	5
20	624	680	-3
21	-453	282	-13

2 k 4

0	3730	3789	-9
1	6070	-6164	-16
2	2027	-1946	16
3	3876	3829	10
4	2162	2186	-5
5	1531	-1479	8
6	3171	-3150	4
7	2507	2445	13
8	1872	1874	0
9	2425	-2543	-26
10	1141	-1115	3
11	1994	2025	-6
12	1918	1914	0
13	1372	-1447	-11
14	-281	-504	-19
15	1906	1914	-1
16	909	1031	-12
17	1272	-1234	4
18	958	-817	12
19	1767	1706	8
20	934	1006	-6
21	1474	-1532	-6

2 k 5

1	826	775	4
2	612	859	-20
3	430	-347	3
4	447	-417	1
5	777	743	3
6	331	262	2
7	494	-322	8
8	-251	0	-4
9	502	615	-8
10	-137	-141	-2
11	810	-815	0
12	407	281	5
13	2046	1979	12
14	-335	67	-6
15	1534	-1525	1
16	-513	-72	-14
17	1023	1132	-11
18	-343	-216	-8
19	1762	-1756	0
20	-458	37	-9
21	1664	1536	15

2 k 6

0	6104	6029	9
1	3739	3808	-14
2	5805	-5846	-7
3	3265	-3144	25
4	3539	3396	30
5	2186	2186	0
6	3170	-3140	6
7	2308	-2381	-15
8	2615	2675	-13
9	2482	2463	4
10	3196	-3174	4
11	2436	-2436	0
12	2657	2609	10
13	2127	2000	23
14	2431	-2496	-12
15	1819	-1899	-13
16	2668	2781	-21
17	1722	1705	2
18	2076	-2242	-26
19	1404	-1377	3
20	1725	1758	-4

2 k 7

1	-519	100	-13
2	699	869	-13
3	788	606	13
4	786	-830	-3
5	964	-1007	-4
6	813	723	8
7	-446	-200	-15
8	967	-1033	-7
9	246	405	-6
10	1855	1907	-9
11	578	272	16
12	2114	-2087	4
13	212	106	1
14	1511	1365	20
15	-370	-264	-11
16	1867	-1963	-15
17	448	315	4
18	1883	1882	0
19	330	-245	2
20	1709	-1602	13

2 k 8

0	4619	-4558	8
1	4353	4359	-1
2	4029	3990	7
3	3959	-3882	15
4	3688	-3638	10
5	2538	2533	1
6	2134	2123	2
7	3026	-2996	6
8	2850	-2741	22
9	2671	2650	4
10	2865	2837	5
11	2546	-2543	0
12	1979	-1958	3
13	2290	2298	-1
14	2407	2364	7
15	2082	-2146	-10
16	1808	-1716	13
17	2223	2210	1
18	1699	1761	-8
19	1941	-1844	13
20	1533	-1466	4

2 k 9

1	596	-533	3
2	-483	128	-13
3	465	298	6
4	268	471	-8
5	1345	-1287	8
6	759	797	-3
7	798	778	1
8	1209	-1119	11
9	1041	-1049	0
10	404	162	7
11	1130	1135	0
12	281	-285	0
13	899	-916	-1
14	-338	131	-6
15	1383	1426	-5
16	291	-268	0
17	1623	-1617	0
18	-204	-205	-3
19	1811	1928	-15
20	675	-130	12

2 k 10

0	3390	-3424	-4
1	2664	-2740	-14
2	1766	1874	-16
3	3115	3132	-3
4	2141	-2212	-12
5	3342	-3318	9
6	1421	1446	-3
7	2957	2919	7
8	1501	-1596	-14
9	1863	-1795	11
10	1772	1800	-4
11	2451	2432	3
12	1431	-1526	-12
13	2361	-2259	17
14	1840	1838	0
15	1982	1969	2
16	1178	-1180	0
17	1742	-1769	-3
18	1169	1157	1
19	1867	1938	-6
20	1123	-1152	-1

2 k 11

1	332	-126	4
2	527	468	2
3	279	559	-11
4	-106	303	-5
5	-323	63	-5
6	-162	-324	-6
7	702	414	16
8	1265	1234	3
9	379	-432	-2
10	680	-719	-2
11	521	-234	11
12	1161	1174	-1
13	-397	116	-8
14	1259	-1202	6
15	402	66	7
16	1195	1042	14
17	375	359	0
18	1007	-1142	-7
19	-562	100	-9
20	1414	1345	4

2 k 12

0	1475	1495	-1
1	2066	-2052	2
2	1897	-1799	13
3	307	634	-14
4	2344	2341	0
5	776	-689	6
6	1998	-1954	7
7	829	808	1
8	2198	2259	-10
9	775	-733	3
10	1685	-1584	13

11	888	964	-6
12	1957	1979	-3
13	886	-701	13
14	1600	-1539	7
15	879	759	8
16	1342	1455	-12
17	487	-775	-9
18	1254	-1260	0
19	312	344	0
20	979	1266	-15

2 k 13

1	664	380	13
2	664	-58	19
3	757	-524	13
4	330	-565	-9
5	222	8	2
6	401	-114	6
7	251	-204	1
8	-355	-52	-6
9	744	740	0
10	359	51	5
11	952	-1085	-11
12	-502	-36	-11
13	619	637	-1
14	-232	-31	-2
15	871	-729	9
16	793	-155	15
17	473	668	-5
18	442	-389	1
19	435	-538	-2
20	498	12	6

2 k 14

0	270	73	2
1	280	-160	2
2	1275	-1307	-3
3	551	-609	-2
4	287	-188	2
5	759	681	4
6	-553	-234	-16
7	857	-758	7
8	475	70	9
9	830	834	0
10	-374	97	-6
11	-227	-494	-12
12	-486	-238	-12
13	667	268	15
14	-727	82	-22
15	601	-656	-1
16	-154	-98	0
17	-608	255	-10
18	575	-65	8
19	669	-494	4
20	-508	142	-7

2 k 15

1	-127	-60	0
2	222	156	1
3	517	-71	10
4	-122	42	0
5	595	316	10
6	-237	-88	-2
7	490	-148	9
8	618	-15	16
9	-380	5	-6
10	743	298	19
11	635	-182	15
12	-149	-200	-2
13	-594	200	-15
14	-628	250	-12
15	110	-4	0
16	-112	-87	0
17	-820	270	-18
18	-1165	3	-32
19	-573	-137	-8
20	476	-92	5

2 k 16

0	1005	1017	0
1	254	1	2
2	40	-945	-12
3	533	275	7
4	969	845	8
5	-527	-55	-11
6	608	-510	4
7	677	689	0
8	936	920	1
9	623	-416	8
10	772	-670	5
11	-712	228	-22
12	661	722	-2
13	-577	-267	-10
14	514	-678	-4
15	196	574	-7
16	770	925	-6
17	-581	-391	-11
18	514	-416	2
19	293	576	-5
20	1226	684	26

2 k 17

1	210	-73	1
2	417	111	5
3	537	4	10
4	528	-344	5
5	-650	400	-21
6	163	474	-7
7	372	-446	-2
8	483	-560	-3
9	-271	272	-5
10	868	433	13
11	276	-527	-5
12	1173	-737	19
13	582	489	2
14	1225	690	25
15	-616	-458	-13
16	-235	-202	-2
17	753	550	6
18	0	295	-2
19	211	-498	-4
20	1208	-830	18

2 k 18

0	305	173	1
1	2244	2263	-2
2	-658	-267	-17
3	1841	-1853	-1
4	-437	254	-8
5	2041	2128	-10
6	658	-750	-4
7	2023	-2007	1
8	381	420	0
9	1641	1793	-11
10	-872	-182	-18
11	1449	-1719	-19
12	659	224	8
13	1609	1543	4
14	679	-300	9
15	1533	-1515	1
16	626	520	2
17	1649	1457	12
18	-123	-250	-1
19	1385	-1390	0
20	657	183	9

2 k 19

1	-653	-14	-9
2	-727	84	-12
3	293	73	1
4	538	-111	6
5	872	-348	14
6	763	57	12
7	-788	589	-21
8	-290	-459	-6
9	760	-790	-1
10	980	715	9
11	-620	346	-11
12	268	-403	-2
13	733	-354	9
14	556	417	3
15	406	695	-7
16	1146	-675	19
17	1022	-917	4
18	1040	784	10
19	920	863	2

2 k 20

0	3141	-3069	6
1	489	175	4
2	2982	2886	9
3	727	122	10
4	2563	-2774	-18
5	-579	-54	-7
6	2608	2688	-7
7	-323	-5	-2
8	2736	-2727	0
9	-366	185	-3
10	2453	2203	20
11	347	-238	1
12	2177	-2020	12
13	581	140	6
14	2369	2094	22
15	906	-11	18
16	1759	-1782	-1
17	-221	25	-1
18	1517	1393	7

2 k 21

1	-732	102	-11
2	-487	-338	-7
3	-282	48	-1
4	-438	376	-7
5	-539	-409	-9
6	536	-327	3
7	504	473	0
8	-765	169	-13
9	765	-265	11
10	1233	-912	13
11	126	626	-7
12	1260	974	13
13	-220	-665	-10
14	931	-753	6
15	794	621	5
16	734	749	0

2 k 22

0	-530	543	-11
1	2939	-2647	24
2	-930	-348	-19
3	2614	2728	-9
4	799	65	14
5	2060	-2184	-8
6	758	-278	9
7	2272	2212	4
8	-224	227	-2
9	2450	-2462	-1
10	-388	-161	-3
11	2333	2265	5
12	-520	325	-7
13	2081	-2019	4
14	1008	-240	22

2 k 23

1	-722	83	-11
2	228	-183	0
3	805	-378	9
4	-351	326	-5
5	-266	278	-2
6	-641	-326	-10
7	639	-542	2
8	-775	203	-12
9	739	514	5
10	497	-187	4
11	266	-481	-3
12	654	447	4

2 k 24

0	2138	2023	7
1	523	492	0
2	1732	-1822	-5
3	790	-608	4
4	1613	1840	-13
5	-528	457	-9
6	1926	-2067	-9
7	547	-440	2
8	1893	1749	9
9	305	756	-9

2 k 25

1	458	-61	4
2	195	-61	0
3	619	-158	6
4	637	-444	4
5	-540	219	-6

3 k 0

0	1413	-1550	-18
1	2625	2607	4
2	650	-601	4
3	566	-384	14
4	1047	892	24
5	1467	1405	13
6	2216	-2236	-5
7	532	-545	-1
8	1218	1200	3
9	726	597	15
10	900	-916	-2
11	570	-486	8
12	1141	965	30
13	1095	1126	-3
14	1347	-1363	-2
15	1490	-1477	1
16	549	414	6
17	424	531	-5
18	923	-777	11
19	495	-737	-13
20	773	830	-3

3 k 1

1	1066	894	16
2	398	-419	0
3	192	-135	1
4	190	121	1
5	457	514	-4
6	617	227	24
7	536	381	8
8	1525	-1443	16
9	1673	-1721	-10
10	1177	1180	0
11	931	895	4
12	661	-644	1
13	773	-746	2
14	338	423	-3
15	690	632	4
16	517	-1025	-40
17	716	-739	-1

18	1071	1143	-7
19	585	428	7
20	1026	-967	5
3 k 2			
0	2898	-2843	8
1	1277	1286	-1
2	4872	4847	4
3	1709	-1671	6
4	2767	-2732	7
5	914	902	1
6	2832	2856	-5
7	860	-867	0
8	2432	-2438	-1
9	1492	1502	-1
10	2825	2800	5
11	1502	-1392	17
12	2179	-2152	5
13	323	616	-16
14	2072	2115	-7
15	1166	-1196	-3
16	1585	-1610	-3
17	591	595	0
18	1748	1855	-15
19	1140	-977	14
20	1486	-1397	10
3 k 3			
1	-470	-107	-11
2	1751	-1801	-8
3	-306	-359	-12
4	197	249	-1
5	541	298	11
6	1587	-1749	-19
7	331	308	0
8	1168	1236	-9
9	343	13	5
10	770	-528	19
11	1073	1061	1
12	693	738	-3
13	1114	-1089	2
14	1202	-1182	2
15	1271	1218	6
16	1175	928	25
17	470	-767	-17
18	803	-827	-1
19	1540	1540	0
20	1128	1213	-8
3 k 4			
0	1920	-1886	3
1	5395	-5406	-1
2	1334	1240	11
3	5851	5783	11
4	1646	-1610	5
5	3779	-3706	15
6	330	552	-11
7	3242	3184	12
8	1167	-1047	15
9	3401	-3331	14
10	-297	67	-5
11	3300	3227	14
12	1296	-1379	-11
13	3474	-3548	-15
14	849	572	21
15	2908	2869	7
16	1007	-852	14
17	2725	-2664	10
18	817	742	5
19	2352	2293	9
20	491	-401	3
3 k 5			
1	514	116	12
2	-511	54	-13
3	265	-18	3
4	1190	1233	-5
5	633	-737	-8
6	834	-787	4
7	905	-882	2
8	589	551	2
9	1415	1419	0
10	923	-869	5
11	1115	-921	21
12	1298	1303	0
13	1028	1103	-8
14	1184	-1168	1
15	1447	-1442	0
16	1376	1382	0
17	1295	1259	4
18	1103	-1193	-8
19	1150	-1059	8
3 k 6			
0	7118	7001	13
1	624	359	12
2	5409	-5453	-7
3	969	1019	-5
4	4631	4553	14
5	905	-721	17
6	3352	-3259	19
7	-596	68	-22
8	3998	4041	-8
9	982	-1005	-2
10	5033	-5033	0
11	603	387	12
12	3201	3304	-20
13	813	-345	29
14	2917	-2942	-4
15	675	362	16
16	3304	3360	-10
17	-560	-56	-15
18	2592	-2513	12
19	529	293	8
3 k 7			
1	506	502	0
2	845	850	0
3	375	-243	4
4	279	-380	-3
5	544	483	3
6	437	287	6
7	380	-646	-15
8	439	-408	1
9	1007	1100	-10
10	-93	206	-2
11	850	-695	13
12	750	-811	-4
13	1082	1170	-9
14	586	889	-22
15	1120	-1042	7
16	708	-765	-3
17	1153	1159	0
18	985	1054	-5
19	1540	-1419	13
3 k 8			
0	480	291	5
1	3972	4005	-6
2	317	78	4
3	4637	-4590	8
4	488	279	8
5	3293	3269	4
6	314	-99	4
7	3243	-3149	18
8	-518	-117	-15
9	3427	3478	-9
10	653	-492	9
11	3121	-3108	2
12	-347	233	-9
13	2412	2362	8
14	-117	-120	-1
15	2274	-2333	-9
16	-369	12	-6
17	2345	2310	5
18	-431	343	-13
3 k 9			
1	533	362	7
2	-64	-203	-2
3	-611	104	-19
4	534	258	11
5	1181	-1125	6
6	764	328	25
7	430	288	5
8	1097	-1057	4
9	838	-531	21
10	526	587	-3
11	-195	519	-15
12	620	-702	-5
13	420	-636	-11
14	917	827	7
15	635	591	2
16	948	-632	21
17	653	-621	1
3 k 10			
0	2251	-2315	-7
1	-229	-513	-15
2	2392	2424	-5
3	362	649	-13
4	2180	-2232	-8
5	388	-575	-8
6	1360	1340	2
7	-267	-205	-5
8	1735	-1692	6
9	252	-298	-1
10	1313	1199	13
11	-476	187	-13
12	1288	-1389	-11
13	228	-36	2
14	1312	1295	1
15	134	598	-15
16	1394	-1311	8
17	490	-302	6
3 k 11			
1	405	-285	3
2	931	-892	3
3	417	168	6
4	-507	-46	-12
5	494	253	8
6	222	-39	2
7	509	590	-4
8	302	254	1
9	178	-254	-1
10	-475	-5	-10
11	603	578	1
12	581	-472	5
13	228	-174	0
14	-413	-41	-7
15	971	784	13
16	-55	-33	0
3 k 12			
0	-298	-45	-2
1	-379	-273	-9
2	-319	40	-4
3	193	-644	-16
4	542	635	-4
5	-183	263	-4
6	827	-642	12
7	358	71	5
8	526	230	10
9	-483	-265	-13
10	501	-325	6
11	522	-252	9
12	314	398	-2
13	330	1	4
14	423	-264	4
15	-645	-11	-17
3 k 13			
1	512	-348	5
2	103	-187	-1
3	-728	57	-22
4	-560	39	-13
5	-270	71	-3
6	608	248	13
7	603	-173	14
8	507	-54	11
9	361	-133	4
10	-445	95	-9
11	-709	109	-21
12	-635	217	-19
13	257	-330	-1
14	-195	-398	-8
3 k 14			
0	986	-1166	-10
1	950	-952	0
2	1325	1239	8
3	-178	186	-2
4	1392	-1545	-16
5	546	-717	-8
6	1709	1670	4
7	631	155	15
8	1578	-1542	4
9	498	-530	-1
10	1114	1076	3
11	328	561	-8
12	1283	-1350	-6
3 k 15			
1	400	369	0
2	164	-296	-2
3	848	-436	19
4	622	670	-2
5	-180	164	-2
6	761	-757	0
7	-225	135	-2
8	703	365	14
9	129	-57	0
10	898	-407	24
11	742	18	21
3 k 16			
0	1471	1555	-5
1	2223	-2207	2
2	1569	-1655	-9
3	1803	1802	0
4	1109	1068	3
5	2234	-2359	-17
6	1318	-1135	15
7	1839	1883	-5
8	1155	1375	-19
9	2008	-2096	-11
3 k 17			
1	703	180	16
2	714	206	16
3	-310	-155	-4
4	-359	-38	-4
5	771	438	13
6	-533	142	-10

4 k 0

0	3301	3307	-1
1	1832	1872	-8
2	4305	-4236	15
3	1840	-1855	-3
4	2764	2741	5
5	1538	1484	11
6	2403	-2322	19
7	1303	-1312	-1
8	4179	4142	8
9	1552	1549	0
10	3537	-3619	-21
11	801	-779	2
12	2436	2334	25
13	507	571	-3
14	2333	-2353	-3
15	1103	-1082	2
16	2364	2254	17
17	840	1025	-15
18	2167	-2281	-17
19	-450	-387	-15

4 k 1

1	-243	-374	-9
2	815	728	6
3	1154	-996	17
4	194	-104	1
5	622	776	-15
6	-496	-245	-22
7	482	620	-11
8	385	-480	-5
9	1016	828	23
10	698	909	-18
11	295	-516	-10
12	1585	-1523	9
13	-253	92	-4
14	1288	1334	-5
15	-142	-400	-9
16	1153	-1186	-3
17	763	544	12
18	1289	1349	-6
19	-200	-151	-2

4 k 2

0	1629	-1818	-20
1	3808	3915	-20
2	1197	1009	19
3	2789	-2781	1
4	2127	-2080	8
5	3871	3888	-3
6	2022	1909	20
7	3829	-3855	-5
8	2209	-2120	12
9	2947	2927	3
10	2487	2564	-15
11	3029	-3033	0
12	1990	-1999	-1
13	2858	2909	-9
14	1326	1400	-9
15	2571	-2624	-9
16	1041	-1147	-10
17	1980	2052	-10
18	1091	1155	-6
19	1958	-1936	3

4 k 3

1	-593	-502	-29
2	27	-68	0
3	281	331	-1
4	326	241	2
5	759	-507	18
6	392	286	4
7	1402	1393	1
8	839	684	13
9	1734	-1641	15
10	217	-234	0
11	1099	1096	0
12	490	-27	12
13	1431	-1513	-11
14	297	362	-2
15	1848	1719	18
16	393	-345	1
17	1473	-1333	16
18	903	543	23

4 k 4

0	2778	-2841	-8
1	2882	-2858	4
2	2899	2901	0
3	2593	2603	-2
4	2633	-2613	3
5	2529	-2520	1
6	1993	2003	-1
7	2118	2037	14
8	2334	-2341	-1
9	1965	-1979	-2
10	2885	2841	8
11	2357	2434	-14
12	1922	-2027	-17
13	1970	-2013	-7
14	2367	2297	11
15	1587	1587	0
16	1772	-1679	12
17	1774	-1687	11
18	1371	1360	1

4 k 5

1	1071	1023	4
2	1196	-1173	2
3	493	-164	11
4	330	18	5
5	399	-180	6
6	636	-209	19
7	521	-357	7
8	1388	1355	4
9	-357	164	-8
10	1020	-1070	-5
11	-213	359	-9
12	921	1019	-9
13	575	-409	8
14	1404	-1496	-11
15	-553	45	-14
16	1606	1451	19
17	423	-526	-4
18	1369	-1241	13

4 k 6

0	1957	1965	0
1	2619	-2650	-5
2	2758	-2889	-24
3	2301	2330	-4
4	2888	2749	26
5	855	-697	12
6	2114	-2188	-13
7	1653	1569	12
8	1681	1624	8
9	1606	-1631	-3
10	1040	-1198	-17
11	1256	1213	5
12	1361	1532	-22
13	1084	-1049	3
14	1258	-1382	-14
15	870	823	3
16	1222	1211	1
17	1208	-1201	0

4 k 7

1	609	363	11
2	986	-824	13
3	-70	102	0
4	-142	0	-1
5	-322	-199	-7
6	94	269	-3
7	293	-98	4
8	597	-328	12
9	-334	51	-5
10	540	-405	6
11	880	-744	10
12	-344	105	-6
13	1077	991	8
14	-332	-11	-5
15	891	-975	-6
16	862	201	31
17	860	1056	-15

4 k 8

0	336	240	1
1	1223	1175	5
2	770	-785	-1
3	696	-727	-2
4	606	899	-20
5	923	876	4
6	942	-995	-5
7	-395	94	-8
8	549	505	2
9	419	536	-5
10	519	-755	-13
11	898	-773	9
12	537	564	-1
13	-422	123	-9
14	573	-585	0
15	743	-732	0
16	699	308	17

4 k 9

1	519	-394	5
2	313	429	-3
3	-441	-109	-9
4	-96	-33	0
5	586	393	8
6	517	-330	7
7	595	-270	13
8	-101	-139	-1
9	338	91	4
10	251	195	1
11	538	-317	8
12	122	-151	0
13	757	736	1
14	687	255	17
15	-34	-160	-1
16	277	-226	1

4 k 10

0	1783	1723	5
1	1065	-1121	-5
2	1050	-1085	-3
3	695	585	6
4	1191	1292	-10
5	776	381	20
6	990	-934	4
7	370	349	0
8	301	633	-14
9	-301	-36	-4
10	1091	-1027	5
11	276	-224	1
12	709	580	6
13	-365	-296	-9
14	687	-559	6
15	253	43	2

4 k 11

1	-72	216	-2
2	673	605	3
3	-152	102	-1
4	-205	287	-5
5	-360	94	-6
6	-705	258	-25
7	-300	167	-5
8	690	-511	9
9	-274	342	-8
10	570	480	3
11	-176	-508	-12
12	-344	165	-6
13	397	358	1
14	-422	523	-17

4 k 12

0	1272	1155	7
1	2839	2856	-2
2	591	-760	-9
3	1959	-2114	-21
4	708	766	-3
5	1739	1831	-11
6	463	-609	-6
7	2233	-2220	1
8	-270	163	-4
9	1720	1692	3
10	767	-623	8
11	1826	-1605	26
12	830	362	21
13	1864	1872	-1

4 k 13

1	586	-472	4
2	498	334	5
3	789	576	11
4	209	-436	-5
5	218	-195	0
6	107	535	-10
7	-211	-160	-2
8	565	-762	-10
9	490	-343	4
10	461	503	-1
11	555	719	-7

4 k 14

0	3206	-2873	36
1	-500	592	-21
2	2619	2670	-7
3	640	-586	2
4	2554	-2694	-20
5	475	618	-5
6	2302	2385	-11
7	110	-705	-17
8	2389	-2430	-5
9	666	528	6
10	2668	2613	7

4 k 15

1	657	471	7
2	868	-685	9
3	621	116	13
4	-409	166	-6
5	552	-382	5
6	-335	-196	-5
7	-229	491	-10
8	558	740	-8

4 k 16

0	-542	-355	-10
1	2902	-2821	11
2	286	583	-8
3	3236	3283	-6
4	658	-59	15

5 k 0

0	5150	5191	-7
1	1579	-1575	0
2	4032	-3949	17
3	957	1020	-8
4	3371	3408	-9
5	1386	-1318	11
6	3996	-3973	5
7	1109	1073	5
8	3202	3194	1
9	827	-749	8
10	3071	-3127	-13
11	484	503	-1
12	2837	2827	2
13	782	-886	-7
14	2846	-2757	15
15	1101	1209	-10
16	2666	2605	9
17	697	-543	7

5 k 1

1	880	928	-3
2	218	-281	-1
3	482	-104	10
4	216	398	-5
5	1107	1179	-7
6	909	602	22
7	991	-991	0
8	201	-504	-10
9	1122	1176	-6
10	865	674	14
11	574	-333	10
12	1017	-1066	-4
13	838	840	0
14	1110	1054	5
15	1234	-1073	15
16	851	-750	6
17	1140	1021	10

5 k 2

0	-459	-117	-7
1	3394	3396	0
2	321	-170	3
3	3887	-3858	5
4	771	599	11
5	2161	2151	1
6	468	-32	11
7	3136	-3240	-19
8	790	776	1
9	2548	2495	9
10	78	-73	0
11	2850	-2880	-5
12	802	586	14
13	2818	2662	26
14	-209	-194	-3
15	2208	-2299	-14
16	280	-41	3

5 k 3

1	1155	-1059	9
2	868	805	4
3	361	-140	5
4	672	-795	-8
5	473	371	4
6	1028	768	22
7	328	-360	-1
8	577	-635	-3
9	631	-355	13
10	289	-89	3
11	607	-12	17
12	439	-667	-11
13	748	-592	9
14	602	729	-7
15	682	356	14
16	879	-860	1

5 k 4

0	2640	-2691	-6
1	905	963	-4
2	636	859	-14
3	-651	256	-22
4	2032	-2042	-1
5	871	-948	-6
6	2289	2332	-7
7	483	639	-8
8	1719	-1662	8
9	507	-362	6
10	1468	1375	11
11	424	226	6
12	1667	-1569	12
13	243	-223	0
14	1212	1287	-7
15	-234	147	-3
16	1499	-1408	10

5 k 5

1	-351	-387	-12
2	-276	-439	-12
3	446	434	0
4	540	317	8
5	229	205	0
6	340	-210	3
7	522	-301	8
8	-287	170	-5
9	-586	0	-16
10	200	307	-2
11	384	4	6
12	292	-28	3
13	435	-147	7
14	382	-124	5
15	572	672	-5
16	323	430	-3

5 k 6

0	-614	-193	-12
1	-387	-486	-17
2	616	195	15
3	448	149	8
4	630	498	6
5	320	-235	2
6	605	-354	11
7	-613	195	-19
8	-556	343	-20
9	740	-289	21
10	121	-163	0
11	-569	45	-14
12	749	636	6
13	626	-216	15
14	594	-289	11
15	509	265	8

5 k 7

1	417	-8	7
2	-591	-261	-18
3	142	10	0
4	45	395	-6
5	404	-169	6
6	346	-418	-2
7	722	634	5
8	391	64	6
9	679	-172	19
10	423	-53	7
11	359	355	0
12	-628	515	-28
13	879	-494	21
14	114	-51	0

5 k 8

0	1745	-1592	13
1	-514	-62	-11
2	1271	1472	-21
3	415	81	6
4	1345	-1398	-5
5	310	-129	3
6	1324	1333	-1
7	-542	-180	-14
8	1200	-1145	5
9	293	-427	-4
10	882	782	6
11	412	-37	7
12	1133	-947	15
13	-771	-89	-24
14	1123	1056	5

5 k 9

1	225	284	-1
2	-623	73	-16
3	614	-466	6
4	-169	143	-2
5	406	-5	6
6	535	-702	-8
7	-473	-300	-12
8	1089	929	12
9	-473	236	-11
10	608	-540	3
11	225	185	0
12	459	419	1
13	291	-192	1

5 k 10

0	1431	1372	4
1	3265	-3256	1
2	1044	-1126	-6
3	2635	2602	5
4	697	891	-11
5	2110	-2214	-14
6	1128	-1285	-14
7	1642	1777	-16
8	1217	1189	2
9	2167	-2262	-13
10	739	-474	12
11	2118	1916	26
12	1005	1191	-14

5 k 11

1	-197	144	-2
2	70	524	-10
3	-204	-654	-17
4	-351	-77	-4
5	658	426	9
6	-226	83	-2
7	537	-721	-8
8	539	349	6
9	603	609	0
10	174	-290	-2
11	1134	-1047	7

5 k 12

0	4180	4220	-4
1	2354	2270	11
2	3599	-3693	-14
3	1770	-1741	3
4	2382	2475	-13
5	1271	1347	-6
6	2579	-2680	-14
7	991	-982	0
8	2518	2595	-10
9	1645	1608	3

5 k 13

1	483	109	8
2	546	437	3
3	207	197	0
4	832	-239	22
5	411	363	1
6	409	496	-2
7	388	-154	4

5 k 14

0	2052	-2096	-3
1	2943	2955	-1
2	2193	2283	-11
3	2569	-2516	7
4	1936	-1924	1

6 k 0

0	1142	1262	-7
1	2218	-2211	1
2	1222	-1079	12
3	1934	1917	2
4	1943	1882	8
5	1795	-1794	0
6	1559	-1370	20
7	1692	1779	-11
8	1481	1529	-5
9	1935	-1955	-2
10	1204	-1035	15
11	1809	1920	-14
12	1314	1254	5
13	1628	-1723	-11
14	1154	-1116	3

6 k 1

1	691	-111	19
2	346	-226	2
3	586	-307	10
4	256	8	2
5	-296	484	-13
6	684	-221	18
7	540	-728	-10
8	185	612	-14
9	568	624	-2
10	-351	-311	-9
11	1017	-855	12
12	490	275	6
13	580	901	-19
14	505	-434	2

6 k 2

0	1884	1935	-4
1	-187	273	-4
2	776	-743	2
3	690	-919	-14
4	713	359	15
5	1357	1510	-16
6	658	-853	-12
7	1156	-925	19
8	705	396	14
9	670	706	-2
10	810	-586	13
11	955	-755	14
12	578	608	-1
13	616	561	2

6 k 3

1	273	361	-2
2	157	295	-2
3	-390	-197	-7
4	-526	-572	-25
5	-261	-182	-4
6	228	298	-1
7	685	189	18
8	413	-211	5

9	249	-13	2
10	517	-99	11
11	-272	-119	-3
12	-598	111	-15
13	-549	194	-13

6 k 4

0	994	866	6
1	327	-265	1
2	357	-347	0
3	-505	-312	-14
4	414	510	-3
5	305	-315	0
6	-538	175	-13
7	67	302	-3
8	364	154	4
9	-228	-149	-3
10	442	-42	7
11	153	546	-10
12	-143	-128	-1
13	167	-625	-14

6 k 5

1	-250	-302	-6
2	-677	29	-18
3	-275	115	-3
4	310	208	2
5	-460	53	-8
6	-536	-26	-11
7	521	224	9
8	-147	-325	-5
9	567	603	-1
10	531	113	11
11	656	-617	2
12	-215	-480	-11

6 k 6

0	920	916	0
1	1823	1918	-12
2	1052	-1124	-5
3	1298	-1322	-2
4	1313	1470	-15
5	1103	1070	2
6	965	-1063	-7
7	1545	-1451	10
8	893	1236	-27
9	1466	1467	0
10	1304	-1192	10
11	1404	-1317	8
12	831	699	7

6 k 7

1	-359	-37	-5
2	353	111	4
3	457	-404	1
4	182	108	0
5	588	-17	13
6	317	313	0
7	349	383	0
8	1081	-712	24
9	896	-928	-2
10	301	423	-3
11	406	267	3

6 k 8

0	2502	-2545	-4
1	780	1161	-26
2	2595	2675	-11
3	1242	-1214	2
4	2237	-2196	5
5	1111	1050	4
6	2350	2496	-20
7	891	-923	-2
8	2032	-1986	5
9	788	859	-4
10	2197	2205	-1

6 k 9

1	-291	74	-3
2	407	-187	4
3	-435	375	-12
4	662	271	13
5	497	-489	0
6	-543	-369	-15
7	635	598	1
8	634	49	14
9	554	-735	-8

6 k 10

0	626	-960	-12
1	2883	-2918	-5
2	1014	880	8
3	2979	2986	0
4	-472	-369	-12
5	2479	-2594	-15
6	756	854	-5
7	2473	2495	-2

6 k 11

1	-376	-93	-5
2	243	-191	0
3	-257	-256	-4
4	-177	-74	-1
5	293	391	-2

7 k 0

0	1077	-549	21
1	228	-380	-3
2	598	292	9
3	359	353	0
4	594	619	-1
5	216	-432	-4
6	-77	-339	-4
7	989	718	16
8	454	292	4
9	655	-393	10

7 k 1

1	205	325	-2
2	233	-133	1
3	524	309	6
4	182	-252	-1
5	582	405	6
6	-585	-28	-12
7	733	-57	19
8	-485	15	-9
9	-412	-21	-6

7 k 2

0	1464	-1456	0
1	438	-439	0
2	825	831	0
3	-237	196	-3
4	1062	-1008	3
5	-627	-11	-14
6	1324	1284	3
7	-480	-233	-10
8	674	-797	-6

7 k 3

1	411	-138	5
2	251	-42	2
3	562	-96	10
4	383	337	1
5	-234	-115	-2
6	382	-162	4
7	464	-314	4
8	-490	-25	-9

7 k 4

0	692	571	3
1	2221	-2199	2
2	850	-390	20
3	2402	2532	-18
4	250	115	1
5	1676	-1851	-18
6	-444	-315	-10
7	2281	2334	-7

7 k 5

1	306	113	2
2	158	18	0
3	310	65	3
4	645	-20	14
5	269	166	1
6	626	-279	11

7 k 6

0	3021	2984	3
1	1020	1122	-7
2	2479	-2406	9
3	914	-971	-3
4	2252	2490	-31
5	923	791	7

7 k 7

1	-293	31	-2
2	697	237	14
3	279	-70	2